**Province of British Columbia**
Ministry of Energy, Mines
and Petroleum Resources
**Hon. Anne Edwards, Minister**

MINERAL RESOURCES DIVISION
Geological Survey Branch

# GEOLOGICAL FIELDWORK 1995

## A Summary of Field Activities and Current Research

**Editors: B. Grant, P.Geo. and J.M. Newell, P. Eng.**

**PAPER 1996-1**

# MINERAL RESOURCES DIVISION

## Geological Survey Branch



**British Columbia Cataloguing in Publication Data**

Main entry under title:
Geological fieldwork: - 1974 -

(Paper, ISSN 0226-9430)
Annual.
Issuing body varies: 1974-1980, Geological Division; 1981-1985, Geological Branch; 1986- , Geological Survey Branch.
Subseries, 1979- , of: Paper (British Columbia. Ministry of Energy, Mines and Petroleum Resources)
"A summary of field activities of the Geological Division, Mineral Resources Branch."
ISBN 0381-243X=Geological fieldwork

1. Geology - British Columbia - Periodicals. 2. Geology, Economic - British Columbia - Periodicals. 3. Mines and mineral resources - British Columbia - Periodicals. I. British Columbia. Geological Division. II. British Columbia. Geological Branch. III. British Columbia. Geological Survey Branch. IV. British Columbia. Ministry of Energy, Mines and Petroleum Resources. V. Series: Paper (British Columbia. Ministry of Energy, Mines and Petroleum Resources)

QE187.G46 557.11'05
Rev. Dec. 1987

VICTORIA
BRITISH COLUMBIA
CANADA

JANUARY 1996

# FOREWORD

Geological Fieldwork: A Summary of Field Activities and Current Research, the 1995 edition, is the twenty-first in this annual publication series. It contains reports on Geological Survey Branch activities and projects during the past year. The base budget of the Branch for the 1995/96 fiscal year is $5.8 million, an increase of 4.7% from the previous year. This budget has been supplemented by an additional $1.07 million, made up of $720 000 from the last year of the current federal-provincial Mineral Development Agreement and $350 000 under the Mineral Potential Initiative; overall funding therefore decreased slightly from the previous year.

As before, the contents of this year's volume reflect the emphasis of Branch programs. The highlight this year has been the initiation of the Nechako Project in central British Columbia. This program, an outgrowth of the Interior Plateau Project completed last year, is a collaborative effort coordinated by the British Columbia Geological Survey Branch and the Geological Survey of Canada. Both agencies fund component projects and the program is financially augmented by the GSC's National Mapping Program (NATMAP). The program will bring the geoscience database for this region, which includes the well mineralized Skeena Arch, up to modern standards. More than fifty scientists from the federal and provincial Surveys, the Canadian Forest Service, North American, Asian and European universities, and the mineral industry, will be involved over the five-year life of the project. More than a dozen component projects were active in 1995, with GSB efforts focused in the Babine Lake area. Papers presented in this volume include reports on both bedrock and surficial geology mapping, geochemistry and an overview outlining the program objectives and progress to date.

Previous multidisciplinary projects on northern Vancouver Island and the southern part of the Nechako Plateau were in the write-up stage this year. Results of this earlier work on the Nechako Plateau are also summarized here, with more detailed papers to be published separately in the spring of 1996. A comphrensive summary of the now-completed mapping in the Tatlayoko Lakes area, south of the Nechako Plateau, is also presented.

Other major contributions include reports on the second field season of 1:50 000 mapping in the Gataga district along the Northern Rocky Mountain Trench and in the northern Selkirk Mountains. A metallogenic study in the Tatogga Lake area, in the headwaters of the Iskut River, is also in its second year. The Red Chris copper gold deposit is the focal point of this study, and was the largest exploration project in the Province in 1995. This year's paper highlights other potential porphyry copper targets in the district.

On other topics, several short papers focus on specific mineral properties, including two wollastonite skarns prospects and four other new industrial minerals targets, emphasizing the Ministry's focus on stimulating industrial mineral development in the province. In this regard, one paper reports on progress towards the development of a complete inventory of the construction aggregate resources of the province. Three other papers on aspects of British Columbia coal deposits will be of more specialized interest. The Branch continues to be much involved in seismic hazard mapping, and heightened public awareness of the potential for a major subduction earthquake beneath Vancouver Island or off the west coast lends a sense of urgency to this work. One paper reports on progress largely as a result of research presently by the Geological Survey of Canada, quantifying the seismic risk in the Fraser Valley area of the Lower Mainland.

An important and time-consuming aspect of the Branch's work over the last two years has been the Mineral Inventory project, now approaching completion. Assessments of mineral potential have been made available to land-use planners throughout the province, and early assessments are constantly being revised; a progress report and a second paper discussing aspects of the methodology used in this project are presented here.

Production of Geological Fieldwork to the camera-ready stage has been by in-house "desktop publishing". Under the general direction of the editors, authors have been responsible for the input, formatting and lay-out of their own papers. The cost savings achieved are substantial and the Branch is moving quickly towards full electronic publishing and print-on-demand for all its geoscience publications. Thanks are due to John Newell for editing and to Brian Grant for guiding the whole process to completion under tight deadlines.

*W.R. Smyth*
*Chief Geologist*
*Geological Survey Branch*
*Mineral Resources Division*

# TABLE OF CONTENTS

## MINERAL POTENTIAL PROJECT



## EXTERNAL PUBLICATIONS

# NATMAP: NECHAKO PROJECT, CENTRAL BRITISH COLUMBIA

By W.J. McMillan, British Columbia Geological Survey Branch

and L.C. Struik, Geological Survey of Canada

*KEYWORDS:* NATMAP, British Columbia, multi-disciplinary studies, bedrock, surficial, geochemical, geophysical, biostratigraphy, paleontology, GIS, multi-agency collaboration.

## INTRODUCTION

The British Columbia Geological Survey Branch, and the Geological Survey of Canada, together with researchers in universities and industry, have initiated a new geoscientific program in central British Columbia (93F, 93K, and parts of 93G, 93L, 93M, 93N). The project is coordinated by both agencies, both fund component projects, and the program is financially augmented by the Geological Survey of Canada's National Mapping Program (NATMAP). Results of bedrock and surficial mapping will be enhanced by integration of isotopic analytical data, paleontology studies, and geophysical and geochemical site studies and interpretations. Ultimately, all data produced will be brought together in computer-accessible format and made available on CD-ROM disks.

The geological database for the central Canadian Cordillera (Figure 1) is poor. The first NATMAP program in British Columbia will address questions that will improve our understanding and guide mineral exploration: Tertiary crustal extension, Mesozoic compression and the manner of accretion of the tectonic terranes that underlie the area, geological and geophysical definitions of the terranes, the history of plutonism, the nature of known mineral deposits and their controls, and the character and dispersion history of glacial deposits.

More than fifty scientists from the Geological Survey of Canada, British Columbia Geological Survey Branch, Canadian Forest Service, universities in North America, Asia and Europe, and mining and exploration companies have major or "in kind" involvement in the program. Over five years, new regional and detailed geological and geophysical maps will be published for the Nechako River (93F), Fort Fraser (93K) and parts of Prince George (93G/12,13), Smithers (93L/16), Hazelton (93M/1), and Manson River (93N/4,5,12) map areas (Figure 1).

The Nechako area was assigned a high priority for new mapping by the GSC/BCGSB cooperation committee (Tempelman-Kluit and Matysek, 1994). Selection of the area was sanctioned by the industry liaison committees of both organizations, and by the local mineral industry.

## NECHAKO NATMAP OBJECTIVES

The study will test the hypothesis that the Eocene volcanic complex in central British Columbia represents the tectonic/magmatic expression of an Eocene regional extensional event (Figure 2; Struik, 1994). Understanding the regional Eocene tectonics, and the structural relationships of the upper and lower plates of the extension complex, will help us understand the potential for epithermal precious metal deposits that could be associated with the contact zone between the upper and lower plates, and to determine the complex history of plutonic events with their potential for new intrusion-related copper-gold and molybdenum deposits. The area will also be evaluated for its potential to host volcanogenic massive sulphide deposits of the Kutcho type.

Some steps to attain these objectives include:

- Bringing obsolete 1:250 000-scale geological maps to modern standards (existing maps are based on fieldwork from the 1940s and 1950s). Revised maps will include bedrock maps for the Babine porphyry belt, 93F and 93K, and surficial maps for the porphyry belt and 93F.
- Unraveling the Triassic-Jurassic volcanic arc sequence of the Skeena Arch by studying stratigraphy, plutonic character, tectonic history and rock distribution, and the copper-gold associations seen so clearly in surrounding areas. More metal production has come from Jurassic mineral deposits in British Columbia than from deposits of any other age.
- Determining the tectonic histories of the three major terranes of the area and testing the hypothesis that the boundary between Stikine and Cache Creek terranes is a regional thrust fault like the Nahlin fault in northern British Columbia.
- Determining changes in the regional Pleistocene ice flow directions through time in central British Columbia, where we know ice sheets from three different directions coalesced (Plouffe, 1995). Retreat of these ice sheets left much of the area covered by unconsolidated glacial deposits. Ice flow information

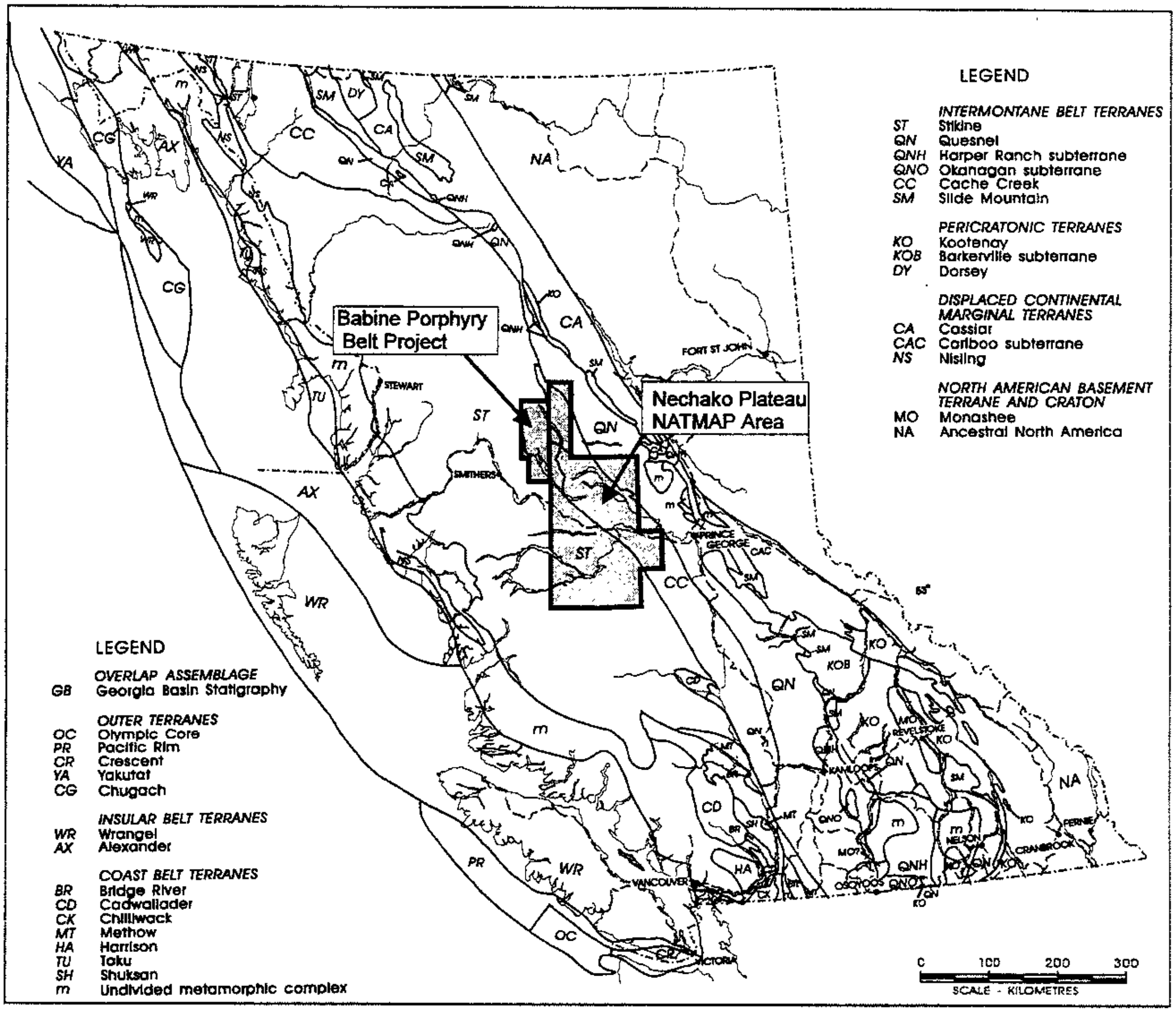


1: Location of the Nechako NATMAP project area. Tectonic boundaries after Wheeler and McFeeley, (1991).

is very important in drift prospecting, in understanding chemical dispersion patterns, and in tracing lithologic units through covered areas during regional bedrock mapping.

The metallogeny of the region can only be interpreted through a knowledge of the nature of the overprinting and coincident Tertiary tectonic history. Answering the fundamental geological questions will require a broad range of expertise and techniques because bedrock exposure in central British Columbia is poor. Further, the prospective Mesozoic and Eocene bedrock often is covered by either local younger Tertiary plateau basalts or extensive Quaternary deposits.

Geoscientific studies planned include:

- Mapping the bedrock and surficial geology at scales appropriate to the problems being tackled. This will be done through coordinated research by a team of experts applying a broad range of techniques to resolve each problem.

- Mapping the surficial geology to determine the glacial history. Till geochemistry and heavy mineral content, combined with measurements of ice flow directions will be used to trace hidden bedrock lithologies and indicate potential mineralized areas.

- Interpreting the aeromagnetic and gravity data to trace units beneath the cover rocks, to map subsurface structures, and to improve interpretations of geology based on mapping of exposed rock.

- Conducting image analysis of satellite spectral and radar data to provide information on the regional distribution of lithologies, structures and lineaments.

- Conducting radiometric surveys to assist in the differentiation of plutonic units directly through their exposed chemical signature and indirectly through their distributed chemical signature in the surficial sediments, and also to locate areas of hydrothermal alteration.

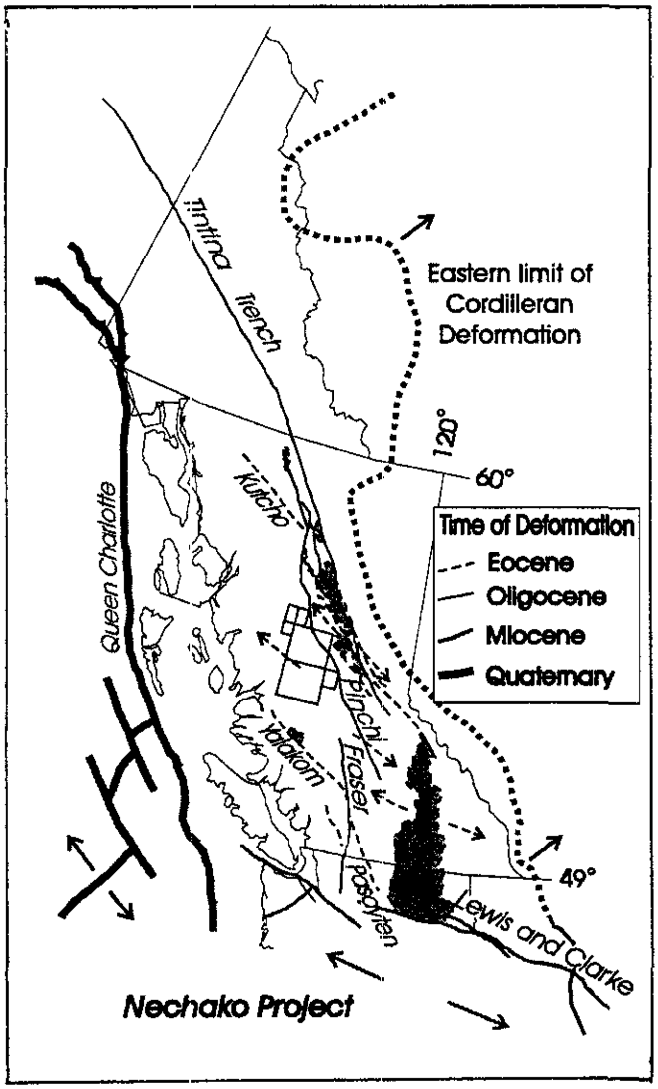


Figure 2: Relationship of the study area to the Eocene tectonic fabric of the North American Cordillera. Shaded areas are metamorphic core complexes.

- Carrying out local gravity and electromagnetic surveys to assist in the delineation of geological structures to depth and to test regional geophysical models.

- Determining paleomagnetic orientations for suites of rocks to assist in determining offsets on terrane contacts and to test for structural rotations that may have accompanied Eocene extension.

- Conducting seismic P-wave crustal studies as a relatively inexpensive way to map the third dimension. This information is needed to solve the contact relationships of the Cache Creek Terrane, and to determine the structural characteristics and geometry of the Eocene extension complex and its upper plate.

- Isotopic dating of all plutonic suites and characterizing them chemically to relate them to tectonic events. These data will aid field identification and classification of the plutonic suites.

- Increasing paleontological control in the area by supporting GSC and university research and determinations, and by providing contracts for identification of radiolarian and fusulinid fauna. Biostratigraphic age controls are needed to clarify internal structural relationships in the Cache Creek and Stikine terranes.
- Collating all the data, using computer technology, into GIS databases that will permit integration and fusion of geoscience information into thematic maps. Providing these datasets to involved researchers and clients, in a simple, easily used format, to encourage analysis of interrelationships of the geoscience data layers.

This research will be published as a series of maps and reports, and as digital databases (Figure 3). We plan to interpret the various data from the perspectives of environmental impact and landuse values to make this pertinent information more widely accessible.

## OVERVIEW OF RESULTS TO DATE

### *BEDROCK MAPPING: BCGSB-GSC-UNIVERSITY-INDUSTRY COLLABORATION*

Don MacIntyre, Ian Webster and Kim Bellefontaine of BCGSB, with the assistance of summer student John Bryant, completed 1:50 000-scale geologic mapping of NTS map-sheet 93L/16 (MacIntyre *et al.*, 1996; Figure 3, D). Significant revisions were made to Carter's 1973 Preliminary Map 12 which was the only published geology map of the porphyry belt other than the

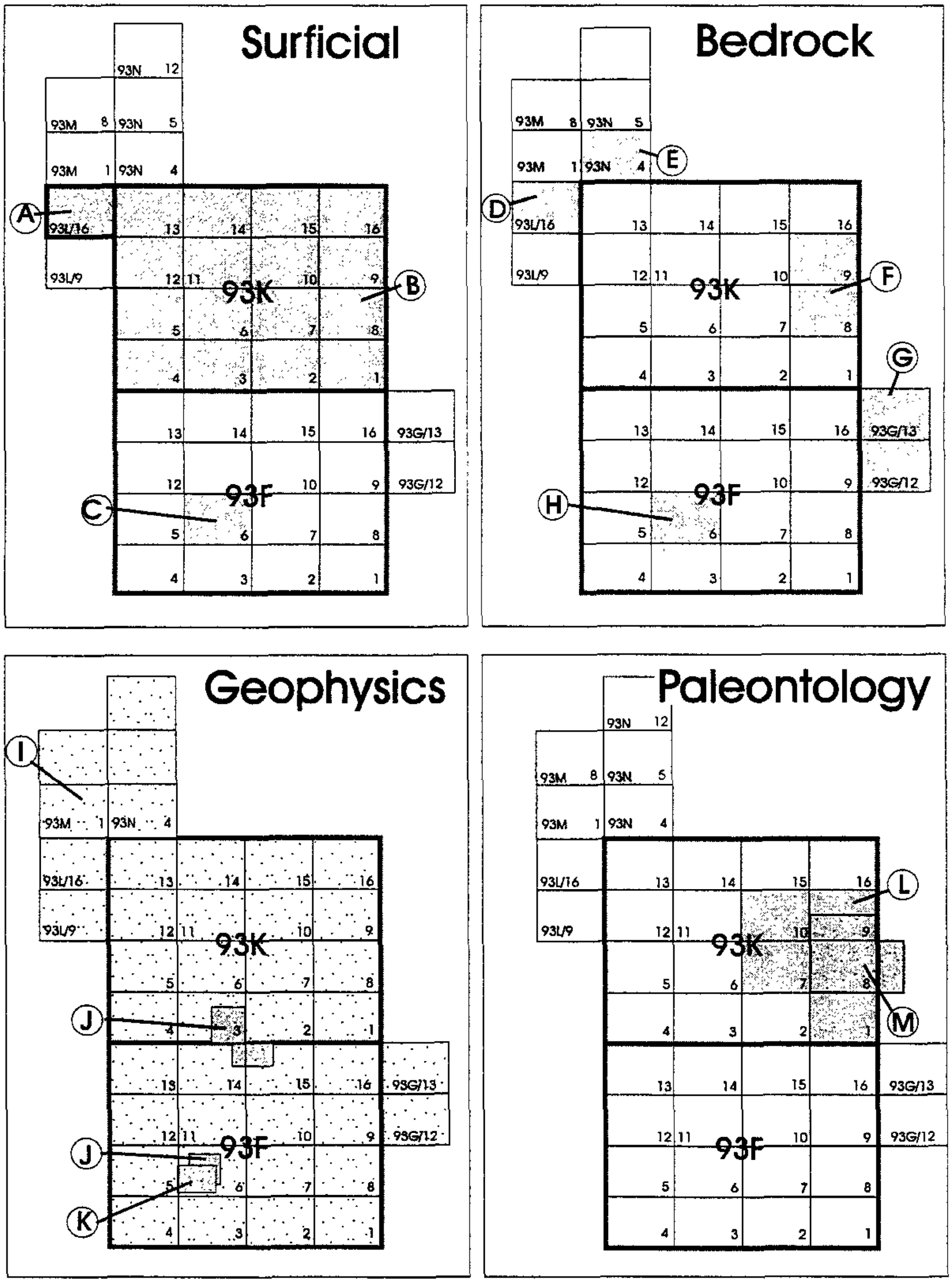


Figure 3: Location of various Nechako NATMAP subprojects active during 1995. Letters are referenced in the text: A. Huntley *et al.* (BCGSB, UNB); B. Plouffe (GSC); C. Levson (BCGSB); D. MacIntyre *et al.* (BCGSB); E. Schiarizza (BCGSB); F. Struik *et al.* (GSC); G. Wetherup and Struik (UA, GSC); H. Diakow *et al.* (BCGSB, GSC); I. Lowe and Seeman (GSC); J. Shives (GSC); K. Enkin (GSC); L. Cordey (contract to GSC); M. Orchard (GSC). Note that not all the projects have publishable results at this early stage in the program.

1:250 000-scale GSC Open File maps (Tipper and Richards, 1976). Carter's geology was placed into a modern stratigraphic framework. Samples were collected for radiometric dating by Mike Villeneuve of the GSC and this information will help to further refine the geology of the area. Several new epithermal systems were located and these appear to be related to either Early Jurassic or post-Eocene hydrothermal events. A stratigraphy was developed for the Eocene Newman volcanics, the extrusive equivalents of the Babine intrusions. Emplacement of porphyries and related extrusive activity appears to predate the main episode of Eocene extensional faulting in the area. Mapping in 1996 will move northward into NTS map-sheet 93M/1.

Paul Schiarizza (BCGSB) spent eight days examining the geology east of Takla Lake (93N/5, 12, 13) in preparation for a geological mapping program that is planned for the area in subsequent years. This project will concentrate on metavolcanic and metasedimentary rocks of the Sitlika assemblage, with the goal of developing an internal stratigraphy and assessing its potential to host volcanogenic massive sulphide (VMS) deposits. The project will establish the relationships between the Sitlika assemblage and adjacent rocks of the Cache Creek Terrane. It will also test the hypothesis that the Sitlika assemblage is a fault-offset correlative of the Kutcho Formation, which hosts the Kutcho VMS deposit in northern British Columbia.

Bert Struik (GSC) and a crew of three university students conducted bedrock mapping of the Vanderhoof Gneiss Complex (93G/12,13 and parts of 93K/5,6 and 11) (Wetherup and Struik, 1996) and began work in the Fort Fraser map area (93K) near Fort St. James (Struik *et al.*, 1996). The Vanderhoof orthogneisses and paragneisses are clearly in fault contact with overlying ultramafic rocks of the Cache Creek Group. Ductile shear in the lower plate gneisses increases toward the contact, and upper plate shear at the contact consists of a narrow zone of brittle gouge. On the eastern side of the complex the upper plate motion was down to the east southeast. Wetherup will be continuing studies of these rocks in the Masters program at the University of Alberta under the supervision of Phillipe Erdmer. Brian Traub mapped the area of metamorphic rocks of southern Babine Lake for a Bachelor's thesis project, also under the guidance of Phillipe Erdmer. This work expands the reconnaissance conducted by Struik and Erdmer (1990).

## *BIOSTRATIGRAPHIC STUDIES: BCGSB-GSC COLLABORATION*

As part of the regional mapping of the Cache Creek Group, contractor Fabrice Cordey has conducted a research project on the radiolarian biostratigraphy (Figure 3, L; Cordey and Struik, 1996). This work will assist in defining the age range, paleogeographic setting, biostratigraphy and structural framework of the Cache Creek Terrane in the central Canadian Cordillera. Preliminary results from this summer are reported by Struik *et al.* (1996). Cordey and Struik (1996) used newly determined age relationships to locate a thrust fault, and have established that Cache Creek ribbon cherts in the Fort St. James area were deposited throughout Triassic time.

Larry Diakow (BCGSB), in concert with Terry Poulton and Howard Tipper (GSC), spent five days revisiting fossil sites in the southern Nechako Plateau area in an effort to better constrain the ages of Lower and Middle Jurassic sedimentary sequences (Figure 3, H). Biostratigraphy is critically important because isotopic dating of interlayered bimodal volcanics has been inconclusive. This work completes a 1:50 000-scale bedrock mapping program funded by the Canada British Columbia Mineral Development Agreement in the Nechako River area. We plan to expand the improved geological coverage provided by this project northward during the NATMAP program, into NTS map sheets 93F/4, 5, 12 and 13.

Mike Orchard (GSC) has brought together a database of existing paleontological information from the project area, particularly conodont fauna from the Cache Creek limestone (Orchard and Struik 1996).

Ed Kimura and Sharon Gardner (Placer Dome Inc.), Glenn Johnston (Endako Mines Limited) and Placer Dome Inc. contributed data from their regional geological mapping of the area around the Endako molybdenum deposit, which is underlain by Mesozoic rocks (93F, 93K). The Placer Dome data are being digitized, and pertinent data elements will appear in the geological compilations for the Nechako NATMAP project.

Joe Whalen (GSC) conducted a reconnaissance of plutonic suites in the Endako/Fraser Lake area (93F/14 and 93K/3) in preparation for mapping and lithogeochemical studies in subsequent years. The plutonic suites show a wide range of genetic types and compositions.

## *SURFICIAL MAPPING AND GEOCHEMICAL SURVEYS: BCGSB-GSC-UNIVERSITY COLLABORATION*

Vic Levson and David Huntley (BCGSB) coordinated regional surficial mapping, drift geochemical sampling and glacial studies in the Babine porphyry belt. They worked closely with Doctoral candidate Andy Stumpf and Masters candidates Erin O'Brien and Gordon Weary under the supervision of Bruce Broster of the University of New Brunswick (93M/01 and 93L/16; Figure 3, A; Huntley *et al.*, 1996; Stumpf *et al.*, 1996).

Surficial geology maps for these two areas will present the kinds of surficial cover, landforms ice flow patterns and the distribution of glacial erratics. The maps will be released at Cordilleran Roundup 1996. Geochemical results from ICP and INA analyses of some 900 samples of basal till (800), mineralized erratics (40) and other sample media were collected in areas of good mineral potential. These will be published when data becomes available. Interpretation of regional paleo-ice flow patterns, physiographic controls of deposition and the history of glacial "Lake Babine" are in progress. These data will be used to interpret the geochemical results to aid future exploration in the area.

Steve Cook (BCGSB) conducted follow-up studies as an outgrowth of MDA-supported lake geochemical surveys (Figure 3, C). In 1995, he and Wayne Jackaman (BCGSB) and Peter Friske, Martin McCurdy and Steven Day (GSC) carried out a regional lake sediment and water geochemistry survey over the northeastern part of the Fort Fraser map area (NTS 93K/9, 10, 15, 16). This survey is a contribution to the continuing objective of completing Regional Geochemical Survey (RGS) coverage of the northern interior. It was funded by the Canada British Columbia Mineral Development Agreement. The survey area also encompassed mercury deposits along the Pinchi fault zone, and will provide valuable regional baseline data for anticipated studies of naturally occurring mercury in the environment.

Alain Plouffe (GSC) has compiled and published the surficial geology of the Fort Fraser map-sheet (93K) at 1:100 000-scale (Figure 3, B). This work derives from mapping that was conducted under the 1991-1995 MDA program. In addition to the geological maps, Plouffe, and Bruce Ballantyne (GSC), have published results of regional till geochemical surveys for the same region. Those geochemical distributions are being interpreted in the context of the glacial flow direction history (Plouffe, 1995).

### *GEOPHYSICAL SURVEYS: GSC-BCGSB COLLABORATION*

Carmel Lowe (GSC) has begun interpreting existing gravity and aeromagnetic data (93G, 93F, 93K, 93L, 93M, 93N). This information will be used to aid bedrock and surficial mapping, and to assist in interpreting the geology to depth.

Rob Shives (GSC) arranged a contract airborne radiometric, aeromagnetic and VLF (very low frequency electromagnetic) survey that covers a pluton-dominated area near Fraser Lake (93K/3, 93F/14) and an area south of the Kemano Reservoir (93F/6). Results from these study areas will be used to aid and accelerate mapping of the various plutonic suites in the two survey areas. The survey was flown in late September and results are pending.

Randy Enkin (GSC) and Larry Diakow (BCGSB) sampled rocks of the Entiako spur and Nagliko uplift for paleomagnetic studies of the Jurassic sequences (93F/6). This work will test the hypothesis that there were plate translations related to terrane accretion, and block rotations possibly related to Tertiary faulting.

### *GEOCHRONOLOGY: GSC-BCGSB-UNIVERSITY (MDRU) COLLABORATION*

Mike Villeneuve (GSC) and Jim Mortensen (UBC, MDRU) conducted a reconnaissance sampling program for isotopic dating of igneous and metamorphic suites throughout the project area. This work will initially concentrate on defining ages for the numerous plutonic and extrusive suites and establishing the relationships between plutonism and ore generation. Villeneuve is coordinating the isotopic dating and has begun compiling existing isotopic dates for the area (93G, 93F, 93K, 93L, 93M, 93N). This database will become part of the Canadian database of isotopic ages that is compiled by the geochronology section of the GSC.

### *DIGITAL DATA/GEOGRAPHIC INFORMATION SYSTEMS: GSC- BCGSB-INDUSTRY COLLABORATION*

Stephen Williams (GSC) is working with Eric Grunsky (BCGSB) and scientific staff of both organizations to compile existing geological, geochemical and geophysical data to be published on CD ROM. These data will be integrated with a common GIS platform. Initially, it will contain information relevant to the Quesnel Trough of north-central British Columbia, including map sheets 93K, 93N, 93J, 93O(SW) and 94C. Placer Dome Inc. is supporting digitization of their exploration mapping database for central British Columbia. This data will be included in future digital data releases. The computer information will be available in several formats and made accessible by software included on the CD ROM. In the future, data from the Interior Plateau (MDA) and NATMAP project areas will also be available in this form.

## ACKNOWLEDGMENTS

This report is a contribution to the Nechako NATMAP program. We thank all those people who worked hard to make this project a reality and for the support of the Geological Survey of Canada, the British Columbia Geological Survey Branch and the geoscience community. We particularly thank Ed Kimura of Placer Dome and Ken Pride of Cominco for their efforts in making company data available to the BC NATMAP projects.

## REFERENCES


Carter, N. (1973): Preliminary Geological map of Northern Babine lake Area (93L/NE, 93M/SE); *B. C. Ministry of Energy, Mines and Petroleum Resources*, Preliminary Map 12.

Cordey, F. and Struik, L.C. (1996): Radiolarian Biostratigraphy, Fort Fraser (93K) and Prince George (93G) Map Areas, Central British Columbia: Scope and Preliminary Results; *in* Current Research 1996-A, *Geological Survey of Canada*, in press.

Huntley, D.H., Stumpf, A., Levson, V.M. and Broster, B.E. 1996. Babine Porphyry Belt Project: Quaternary Geology and Regional Till Geochemistry Sampling in the Old Fort (93M/01) and Fulton Lake (93L/16) Map Areas, British Columbia; in Geological Fieldwork 1995, Grant, B. and Newell, J. M., Editors, *B.C. Ministry of Energy, Mines and Petroleum Resources*, Paper 1996-1.

MacIntyre, D.G., Webster, I.C.L. and Bellefontaine 1996. Babine Porphyry Belt Project: Bedrock Geology of the Fulton Lake Map Sheet (93L16), British Columbia; in Geological Fieldwork 1995, Grant, B. and Newell, J. M., Editors, *B.C. Ministry of Energy, Mines and Petroleum Resources*, Paper 1996-1.

Orchard, M.J. and Struik, L.C. (1996): Conodont biostratigraphy, lithostratigraphy and correlations of the Permo-Carboniferous Cache Creek Group Limestones Near Fort St. James, British Columbia; *in* Current Research 1996-A, *Geological Survey of Canada*, in press.

Plouffe, A. (1995): Glacial History of North Central British Columbia; *in* Final Program and Abstracts, Volume 20, *Geological Association of Canada*, p. A84.

Struik, L.C. (1994) Intersecting Intracratonal Tertiary Transform Fault Systems in the North American Cordillera: *Canadian Journal of Earth Sciences*, Volume 30, p. 1262-1274.

Struik, L.C. and Erdmer, P. (1990): Metasediments, Granitoids, and Shear Zones, Southern Babine Lake, British Columbia; *in* Current Research, Part E, *Geological Survey of Canada*, Paper 90-1E, p. 59-63.

Struik, L.C., Floriet, C. and Cordey, F. (1996): Geology of the Fort St. James Area, Central British Columbia; *in* Current Research 1996-A, *Geological Survey of Canada*, in press.

Stumpf, A.J., Huntley, D.H., Broster, B.E. and Levson, V.M. 1996. Babine Porphyry Belt Project: Detailed Drift Exploration Studies: Babine Porphyry Belt in the Fulton Lake (93L/16) and Old Fort Mountain (93L/16) Map Areas, British Columbia; in Geological Fieldwork 1995, Grant, B. and Newell, J. M., Editors, *B.C. Ministry of Energy, Mines and Petroleum Resources*, Paper 1996-1.

Tempelman-Kluit, D. J. and Matysek, P. (1994): Geoscience Information Needs for the Future of British Columbia; internal report, *Geological Survey of Canada* and *B. C. Geological Survey Branch.*

Tipper, H.W. and Richards, T.A. (1976): Geology of the Smithers a Area; *Geological Survey of Canada*, Open File 351.

Wetherup, S. and Struik, L.C. (1996): Vanderhoof Metamorphic Complex and Surrounding Rocks, Central British Columbia; *in* Current Research 1996-A, *Geological Survey of Canada*, in press.

Wheeler, J.O. and McFeeley, P. (1991): Tectonic Assemblage Map of the Canadian Cordillera and Adjacent Portions of the United States of America; *Geological Survey of Canada*, Open File 1712A.

NOTES

# BABINE PORPHYRY BELT PROJECT: BEDROCK GEOLOGY OF THE FULTON LAKE MAP AREA (93L/16), BRITISH COLUMBIA

By D.G. MacIntyre, I.C.L. Webster and K.A. Bellefontaine

*(British Columbia Ministry of Energy, Mines and Petroleum Resources contribution to the Nechako National Mapping Program)*

*KEYWORDS:* porphyry copper deposits, transtensional tectonics, Stuhini Group, Permo-Triassic, Telkwa Formation, Topley intrusions, Bulkley intrusions, Babine intrusions, Newman volcanics, Granisle, Lennac Lake, Babs, Babine Lake, Fulton Lake.

## INTRODUCTION

The Babine porphyry belt project is part of the new Nechako National Mapping Program (NATMAP), a joint effort of the Geological Survey of Canada and the British Columbia Geological Survey Branch of the Ministry of Energy, Mines and Petroleum Resources (McMillan and Struik, 1996, this volume). This is a multidisciplinary project with separate components for bedrock and surficial geology, till and silt geochemistry. The objective of the Babine Porphyry Belt project is to map the Fulton Lake (93L/16), Old Fort Mountain (93M/1) and Nakinilerak Lake (93M/8) map sheets over the next four years (Figure 1). This report summarizes the results of bedrock mapping completed in 1995. The reader is cautioned that this report is very preliminary and is being written without the benefit of paleontological identifications, radiometric age dating, whole-rock and trace element geochemistry or petrographic analysis, any of which may significantly change our understanding of the geology of the Fulton Lake map sheet.

## PROJECT DESCRIPTION

The Babine porphyry belt is located in west-central British Columbia and is centred on the northern third of Babine Lake (Figure 1). The belt is approximately 80 kilometres long and includes twelve significant porphyry copper deposits and prospects including the Bell and Granisle past producers. The mineral potential of the area was ranked the fourth highest of the 97 tracts evaluated in the Skeena-Nass mineral potential project (MacIntyre *et al.*, 1995). The estimated value of known in-ground mineral resources in the area is $1.96 billion and the value of past production is estimated at $1.13 billion (1986 dollars). In spite of the high mineral potential and obvious economic significance of the area, the most recent published geological mapping in the belt was by Carter (1973). Since then there has been extensive logging in the area, providing new access and

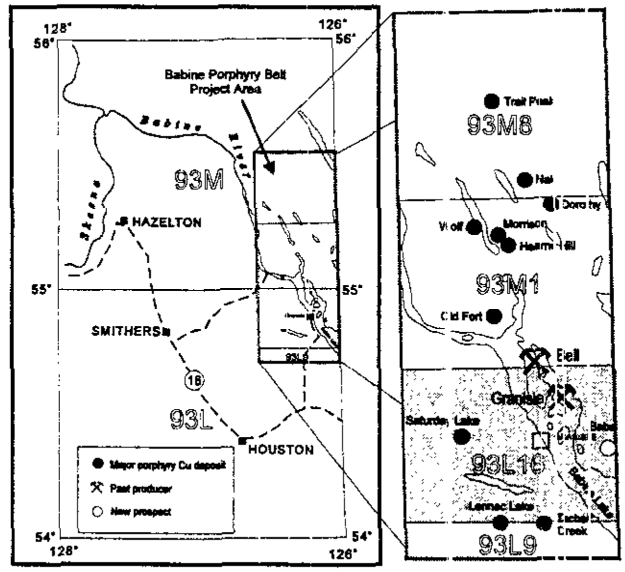


Figure 1. Location of the Babine Porphyry Belt project area, West-central British Columbia. Shaded area was mapped in 1995 and is the subject of this report.

better bedrock exposure, especially in areas of extensive drift cover. This, coupled with renewed interest in porphyry copper deposits as an exploration target and the need for economic diversification in the economy of the area, make this project particularly timely. It is hoped that new bedrock and surficial mapping, together with regional geochemistry and airborne geophysical surveys, will stimulate additional exploration in the belt and lead to new discoveries. Drift prospecting, lake geochemistry and airborne geophysics will be especially important in defining new targets in drift-covered areas. The Quaternary geology and till geochemical sampling completed in 1995 are discussed in separate reports (Huntley *et al.*, 1996, this volume; Stumpf *et al.*, 1996, this volume)

## ACCOMPLISHMENTS

The 1995 bedrock mapping crew consisted of Don MacIntyre, Ian Webster and Kim Bellefontaine of the British Columbia Geological Survey Branch in Victoria, and John Bryant, a Geological Survey of Canada summer student. This crew completed 1:50 000-scale geological mapping of the Fulton Lake map sheet

(93L/16). In addition to regional bedrock mapping, major mineral deposits and new prospects in the area were mapped in detail and sampled. Samples were also collected for radiometric dating in conjunction with Mike Villeneuve of the Geological Survey of Canada and this information will help to further refine the geology of the area. Major geological accomplishments made during the 1995 field season are summarized below.

- Development of a possible Permo-Triassic statigraphy in the area west of Granisle. Permian rocks are tentatively correlated with the Asitka Group, Triassic rocks with the Stuhini Group.
- Recognition of possible Triassic rocks on the Newman Peninsula (Bell mine). These rocks were previously mapped as Lower Jurassic Telkwa Formation.
- Correlation of Lower Jurassic stratigraphy in the Babine Lake area with the type area of the Telkwa Formation in the Telkwa Range. This suggests the Howson subaerial facies extends much farther east than originally thought.
- Recognition of several distinct phases within the Late Triassic - Early Jurassic Topley intrusions.
- Collection of samples for U-Pb and Ar-Ar dating by Mike Villeneuve of the Geological Survey of Canada. These data will help refine the ages of some of the map units in the area.
- Development of a stratigraphy for the Eocene Newman volcanics. Argon-argon age dating and whole-rock geochemistry will be used to help refine our understanding of the relationships between these rocks and the Babine Plutonic Suite.
- Location of two new epithermal systems, one of which has elevated zinc values, three new copper showings, one of which carries anomalous gold and a new molybdenum showing.
- Discovery of a biotite-feldspar porphyry (bfp) dike cutting Topley intrusions on the Babs property. This was the first time bfp was found in outcrop and indicates that the mineralized porphyry float may be locally derived.
- Mapping and sampling of recent trenching at the Lennac Lake porphyry prospect. This work documents a new zone on the property which was trenched by Cominco and Kennecott in 1992 and 1993. Although low grade copper mineralization occurs over a wide area, this zone has never been tested by drilling.

## SUMMARY STATISTICS

A total of 223 person days was required to complete 1:50 000-scale mapping of Fulton Lake map sheet (93L/16). A total of 796 geologic stations were recorded in the 89 000 hectare map area. The station density was approximately 9 stations per 1000 hectares. This relatively low density reflects the lack of bedrock exposure in a large part of the map area. A summary of the samples collected from the area is given below.

| Sample Type | Number |
|---|---|
| Conodonts | 7 |
| Macrofossils | 7 |
| U-Pb zircon | 4 |
| Ar-Ar | 8 |
| Assay | 40 |
| Whole rock | 21 |
| Silt | 44 |

## FUTURE PLANS

Geoscientific studies will continue in the Babine Lake area contingent upon funding of the Nechako NATMAP program. The target for bedrock mapping in 1996 will be to complete 1:50 000-scale mapping of the Old Fort Mountain map sheet (93M/1, Figure 1). The major porphyry copper deposits on this map sheet include Bell, Morrison and Hearne Hill. Hopefully regional silt and lake geochemistry, detailed mineral deposit studies and possibly airborne geophysical surveys can be added as components of the project next year.

## PREVIOUS WORK

Geologic mapping and mineral property evaluations by the Geological Survey of Canada and the British Columbia Department of Mines (now Ministry of Energy, Mines and Petroleum Resources) date back to the turn of the century. Earliest reports on the geology of west-central British Columbia are by G.M. Dawson (1881) who described porphyritic flows in the Francois Lake and Skeena River areas. Volcanic rocks in the Hazelton and Smithers area were first described by Leach (1910) who proposed a two-fold subdivision between Jurassic volcanics, which he called the Hazelton Group, and Cretaceous sedimentary strata which he named the Skeena series. Hanson (1925) further subdivided the Hazelton Group into a lower volcanic division, a middle sedimentary division and an upper volcanic division. This division remained unchanged for many years until Armstrong (1944a, 1944b) included the Skeena series with the Hazelton Group

In 1976, the Geological Survey of Canada published Tipper and Richards (1976a) bulletin *Jurassic Stratigraphy and History of North-central British Columbia*. This comprehensive publication included previously unpublished data on numerous fossil localities and measured stratigraphic sections, including several in the Babine Lake area. This bulletin complimented the release of an open file, 1:250 000-

scale, geological map of the Smithers area (Tipper and Richards, 1976b).

Tipper and Richards subdivided the Hazelton Group into several different formations. They also resurrected the name Skeena Group for Early Cretaceous coal-bearing, overlap sedimentary strata that Armstrong (1944a, 1944b) originally placed in the Hazelton Group.

Carter mapped the Babine porphyry belt in detail between 1965 and 1972 as part of a British Columbia Ministry of Mines regional study of porphyry deposits in west-central British Columbia. This excellent work was released as Preliminary Map 12 (Carter, 1973) and remains the only published geological map of the belt. Because of improved access via logging roads, better bedrock exposure in clear-cuts and a better understanding of regional stratigraphic relationships, we were able to expand on this earlier mapping and place it in a modern stratigraphic framework.

The Babine porphyry belt is one of the most important mineral camps in British Columbia (Carter *et al.* 1995). Numerous reports have been published on individual deposits. Carson and Jambor (1974), Wilson *et al.* (1980) and Zaluski *et al.* (1994) have discussed hydrothermal alteration and fluid geochemistry in the district; Fahrni *et al.* (1976), Carson *et al.* (1976) and Dirom *et al.* (1995) have described the geology and mineralization at the Granisle and Bell mines; Carson and Jambor (1976) and Ogryzlo *et al.* (1995) have described the Morrison and Hearne Hill deposits.

## ACCESS

The main access to the area is from Highway 16, which follows the Bulkley River valley from the town of Houston through Telkwa and Smithers and north to Hazelton (Figure 1). Smithers, located approximately half way between Prince George and Prince Rupert, is the largest town in the area and is a major transportation centre with daily jet service to Vancouver, Terrace and Prince George.

There are two main routes into the study area from Highway 16. The Smithers Landing - Granisle connector route which leaves Highway 16 south of Smithers and goes through McKendrick Pass on its way to Granisle is 78 kilometres long and is mainly gravel. The Topley - Granisle road is paved; it leaves Highway 16 at Topley and terminates at Granisle, a distance of 48 kilometres. An extensive network of logging roads provides access to much of the map area, especially east of Babine Lake. The east side of the lake is accessible by ferry between Mill Bay, just north of Topley Landing, and Nose Bay on the east side of the lake. Crossing time is approximately 20 minutes. The ferry is run by Northwood Lumber Co. based in Houston, and is free to the public with the acquisition of a permit. On the east side of the lake, the Hagan, Jinx and Nose Bay haulage roads, which are radio controlled and heavily used by logging trucks, are the main access routes.

## PHYSIOGRAPHY

The physiography of the Babine Lake area is characterized by rolling hills and extensive drift-covered areas of low relief. Bedrock exposure is found on the crests of small glaciated knolls, in deeply incised creek valleys and along the shores of Babine and Fulton lakes. Clear-cut logging in the area has also exposed bedrock along road cuts and in areas subject to soil erosion. Huntley *et al.* (this volume) discuss the physiography and Quaternary history of the study area.

## TECTONIC HISTORY AND REGIONAL GEOLOGIC SETTING

The study area is entirely within Stikinia, which is the largest terrane of the Intermontane tectonic belt (Figure 1, McMillan and Struik, 1996, this volume). Stikinia includes Lower Devonian to Middle Jurassic volcanic and sedimentary strata of the Asitka, Stuhini, Lewes River and Hazelton assemblages and related comagmatic plutonic rocks. The oldest rocks are upper Paleozoic carbonates and island-arc volcanic and volcaniclastic rocks locally referred to as the Stikine assemblage (Monger, 1977; Brown *et al.*, 1991). Areas with this assemblage, which east of the Bowser Basin is called the Asitka Group, represent remnants of a tectonically dismembered, shallow-water island-arc environment with carbonate buildups fringing emergent volcanic islands. Permian and possibly older rocks occur in the study area and these rocks are tentatively correlated with the Asitka Group.

The Paleozoic island-arc regime was followed by a depositional hiatus prior to development of a Late Triassic volcanic arc and eruption of the predominantly basaltic Stuhini Group. By Early Jurassic time the area was part of the regionally extensive Hazelton calcalkaline volcanic arc. The orientation of this arc and the polarity of related subduction zones is still much in debate. However, facies relationships suggest there was a central marine trough that was bounded by northwest-trending island-arcs. This apparent paleogeography is complicated by significant right-lateral displacement of the Hazelton rocks along northeast-trending transcurrent faults. A northeast-dipping subduction zone seems likely for the western part of the Hazelton arc. The basaltic to andesitic island-arc volcanics exposed in the study area can be correlated with the Stuhini and Hazelton groups on the basis of lithology and inferred stratigraphic position.

Collision of Stikinia with the Cache Creek Terrane in Middle Jurassic time resulted in uplift of the Skeena Arch and formation of the Bowser Basin. From Late Jurassic to Early Cretaceous time, continued uplift and erosion of the Skeena Arch and Omineca crystalline belt resulted in deposition of thick molasse deposits in the Bowser Basin, which lies just north of the study area. In the Early Cretaceous, rocks of the Skeena Group were deposited in fault-controlled basins along the southern

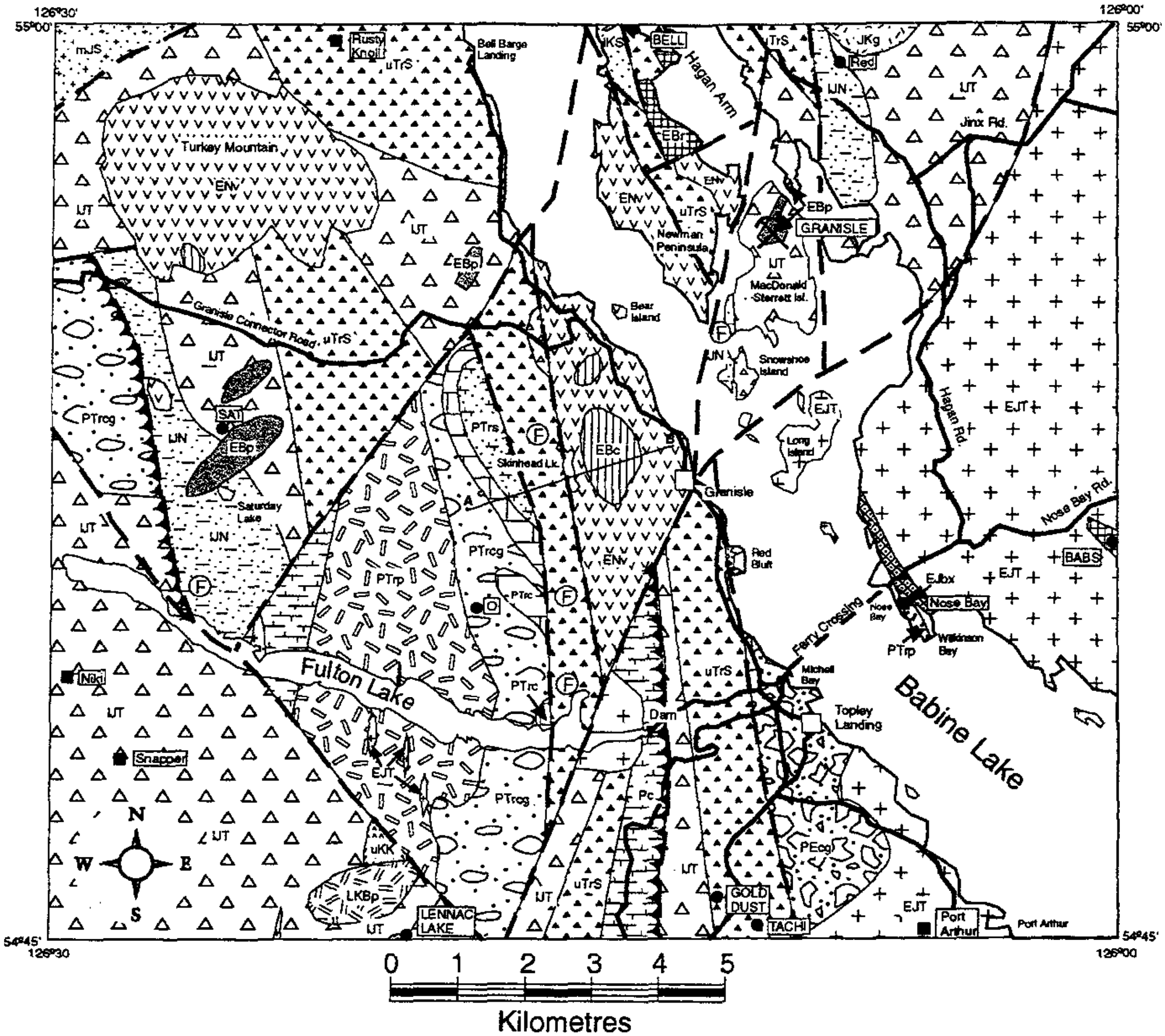


Figure 2. Generalized bedrock geology of the Fulton Lake map sheet, 93L/16. See Figure 3 for legend. Solid squares are new mineral showings; solid circles are know occurrences discussed in this report. Line A-B is the location of section shown in Figure 5.

margin of the Bowser Basin. The Upper Jurassic to Lower Cretaceous rocks of the Bowser Lake and Skeena groups host important coal deposits. Although these overlap assemblages are well represented elsewhere in the Babine Lake area, they underlie less than 5% of the area mapped in 1995.

A major plate collision in middle Cretaceous time resulted in uplift of the Coast Mountains and extensive folding and thrust faulting of rocks to the east. Debris from rising metamorphic-plutonic complexes was shed eastward and deposited in the Sustut basin. This was followed by the growth of north-trending, eastward-migrating Andean-type volcanic arcs in middle Cretaceous to Eocene time. These arcs are believed to be the result of oblique, eastward subduction of oceanic crust along the leading edge of the North American plate, with volcanic centres localized along zones of extension within a transtensional tectonic regime. Calcalkaline volcanic rocks of the Upper Cretaceous Kasalka Group and Eocene Ootsa Lake Group are the remnants of these arcs which were built on uplifted and eroded blocks of Stikinia and its Upper Jurassic to Lower Cretaceous overlap assemblages. In the study area, Eocene porphyritic flows and breccias of

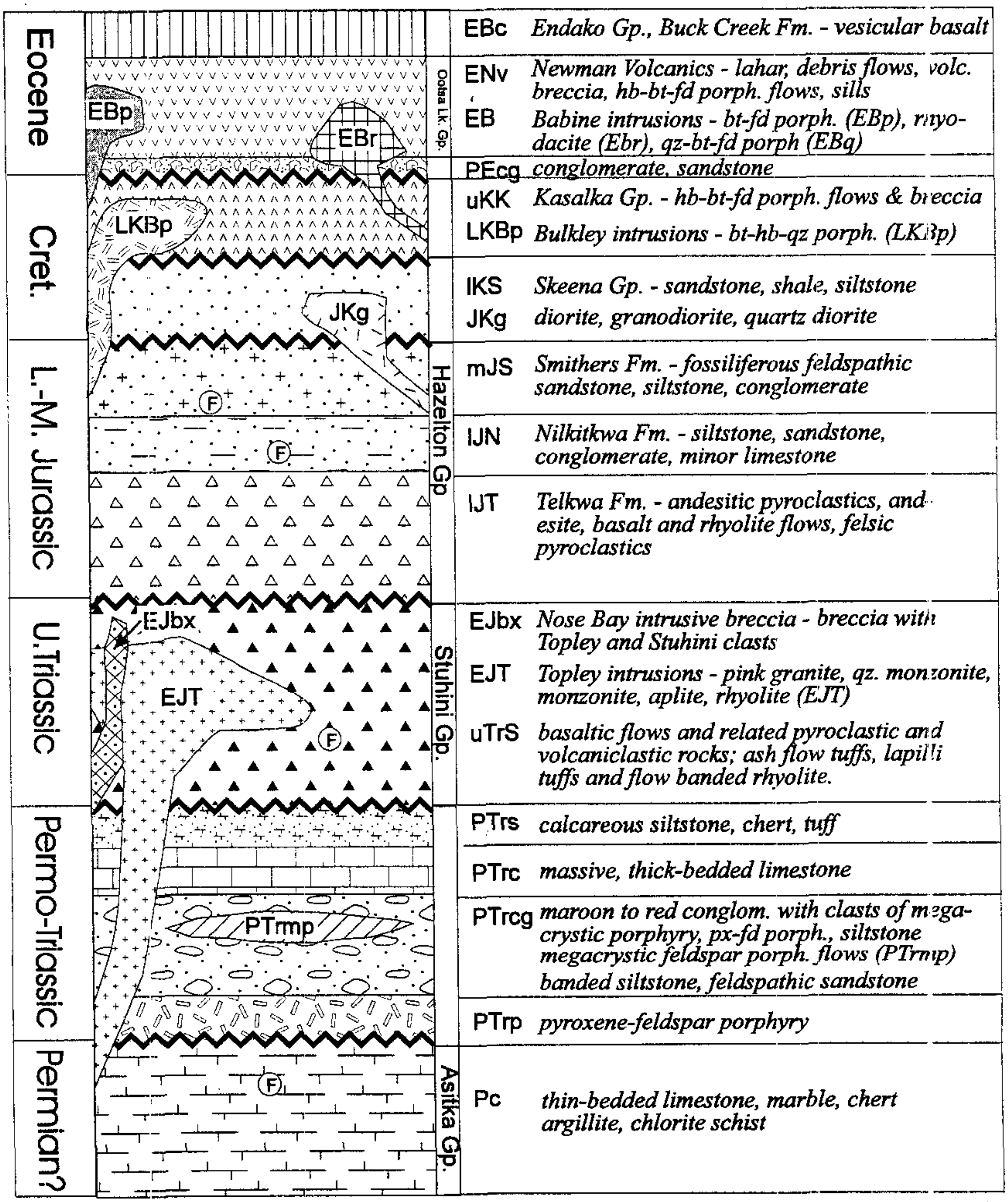


Figure 3. Stratigraphic column for the Fulton Lake map area. Fossil control shown by F inside a circle.

the Newman volcanics are correlated with the Ootsa Lake Group; the Kasalka Group is not well represented, being restricted to one small outlier. The Middle to Late Cretaceous Bulkley intrusions and the Eocene Babine intrusions (Carter, 1981) are the plutonic roots of these younger continental volcanic arcs. Mineral deposits in the study area are associated with emplacement of these intrusions. The most economically important exploration targets are porphyry copper and molybdenum deposits and related mesothermal precious metal veins.

The middle Cretaceous to Late Eocene transtensional tectonic regime produced the basin-and-range geomorphology that controls the current map pattern of the area. The latest tectonic event appears to be northeast displacement along right-lateral transcurrent faults and tilting of fault blocks to the southeast. This right-lateral displacement has offset earlier northwest-trending grabens and horsts containing Eocene and younger volcanic and sedimentary strata (MacIntyre *et al.*, 1989). Extension of the crust in Eocene to Miocene time was accompanied by extensive outpouring of continental lava flows of the Endako and Chilcotin groups which now cover large parts of the Interior Plateau.

## LITHOLOGIC UNITS

The geology of the study area, based on mapping completed in 1995 and the earlier mapping of Carter (1973), Tipper and Richards (1976) and Richards (in press), is shown in Figure 2. Figure 3 illustrates our current understanding of the stratigraphic relationships between the different map units; Figure 4 is a diagrammatic section across the map area.

The geologic framework of the study area consists of a series of uplifted, tilted and folded fault blocks containing rocks ranging from possibly pre-Permian to Eocene. A north-trending graben centred on Babine Lake is defined by a series of inward dipping, progressively down-dropped fault blocks. Eocene and possibly younger volcanic rocks are preserved in the core of this graben. The graben and surrounding geology are truncated and offset by several northeast-trending dextral shear zones of probable Late Eocene age.

### *PERMIAN AND OLDER? ROCKS (Pc)*

The oldest rocks in the map area are probably exposed in the canyon below the Fulton River dam. These rocks are distinct because they often have a well-developed schistosity. This section, which includes partly recrystallized limestone, chert, slate, phyllite, chlorite schist, amygdaloidal basalt and maroon tuff, is structurally complex and may include imbricated thrust panels of rocks ranging in age from Permian to Jurassic.

A steeply dipping, partly recrystallized limestone containing coral debris is exposed in the canyon walls at the Fulton River dam site and in a quarry just west of the dam. The limestone is thin to medium bedded, with alternating dark grey and white bands and is at least 50 metres thick. Outcrops at the dam site were sampled for radiolaria by Bert Struik of the Geological Survey of Canada. These sedimentary rocks are cut by near-vertical feldspar porphyry dikes. Near the dikes, the sediments are rusty weathering due to the presence of disseminated pyrite. Above the dam the sediments are tightly folded next to one of the dikes. The dikes may be related to a large stock of Topley quartz monzonite which crops out on the shores of Fulton Lake a few hundred metres west of the limestone outcrops.

The limestone exposed at the Fulton River dam apparently contains Permian fossils (H.W. Tipper, personal communication, 1995). Based on this assumed age these rocks are tentatively correlated with the Asitka Group (Lord, 1948; Monger, 1977) which is found east of the Bowser Basin in the McConnell Creek map area (94D).

The limestone member is overlain by dark grey chert, silty argillite and chlorite schist. Maroon tuffs and amygdaloidal basalt flows are exposed further up section, but these rocks are probably part of the Lower Jurassic Telkwa Formation. The contact is probably a high-angle thrust fault, with the Telkwa Formation rocks thrust northeastward over strongly magnetic chlorite schists. These metavolcanics may be Triassic in age.

### *PERMO-TRIASSIC ROCKS*

Limestone and mafic volcanics that have previously been mapped as Permian and Triassic in age (Tipper and Richards, 1976b) crop out as a series of uplifted fault blocks in the centre of the map area. The best section is exposed in the large clearcut west of Granisle (Figure 5).

The Permo-Triassic succession includes a distinctive, thick-bedded limestone member which has previously been mapped as Permian. However, there are no fossil data to confirm this age and the limestone may actually be Triassic (H.W. Tipper, personal communication, 1995). Our mapping suggests the limestone is conformably underlain by a red to maroon polymictic conglomerate that contains coarse, bladed feldspar porphyry clasts. Although outcrop is limited, it appears that the conglomerate sits on pyroxene-feldspar porphyry flows that are strongly magnetic.

Limestone is the most distinctive lithology of the Permo-Triassic succession and can be several hundred metres thick. The limestone contains coral debris. Seven samples were collected from this member and these are currently being dissolved for possible conodont extraction.

#### PYROXENE-FELDSPAR PORPHYRY (PTrp)

Medium to coarse-grained, greenish grey pyroxene-feldspar porphyry crops out north and south of Fulton Lake. These porphyritic rocks are interpreted to be basaltic flows that formed islands within an island-arc environment. They, have equant to tabular feldspar phenocrysts up to 3 millimetres in length and pyroxene phenocrysts to 1 millimetre. Hornblende and rare biotite phenocrysts may be present. The flows locally have chlorite, quartz or carbonate-filled amygdules and are often strongly magnetic. Not surprisingly, areas underlain by these rocks produce a strong aeromagnetic

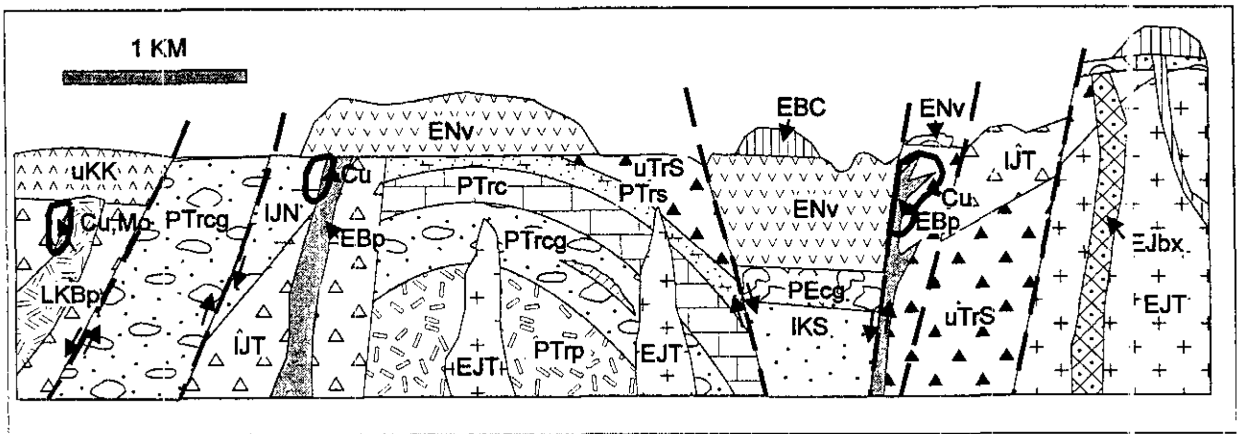


Figure 4. Diagrammatic section showing relationships of the map units in the Fulton Lake area. See Figure 3 for legend.

response and this characteristic has helped to define their extent in areas of limited or no outcrop.

The stratigraphic position of the pyroxene-feldspar porphyry flows is not certain. Based on sporadic outcrops, and assuming there are no major fault displacements, they would form the core of a north-trending antiform with its axis located near the centre of Fulton Lake. If this interpretation is correct, the porphyritic flows are overlain by interbedded tuffaceous siltstones, maroon mudstones and volcanic conglomerates. As clasts of pyroxene-feldspar porphyry occur in these conglomerates, this stratigraphic position seems likely.

## CONGLOMERATE AND SANDSTONE (PTrcg)

A unit of red to maroon-weathering, poorly sorted, polymictic boulder to pebble conglomerate, and lesser greenish grey feldspathic sandstone and siltstone, crops out in a large clear-cut north of Fulton Lake. These rocks strike northwest and dip steeply northeastward below the main cliff exposures of limestone (Figure 5). Because of similar bedding attitudes, we believe the conglomerate member conformably underlies the limestone. Alternatively the limestone and overlying strata may have been thrust to the southwest over the conglomerate.

A distinctive feature of the conglomerate is the occurrence of coarse-grained tabular feldspar porphyry boulders up to 30 centimetres in diameter. The same porphyry occurs as massive sills or flows within the unit, suggesting the boulders are locally derived. Other clasts in the conglomerate are greenish chert, sandstone, siltstone, lapilli tuff and fine-grained porphyritic andesite. The conglomerate is also cut by northeast-trending, steeply dipping, epidote-rich basaltic dikes which are probably feeders for flows higher in the stratigraphic succession.

A southeasterly trending series of resistant ridges and knolls extends from the Smithers connector road at the western edge of the map area to Fulton Lake. They are underlain by conglomerate, coarse feldspathic sandstone, siltstone, minor mudstone and pyroxene-feldspar porphyry. The conglomerate is greenish grey to maroon, poorly sorted, feldspar rich and matrix-supported with subangular to subrounded, 2 to 30-centimetre clasts of bladed pyroxene-feldspar porphyry, banded tuffaceous siltstone, fine-grained felsic volcanics, chert and rare limestone. The dark green sandstone and conglomerate contain angular feldspar crystals and crystal fragments, that are often interlocking, and locally contain pyroxene crystals that comprise up to 8% of the rock. Minor pale green, thin mudstone beds have rare belemnite holes whereas the grey coarse feldspathic sandstone is generally massive, contains approximately 30% feldspar and is devoid of fossils. The conglomerate is tentatively correlated with the maroon to red-weathering conglomerate that apparently lies stratigraphically below massive, thick-bedded limestone.

A distinctive member of thin-bedded, dark grey tuffaceous mudstone, siltstone and granule conglomerate crops out in the northwest corner of the map area. These rocks may overlie, and in part be interbedded with, the pyroxene-feldspar porphyry flows. The siltstone is strongly contorted in places and much of this deformation appears to have occurred prior to lithification. Irregular, wispy rip-up clasts of siltstone also occur in overlying conglomerates, suggesting erosion of the siltstone prior to complete lithification. It seems that the siltstone and conglomerate have similar ages, with no major depositional hiatus between them.

The conglomerate and interbedded maroon and green sandstones are interpreted to be intervolcanic sediments derived from the exposure and erosion of volcanic islands comprised mainly of pyroxene-feldspar porphyry flows and associated poorly lithified marine and nonmarine sediments.

## MEGACRYSTIC FELDSPAR PORPHYRY (PTrmp)

A distinctive porphyry (Photo 1), which has bladed to equant feldspar phenocrysts up to 3 centimetres long, in

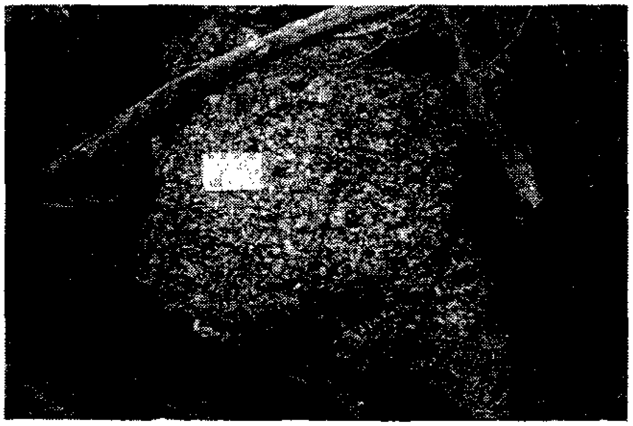
Photo 1. Megacrystic porphyry, unit PTrmp

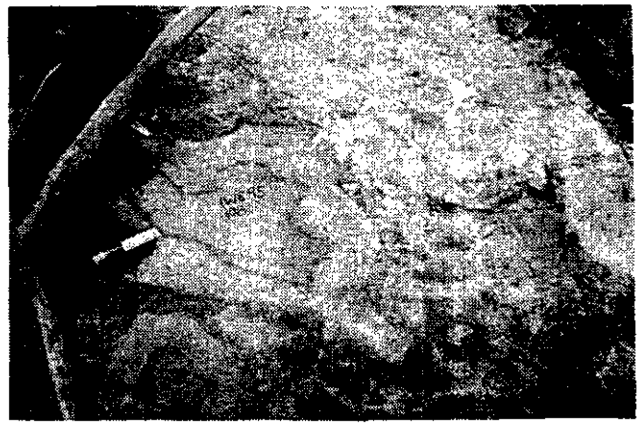
Photo 2. Volcanic breccia with rhyolitic bombs, uTrS

a greenish grey chloritic groundmass, crops out in the large clear-cut area west of Granisle and north of Fulton Lake. The porphyry, which is locally amygdaloidal, forms massive, conformable bodies within the maroon to red conglomerate-sandstone member. As mentioned earlier, clasts of this porphyry occur within the conglomerate suggesting the porphyry is the same age as its hostrocks and is more likely a flow than a sill. The same megacrystic porphyry has been noted in the conglomerate-sandstone unit south of Fulton Lake and west of Saturday Lake.

**LIMESTONE (PTrc)**

The most distinctive member of the Permo-Triassic succession is a medium to thick-bedded white to grey weathering, cliff-forming limestone. The limestone is best exposed along the west-facing slope of a north-trending ridge near the centre of the map sheet. Here the limestone member dips 45° to 50° to the northeast and is well exposed along several near-vertical cliff faces. This location has been examined for its industrial mineral potential (Cart prospect, MINFILE 93L 306). A similar limestone member occurs west of the dam on the north shore of Fulton Lake and dips moderately to the west.

**CALCAREOUS SILTSTONE (PTrs)**

Well bedded calcareous siltstones and pebble conglomerates conformably overlie the limestone member (Figure 5). These rocks are exposed on the crest of a ridge immediately east of the chain of limestone cliffs in the centre of the map area. They are in fault contact with overlying Stuhini volcanic rocks.

***UPPER TRIASSIC STUHINI GROUP***

A bimodal volcanic sequence overlies Permo-Triassic limestone and calcareous sediments and is tentatively correlated with the Upper Triassic Stuhini Group (uTrS) based on the occurrence of the fossil *Halobia* (H.W. Tipper, personal communication, 1995). The volcanic rocks are well exposed as a series of north-trending ridges in the large clear-cut west of Granisle and appear to be part of a continuous stratigraphic succession that dips moderately to the northeast (Figure 5). In general there is a change from maroon to green colour up section, suggesting a change from subaerial to submarine conditions. This succession is comprised of volcanic breccia, aquagene tuff and autobrecciated basaltic flows, interbedded with lapilli tuff, volcanic conglomerate and sandstone. The most distinctive lithology within the suspected Triassic succession is a greenish grey to slightly maroon volcanic breccia. The breccia is poorly sorted and contains lapilli to block-sized, rounded to subrounded volcanic clasts in a greenish grey feldspathic matrix. The clasts vary from light grey to dark green in colour and from dense, aphanitic to feldspar phyric and amygdaloidal. Medium to strong epidote alteration, often with quartz, occurs either pervasively or as veins and clots. White-weathering, flow-banded rhyolite and weakly welded ash-flow tuff members occur near the middle of the succession. A minor amount of marine sediment also occurs in the upper half of the section and contains poorly preserved bivalve fossils and possible corals. Attitudes are measured from thin tuffaceous sandstone, feldspar crystal tuff and ash tuff beds that are intercalated with the more massive volcanic rocks.

The lower part of the Triassic section is mainly massive beds of volcanic breccia with feldspar-phyric clasts in a fine-grained dark maroon matrix, separated by thin intervals of well bedded feldspar crystal tuff and volcanic conglomerates. The crystal tuffs sometimes contain minute quartz and biotite crystal fragments. Very fine grained dark maroon veinlets cut these rocks and epidote occurs as clots. Grading in the conglomerates indicates stratigraphic top is to the northeast.

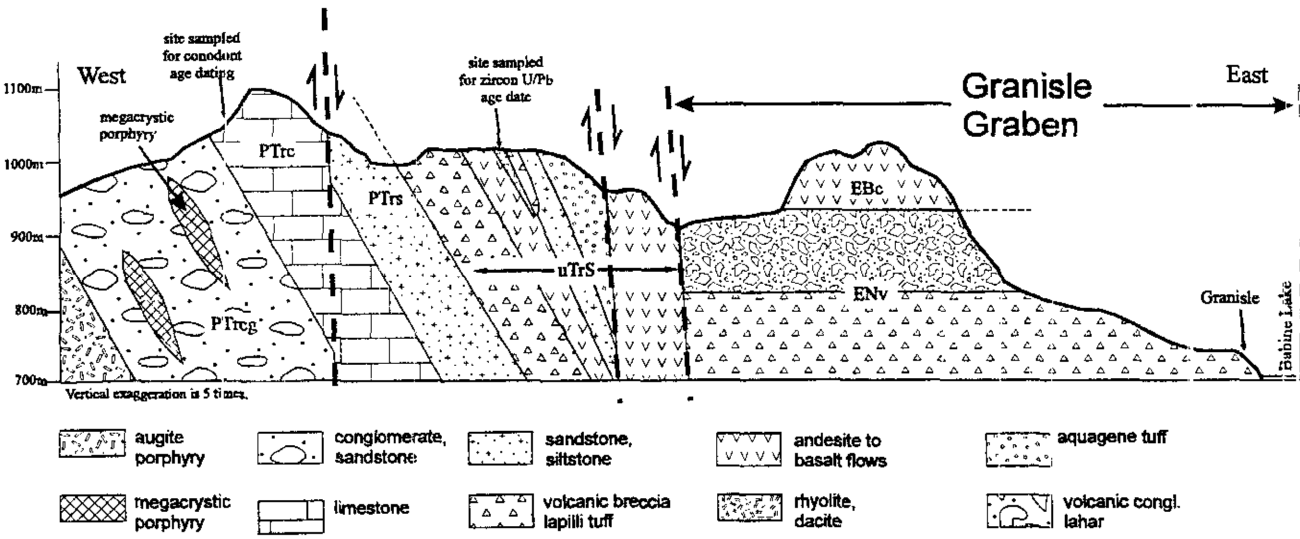


Figure 5. Section through Permo-Triassic and Eocene rocks, west of Granisle. See Figure 2 for section location, Figure 3 for legend.

Overlying the breccias is a unit of basalt to andesite flows. The flows are typically amygdaloidal and locally autobrecciated. Intense epidote alteration and veining is common. The flows weather a light brown colour and vary from maroon to greenish grey on fresh surfaces. They appear to be mostly subaerial in origin.

Overlying the flows, or possibly intruding them, are light grey weathering, discontinuous, lensoidal to dome-like bodies of flow-banded rhyolite. Flow banding is defined by cream and maroon bands, approximately 1 to 2 millimetres wide. Some of the bands are comprised almost entirely of white spherulites. The maximum thickness of this member is approximately 15 metres.

The next member in the sequence is a heterolithic, clast-supported volcanic breccia or agglomerate that contains white-weathering, 25-centimetre to 1-metre subrounded bombs of the flow-banded rhyolite. The bombs have deep reaction rims indicating that they were hot at the time of lithification (Photo 2). The breccia was probably the result of a phreatic explosion. Immediately overlying this breccia is a thin amygdaloidal basalt flow.

The next prominent ridge in the section is comprised of light grey to white-weathering, well bedded lapilli tuffs, ash-flow tuffs and volcanic debris-flows. The ash-flow tuffs are weakly welded to unwelded and contain light coloured, lapilli-sized clasts that include aphanitic rhyolite, flow-banded rhyolite and scoriaceous tuff in a fine-grained, greyish green, feldspar-phyric matrix (Photo 3). Mike Villeneuve of the Geological Survey of Canada collected a sample from this unit for U-Pb isotopic dating of zircons. Debris flows in the section contain clasts of the ash-flow tuffs and are probably locally derived.

Overlying the felsic lapilli and ash-flow tuffs is a section of interbedded medium to coarse-grained volcanic wacke, aquagene tuff and autobrecciated, amygdaloidal basalt flows. These rocks weather a distinctive orange-tan colour and have a dark green chloritic matrix. The volcanic wackes have poorly defined cross and graded bedding and locally contain poorly preserved bivalve fossils *(Halobia?)* indicating a marine depositional environment. Irregular bodies of light grey, recessive, lime mud are also associated with the fossil bearing beds and these have been sampled for conodonts.

A high-angle, north-trending normal fault displaces the Triassic section downward just west of Skinhead Lake. A sequence of greenish grey weathering, autobrecciated basaltic flows and aquagene tuffs crops out east of the fault and these rocks presumably occur near the top of the Triassic section. The flows vary from aphanitic to intensely amygdaloidal. Epidote alteration and veining is locally intense. In one locality, an aphanitic flow has a bulbous weathering pattern that is suggestive of pillows.

The Triassic section is truncated by a north-trending normal fault that traces through Skinhead Lake. East of the fault is the Granisle graben which contains flat-lying Eocene Newman and Buck Creek volcanics. The bedding attitude in the Triassic section becomes more northerly and near vertical towards the edge of the graben, probably due to downward movement on bounding faults.

Rocks similar to those exposed in the Skinhead Lake section crop out down the middle of the Newman Peninsula and on the east shore of the Hagan Arm of Babine Lake. These rocks were previously mapped as part of the Lower Jurassic Telkwa Formation, but we believe they are Triassic in age and correlative with the Stuhini Group. This conclusion is based on lithologic similarity. In both areas the rocks are mixed basalt and rhyolite in composition with pyroclastic and epiclastic members characterized by angular felsic clasts in a green chloritic matrix. The section may include minor amounts of marine siltstone and limestone.

Photo 3. Lapilli tuff with felsic clasts, unit uTrS.

Photo 4. View looking northwest toward Turkey Mountain.

## *PRE-TOPLEY FOLIATED DIORITE*

Medium-grained equigranular, hornblende-biotite diorite underlies the high hills just outside of the northeast corner of map sheet 93L/16. The diorite has a pronounced mineral foliation defined by the alignment of hornblende and biotite. In one locality this foliation has an attitude of 095/65S. Xenoliths of biotite microdiorite, up to 10 centimetres in diameter, have indistinct (resorbed?) margins and are abundant in the intrusive. Fine-grained, pink aplitic dikes of the Topley intrusive suite cut the diorite, suggesting that the latter is an older phase and may possibly be comagmatic with Upper Triassic Stuhini volcanics. In general, the diorite does not resemble any phase of the Topley suite due to its apparent lack of potassium feldspar. An Ar-Ar geochronology sample collected from this intrusion may yield important age constraints and cooling history information.

## *LATE TRIASSIC TO EARLY JURASSIC TOPLEY INTRUSIONS (EJT)*

The Topley intrusions, as defined by Carter (1981), include quartz diorite to quartz monzonite of Late Triassic to Early Jurassic age. Earlier studies (Carr, 1966; Kimura *et al.*, 1976) used the term Topley intrusions for granite, quartz monzonite, granodiorite, quartz diorite, diorite and gabbro intrusions of probable Jurassic age that intrude Triassic volcanic rocks from Babine Lake to Quesnel. Included in this Topley suite were high-potassium intrusions associated with the Endako porphyry molybdenum deposit. However, subsequent K-Ar isotopic dating showed most of these intrusions were Late Jurassic to Early Cretaceous in age. Consequently, the intrusions around Endako were renamed the Francois Lake intrusions to distinguish them from the older Topley suite.

Potassium-argon isotopic dates for the Topley intrusions, as defined by Carter (1981), would include ages as young as 178 Ma, but most are between 199 and 210 Ma (Early Jurassic) using the old decay constants. Most of these dates are from large plutons in the Topley area and southwest of Babine Lake. In the current study, we restrict the term Topley intrusions to typically pink, potassium feldspar rich granite and quartz monzonite of apparent Late Triassic to Early Jurassic age. We consider the type area to be the southeast corner of the Fulton Lake map sheet where a large, multiphase intrusive body, the Tachek stock, is well exposed in clear-cuts and along the shores of Babine Lake. The high-potassium composition of these rocks distinguishes them from older and younger plutonic suites that are mainly granodiorite to quartz diorite. Phases of the Topley intrusions, as defined in this study, intrude rocks believed to be correlative with the Permian Asitka and Late Triassic Stuhini groups. The only locality where a Topley intrusion has been observed cutting Telkwa Formation rocks is in a creek exposure 3 kilometres west of Lennac Lake. Here, a fine-grained, pink aplitic dike, typical of the youngest phase of the Topley suite, cuts maroon lapilli tuffs.

In the current study area there are only two localities where the Topley intrusions have been dated (Table 1). A 205±9 Ma age (210 Ma revised) was determined on hornblende extracted from coarse-grained porphyritic monzonite exposed on a small island 8 kilometres north of Topley Landing (Wanless, 1974); a 176 Ma±7 Ma age (178 Ma revised) was determined on biotite from a biotite-quartz-feldspar porphyry dike at the Tachek porphyry copper prospect (Carter, 1981). Based on lithology and apparent age we do not consider the dikes at the Tachek property to be part of the Topley suite. They are more likely related to compositionally similar rocks in the Telkwa Formation although the 178 Ma age is too young even for this correlation.

### TOPLEY INTRUSIVE PHASES

The Topley intrusions have been divided into several mappable phases based on macroscopic field

**TABLE 1. K-Ar DATES IN THE FULTON LAKE MAP AREA.**

| NTS Map | UTM Easting | UTM Northing | Description | Type | Lab Number | Reference | Original date | Revised date | error |
|---|---|---|---|---|---|---|---|---|---|
| 93L/16 | 677314 | 6091091 | Newman BFP; Bear Isl., Babine L. | bt | GSC 73-43 | Wanless et al., 1974 | 44.3 | 45.1 | 2 |
| 93L/16 | 665878 | 6094217 | Newman HFP; 12.9 km N of Saturday L. | hb | GSC 73-37 | Wanless et al., 1974 | 45.3 | 46.8 | 2.7 |
| 93L/16 | 662856 | 6089781 | Newman HFP, small stock; 6.4 km NW Saturday L. | hb | GSC 73-39 | Wanless et al., 1974 | 49.0 | 50.2 | 3 |
| 93L/16 | 662856 | 6089781 | Newman HBFP stock; 6.4km NW Saturday L. | bt | GSC 73-40 | Wanless et al., 1974 | 48.9 | 50.2 | 3 |
| 93L/16 | 677036 | 6096223 | Babine BFP, late phase, weakly mineralized; S central part of Bell Cu plug | bt | NC-67-22 | Carter, 1981 | 49.8 | 50.7 | 2.1 |
| 93L/16 | 682022 | 6091781 | quartz, biotite, apatite, chalcopyrite and bornite vein; S end of Granisle orebody | bt | NC-69-8 | Carter, 1981 | 50.2 | 51.0 | 2.1 |
| 93L/16 | 677036 | 6096223 | Babine BFP, late phase, mineralized; NE part of intrusion at Bell mine | bt | NC-67-23 | Carter, 1981 | 51.0 | 51.5 | 3 |
| 93L/16 | 682022 | 6091781 | Babine BFP, late dike; E. side Granisle pit | bt | NC-68-1 | Carter, 1981 | 51.0 | 51.5 | 2 |
| 93L/16 | 682022 | 6091781 | Babine BFP, late dike, unmineralized; 900 m SW of Granisle orebody | bt | NC-67-5 | Carter,1981 | 51.0 | 51.6 | 2 |
| 93L/16 | 679391 | 6090746 | Newman HFP; SW end of Newman Peninsula | hb | NC-67-43 | Carter, 1981 | 51.5 | 52.4 | 1.9 |
| 93L/16 | 682022 | 6091781 | Babine BFP, mineralized; SW part of Granisle orebody | bt | NC-67-4 | Carter, 1981 | 55.0 | 55.8 | 3 |
| 93L/16 | 681279 | 6070396 | Topley hornblende-biotite-quartz porphyry, late dike, *mineralized; Tachek Creek* | bt | NC-69-4 | Carter, 1981 | 176 | 178 | 7 |
| 93L/16 | 683883 | 6082888 | Topley monzonite, coarsely porphyritic, slightly foliated; island 8 km N of Topley Landing | hb | GSC 73-45 | Wanless et al., 1974 | 205 | 210 | 9 |
| 93L/09 | 671768 | 6066311 | Bulkley hornblende-biotite-quartz-feldspar porphyry, mineralized; Lennac Lake (Thezar) property | bt | NC-72-1 | Carter, 1981 | 77.0 | 78.3 | 2.5 |

HBFP = hornblende-biotite-feldspar porphyry
BFP = biotite-feldspar porphyry

hb=hornblende
bt=biotite

observations and modal abundances. Names of phases were assigned using the IUGS classification scheme for intrusive rocks. Future work, to better characterize the intrusive suite, will involve staining, thin section examination and whole-rock geochemistry. Following is a brief description of the plutonic phases from oldest to youngest.

### *Monzonite to Quartz Monzonite Phase*

This phase occupies the eastern part of the Tachek stock on the Fulton Lake map sheet. It typically weathers orange and forms some of the conspicuous, large orange outcrops in clear-cuts on the east side of Babine Lake. This phase is mainly a leucocratic, medium to coarse-grained, equigranular and plagioclase-phyric intrusive that varies from monzonite to predominantly quartz monzonite in composition. The groundmass is composed of intergrown potassium feldspar and quartz crystals. Slightly larger plagioclase phenocrysts (up to 7 mm) sometimes give the rock a porphyritic appearance. The rocks commonly contain biotite with or without hornblende, with mafics totalling less than 3% by volume. Miarolitic cavities occur only in this phase of the Topley suite. They are filled with terminated quartz crystals which may have a black coating, and less frequently with epidote crystals. The cavities vary from several millimetres to 2 centimetres in diameter with the average being 1 centimetre. Mike Villeneuve of the Geological Survey of Canada collected a sample from this phase for U-Pb isotopic dating, in an overgrown clear-cut on the east side of the lake.

A slightly different monzonite was observed in contact with the coarse-grained main monzonite phase in two localities. Although noteworthy, this unit may not be of regional significance. The phase is a very fine grained monzonite with densely packed, bladed feldspars on a millimetre scale. The contact between it and the main monzonite is diffuse and suggests that both rocks were molten when intruded and that they could possibly be segregations of the same magma. In another locality, an apophysis of the coarse-grained monzonite has invaded a fine-grained phase that also appears to have been only partially crystallized.

Other variations in the monzonite include a fine-grained phase with bladed hornblende crystals and small areas of finer grained intrusive with lesser plagioclase, which may be closer to syenite in composition.

### *Granite Phase*

The granite phase, which crops out on the east and west shores of Babine Lake and on Long and Double islands, comprises the largest proportion of the Topley intrusions in the study area. The granite is more monotonous in composition and visual appearance than the quartz monzonite phase. It typically has a medium to coarse-grained equigranular texture and weathers pale pink. Locally the granite is sparsely porphyritic with scattered orthoclase megacrysts up to 2 centimetres long. Quartz phenocrysts up to 1 centimetre long occur as irregularly shaped, elongate crystals that are intergrown with a groundmass of orthoclase, plagioclase and lesser quartz. This phase may also carry up to 2% biotite and/or hornblende phenocrysts. A very weak foliation, defined by the alignment of quartz and mafic minerals locally occurs in the granite. A stronger foliation, with a gentle to moderate northeast dip, is present in outcrops on Double Island. This foliation is probably structurally controlled.

In one clear-cut near the Jinx Road, the granite grades into crowded porphyritic granodiorite. Although the granodiorite is more plagioclase rich than the granite, it still has sporadic potassium feldspar megacrysts and occasional large quartz grains. The groundmass of the granodiorite is composed of rounded plagioclase crystals up to 5 millimetres in diameter with very fine grained mafic minerals comprising 7 to 10% of the rock. This phase contains small xenoliths of dark grey microdiorite and clusters of hornblende crystals up to 3 centimetres long.

The coarse-grained phase is more recessive than the quartz monzonite and therefore not as well exposed. Intrusive relationships between the two phases have not yet been observed. However, in one locality, on the east side of Babine lake, a brecciated zone in the granite contains a single rounded clast of quartz monzonite, suggesting that the latter is slightly older. Overall, the two phases are considered to be very similar in age and derived from the same magmatic source. Mike Villeneuve of the Geological Survey of Canada collected a sample of the granite for U-Pb radiometric dating from an excellent exposure in a quarry near the Port Arthur landing on the west shore of Babine Lake, south of Topley Landing. A basalt dike of probable Eocene age cuts the granite near the northeast end of the quarry.

### *Pink Aplite to Rhyolite Phase*

There are several later dike phases that intrude both the quartz monzonite and granite phases of the Tachek stock and surrounding rocks. The dikes appear to have a similar potassium-rich composition to the main granitoid phases and are therefore included as part of the intrusive suite. They typically have vertical contacts and a predominant northeast trend. All of the dikes have an aphanitic to sugary textured groundmass that can be pink, orange, orange-brown, orange-tan or light grey in colour. The dikes are locally sparsely porphyritic with two distinct phenocryst assemblages. One has orthoclase phenocrysts up to 4 millimetres long, the other has both orthoclase and glassy quartz eyes up to 3 millimetres.

The composition of these fine-grained, dense rocks is unknown until staining and thin section work can be completed. Rock names such as aplite, rhyolite, syenite and monzonite all seem appropriate, depending on the colour of the rock and its mineralogy. This apparent variation in dike chemistry may mimic the range of compositions in the main phases of the Topley suite. In several localities, the borders of dikes are flow banded and/or spherulitic, suggesting these are high-level, volatile-rich rhyolitic intrusions. An excellent example of flow banded dikes crops out on the western shore of Double Island. Occasionally the flow banded dikes are chalky weathering and this is probably due to devitrification.

## XENOLITHS

Xenoliths are rare in the Topley intrusions. All of the xenoliths occur as pods several metres in diameter and are composed of mafic volcanic rocks of probable Triassic age. Although few of the contacts are exposed, the xenoliths show no apparent sign of metamorphism or assimilation and no fingers of Topley intrude them. In one locality, a xenolith of dark grey mafic volcanic flow, with 1 to 2-millimetre feldspar laths, grades into a fine-grained flow-top breccia with recessive calcite-filled cavities.

## ALTERATION

Most of the Topley rocks are relatively fresh, with only minor chlorite alteration of hornblende and biotite. Fractures sometimes have potassium feldspar alteration envelopes around them, typically a few millimetres wide. This alteration is probably related to discharge of volatile-rich fluids during the final stages of crystallization. Epidote veins and clots are locally observed and generally have no consistent orientation. Rarely a criss-crossing network of chloritic veinlets penetrates the rock. Some of the Topley rocks near the Babs prospect have a chalky, whitish appearance. This argillic alteration may be related to a younger hydrothermal system active during emplacement of biotite-feldspar porphyry dikes.

## CORRELATION OF THE TOPLEY SUITE

The high potassium content of the Topley intrusions is reflected in the presence of potassium feldspar either as large 2 to 3-centimetre phenocrysts or as a pervasive fine-grained groundmass. Previous workers (Carter, 1981) felt these intrusions were comagmatic with the Lower Jurassic Telkwa Formation. However, the Telkwa Formation is a typical calcalkaline andesitic arc assemblage. The plutonic equivalents of such an arc should be granodiorites and quartz diorites, not the potassium-rich granites and monzonites exposed in the Babine Lake area. The Topley suite appears to be too potassium rich (and possibly too old) to be related to the Telkwa Formation andesites. Intrusions that may be comagmatic with the Telkwa Formation do occur elsewhere in the Skeena Arch and in the Coast Plutonic Complex and some of them were previously included in the Topley suite. We feel these intrusions, which are possibly younger and clearly compositionally different from the type intrusions of the Topley suite, should be treated separately.

In terms of composition and age, the Topley intrusions (as defined in this report) are most similar to the Black Lake intrusions in the Toodoggone River area. These rocks are believed to be comagmatic with the high-potassium Early Jurassic Toodoggone volcanics which host important epithermal deposits (Diakow *et al.*, 1991). This raises an intriguing question: are the Black Lake intrusions in the Toodoggone River area the northwardly displaced equivalent of the Topley intrusions? This would require over 200 kilometres of right-lateral displacement on the Takla-Ingenika-Finlay fault system, considerably more than the 115 kilometres proposed by Gabrielse (1991). However, if this correlation is correct then it has important implications for the mineral potential of Jurassic volcanic rocks southeast of the Topley intrusions. Some of these rocks may be equivalent to the Toodoggone Formation and may host epithermal gold deposits. The southern extent of the Takla fault projects into the Fulton Lake map sheet. However, low topography and limited outcrop makes establishing the true trace and nature of this structure impossible. We currently believe that the contact of the Tachek stock in the southeast corner of the study area is a fault and may in fact connect to the Takla fault system. Telkwa Formation rocks adjacent to this fault are not thermally metamorphosed, do not contain Topley dikes and are locally sheared, further evidence that the contact is a fault.

## *NOSE BAY INTRUSIVE BRECCIA*

A distinctive breccia, which we believe to be intrusive, crops out on the east shore of Babine Lake, just south of Nose Bay. This breccia, which we have named the Nose Bay intrusive breccia, trends northwest, has near-vertical contacts with surrounding Topley rocks, and is over 5 kilometres long and up to 1 kilometre wide. One of the best exposures occurs at the Nose Bay ferry landing on the east side of Babine Lake. Here, the breccia crosscuts the main granite phase of the Early Jurassic Tachek stock. Clast types are dominated by milled and broken fragments of Topley granite with lesser monzonite and fine-grained aplitic phases. The breccia can be both matrix and clast-supported. The matrix is greenish in colour and appears to be mainly basaltic in composition. In many exposures it is evident that the matrix, despite its apparent volcanic composition, has forcibly intruded the host granite, breaking, injecting and milling the rock into fragments during the process.

One of the best examples of fragment milling is exposed at Wilkinson Bay where the matrix of the breccia contains abundant broken crystals of quartz and feldspar. At this locality the breccia also contains larger clasts of granite, augite-porphyritic basalt and rare limestone. The latter are probably Permian or Upper Triassic in age and indicate that the breccia cuts through these rocks at depth. This also suggests that the Tachek stock is a large, epizonal, mushroom-shaped body, which is partially floored by older Asitka and/or Stuhini rocks.

Other exposures of the Nose Bay intrusive breccia, especially those along the main logging road, have a larger proportion of volcanic clasts than Topley clasts. The volcanic clasts include dense augite-phyric basalt, augite-plagioclase-phyric basalt, amygdaloidal basalt, equigranular diorite, quartz, and strongly epidotized volcanic rock, all of which are believed to be derived from the Stuhini Group.

The Nose Bay breccia is clearly younger than the main granitoid phases of the Topley intrusions which it cuts. It is also located close to the contact between quartz monzonite and granite phases and a fault-bounded panel of augite-phyric basalt that is probably Triassic in age. This implies emplacement of the breccia was in part structurally controlled. In one locality along the road it appears that the intrusive breccia is cut by vertical, late-stage Topley aplitic dikes. If these dikes are in fact part of the Topley suite, it indicates formation of the intrusive breccia occurred during the waning stages of Topley plutonism. However, a younger age for the breccia cannot be ruled out. Mafic dikes of possible Eocene or younger age also cut the breccia.

The Nose Bay breccia unequivocally intrudes a large structural zone. Many questions arise about how it fits into the regional tectonic framework of the Babine Lake area and where its eruptive equivalents, if any, may be. One possible locality where such rocks may occur is adjacent to and within the Topley intrusive body exposed south of Tachek creek. Here, maroon, feldspar-phyric volcanic breccias contain angular, pink-weathering clasts of the Topley intrusions. These breccias, which were originally called the Tachek Group by Carter (1973), appear to have been deposited directly on exposures of Topley intrusive rocks. Although the breccias may be correlative with the Lower Jurassic Telkwa Formation, they are also lithologically similar to the Nose Bay intrusive breccia and may be the extrusive equivalent of these rocks. More work is needed to better define these relationships.

South of the map area, Eocene basaltic flows of the Buck Creek Formation disconformably overlie both the Topley intrusions and surrounding Triassic and Jurassic volcanic rocks. This indicates that the intrusions were unroofed sometime prior to the Eocene and perhaps as early as Middle Jurassic when the Skeena Arch was formed.

## *LOWER TO MIDDLE JURASSIC HAZELTON GROUP*

The Hazelton Group (Leach, 1910) is a calcalkaline island-arc assemblage that evolved in Early to Middle Jurassic time. Tipper and Richards (1976a) divided the group into three major formations. These are, from oldest to youngest, the subaerial to submarine, predominantly calcalkaline volcanic Telkwa Formation, the marine sedimentary and volcanic Nilkitkwa Formation and the shallow water, marine transgressive Smithers Formation. The Telkwa Formation underlies the southwest and northeast corners of the study area, whereas only minor exposures of the Nilkitkwa and Smithers formations are present.

## LOWER JURASSIC TELKWA FORMATION (lJT)

The type area for the Telkwa Formation is in the Telkwa Range, where a thick section of Early Jurassic volcanic rocks is well exposed. Regionally, the formation varies from marine to nonmarine and ranges from Sinemurian to early Pliensbachian in age. In the type area the predominant lithologies are air-fall tuffs, volcanic breccias and amygdaloidal basalt flows; these rocks constitute the Howson subaerial facies of the formation (Tipper and Richards, 1976a).

Previous mapping in the type area (MacIntyre *et al.*, 1989) suggests the Telkwa Formation is divisible into three members, each representing a distinct cycle of arc volcanism. These members are characterized by their predominant lithologies, although internal facies variations are common. In ascending stratigraphic order they are: (1) an andesitic pyroclastic member comprised of thick-bedded, massive, maroon andesitic lapilli, crystal and ash tuffs with minor interbeds of siliceous-banded ash flows and grey, welded lapilli tuffs; (2) a basaltic flow member which is predominantly dark green to maroon, amygdaloidal to aphyric basalt; and (3) a felsic pyroclastic member that includes interbedded ash-flow tuff, felsic lapilli and crystal tuff, flow-banded spherulitic rhyolite, volcanic breccia and related epiclastic rocks.

A succession of maroon tuffs and amygdaloidal basalt flows crops out in the southwest and northeast corners of the Fulton Lake map sheet and on MacDonald-Sterrett Island. Lithologically and stratigraphically these rocks are identical to the Howson subaerial facies of the Telkwa Formation in the type area west of Telkwa. Both the andesitic pyroclastic and basaltic flow members are present in the Babine Lake area although the upper felsic pyroclastic member is absent or very thin. Here, as in the type area, air-fall tuffs predominate and typically contain feldspar-phyric maroon and grey andesite clasts in a feldspar-rich matrix. In the Babine Lake area, lapilli tuffs and volcanic breccias predominate near the top of the Telkwa section and finer grained maroon ash and crystal tuff interbedded with tuffaceous sandstone and mudstone occur near the base of the section.

The Telkwa rocks are assumed to rest unconformably on Triassic Stuhini rocks although this contact has not yet been observed. Everywhere in the current study area the contact between suspected Triassic or older rocks and the Telkwa Formation is a fault.

The best section through the Telkwa Formation is on MacDonald-Sterrett Island (Granisle mine). Here the Telkwa rocks dip moderately to the northwest and are overlain conformably by fossiliferous marine sedimentary rocks of the Nilkitkwa Formation. Underlying the sedimentary rocks are amygdaloidal basalt flows which we correlate with the middle member of the Telkwa Formation (the upper felsic pyroclastic member is absent or very thin here). The basaltic flow member is underlain by the andesitic pyroclastic member which, going from highest statigraphic position to lowest, includes maroon volcanic breccia, ridge-forming, massive porphyryitic andesite flows and recessive, interbedded maroon crystal and ash tuff.

East of Babine Lake, maroon volcanic breccias and lapilli tuffs, similar to those on MacDonald-Sterrett island, are found in sporadic outcrops west and east of the Hagen and Jinx haulage roads. Here, as on the island, the Telkwa rocks dip moderately to the northwest. The occurrence of coarse volcanic breccias and porphyritic flows suggests a proximal, subaerial volcanic environment similar to the Howson subaerial facies as defined by Tipper and Richards (1976) in the type area of the Telkwa Formation. However, Tipper and Richards assign the Telkwa rocks in the Babine Lake area to the submarine Kotsine facies. Our work does not support this correlation. We feel all of the Telkwa rocks in the Babine Lake area are vent-proximal, subaerial calcalkaline volcanics. The occurrence of these rocks as far east as Babine Lake implies that Telkwa subaerial volcanism extends much further east than originally thought.

Although the andesitic pyroclastic member of the Telkwa Formation is predominantly air-fall tuff, flow-banded, spherulitic rhyolite domes and welded ash-flow tuffs do crop out in the west-central part of the map area, just south of Fulton Lake. These siliceous rocks appear to sit stratigraphically above amygdaloidal basalt flows and are, therefore, tentatively correlated with the upper felsic pyroclastic member of the Telkwa Formation. The felsic pyroclastic member, which represents the final explosive stages of Telkwa volcanism, is very thin or absent elsewhere in the Babine Lake area.

## LOWER JURASSIC NILKITKWA FORMATION (lJN)

Tipper and Richards (1976a) assigned thick sections of Pliensbachian to Toarcian shale, greywacke, tuff, breccia and minor limestone, that are well exposed in the Nilkitkwa and Bait ranges, to the Nilkitkwa Formation. In the type area the formation is as much as 1000 metres thick. Limestone and chert beds occur in the lower part of the section and help distinguish Nilkitkwa rocks from younger, lithologically similar formations. Shallow-water fossiliferous limestone, interbedded with pebble conglomerate and feldspathic sandstone, is particularly common where Nilkitkwa sediments onlap Telkwa volcanics.

The only known occurrences of the Nilkitkwa Formation in the current study area are on the northwest shore of MacDonald-Sterrett Island and in Broughton Creek, west of Saturday Lake. On MacDonald-Sterrett

Island, fossiliferous feldspathic sandstone, siltstone and pebble conglomerate conformably overlie the amygdaloidal basalt member of the Telkwa Formation. Fossils from this locality, including well preserved *Weyla*, are similar to fossils found in late Sinemurian to early Pliensbachian beds in the Telkwa Range (MacIntyre *et al.*, 1989). One locality on a small island just south of Sterrett Island is Late Sinemurian in age (H.W. Tipper, personal communication, 1995). The Broughton Creek locality is younger and contains late Pliensbachian macrofossils (H.W. Tipper, personal communication, 1995).

Although outliers of Nilkitkwa Formation were mapped south and north of Fulton Lake by Tipper and Richards (1976a), we believe these rocks are actually older and part of the Permo-Triassic succession because of their apparent stratigraphic position and lithology.

## MIDDLE JURASSIC SMITHERS FORMATION (mJS)

The only known exposures of the Smithers Formation are in the extreme northwest corner of the study area. Here, a northeast-trending fault separates a down-dropped block of Smithers Formation and older Jurassic and Triassic volcaniclastic rocks. Smithers Formation lithologies include maroon to greenish grey glauconitic feldspathic sandstone, siltstone and shale, lithic wacke, tuff and minor pebble conglomerate and limy siltstone. The sediments, which were deposited in a shallow-water marine to nonmarine environment, are locally fossiliferous with numerous Belemnite holes.

## *UPPER JURASSIC TO LOWER CRETACEOUS BOWSER LAKE GROUP*

There are no known outcrops of Bowser Lake Group in the Fulton Lake map area. This may be due to the fact that it lies between the Bowser Basin and the Skeena Arch and Bowser Lake Group rocks were not deposited in this area, or alternatively they were deposited and subsequently removed by erosion. Coal-bearing chert-pebble conglomerates of the Trout Creek Formation do occur in down-thrown fault blocks immediately west and north of the map area. These rocks are at the base of the Bowser Lake Group and were deposited in a high-energy, near-shore environment that probably bordered uplifted areas in Late Jurassic to Early Cretaceous time.

## *JURA-CRETACEOUS INTRUSIONS (JKg)*

A stock of medium-grained diorite crops out in a clear-cut in the northeast corner of the study area. The stock apparently intrudes Lower Jurassic Nilkitkwa Formation sedimentary rocks and is therefore Jurassic or younger. The diorite is similar to other intrusions in the district that have yielded 100 Ma ages.

## *LOWER CRETACEOUS SKEENA GROUP (lKS)*

The Skeena Group (Leach, 1910) is characterized by well bedded, quartz and muscovite-bearing, marine sedimentary rocks that overlap Jurassic and older rocks along the southern margin of the Bowser Basin. The main Skeena lithologies are dark grey shaly siltstone, greywacke and chert-pebble conglomerate These sediments were deposited in a fluviodeltaic, near-shore marine environment (Basset, 1991). The only rocks in the current study area that may be part of the Skeena Group are siltstones and sandstones immediately west of the Bell mine and sporadic outcrops in a large clear-cut that parallels the northern edge of the map area.

## *LATE CRETACEOUS BULKLEY INTRUSIONS (LKBp)*

The term Bulkley Intrusions was first used by Kindle (1954) for granitic rocks in the Hazelton area. This suite of intrusions is Late Cretaceous in age and includes large porphyritic and equigranular stocks of quartz monzonite, granodiorite and quartz diorite and smaller plutons and dikes of feldspar porphyry, hornblende-biotite-quartz-feldspar porphyry and quartz porphyry. Potassium argon isotopic ages range from 70 to 84 Ma (Carter, 1976). The plutons define a north-trending belt that extends from north of the Babine River south to the Eutsuk Lake area. They are believed to be the roots of an eastward-migrating magmatic arc that formed during a major transtensional tectonic event in Middle to Late Cretaceous time.

In the study area, the only known Bulkley intrusions crop out northeast of Lennac Lake. These intrusions, which cut maroon tuffs of the Telkwa Formation and have associated porphyry copper mineralization, are coarse-grained crowded porphyries with 30 to 40% biotite and plagioclase phenocrysts in a medium-grained quartz-plagioclase groundmass. Phases containing hornblende and quartz phenocrysts are also common. A characteristic of the intrusions near Lennac Lake is the presence of 0.5 to 1 centimetre wide books of biotite. A 77.0±2.5 Ma K-Ar age (78.3 Ma using new decay constants, Table 1) was determined on biotite from a biotite-hornblende-feldspar porphyry intrusion at the west zone on the Lennac Lake property (Carter, 1976).

## *UPPER CRETACEOUS KASALKA GROUP (uKK)*

The type area for the Kasalka Group is at Tahtsa Lake where Middle to Upper Cretaceous calcalkaline volcanics overlie the Skeena Group with angular discordance (MacIntyre, 1985). These volcanics are part of a north-trending continental volcanic arc that transected west-central British Columbia in Late

Cretaceous time. The predominant rock types are hornblende-feldspar-phyric latite-andesite and andesite, volcanic breccia, lapilli tuff and lahar. Sutherland Brown (1960) mapped similar rocks as the Brian Boru Formation in the Rocher Déboulé Range north of Smithers and MacIntyre and Desjardins (1988) documented Kasalka Group rocks in the Babine Range west of the study area. Our mapping suggests a small, fault-bounded block of Kasalka volcanics occurs 3 kilometres north of the west zone at the Lennac Lake property. Although outcrop is very limited, two small outcrops of volcanic breccia with clasts of medium-grained, crowded, hornblende-biotite phyric andesite, typical of the Kasalka Group, were located. One of the breccias contains clasts of coarse-grained quartz-biotite-feldspar porphyry that is identical to a large intrusive body less than 2 kilometres to the south. This suggests the breccia is slightly younger than the intrusions.

## *EOCENE BABINE INTRUSIONS*

The Babine intrusions (Carter, 1976; 1981) include small plugs and dikes of crowded biotite-feldspar porphyry (bfp) and lesser granodiorite, quartz diorite and rhyodacite that occur as multi-phase intrusive centres in a north-trending belt that extends from Fulton Lake to Trail Peak (Figure 1). Potassium-argon isotopic ages range from 49 to 55 Ma (50.2 to 55.8 using new decay constants, see Table 1) indicating the intrusions are early Eocene in age. The intrusions, which are believed to be the subvolcanic roots of a calcalkaline magmatic arc, cut volcanic and sedimentary strata ranging in age from Triassic to Early Cretaceous. The Newman volcanics are the extrusive equivalents of the intrusions and these rocks are preserved close to intrusive centres on the Newman Peninsula and at Saturday Lake. The fact that the volcanic edifices have not been completely removed by erosion is further evidence that the Babine intrusions and associated porphyry copper deposits such as Bell and Granisle are exposed at a subvolcanic level.

Compositionally, the Babine intrusions and Newman volcanics are very similar to the older Bulkley intrusions and Kasalka volcanics found further to the west. This suggests similar, transtensional, volcanic environments prevailed during the Late Cretaceous and, Eocene, with the locus of volcanism moving progressively eastward with time.

### BIOTITE-FELDSPAR PORPHYRY (EBp)

The most characteristic rock type of the Babine intrusive suite is a crowded, dark grey biotite-feldspar porphyry which typically occurs as small plugs and dikes. This rock type contains 40 to 60%, 2 to 3-millimetre phenocrysts of biotite, plagioclase and rarely hornblende and quartz, in a finer grained groundmass of plagioclase, quartz, biotite and minor potassium feldspar. The porphyries are quartz diorite to granodiorite in composition and are typical of plutonic rocks found in a continental calcalkaline magmatic arc environment.

### QUARTZ-BIOTITE-FELDSPAR PORPHYRY AND QUARTZ FELDSPAR PORPHYRY (EBq)

Quartz-phyric intrusions with or without biotite postdate the main phase of stockwork mineralization at the Bell mine and apparently cut the earlier biotite-feldspar porphyry phase (Dirom *et al.*, 1995). The quartz-phyric rocks are weakly mineralized relative to the bfp phase and contain partially resorbed quartz phenocrysts. This intrusive phase is restricted to the area around the Bell pit and is not found elsewhere in the map area other than perhaps at the Babs property where quartz eyes have been noted in altered rhyolitic rocks.

### RHYODACITIC INTRUSIVE-EXTRUSIVE COMPLEX (EBr)

An intrusive-extrusive complex of probable Eocene age crops out on the Newman Peninsula south of the Bell mine. It is comprised of interbedded amygdaloidal basalt or andesite and greenish grey feldspar porphyry, with distinctive, zoned, partly resorbed, 1 to 5-millimetre plagioclase phenocrysts, intruded by dikes and plugs of white to cream, flow-banded rhyodacite. Rhyodacite plugs and dikes also crop out in the vicinity of the Bell deposit and appear to bracket the main phase of biotite-feldspar porphyry. It is uncertain whether rhyodacite in this complex is the same age as rhyodacite intrusions in the vicinity of the Bell pit. The intrusive-extrusive complex is interpreted to be an eruptive centre coeval with the main phase of Newman volcanism.

## *EOCENE OOTSA LAKE GROUP*

The Ootsa Lake Group, as defined by Duffell (1959), is a succession of continental calcalkaline volcanic rocks with minor nonmarine sedimentary interbeds. In the type area around Ootsa Lake, the volcanic members are differentiated andesites, dacites and rhyolites. The dacites and rhyolites occur both as flows and flow-breccia dome complexes of limited areal extent; the andesites and tuffs are more extensively distributed. Several dates determined in the Whitesail Lake area indicate that the Ootsa Lake volcanics erupted 50 million years ago for a period as short as 1 million years (Diakow and Mihalynuk, 1987). In the study area, hornblende-biotite-phyric andesite flows, breccias and lahars of the Newman volcanics yield similar ages and are therefore mapped as part of the Ootsa Lake Group.

### NEWMAN VOLCANICS (ENv)

In the Babine Lake area, hornblende-biotite-plagioclase porphyry flows, breccias and lahars sit with angular discordance on Triassic and Jurassic volcanic

Photo 5. Columnar-jointed hornblende-biotite-feldspar porphyry, Newman Peninsula.

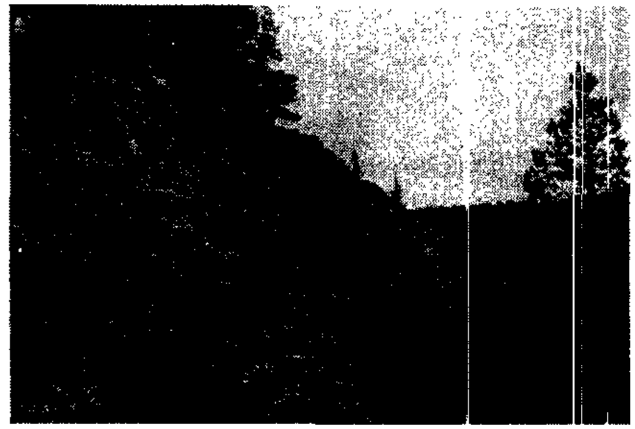

Photo 6. Stratified lahar of the Newman volcanics exposed on the west side of Turkey Mountain.

and sedimentary rocks. These rocks are well exposed on both sides of the Newman Peninsula and were given the name Newman volcanics by Tipper and Richards (1976a). On the east side of the peninsula the Newman volcanics appear to rest with angular discordance on folded Triassic or Jurassic volcanics. They also form a subcircular volcanic plateau in the northwest corner of the study area. This plateau, which is locally known as Turkey Mountain, may be the eroded remains of a large volcanic cone (Photo 4). Good exposures of the Newman volcanics also occur sporadically along the western shore of Babine Lake and on Bear Island.

The Newman volcanics are Early Eocene based on previous K-Ar dating which ranges from 44.3±2 to 51.5±1.9 Ma (45.1 to 52.4 using new decay constants, Table 1). These ages overlap those determined for lithologically identical porphyries of the Babine intrusions and the volcanics are, therefore, considered to be the extrusive equivalent of these rocks.

The Newman volcanics can be subdivided into three units or members. The lowest member is mainly columnar to sheet-jointed hornblende-biotite-feldspar porphyry flows and/or sills that are lithologically similar to biotite-feldspar porphyries of the Babine intrusions. These rocks are overlain by a middle member which is mainly volcanic breccia composed of angular clasts identical to the underlying porphyries. Towards the top of the section lahars, debris flows and volcanic-pebble conglomerate predominate. A gently east dipping, heterolithic conglomerate exposed in Tachek Creek, and sitting with angular discordance on Triassic volcanic rocks, may be the basal member of the Newman volcanics.

### *Hornblende±Biotite-Feldspar Porphyry Member*

The best exposures of the hornblende±biotite-feldspar porphyry member are along the west side of the Newman Peninsula. Here, a columnar jointed flow or sill is well exposed along the shoreline for several hundred metres (Photo 5). A sheet-jointed flow or sill crops out higher up on the steep west face of a prominent knoll near the end of the peninsula. Across the lake, to the west, columnar jointed porphyry is exposed on the shoreline cliffs of Bear Island.

Northwest of Saturday Lake and south of Turkey Mountain, columnar jointed hornblende-biotite-feldspar porphyry crops out as a small, steep-sided knoll. The porphyry is either a flow that rests on folded sediments of the Nilkitkwa Formation or the remnants of a steep-sided plug or volcanic neck.

### *Volcanic Breccia Member*

A northeast-dipping section through the Newman volcanics is well exposed along the access road on the east side of the Newman Peninsula. Massive hornblende±biotite-feldspar porphyry crops out at the south end of the road and is probably near the base of the section. The porphyry grades into a volcanic breccia that contains angular clasts identical to underlying flows but in a finer grained, greenish grey hornblende±biotite-feldspar phyric andesitic matrix. Near the top of the section, the breccias become more recessive and are interbedded with monolithic lahar and volcanic conglomerate. The volcanic breccia member appears to occupy a similar stratigraphic position on the west side of the peninsula although these relationships are complicated by a series of northwest-trending faults.

### *Lahar Member*

The upper part of the Newman volcanics is dominated by chaotic debris flows or lahars with lesser interbedded volcanic conglomerate. These rocks are well exposed on steep cliff faces surrounding Turkey Mountain in the northwest corner of the map area (Photo 6). The lahars are typically very poorly sorted with subangular to subrounded, hornblende-biotite-feldspar porphyry clasts, ranging from several metres to less than 10 centimetres in diameter, floating in a matrix of poorly consolidated light grey ash and 1 to 2-

**TABLE 2. MINERAL OCCURRENCES**

| MINFILE Number | Name | Status | NTS Map | UTM Easting | UTM Northing | Commodity | Type |
|---|---|---|---|---|---|---|---|
| 093L 144 | Tachi | show | 93L16 | 681534 | 6070716 | Cu,Mo | Porphyry |
| 093L 145 | Newman | show | 93L16 | 680973 | 6091274 | Pb, Zn, Ag, Au, Cu | Vein |
| 093L 146 | Granisle | pp | 93L16 | 682187 | 6092097 | Cu, Ag, Au, Mo | Porphyry |
| 093L 163 | O | show | 93L16 | 673355 | 6080915 | Cu | unknown |
| 093L 164 | Mine | show | 93L16 | 673510 | 6088875 | Cu | unknown |
| 093L 167 | Alp | show | 93L16 | 669203 | 6077353 | Cu | unknown |
| 093L 190 | Thezar 75 | pros | 93L09 | 671448 | 6070012 | Cu, Mo | Porphyry |
| 093L 191 | Thezar 81 | show | 93L09 | 671638 | 6069710 | Cu | Porphyry |
| 093L 192 | Cortina | show | 93L16 | 675772 | 6073892 | Cu | Porphyry |
| 093L 199 | Totem | show | 93L09 | 687176 | 6070637 | Cu | Porphyry |
| 093L 207 | Hag | show | 93L16 | 683966 | 6096502 | Cu, Pb, Zn | Vein |
| 093L 208 | Trek | show | 93L16 | 683991 | 6095884 | Cu, Pb, Zn | Stratiform |
| 093L 209 | Mag | show | 93L16 | 683577 | 6095008 | Cu, Pb, Zn | Vein |
| 093L 212 | Donna | show | 93L16 | 679091 | 6075879 | Cu | Porphyry |
| 093L 215 | Badge | show | 93L16 | 671274 | 6079288 | Fe, magnetite | Porphyry |
| 093L 219 | Ketza | show | 93L16 | 679012 | 6093516 | Cu | Porphyry |
| 093L 220 | Kare | show | 93L16 | 686747 | 6093832 | Cu | Porphyry |
| 093L 224 | Sat | show | 93L16 | 665361 | 6084637 | Cu | Porphyry |
| 093L 225 | Pro | show | 93L16 | 680668 | 6072229 | Cu, Mo | Porphyry |
| 093L 306 | Cart | show | 93L16 | 672949 | 6082168 | limestone | Limestone |
| 093L 308 | Calcite | show | 93L16 | 674235 | 6077545 | limestone | Limestone |
| 093L 315 | Gold Dust | show | 93L16 | 681229 | 6071633 | Cu, Mo, Au, Ag | Vein |
| 093L 325 | Babs | show | 93L16 | 692500 | 6082500 | Cu, Au | Porphyry |

Note: show = showing, pros = prospect, pp = past producer.

millimetre hornblende and plagioclase crystal fragments. The lahars are very susceptible to weathering and decompose easily, producing residual deposits of porphyry boulders in a feldspar, quartz and hornblende-rich sand. North of the Granisle connector road, differential erosion of lahars and breccias along a steep cliff has produced spectacular hoodoos.

### *EOCENE ENDAKO GROUP*

The Endako Group is comprised of basaltic flows that conformably overlie the Ootsa Lake Group. They represent the last stage of volcanic activity in the evolution of an Eocene transtensional volcanic arc. Endako Group rocks also sit directly on the large Tachek stock located immediately south of the study area in 93L/9. Within the study area there is one small outlier of the Endako Group which is tentatively correlated with the Buck Creek Formation (Church 1973).

#### BUCK CREEK FORMATION (EBC)

A circular knoll immediately west of Granisle is comprised of flat-lying, very vesicular basalt flows. Sporadic outcrops near the base of the knoll are lahar of the Newman volcanics, suggesting the basalt flows are stratigraphically above these rocks. The basalt flows, which are clearly Eocene or younger, have been previously mapped as the Buck Creek Formation of the Endako Group (Tipper and Richards, 1976b).

A large, north-trending dike and a plug of massive basalt cut the Newman volcanics on Turkey Mountain. These intrusions may have been feeders to Buck Creek flows.

## STRUCTURE

The structure of the Babine Lake area is characterized by north-trending grabens offset by northeast-trending, right-lateral shear zones. Both graben development and right-lateral displacement of fault blocks are believed to be related to an Eocene transtensional event that is widely recognized within the Nechako and Interior plateaus. At least some crustal subsidence occurred after the main period of magmatic and hydrothermal activity, as both the Babine intrusions and Newman volcanics have been displaced by movement on faults bounding the grabens. Arc volcanism and porphyry copper mineralization appear to have been early events in the Eocene transtensional tectonic regime.

The Permo-Triassic and Early to Middle Jurassic rocks of the area are folded and locally have a well developed penetrative cleavage. This deformation is believed to be related to the Middle Jurassic collision of Stikinia with the Cache Creek Terrane. Folds are offset and truncated by high-angle faults which are probably Eocene or younger in age. Eocene volcanics rest with angular discordance on Triassic and Jurassic volcanics and also on the Topley intrusions, suggesting considerable uplift and erosion prior to the Eocene.

The most intense deformation is in Permo-Triassic and possibly Early Jurassic rocks that crop out between the Fulton Lake dam and north of Shoulder Mountain. Here a strong north-trending, steeply dipping foliation is developed in intensely folded and possibly thrust faulted volcanics and sediments. The area of penetrative cleavage is bounded to the north and south by unfoliated rocks. The northerly trend of foliation and fold axes within this anomalously deformed zone are consistent with stress generated between northeast-trending dextral shear zones. These shear zones may be the southwest extension of the Takla fault system, a major zone of dextral displacement.

## MINERAL OCCURRENCES

The most important mineral occurrences in the Babine Lake area are porphyry copper deposits associated with the Eocene Babine intrusions and Late Cretaceous Bulkley intrusions (Carter, 1981; Carter *et al.*, 1995). The Granisle past producer and the Saturday Lake and Babs prospects are the main porphyry copper occurrences in the study area (Table 2). In addition, the Lennac Lake and Tachek porphyry prospects occur on or just south of the southern boundary of the study and are also discussed in this report. A detailed description of these deposits is not included here and the reader is referred to excellent review papers by Fahrni *et al.* (1976), Carson *et al.* (1976) and Dirom *et al.* (1995).

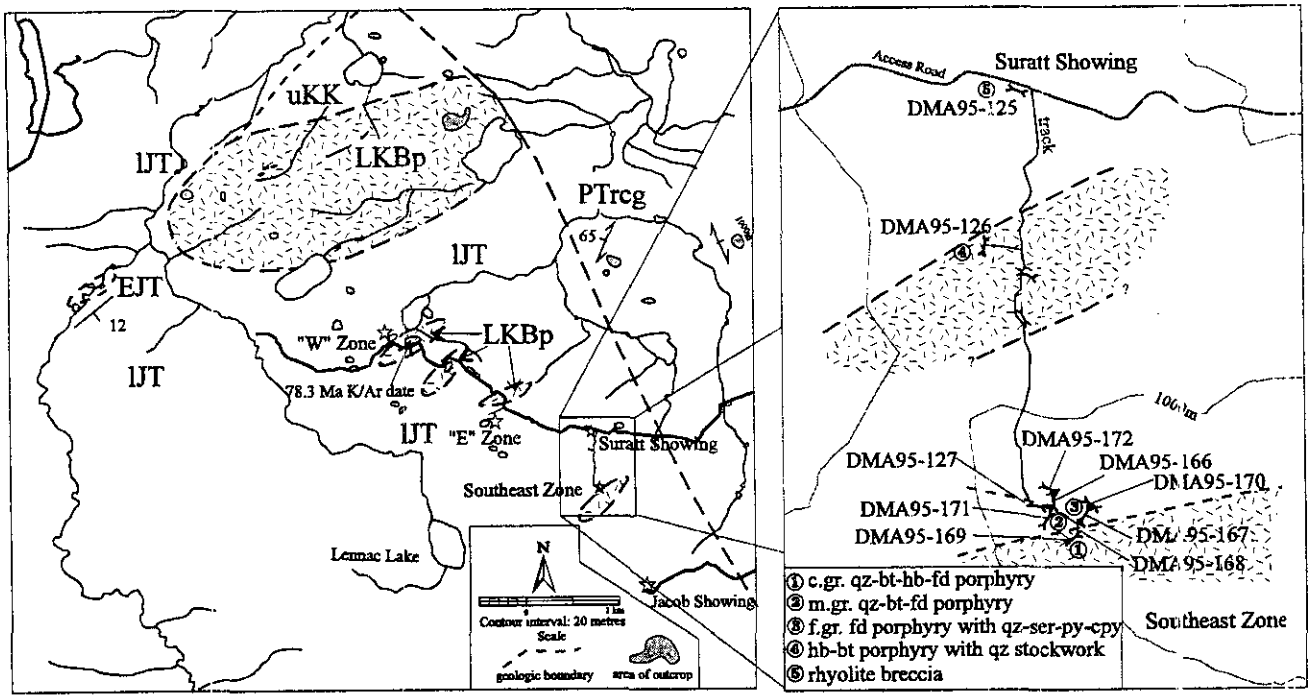


Figure 6. Geology of the Lennac Lake porphyry copper property. Inset shows sample location sites in the southeast zone. Analytical results are given in Table 3. See Figure 2 for property location; Figure 3 for legend.

## *GRANISLE (MINFILE 93L 146)*

The Granisle pit is located on MacDonald-Sterrett Island (Figure 2). The mine was in production from 1966 to 1982 during which time 214 300 tonnes copper, 6833 kilograms gold and 69 753 kilograms of silver were produced from 52.7 million tonnes of ore (Dirom *et al.*, 1995). The average grade was 0.47% Cu and the average waste to ore ratio was 1.37:1. The town of Granisle was built to provide accommodation for workers at the mine.

The Granisle porphyry copper deposit is asymmetrically zoned about a northeast-trending multiphase stock that cuts Lower Jurassic Telkwa Formation tuffs and amygdaloidal flows. The main intrusive phases, in order of relative age, are quartz diorite microporphyry and biotite-feldspar porphyry. Alteration assemblages include biotite-magnetite, carbonate-sericite-quartz-pyrite and chlorite-carbonate-epidote. The geology and mineralogy of the Granisle mine are described in detail by Fahrni *et al.* (1976) and Dirom *et al.* (1995).

## *RED (MINFILE 93L 207,208,209)*

The Red property is located 6 kilometres north of the Granisle mine-site in an area of very limited outcrop. Granby Mining Company Limited first explored the property in the mid 1960's followed in 1966 by Bethex Explorations Ltd. Bethex drilled nine holes in 1967. Canadian Superior Exploration Limited and Quintana Minerals Corporation completed induced polarization and geochemical surveys in 1972. The property was restaked by Gerard Auger in 1984 and he subsequently optioned it to Anglo Canadian Mining Corporation. Anglo in turn optioned the property to Equity Silver Mines Limited. In 1987; Equityt completed 963 metres of diamond drilling in seven inclined holes. An additional 914 metres was drilled in six holes in 1989.

The only mineral occurrence exposed on surface is a 0.3 metre wide quartz-carbonate vein with galena, sphalerite and chalcopyrite, in sheared, rusty sedimentary rocks near the northwest corner of the property. The main target is a pyrite-pyrrhotite zone that produces a strong geophysical conductor. The zone has been drill-tested over a strike length of 2?0 metres. Drill intersections with core lengths of between 30 and 50 metres have contained massive and stringer sulphides with elevated copper, zinc, lead, silver and gold values (N.C. Carter, personal communication, 1995). Hostrocks are Lower Jurassic Nilkitkwa Formation argillaceous siltstones and greywackes with interbedded felsic and intermediate volcanic rocks. One outcrop of the sedimentary rocks occurs in a south-flowing creek gully on the west side of the property. Here, the beds strike north and dip moderately to the west. A Jura-Cretaceous diorite stock crops out in the large clear-cut on the north end of the property.

## *O-SHOWING (MINFILE 93L 163)*

The O showing (MINFILE 93L 163) is located near three small lakes, approximately 3 kilometres north of Fulton Lake and 7.5 kilometres west of Babine Lake. Very coarse, bladed feldspar porphyry flows, brick-red to maroon conglomerate and green coarse sandstone to grit underlie the property. These rocks are believed to be Triassic or older based on our mapping in 1995. Bedding strikes 033° and has a near vertical dip. The feldspar porphyry is locally amygdaloidal and is probably a flow. The red conglomerate contains coarse plagioclase crystals which were probably derived from the porphyry. The conglomerate is very similar to that seen in drill core at the Cortina showing (MINFILE 93L 192) 7 kilometres to the south.

Minor amounts of bornite, chalcocite and malachite have been reported at the O showing, but this mineralization was not located. A small outcrop with an orange-buff weathering quartz and calcite stockwork was sampled (IWE95-290) but no significant assays were returned (Table 3). Previous soil sampling has defined four areas with copper concentrations greater than 400 ppm and one greater than 600 ppm. The source of these anomalies is still unknown. Till sampling in the area may help define new targets on the property.

## *TACHI (MINFILE 93L 144)*

The Tachi showings (MINFILE 93L 144) are centred on Tachek Creek, just below the scenic lookout on the Topley-Granisle highway. The best exposure occurs on steep canyon walls where medium-grained porphyritic hornblende-biotite granodiorite dikes, trending approximately 155°, cut fractured and altered siliceous volcanic rocks of Permo-Triassic or Jurassic age. Rare, green and orange gossanous patches, 1 metre wide, also occur on the canyon face. Orange-weathering potassium feldspar with minor chlorite and sericite occurs as diffuse patches and fracture coatings throughout the volcanic rock. Associated mineralization includes pyrite, chalcopyrite and minor molybdenite as disseminations and veinlets. One sample (IWE95-9, Table 3) returned low copper and molybdenum assays. A K-Ar isotopic age of 176±7 Ma (178 Ma using new decay constants, Table 1) was determined by Carter (1981) for one of the dikes at the Tachi showing. Medium-grained quartz monzonite also crops out in the creek but crosscutting relationships with the porphyry dikes could not be determined.

## *GOLD DUST (MINFILE 93L 315)*

The Gold Dust (MINFILE 93L 315) showing is situated north of the Tachi prospect, on the north side of the Topley-Granisle highway. Here, a 2-metre section of chlorite schist of probable Triassic age is cut by numerous quartz veins, 20 centimetres wide. The veins and schistosity strike approximately 010° and are vertical. The schistosity is imparted by 1-millimetre bands of chlorite and very fine magnetite that pinch and swell, locally giving the rock a spotted appearance. The white quartz veins are often rimmed by coarse potassium feldspar crystals. No sulphide minerals were seen in these rocks which are well exposed at the top of a prominent knoll. A grab sample (IWE95-25, Table 3) returned very low assay values.

## *LENNAC LAKE (MINFILE 93L 190,191)*

Amax Exploration Inc. discovered the Lennac Lake porphyry copper-molybdenum prospect in 1971 while following up a soil anomaly on its regional soil sampling grid. Sampling on this grid, which covered most of the Babine Lake area, was done every 500 feet (approximately 150 metres) on parallel, northeast-trending lines 0.5 mile (approximately 800 metres) apart. Subsequent work on the property defined four areas of low-grade copper mineralization, namely the west, east, southeast and Jacob zones, over a distance of approximately 4 kilometres (Figure 6).

The Lennac Lake property was originally staked as the Thezar claims (Leary and Allen, 1972). Following induced polarizaton, magnetometer and soil geochemical surveys in 1971 and 1972, Amax drilled 44 percussion holes (3462 metres) in 1973 and five diamond-drill holes (919 metres) in 1974. This work confirmed the presence of low-grade copper mineralization in the west and east zones. The west zone was shown to contain approximately 0.2% copper over an area of 300 by 300 metres and to a depth of 100 metres, and the east zone approximately 0.1% copper over an area of 800 by 800 metres. At the same time British Newfoundland Exploration Limited drilled eleven percussion (450 metres) and three diamond-drill holes (180 metres) on the Jacob showing near Baboon Lake. The claims were subsequently allowed to lapse.

In 1990 the Lennac Lake property was restaked by L. Bourgh and optioned to Kennecott Explorations (Canada) Limited. Kennecott completed geological mapping, prospecting and trenching and discovered additional copper showings on the east side of the property (southeast zone). Cominco Limited optioned the property in 1993 and did additional prospecting, soil geochemistry and trench sampling (Jackisch, 1993) in the southeast zone.

## TABLE 3. ANALYTICAL RESULTS FOR ROCK SAMPLES COLLECTED FROM THE 1995 STUDY AREA

| Lab Number | Field Number | NTS Map | UTM Zone | UTM Easting | UTM Northing | Mo ppm | Cu ppm | Pb ppm | Zn ppm | Ag ppm | Au ppb | Ni ppm | Mn ppm | As ppm | Sr ppm | Sb ppm | V ppm | La ppm | Ba ppm | Ti % | Al % | Na % | Ca % | Fe % | Mg % | K % |
|---|---|---|---|---|---|---|---|---|---|---|---|---|---|---|---|---|---|---|---|---|---|---|---|---|---|---|
| 51025 | DMA95-2 | 93 K/13 | 10 | 307464 | 6082464 | 74 | 10491 | < 3 | 31 | 1.9 | 411 | 20 | 109 | 3 | 40 | < 2 | 76 | 9 | 91 | 0.19 | 1.4 | 0.12 | 0.47 | 3.6 | 0.9 | 1.06 |
| 51026 | DMA95-3 | 93 K/13 | 10 | 307717 | 6082752 | 11 | 16 | < 3 | 18 | 0.3 | 15 | 1 | 8 | 3 | 6 | < 2 | < 1 | 9 | 26 | < .01 | 0.5 | 0.17 | 0.01 | 0.3 | 0 | 0.24 |
| 51036 | DMA95-25 | 93 M/1 | 9 | 666404 | 6122098 | 20 | 614 | < 3 | 41 | < .3 | 5 | 38 | 358 | 66 | 142 | 17 | 54 | 18 | 131 | < .01 | 1.6 | 0.01 | 2.81 | 3.1 | 1.2 | 0.1 |
| 51050 | DMA95-29 | 93 M/8 | 9 | 675341 | 6130074 | 3 | 3362 | < 3 | 20 | 1 | 23 | 8 | 100 | 9 | 50 | < 2 | 24 | 16 | 389 | < .01 | 1 | 0.05 | 1.98 | 1 | 0.6 | 0.33 |
| 51053 | DMA95-40 | 93 M/8 | 9 | 674809 | 6130655 | 1 | 15 | 5 | 18 | < .3 | 4 | 9 | 198 | 73 | 17 | 2 | 40 | 15 | 150 | 0.01 | 1.2 | 0.21 | 0.14 | 2.9 | 0.4 | 0.2 |
| 51052 | DMA95-42 | 93 M/8 | 9 | 676500 | 6130500 | 7 | 226 | 23 | 65 | < .3 | 14 | 28 | 469 | 26 | 28 | < 2 | 33 | 19 | 78 | < .01 | 1.7 | 0.01 | 1.74 | 2 | 0.5 | 0.06 |
| 51037 | DMA95-99 | 93 L/16 | 9 | 671945 | 6077317 | < 1 | 8 | < 3 | 5 | < .3 | < 2 | < 1 | 3685 | < 2 | 106 | < 2 | 7 | 6 | 17 | < .01 | 0.1 | < .01 | 37 | 1.1 | 0.1 | < .01 |
| 51030 | DMA95-100 | 93 L/16 | 9 | 671148 | 6077897 | 1 | 192 | 7 | 70 | 0.3 | 26 | 8 | 580 | 15 | 38 | < 2 | 78 | 7 | 75 | < .01 | 0.9 | 0.02 | 3.55 | 3.9 | 0.8 | 0.37 |
| 51032 | DMA95-107 | 93 L/16 | 9 | 665144 | 6087027 | 1 | 76 | < 3 | 52 | < .3 | 5 | 131 | 629 | 2 | 44 | < 2 | 153 | 1 | 29 | 0.42 | 2 | 0.05 | 7.86 | 4.1 | 2.7 | 0.01 |
| 51018 | DMA95-125 | 93 L/9 | 9 | 673391 | 6068992 | 8 | 3287 | 29 | 89 | 5.2 | 16 | 3 | 455 | 534 | 28 | 27 | 6 | 12 | 110 | < .01 | 0.9 | 0.01 | 0.63 | 0.6 | 0.3 | 0.29 |
| 51019 | DMA95-126 | 93 L/9 | 9 | 673335 | 6068771 | 58 | 877 | 3 | 53 | 0.6 | 45 | 6 | 223 | 185 | 32 | 8 | 39 | 6 | 87 | 0.01 | 0.7 | 0.07 | 1.13 | 0.9 | 0.3 | 0.29 |
| 51022 | DMA95-127 | 93 L/9 | 9 | 673420 | 6068375 | 31 | 392 | 6 | 51 | 1 | 12 | 1 | 274 | 52 | 92 | < 2 | 31 | 11 | 784 | 0.01 | 1.2 | 0.09 | 1.83 | 2.5 | 0.5 | 0.39 |
| 51040 | DMA95-166 | 93 L/9 | 9 | 673451 | 6068378 | 12 | 1215 | 11 | 106 | 2.4 | 32 | 1 | 441 | 313 | 32 | 7 | 23 | 22 | 180 | < .01 | 1 | 0.04 | 1.05 | 1.9 | 0.2 | 0.5 |
| 51042 | DMA95-167 | 93 L/9 | 9 | 673487 | 6068349 | 4 | 192 | 7 | 121 | 0.6 | 27 | 1 | 475 | 44 | 17 | 3 | 25 | 8 | 195 | < .01 | 0.9 | 0.06 | 0.58 | 2.9 | 0.2 | 0.45 |
| 51043 | DMA95-169 | 93 L/9 | 9 | 673472 | 6068322 | 1 | 16 | 11 | 325 | 0.4 | 8 | 4 | 660 | 7 | 23 | 2 | 19 | 15 | 271 | < .01 | 0.9 | 0.03 | 0.9 | 1.9 | 0.1 | 0.38 |
| 51044 | DMA95-170 | 93 L/9 | 9 | 673503 | 6068378 | 2 | 265 | 9 | 55 | 0.5 | 23 | 1 | 510 | 77 | 18 | 5 | 18 | 7 | 74 | < .01 | 0.7 | 0.03 | 1.15 | 3.3 | 0.2 | 0.47 |
| 51045 | DMA95-171 | 93 L/9 | 9 | 673439 | 6068356 | 43 | 313 | 4 | 68 | 1.5 | 11 | 1 | 532 | 67 | 21 | 20 | 10 | 10 | 281 | < .01 | 0.3 | 0.01 | 1.12 | 1.3 | 0.2 | 0.16 |
| 51046 | DMA95-172 | 93 L/9 | 9 | 673442 | 6068395 | 6 | 440 | 14 | 128 | 3.2 | 15 | 1 | 940 | 148 | 17 | 71 | 4 | 8 | 135 | < .01 | 0.7 | 0.01 | 0.5 | 0.8 | 0.2 | 0.51 |
| 51021 | IWE95-9 | 93 L/16 | 9 | 681440 | 6070665 | 102 | 536 | < 3 | 33 | 0.7 | 6 | 4 | 248 | 4 | 145 | < 2 | 53 | 8 | 91 | 0.16 | 1.3 | 0.16 | 0.71 | 2.9 | 1.1 | 0.21 |
| 51024 | IWE95-25 | 93 L/16 | 9 | 680773 | 6071902 | 1 | 4 | < 3 | 39 | < .3 | 2 | < 1 | 321 | 2 | 6 | < 2 | 3 | 4 | 46 | 0.04 | 0.3 | 0.04 | 0.15 | 0.8 | 0.1 | 0.14 |
| 51033 | IWE95-39 | 93 L/16 | 9 | 680525 | 6077345 | 1 | 32 | 3 | 50 | < .3 | 3 | 12 | 385 | 11 | 149 | < 2 | 106 | 1 | 13 | 0.36 | 2 | 0.1 | 2.04 | 4.1 | 1.3 | 0.07 |
| 51028 | IWE95-51 | 93 L/16 | 9 | 679696 | 6077233 | 3 | 9 | < 3 | 29 | 0.6 | 5 | 2 | 170 | 3 | 23 | < 2 | 3 | 63 | 979 | < .01 | 0.4 | 0.2 | 0.12 | 1.6 | 0.1 | 0.12 |
| 51029 | IWE95-54 | 93 L/16 | 9 | 686771 | 6070873 | 819 | 4 | < 3 | 7 | 3.5 | < 2 | < 1 | 94 | 3 | 7 | < 2 | 3 | 1 | 33 | < .01 | 0.1 | 0.02 | 0.07 | 0.1 | 0 | 0.06 |
| 51027 | IWE95-85 | 93 L/16 | 9 | 675003 | 6082129 | 2 | 6 | 4 | 62 | < .3 | 4 | 11 | 521 | 6 | 129 | < 2 | 92 | 5 | 56 | 0.4 | 2.7 | 0.07 | 2.13 | 3 | 1.6 | 0.05 |
| 51054 | IWE95-117 | 93 L/16 | 9 | 675437 | 6085512 | 1 | 36 | 9 | 50 | < .3 | < 2 | 2 | 406 | 3 | 42 | 2 | 35 | 10 | 137 | 0.3 | 1.2 | 0.12 | 0.68 | 1.9 | 0.5 | 0.32 |
| 51034 | IWE95-155 | 93 L/16 | 9 | 668425 | 6097164 | 14 | 187 | 6 | 213 | < .3 | 8 | 31 | 511 | 20 | 97 | 2 | 135 | < 1 | 68 | 0.38 | 3.4 | 0.44 | 1.86 | 4.6 | 1.5 | 0.12 |
| 51061 | IWE95-237 | 93 L/16 | 9 | 686875 | 6079930 | < 1 | 10838 | 5 | 158 | 18 | 246 | 76 | 1155 | 7 | 296 | < 2 | 110 | 2 | 18 | 0.27 | 2.8 | 0.11 | 2.51 | 5.7 | 2.5 | 0.09 |
| 51059 | IWE95-249 | 93 L/16 | 9 | 681425 | 6087800 | 3 | 128 | 30 | 142 | 1.7 | 3 | 2 | 574 | 12 | 9 | 2 | 67 | 5 | 125 | 0.01 | 1.7 | 0.08 | 0.04 | 4.7 | 1 | 0.17 |
| 51058 | IWE95-275 | 93 L/16 | 9 | 668800 | 6096920 | 1 | 281 | 4 | 481 | 0.7 | 23 | 16 | 680 | 22 | 87 | < 2 | 121 | 1 | 75 | 0.29 | 3.3 | 0.45 | 3.13 | 5 | 1.1 | 0.23 |
| 51060 | IWE95-290 | 93 L/16 | 9 | 673655 | 6080200 | 1 | 4 | 6 | 42 | < .3 | 2 | < 1 | 495 | 2 | 16 | 2 | 18 | 11 | 50 | 0.01 | 0.9 | 0.09 | 1.97 | 1.4 | 0.5 | 0.1 |
| 51039 | KBE95-4 | 93 M/1 | 9 | 683900 | 6101500 | 1 | 28 | 3 | 105 | < .3 | 2 | 11 | 799 | 15 | 56 | < 2 | 54 | 10 | 98 | 0.01 | 2 | 0.06 | 1.97 | 4.2 | 1 | 0.38 |
| 51020 | KBE95-25 | 93 L/16 | 9 | 663011 | 6078619 | 1 | 134 | 54 | 84 | < .3 | < 2 | 2 | 640 | 3 | 15 | < 2 | 32 | 10 | 134 | 0.04 | 0.7 | 0.09 | 1.96 | 1.9 | 0.3 | 0.23 |
| 51023 | KBE95-28 | 93 L/16 | 9 | 662963 | 6079059 | < 1 | 182 | 29 | 153 | 0.7 | 2 | < 1 | 1062 | 4 | 18 | < 2 | 95 | 10 | 321 | 0.04 | 0.8 | 0.01 | 2.36 | 4 | 0.2 | 0.37 |
| 51038 | KBE95-44 | 93 L/16 | 9 | 665050 | 6094174 | < 1 | 32 | 6 | 88 | 0.3 | 5 | 17 | 355 | 3 | 98 | < 2 | 78 | 7 | 162 | 0.12 | 1.4 | 0.19 | 0.75 | 3 | 0.8 | 0.36 |
| 51047 | KBE95-51 | 93 L/16 | 9 | 662841 | 6073790 | < 1 | 12 | 11 | 84 | 0.3 | 2 | 14 | 1095 | 9 | 59 | < 2 | 123 | 6 | 70 | 0.05 | 1.4 | 0.11 | 2.28 | 5 | 0.9 | 0.07 |
| 51049 | KBE95-58 | 93 L/16 | 9 | 662841 | 6074730 | 1 | 1314 | < 3 | 46 | 4.9 | 4 | 2 | 601 | < 2 | 95 | 4 | 26 | 12 | 67 | 0.07 | 1.3 | 0.12 | 0.68 | 1.9 | 0.7 | 0.13 |
| 51048 | KBE95-61 | 93 L/16 | 9 | 660888 | 6027293 | 1 | 4196 | 19 | 59 | < .3 | 4 | 29 | 699 | 3 | 177 | < 2 | 164 | 4 | 18 | 0.3 | 1.4 | 0.07 | 6.1 | 4.6 | 1.2 | 0.02 |
| 51055 | KBE95-146A | 93 L/16 | 9 | 691150 | 6083300 | 1 | 3 | 4 | 78 | < .3 | 6 | 3 | 825 | 3 | 92 | < 2 | 57 | 10 | 41 | 0.06 | 2.2 | 0.09 | 0.78 | 3.4 | 1.8 | 0.1 |
| 51056 | KBE95-146B | 93 L/16 | 9 | 691150 | 6083300 | 2 | 8 | 7 | 46 | < .3 | 2 | 4 | 452 | 2 | 34 | < 2 | 26 | 7 | 86 | 0.01 | 1 | 0.18 | 0.15 | 1.7 | 0.7 | 0.17 |
| 51057 | KBE95-152 | 93 L/16 | 9 | 692300 | 6087300 | 6 | 4 | 3 | 13 | < .3 | 5 | < 1 | 155 | 2 | 19 | < 2 | 5 | 13 | 153 | 0.06 | 0.7 | 0.12 | 0.16 | 0.8 | 0.2 | 0.29 |
| | | | | | Detection limit | 1 | 1 | 3 | 1 | 0.3 | 2 | 1 | 2 | 2 | 1 | 2 | 1 | 1 | 1 | 0.01 | 0 | 0.01 | 0.01 | 0 | 0 | 0.01 |

Method: aqua regia-ICP, Au by fire assay and ICP finish; analysis by ACME Analytical

Porphyry copper mineralization and alteration are associated with a series of northeast-trending dikes of biotite-hornblende-feldspar±quartz porphyry that intrude maroon lapilli tuffs and volcaniclastic rocks of the Lower Jurassic Telkwa Formation. The porphyry, which is quartz monzonite to granodiorite in composition and typical of the Late Cretaceous Bulkley intrusions, contains euhedral biotite books, hornblende, plagioclase and locally quartz eyes up to 1 centimetre in diameter. Phenocrysts comprise up to 30% of the rock.

The main areas of mineralization on the Lennac Lake property are the west, east, southeast and Jacob zones. The west zone, which was discovered first, is mainly disseminated and fracture-coating pyrite, chalcopyrite and trace molybdenite in relatively fresh, coarse-grained porphyry and hornfelsed volcanics. The east zone is mainly fracture coatings and veinlets of pyrite and chalcopyrite with associated chlorite-epidote alteration envelopes. This alteration is superimposed on biotite hornfelsed Telkwa volcanic rocks.

The Suratt showing comprises chalcopyrite, pyrite and tetrahedrite in a rhyolite breccia that has been exposed by trenching along the main access road. A zone of quartz-molybdenite stockwork in a quartz-sericite-altered quartz-biotite-feldspar porphyry intrusion is exposed in trenches along a cat trail that heads south from the Suratt showing. The trail ends 600 metres to the south (inset, Figure 6) where several trenches have exposed disseminated and fracture controlled chalcopyrite and pyrite in fine-grained quartz-sericite-altered feldspar porphyry (altered Telkwa Formation andesite?) and a medium to coarse-grained quartz-biotite-feldspar porphyry intrusion. Samples DMA95-127 and 166-172 were collected from these trenches. These chip samples returned only low copper assays (Table 3). However, the area is still considered favourable because copper mineralization occurs in widely space trenches within an area of no outcrop and there is strong quartz-sericite alteration and quartz vein stockworking in a multi-phase porphyryitic intrusion. To date this area has not been tested by diamond drilling.

## *SAT (MINFILE 93L 224)*

The Saturday Lake porphyry copper occurrence (SAT claims) was staked by Amoco Canada Peroleum Company Ltd. in 1972. Amoco conducted induced polarization, magnetometer and electromagnetic surveys and soil, silt and rock geochemistry, followed by 2000 metres of diamond drilling in 19 holes. The results of this drilling were never published but Leahey (1982) states that one hole (72-3) apparently intersected 40 metres of 0.10% copper. Amoco allowed the claims to lapse in 1974. The property was subsequently restaked by Cities Services Minerals Corporation in 1974 and Great Western Petroleum Corporation in 1980, who subsequently optioned the property to Noranda. Additional IP, magnetometer and soil geochemical surveys by Noranda failed to define any new targets (Leahey, 1982).

A cursory examination of the drill core still at the old Saturday Lake campsite confirms the presence of biotite-feldspar porphyry intrusions of the Babine intrusive suite cutting volcanic and sedimentary rocks of probable Triassic age. Low grade copper mineralization in the form of disseminated and fracture controlled chalcopyrite is present in some of the core but much of the remaining core appears to be unmineralized and has never been split or assayed. The core boxes for several holes could not be found.

## *BABS (MINFILE 93L 325)*

The Babs property is located in the southeast corner of the map area and straddles the border between 93L/16 and 93K/13 (Figure 7). Although the property has been known for some time it has only recently been assigned a MINFILE number (93L 325). An unrelated property (MINFILE 93L 220) with the same name is located 16 kilometres to the northwest and this has caused some confusion in the past.

The Babs property, which has very little outcrop, was staked to cover a southeast-trending train of well-mineralized, subangular biotite-feldspar porphyry boulders. The boulders are typical of the Eocene Babine intrusions, which are the hostrocks at the Bell and Granisle mines. Over 80 boulders, ranging from 10 to 150 centimetres in diameter, have been located within an area of 150 by 300 metres.

Work on the Babs property has defined coincident chargeability and soil geochemical anomalies. In 1992, Equity Silver Mines Ltd. drilled seven NQ holes peripheral to, but not within, the boulder train. All of these holes were terminated shortly after encountering bedrock, with the maximum depth of bedrock penetration being 4.1 metres. One of the holes, BB92-6, was resampled by Noranda and returned 0.34% Cu for the 3 metres of bedrock that was cored. This hole was collared 300 metres east of the boulder train and 300 metres west of copper showings in a borrow bit on Pat's road. In 1992, Noranda drilled two 100-metre holes (BS93-8 and BS93-9) within the area of the boulder train. The top 10.4 metres of hole BS93-8 returned 0.21% Cu and 12.0 g/t Ag (Kemp and Robertson, 1994). Two additional holes were drilled in 1994 (NB94-10 and NB94-11) and these were 400 and 1000 metres east of the boulder train, respectively (Kemp and Robertson, 1994). Surprisingly, none of the drilling to date has tested the up-ice area of the boulder train.

The best bedrock exposure is along the eastern margin of the Babs boulder train, in a stripped area (borrow pit) along the east side of Pat's road. Here, over 30 metres of gossanous, clay-altered, quartz-phyric crystal and lapilli tuffs containing minor disseminated pyrite, chalcopyrite and malachite are exposed. Kemp and Robertson (1994) report assay values up to 726 ppm Cu and 16 ppm Ag. Noranda diamond-drill hole NB94-10, which was drilled 125 metres northwest of the borrow pit, intersected 0.19% Cu over 77.3 metres.

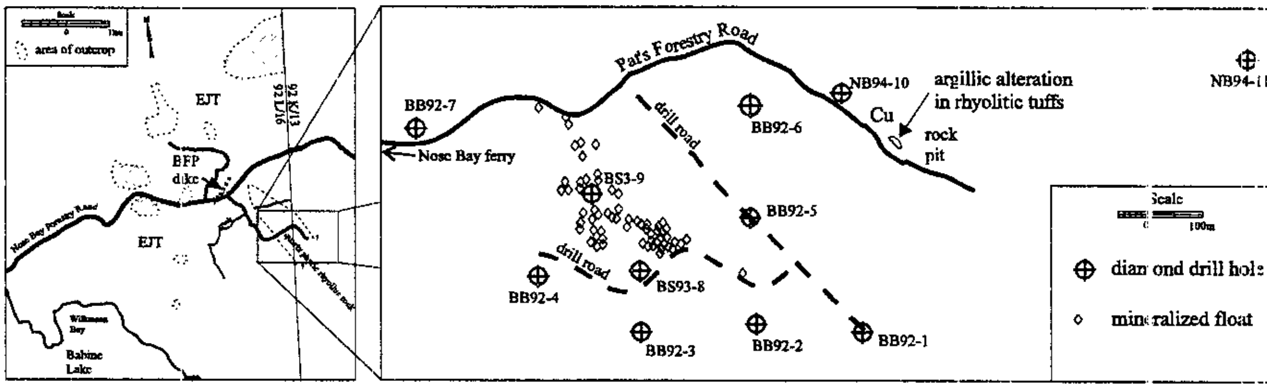


Figure 7. Geology and drill hole locations on the Babs property. See Figure 2 for property location; Figure 3 for legend.

Another small outcrop of clay-altered quartz-phyric tuffs occurs on the south side of Pat's road, near the northern limit of the boulder train. Similar rocks occur as large angular blocks or subcrop within the area of the boulder train and were also intersected in drilling in this area by Equity Silver in 1992 and Noranda in 1994.

Many of the boulders on the Babs property are strongly magnetic, have intense stockwork veining or crackle breccia textures and contain secondary biotite. The boulders are very similar to ore grade material at the Granisle mine, 14 kilometres up-ice to the northwest. Because of this it was believed for many years that the boulders were glacially transported from Granisle and little work was done on the property . However, subsequent drilling has shown that low-grade copper-silver mineralization occurs in clay-altered, quartz-phyric tuffs that underlie the boulder train and the boulders may be locally derived (see Stumpf *et al.*, 1996, this volume). Although the source of the boulders has not yet been located, a northeast-trending dikelet of dark grey biotite-feldspar porphyry was found cutting Topley monzonite in a small drainage ditch near the junction of the Nose Bay and Pat's haulage roads. Disseminated pyrite is associated with the dikelet, which is up-ice from the mineralized boulder train.

A large angular block of biotite-feldspar porphyry with a chalcopyrite-pyrite quartz stockwork was located by prospector and property owner Ralph Keefe in a new clear-cut at the southeast limit of the boulder train. A sample from this block (DMA95-2, Table 3) assayed 1.05% Cu and 0.41 g/t Au.

The Babs occurrence is in a northwest-trending belt of altered quartz-phyric pyroclastic rocks enclosed in a large, multi-phase stock of the Topley intrusions. Although the contact with the Topley rocks is not exposed, it is most likely a fault. The felsic pyroclastics are probably Eocene in age and part of the Babine intrusive suite based on lithologic similarity to quartz-phyric rocks on the Newman Peninsula.

## *NEW SHOWINGS*

Several new mineral showings were located during the 1995 bedrock mapping program and these are briefly described below. Locations are shown on Figure 2. Some of these showings may have been found by exploration companies working in the district in the past but this information has never been put in the public record. None appear to be significant.

### NIKI AND SNAPPER Cu SHOWINGS

Two small copper showings were found in a large clear-cut, approximately 6 kilometres south of the west end of Fulton Lake (Figure 2). One of these (sample KBE95-61, Table 3) is from a southeast-striking, northwest-dipping quartz-epidote veinlet, 5 millimetres wide, containing pyrite and malachite. The vein cuts maroon crystal-lithic tuff beds of the Lower Jurassic Telkwa Formation that strike 124° and dip 40° southwest. We have named this showing the Niki.

Sample KBE95-58 (Table 3) is from malachite-coated quartz-epidote veins and veinlets that cut at least four small bodies of orange-weathering quartz monzonite. These rocks intrude contorted maroon ash and crystal tuff beds of the Telkwa Formation. We have named this showing the Snapper.

### NOSE BAY Cu-Ag-Au SHOWING

Copper mineralization was found in a poorly defined fault zone cutting a shoreline bluff of Stuhini augite-phyric basalt, 2 kilometres south of Nose Bay, on the east shore of Babine Lake. A sample from the shear zone (IWE95-237, Table 3) contained disseminated malachite and chalcocite and assayed 1.08% Cu, 17.5 g/t Ag and 0.246 g/t Au .

### RUSTY KNOLL Zn SHOWING

A strongly gossanous, cliff face occurs on the southwest side of a prominent knoll, 160 metres high near the north edge of the study area, 4 kilometres west of Babine Lake. The rock at the base of the cliff is strongly altered and light bluish-grey in colour. Alteration is associated with a crackle breccia of very thin microcrystalline quartz veinlets that carry fine-grained magnetite, an unidentified silver-white metallic mineral and a fine acicular green mineral which may be pyrophyllite. Larger veinlets roughly parallel widely spaced, near vertical gossanous fractures that trend approximately 020°. The protolith within the mineralized zone is masked by the intense veining and alteration. However, away from this zone, further up the knoll the rock is a medium grey augite-phyric basalt of probable Triassic age. Samples of intensely veined rock (IWE95-155, IWE95-275, Table 3), with approximately 1% disseminated pyrite, had elevated zinc and copper concentrations. The mineralized knoll is only a few kilometres southeast of the Fireweed prospect and a similar geochemical signature suggests these occurrences may be related to the same mineralizing system. A major northeast-trending fault occurs just north of the knoll and may also have controlled localization of mineralizing fluids. The nature of the mineralization suggests an epithermal environment.

### PORT ARTHUR Mo SHOWING

A new molybdenum showing was discovered 8 kilometres south-southeast of Topley Landing. Here, a small outcrop exposes a quartz vein 20 centimetres wide cutting pale orange aplitic Topley intrusive rocks. The vein contains approximately 1% finely disseminated molybdenite. A sample returned anomalous molybdenum values (sample IWE95-54, Table 3). The extent of the vein was not determined but the amount of float present suggests other veins may be present and further exploration may be warranted.

## ACKNOWLEDGMENTS

The authors gratefully acknowledge the Geological Survey of Canada and the Nechako NATMAP program, for logistical support during the 1995 field season. Mike Villeneuve of the Geological Survey of Canada also provided invaluable support and advice for the collection of samples for U-Pb and Ar-Ar isotopic age dating. The authors would also like to thank John Bryant and Roger White for their excellent assistance in the field. We also appreciate the assistance and camaraderie of our surficial geology coworkers on this project, namely David Huntley, Andrew Stumpf, Erin O'Brien, Gordon Weary and Jennifer Hobday. Finally, we thank John Newell for his critical review of the original manuscript and many helpful suggestions towards improving the final product.

## REFERENCES

Armstrong, J.E. (1944a): Smithers, British Columbia; *Geological Survey of Canada*, Paper 44-23.

Armstrong, J.E. (1944b): Hazelton, British Columbia; *Geological Survey of Canada* Paper 44-24.

Bassett, K.N. (1991): Preliminary Results of the Sedimentology of the Skeena Group in West-central British Columbia; *in* Current Research, Part A, *Geological Survey of Canada*, Paper 91-1A, pages 131-141.

Brown, D.A., Logan, J.M., Gunning, M.H., Orchard, M.J. and Bamber, W.E. (1991): Stratigraphic Evolution of the Paleozoic Stikine Assemblage in the Stikine and Iskut Rivers Area, Northwestern British Columbia; *Canadian Journal of Earth Sciences*, Volume 28, pages 958-972.

Carr, J.M. (1965): The Geology of the Endako Area; *in* Lode Metals in British Columbia 1965, *B.C. Ministry of Energy, Mines and Petroleum Resources*, pages 114-135.

Carson, D.J.T. and Jambor, J.L. (1974): Mineralogy, Zonal Relationships and Economic Significance of Hydrothermal Alteration at Porphyry Copper Deposits, Babine Lake Area, British Columbia, *Canadian Institute of Mining and Metallurgy*, Bulletin, Volume 67, pages 110-133.

Carson, D.J.T. and Jambor, J.L. (1976): Morrison: Geology and Evolution of a Bisected Annular Porphyry Copper Deposit. *in* Porphyry Deposits of the Canadian Cordillera, Sutherland Brown, A., Editor, *Canadian Institute of Mining and Metallurgy*, Special Volume 15, pages 264-273.

Carson, D.J.T., Jambor, J.L., Ogryzlo, P.L., and Richards, T.A. (1976): Bell Copper: Geology, Geochemistry and Genesis of a Supergene-enriched, Biotitized Porphyry Copper Deposit with a Superimposed Phyllic Zone. *in* Porphyry Deposits of the Canadian Cordillera, Sutherland Brown, A., Editor, *Canadian Institute of Mining and Metallurgy*, Special Volume 15, pages 245-263.

Carter, N.C. (1973): Geology of the Northern Babine Lake Area; *B.C. Ministry of Energy, Mines and Petroleum Resources*, Preliminary Map 12 (93L).

Carter, N.C. (1976): Regional Setting of Porphyry Deposits in West-central British Columbia. *in* Porphyry Deposits of the Canadian Cordillera, Sutherland Brown, A., Editor, *Canadian Institute of Mining and Metallurgy*, Special Volume 15, pages 245-263.

Carter, N.C. (1981): Porphyry Copper and Molybdenum Deposits West Central British Columbia; *B.C. Ministry of Energy, Mines and Petroleum Resources*, Bulletin 64.

Carter, N.C., Dirom, G.E., and Ogryzlo, P.L. (1995): Porphyry Copper-gold Deposits, Babine Lake Area, West-central British Columbia, *in* Porphyry Deposits of the Northwestern Cordillera of North America, Schroeter, T.G., Editor, *Canadian Institute of Mining, Metallurgy and Petroleum*, Special Volume 46.

Church, B.N. (1973): Geology of the Buck Creek Area; *in* Geology, Exploration and Mining in British Columbia 1972, *B.C. Ministry of Energy, Mines and Petroleum Resources*, pages 353-363.

Dawson, G.M., (1881): On the Geology of the Region between the 54th and 56th Parallels, from the Pacific Coast to Edmonton; *in* Report on an Exploration from Port Simpson on the Pacific Coast, to Edmonton on the Saskatchewan, Embracing a Portion of the Northern Part of British Columbia, and the Peace River Country; *Geological Survey of Canada*, Report on Progress 1879-1880, pages 99B-142B.

Diakow, L. and Mihalynuk, M. (1987): Geology of Whitesail Reach and Troitsa Lake Map Areas; *in* Geological Fieldwork 1986, *B.C. Ministry of Energy, Mines and Petroleum Resources*, Paper 1987-1, pages 171-180.

Diakow, L.J., Panteleyev, A. and Schroeter, T.G. (1991): Jurassic Epithermal Deposits in the Toodoggone River Area, Northern British Columbia: Examples of Well-preserved, Volcanic-hosted, Precious Metal Mineralization; *Economic Geology*, Volume 88, pages 529-554.

Dirom, G.E., Dittrick, M.P., McArthur, D.R., Ogryzlo, P.L., Pardoe, A.J. and Stothart, P.G. (1995): Bell and Granisle Porphyry Copper-Gold Mines, Babine Region, West-central British Columbia; *in* Porphyry Deposits of the Northwestern Cordillera of North America, Schroeter, T.G., Editor, *Canadian Institute of Mining, Metallurgy and Petroleum,* Special Volume 46.

Duffell, S. (1959): Whitesail Lake Map-area, British Columbia; *Geological Survey of Canada*, Memoir 299.

Fahrni, K.C., Kim, H., Klein, G.H. and Carter, N.C. (1976): Granisle; *in* Porphyry Deposits of the Canadian Cordillera, Sutherland Brown, A., Editor, *Canadian Institute of Mining and Metallurgy,* Special Volume 15, pages 239-244.

Gabrielse, H. (1991): Structural Styles, Chapter 17; *in* Geology of the Cordilleran Orogen in Canada, Gabrielse, H. and Yorath, C.J., Editors, *Geological Survey of Canada*, Geology of Canada, Number 4, pages 571-675.

Hanson, G. (1925): Driftwood Creek Map-area, Babine Mountains, British Columbia; *Geological Survey of Canada*, Summary Report 1924, Part. A.

Huntley, D.H., Stumpf, A., Levson, V.M. and Broster, B.E. (1996): Babine Porphyry Belt Project: Quaternary Geology and Regional Till Geochemistry Sampling in the Old Fort Mountain (93M/1) and Fulton Lake (93L/16) Map Areas, British Columbia; *in* Geological Fieldwork 1995, Grant, B. and Newell, J.M., Editors, *B.C. Ministry of Energy, Mines and Petroleum Resources*, Paper 1996-1, this volume.

Jackisch, I. (1993): I.P./Resistivity Survey on the Lennac Property: *B.C. Ministry of Energy, Mines and Petroleum Resources*, Assessment Report 23048.

Kemp, R. and Robertson, K.A. (1994): Geological, Geochemical and Geophysical Report on the Babs Claim Group Located in the Omineca Mining Division (NTS 93L/16E and 93K/13W); *B.C. Ministry of Energy, Mines and Petroleum Resources*, Assessment Report 23536, 13 pages.

Kimura, E.T., Bysouth, G.D. and Drummond, A.D. (1976): Endako; *in* Porphyry Deposits of the Canadian Cordillera, Sutherland Brown, A., Editor, *Canadian Institute of Mining and Metallurgy,* Special Volume 15, pages 444-454.

Kindle, E.D. (1954): Mineral Resources, Hazelton and Smithers Areas, Cassiar and Coast Districts, British Columbia; *Geological Survey of Canada*, Memoir 223.

Leach, W.W. (1910): The Skeena River District; *Geological Survey of Canada*, Summary Report 1909.

Leahey, M.W. (1982): Linecutting, Geology, Geophysics and Geochemistry on the Sat 1-4 Mineral Claims; British Columbia; *B.C. Ministry of Energy, Mines and Petroleum Resources*, Assessment Report 10688, 10 pages.

Leary, G.M. and Allen, J.F. (1972): 1971 Geochemical and Geological Report, Lennac Lake Cu Property; *B.C. Ministry of Energy, Mines and Petroleum Resources*, Assessment Report 3807.

Lord, C.S. (1948): McConnell Creek Map-area, Cassiar District, British Columbia; *Geological Survey of Canada*, Memoir 251, 72 pages.

MacIntyre, D.G. (1985): Geology and Mineral Deposits of the Tahtsa Lake District, West Central British Columbia; *B.C. Ministry of Energy, Mines and Petroleum Resources*, Bulletin 75.

MacIntyre, D.G. and Desjardins, P. (1988): Geology of the Silver King - Mount Cronin Area; *B.C. Ministry of Energy, Mines and Petroleum Resources*, Open File 1988-20.

MacIntyre, D.G. and Desjardins, P. (1989): Geology of the Telkwa River Area; *B.C. Ministry of Energy, Mines and Petroleum Resources*, Open File 1989-16.

MacIntyre, D.G., Ash, C.H., Britton, J.B., Kilby, W. and Grunsky, E. (1995): Mineral Potential Assessment of the Skeena-Nass Area (93E,L,M,94D,103G,H, I,J,P,104A,B); *in* Geological Fieldwork 1994, Grant, B. and Newell, J.M., Editors, *B.C. Ministry of Energy, Mines and Petroleum Resources*, Paper 1995-1, pages 459-468.

MacIntyre, D.G., Desjardins, P. and Tercier, P (1989): Jurassic Stratigraphic Relationships in the Babine and Telkwa Ranges; *in* Geological Fieldwork 1988, *B.C. Ministry of Energy. Mines and Petroleum Resources*, Paper 1989-1, pages 195-208.

McMillan, W.J. and Struik, B., (1996): NATMAP: Nechako Project, Central British Columbia; *in* Geological Fieldwork 1995, Grant, B. and Newell, J.M., Editors, *B.C. Ministry of Energy, Mines and Petroleum Resources*, Paper 1996-1, this volume.

Monger, J.W.H. (1977): Upper Paleozoic Rocks of the Western Canadian Cordillera and their Bearing on Cordillera Evolution; *Canadian Journal of Earth Sciences*, Volume 14, pages 1832-1859.

Ogryzlo, P.L., Dirom, G.E. and Stothart, P.G. (1995): Morrison - Hearne Hill Copper-Gold Deposits, Babine Region, West-central British Columbia; *in* Porphyry Deposits of the Northwestern Cordillera of North America, Schroeter, T.G., Editor, *Canadian Institute of Mining, Metallurgy and Petroleum,* Special Volume 46.

Richards, T.A. (1990): Geology of the Hazelton Map Area (93M); *Geological Survey of Canada*, Open File 2322.

Richards, T.A. (in press): Geologic Map and Mineral Deposit Tables for the Smithers Area (93L); *Geological Survey of Canada*.

Stumpf, A.J., Huntley, D.H., Broster, B.E. and Levson, V.M. (1996): Babine Porphyry Belt Project: Detailed Drift Exploration Studies in the Fulton Lake (93L/16) and Old Fort Mountain (93M/01) Map Areas; *in* Geological Fieldwork 1995, Grant, B. and Newell, J.M., Editors, *B.C. Ministry of Energy, Mines and Petroleum Resources*, Paper 1996-1, this volume.

Sutherland Brown, A. (1960): Geology of the Rocher Déboulé Range; *B.C. Ministry of Energy, Mines and Petroleum Resources*, Bulletin 43.

Tipper, H.W. and Richards, T.A. (1976a): Jurassic Stratigraphy and History of North-Central British Columbia; *Geological Survey of Canada*, Bulletin 270, 73 pages.

Tipper, H.W. and Richards, T.A. (1976b), Geology of the Smithers Area; *Geological Survey of Canada*, Open File 351.

Wanless, R.K. (1974): Age Determinations and Geological Studies, K-Ar Isotopic Ages; *Geological Survey of Canada*, Report 11, Paper 73-2, pages 22-23.

Wilson, J.W.J., Kesler, S.E., Cloke, P.L. and Kelly, W.C. (1980): Fluid Inclusion Geochemistry of the Granisle and Bell Porphyry Copper Deposits, British Columbia; *Economic Geology*, Volume 75, pages 45-61.

Zaluski, G., Nesbitt, B. and Muehlenbachs, K. (1994): Hydrothermal Alteration and Stable Isotope Systematics of the Babine Porphyry Cu Deposits, British Columbia: Implications for Fluid Evolution of Porphyry Systems; *Economic Geology*, Volume 89, pages 1518-1541.

# NOTES

# BABINE PORPHYRY BELT PROJECT: DETAILED DRIFT EXPLORATION STUDIES IN THE OLD FORT MOUNTAIN (93M/01) AND FULTON LAKE (93L/16) MAP AREAS, BRITISH COLUMBIA

By A.J. Stumpf[1], D.H. Huntley[2], B.E. Broster[1] and V.M. Levson[2]

[1] University of New Brunswick, Fredericton
[2] British Columbia Geological Survey Branch

*(B.C. Ministry of Energy, Mines and Petroleum Resources Contribution to the Nechako National Mapping Program)*

*KEYWORDS:* Drift exploration, geochemistry, porphyry copper mineralization, Babs, Hearne Hill, Lennac Lake, Bell mine, Saddle Hill

## INTRODUCTION

In conjunction with bedrock mapping (MacIntyre *et al.*, 1996, this volume) and regional till geochemistry surveys (Huntley *et al.*, 1996, this volume) in the Babine Lake area, detailed drift exploration studies were undertaken on five porphyry-related copper properties: Babs, Hearne Hill, Lennac Lake, Bell mine (Newman Peninsula), and Saddle Hill (Figure 1). The objective of our study was to investigate the effects of glacial and postglacial processes on geochemical dispersal patterns at properties in three contrasting physiographic settings. It is hoped this will help better define potential zones of mineralization, and provide models for future drift exploration programs.

The properties examined in this report are located in 93L/16 (Fulton Lake) and 93M/01 (Old Fort Mountain) map areas, and lie at the northern limit of the Nechako Plateau (Figure 1; see also Huntley *et al.*, 1996, this volume). All five mineral properties border Babine Lake and its tributary waters, including Fulton and Morrison lakes (Figure 1). Valleys in the Babine Lake area are broad, with gently sloping sides reflecting glacial modification. Regional iceflow directions in the study area are predominantly toward the south-southeast, paralleling these major topographic features (Armstrong and Tipper, 1948; Tipper, 1971a, 1994; Plouffe, 1991; Huntley *et al.*, 1996, this volume),

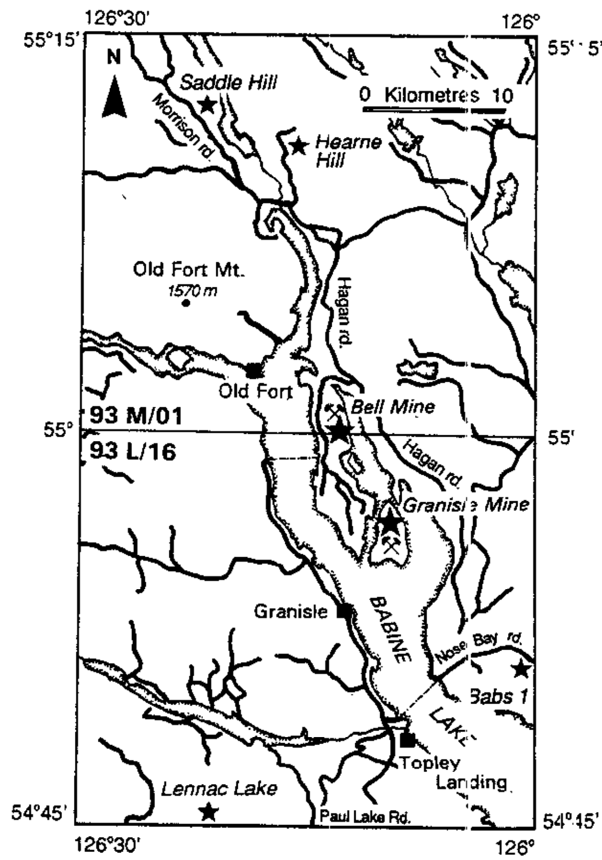


Figure 1. Location of properties studied in this report. For location of map sheets 93L/16 (Fulton Lake) and 93M/01 (Old Fort Mount Mountain), see Figure 1 in Huntley *et al.*, 1996, this volume.

## THE APPROACH

In areas with extensive surficial cover, traditional bedrock mapping alone is insufficient to define mineral potential. The most effective means to address this problem is to combine bedrock mapping with drift, lake and stream sediment geochemical sampling programs (Levson *et al.*, 1994). For regional scale (1: 50 000) drift exploration programs, sampling focuses on collection and geochemical analysis of basal tills. At this scale, till is usually sufficiently abundant to be an effective sample medium for detecting regional mineral dispersal patterns (Giles and Levson, 1994). At larger scales of mapping (*e.g.*, 1:10 000), supraglacial till, glaciofluvial sediments and colluvium must also be sampled in order to define dispersal patterns (O'Brien *et al.*, 1995). In this paper, we outline an approach that uses regional-scale drift exploration techniques modified for mapping and sampling at a property scale of 1:10 000.

## *FIELD METHODS*

Prior to fieldwork, the MINFILE database and assessment reports were examined for criteria critical to designing an effective drift sampling program. Preliminary surficial geology mapping of each property was completed using 1:63 500 and 1:50 000 aerial photographs. Measurements of glaciated landforms, including crag-and-tail features, flutings and drumlins, were recorded to interpret local iceflow histories. These measurements were confirmed in the field by direct measurement of striae and landforms. Existing B-horizon soil data from the selected properties were also replotted to better define sampling strategies.

A sampling grid was established at each mineral property. Sampling along pre-cut grid lines was completed at the Babs and Hearne Hill properties, using a sample spacing of 200 to 400 metres. Elsewhere, sampling was completed along roads accessible by truck or foot traverse, using a sampling interval of 250 to 1000 metres. Typically, samples were collected from roadcuts, mine-pit exposures and hand-dug pits. Vertical profiles were sampled along exploration trenches at both the Hearne Hill and Lennac Lake properties, and along the eastern face of the open pit at Bell mine.

Basal till was the preferred drift sample medium. Colluvium, glacigenic debris flows, supraglacial till, glaciofluvial and glaciolacustrine deposits were also sampled to investigate the applicability of various media in geochemical sampling programs. Where possible, sample locations were chosen to coincide with soil anomalies (detected by previous exploration programs) in order to examine the degree to which pedogenic processes have influenced the geochemical composition of the near-surface medium.

In total, 173 sediment samples, weighing from 2 to 5 kilograms, were collected from the five properties. The samples were dried, split and passed through a -230 mesh (<63 µm) sieve. This fraction was analyzed by instrumental neutron activation analysis (INA) and inductively coupled plasma analysis - atomic emission spectroscopy (ICP-ES) for 47 elements.

At each property, attempts were made to trace mineralized boulders to their source. Till-clast lithologies were also studied each property. Balzer and Broster (1994) and Stumpf (1995) suggest clasts delineate much larger dispersal trains than matrix components, allowing target areas to be defined more easily. At selected sites, 20 to 25 pebble-sized clasts were collected and information was recorded pertaining to their lithology, size, degree of roundness, and presence of striated or faceted surfaces. Mineralized clasts showing evidence of mineralization were described and sampled for assay.

## BABS

The Babs property comprises 21 mineral claims on the east side of Babine Lake, 6 kilometres southeast of the Granisle mine. The property has only recently been assigned a MINFILE number (93L 325). The property is currently under option to Northern Dynasty Minerals Ltd. Detailed studies were carried out on the Babs 1 claim, centred at 54°51'N, 126°W. The claim area lies on a gently sloping spur between two streams that drain into Babine Lake. Elevation ranges from 855 to 975 metres. Access is by the Nose Bay road to the junction with Pat road, 7 kilometres east of Topley Landing and the Northwood barge crossing.

Much of the east flank of the Babine valley in the vicinity of the property is underlain by granite, quartz monzonites and rhyolitic equivalents of the Early Jurassic Topley Plutonic Suite (Carter, 1981; MacIntyre *et al.*, 1996, this volume). Outcrop on the property is rare and exposed only in borrow pits, road cuts and stream cut banks. Outcrops include gossanous, sericite-clay-altered quartz-phyric crystal and lapilli tuffs, and a northeast-trending biotite feldspar porphyry dike (Figure 2). Tuffaceous rocks contain disseminated pyrite and chalcopyrite, and have iron and malachite staining on fracture surfaces. These rocks have returned anomalous values at surface of 726 ppm copper and 16 ppm silver, and up to 0.19% copper over 77.3 metres in core from limited drilling (Kemp and Roberston, 1994). Pyrite is sparsely, but not uniformly disseminated in the porphyry dike.

## *DRIFT EXPLORATION RESULTS*

Much of the property is mantled by an undulating to gently rolling ground moraine. The surface is locally fluted, indicating regional iceflow toward 150° (Figure 2). Washed till is the dominant morainal sediment and is a pervasively oxidized, massive, poorly consolidated, matrix-supported diamicton. Basal till is subordinate, and is a dense, fissile matrix-supported diamicton with a clay-silt matrix. Extensive areas of moraine are washed, winnowed and blanketed by massive gravel and sand lag deposits with an inferred glaciofluvial origin. Additional evidence for meltwater flow is suggested by numerous small eskers and meltwater channels that apparently drained southward (Figure 2). The abundant evidence for meltwater flow on this property should be considered when interpreting geochemical dispersal patterns in soils and underlying glacial materials.

Twenty five samples of till and glaciofluvial sediments were collected over a recently cut survey grid, and in the vicinity of a 1.2 kilometre long train of well-mineralized angular biotite feldspar porphyry cobbles and boulders. Additional basal till samples were collected north and northwest of the claim area as part of the regional till sampling program to determine geochemical background (Huntley *et al.*, 1996, this volume).

Boulders in the main body of the train contain abundant chalcopyrite as disseminations and fracture fillings, and grade up to 0.9% Cu and 1.3 g/t Au (Kemp and Robertson, 1994). Six cobble to boulder-sized erratics exposed at the surface of washed till were sampled (Figure 2). A biotite feldspar porphyry clast recovered in the vicinity of the biotite feldspar porphyry

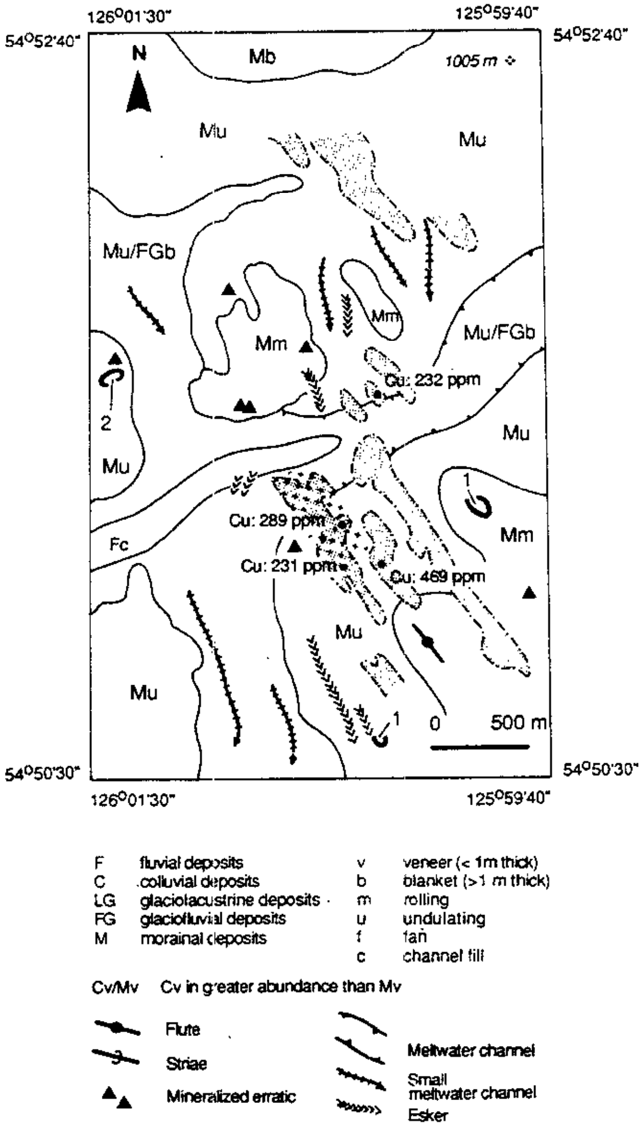


Figure 2. Simplified surficial geology of the Babs 1 property. 1. Altered quartz-phyric crystal and lapilli tuffs; 2. Biotite feldspar porphyry dike. Small crosses - approximate location of mineralized boulder train. Shaded areas - copper values in soils above 40 ppm; maximum concentrations given as point values (data modified from Kemp and Robertson, 1994).

dike returned very low copper values (5 ppm Cu). A boulder sampled 100 metres east of central part of the boulder train assayed 126 ppm lead and 2039 ppm zinc, but returned low copper values (3 ppm). In contrast, a biotite feldspar porphyry boulder found beyond the southeastern limit of the train has assayed 10 491 ppm copper and 411 ppb gold (MacIntyre *et al.*, 1996, this volume). Sparsely mineralized cobble-sized float samples, found up to 700 metres northwest of the boulder train, were not submitted for assay. The source of the mineralized erratics is unknown. Most cobbles and boulders resemble biotite feldspar porphyry exposed at the Granisle and Bell mines and lie approximately down-ice from these areas (Figure 1). However, a more local source is suggested by the angularity, abundance and size of erratics within reworked till. Erratics also closely resemble biotite feldspar porphyry dike rocks exposed close to west-central part of the map area (Figure 2). The trend of this dike crosses the up-ice projection of the main body of the boulder train (Figure 2). In addition, the boulder train is near an induced polarization chargeability anomaly attributed to significant intervals of low-grade porphyry-style copper mineralization over an area of 2 square kilometre and located approximately on the same structural trend as the Bell and Granisle deposits (B. Youngman, personal communication, 1995)

Copper values up to 467 ppm are reported from B-horizon soil samples (Kemp and Robertson, 1994). As originally plotted, copper values above a 40 ppm background, define a circular anomaly flanking the boulder train. This pattern has been reinterpreted as a linear plume reflecting southeast dispersal of copper by ice and secondary southwest dispersal by meltwater Figure 2). There is little evidence to support significant dispersal by postglacial colluviation.

## HEARNE HILL (MINFILE 93M 6)

The Hearne Hill prospect lies 2 kilometres east of Morrison Lake and 32 kilometres north of Granisle. Studies focused on a 3 square kilometre area over the crest and steep western flank of Hearne Hill, centred around the "discovery showing" at 55°11' N and 126°17' W (Figure 3). The property, currently under exploration by Booker Gold Explorations Ltd., lies 1.2 kilometres east of the Morrison Lake deposit. The prospect is reached by following a steep dirt track for 6 kilometres off the Hagan road at about 46 kilometres from Topley Landing and the Northwood barge crossing (Figure 1).

Hearne Hill is underlain by Lower to Middle Jurassic lapilli crystal tuffs, andesite flows and volcaniclastic sedimentary rocks (Hazelton Group). These rocks have been intruded by a small, Early Jurassic quartz diorite stock (Topley Plutonic Suite), and a northeast-trending biotite feldspar porphyry plug and dikes of the Eocene Babine Plutonic Suite (Figure 3; Ogryzlo, 1990). The western flank of Hearne Hill is apparently the escarpment of the southeast-trending Morrison fault (Ogryzlo, 1990). West of the fault, younger Jurassic to Cretaceous Bowser Lake Group sediments and biotite feldspar porphyry of the Morrison deposit occupy the downthrown block.

Earlier studies showed that mineralization is widespread, but not uniformly distributed. Chalcopyrite, bornite and molybdenite occur as fracture fillings, and are disseminated throughout intrusive and country rocks. Mineralization is related to a weakly developed porphyry copper system (Ogryzlo, 1990) carrying between 0.1 and 0.2% Cu. This system is cut by an east-dipping breccia pipe, 50 to 60 metres in diameter. Breccia clasts are cemented with interstitial chalcopyrite, subordinate pyrite, malachite and azurite. Copper grades from the pipe range from 0.01 to 2.75% Cu. The 1995 exploration program has extended drilling northward from the breccia body into a potentially large zone of copper porphyry mineralization in breccia and vein stockwork. One drill hole has returned an assay of 0.75% Cu and 0.32 g/t over the total length of the hole (301 m). Host volcanic rocks are strongly silicified. Alteration of intrusive rocks includes replacement of plagioclase phenocrysts by sericite, and biotite by chlorite. Pyrite mineralization is associated with sericite alteration. The most intense alteration is found in the breccia pipe and adjacent wallrock.

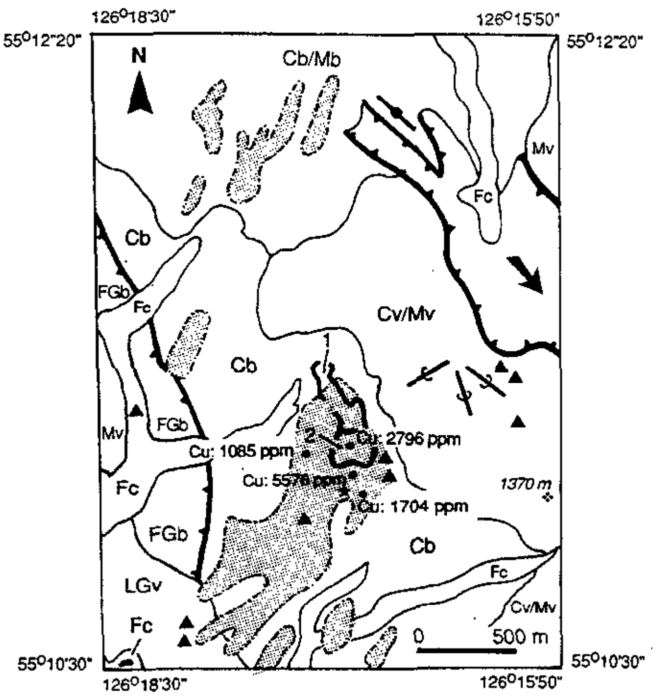


Figure 3. Simplified surficial geology of the Hearne Hill property. See Figure 2 for legend. 1. Early Jurassic quartz diorite (Topley Plutonic Suite); 2. Eocene biotite feldspar porphyry (Babine Pluton Suite). Shaded areas - copper values in soils above 100 ppm; maximum concentrations given as point values (data modified from Dirom, 1967 and Ogryzlo, 1990). Small pentangle - "discovery showing".

### *DRIFT EXPLORATION RESULTS*

Hearne Hill is a montane upland flanking the glaciated Morrison valley. Prominent southeast-trending troughs and ridges occur along the hill crest. Fluted bedrock and striae exposed on trough walls and ridges, indicate iceflow between 120° and 160°. Striae near the summit locally crosscut this direction and indicate secondary flow at 240° into the Morrison valley (Figure 3).

Glacial deposits are rare or absent on the steep, west-facing hillside. Here, bedrock is mantled by talus and hill-slope colluvium (Figure 3). Deposits range in thickness from 0.5 to greater than 2 metres, and are commonly oxidized to bedrock. Talus consists of coarse, angular rubble derived from subaerially weathered outcrops. Hill-slope colluvium comprises poorly consolidated, massive or stratified, clast-supported diamictons. These latter sediments are interpreted as glacigenic debris flows, glaciofluvial deposits and weathered bedrock. On the hill crest, glaciofluvial gravels and sands are confined to trough floors. Adjacent ridges are mantled by morainal deposits consisting of washed basal till and supraglacial tills. These tills are poorly consolidated, massive diamictons with oxidized sandy matrices.

Forty-three colluvium, till and glaciofluvial samples were collected on, or around a recently cut survey grid. Vertical profiles were sampled at three trenches to determine vertical variations in geochemical signatures within the surficial cover. Talus and mineralized boulders were sampled for assay, and will be compared to erratics found in a linear boulder train 2.5 kilometres down-ice from the property (Huntley *et al.*, 1996, this volume). One boulder sampled from this train has assayed 591 ppm copper. It is uncertain whether these erratics are derived from the property or from an undiscovered zone of mineralized outcrop on the southwest flank of Hearne Hill.

Three copper anomalies were identified within a 200 metre radius of the discovery showing during an earlier B-horizon soil sampling program (Dirom, 1967; Ogryzlo, 1990). Copper values above 100 ppm have been replotted in Figure 3 (background threshold for copper in soils is 65 ppm). The resultant dispersal pattern is thought to primarily reflect down-slope transport of weathered bedrock and surficial deposits. This suggests that mineralized float and soil geochemical anomalies are probably sourced northeast of past exploration activity. This conclusion is supported by preliminary reports of higher grades from recent drilling in the northeast part of the property. Additional, down-slope replenishment at lower elevations is anticipated from a mineralized dike swarm extending southwest from the porphyry plug (J.M. Newell, personal communication, 1995).

## LENNAC LAKE (MINFILE 93L 190,191)

The Lennac Lake property is located approximately 20 kilometres south-southwest of Granisle (Figure 1). The area is characterized by a subdued, undulating to hummocky topography, with elevations ranging from 880 to 1065 metres. Many of the ridges and knobs are bedrock cored, but locally these features are draped by a veneer or blanket of glacial sediment. Low-lying areas within the property are poorly drained by numerous streams and swamps. The area includes the Thezar #75 (West) (54°44'N, 126°20'W), Thezar #81 (East) (54°45'N, 126°20W), and Jacob (54°43'N, 126°17'W) mineral claims. Thezar #75 and #81 are currently owned by Cominco Ltd. The Jacob property was drilled by Cominco in 1993. The Lennac Lake property straddles the boundary between 93L/16 and 93L/09 map sheets (Figure 1). Access is by a four-wheel-drive road which joins the Paul Lake Recreation Road, approximately 10 kilometres northwest of the Highway 16 intersection.

Country rocks are Lower Jurassic volcanic and volcaniclastic rocks of the Telkwa Formation (MacIntyre *et al.*, 1996, this volume). Intrusions are hornblende-biotite-feldspar and quartz-hornblende-biotite-feldspar porphyries with a granodiorite composition, related to the late Cretaceous Bulkley Plutonic Suite (Plicka, 1981). They parallel northeast trending fault systems, mapped to the east of the area and occur within the Amax west and east zones of the former Thezar claims.

Mineralization is related to a hydrothermal system active during emplacement of the Bulkley intrusive rocks. Well-developed propylytic alteration zones occur in Telkwa Formation volcanic and volcaniclastic rocks to the north of the Lennac Lake area. Sulphide mineralization (pyrite, chalcopyrite, molybdenite and minor sphalerite) borders the main porphyry bodies (Plicka, 1981). Quartz-sericite-pyrite alteration occurs in intrusive rocks along the eastern margin of the Amax E zone. Azurite, malachite and bornite mineralization is exposed in a trench along the access road at the eastern limit of the property. This is the Suratt showing. Felsic volcanics exposed in trenches southeast of the Amax E zone carry gold up to 6000 ppb (Plicka, 1981).

### *DRIFT EXPLORATION RESULTS*

In the property area, glacial flutings indicate the last major iceflow was toward the east-southeast (090° to 120°). A southeast-trending train of maroon, andesitic lapilli tuff and agglomerate, identified during a soil sampling program (Plicka, 1981) is additional confirmation of iceflow direction.

Till, glaciofluvial and glaciolacustrine sediments of variable thickness overlie undulating bedrock, including deep-weathered quartz-biotite-feldspar porphyry. Sediment cover ranging from a thin veneer (<10 cm) to several metres in thickness has hampered past exploration efforts. At several sample sites, supraglacial or washed basal till overlies compact clay-rich lodgement till. The upper till unit, although visually similar to the underlying basal till, is less compact and much sandier in texture.

Twenty-six till and meltwater sediment samples were collected from hand-dug pits and exploration trenches. Three of these samples were collected up-ice and one sample down-ice from the property to better define geochemical dispersal in till. Vertical profile samples were taken along an exposure 2 metre high in an exploration trench at the Surrat copper showing. Three samples were collected from a compact clay-rich till at the base of the section, over a distance of 4 metres. Three samples of the upper, sandy supraglacial till were collected. Data from these profiles will be used to study the geochemical variability in till, both vertically and laterally (*cf.* Broster, 1986). Examinations of clast lithologies were completed at several sites across the property. Clast samples were collected from both hand-dug pits and exploration trenches overlying bedrock. These data will be used to define local clast dispersal patterns.

## BELL MINE AND NEWMAN PENINSULA (MINFILE 93M 1)

The Bell mine is situated on Newman Peninsula, within the Babine Lake basin. It is located 8 kilometres north of Granisle, at 54°58'N and 126° 12'W, and straddles the 93M/01 and 93L/16 map boundary (Figure 1). Much of the area is low lying, with elevations ranging from 715 to 915 metres. The property is presently owned by Noranda Mines Limited. Access is by the Hagan road via the Northwood barge or by private ferry operated from the property to a gravel road 10 kilometres north of Granisle (Figure 1).

Hazelton volcanics (possibly older Stuhini Group; see MacIntyre *et al.*, 1996, this volume) and Skeena sedimentary rocks are intruded by rhyodacite, biotite feldspar porphyry, and quartz feldspar porphyry. These intrusive rocks are part of the Eocene Babine Plutonic Suite.

The orebody at the Bell mine is a high-level porphyry copper-gold deposit containing symmetrical zones of biotite-magnetite and propylytic alteration associated with multiple phase Babine intrusions (Carter, 1981). Copper and gold occur in the intrusive rocks, where the Newman fault intersects an east to northeast-trending fault. These intrusions are overprinted by pervasive quartz-sericite alteration. Pyrite and chalcopyrite occur as disseminations and fracture fillings in the main stockwork and the propylytic and biotite alteration zones. Bornite and minor molybdenite are also present in the biotite-altered biotite-feldspar porphyry. Chalcopyrite, pyrite, and minor bornite occur in quartz-sericite altered rocks.

### *DRIFT EXPLORATION RESULTS*

The Newman Peninsula has been intensely glaciated. Well formed fluting and striae are exposed on bedrock surfaces. Predominant iceflow in the area was from 120° to 180° (Armstrong and Tipper, 1948; Tipper, 1971b, 1994; Plouffe, 1991). Locally, iceflow directions deviate toward 220°, possibly due to topographic control of iceflow during early glaciation. Similar local iceflow patterns have been observed to the north and east of Babine Lake by Huntley *et al.* (1996, this volume).

Variable thicknesses of glacial, postglacial and anthropogenic sediments are exposed at the Bell mine property. Along the Babine valley and in topographic lows, sediment thicknesses reach 120 metres (Harrington *et al.*, 1974). Elsewhere, sediment occurs as a thin veneer over bedrock. Deformed laminated clays and silts are exposed along the east side of the Bell open pit. These sediments may be equivalent to mid-Wisconsinan lacustrine sediments dated at 34000±690 BP (Harrington *et al.*, 1974). Approximately 5.5 metres of grey to dark brown clayey, very dense and fissile basal till overlies this unit. The contact between these units is not exposed, and it is not certain whether silts and clays stratigraphically underlie the till. Elsewhere, till overlies deeply weathered bedrock. Locally, dense basal till is capped by a layer of supraglacial or washed till, having characteristics similar to the upper till unit, but less compact and sandier. Locally, colluvium and glaciofluvial sediments overlie basal till. Along the Babine valley, below the 760-metre level, glaciolacustrine deposits drape older sediments and bedrock.

A significant portion of the overburden cover has been disturbed by mining activity. Caution was therefore used when locating suitable sampling sites. Sixty-four till and colluvial samples were collected from hand-dug pits, road cuts and mine pit exposures. Two samples of preglacial silts and clays were collected to compare the geochemistry of the glaciolacustrine sediments with the overlying basal till, and investigate the possible presence of microfossils. Vertical profiles were sampled around Bell open pit, where till exposures are in excess of 3 metres thick. Till-clast lithologies were examined to define clast dispersal trains of distinct bedrock lithologies.

## SADDLE HILL (MINFILE 93M 8)

The Saddle Hill property, 36 kilometres north of Granisle, is a rolling montane upland flanked by Morrison Lake and a tributary valley. The property comprises the Double R1 to R8 claims, and includes the former Wolf claims (Fraser, 1980). Detailed studies focused on the Double R1 to R4 claims, centred at 55°12'N, 126°23'W (Figure 4). This area covers the crest of a southeast-trending hill, and the western shore of Morrison Lake. The claims are accessed on foot, by following a disused road that intersects the Morrison road 56 kilometres north of Topley Landing and the Northwood barge landing (Figure 1).

The area is underlain by Triassic siltstones, greywackes and mudstones and Jurassic andesites, rhyolites and subordinate volcaniclastic sediments. Country rocks are intruded and hornfelsed by an Eocene composite biotite granodiorite stock that is part of the Babine Plutonic Suite (Fox, 1993). The stock is approximately 700 metres in diameter and forms an east-west oriented ellipse with a bulge to the north (Figure 4; Fraser, 1980). Granodiorite and country rocks are intruded by biotite feldspar porphyry dikes.

Mineralization is associated with the dikes. In country rocks and granodiorite, pyrite and chalcopyrite occur as fine-grained disseminations or fracture coatings. Up to 2% disseminated pyrite and 3% fracture-coating chalcopyrite is reported in granodiorite (Fox, 1993). Quartz veins and thin, sulphide-rich veins in dikes and granodiorite carry disseminated chalcopyrite, molybdenite and pyrite. Weak to intense argillic alteration occurs adjacent to fractures and quartz veins in granodiorite and dike rocks. Alteration zones are up to 10 metres wide. Biotite and hornblende phenocrysts are destroyed and sericite is present along fracture surfaces. Hornblende is replaced by secondary biotite. Secondary biotite is also associated with copper mineralization (Fraser, 1980).

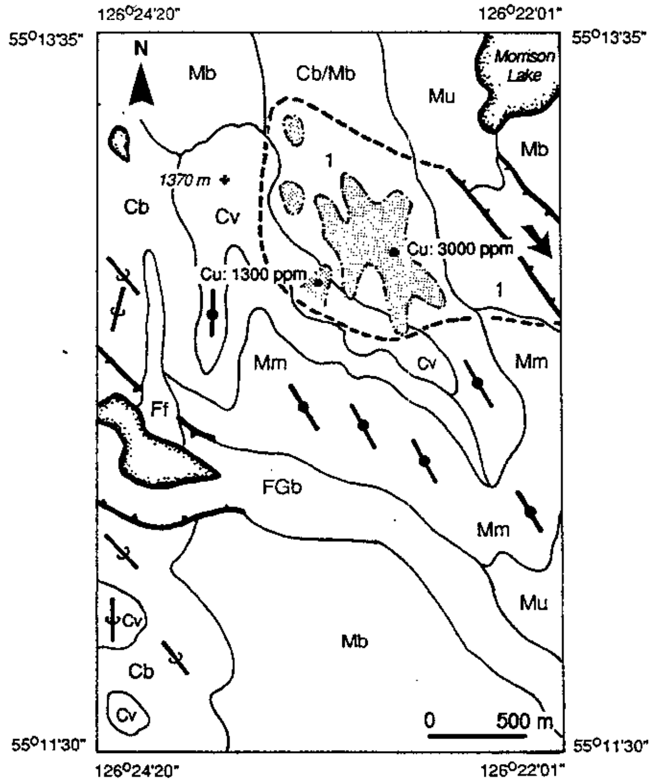


Figure 4. Simplified surficial geology of the Saddle Hill property. See Figure 2 for legend. 1. Eocene biotite granodiorite (Babine Plutonic Suite); approximate position indicated by dashed line. Shaded areas - copper values in soils above 100 ppm; maximum concentrations given as point values (data modified from Fox, 1993).

### *DRIFT EXPLORATION RESULTS*

Glacially streamlined ridges and striae are exposed on the hill crest, spurs and valley walls (Figure 4). These features indicate iceflow between 140° and 167°. Crosscutting striae on west-facing valley walls indicate later local flow between 180° and 195°. This deviation probably reflects local topographic control on iceflow.

Massive, matrix-supported basal and supraglacial tills are confined to lower valley sides. Tills form an undulating to rolling moraine mantling bedrock. Matrices range from dense, fissile clayey silt to moderately dense, weakly fissile sandy silt. Oxidation is moderate to strong in sandier tills. Valley floors are blanketed by up to 5 metres of cobble-rich glaciofluvial sediments. On steeper slopes and over the hill crest, bedrock is locally covered by poorly consolidated, sandy supraglacial till, and massive or stratified, clast-supported hill-slope colluvium. Deposit thicknesses range from 0.2 to 1 metre. These latter deposits are commonly oxidized to bedrock.

Eleven till and three colluvium samples were taken at a spacing of 1 kilometre. Additional basal till samples were collected around the property as part of the regional till sample program (Huntley *et al.*, 1996, this volume). High values for copper (from 1000 to 3000 ppm), molybdenum (up to 80 ppm) and zinc (up to 2500 ppm) were reported in thin B-horizon soil samples collected over the stock (Fraser, 1980). Copper values above 100 ppm are replotted in Figure 4 (above a 60 ppm background threshold; Fraser, 1980). This dispersal pattern is thought to reflect primary dispersal of pyrite and chalcopyrite in till, secondary dispersal by postglacial colluviation and dispersion during pedogenesis.

## SUMMARY

In montane uplands, characterized by Hearne Hill and Saddle Hill, steep bedrock slopes are predominantly mantled by veneers and blankets of postglacial hill-slope colluvium and talus. These deposits are first or second derivative products of erosion and deposition with short and simple transport histories. Dispersal patterns observed in soils and boulders in colluvium indicate a dominant down-slope dispersal of mineralized material from potential sources. On gentler slopes and hill crests, bedrock is covered by colluvium and morainal sediments, including basal till and supraglacial till. Dispersal patterns in these deposits are anticipated to reflect a dominant trend in the direction of iceflow.

In plateau areas, characterized by the Babs and Lennac Lake properties, thick, undulating or rolling moraines blanket bedrock. Moraines contain basal, washed and supraglacial tills, and subordinate glaciofluvial deposits. Because these moraines include proximally and distally-sourced mineralized float and matrix, careful interpretation of data from soil surveys, drift geochemistry, landforms and boulder trains is required to evaluate dispersal patterns. Generally, patterns reflect primary dispersal consistent with down-ice transport. Secondary dispersal down-slope or toward local topographic lows is effected by washing of finer material by glaciofluvial action and postglacial colluviation.

In valley settings, characterized by Newman Peninsula, glaciolacustrine silts are ubiquitous below 760 metres and drape other deposits. These sediments have potentially complex transport and sedimentary histories and probably mask geochemical signatures in underlying sediments. It is necessary to sample beneath glacial lake silts to gain a better assessment of geochemical values in drift.

We recommend that future drift exploration in the Babine porphyry belt should focus primarily on sampling of basal till and colluvium. These first derivative products of erosion and deposition have relatively simple transport histories and can be readily used to trace and define mineral dispersal patterns. It is stressed, however, that where possible, drift sampling should be supported by other surficial exploration techniques, including B-horizon soil sampling, landform analysis and boulder tracing.

## ACKNOWLEDGMENTS

Logistical and financial assistance was provided through the Geological Survey of Canada NATMAP Babine Porphyry Belt project and British Columbia Geological Survey Branch mapping project budgets to Levson. Additional support was provided through a British Columbia Geological Survey Branch research grant to Broster and an Natural Sciences and Engineering Research Council scholarship to Stumpf. The authors would like to thank Erin O'Brien, Jennifer Hobday and Gordon Weary for assistance in the field. We also appreciate the insights of our colleagues, prospectors and the mining community working in the Babine area. Earlier versions of this manuscript were edited by Bill McMillan, John Newell and Bruce Youngman.

## REFERENCES

Armstrong, J.E. and Tipper, H.W. (1948): Glaciation in North-central British Columbia; *American Journal of Science*, Volume 246, pages 283-310.

Balzer, S.A. and Broster, B.E. (1994): Comparison of Clast and Matrix Dispersal in Till: Canterbury Area, New Brunswick; *Atlantic Geology*, Volume 30, pages 9-17.

Broster, B.E. (1986): Till Variability and Compositional Stratification Examples from the Port Huron Lobe; *Canadian Journal of Earth Sciences*, Volume 23, pages 1823-1841.

Carter, N.C., (1981): Porphyry Copper and Molybdenum Deposits West-Central British Columbia; *B. C. Ministry of Energy, Mines and Petroleum Resources*, Bulletin 64, 150 pages.

Dirom, G.A. (1967): Geochemical and Magnetometer Report "K" Group of Mineral Claims, Morrison Lake; *B.C. Ministry of Energy, Mines and Petroleum Resources*, Assessment Report 1102, 7 pages.

Fox, P.E. (1993): Geophysical and Diamond Drilling Report, Saddle Hill Prospect, Babine Lake Area, British Columbia; *B.C. Ministry of Energy, Mines and Petroleum Resources*, Assessment Report 23536, 13 pages.

Fraser, J.R. (1980): Geochemical Survey on the Wolf 1 Claim (Saddle Hill Property) 93M/01W; *B.C. Ministry of Energy, Mines and Petroleum Resources*, Assessment Report 8176, 7 pages.

Giles, T.R. and Levson, V.M. (1994): Surficial Geology and Drift Exploration Studies in the Tsacha Lake (93F/02) and Chedazuk Creek (93F/07) Map Areas, *in* Geological Fieldwork 1993, Grant B. and Newell, J.M., Editors, *B.C. Ministry of Energy, Mines and Petroleum Resources*, Paper 1994-1, pages 27-37.

Harrington, C.R., Tipper, H.W. and Mott, J.R. (1974): Mammoth from Babine Lake, British Columbia. *Canadian Journal of Earth Sciences*, Volume 11, pages 285-303.

Huntley, D.H., Stumpf, A.J., Levson, V.M., and Broster, B.E. (1996): Quaternary Geology and Regional Till Geochemical Sampling, Central Babine Lake Area (93L/16 and 93M/01), British Columbia; *in* Geological Fieldwork 1995, Grant B. and Newell, J.M., Editors, *B.C. Ministry of Energy, Mines and Petroleum Resources*, Paper 1996-1, this volume.

Kemp, R. and Robertson, K.A. (1994): Geological, Geochemical and Geophysical Report on the Babs Claim Group Located in the Omineca Mining Division (NTS 93L/16E and 93K/13W); *B.C. Ministry of Energy, Mines and Petroleum Resources*, Assessment Report 23536, 13 pages.

Levson, V.M., Giles, T.R., Cook, S.J., and Jackaman, W. (1994): Till Geochemistry of the Fawnie Creek Area (93F/03); *B.C. Ministry of Energy, Mines and Petroleum Resources*, Open File 1994-18, 34 pages with appendices.

MacIntyre, D.G., Webster, I.C.L. and Bellefontaine, K.A. (1996): Babine Porphyry Belt Project: Bedrock Geology of the Fulton Lake Map Area (NTS 93L/16); *in* Geological Fieldwork 1995, Grant B. and Newell, J.M., Editors, *B.C. Ministry of Energy, Mines and Petroleum Resources*, Paper 1996-1, this volume.

O'Brien, E.K., Broster, B.E., Giles, T.R., and Levson, V.M. (1995): Till Geochemical Sampling: CH, Blackwater-Davidson and Uduk Lake Properties, British Columbia: Report of Activities; *in* Geological Fieldwork 1994, Grant B. and Newell, J.M., Editors, *B.C. Ministry of Energy, Mines and Petroleum Resources*, Paper 1995-1, pages 207-211.

Ogryzlo, P. (1990): Geochemical and Diamond Drilling Assessment Report of the Hearne Hill Breccia Pipe; *B.C. Ministry of Mines, Energy and Petroleum Resources*, Assessment Report 20084, 19 pages.

Plicka, P. (1981): Report on the Jery Claims of Pola Resources Limited, Omineca Mining Division, Babine Lake Area, (NTS 93 L/16; Latitude 54 45 N, Longitude 126 22 W); *B.C. Ministry of Energy, Mines and Petroleum Resources*, Assessment Report 9934, 10 pages.

Plouffe, A. (1991): Preliminary Study of the Quaternary Geology of the Northern Interior of British Columbia; *in* Current Research, Part A; *Geological Survey of Canada*, Paper 91-1A, pages 7-13.

Stumpf, A.J. (1995): Quaternary Geology and Dispersal Patterns of the McAdam (NTS 21G/11) Map Area, York County, New Brunswick; *New Brunswick Department of Natural Resources and Energy, Mineral Resources* Branch, Open File Report, 217 pages.

Tipper, H.W (1971a): Smithers Map-area, British Columbia; *in* Report of Activities, *Geological Survey of Canada*, Paper 71-1, Part A, pages 34-37.

Tipper, H.W. (1971b): Glacial Geomorphology and Pleistocene History of Central British Columbia; *Geological Survey of Canada*, Bulletin 196, 89 pages.

Tipper, H.W. (1994): Preliminary Interpretation of Glacial Features and Quaternary Information from the Smithers Map Area (93L), British Columbia; *Geological Survey of Canada*, Open File 2837, scale 1:250 000)

# BABINE PORPHYRY BELT PROJECT: QUATERNARY GEOLOGY AND REGIONAL TILL GEOCHEMISTRY SAMPLING IN THE OLD FORT MOUNTAIN (93M/01) AND FULTON LAKE (93L/16) MAP AREAS, BRITISH COLUMBIA

By D.H. Huntley[1], A. Stumpf[2], V.M. Levson[1] and B.E. Broster[2]

[1] British Columbia Geological Survey Branch
[2] University of New Brunswick, Fredericton

*(B.C. Ministry of Energy, Mines and Petroleum Resources Contribution to the Nechako National Mapping Program)*

*KEYWORDS:* Babine Lake, regional drift geochemistry, surficial sediments, geomorphology, Quaternary history

## INTRODUCTION

The Babine porphyry belt in the northern Nechako Plateau has long been known as an area of productive copper, molybdenum and gold mineralization (Carter, 1981). A regional mapping program was initiated as part of the Nechako Plateau National Mapping Program to stimulate further exploration and define new mineralization targets in the Babine Lake area (MacIntyre *et al.*, 1996, this volume; McMillan and Struik, 1996, this volume). The surficial geology component of this integrated project focused on the Old Fort Mountain (93M/01) and Fulton Lake (93L/16) map areas (Figure 1). In this paper we report:

- An outline of field methods used in surficial mapping and till geochemistry sampling.
- A descriptive inventory of Quaternary deposits and selected glacial landforms.
- A preliminary discussion of the local glacial history.

Details of supplementary research at several mineral prospects in the map area are discussed elsewhere (Stumpf *et al.*, 1996, this volume).

### *PHYSIOGRAPHIC SETTING*

The glaciated Babine and Hautête drainage basins lie close to the northern edge of the Nechako Plateau (Figure 1; Holland, 1980). Three physiographic elements are common to these basins (Figure 2). Broad valleys are occupied by numerous lakes. Fulton and Morrison lakes drain east and southeast into Babine Lake, which in turn drains northward into the Skeena River. Hautête Creek lies within the Fraser River catchment and drains southeast, through Hautête and Natowite lakes into Takla Lake. Valleys are flanked by undulating to rolling plateaus and uplands (Figure 2). The central and northeastern portions of the 93M/01 map area are more mountainous than other parts of the study area, and contain several peaks over 1200 metres (4000 feet), including Old Fort Mountain (1570 m; 5146 ft), Hearne Hill (1370 m; 4500 ft) and Wedge Mountain (1250 m;

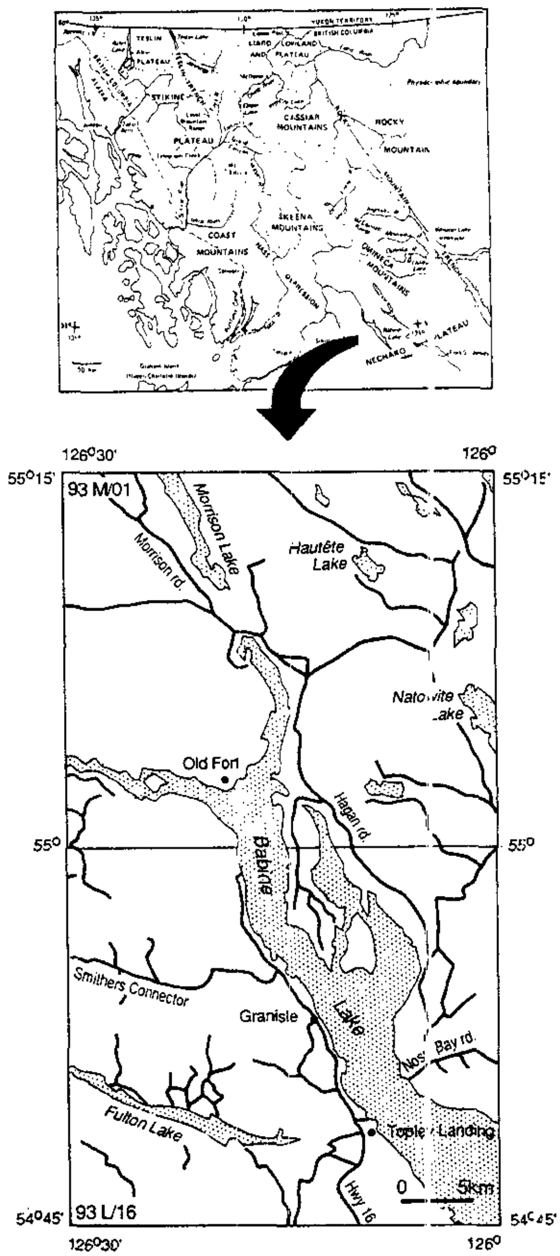


Figure 1. Location of the Old Fort (93M/01) and Fulton Lake (93L/16) map areas. Upper map modified from Ryder and Maynard (1991).

4100 ft). In contrast, the western part of 93M/01 and much of the 93L/16 map area are dominated by plateau terrain, with glacially eroded hills standing 100 to 150 metres above surrounding lowlands.

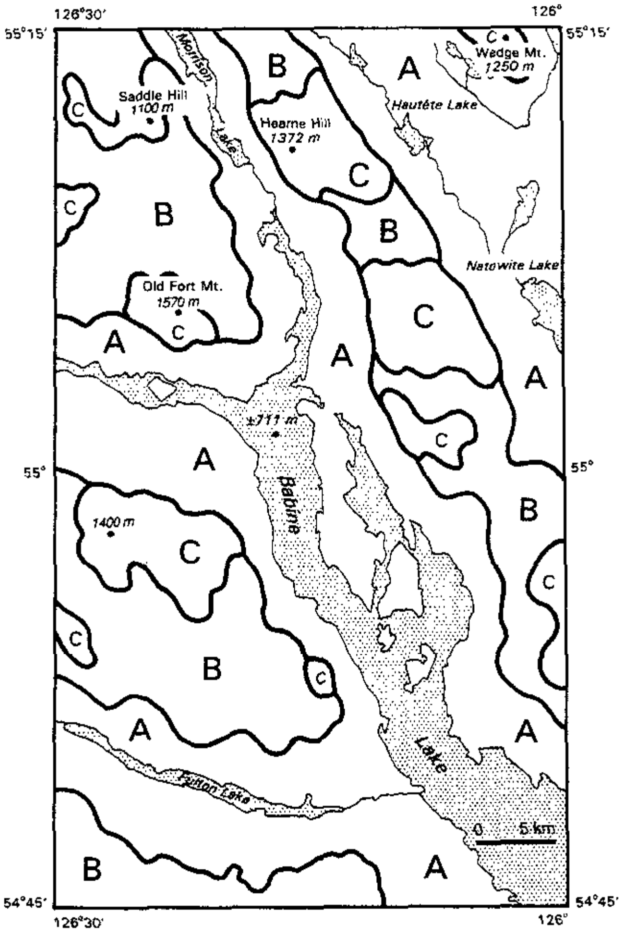


Figure 2. Phyiosography of study area. A - Ponded and free-draining valleys; B - Undulating and rolling plateaus; C - Uplands.

# FIELD METHODS

## *SURFICIAL GEOLOGY*

Preliminary 1:50 000-scale surficial geology maps were prepared before fieldwork using existing soils and terrain classification maps (*e.g.*, Wittneben, 1981) and airphotos (suites BC 86048 and BC 87062). Terrain unit polygons were defined according to surficial material type and surface expression. These criteria were coded and landforms symbolized using mapping standards similar to those detailed in Howes and Kenk (1988). Preliminary mapping and airphoto interpretations were verified during field traverses.

The town of Granisle is reached by driving 48 kilometres north from Highway 16 at Topley. Much of the area was accessed by an extensive network of gravel roads (Figure 1). Access to eastern and northern parts was provided by a private barge crossing operated by Northwood Forest Products. Off-road access was by helicopter, boats, mountain bikes, or on foot. A variety of natural and anthropogenic sites exposed overburden cover, including stream cutbanks, forest blowdowns, borrow pits, trenches and roadcuts. Where exposure was poor or lacking, observation pits were dug by hand.

Surficial sediments and glacial landforms were described to aid the interpretation of till geochemistry data. Regional and local paleo-iceflow patterns were defined by plotting the distribution of directional glacial indicators, including troughs, roches moutonnées, crag-and-tails, flutes and striae, on preliminary surficial geology maps. Glacier margins were identified from the spatial distribution of morainal, glaciofluvial and glaciolacustrine deposits. Between 20 and 50 pebble to cobble-sized clasts and surface boulders in surficial deposits identified as basal tills were examined for mineralization and rock type at till sample sites (*cf.* Giles *et al.*, 1995). Thirty mineralized boulders were sampled for assay. These data will be useful for tracing mineralized float to source and determining bedrock lithology in areas of extensive drift cover.

## *REGIONAL DRIFT GEOCHEMISTRY*

Regional drift geochemistry sampling focused on basal tills (lodgement and basal melt-out till). These sediments are first derivative products of erosion and deposition with relatively simple transport histories (Shilts, 1993; Levson *et al.*, 1994). As such, mineralized debris dispersed within basal tills can be more readily traced to origin than in most other deposits. Undisturbed basal till matrix samples (1 to 3 kg per sample) were collected at 293 stations on the 93M/01 map sheet and 304 stations on map sheet 93L/16 (Figure 3). Sample sites were located with a Trimble "Scoutmaster" global positioning system (accuracy ± 50 m) or by compass triangulation, then plotted on a base map using the UTM coordinate system (North American datum 1927). Elevations were determined using a Thommen altimeter, periodically benchmarked to spot heights and contours. At each site, exposures were logged using traditional Quaternary geology mapping techniques to document the drift cover. Observations included general attributes such as map unit, sample medium, depth to bedrock, depth of oxidation, surface expression, slope and vegetation cover. Additional records were made of the internal structure (fissility and jointing), texture, density, colour and clast characteristics (mode, shape and presence of striae) in surficial deposits. Sampling was confined to the unweathered C-horizon, which ranged from 0.2 to 6 metres below surface. An average density of one sample per 2.5 square kilometres was achieved. The greatest density of samples was along transects perpendicular to inferred iceflow direction, in areas of perceived higher mineral potential or around known mineral prospects. Sample density parallel to regional iceflow was lower (Figure 3). This sample design is consistent with similar regional till geochemistry surveys (Levson *et al.*, 1994; Giles *et al.*, 1995). An additional 173 samples of basal and ablation tills, glaciofluvial and glaciolacustrine sediments and colluvium were collected at five mineral prospects (Table 1; Stumpf *et al.*, 1996, this volume).

Samples were stored in heavy-mil plastic bags, air dried (at 25-30°C), split, crushed and sieved to -230 mesh (<63 μm) in the laboratory. Ninety-six analytical duplicates, field duplicates and analytical standards were integrated into the sample database prior to analysis for quality control. Representative splits have been submitted for aqua regia inductively coupled plasma emission spectroscopy (ICP-ES) and instrumental neutron activation (INA) analysis for 47 elements.

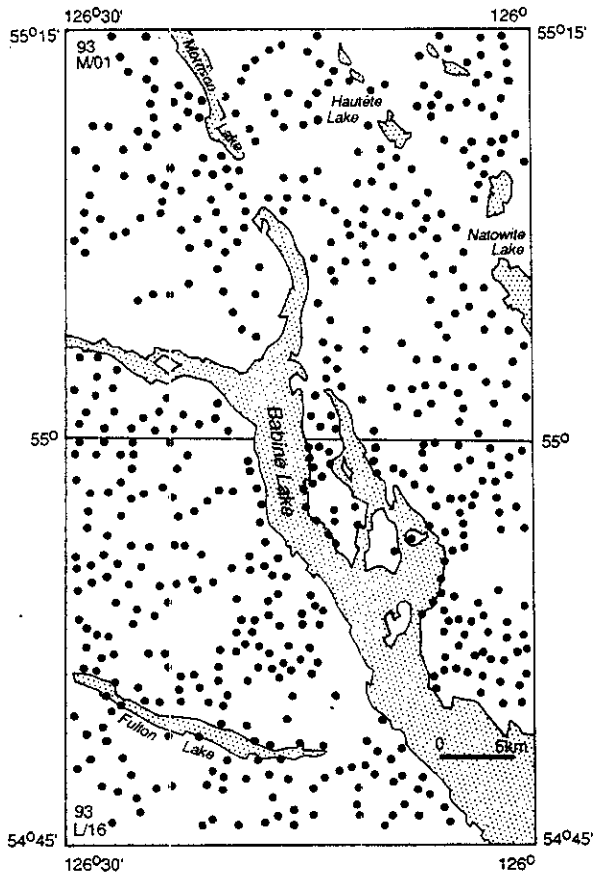


Figure 3. Location of till geochemistry samples.

## SURFICIAL SEDIMENTS

Six surficial sediment types occur in the study area: tills, glaciofluvial, glaciolacustrine, colluvial, fluvial and organic deposits (Figure 4). Their relative abundance and areal distribution are physiographically controlled. The greatest range of sediment types is observed in ponded and free-draining valleys, where complex sediment assemblages may be preserved (Figure 5A). Deposit thicknesses in valleys can exceed 10 metres (*e.g.*, Babine Lake valley). Undulating and rolling plateaus are covered by till, colluvium and glaciofluvial sediments (Figure 5B and C). In upland settings, colluvial deposits dominate on steeper slopes; tills and glaciofluvial sediments are confined to more gentle slopes (Figure 5D).

### *BASAL TILLS*

Throughout the area, glacially streamlined bedrock is mantled by massive, matrix-supported diamicton. Deposit thicknesses range from less than 1 metre in montane uplands, to greater than 5 metres along valley sides (log 1; Figure 4; Figure 5A). Surface expressions of deposits range from gently undulating to drumlinized or fluted. The matrix component ranges from about 70 to 90%, and is composed of moderately to well compacted sand, silt and clay. Moderate to strong bedding-parallel fissility and moderate to strong jointing are characteristic. Colour is variable and is often reflective of underlying bedrock. As such, it is not a distinguishing characteristic. Oxidation, if present, is predominantly confined to joints or fissility planes and discolours matrices orange to red-brown. Clasts range in size from small pebbles to large cobbles, and consist of subrounded to subangular local and distally derived lithologies. Subrounded, prolate clasts usually have striated, faceted surfaces and show alignment parallel to palaeo-iceflow. Massive, matrix-supported diamictons are interpreted as lodgement tills deposited at the base of active glacier ice (Dreimanis, 1988). Lodgement tills are occasionally interbedded with thin lenses of dense, stratified, matrix-supported diamictons, gravel and sand. Subordinate interbeds may represent basal melt-out till and subglacial fluvial deposits.

### *SUPRAGLACIAL TILLS AND GLACIGENIC DEBRIS FLOWS*

In many areas, bedrock and basal till are mantled by massive and stratified, matrix-supported diamictons (log 2, Figure 4; Figure 5B). Deposits typically have undulating or hummocky surface expressions. Basal contacts with underlying till are either gradational (for massive diamictons) or erosional (for stratified diamictons). In contrast to basal tills, these diamictons are less compact, have silt and clay-deficient matrices and are pervasively oxidized. Massive diamictons have clast contents ranging from about 20 to 40%. Subangular to subrounded pebbles and cobbles are the dominant clast sizes, although boulders (up to 3 m in diameter) are exposed close to upper surfaces. Distally derived lithologies predominate. Massive diamictons are interpreted as supraglacial tills, deposited by retreating or stagnating glacier ice. Stratified diamictons may be lithogically similar to underlying tills, and are interbedded with subordinate silt, sand or gravel. Stratified diamictons resemble glacigenic debris flows derived from steep, debris-covered ice margins or remobilized tills exposed in ice-proximal settings (*cf.* Lawson, 1988). Below 760 metres (2500 ft), linear diamicton-filled ridges, lying perpendicular to inferred iceflow, drape till. These ridges are interpreted as crevasse fills.

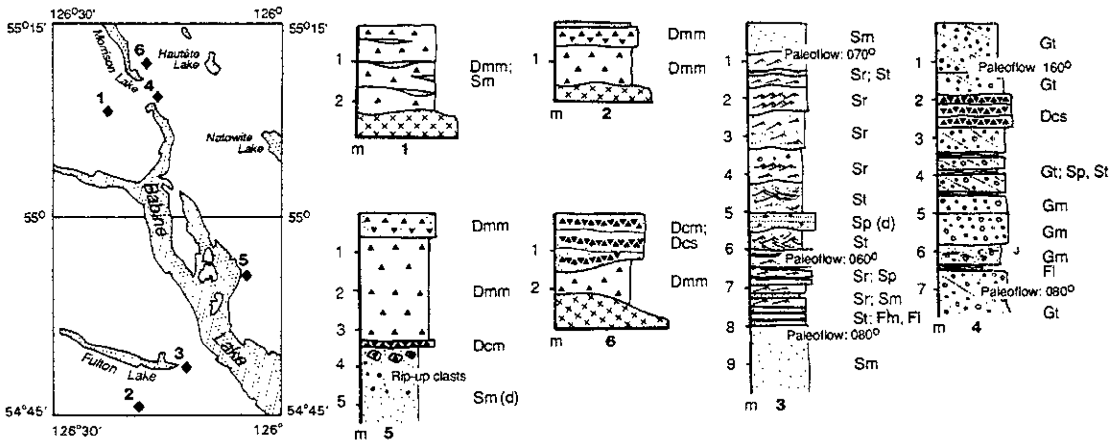


Figure 4. Selected logged profiles. Legend: Dmm - massive, matrix-supported diamicton; Dcm- massive, clast-supported diamicton; Dcs - stratified, clast-supported diamicton; G - massive gravel; Gt - cross-trough-bedded gravel; Sm - massive sand; Sp - planar bedded sand; Sr - ripple bedded sand; Fm - massive silt and clay; Fl - laminated silt and clay. Additional qualifiers: d - dropstones.

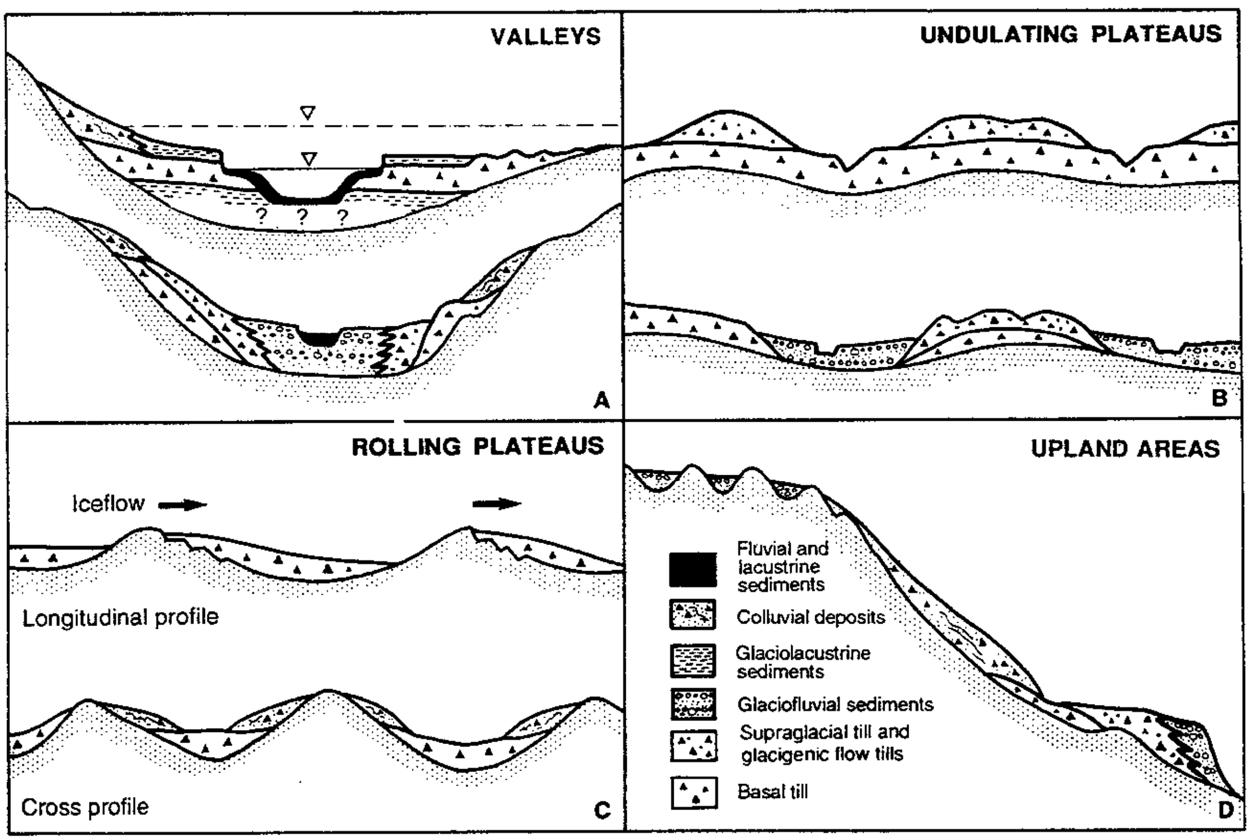


Figure 5. Simplified depositional models for valleys, plateau and upland areas in the Old Fort (93M/01) and Fulton Lake (93L/16) map areas. Note figures are not to scale.

## *GLACIOFLUVIAL SEDIMENTS*

Sequences of interbedded clast-supported gravel, subordinate sand and stratified, matrix-supported diamictons are confined to bedrock and till-walled channels in upland areas (Figure 5D). In valleys and plateaus, similar sediment assemblages form terraced benches (kames), sinuous ridges (eskers) or undulating terraces (spillways and outwash plains) in proximity to ablation and basal till (Figure 5A and B). Raised deltaic sequences (fan deltas) are also preserved above contemporary lake margins. Thickest deposits (> 5 m) occur along valley floors (log 3, Figure 4). Gravels are composed of poorly sorted, rounded, polymictic clasts, ranging in size from pebbles to cobbles. Crude may be imbricated. Upward coarsening is seen in some fan delta sequences (log 4; Figure 4). Sand interbeds are well sorted and normally graded. Planar cross-bedding, trough-cross bedding and ripple-drift bedding are preserved and frequently indicate paleoflows contrary to contemporary drainage directions. Locally, in the Fulton Lake basin, sand beds contain numerous calcite concretions of unknown origin. Gravel, sand and diamicton assemblages are interpreted as ice-proximal glaciofluvial deposits (Rust and Koster, 1984). Interbedded diamictons closely resemble glacigenic debris flows.

### *GLACIOLACUSTRINE SEDIMENTS*

On the Newman Peninsula and the south-central flank of Babine Lake, massive clays and sands with dispersed dropstones, outcrop to a maximum elevation of 790 metres (2600 ft). These deposits are truncated and overlain by thin clast-supported debris-flow diamictons and basal till. Rip-up clasts, containing diamicton, are locally preserved in the sand unit close to the overlying contact (log 5; Figure 4). Along the valley margins of Hautête Creek, rhythmically bedded silts and sands locally overlie kame deposits up to an elevation of 885 metres (2900 ft). Around the margins of Babine and Natowite lakes, massive and laminated fine sand, silt and clay beds are draped over winnowed tills up to elevations of 760 metres (2500 ft) and 790 metres (2600 ft), respectively. Generally, unit thicknesses range from 0.2 to 1.5 metres. Deposits up to 3 metres thick occur close to flanks of fan deltas and other stream outlets. Crevasse fills, glacigenic debris flows and fan delta deposits are locally interbedded with, or prograde over finer sediments, for example in the Morrison Creek and Fulton River areas (logs 3 and 4; Figure 4). Faceted and striated clasts (interpreted as dropstones) are dispersed throughout these deposits and frequently display load structures. Similar sediments are rare in the Morrison Lake valley, where sediment assemblages, bedding characteristics and grain-size distributions are consistent with deposition in ice-proximal glacial lakes.

### *COLLUVIUM*

Bedrock and glacial deposits on slopes greater than 15° are commonly mantled by massive and stratified, clast-supported diamictons, and massive deposits of bouldery rubble (Figure 5D). Proportionally, these sediments are most common in upland areas. Deposit form varies from homogenous blankets to fan aprons (log 6, Figure 4). When seen, basal contacts with underlying glacigenic deposits are predominantly erosional. Diamicton matrices comprise predominantly poorly consolidated sand that may display slope-parallel fissility and bedding. Diamictons are primarily composed of subangular, mechanically weathered bedrock fragments; subrounded, distal clasts may be present if diamictons are derived from glacigenic sediments. Clast contents range from 45 to 80%. Prolate clasts are crudely aligned parallel to slope. Boulder deposits are generally monolithic and composed of locally weathered bedrock. Clast-supported diamictons and boulder deposits are interpreted as postglacial sequences derived from subaerial weathering and gravity-induced mass movement, and include hill-slope colluvium and talus

### *FLUVIAL AND ORGANIC SEDIMENTS*

Throughout the area, streams have incised gullies and channels into older deposits or bedrock (Figure 5A and B). Along active stream beds, sands and gravels are stored in migrating point, and in-channel bars. More stable deposits are found in broad, relict floodplains, now drained by underfit streams. Sand beds are generally well sorted and normally graded. Gravel clasts are rounded to well rounded, range from pebble to cobble size, and have highly variable provenance. When seen, paleoflow indicators (*e.g.*, trough-cross and ripple-drift bedding) are consistent with contemporary drainage directions. In plateau and montane areas, organic deposits are confined to hummocky depressions, and overlie till and glaciofluvial sediments. In ponded valley reaches, organic deposits form floating vegetation mats that encroach upon open water.

## GLACIAL GEOMORPHOLOGY

### *EROSIONAL LANDFORMS*

Cirques, horns, arêtes, and other landforms indicative of alpine glacier accumulation areas, are found northwest of the study area, in the Babine Range and Skeena Mountains (Figure 1). Within the area, glacial troughs, crag-and-tails, roches moutonnées, drumlins and flutes occur where southeasterly iceflow from these sources followed the prominent regional structural grain. These features probably record the last dominant regional iceflow direction (Figure 6A). Small-scale grooves, rat-tails and striae are best preserved on fine-grained volcanic and clastic rocks, and chert-pebble conglomerate. Striae in some montane areas, and on larger streamlined landforms, indicate localized south to southwest deflection of regional iceflow (Figure 6A). These deviations imply that small bedrock obstacles controlled basal iceflow patterns at a local scale. No limit to glaciation was observed in the study area.

### *MORAINAL COMPLEXES*

In montane uplands, bedrock is covered by veneers or patchy morainal blankets, comprising glacigenic debris flows, subordinate glaciofluvial sediments and basal till. Postglacial talus and hill-slope colluvium unconformably overlie moraine sediments on steeper

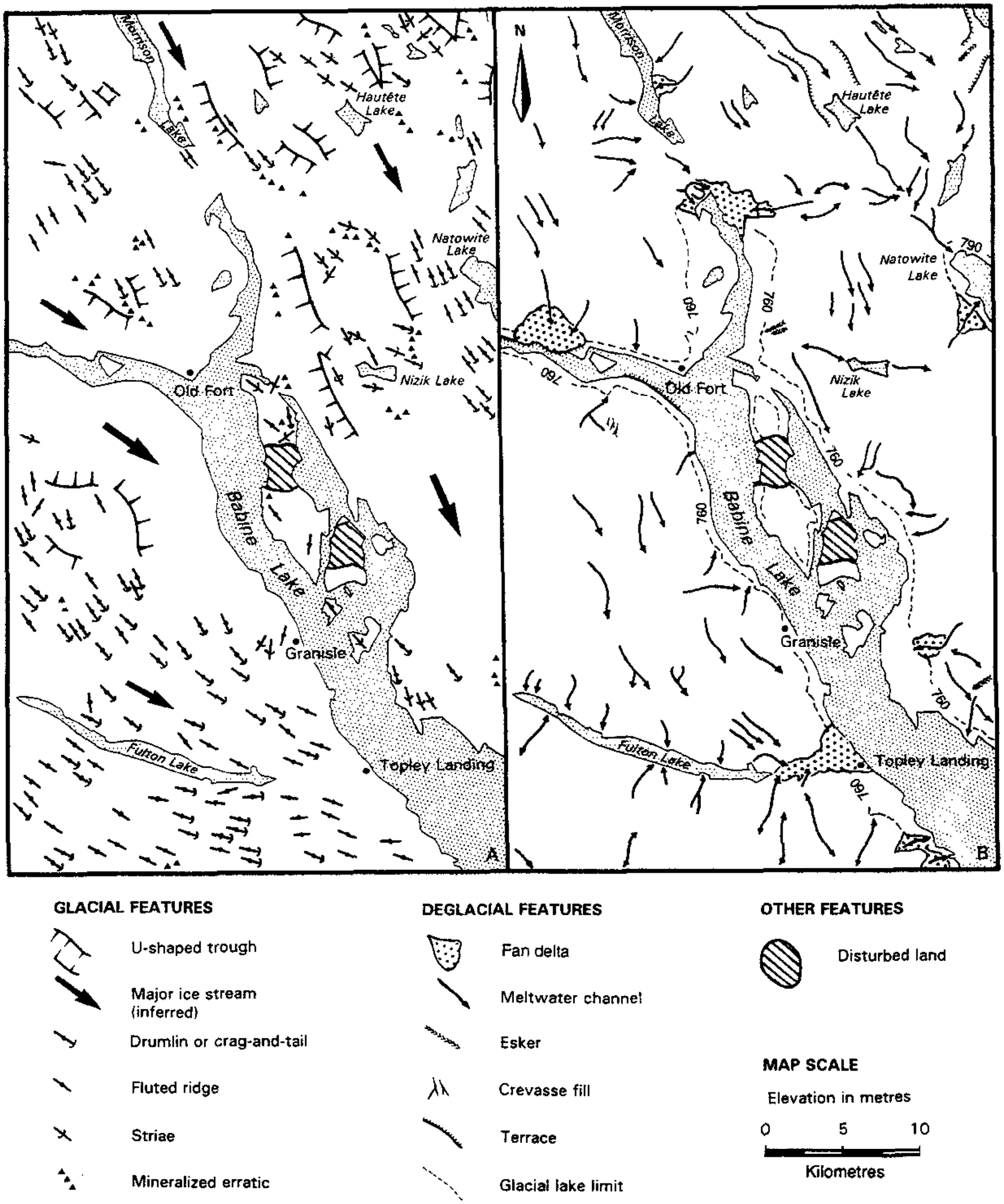


Figure 6. Glacial geomorphology of the study area.

slopes (*e.g.*, Figure 5D). Plateaus are mantled by fluted and drumlinized ground moraines composed of basal till, with subordinate supraglacial till and glaciofluvial sediments (*e.g.*, Figure 5C). Colluvium is locally dominant in hilly areas. Ground moraines deposited in the Babine, Fulton and Hautête valleys comprise undulating, hummocky or kettled blankets of basal and supraglacial tills in equal abundance (Figure 5B, upper diagram). A lateral moraine is preserved in the northeast corner of the map area. Subordinate glaciofluvial deposits form outwash plains, eskers and kame terraces (*e.g.*, Figure 5A, lower diagram; Figure 5B, lower diagram). Morrison and Babine lakes are separated by a morainal complex of basal and supraglacial till, with a maximum surface elevation of 780 metres (2560 ft). The moraine is incised by meltwater channels that drain south to fan deltas formed at 760 metres (2500 ft; Figure 6B). Below this elevation, washed tills are overlain by fan delta sequences, crevasse fills and massive glaciolacustrine silts around much of Babine Lake.

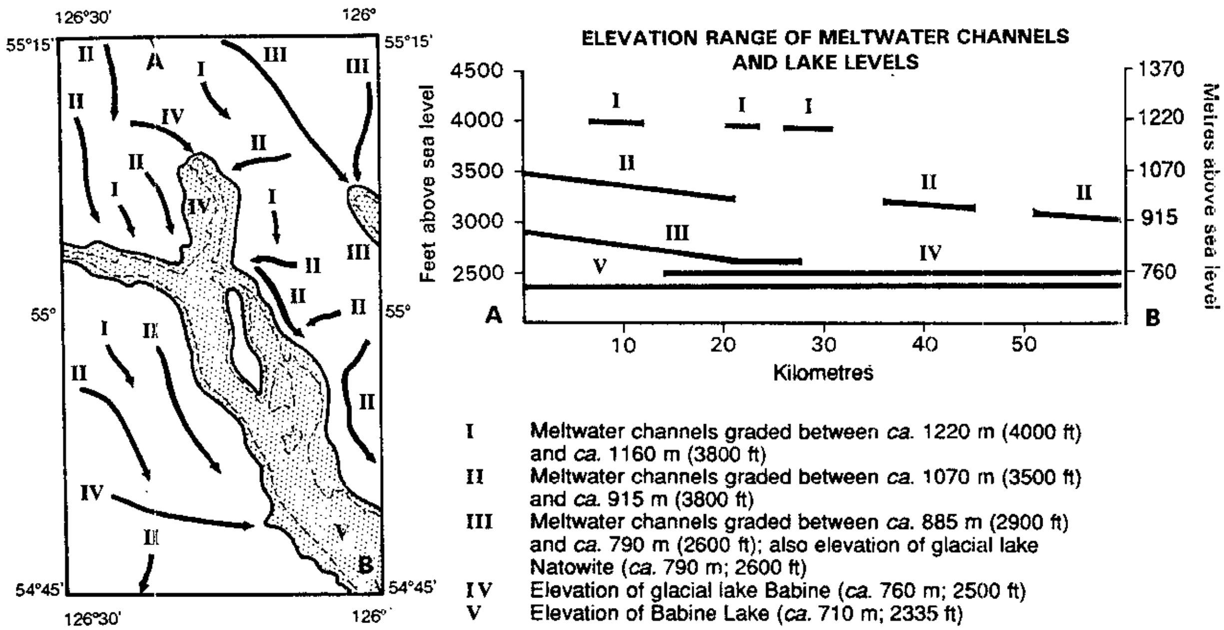


Figure 7. Simplified elevational distribution and drainage directions of meltwater channels and lakes in the study area.

## *ERRATICS, INDICATORS AND BOULDER TRAINS*

Mineralized erratics are found throughout the area (Figure 6A). Linear boulder trains, up to 5 kilometres long, originate 2.5 and 7 kilometres southeast of Hearne Hill, and 2 kilometres east of Hautête Lake (Figure 6A). Although dispersal patterns are consistent with southeasterly transport by ice, identification of sources is complicated as many boulder lithologies are superficially similar, or have several potential provenances. Two indicator lithologies are recognized and provide a first order approximation of clast transport distances. In the western half of the 93L/16 map area, ground moraine and glaciofluvial sediments contain a significant proportion of granodiorite boulders and pebbles. A probable source area for this lithology lies 70 kilometres northwest, near Mount Thoen (D.G. MacIntyre, personal communication, 1995). Chert-pebble conglomerate, eroded from outcrops in the northwest part of the 93M/01 map sheet, is observed in moraines throughout the study area. Generally, clast size decreases and roundness increases down-ice from source. The distribution of conglomerate boulders suggests potential debris transport distances of a minimum of 60 kilometres from source.

## *GLACIOFLUVIAL AND GLACIOLACUSTRINE LANDFORMS*

In montane uplands, meltwater flow was focused in bedrock channels formed on hill crests (Figure 6B; Figure 7). These relict landforms are graded between *ca.* 1220 metres (4000 ft) and 1160 metres (3800 ft); paleoflow was to the southeast. Hydrological continuity between hill crests was probably maintained by supraglacial channels formed on ice below 1220 metres. A second system of meltwater channels, with originating elevations *ca.* 975 metres (3200 ft), drained westward from Hautête valley to kame terraces formed at about 915 metres (3000 ft.) along the eastern flank of the Babine valley (Figure 6B; Figure 7). This drainage pattern implies that glacier ice occupied the Hautête valley to a minimum elevation of 975 metres (3200 ft). Elsewhere in the Babine valley, southeasterly paleoflow was confined to ice-marginal spillways incised into morainal sediments over the plateau. The presence of eskers in the Babine and Fulton valleys indicates that drainage was partly through subglacial conduits. Westward drainage into the Babine valley ended when ice levels in the Hautête valley fell to below *ca.* 975 metres (3200 ft). Below this elevation, kame terraces, eskers and spillways in the Hautête valley have profiles graded from *ca.* 885 metres (2900 ft) to *ca.* 790 metres (2600 ft; Figure 7). This latter elevation is the minimum water level of an ancestral Natowite Lake, informally named "glacial lake Natowite". In the Babine valley, another system of meltwater channels and fan deltas is graded to 760 metres (2500 ft; Figure 7). By this stage, contemporary drainage patterns were established. The 760-metre elevation defines a minimum water level for a deglacial lake partly impounded by morainal sediments between Morrison and Babine lakes (Figure 6B). This lake is informally named "glacial lake Babine".

## QUATERNARY HISTORY

The contemporary landscape of the central Babine Lake area is the product of multiple glacial and fluvial cycles operating throughout the Quaternary. Pre-late Wisconsinan fluvial and lake deposits are documented in the study area (Harrington *et al.*, 1974). Mammoth skeletal remains and plant material provide an Olympia nonglacial interval age of *ca.* 34 ka for these sediments. Pre-late Wisconsinan deposits rest unconformably on glacially eroded bedrock, which suggests at least one phase of pre-Fraser glaciation in the area.

Most sediments and landforms are inferred to be the product of the late Wisconsinan Fraser Glaciation. Glacier advance was probably marked by ice accumulation in the southern Skeena Mountains and Babine Range, northwest of the study area (Figure 1). Broad valley glaciers from these sources probably flowed southeast into the Babine and Hautête valleys. Glaciolacustrine sediments overlain by basal till indicate that a glacial lake was ponded in the Babine valley during ice advance. Deposition in this lake continued to a minimum upper elevation of 790 metres (2600 ft) before being overridden by Fraser Glaciation ice (log 5; Figure 4). It is unclear how this lake was impounded.

No limit to glaciation was observed. This suggests that by the glacial maximum, ice had inundated the entire area. At this time, the dominant iceflow was southeast. Minor deviations in this pattern occurred in upland areas, or in areas with ice-sculpted bedrock. In many areas, bedrock is mantled by Fraser Glaciation basal till. These tills are the dominant components of extensive drumlinized and fluted ground moraines. Recent studies by Plouffe (1991) and Tipper, (1994) have identified an area of glacial ice coalescence along the southern part of Babine Lake. Glaciers moving southward out of the Skeena Mountains, across the Babine Lake valley, were diverted eastward by glaciers originating in the Coast Mountains and flowing northeast along the Nechako valley.

The distribution and composition of moraines and glaciofluvial landforms is consistent with frontal recession of active glaciers and downwasting of stagnant ice confined to valleys (Ryder and Maynard, 1991). During the later stages of ice retreat, Babine and Natowite lakes were dammed by moraines, outwash and ice, and ponded to elevations of 760 metres (2500 ft) and 790 metres (2600 ft). Outlets for these deglacial lakes have yet to be identified. In addition, the hydrologic relationship of these lakes to glacial lake Fraser, which had a similar range of surface elevations (Clague, 1988), has yet to be investigated.

## CONCLUDING REMARKS

Current research in the central Babine Lake area has been directed to understanding sediment and iceflow patterns in a landscape extensively modified by multiple glacial cycles throughout the Quaternary. Physiographic setting and topographic position during glacial advance and retreat largely determine the areal distribution and sediment characteristics of glacigenic sediments. Glacially streamlined landforms and striae indicate regional iceflow toward the southeast. Localized deviations in basal iceflow patterns were effected by smaller bedrock obstacles. The possibility of interaction between coalescing glaciers from multiple sources suggests a complex depositional history for the area. This observation has important implications when interpreting geochemical dispersion patterns in basal tills.

At least three glacial meltwater systems evolved during deglaciation, progressively grading to lower base levels. Not only do these drainage networks appear to be interconnected with the evolution of glacial lake Fraser, but the lowest base level is coincident with a lake impounded behind morainal sediments, informally named glacial lake Babine. Further work will be undertaken to investigate the complex relations between the glacial lake Fraser and glacial lake Babine drainage systems.

The extent to which physiographic setting and topography have influenced iceflow, sedimentation patterns, and geochemical distribution patterns, down-ice from known mineral prospects remains unclear. We are currently developing an effective drift exploration model to study the glacial and sedimentation processes occurring in mineralized areas with variable relief and complex geology.

## ACKNOWLEDGMENTS

Fieldwork was undertaken as part of the multidisciplinary Babine Porphyry Belt project, a component of the ongoing NATMAP Nechako Project in central British Columbia. Preliminary findings outlined here form the basis of a Ph.D. research project by Andrew Stumpf. We thank Erin O'Brien, Jennifer Hobday and Gordon Weary; who, despite the draconian field program, eight foot high devil's club and voracious bugs, kept digging holes all summer. We also appreciate the frequent assistance and insights of Don MacIntyre, Ian Webster, Kim Bellafontaine and John Bryant. The manuscript was edited by W.J. McMillan and J.M. Newell.

## REFERENCES

Carter, N.C., (1981): Porphyry Copper and Molybdenum Deposits West-central British Columbia; *B. C. Ministry of Energy, Mines and Petroleum Resources*, Bulletin 64, 150 pages.

Clague, J.J. (1988): Quaternary Stratigraphy and History, Quesnel, British Columbia; *Géographie Physique et Quaternaire*, Volume 42, pages 279-288.

Dreimanis, A. (1988): Tills: Their Genetic Terminology and Classification; *in* Genetic Classification of Glacigenic Deposits, Goldthwait, R.P. and Matsch, C.L., Editors, *Balkema*, pages 17-67.

Harrington, C.R., Tipper, H.W. and Mott, J.R. (1974): Mammoth from Babine Lake, British Columbia; *Canadian Journal of Earth Sciences*, Volume 11, pages 285-303.

Holland, S.S. (1980): Landforms of British Columbia, A Physiographic Outline; *B.C. Ministry of Energy, Mines and Petroleum Resources*, Bulletin 48, 138 pages.

Howes, D.E. and Kenk, E. (1988): Terrain Classification System for British Columbia (Revised Edition); *B.C. Ministry of Environment, Lands and Parks, Surveys and Resource Mapping Branch*, MOE Manual 10, 90 pages.

Giles, T.R., Levson, V.M. and Weary, G.F. (1995): Surficial Geology and Drift Exploration Studies in the Tsacha Lake and Chedakuz Creek Areas (93F/2, 7), Central British Columbia; *in* Geological Fieldwork 1994, Grant B. and Newell, J.M., Editors, *B.C. Ministry of Energy, Mines and Petroleum Resources*, Paper 1995-1, pages 199-205.

Lawson, D.E. (1988): Glacigenic Resedimentation: Classification Concepts and Applications to Mass-movement Processes and Deposits; *in* Genetic Classification of Glacigenic Deposits, Goldthwait, R.P. and Matsch, C.L., Editors, *Balkema*, pages 19-22

Levson, V.M., Giles, T.R., Cook, S.J. and Jackaman, W. (1994): Till Geochemistry of the Fawnie Creek Area (93 F/03); *B.C. Ministry of Energy, Mines and Petroleum Resources*, Open File 1994-18, 34 pages with appendices.

MacIntyre, D.G., Webster, I.C.L. and Bellefontaine, K.A. (1996): Babine Porphyry Belt Project Bedrock Geology of the Fulton Lake Map Area (NTS 93L/16); *in* Geological Fieldwork 1995, Grant B. and Newell, J.M., Editors, *B.C. Ministry of Energy, Mines and Petroleum Resources*, Paper 1996-1, this volume.

McMillan, W.J. and Struik, B. (1996): Natmap: Nechako Plateau, British Columbia; *in* Geological Fieldwork 1995, Grant B. and Newell, J.M., Editors, *B.C. Ministry of Energy, Mines and Petroleum Resources*, Paper 1996-1, this volume

Plouffe, A. (1991): Preliminary Study of the Quaternary Geology of the Northern Interior of British Columbia; *in* Current Research, Part A; *Geological Survey of Canada*, Paper 91-1A, pages 7-13.

Rust, B.R. and Koster, E.H. (1984): Coarse Alluvial Deposits; *in* Facies Models, Walker, R.G., Editor, *Geological Association of Canada*, Geoscience of Canada Reprint Series, pages 53-70.

Ryder, J.M. and Maynard, D. (1991): The Cordilleran Ice Sheet in Northern British Columbia, *Géographie Physique et Quaternaire*, Volume 45, pages 355 363.

Shilts, W.W. (1993): Geological Survey of Canada Contributions to Understanding the Composition of Glacial Sediments; *Canadian Journal of Earth Sciences*, Volume 30, pages 333-353.

Stumpf, A.J., Huntley, D.H., Broster, B.E. and Levson, V.E., (1995): Detailed Drift Exploration Studies in the Babine Porphyry Belt (93l/16 and 93m/01), British Columbia; *in* Geological Fieldwork 1995, Grant B. and Newell, J.M., Editors, *B.C. Ministry of Energy, Mines and Petroleum Resources*, Paper 1996-1, this volume.

Tipper, H.W. (1994): Preliminary Interpretation of Glacial Features and Quaternary Information from the Smithers Map Area (93L), British Columbia; *Geological Survey of Canada*, Open File 2837, (scale 1:250 000).

Wittneben, U. (1981): Terrain Classification, Old Fort Mountain Map Area (93M/01). *B.C. Ministry of Environment, Lands and Parks, Surveys and Resource Mapping Branch.*

NOTES

# NORTHERN VANCOUVER ISLAND INTEGRATED PROJECT

By A. Panteleyev, P.T. Bobrowsky, G.T. Nixon and S.J. Sibbick

*KEYWORDS*: Northern Vancouver Island, regional geology, surficial geology, drift exploration, economic geology, hydrothermal alteration, mineral deposits, exploration geochemistry.

## INTRODUCTION

The Northern Vancouver Island integrated project (Figure 1) was initiated in 1993 as part of an effort by the Ministry to revitalize base metal exploration in the province. This "targeted" geoscience program (Panteleyev et al., 1994) includes bedrock and surficial geological mapping; water, till and bedrock geochemistry; and alteration and mineral deposits studies. A major focus is to provide a clearer understanding of the nature of the Bonanza volcanics, their geochemical expression and their mineral potential. The original plan was to have a two-year program ending in 1994; the regional bedrock mapping component was extended in 1995 for one additional year. The program is jointly funded by the Canada/British Columbia Mineral Development Agreement (MDA). Results of the most recent studies are described below. A final report summarizing the various component studies and specialized stratigraphic, geochronological, remote sensing, paleontological, geophysical, and other support investigations, will be made ready in 1996.

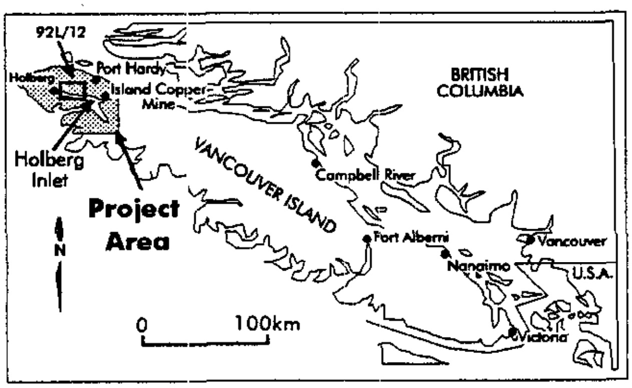


Figure 1. Location map.

## REGIONAL BEDROCK MAPPING

Mapping in the 1995 field season covered the Alice Lake map sheet (92L/6) which extends from the southeastern extremity of Quatsino Sound (Neroutsos Inlet) eastward to the northwestern shore of Nimpkish Lake. The northeastern part of the map area is underlain extensively by subaerial flood basalts of the Upper Triassic Karmutsen Formation; the southern and western parts of the area by northwesterly striking, southwesterly dipping units of the overlying Upper Triassic Quatsino and Parson Bay formations and Lower to Middle Jurassic Bonanza group volcanic and sedimentary sequences. The area is intruded by granitoids of the Island Plutonic Suite, the most important of which, the Coast Copper stock, is exposed south of Benson Lake and is genetically related to past-producing copper-iron-gold skarn deposits in the vicinity of Merry Widow Mountain. The most significant results of the 1995 field program are summarized below. Previous project work has been described by Hammack *et al.* (1994), Nixon *et al.* (1994; 1995) and Archibald and Nixon (1995).

Major mafic to intermediate pyroclastic and proximal epiclastic deposits are intercalated with typical Parson Bay lithologies, namely dark to medium grey, thin to medium-bedded, locally coralline, carbonaceous lime mudstone, and argillaceous to silty limestone. The volcanic rocks are dark grey-green, thin to thick bedded, predominantly laharic breccias and lapilli tuffs of probable phreatomagmatic origin, containing clinopyroxene and sparse amphibole phenocrysts and commonly clasts of Quatsino limestone. The lowest pyroclastic horizons occur within the upper few metres of the Quatsino limestone that is locally rich in corals, bivalves and ammonoids The stratigraphic position of the volcanic rocks implies that they are Upper Triassic, which makes them the only volcanics of this age presently known on Vancouver Island. This conclusion is presently being tested in the laboratories of M.J. Orchard of the Geological Survey of Canada by the processing of samples collected for conodonts, and by laser $Ar^{40}/Ar^{39}$ dating of amphiboles separated from the tuffs by D.A. Archibald of Queen's University.

Metasomatism at the periphery of epidote and garnet-bearing skarns in the Merry Widow area preferentially affects the upper parts of the Quatsino limestone and lowermost Parson Bay sediments, especially the coarser volcaniclastic sequences which are more permeable. Such controls on magnetite-rich skarns and associated sulphide ore deposits were noted by previous workers.

Major sequences of subaerial aphyric to plagioclase-phyric basalt of probable tholeiitic affinity characterize Bonanza volcanic stratigraphy around the shores of Victoria Lake and south of the Benson River. These flows may be genetically linked to the younger Coast Copper stock, a composite hornblende-bearing gabbroic to monzonitic intrusion. Lithogeochemical studies of the Bonanza volcanic rocks and Island Plutonic Suite are currently in progress.

## SURFICIAL GEOLOGY

Surficial geological investigations on Northern Vancouver Island have stressed three components during the life of the project: Quaternary geologic history, till geochemistry and new geophysical applications. To date, preliminary and/or final results of all three elements have been addressed in a series of reports and maps presented elsewhere (Bobrowsky and Meldrum, 1994; Bobrowsky *et al.* 1995; Huntley and Bobrowsky, 1995).

Fieldwork in 1995 consisted of follow-up studies in geophysical applications. A max-min frequency-domain electromagnetic survey was completed at site 2, Mine View Road, near Island Copper mine, to improve the interpretation of bedrock lithology and shear zone location under the monotonous drift cover. Detailed magnetic measurements were also taken at site 3, near the Red Dog property, to complete the "frontier studies" aspect of the project. Interpretive papers on the geophysical studies are in progress to complement a recently released open file (Lowe *et al.* 1995). The till geochemistry data will be published in a separate open file (Bobrowsky and Sibbick, 1996). The latter provides a documentation and synthesis of the till geochemistry samples collected in NTS sheets 92L/5,6,11 and 12 over the past several years by the Geological Survey Branch.

## MINERAL DEPOSITS STUDIES

The mineral deposits component of the integrated project investigated porphyry copper, and other intrusion-related mineralization, in a belt of mainly Bonanza volcanics and Island intrusions west of Island Copper mine. The study focused on the potential for additional types of copper-gold-silver mineralization in both "transitional" and epithermal high-sulphidation environments. The transitional hydrothermal environment can be considered to occur between the tops of porphyry copper deposits, and their uppermost expressions at ground surface, as acidic crater lakes or solfateras.

The study of intrusion-related transitional hydrothermal environments is provincial in scope. It was initiated in 1991 in northern Vancouver Island and continued in 1992 in the well exposed high-level, siliceous, advanced argillic alteration zone at Mount McIntosh, its underlying porphyry copper deposit, the Hushamu prospect, and elsewhere in the province. In 1993 the study concentrated on northern Vancouver Island and was incorporated into the integrated project. In 1994, fieldwork was limited, but core from a number of diamond-drill holes on the Hushamu deposit was examined and representative samples selected; additional drill core from Hushamu/Mount McIntosh was examined in 1995. Summaries of previous work are given in Panteleyev and Koyanagi (1993, 1994).

The current project's field component is now concluded. A mineral occurrence model can be formulated. Much of the present interpretation is based on comparisons with circum-Pacific mineral deposits, active volcanoes and geothermal systems in the Philippines, Japan, Chile, and elsewhere, that are described in the scientific literature. The key issue in this study is to determine whether the extensive advanced argillic alteration zones, and their contained acid-leached rocks, are parts of productive, magmatically influenced hydrothermal systems, and can be mineralized or, alternatively, are products of boiling, vapour-dominated acid-leaching systems, which are barren. We cannot, nor can anybody else without much additional expenditure and exploration effort, provide a conclusive and definitive answer for the northern Vancouver Island study area. Certainly the Mount McIntosh/Hushamu example testifies that rocks in high-level, advanced argillic, acid sulphate hydrothermal systems contain (weakly developed) high-sulphidation mineralization. Based on this example, other zones in the belt appear to be permissive for transitional to high-sulphidation epithermal precious and base metal mineralizaton.

The geochemical expression of the porphyry copper, and related high-sulphidation mineralization and advanced argillic/acid sulphate alteration in acidic waters derived from the weathered (oxidized and leached) hostrocks is summarized elsewhere (Panteleyev *et al.* 1996, this volume).

## EXPLORATION GEOCHEMISTRY

Fieldwork was conducted during 1995 on the exploration geochemistry component of the project. A small number of water, moss sediment and stream sediment samples were collected in the Macjack River area and from Hepler Creek, which drains the Hushamu deposit. Data from these samples will be incorporated into the final Northern Vancouver Island project report. The geochemistry section of the report will focus on two main topics:

- The application of catchment basin GIS analysis to RGS data.
- The mineral concentration properties of moss mats.

Preliminary results from these studies are already published. Open File 1995-12 (Sibbick and Laurus, 1995a) reports on the integration of geological and RGS data to predict potential areas for intrusion-related mineralization. Initial work on the concentration of heavy minerals by moss-mats was published in the journal Explore (Sibbick and Laurus, 1995b).

## REFERENCES


Archibald, D.A. and Nixon, G.T. (1995): $^{40}Ar/^{39}Ar$ Geochronometry Of Igneous Rocks in the Quatsino - Port McNeill Map Area, Northern Vancouver Island (92L/12,11); *in* Geological Fieldwork 1994, Grant, B. and Newell, J. M., Editors, *B.C. Ministry of Energy, Mines and Petroleum Resources*, Paper 1995-1, pages 49-59.

Bobrowsky, P.T. and Meldrum, D. (1994): Preliminary Drift Exploration Studies, Northern Vancouver Island (92L/6, 92L/11); *in* Geological Fieldwork 1993, Grant, B. and Newell, J. M., Editors, *B.C. Ministry of Energy, Mines and Petroleum Resources*, Paper 1994-1, pages 87-99.

Bobrowsky, P.T. and Sibbick, S.J.N. (1996): Till Geochemistry of the Northern Vancouver Island Area (92L/5,6,11 and 12); *B.C. Ministry of Energy, Mines and Petroleum Resources*, Open File 1996-7.

Bobrowsky, P.T., Best, M., Dunn, C.E., Huntley, D.H., Lowe, C., Roberts, M., Seeman, D.A. and Sibbick, S.J.N. (1995): Integrated Drift Exploration Studies on Northern Vancouver Island (92L); *in* Geological Fieldwork 1994, Grant, B. and Newell, J. M., Editors, *B.C. Ministry of Energy, Mines and Petroleum Resources*, Paper 1995-1, pages 23-33.

Hammack, J.L., Nixon, G.T., Koyanagi, V.M., Payie, G.J., Panteleyev, A., Massey, N.W.D., Hamilton, J.V. and Haggart, J.W. (1994): Preliminary Geology of the Quatsino - Port McNeill Area, Northern Vancouver Island, NTS 92L/11W,12; *B. C. Ministry of Energy, Mines and Petroleum Resources*, Open File 1994-26, Scale 1:50 000, 2 sheets.

Huntley, D.H. and Bobrowsky, P.T. (1995): Surficial Geology and Drift Exploration; Mahatta Creek Map Area (92L/5); *in* Geological Fieldwork 1994, Grant, B. and Newell, J. M., Editors, *B.C. Ministry of Energy, Mines and Petroleum Resources*, Paper 1995-1, pages 35-48.

Lowe, C., Best, M.E., Seeman, D.A. and Bobrowsky, P.T. (1995): Shallow Subsurface Mapping Using an Integrated Geophysical Approach, Northern Vancouver Island, British Columbia; *Geological Survey of Canada*, Open File 3195.

Nixon, G.T., Hammack, J.L., Koyanagi, V.M., Payie, G.J., Massey, N.W.D., Hamilton, J.V. and Haggart, J.W. (1994): Preliminary Geology of the Quatsino - Port McNeill Map Areas, Northern Vancouver Island (92L/12, 11); *in* Geological Fieldwork 1993, Grant, B. and Newell, J. M., Editors, *B. C. Ministry of Energy, Mines and Petroleum Resources*, Paper 1994-1, pages 63-85.

Nixon, G.T., Hammack, J.L., Payie, G.J. Snyder, L.D., Archibald, D.A. and Barron, D.J. (1995): Quatsino - San Josef Map Area, Northern Vancouver Island: Geological Overview (92L/12, 102I/8,9); *in* Geological Fieldwork 1994, Grant, B. and Newell, J. M., Editors, *B. C. Ministry of Energy, Mines and Petroleum Resources*, Paper 1995-1, pages 9-21.

Panteleyev, A. and Koyanagi, V.M. (1993): Advanced Argillic Alteration in Bonanza Volcanic Rocks, Northern Vancouver Island - Transitions Between Porphyry Copper and Epithermal Environments; *in* Geological Fieldwork 1992, Grant, B and Newell, J. M., Editors, *B. C. Ministry of Energy, Mines and Petroleum Resources*, Paper 1993-1, pages 287-293.

Panteleyev, A. and Koyanagi, V.M. (1994): Advanced Argillic Alteration in Bonanza Volcanic Rocks, Northern Vancouver Island - Lithologic and Permeability Controls; *in* Geological Fieldwork 1993, Grant, B. and Newell, J. M., Editors, *B. C. Ministry of Energy, Mines and Petroleum Resources*, Paper 1994-1, pages 101-109.

Panteleyev, A., Bobrowsky, P.T., Nixon, G.T. and Sibbick, S.J. (1994): Northern Vancouver Island Integrated Project; *in* Geological Fieldwork 1993, Grant, B. and Newell, J. M., Editors, *B. C. Ministry of Energy, Mines and Petroleum Resources*, Paper 1994-1, pages 59-62.

Panteleyev, A., Sibbick, S.J. and Koyanagi, V.M. (1996): Natural Acidic Drainage in Northern Vancouver Island - Its Place In Geoenvironmental Ore Deposit Models; *in* Geological Fieldwork 1995, Grant. B. and Newell, J. M., Editors, *B. C. Ministry of Energy, Mines and Petroleum Resources*, Paper 1996-1, this volume.

Sibbick, S.J. and Laurus, K.A. (1995a) Integrated Geological and Geochemical Map for the Prediction of Intrusion-related Mineralization, Northern Vancouver Island; *B.C. Ministry of Energy, Mines and Petroleum Resources*, Open File 1995-12.

Sibbick, S.J. and Laurus, K.A. (1995b): Accumulation of Gold and Heavy Minerals in a Northern Vancouver Island Stream; *Explore*, Number 86, pages 8-12.

# NOTES

British Columbia Geological Survey
Geological Fieldwork 1995

# NATURAL ACIDIC DRAINAGE IN NORTHERN VANCOUVER ISLAND - ITS PLACE IN GEOENVIRONMENTAL ORE DEPOSIT MODELS

By A. Panteleyev, S.J. Sibbick and V.M. Koyanagi

*KEYWORDS:* acid rock drainage, pH, dissolved metals, northern Vancouver Island, geoenvironmental ore deposit models, acidic water geochemistry, advanced argillic alteration.

## INTRODUCTION

During the course of mineral deposits studies in Northern Vancouver Island (Figure 1) as part of an integrated project (Panteleyev *et al.*, 1994), stream waters emanating from, and flowing through, large areas of pyritic rocks were found to be strongly acidic (commonly <4 pH). The bedrock sources for the acidic waters are hydrothermally altered and mineralized Bonanza volcanic rocks and some Island intrusions containing porphyry copper mineralization and large zones of advanced argillic alteration.

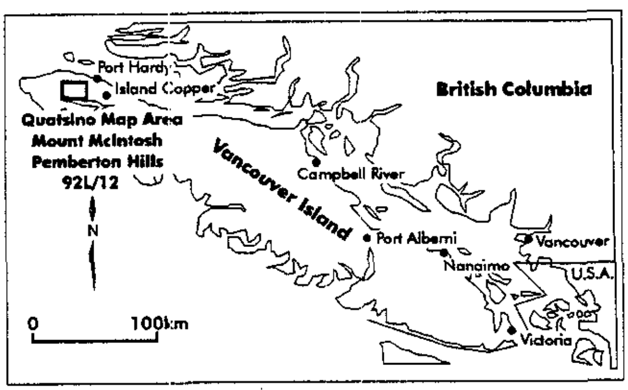


Figure 1. Location of water sampling in Quatsino map area (NTS 92L/12).

## GEOLOGICAL SETTING AND MINERALIZATION

The regional geological setting of the Quatsino Sound area is described by Nixon *et al.* (1994) and Hammack *et al.* (1994). The style of mineralization and alteration 15 to 40 kilometres to the west of Island Copper mine, mainly in the Bonanza volcanic rocks and to a lesser extent in the Island intrusions, is discussed by Panteleyev and Koyanagi (1993, 1994). Ages of hostrocks, hydrothermal systems and alteration minerals are summarized by Archibald and Nixon (1995) and Panteleyev *et al.* (1995).

The principal mineral deposits in the study area are the intrusion-related, pyrite-rich Hushamu and Red Dog porphyry copper deposits. A number of related, smaller pyritic zones are also present, for example the Hep deposit. The Hushamu deposit has an overprint of advanced argillic alteration that is expressed as the siliceous "capping" on Mount McIntosh. The alteration (quartz-pyrophyllite-kaolinite-alunite-zunyite-diaspore) is superimposed, together with vuggy quartz, and weakly developed, high-sulphidation epithermal mineralization, on the deeper, underlying Hushamu porphyry copper deposit. The advanced argillic overprinting occurred when the late hydrothermal system collapsed onto the deeper copper-bearing, predominantly quartz-sericite/illite-pyrite and quartz-amphibole-magnetite-chlorite alteration zones. Both the upper Mount McIntosh and the underlying Hushamu zones are cut by younger, siliceous hydrothermal breccias. The weakly developed epithermal mineralization that accompanies the advanced argillic and vuggy quartz alteration contains abundant pyrite with minor enargite, chalcopyrite, covellite and chalcocite (Panteleyev and Koyanagi, 1994; Dasler *et al.*, 1995).

There is widespread advanced argillic alteration to the east of the Hushamu deposit throughout the Pemberton Hills over a distance of about 11 kilometres, and in the western part of the study area at the Red Dog deposit and the nearby Northwest Expo claim area. It is evident as pyritic quartz-kaolinite-alunite alteration in the rhyolitic Bonanaza map units. Centres of most intense alteration seem to be associated with rhyolite dome emplacement, associated vent deposits and hydrothermal breccia bodies. In addition to abundant pyrite, quartz-alunite is widespread and there is rare enargite, covellite and chalcocite; native sulphur is locally abundant. The strongly altered, siliceous, aluminous rocks have been hydrothermally acid leached. They lack buffering (acid neutralizing) capacity and weathering of the highly pyritic rocks gives rise to extensive zones of near-surface, secondary (supergene) acid-leached limonitic rocks.

## GEOCHEMICAL WATER SAMPLING

Starting in 1991, and continuing in 1992 and 1993, stream and various standing waters were measured directly in the field for pH, conductivity and total dissolved solids (TDS) at 248 sites, using a Corning Checkmate™ M90 portable microprocessor. Preliminary results are summarized by Koyanagi and Panteleyev (1993, 1994). Water geochemical samples were taken

## TABLE 1: WATER CHEMISTRY - MOUNT McINTOSH/PEMBERTON HILLS AREA, NORTHERN VANCOUVER ISLAND, IN ppm

| Sample | pH | Cond | TDS | UTM Zone 10 | | Location | SO4 | Fe | Si | Al | Mg | Ca | Mn | Cu | Pb | Zn | Ba | Co | Ni | As |
|---|---|---|---|---|---|---|---|---|---|---|---|---|---|---|---|---|---|---|---|---|
| No. | | μs | g/ml | Easting | Northing | | | | | | | | | | | | | | | |
| 1991 samples | | | | | | | | | | | | | | | | | | | | |
| EC91AP-16 | 3.9 | 163 | 82 | 583092 | 5609526 | Hushamu Creek | 31 | 0.01 | 6.8 | 1.9 | 1.7 | 5.2 | 0.11 | 0.01 | 0.02 | 0.01 | 0.03 | <0.01 | <0.01 | 0.05 |
| EC91AP-19 | 3.8 | 177 | 92 | 583209 | 5611889 | Hushamu Ck. tributary | 39 | 0.01 | 8.7 | 1.9 | 2.2 | 4.0 | 0.12 | 0.00 | 0.01 | 0.01 | 0.04 | <0.01 | <0.01 | 0.03 |
| EC91AP-20 | 4.3 | 120 | 61 | 582996 | 5612577 | Hushamu Creek | 18 | 0.01 | 5.9 | 1.0 | 1.9 | 4.7 | 0.07 | 0.01 | 0.00 | 0.01 | 0.01 | <0.01 | <0.01 | 0.01 |
| EC91AP-22 | 3.5 | 244 | 126 | 581785 | 5613442 | Hushamu Ck. tributary | 50 | 0.21 | 8.9 | 6.3 | 1.4 | 0.2 | 0.30 | 0.01 | 0.02 | 0.01 | 0.02 | 0.01 | <0.01 | 0.06 |
| EC91AP-23 | 4.3 | 141 | 71 | 581451 | 5613942 | Hushamu Lake | 32 | 0.01 | 5.8 | 1.5 | 2.3 | 6.4 | 0.10 | 0.02 | 0.02 | 0.01 | 0.01 | 0.01 | <0.01 | 0.03 |
| EC91AP-24 | 3.7 | 54 | 27 | 581488 | 5614083 | Hushamu Ck. tributary | 228 | 0.55 | 21.5 | 16.5 | 10.9 | 23.3 | 0.47 | 0.32 | 0.05 | 0.04 | 0.01 | 0.04 | 0.04 | 0.09 |
| EC91AP-25 | 6.2 | 51 | 25 | 582901 | 5609635 | Hushamu Ck. tributary | 1 | 0.10 | 1.9 | 0.1 | 0.6 | 2.1 | 0.01 | 0.00 | 0.01 | 0.03 | 0.05 | <0.01 | <0.01 | 0.02 |
| EC91AP-30 | 4.1 | 100 | 50 | 579683 | 5614349 | Hepler Ck. tributary | 18 | 0.01 | 3.7 | 0.8 | 0.9 | 3.0 | 0.30 | 0.07 | 0.01 | 0.01 | 0.01 | <0.01 | <0.01 | 0.04 |
| EC91AP-31 | 3.9 | 119 | 62 | 579689 | 5614255 | Hepler Ck. tributary | 20 | 0.07 | 3.7 | 1.2 | 1.2 | 3.2 | 0.06 | 0.00 | 0.01 | 0.01 | 0.03 | <0.01 | <0.01 | 0.04 |
| EC91AP-34 | 5.6 | 40 | 20 | 578313 | 5612787 | Goodspeed R. tributary | 3 | 0.01 | 1.4 | 0.2 | 0.5 | 1.5 | 0.01 | 0.00 | 0.00 | 0.03 | 0.01 | <0.01 | 0.01 | 0.01 |
| EC91AP-35 | 4.8 | 15 | 8 | 580888 | 5613535 | Mount McIntosh | 7 | 0.29 | 0.3 | 0.3 | 0.1 | 0.0 | 0.01 | 0.00 | 0.01 | 0.01 | 0.01 | <0.01 | <0.01 | 0.01 |
| EC91AP-37 | 3.6 | 88 | 45 | 580956 | 5612541 | Mount McIntosh | 14 | 0.56 | 0.7 | 1.0 | 0.8 | 0.0 | 0.01 | 0.00 | 0.00 | 0.01 | 0.02 | <0.01 | <0.01 | 0.01 |
| EC91AP-42 | 3.9 | 159 | 79 | 581612 | 5610201 | South McIntosh | 29 | 0.01 | 5.4 | 1.9 | 1.7 | 6.9 | 0.25 | 0.00 | 0.01 | 0.01 | 0.03 | <0.01 | <0.01 | 0.01 |
| 1992 samples | | | | | | | | | | | | | | | | | | | | |
| EC92AP-1 | 5.6 | 76 | 38 | 577726 | 5611934 | Goodspeed R. tributary | 13 | 0.13 | 3.9 | 0.2 | 1.2 | 9.0 | <0.01 | 0.01 | 0.01 | 0.03 | 0.06 | <0.01 | <0.01 | <0.01 |
| EC92AP-3 | 5.6 | 23 | 12 | 583032 | 5615140 | Mead Creek | 10 | 0.41 | 2.2 | 0.5 | 0.2 | 1.8 | <0.01 | 0.00 | 0.01 | 0.04 | 0.05 | <0.01 | <0.01 | <0.01 |
| EC92AP-6 | 6.5 | 35 | 18 | 584095 | 5616670 | Mead Creek | 10 | 0.19 | 2.9 | 0.2 | 0.5 | 4.3 | <0.01 | 0.01 | 0.01 | 0.11 | 0.03 | <0.01 | <0.01 | <0.01 |
| EC92AP-10 | 5.0 | 74 | 36 | 579235 | 5617182 | Hepler Creek | 26 | 0.45 | 5.3 | 0.5 | 1.2 | 5.7 | 0.04 | 0.01 | 0.01 | 0.01 | 0.05 | <0.01 | <0.01 | <0.01 |
| EC92AP-13 | 3.9 | 152 | 75 | 578378 | 5615969 | Hepler Ck. tributary | 51 | 0.35 | 7.8 | 3.5 | 1.1 | 7.5 | 0.02 | 0.03 | 0.01 | 0.08 | 0.05 | <0.01 | <0.01 | 0.02 |
| EC92AP-15 | 4.7 | 51 | 26 | 583015 | 5612783 | Hushamu Ck. tributary | 17 | 0.29 | 4.5 | 0.3 | 0.6 | 3.8 | 0.02 | 0.00 | 0.01 | 0.02 | 0.04 | <0.01 | <0.01 | <0.01 |
| EC92AP-16 | 4.4 | 151 | 75 | 582246 | 5613217 | Mount McIntosh | 54 | 9.20 | 8.5 | 1.6 | 2.8 | 7.6 | 0.07 | 0.02 | 0.01 | 0.02 | 0.10 | <0.01 | <0.01 | <0.01 |
| EC92AP-18 | 3.2 | 259 | 128 | 580958 | 5612530 | Mount McIntosh | 58 | 0.14 | 3.3 | 0.1 | 0.7 | 5.5 | 0.02 | 0.01 | 0.01 | 0.06 | 0.30 | <0.01 | <0.01 | 0.02 |
| EC92AP-19 | 5.4 | 55 | 27 | 579806 | 5611551 | Cleskiagh Creek | 10 | 2.30 | 1.1 | 2.9 | 1.8 | 1.4 | <0.01 | 0.01 | 0.01 | 0.01 | 0.14 | <0.01 | <0.01 | <0.01 |
| EC92AP-20 | 3.9 | 184 | 93 | 580697 | 5609698 | Cleskiagh Creek | 72 | 0.68 | 8.2 | 3.2 | 2.3 | 14.3 | 0.39 | 0.01 | 0.01 | 0.03 | 0.08 | <0.01 | <0.01 | 0.02 |
| EC92AP-21 | 2.0 | 2400 | 1190 | 580439 | 5611893 | South McIntosh ditch | 1300 | 88.80 | 36.6 | 45.7 | 9.6 | 165.0 | 10.00 | 0.15 | 0.11 | 0.65 | 0.06 | 0.15 | 0.03 | 0.3 |
| EC92AP-24 | 3.6 | 219 | 105 | 582100 | 5610975 | South McIntosh | 67 | 0.29 | 5.4 | 1.7 | 2.0 | 14.0 | 0.79 | 0.01 | 0.01 | 0.02 | 0.10 | <0.01 | <0.01 | <0.01 |
| EC92AP-26 | 4.8 | 53 | 25 | 584759 | 5608931 | Hushamu Ck. tributary | 12 | 2.98 | 3.5 | 0.6 | 0.9 | 4.5 | 0.08 | 0.00 | 0.01 | 0.01 | 0.05 | <0.01 | <0.01 | <0.01 |
| EC92AP-27 | 3.1 | 252 | 124 | 585996 | 5609231 | Youghpan Creek | 72 | 2.23 | 6.9 | 3.5 | 1.3 | 11.7 | 0.18 | 0.01 | 0.01 | 0.02 | 0.09 | <0.01 | <0.01 | 0.01 |
| EC92AP-28 | 2.9 | 311 | 157 | 585514 | 5609187 | Youghpan Ck. tributary | 113 | 5.60 | 11.3 | 4.0 | 2.7 | 14.7 | 0.44 | 0.01 | 0.01 | 0.03 | 0.12 | <0.01 | <0.01 | 0.02 |
| EC92AP-30 | 5.3 | 90 | 28 | 585853 | 5611835 | N. Youghpan Creek | 17 | 0.17 | 2.9 | 0.3 | 0.7 | 3.0 | 0.06 | 0.00 | 0.01 | 0.01 | 0.06 | <0.01 | <0.01 | <0.01 |
| EC92AP-33 | 4.2 | 166 | 83 | 582226 | 5606791 | Mouth Youghpan Creek | 69 | 0.89 | 8.4 | 1.7 | 1.9 | 17.9 | 0.26 | 0.01 | 0.01 | 0.02 | 0.09 | <0.01 | <0.01 | 0.03 |
| EC92AP-52 | 4.0 | 91 | 43 | 586391 | 5608915 | Youghpan Ck. tributary | 18 | 1.21 | 5.2 | 0.7 | 0.9 | 2.8 | 0.07 | 0.01 | 0.06 | 0.01 | 0.10 | <0.01 | <0.01 | <0.01 |
| EC92AP-55 | 3.4 | 240 | 119 | 586954 | 5608357 | Youghpan Ck. tributary | 60 | 2.25 | 7.0 | 2.4 | 1.7 | 5.5 | 0.14 | 0.01 | 0.01 | 0.03 | 0.09 | <0.01 | <0.01 | 0.02 |
| EC92AP-58 | 3.5 | 264 | 131 | 587799 | 5608199 | Youghpan Ck. tributary | 84 | 2.73 | 7.8 | 3.9 | 1.8 | 13.9 | 0.16 | 0.01 | 0.02 | 0.03 | 0.11 | <0.01 | <0.01 | 0.04 |
| EC92AP-60 | 5.4 | 146 | 70 | 588699 | 5607854 | Youghpan Ck. tributary | 49 | 1.12 | 6.7 | 0.4 | 1.5 | 16.4 | 0.13 | 0.01 | 0.01 | 0.01 | 0.05 | <0.01 | <0.01 | <0.01 |
| 1993 samples | | | | | | | | | | | | | | | | | | | | |
| S493VK-01 | 3.6 | 206 | 102 | 572115 | 5618055 | Red Dog | 62 | 0.24 | 9.0 | 3.2 | 3.4 | 5.4 | 0.28 | 0.38 | 0.01 | 0.02 | 0.05 | <0.01 | <0.01 | 0.02 |
| S493VK-02 | 5.4 | 76 | 38 | 571641 | 5618113 | Red Dog | 23 | 0.39 | 6.6 | 0.1 | 1.9 | 7.8 | 0.01 | 0.01 | 0.00 | 0.00 | 0.04 | <0.01 | <0.01 | <0.01 |
| S493VK-03 | 5.2 | 88 | 43 | 571690 | 5617375 | Red Dog | 23 | 0.49 | 13.2 | 5.4 | 3.8 | 28.7 | 0.49 | 0.02 | 0.02 | 0.04 | 0.08 | 0.01 | <0.01 | 0.03 |
| S493VK-04 | 3.2 | 471 | 240 | 580731 | 5611275 | Cleskiagh Ck. tributary | 150 | 1.30 | 6.2 | 0.5 | 1.7 | 7.2 | 0.04 | 0.09 | 0.01 | 0.00 | 0.01 | <0.01 | <0.01 | <0.01 |
| S493VK-05 | 4.1 | 230 | 120 | 580630 | 5609747 | Cleskiagh Creek | 70 | 0.52 | 8.6 | 2.9 | 2.4 | 14.6 | 0.36 | 0.01 | 0.02 | 0.02 | 0.04 | <0.01 | <0.01 | 0.02 |
| S493VK-06 | 3.4 | 158 | 80 | 583092 | 5609526 | Hushamu Creek | 51 | 0.46 | 8.7 | 2.0 | 2.2 | 7.9 | 0.12 | 0.02 | 0.03 | 0.02 | <0.01 | <0.01 | <0.01 | <0.01 |
| S493VK-07 | 3.8 | 436 | 219 | 582069 | 5610698 | South McIntosh | 149 | 0.21 | 14.2 | 5.7 | 4.2 | 32.2 | 0.72 | 0.01 | 0.03 | 0.03 | 0.09 | 0.01 | <0.01 | 0.06 |
| S493VK-08 | 5.5 | 73 | 35 | 579603 | 5614379 | Hepler Ck. swamp | 76 | 1.58 | 5.1 | 0.4 | 1.2 | 4.9 | 0.02 | 0.02 | 0.02 | 0.00 | 0.03 | <0.01 | <0.01 | <0.01 |
| S493VK-09 | 3.8 | 190 | 96 | 579235 | 5617182 | Hepler Creek, S. fork | 58 | 1.44 | 8.0 | 1.8 | 2.5 | 11.0 | 0.14 | 0.01 | 0.03 | 0.01 | 0.04 | <0.01 | <0.01 | <0.01 |
| S493VK-10 | 2.9 | 1017 | 527 | 58007 | 5614325 | Hushamu deposit ditch | 338 | 2.40 | 14.8 | 20.1 | 9.3 | 36.1 | 0.43 | 1.37 | 0.08 | 0.16 | <0.01 | 0.04 | 0.01 | 0.12 |
| S493VK-11 | 4.3 | 137 | 70 | 582034 | 5613403 | Hushamu Ck. headwater | 51 | 1.35 | 6.9 | 1.3 | 2.9 | 8.1 | 0.09 | 0.03 | 0.03 | 0.02 | <0.01 | <0.01 | <0.01 | <0.01 |
| S493VK-12 | 5.2 | 58 | 29 | 582993 | 5612749 | Hushamu Creek | 14 | 0.38 | 4.4 | 0.3 | 1.0 | 3.7 | 0.09 | 0.01 | 0.01 | 0.01 | 0.02 | <0.01 | <0.01 | <0.01 |
| S493VK-13 | 3.7 | 181 | 90 | 583227 | 5611897 | Hushamu Ck. tributary | 58 | 1.48 | 11.0 | 2.1 | 2.9 | 7.0 | 0.16 | 0.01 | 0.03 | 0.01 | 0.02 | <0.01 | <0.01 | <0.01 |

## TABLE 2: WATER CHEMISTRY - MOUNT McINTOSH/PEMBERTON HILLS AREA, NORTHERN VANCOUVER ISLAND, IN ppm

| Sample | pH | Cond | TDS | UTM Zone 10 | | Location | SO4 | Fe | Si | Al | Mg | Ca | Mn | Cu | Pb | Zn | Ba | Co | Ni | As |
|---|---|---|---|---|---|---|---|---|---|---|---|---|---|---|---|---|---|---|---|---|
| No. | | μs | g/ml | Easting | Northing | | | | | | | | | | | | | | | |
| 1993 samples (continued) | | | | | | | | | | | | | | | | | | | | |
| S493VK-14 | 3.9 | 215 | 88 | 581533 | 5610239 | Clesklagh Ck. tributary | 61 | 0.47 | 6.8 | 1.8 | 2.9 | 10.4 | 0.28 | 0.02 | 0.05 | 0.01 | 0.19 | 0.01 | <0.01 | 0.01 |
| S493VK-15 | 5.9 | 65 | 32 | 585572 | 5611986 | top H600 Road | 17 | 4.03 | 3.0 | 0.3 | 1.2 | 3.3 | 0.57 | 0.00 | 0.01 | 0.00 | 0.04 | 0.01 | <0.01 | <0.01 |
| S493VK-16 | 5.4 | 56 | 28 | 585896 | 5611834 | top H600 Road | 12 | 0.15 | 3.7 | 0.2 | 1.0 | 2.7 | 0.08 | 0.01 | 0.02 | 0.00 | 0.05 | <0.01 | <0.01 | <0.01 |
| S493VK-17 | 3.5 | 408 | 203 | 585155 | 5609947 | Youghpan Creek, head | 138 | 1.21 | 15.0 | 5.9 | 4.5 | 20.1 | 0.51 | 0.02 | 0.06 | 0.05 | 0.03 | 0.02 | <0.01 | 0.04 |
| S493VK-18 | 3.3 | 449 | 232 | 585523 | 5609163 | Youghpan Creek | 126 | 2.53 | 10.6 | 3.9 | 3.4 | 13.9 | 0.42 | 0.02 | 0.06 | 0.04 | <0.01 | 0.02 | <0.01 | <0.01 |
| S493VK-19 | 3.7 | 250 | 130 | 586195 | 5609062 | Youghpan Creek | 65 | 2.04 | 6.4 | 3.2 | 1.8 | 10.8 | 0.17 | 0.02 | 0.04 | 0.02 | <0.01 | 0.01 | <0.01 | <0.01 |
| S493VK-20 | 4.2 | 176 | 88 | 582226 | 5606791 | Youghpan Ck. at Main | 65 | 0.41 | 5.6 | 1.5 | 1.8 | 13.0 | 0.19 | 0.01 | 0.03 | 0.01 | <0.01 | <0.01 | <0.01 | <0.01 |
| S493VK-21 | 6.4 | 189 | 95 | 593651 | 5606900 | Wakalish Ck. mouth | 18 | 0.01 | 2.9 | 0.1 | 2.8 | 4.7 | 0.01 | 0.01 | 0.02 | 0.00 | 0.02 | <0.01 | <0.01 | <0.01 |
| 1995 samples | | | | | | | | | | | | | | | | | | | | |
| EC95-01 | 6.2 | | | 591015 | 5606839 | Wanokana R. at Main | 11 | 0.39 | 3.3 | 0.1 | 0.7 | 3.5 | 0.01 | 0.01 | 0.00 | 0.00 | <0.01 | <0.01 | <0.01 | <0.01 |
| EC95-02 | 4.5 | | | 582226 | 5606791 | Youghpan Ck. at Main | 56 | 0.52 | 6.3 | 1.1 | 1.5 | 13.6 | 0.15 | 0.01 | 0.02 | 0.01 | 0.05 | 0.01 | <0.01 | <0.01 |
| EC95-03 | 6.3 | | | 584949 | 5608906 | H600 Road, at Main | 9 | 0.99 | 3.8 | <.0.1 | 1.0 | 6.0 | 0.04 | 0.01 | 0.03 | 0.10 | 0.01 | <0.01 | <0.01 | <0.01 |
| EC95-04 | 4.2 | | | 583092 | 5609526 | Hushamu Ck. at Main | 43 | 0.75 | 7.4 | 1.0 | 1.7 | 7.1 | 0.09 | 0.02 | 0.06 | 0.02 | 0.03 | 0.01 | <0.01 | <0.01 |
| EC95-05 | 3.7 | | | 582069 | 5610698 | H1000 Road, S. McIntosh | 100 | 4.00 | 14.1 | 4.6 | 4.2 | 17.6 | 0.43 | 0.01 | 0.31 | 0.03 | 0.04 | 0.01 | 0.01 | <0.01 |
| EC95-06 | 4.5 | | | 581427 | 5610561 | Clesklagh Ck. tributary | 61 | 0.54 | 8.1 | 1.2 | 2.3 | 14.6 | 0.25 | 0.01 | 0.00 | 0.01 | 0.04 | <0.01 | <0.01 | <0.01 |
| EC95-07 | 3.8 | | | 580731 | 5611275 | Clesklagh Ck at CL130 | 110 | 4.14 | 11.9 | 3.2 | 3.5 | 29.6 | 0.39 | 0.02 | 0.21 | 0.03 | 0.04 | 0.01 | <0.01 | <0.01 |
| EC95-08 | 4.2 | | | 579235 | 5617182 | Hepler Creek | 54 | 1.61 | 7.4 | 1.1 | 2.0 | 9.9 | 0.11 | 0.01 | 0.10 | 0.01 | <0.01 | <0.01 | <0.01 | <0.01 |
| EC95-09 | 4.7 | | | 581451 | 5613942 | Hushamu Lake | 49 | 0.44 | 8.8 | 1.7 | 3.0 | 10.4 | 0.11 | 0.05 | 0.01 | 0.04 | 0.01 | 0.01 | <0.01 | <0.01 |
| EC95-10 | 4.6 | | | 582996 | 5612577 | Hushamu Ck. headwater | 38 | 0.80 | 7.1 | 0.7 | 2.1 | 7.1 | 0.06 | 0.02 | 0.00 | 0.02 | 0.04 | <0.01 | <0.01 | <0.01 |

1995 samples were filtered and acidified; 1992 and 1993 samples were acidified but not filtered; 1991 samples were untreated.

Analytical method: ICP. Laboratory: 1991 - MinEn; 1992, 1993 - Eco-Tech; 1995 - CanTech. ICP data for other elements are available, upon request, from the senior author.

## TABLE 3: REPLICATE WATER SAMPLES, NORTHERN VANCOUVER ISLAND, IN ppm

| Sample | pH | Cond | TDS | UTM Zone 10 | | Location | SO4 | Fe | Si | Al | Mg | Ca | Mn | Cu | Pb | Zn | Ba | Co | Ni | As |
|---|---|---|---|---|---|---|---|---|---|---|---|---|---|---|---|---|---|---|---|---|
| No. | | μs | g/ml | Easting | Northing | | | | | | | | | | | | | | | |
| EC95-02 | 4.5 | | | 582226 | 5606791 | Youghpan Ck. at Main | 56 | 0.52 | 6.3 | 1.1 | 1.5 | 13.6 | 0.15 | 0.01 | 0.10 | 0.01 | 0.05 | 0.01 | <0.01 | <0.01 |
| EC92AP-33 | 4.2 | 166 | 83 | 582226 | 5606791 | Mouth Youghpan Creek | 69 | 0.89 | 8.4 | 1.7 | 1.9 | 17.9 | 0.26 | 0.01 | 0.01 | 0.02 | 0.09 | <0.01 | <0.01 | 0.03 |
| S493VK-20 | 4.2 | 176 | 88 | 582226 | 5606791 | Youghpan Ck. at Main | 65 | 0.41 | 5.6 | 1.5 | 1.8 | 13.0 | 0.19 | 0.01 | 0.03 | 0.01 | <0.01 | <0.01 | <0.01 | <0.01 |
| EC95-04 | 4.2 | | | 583092 | 5609526 | Hushamu Ck. at Main | 43 | 0.75 | 7.4 | 1.0 | 1.7 | 7.1 | 0.09 | 0.02 | 0.14 | 0.02 | 0.03 | 0.01 | <0.01 | <0.01 |
| EC91AP-16 | 3.9 | 163 | 82 | 583092 | 5609526 | Hushamu Creek | 31 | 0.01 | 6.8 | 1.9 | 1.7 | 5.2 | 0.11 | 0.01 | 0.02 | 0.01 | 0.03 | <0.01 | <0.01 | 0.05 |
| S493VK-06 | 3.4 | 158 | 80 | 583092 | 5609526 | Hushamu Creek | 51 | 0.46 | 8.7 | 2.0 | 2.2 | 7.9 | 0.12 | 0.02 | 0.03 | 0.02 | <0.01 | <0.01 | <0.01 | <0.01 |
| EC95-05 | 3.7 | | | 582069 | 5610698 | H1000 Road, S. McIntosh | 100 | 4.00 | 14.1 | 4.6 | 4.2 | 17.6 | 0.43 | 0.01 | 0.39 | 0.03 | 0.04 | 0.01 | <0.01 | <0.01 |
| S493VK-07 | 3.8 | 436 | 219 | 582069 | 5610698 | South McIntosh | 149 | 0.21 | 14.2 | 5.7 | 4.2 | 32.2 | 0.72 | 0.01 | 0.03 | 0.03 | 0.09 | 0.01 | <0.01 | 0.06 |
| EC95-08 | 4.2 | | | 579235 | 5617182 | Hepler Creek | 54 | 1.61 | 7.4 | 1.1 | 2.0 | 9.9 | 0.11 | 0.01 | 0.18 | 0.01 | <0.01 | <0.01 | <0.01 | <0.01 |
| S493VK-09 | 3.8 | 190 | 96 | 579235 | 5617182 | Hepler Creek, S. fork | 58 | 1.44 | 8.0 | 1.8 | 2.5 | 11.0 | 0.14 | 0.01 | 0.03 | 0.01 | 0.04 | <0.01 | <0.01 | <0.01 |
| EC95-09 | 4.7 | | | 581451 | 5613942 | Hushamu Lake | 49 | 0.44 | 8.8 | 1.7 | 3.0 | 10.4 | 0.11 | 0.05 | 0.08 | 0.04 | 0.01 | 0.01 | <0.01 | <0.01 |
| EC91AP-23 | 4.3 | 141 | 71 | 581451 | 5613942 | Hushamu Lake | 32 | 0.01 | 5.8 | 1.5 | 2.3 | 6.4 | 0.10 | 0.02 | 0.02 | 0.01 | 0.01 | 0.01 | <0.01 | 0.03 |
| EC95-10 | 4.6 | | | 582996 | 5612577 | Hushamu Ck. headwater | 38 | 0.80 | 7.1 | 0.7 | 2.1 | 7.1 | 0.06 | 0.02 | 0.06 | 0.02 | 0.04 | <0.01 | <0.01 | <0.01 |
| EC91AP-20 | 4.3 | 120 | 61 | 582996 | 5612577 | Hushamu Creek | 18 | 0.01 | 5.9 | 1.0 | 1.9 | 4.7 | 0.07 | 0.01 | 0.00 | 0.01 | 0.01 | <0.01 | <0.01 | 0.01 |

1995 samples were filtered and acidified; 1993 and 1992 samples were acidified but not filtered; 1991 samples were untreated.

Analytical method: ICP. Laboratory. 1991 - MinEn, 1992, 1993, 1994 - Echo-Tech. ICP data for other elements are available, upon request, from the senior author.

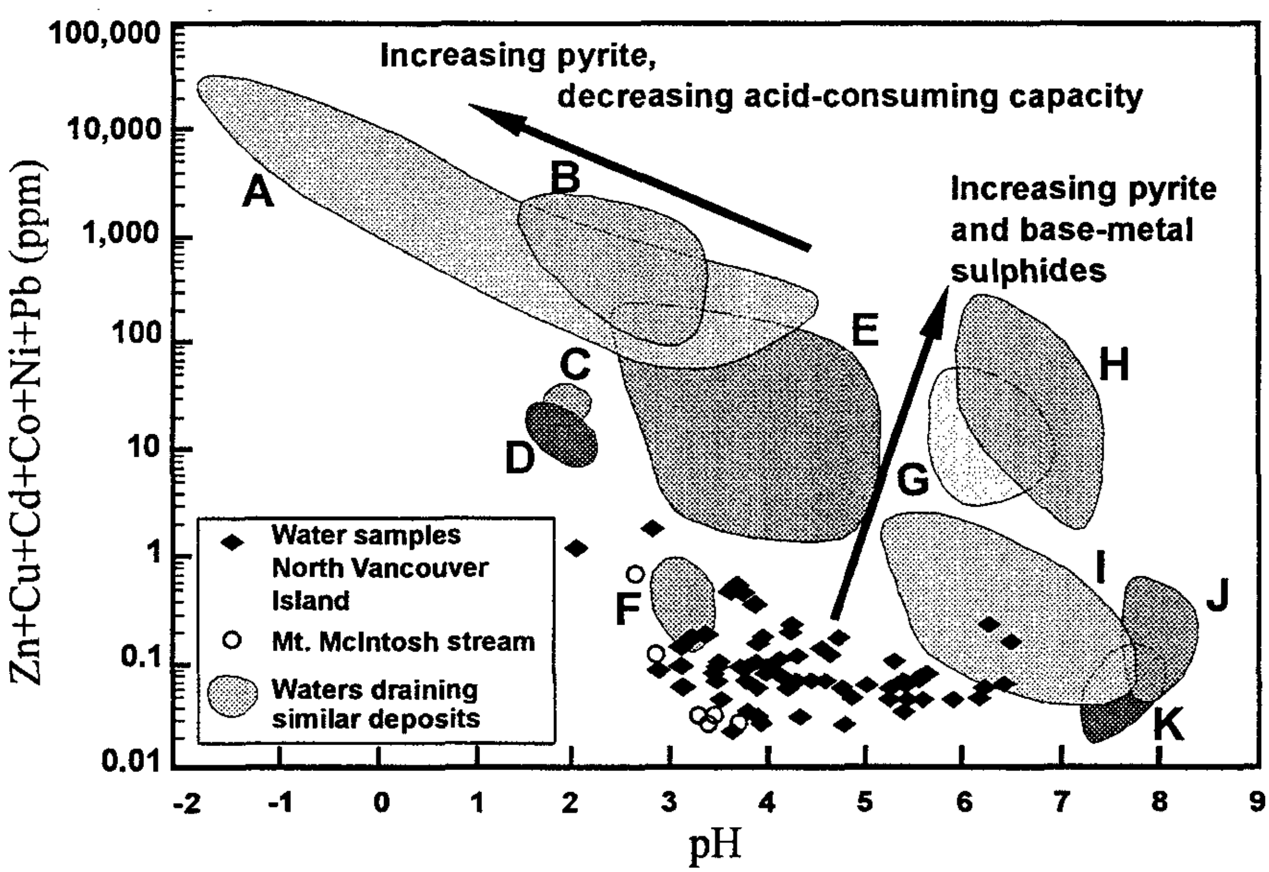


Figure 2. 'Ficklin' diagram of pH and dissolved base metal contents of waters draining diverse mine and mineral deposit types, from Plumlee *et al.* (1994). Fields are: **A** - pyrite-rich massive sulphides; **B** - sulphide-rich ores in silica-alunite-kaolinite-clay altered rocks (advanced argillic alteration); **C** - high-sulphide, low- base metal hotspring ores in acid-altered wallrocks; **D** - high-sulphide, low-base metal porphyry Mo ores in igneous wallrocks; **E** - pyrite and base metal-rich polymetallic veins and disseminations in wallrocks with low acid-buffering capability; **F** - pyrite-rich, base metal-poor veins and disseminations in wallrocks with low acid-buffering capacity; **G** - pyrite and base metal-rich polymetallic veins with carbonate gangue or carbonate-altered wallrocks; **H** - pyrite and base metal-rich, polymetallic replacements and veins in carbonate-rich sediments; **I** - polymetallic veins with moderate to low pyrite and base metal content with carbonate gangue and/or carbonate wallrock alteration; **J** - pyrite-poor polymetallic replacements in carbonate-rich sediments; **K** - pyrite-poor, Au-Te veins and breccias with carbonate gangue.

from 55 of the sites and analyzed for their $SO_4$ and metal contents. Two water samples were submitted; one for $SO_4$ and the other, acidified with nitric acid, for dissolved metals. In 1995, ten additional water samples were taken for analysis and the pH measured *in situ* using a Cole Parmer model 5941-00 pocket digital pH meter. All the geochemical analytical results are summarized in Tables 1 and 2.

Water samples taken in 1991 were neither acidified nor filtered. Replicate sampling of some sites in subsequent years with acidified samples shows no appreciable differences between the acidified and non-acidified samples for most metals. However the unacidified waters do appear to have lower iron contents and inconsistent lead values compared to acidified samples taken in later years. The 1995 sample suite provided both acidified and filtered samples and used acid-washed, ultra-clean sample bottles. For most metals there is no evident difference between metal content of these most recent, filtered samples and the earlier unfiltered ones. All waters analyzed contain very little dissolved ore metals though iron, and other metals derived from silicate mineral breakdown such as aluminum, calcium and magnesium, are present in abundance. Results of replicated sampling are given in Table 3.

## GEOENVIRONMENTAL ORE DEPOSIT MODEL

Geochemical classification and description of metal distributions within, and in waters derived from, various mineralized environments and ore deposits is currently being undertaken and is referred to as 'geoenvironmental' mineral deposit modeling. The work of the United States Geological Survey, by Ficklin *et al.* (1992) and Plumlee *et al.* (1992, 1994), among others, has documented and classified a large number of mine and natural drainages derived and evolved from various mineralized settings. The information is presented graphically in what has been referred to as a 'Ficklin' plot (Figure 2).

The data from the measured and analyzed natural drainages in this study on Vancouver Island are illustrated on Figure 2. Numerous samples have low pH (pH 2 to 4), elevated iron, magnesium, manganese and aluminum, but low levels of copper and zinc (tens to hundreds of ppb) compared to mine drainages. The waters all display low levels of metal loading, rarely greater than 3 ppm combined Zn+Cu+Cd+Co+Ni+Pb.

The effects of dilution are described by Sibbick and Laurus (1995). Their detailed follow-up work in a stream undisturbed by logging in the the Mount McIntosh area, shows that stream acidity and dissolved metals have their sources, and are most concentrated, in the strongly altered rocks from which the streams emanate or pass over. Downstream from the source areas, metal concentrations and acidity decrease due to dilution by tributary streams. Their results are shown on Figure 2 as open circles. The most acidic samples are at the source of the stream in the altered and mineralized rocks; the other circles are sample sites at 100 to 200-metre intervals downstream, where progressively greater dilution effects are evident over the measured distance of 800 metres.

## CONCLUSIONS

The main factors determining the pH and metal contents of drainages are, according to Plumlee *et al.* (1992): the acid-buffering capacity of the gangue minerals and hostrocks in which the mineralization occurs; the types and abundances of metal-bearing sulphide minerals present; the availability of sulphides for weathering; and the availability of dissolved oxygen during sulphide weathering and drainage generation. Geologic factors influencing the stream geochemistry are: deposit size, hostrock composition, wallrock alteration, surrounding geological and surficial terrains, nature of ore, trace element geochemistry, ore and gangue mineralogy and zonation, mineral characteristics, secondary mineralogy, topography and physiography, hydrology and degree of surface disruption or exploitation.

The natural acidity in the northern Vancouver Island study area is due to the abundance of pyrite in the extensive zones of advanced argillic alteration and the locally underlying porphyry copper mineralization. There is a lack of neutralizing capability in the hydrothermally altered, rhyolitic Bonanza volcanic rocks, and their related granitic bodies. Pyrite, mainly as fine-grained disseminations and fracture fillings, is abundant but little ore metal is present in the acidic leaching solutions, due to an apparent lack of ore minerals in the near-surface (weathering) environment.

In the generally wet coastal climate, rainwater with pH of about 5.6, and the augmentation of streams by surface, groundwater and tributary stream additions, results in downstream dilution of pH and metal contents. Nevertheless, streams maintain their acid character (pH <5) over distances of a few kilometres from the sources of acidity unless they flow across neutralizing rocks. In the study area, the most effective neutralization takes place in sedimentary rocks of the Parson Bay and Quatsino limestone map units and the weakly altered, zeolite and calcite-bearing basaltic units of the Bonanza volcanics.

The sources of ferruginous, base metal deficient acidic drainages derived from hydrothermally acid-leached rocks of northern Vancouver Island can be classified as 'pyrite-rich, base metal-poor veins and disseminations in wallrocks with low acid-buffering capacity' (category F on Figure 2), or more simply, (an) "acid, low-metal environment".

## REFERENCES


Archibald, D. A. and Nixon, G. T., (1995): $^{40}Ar/^{39}Ar$ Geochronometry of Igneous Rocks in the Quatsino - Port McNeill Area, Northern Vancouver Island (92L/12, 11); *in* Geological Fieldwork 1994, Grant, B. and Newell, J. M., Editors, *B. C. Ministry of Energy, Mines and Petroleum Resources*, Paper 1995-1, pages 49-59.

Dasler, P.G., Young, M.J., Perelló, J. and Giroux, G. (1995): The Hushamu Porphyry Copper-Gold Deposit, Northern Vancouver Island, British Columbia; *in* Porphyry Deposits of the Northern Cordillera of North America, Schroeter, T.G., Editor, *Canadian Institute of Mining, Metallurgy and Petroleum*, Special Volume 46, in press.

Ficklin, W.H., Plumlee, G.S., Smith, K.S. and McHugh, J.B. (1992): Geochemical Classification of Mine Drainages and Natural Drainages in Mineralized Areas; *in* Water-Rock Interaction, Proceedings of the 7th International Symposium on Water-rock Interactions, Kharaka, Y.K. and Maest, A.S., Editors, A.A. *Balkema* , Rotterdam, pages 381-384.

Hammack, J.L., Nixon, G.T., Koyanagi, V.M., Payie, G.J., Panteleyev, A., Massey, N.W.D., Hamilton, J.V. and Haggart, J.W. (1994): Preliminary Geology of the Quatsino - Port McNeill Area, Northern Vancouver Island, NTS 92L/11W,12; *B. C. Ministry of Energy, Mines and Petroleum Resources,* Open File 1994-26, Scale 1:50 000, 2 sheets.

Koyanagi, V.M. and Panteleyev, A. (1993): Natural Acid Rock-drainage in the Red Dog - Hushamu - Pemberton Hills Area, Northern Vancouver Island (92L/12); *in* Geological Fieldwork 1992, Grant, B. and Newell, J. M., Editors, *B. C. Ministry of Energy, Mines and Petroleum Resources*, Paper 1993-1, pages 445-450.

Koyanagi, V.M. and Panteleyev, A. (1994): Natural Acid Rock-drainage in the Red Dog - Hushamu - Pemberton Hills Area, Northern Vancouver Island; *in* Geological Fieldwork 1993, Grant, B. and Newell, J. M., Editors, *B. C. Ministry of Energy, Mines and Petroleum Resources*, Paper 1994-1, pages 119-125.

Nixon, G.T., Hammack, J.L., Koyanagi, V.M., Payie, G.J., Massey, N.W.D., Hamilton, J.V. and Haggart, J.W. (1994): Preliminary Geology of the Quatsino - Port McNeill Map Areas, Northern Vancouver Island (92L/12, 11); *in* Geological Fieldwork 1993, Grant, B. and Newell, J. M., Editors, *B. C. Ministry of Energy, Mines and Petroleum Resources,* Paper 1994-1, pages 63-85.

Panteleyev, A. and Koyanagi, V.M. (1993): Advanced Argillic Alteration in Bonanza Volcanic Rocks, Northern Vancouver Island - Transitions Between Porphyry Copper and Epithermal Environments; *in* Geological Fieldwork 1992, Grant, B. and Newell, J. M., Editors, *B. C. Ministry of Energy, Mines and Petroleum Resources*, Paper 1993-1, pages 287-293.

Panteleyev, A. and Koyanagi, V.M. (1994): Advanced Argillic Alteration in Bonanza Volcanic Rocks, Northern Vancouver Island - Lithologic and Permeability Controls; *in* Geological Fieldwork 1993, Grant, B. and Newell, J. M., Editors, *B. C. Ministry of Energy, Mines and Petroleum Resources*, Paper 1994-1, pages 101-109.

Panteleyev, A., Bobrowsky, P.T., Nixon, G.T. and Sibbick, S.J. (1994): Northern Vancouver Island Integrated Project; *in* Geological Fieldwork 1993, Grant, B. and Newell, J. M., Editors, *B. C. Ministry of Energy, Mines and Petroleum Resources*, Paper 1994-1, pages 59-62.

Panteleyev, A., Reynolds, P.H. and Koyanagi, V.M. (1995): $^{40}Ar/^{39}Ar$ Ages of Hydrothermal Minerals in Acid Sulphate-altered Bonanaza Volcanics, Northern Vancouver Island; *in* Geological Fieldwork 1994, Grant, B. and Newell, J. M., Editors, *B. C. Ministry of Energy, Mines and Petroleum Resources*, Paper 1995-1, pages 61-65.

Plumlee, G.S., Smith, K.S., Ficklin, W.H. and Briggs, P.H. (1992): Geological and Geochemical Controls on the Composition of Mine Drainages and Natural Drainages in Mineralized Areas; *in* Water-Rock Interaction, Proceedings of the 7th International Symposium on Water-rock Interactions, Kharaka, Y.K. and Maest, A.S., Editors, *A.A. Balkema*, Rotterdam, pages 419-422.

Plumlee, G.S., Smith, K.S., and Ficklin, W.H (1994): Geoenvironmental Models of Mineral Deposits, and Geology-Based Mineral-Environmental Assessments of Public Lands; *U. S. Geological Survey*, Open-File Report 94-203, 7 pages.

Sibbick, S.J. and Laurus K.A. (1995): Investigation of a Natural Acid Rock Drainage and an Anomalous Mercury-bearing Stream, Northern Vancouver Island; *in* Geological Fieldwork 1994, Grant, B. and Newell, J. M., Editors, *B. C. Ministry of Energy, Mines and Petroleum Resources*, Paper 1995-1, pages 67-70.

# SUMMARY OF THE INTERIOR PLATEAU PROGRAM: ACTIVITIES BY THE BRITISH COLUMBIA GEOLOGICAL SURVEY IN THE SOUTHERN NECHAKO PLATEAU (Parts of 93F,C,K)

**By L.J. Diakow, S.J. Cook, R.A. Lane, V.M. Levson and T.G. Schroeter**

*(B.C. Ministry of Energy, Mines and Petroleum Resources Contribution to the Interior Plateau Program, Canada - British Columbia Mineral Development Agreement 1991 - 1995)*

*KEYWORDS:* Southern Nechako Plateau, Interior Plateau, regional geology, surficial geology, mineral deposits, lake sediment geochemistry, till geochemistry.

## INTRODUCTION

The Interior Plateau Program is a federal-provincial multidisciplinary geoscience initiative funded under the guidelines of the Mineral Development Agreement. The program, ongoing since 1992, and involving projects by geoscientists from the Geological Survey of Canada and the British Columbia Geological Survey Branch, concluded in 1995. Individual projects are currently in the write-up stage, with final reports to be collated in a volume that is scheduled for publication in March, 1996.

Prospective geological environments for a variety of mineral deposits exist in the Interior Plateau as inferred from some important mines located in the region (Figure 1). However, mineral exploration in this region has generally been hampered by a number of factors, some of which include: inaccessibility, vegetation and glacial cover, and a blanket of Neogene lava flows. Outdated bedrock mapping and lack of surficial mapping, regional gochemistry and modern geophysical coverage were major deficiencies in the geoscience database prior to the start of the Interior Plateau Program. The purpose of this program was to identify mineral potential and promote mineral exploration through improved understanding of the geology of the region. Furthermore, there is a need to develop and evaluate drift exploration models and geochemical exploration techniques applicable to drift-covered plateau regions, and to determine geochemical pathfinder elements and their significant thresholds in tills and lake sediments on the Interior Plateau.

Projects directed by the British Columbia Geological Survey Branch include bedrock and surficial geology mapping at 1:50 000 scale, till and lake sediment geochemistry and mineral deposit investigations (Figures 2 and 3). Most of these scientific studies were fully integrated and conducted in the Nechako Plateau. The exception is in the southern Fraser Plateau, where bedrock mapping along the Coast-Intermontane belt boundary was completed in 1995 (see Schiarizza, 1996; this volume).

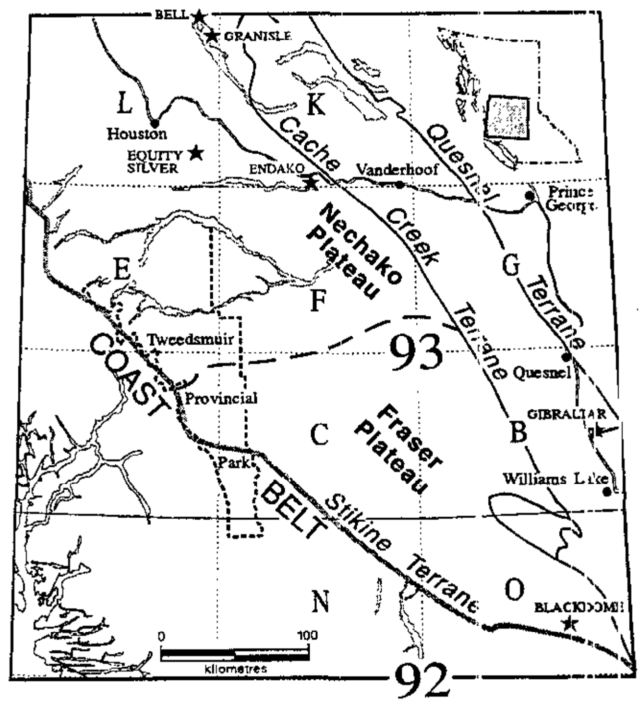


Figure 1. Tectonstratigraphic terranes and physiographic subdivisions in central British Columbia.

The integrated approach of projects in the Nechako area has been highly successful; significantly improving geological understanding and having a profound impact on grassroots mineral exploration. During the 1993 field program, new mineral occurrences such as the Tommy gold prospect was discovered. More than 1300 claim units were staked in 1994; more than ten times the 1993 level, and a 35% increase over 1992. This activity is the direct result of new discoveries and publication of new geoscience data, specifically bedrock, till and regional geochemical maps.

## BEDROCK MAPPING

Bedrock mapping at 1:50 000 scale, conducted over three field seasons in the southern Nechako Plateau, has been completed in four mapsheets covering roughly 3500 square kilometres, centred on the Fawnie and Nechako ranges and connected east-west trending ridges of the Entiako Spur and Naglico Hills. These studies include mapping in the Natalkuz Lake (93F/6, Diakow *et al.*, 1993; Green and Diakow, 1993), Fawnie Creek (93F/3, Diakow and Webster, 1994; Diakow *et al.*, 1994), Tsacha Lake (93F/2, Diakow *et al.*, 1995a, b) and Chedakuz Creek (93F/7, Diakow *et al.*, 1995c) map areas.

Objectives of the mapping project were to determine stratigraphic, plutonic and structural relationships, establish a framework of geological events and identify favorable environments to focus exploration for epithermal precious metals and porphyry style mineralization. The main conclusions of this program are summarized here.

### *LITHOSTRATIGRAPHY*

The southern Nechako Plateau region is underlain by rocks that vary in age from Late Triassic to Neogene. The stratigraphy comprises rare Late Triassic marine sediments at the base, succeeded by two sequences of interlayered volcanic rocks and volcaniclastic sediments containing fossils that range in age from early Toarcian to early Bajocian. Early volcanism (Toarcian and Aalenian?) is exclusively rhyolitic in composition; it contrasts with a younger (Bajocian?), predominately basaltic event. Both sequences record island arc volcanic activity and associated intrabasinal sedimentation. Early Callovian marine siltstone and shale are sporadically exposed. In places, sections feature chert-bearing conglomerate interbeds that become more prevalent eastward from the Fawnie Range towards the Nechako Range. The probable provenance of chert detritus is the Cache Creek Terrane lying immediately to the east. New radiometric dates from areally restricted, unnamed volcanic remnants suggest that subaerial eruptions recurred during Late Jurassic (*ca.* 152 Ma), Jura-Cretaceous (*ca.* 144 Ma) and Late Cretaceous time (*ca.* 65 Ma).

Tectonic uplift of the Fawnie and Nechako ranges preceeded a regional episode of high-potassium calcalkaline volcanism that characterizes Paleogene time. During Middle Eocene time the Ootsa Lake Group, dominated by continental arc rhyolitic and less voluminous andesitic rocks, formed an extensive volcanic field. At present these strata occupy a small area of the uplifted region; however, they are widespread in topographically lower regions to the north and south. In the Fawnie Range these rocks record the growth of flow

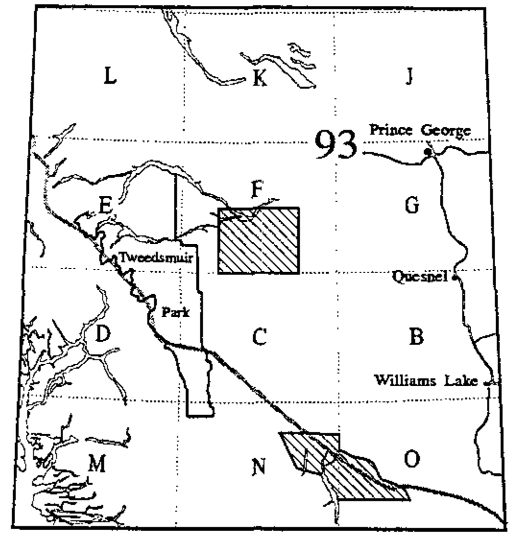


Bedrock Mapping

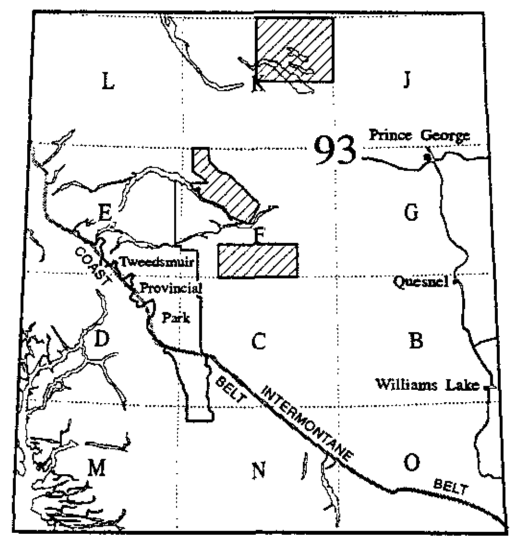


Regional Lake Sediment Geochemistry

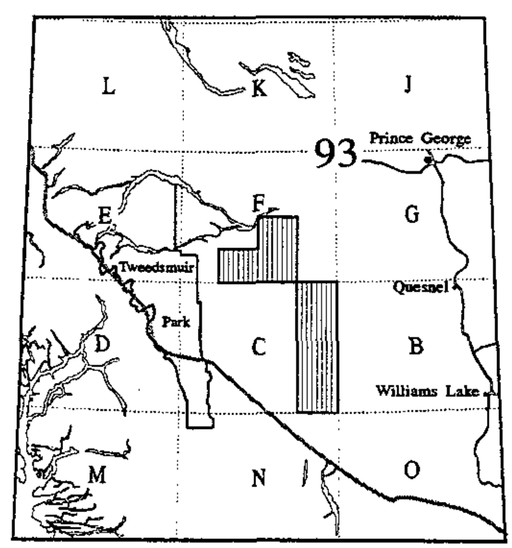


Surficial Geology and Till Geochemistry

Figure 2. Location of geoscience projects in the Interior Plateau region.

domes and the development of a relatively small volcanic subsidence structure superposed on older Jurassic plutonic and volcanic rocks. The Endako Group is a sequence of high-potassium andesitic flows that have compositional continuity with volcanic rocks of the Ootsa Lake Group. Their source is believed to be broad volcanic centres that lay to the north of the uplifted region. By Neogene time, alkaline shield volcanoes and probable fissures erupted extensive sheets of basaltic flows assigned to the Chilcotin Group. The Chilcotin Group, restricted to the southern flank of the Nechako and Fawnie ranges, apparently thickens southward toward stratovolcanoes comprising the Anahim volcanic belt.

## *PLUTONIC EVENTS*

The oldest plutonic rocks are small stocks and plugs of augite porphyry that are interpreted as subvolcanic feeders for Middle Jurassic augite phyric basaltic rocks. The Jura-Cretaceous (*ca.* 141 Ma) Capoose batholith underlies much of the western part of the Fawnie Range. The composition of this intrusion is relatively uniform, varying from hornblende-biotite granodiorite to quartz monzonite. Several newly discovered epithermal precious metal prospects are related to hydrothermal activity localised along the margin of the pluton. A single small outcrop of biotite-bearing dacite flows yields a radiometric age (K-Ar, 144 Ma) that is contemporaneous with the Capoose batholith, suggesting that Jura-Cretaceous magmatism may have had an extrusive component, much of which either has been subsequently eroded or is indistinguishable in the field from older volcanic rocks.

Late Cretaceous magmatism is restricted to the northern part of the Fawnie Range where felsic sills and dikes on the Capoose property contain disseminated silver. These hypabyssal intrusions have radiometric ages of 64 to 68 Ma, identical to granodiorite that was dated previously (Andrew, 1988), and mapped in this study as part of the Capoose batholith. New radiometric dates, however, suggest the batholith is significantly older (*ca.* 141 Ma). The discrepancy in ages suggests that the batholith may be a composite body, cut by a younger, compositionally similar pluton that is comagmatic with felsic hypabyssal rocks on the Capoose property. Uranium-lead zircon geochronology is in progress to better define the age of the Capoose batholith. Throughout the Nechako Range, dioritic stocks, sills and dikes cut penetratively cleaved Callovian and older strata. Locally they are weakly mineralized, carrying disseminated copper. Eocene intrusions occur in several widely spaced areas with volcanic rocks of the Ootsa Lake Group. At the Wolf precious metal prospect, an Eocene potassium feldspar megacrystic sill, believed to be comagmatic with felsic extrusive rocks, forms a resistive caprock on the deposit. Quartz feldspar porphyry sills and small plugs occur mainly in the central Fawnie Range, near outliers of the Ootsa Lake Group. The CH pluton has recently determined K-Ar dates on hornblende and biotite of 52 Ma and 49 Ma, respectively; it crops out about 1 kilometre west of porphyry copper showings on the CH property.

## *STRUCTURE*

Mesozoic rocks dominate the Fawnie and Nechako ranges, but they terminate abruptly to the north and south, where topographically subdued terrain is underlain primarily by Eocene and younger volcanic successions. These dramatic changes in physiography and stratigraphy reflect a broad horst, called the Nechako uplift. A series of northeast-trending faults delimit the horst to the north and south, and internally offset stratigraphy as young as Middle Eocene.

The timing of structural uplift is uncertain, but it may be contemporaneous with deformation that imparted a pervasive penetrative cleavage and local mylonitic fabric on Jurassic strata in the Nechako Range. $^{40}Ar/^{39}Ar$ dating of sericite developed on the cleavage planes of probable Aalenian volcanic rocks is suggestive of Late Cretaceous deformation. Undated dioritic plutons and the Eocene CH stock truncate the predominant northwest-trending structural fabric in the Nechako Range.

The Nechako horst may have remained a slightly elevated region for much of Tertiary time. The distribution and thickness of Eocene and younger volcanic units diminishes over the horst, relative to extensive volcanic fields to the north and south. In the uplifted region Eocene strata are restricted to several outliers that rest upon Middle Jurassic rocks. Block faults, accompanied locally by caldera subsidence and the emplacement of hypabyssal and epizonal plutons, all emphasize the extensional regime that characterized the Nechako uplift during Eocene time.

# MINERAL DEPOSIT STUDIES

Twenty metallic mineral occurrences ranging from newly discovered showings to developed prospects, were studied in parts of the Nechako (NTS 93F) and Anahim (NTS 93C) map areas (Figure 3). Each occurrence was characterized in terms of geologic setting, structural controls, style of mineralization, ore mineralogy and alteration assemblage. The Holy Cross and Wolf occurrences were mapped at 1:10 000 scale, and a map of the former published (Lane, 1995). Descriptions of most other mineral occurrences have also been published (Lane and Schroeter, 1995; Schroeter and Lane, 1992, 1994). At present, K-Ar and U-Pb geochonology and trace lead analysis for specific deposits are in progress at the University of British Columbia.

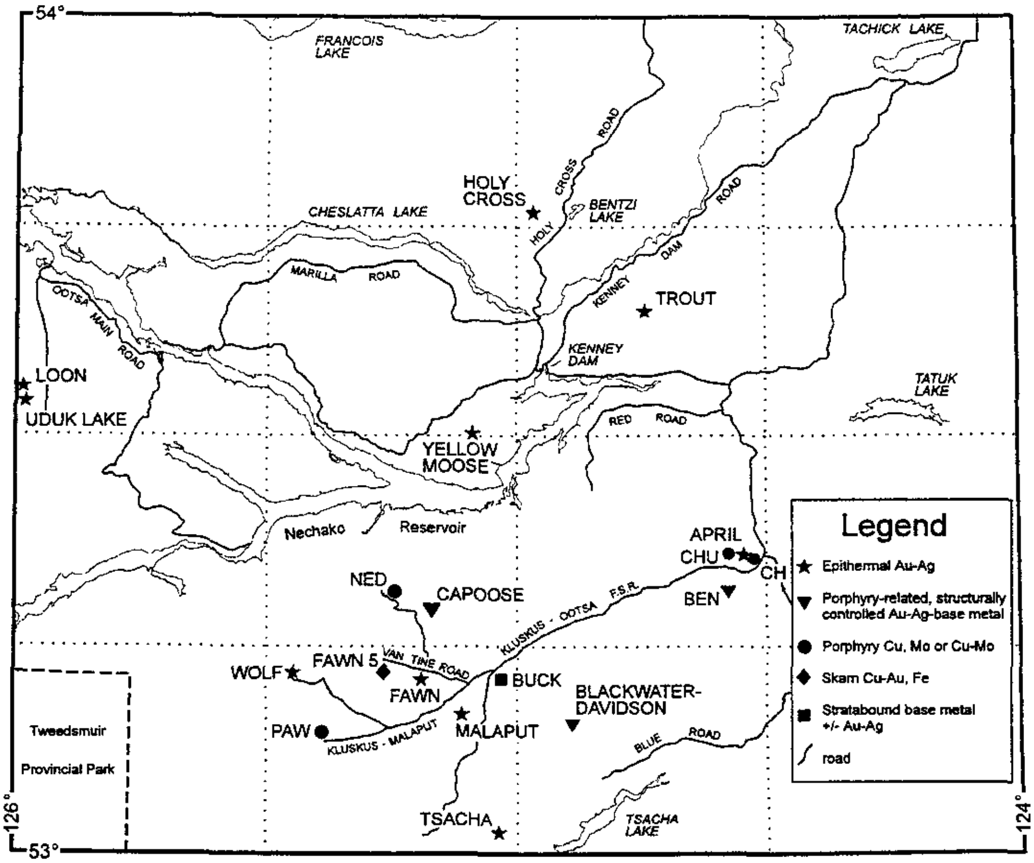


Figure 3. Location of metallic mineral occurrences investigated in the southern Nechako Plateau.

Mineral occurrences appear to be associated with three magmatic episodes: Eocene (*ca.* 50 Ma) and Late Cretaceous (*ca.* 65 Ma.) felsic volcanism and plutonism and Jura-Cretaceous calcalkaline intrusive activity (*ca.* 141 Ma.). Eocene mineral occurrences consist of:

- low-sulphidation, adularia-sericite epithermal gold-silver quartz vein systems related to northerly trending structures and rhyolitic volcanic activity that characterizes the Ootsa Lake Group throughout much of the Nechako area. Such occurrences have bonanza vein and bulk-tonnage potential; examples include the Wolf, Clisbako and Holy Cross prospects.
- Porphyry copper and/or molybdenum prospects in Jurassic country rocks are spatially associated with Eocene granodiorite of the CH stock.

Older deposits are associated with probable Late Cretaceous or older (?) subvolcanic rhyolitic intrusions carrying disseminated and fracture-controlled silver-gold-zinc mineralization at the Capoose prospect or within thermally altered and hornfelsed Middle Jurassic volcanic rocks marginal to the Jura-Cretaceous Capoose batholith. Notable examples include porphyry molybdenum-copper occurrences (Ned); iron and copper-gold skarn (Fawn 5) and, gold and silver-bearing epithermal quartz-vein stockworks (Tsacha).

## LAKE SEDIMENT GEOCHEMISTRY STUDIES

A variety of lake sediment geochemistry studies were conducted in the Nechako Plateau region between 1992 and 1995 (Cook, 1993, 1995; Cook and Jackaman, 1994a, b; Cook and Luscombe, 1995; Cook *et al.*, 1994, 1995). The lake sediment geochemistry program had two major components: (1) detailed case studies of individual lakes, to provide a better understanding of how sediment geochemistry reflects the presence of adjacent mineral deposits, and (2) regional geochemical surveys, to provide baseline data for mineral exploration and environmental studies.

### *LAKE SEDIMENT CASE STUDIES*

Case studies were completed at 25 lakes in 18 localities. The main objective was to determine the effectiveness of lake sediments as a sample medium for future regional geochemical surveys. A secondary objective was to determine their usefulness in more advanced, property-scale stages of geochemical exploration, by characterizing metal distribution patterns in different types of lake sediments typically found in the area. The main conclusions are as follows:

- Metal concentrations in lake sediment reflect the presence of adjacent epithermal gold and porphyry copper or molybdenum mineralization in each of seven case studies. Specifically, centre-lake gold concentrations of 4 ppb or greater, and molybdenum concentrations of 12 ppm or greater at these sites reflected the presence of epithermal and porphyry prospects, respectively.
- Considerable within-lake geochemical variations occur between individual sub-basins of the same lake, and between near-shore and profundal sediment within sub-basins.
- In the case of gold, centre-lake sediments may, but do not necessarily, contain the highest gold concentrations present in the surveyed lakes. Greater gold concentrations may occur in near-shore organic-rich sediments, particularly near drainage in-flows. Gold distribution patterns in the sediment may reveal the locations of stream water and ground water in-flows draining upstream or upslope mineralized bedrock, or its dispersed remnants within till or colluvium.
- Different types of lakes (seepage and drainage) with anomalous sediment geochemistry may require different follow-up exploration strategies. At a minimum, follow-up sampling of any lake sediment anomaly should involve resampling of the original site and verification of the analytical result. However, the data suggest that drainage lakes, which lose water by stream flow through an outlet, are more likely to show near-shore zonation patterns than the generally smaller and more geochemically homogenous seepage lakes, which lack stream in-flows or out-flows. Detailed sampling of anomalous drainage lakes may be an effective tool to map out potential metal zonation patterns and to determine the general direction toward any covered mineral occurrences within a watershed.

### *REGIONAL LAKE SEDIMENT GEOCHEMISTRY SURVEYS*

Much of the Nechako Plateau region, with its subdued topography and abundance of lakes, is better suited for regional lake sediment than stream sediment geochemical surveys. Prior to the beginning of the Interior Plateau Program large tracts of the Nechako and Fraser plateaus lacked regional lake sediment geochemical coverage, and available RGS data were restricted to the eastern parts of the Whitesail Lake (NTS 93E-RGS 16) and Smithers (NTS 93L-RGS 17) map areas.

Three small regional lake sediment geochemical surveys were completed in the Nechako (NTS 93F) and Fort St. James (NTS 93K- results not yet released) areas between 1993 and 1995. They cover an area of about 7300 square kilometres at an average sampling density of about 1 site per 8.3 square kilometres. Objectives of this program are to provide baseline geochemical data necessary for both grassroots mineral exploration and for environmental studies. Geochemical patterns corroborate earlier lake sediment anomalies (e.g., Wolf prospect), enlarge target areas around currently known deposits, and outline new prospective areas (e.g., Tsacha prospect). Significantly, regional lake sediment geochemistry results highlight the epithermal precious metal potential of Jurassic, as well as Eocene, volcanic units. Furthermore, the locations of all five precious and base-metal prospects recorded in the MINFILE database in the Fawnie Creek map area (NTS 93F/3), and located near lakes, were reflected by elevated metal concentrations greater than the 95th percentile of the regional data set.

Implementation of the regional surveys was guided by the results of prior orientation case studies. The following guidelines are useful for conducting regional geochemical surveys in the Nechako Plateau:

- Centre-basin sediment is most suitable for regional surveys, due to its greater homogeneity and higher proportion of fine-grained organic material relative to near-shore sediment.
- Lake sediment geochemical surveys are most effective in this area if every lake in the survey area is sampled, rather than sampling only a selection of lakes at a fixed site density.
- Sampling designs must accomodate the geochemical variation which may be present between separate sub-basins of any one lake. Collection of a single centre-basin sample is sufficient for ponds and smaller lakes, but additional samples should also be obtained from the centres of any major sub-basins.
- There are no simple guidelines for metal signatures in anomalous lakes adjacent to epithermal prospects. Sediment geochemistry in anomalous lakes is related to the geochemistry of the mineralized system, and sediments may, but do not necessarily, exhibit multi-element geochemical signatures. Metal signatures range from multi-element (gold-silver-arsenic-molybdenum-zinc) at the Wolf prospect, to single element (gold) at the Tsacha prospect.

## SURFICIAL GEOLOGY MAPPING AND REGIONAL TILL GEOCHEMISTRY

Regional till geochemical surveys and 1:50 000-scale surficial geology mapping were conducted to aid mineral exploration in areas of thick glacial drift. Stratigraphic and sedimentologic studies of Quaternary deposits were also completed in order to define the glacial history and help in interpreting till geochemical data. The main objectives of the program were to map the distribution of Quaternary deposits, decipher the glacial history, identify geochemically anomalous areas, refine models of glacial dispersal and develop methods of drift exploration applicable to the Interior Plateau.

A number of publications relating to this program have been released, including surficial geology and till geochemistry data for the Fawnie Creek map area (NTS 93F/3), Giles and Levson (1994a,b), Levson and Giles (1994) and Levson *et al.* (1994). Recent surficial geology data are available for the Chilanko Forks - Chezacut map areas (93C/1 and 8, respectively), Giles and Kerr (1993), Kerr and Giles (1993a,b); the Clusko River - Toil Mountain map areas (93C/9 and 16, respectively), Proudfoot (1993), Proudfoot and Allison, (1993a,b); the Tsacha Lake - Chedakuz Creek map areas (93F/2 and 7, respectively), Giles and Levson (1995), Giles *et al.* (1995), Weary *et al.* (1995); and Fulton Lake - Old Fort Mountain map areas (93L/16 and 93M/1, respectively), Huntley *et al.*, (1996, this volume). Detailed investigations around areas of known mineralization have also been conducted as part of this program (Levson and Giles, 1995; O'Brien *et al.*, 1995; Stumpf *et al.* (1996, this volume).

### *RESULTS*

Results of Quaternary geology studies indicate that glacial dispersal processes in the region are dominated by the last (Late Wisconsinan) glaciation. In most areas there was one dominant ice-flow direction, influenced by topography during both early and late stages of the Late Wisconsinan (*e.g.*, Levson and Giles, 1994; Levson *et al.*, 1994). Morainal sediments are widespread in the Interior Plateau region; they form a cover, varying in thickness from a few metres to several tens of metres in low-lying areas, to less than 2 metres in upland regions. Glaciofluvial sediments are also common, occurring as eskers, kames, terraces, fans and outwash plains in valley bottoms and along valley flanks. They consist mainly of poorly to well sorted, stratified, pebble and cobble gravels and sands. Glaciolacustrine sediments are common in some valleys, generally at elevations below 750 to 950 metres, often near modern lakes. Stratigraphic studies of Quaternary deposits indicate ice damming during both advance and retreat stages of the last glaciation.

Geochemical anomalies associated with glacial dispersal of mineralized bedrock in the region are up to a few kilometres long and several hundred metres or more wide, but some anomalies cover much larger areas (Levson and Giles, 1995). Erratics trains are typically up to several kilometres long and more readily detected than till anomalies. Both erratics trains and geochemical anomalies in till show a pronounced elongation parallel to ice-flow direction. In areas of thick till, near-surface anomalies may be displaced by 500 metres or more down-ice from their bedrock source. As the till geochemistry reflects up-ice bedrock sources and not the immediately underlying bedrock, subsurface exploration targets should be up-ice, rather than at the head of the anomaly.

Basal till sampling is an effective tool for regional exploration programs in drift-covered parts of the Interior Plateau (Levson *et al*, 1994, Cook *et al.*, 1995; Kerr and Levson, 1995). To reflect mechanical dispersal processes, samples should be collected from the C soil horizon. For property-scale exploration programs, where sediment types other than basal tills may be sampled, sedimentologic data should be collected at all sample sites in order to distinguish till from glacigenic debris-flow, colluvial, glaciofluvial or glaciolacustrine sediments. These sediments have different processes of transportation and deposition which must be recognized in order to understand associated mineral anomaly patterns. Similarly, an understanding of ice-flow history, glacial dispersal processes, transportation distances and Quaternary stratigraphy are considered essential for successful drift exploration programs in this region.

## INTEGRATED GEOLOGICAL STUDIES

An important focus of the Interior Plateau Program has been the integration of geological studies from a number of different disciplines. One of the first products of these multidisciplinary studies was the production of a combined bedrock and surficial geology map of the Fawnie Creek map area (Diakow *et al.*, 1994). This was the first map of this type produced by the B.C. Geological Survey Branch in many years and, due to the positive reception it received from mineral exploration companies working in the region, two more maps of this type were produced after the 1994 field season (Diakow *et al.*, 1995b,c). Other integrated studies include: a detailed comparison of geochemical results from till and lake sediment surveys conducted in the Fawnie Creek map area (Cook *et al.*, 1995), the identification of several new exploration targets in the same area using data from bedrock geology as well as till and lake sediment geochemical studies (Diakow *et al.*, 1994; Cook *et al.*, 1994; Levson *et al.*, 1994) and an electromagnetic survey conducted to help delineate the margins of the Capoose batholith and till thickness in areas with anomalous till geochemistry (Best *et al.*, in press). Further interdisciplinary work is planned for the Nechako Plateau during the Nechako NATMAP program and may lead to the identification of other areas with high mineral potential as well as the development of exploration techniques specifically suited to this part of British Columbia.

## ACKNOWLEDGMENTS

The authors thank John Newell and Paul Matysek for critical review of the original manuscript and helpful suggestions that improved the final version.

## REFERENCES

Andrew, K.P.E. (1988): Geology and Genesis of the Wolf Precious Metal Epithermal Prospect and the Capoose Base and Precious Metal Porphyry-style Prospect, Capoose Lake Area, Central British Columbia; unpublished M.Sc. thesis, *The University of British Columbia*, 334 pages.

Best M.E., Levson, V.M. and Diakow, L.J. (in press): Time-domain Electromagnetic Surveys in Drift Covered Regions of the Fawnie Creek Map Area, British Columbia; *in* Current Research, *Geological Survey of Canada*, 1996.

Cook, S.J. (1993): Preliminary Report on Lake Sediment Studies in the Northern Interior Plateau, Central British Columbia (93C, E, F, K, L); *in* Geological Fieldwork 1992, Grant, B. and Newell, J.M., Editors, *B.C. Ministry of Energy, Mines and Petroleum Resources*, Paper 1993-1, pages 475-481.

Cook, S.J. (1995): Gold Distribution in Lake Sediments near Epithermal Gold Occurrences in the Northern Interior Plateau, British Columbia; *in* Drift Exploration in Glaciated and Mountainous Terrain, Bobrowsky, P.T., Sibbick, S.J. and Newell, J.M., Editors, *B.C. Ministry of Energy, Mines and Petroleum Resources*, Paper 1995-2.

Cook, S.J. and Jackaman, W. (1994a): Regional Lake Sediment and Water Geochemistry Surveys in the Northern Interior Plateau, B.C. (93F/2, 3, 6, 11, 12, 13, 14); *in* Geological Fieldwork 1993, Grant, B. and Newell, J.M., Editors, *B.C. Ministry of Energy, Mines and Petroleum Resources*, Paper 1994-1, pages 39-44.

Cook, S.J. and Jackaman, W. (1994b): Regional Lake Sediment and Water Geochemistry of Part of the Nechako River Map Area, (NTS 93F/2,3; Parts of 93F/6, 11, 12, 13, 14); *B.C. Ministry of Energy, Mines and Petroleum Resources*, Open File 1994-19.

Cook, S.J. and Luscombe, M.E. (1995): Update on 1994 Lake Sediment Geochemistry Studies in the Northern Interior Plateau, Central British Columbia (93 F); *in* Geological Fieldwork 1994, Grant, B. and Newell, J.M., Editors, *B.C. Ministry of Energy, Mines and Petroleum Resources*, Paper 1995-1, pages 193-197.

Cook, S.J., Levson, V.M., Giles, T.R., Diakow, L.J. and Webster, I.C.L. (1994): Drift Exploration in the Northern Interior Plateau: Application of Surficial Mapping and Integrated Geochemical Studies to Mineral Exploration; *Canadian Institute of Mining, Metallurgy, and Petroleum*, District 6 Annual General Meeting, Proceedings, pages G13-G14.

Cook, S.J., Levson, V.M., Giles, T.R. and Jackaman, W. (1995): A Comparison of Regional Lake Sediment and Till Geochemistry Surveys: A Case Study from the Fawnie Creek Area, Central British Columbia; *Exploration and Mining Geology*, Volume 4, Number 2, pages 93-110.

Diakow, L.J., Green, K., Whittles, J. and Perry, A. (1993): Geology of the Natalkuz Lake Area, Central British Columbia (NTS 93F/6); *B.C. Ministry of Energy, Mines and Petroleum Resources*, Open File 1993-14.

Diakow, L.J. and Webster, I.C.L. (1994): Geology of the Fawnie Creek Map Area (93F/3); *in* Geological Fieldwork 1993, Grant, B. and Newell, J.M., Editors, *B.C. Ministry of Energy, Mines, and Petroleum Resources*, Paper 1994-1, pages 15-26.

Diakow, L.J., Webster, I.C.L., Levson, V.M. and Giles, T.R. (1994): Bedrock and Surficial Geology of the Fawnie Creek Map Area (NTS 93F/3); *B.C. Ministry of Energy, Mines and Petroleum Resources*, Open File 1994-2.

Diakow, L.J., Webster, I.C.L., Whittles, J.A. and Richards, T.A. (1995a): Stratigraphic Highlights of Bedrock Mapping in the Southern Nechako Plateau, Northern Interior Plateau Region; *in* Geological Fieldwork 1994, Grant, B. and Newell, J.M., Editors, *B.C. Ministry of Energy, Mines and Petroleum Resources*, Paper 1995-1, pages 171-176.

Diakow, L.J., Webster, I.C.L., Whittles, J.A., Richards, T.A., Giles, T.R. and Levson, V.M. (1995b): Bedrock and Surficial Geology of the Tsacha Lake Map Area (NTS 93F/2); *B.C. Ministry of Energy, Mines and Petroleum Resources*, Open File 1995-16.

Diakow, L.J., Webster, I.C.L., Whittles, J.A., Richards, T.A., Giles, T.R. Levson, V.M. and Weary, G.F. (1995c): Bedrock and Surficial Geology of the Chedakuz Creek Map Area (NTS 93F/7); *B.C. Ministry of Energy, Mines and Petroleum Resources*, Open File 1995-17.

Giles, T.R. and Kerr, D.E. (1993): Surficial Geology in the Chilanko Forks and Chezacut Areas (93C/1, 8); *in* Geological Fieldwork 1992, Grant, B. and Newell, J.M., Editors, *B.C. Ministry of Energy, Mines and Petroleum Resources*, Paper 1993-1, pages 483-490.

Giles, T.R. and Levson, V.M. (1994a): Surficial Geology and Drift Exploration Studies in the Fawnie Creek Area (93F/3); *in* Geological Fieldwork 1993, Grant, B. and Newell, J.M., Editors, *B.C. Ministry of Energy, Mines and Petroleum Resources*, Paper 1994-1, pages 27-37.

Giles, T.R. and Levson, V.M. (1994b): Drift Prospecting Potential of the Fawnie Creek Area (NTS 93F/3); *B.C. Ministry of Energy, Mines and Petroleum Resources*, Open File 1994-10 (1:50 000 map).

Giles, T.R. and Levson, V.M. (1995): Surficial Geology and Quaternary Stratigraphy of the Tsacha Lake Area (NTS 93F/2); *B.C. Ministry of Energy, Mines and Petroleum Resources*, Open File 1995-10 (1:50 000 map).

Giles, T.R., Levson, V.M. and Weary, G.F. (1995): Surficial Geology and Drift Exploration Studies in the Tsacha Lake and Chedakuz Creek Areas (NTS 93F/2, 7), Central British Columbia; *in* Geological Fieldwork 1994, Grant, B. and Newell, J.M., Editors, *B.C. Ministry of Energy, Mines and Petroleum Resources*, Paper 1995-1, pages 199-205.

Green, K.C. and Diakow, L.J. (1993): The Fawnie Range Project - Geology of the Natalkuz Lake Map Area (93F/6); *in* Geological Fieldwork 1992, Grant, B. and Newell, J.M., Editors, *B.C. Ministry of Energy, Mines and Petroleum Resources*, Paper 1993-1 pages 57-67.

Huntley, D.H., Stumpf, A., Levson, V.M. and Broster, B.E. (1996): Babine Porphyry Belt Project: Quaternary Geology and Regional Till Geochemistry Sampling in the Old Fort Mountain (93M/01) and Fulton Lake (93L/16) Map Areas, British Columbia; *in* Geological Fieldwork 1995, Grant, B. and Newell, J.M., Editors, *B.C. Ministry of Energy, Mines and Petroleum Resources*, Paper 1996-1, this volume.

Kerr, D.E. and Giles, T.R. (1993a): Surficial Geology of the Chilanko Forks Area (NTS 93C/1); *B.C. Ministry of Energy, Mines and Petroleum Resources*, Open File 1993-16 .

Kerr, D.E. and Giles, T.R. (1993b): Surficial Geology of the Chezacut Area (NTS 93C/8); *B.C. Ministry of Energy, Mines and Petroleum Resources*, Open File 1993-17.

Kerr, D.K. and Levson, V.M. (1995): Annotated Bibliography of Drift Prospecting Activities in British Columbia; *in* Drift Exploration in Glaciated and Mountainous Terrain, Bobrowsky, P.T., Sibbick, S.J. and Newell, J.M., Editors, *B.C. Ministry of Energy, Mines and Petroleum Resources*, Paper 1995-2.

Lane, R.A. (1995): Preliminary Bedrock Geology, Holy Cross Mountain to Bentzi Lake, Central British Columbia (NTS 93F/14E and 15W); B.C. Ministry of Energy, Mines and Petroleum Resources, Open File 1995-22.

Lane, R.A. and Schroeter, T.G. (1995): Mineral Occurrence Investigations and Exploration Monitoring in the Interior Plateau (93F/2, 7, 10, 11, 12, 14, 15 and 93C/9 and 16); *in* Geological Fieldwork 1994, Grant, B. and Newell, J.M., Editors, *B.C. Ministry of Energy, Mines and Petroleum Resources*, Paper 1995-1, pages 177-191.

Levson, V.M. and Giles, T.R. (1994): Surficial Geology and Quaternary Stratigraphy of the Fawnie Creek Area (NTS 93F/3); *B.C. Ministry of Energy, Mines and Petroleum Resources*, Open File 1994-9 .

Levson, V.M. and Giles, T.R. (1995): Glacial Dispersal Patterns of Mineralized Bedrock with Examples from the Nechako Plateau, Central British Columbia; *in* Drift Exploration, Bobrowsky, P.T., Sibbick, S.J. and Newell, J.M., Editors, *B.C. Ministry of Energy, Mines and Petroleum Resources*, Paper 1995-2.

Levson, V.M., Giles, T.R., Cook, S.J. and Jackaman, W. (1994): Till Geochemistry of the Fawnie Creek Area (93F/03); *B.C. Ministry of Energy, Mines and Petroleum Resources*, Open File 1994-18, 34 pages.

O'Brien, E.K. Broster, B.E. Giles, T.R. and Levson, V.M. (1995) Till Geochemical Sampling: CH, Blackwater-Davidson, and Uduk Lake Properties, British Columbia: Report of Activities; *in* Geological Fieldwork 1994. Grant, B. and Newell, J.M., Editors, *B.C. Ministry of Energy, Mines and Petroleum Resources*, Paper 1995-1, pages 207-211.

Proudfoot, D.N. (1993): Drift Exploration and Surficial Geology of the Clusko River (93C/9) and Toil Mountain (93C/16) Map Sheets; *in* Geological Fieldwork 1992, Grant, B. and Newell, J.M., Editors, *B.C. Ministry of Energy, Mines and Petroleum Resources*, Paper 1993-1, pages 491-498.

Proudfoot, D.N. and Allison, R.F. (1993a): Surficial Geology of the Clusko River Area (NTS 93C/9); *B.C. Ministry of Energy, Mines and Petroleum Resources*, Open File 1993-18.

Proudfoot, D.N. and Allison, R.F. (1993b): Surficial Geology of the Toil Mountain Area (NTS 93C/16); *B.C. Ministry of Energy, Mines and Petroleum Resources*, Open File 1993-19.

Schiarizza, P. (1996): Tatlayoko Project Update (92N/8,9,10; 92O/5,6,12); *in* Geological Fieldwork 1995, Grant, B. and Newell, J.M., Editors, *B.C. Ministry of Energy, Mines and Petroleum Resources*, this volume.

Schroeter, T. and Lane, B. (1992): Clisbako; *in* Exploration in British Columbia 1991, *B.C. Ministry of Energy, Mines and Petroleum Resources*, pages 103-111.

Schroeter, T.G. and Lane, R.A. (1994): Mineral Resources: Interior Plateau Project (93F/3 and parts of 93F/2,6, and 7); *in* Geological Fieldwork 1993, Grant, B. and Newell, J.M., Editors, *B.C. Ministry of Energy, Mines and Petroleum Resources*, Paper 1994-1, pages 45-55.

Stumpf, A., Huntley, D.H., Broster, B.E. and Levson, V.M. (1996): Babine Porphyry Belt Project: Detailed Drift Exploration Studies in the Old Fort Mountain (93M/01) and Fulton Lake (93L/16) Map Areas, British Columbia; *in* Geological Fieldwork 1995, Grant, B. and Newell, J.M., Editors, *B.C. Ministry of Energy, Mines and Petroleum Resources*, Paper 1996-1, this volume.

Weary G.F., Giles, T.R., Levson, V.M. and Broster, B.E. (1995): Surficial Geology and Quaternary Stratigraphy of the Chedakuz Creek Area (NTS 93F/7); *B.C. Ministry of Energy, Mines and Petroleum Resources*, Open File 1995-13.

# TATLAYOKO PROJECT UPDATE (92N/8, 9, 10; 92O/5, 6, 12)

By Paul Schiarizza

*(Contribution to the Canada - British Columbia Mineral Development Agreement 1991-1995)*

*KEYWORDS:* Tatlayoko Lake, Niut Mountain, Fish Lake, Mount Moore Formation, Relay Mountain Group, Methow Terrane, Tyaughton-Methow basin, Skinner gold-quartz vein.

## INTRODUCTION

The Tatlayoko bedrock mapping program, funded by the 1991-1995 Canada - British Columbia Mineral Development Agreement, was designed to update the geological database for the eastern Coast Belt in parts of the Mount Waddington and Taseko Lakes map areas, and to integrate the structural and stratigraphic relationships established within this area with rapidly evolving concepts regarding the tectonic and stratigraphic framework of the region. This will provide an improved geological framework for understanding the settings and controls of known mineral occurrences in the area (*e.g.*, Fish Lake, Skinner) and for evaluating the potential for additional discoveries. The program was initiated in 1992 with geological mapping of the Mount Tatlow map area (Riddell *et al.*, 1993a,b). No fieldwork was done in 1993, but the project was continued in 1994 with geological mapping of the Tatlayoko Lake map area (Schiarizza *et al.*, 1995a,b). Fieldwork was completed in July of 1995, when two and a half weeks were spent mapping in the Niut Range in the northwestern corner of the project area, and two days were spent revisiting the geology near Fish Lake. The present report summarizes the findings of this 1995 fieldwork, and also presents a simplified map, tectonostratigraphic assemblage diagram and table of mineral occurrences, which provide an overview of the geology of the entire study area (Figures 3 and 4; Table 1).

The Tatlayoko project area covers the transition from the rugged Coast Mountains in the southwest, to gently rolling topography of the Fraser Plateau to the northeast. Mount Nemaia, in the central part of the area, is 250 kilometres north-northwest of Vancouver and 155 kilometres southwest of Williams Lake (Figure 1). The eastern part of the area is accessed by an all-season road that extends southwestward from Highway 20 at Hanceville to the Nemaia valley. A seasonal road branches off it at the Taseko River and continues southward to the Taseko Lakes. Tatlayoko Lake, in the western part of the area, is accessed by an all-season road that extends south from Highway 20 at Tatla Lake. A

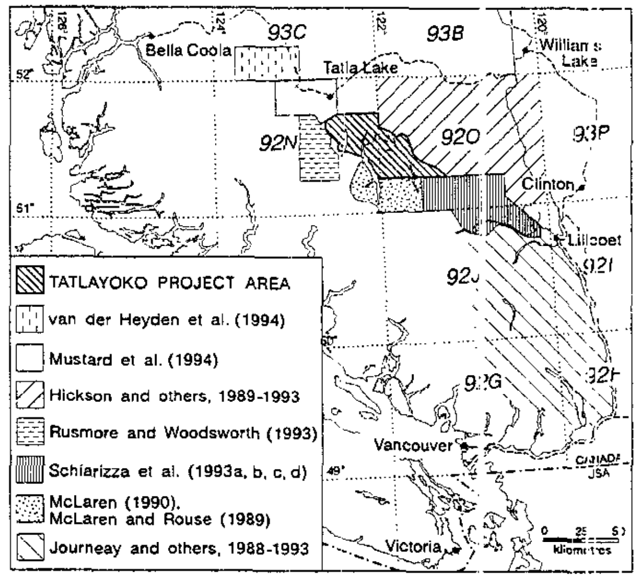


Figure 1. Location of the Tatlayoko project area. This map also provides an index to recent geological mapping by the British Columbia Geological Survey Branch and Geological Survey of Canada in adjacent parts of the southeastern Coast Belt and adjacent Intermontane Belt.

branch from this road extends eastward to the north end of Chilko Lake, and a seasonal road crosses the Chilko River and continues southward to Tsuniah Lake and the Nemaia valley.

## REGIONAL GEOLOGIC SETTING

The geologic setting of the Tatlayoko project area is summarized in Figure 2. It encompasses the boundary between the Coast and Intermontane morphogeologic belts. Within the Tatlayoko project area this boundary corresponds to the Yalakom fault, a major linear feature that extends for about 300 kilometres and was the locus of more than 100 kilometres of Late Cretaceous(?) to early Tertiary dextral displacement (Riddell *et al*, 1993a).

The eastern Coast Belt in the region of the Tatlayoko project area can be subdivided into the south Chilcotin, Methow and Niut domains of contrasting stratigraphy and structural style (Figure 2). The south Chilcotin domain includes Mississippian to Jurassic oceanic rocks of the Bridge River accretion-subduction complex, Upper

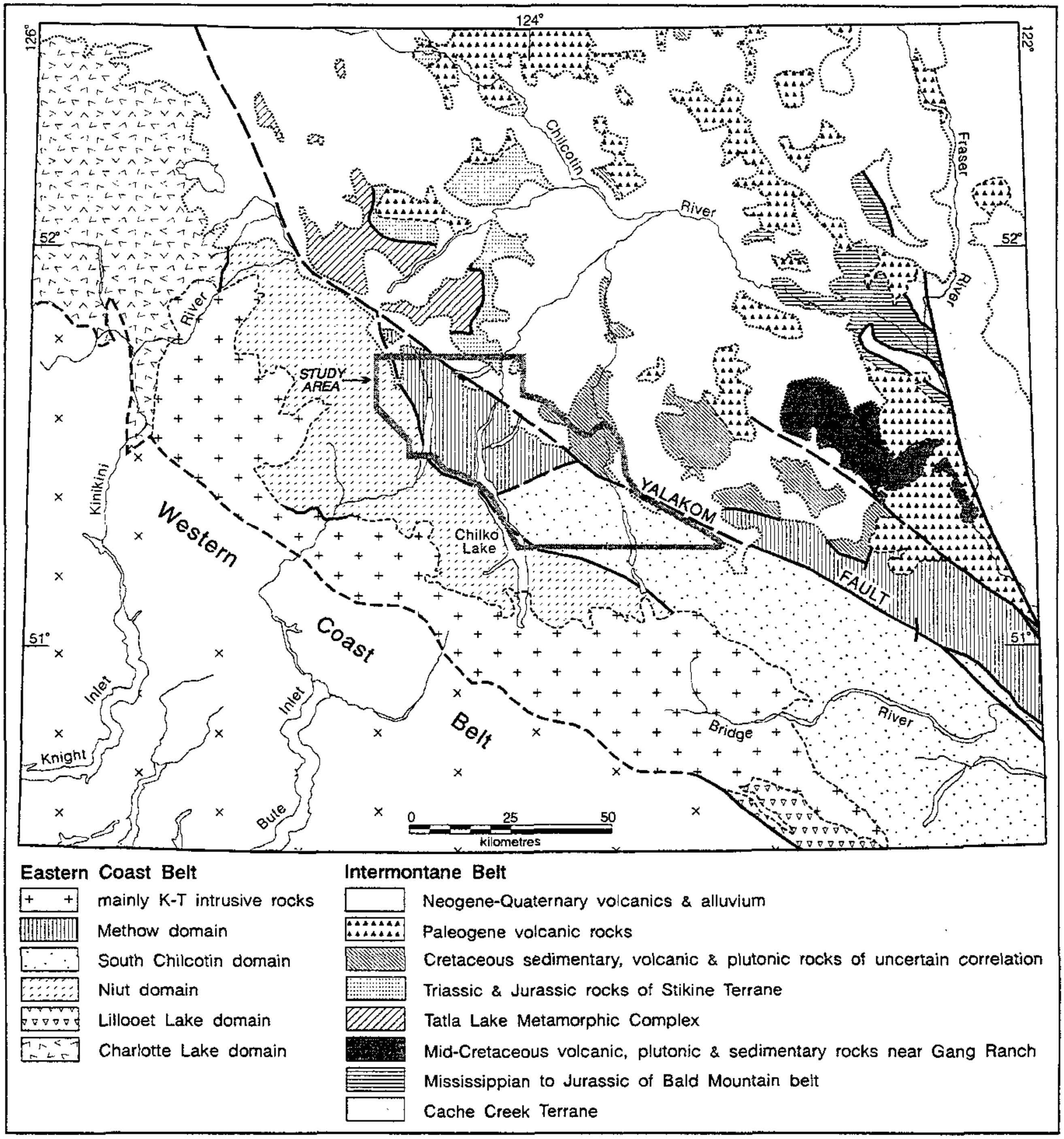


Figure 2. Geologic setting of the Tatlayoko project area.

Triassic to Middle Jurassic arc-derived volcanic and clastic sedimentary rocks of Cadwallader Terrane, Permian ophiolitic rocks of the Shulaps and Bralorne - East Liza complexes, Upper Jurassic to mid-Cretaceous clastic sedimentary rocks of the Tyaughton-Methow basin, and Upper Cretaceous subaerial volcanic rocks of the Powell Creek formation (informal). These partially coeval lithotectonic assemblages are juxtaposed across a complex network of structures that is dominated by middle to Late Cretaceous southwest-directed contractional faults, and Late Cretaceous to early Tertiary dextral strike-slip faults.

The Methow domain occurs to the north and northeast of the south Chilcotin domain, and is distinguished by a less complex structural style dominated by widely spaced faults and broad folds. The two domains are separated in part by the Yalakom fault, and in part by an earlier structure that is offset by the Yalakom fault. This earlier structure is referred to as the Camelsfoot fault in the south (Schiarizza *et al.*, 1993b; Schiarizza and

Garver, 1995) and the Konni Lake fault in the north (Riddell *et al.*, 1993a). Methow domain is underlain mainly by Lower to Middle Jurassic sedimentary and volcanic rocks of the Methow Terrane, and overlying Upper Jurassic to mid-Cretaceous clastic sedimentary rocks of the Tyaughton-Methow basin. Older rocks are exposed locally and include Middle to Late Triassic quartz dioritic intrusions and overlying Upper Triassic sedimentary rocks that outcrop near Tatlayoko Lake. The Jurassic rocks of Methow Terrane are lithologically distinct from age-equivalent rocks found within the Cadwallader and Bridge River terranes of the south Chilcotin domain. The upper part of the Tyaughton-Methow basin, within the Methow domain (the Jackass Mountain Group), is also distinct from coeval rocks comprising the upper part of the basin in the south Chilcotin domain (the Taylor Creek Group). The lower part of the Tyaughton-Methow basin, represented by the Jura-Cretaceous Relay Mountain Group, is, however, common to both domains (Figure 3).

The Niut domain is underlain largely by Upper Triassic volcanic and sedimentary rocks of the Mount Moore and Mosley formations, associated Late Triassic plutons, and Lower Cretaceous volcanic and sedimentary rocks assigned to the Ottarasko and Cloud Drifter formations (Rusmore and Woodsworth, 1991a; Mustard and van der Heyden, 1994). Both the Triassic rocks, which have been correlated with those of the Stikine Terrane, and the Lower Cretaceous rocks are distinct from age-equivalent rocks to the east, but the Niut domain also includes middle to Upper Cretaceous rocks that correlate with the upper Tyaughton basin and Powell Creek formation of the south Chilcotin domain. The stratigraphic elements of the Niut domain are deformed by early Late Cretaceous faults of the northeast-vergent Eastern Waddington thrust belt (Rusmore and Woodsworth, 1991b; van der Heyden *et al.*, 1994a). The northeast boundary of the domain is a system of faults that juxtaposes it against the south Chilcotin domain in the area east of Chilko Lake, and against the Methow domain to the west of the lake (Figure 2).

The Intermontane Belt is characterized by subdued topography and sparse bedrock exposure. Pre-Neogene strata north of Chilko Lake comprise volcanic and volcaniclastic rocks that have been correlated with the Lower to Middle Jurassic Hazelton Group of the Stikine Terrane (Tipper, 1969a,b). To the west, these rocks are juxtaposed against penetratively deformed meta-sedimentary, metavolcanic and metaplutonic rocks of the Tatla Lake Metamorphic Complex across an east to northeast-dipping normal fault. This fault formed late in the structural history of the complex, which was ductilely sheared and exhumed in Eocene time (Friedman and Armstrong, 1988), possibly in a structural regime linked to dextral movement along the Yalakom fault (Schiarizza *et al.*, 1995a).

To the southeast is a belt of mainly Cretaceous sedimentary, volcanic and plutonic rocks that extends from the Taseko River to the Fraser River. Exposures near the Taseko River include Hauterivian sedimentary and volcanic rocks that may correlate with those of Niut domain, as well as younger Aptian-Albian conglomerates that resemble the Jackass Mountain Group of the Methow domain (Fish Lake area of Figure 3). Farther to the southeast, near the Fraser River, this belt comprises Lower Cretaceous volcanic rocks of the Spences Bridge Group and an overlying succession of middle to Upper Cretaceous sedimentary and volcanic rocks (Green, 1990; Hickson, 1992; Gang Ranch area of Figure 2). Underlying rocks are not exposed, but correlative rocks to the east of the Fraser fault overlap Quesnel and Cache Creek terranes (Monger and McMillan, 1989).

## GEOLOGY OF THE FISH LAKE - CHAUNIGAN LAKE AREA

Pre-Miocene bedrock exposures on the northeast side of the Yalakom fault, near Fish Lake, are largely restricted to the steep slopes bordering the Taseko River, the Elkin Creek canyon, and a wooded ridge system to the northwest of Chaunigan Lake (Figure 4). The exposures in this area comprise sedimentary and volcanic rocks that were assigned to the Upper Cretaceous Kingsvale Group by Tipper (1978), which also included rocks now assigned to the Powell Creek formation on the southwest side of the fault. The sedimentary rocks in this area were remapped as the Lower Cretaceous Jackass Mountain Group by Riddell *et al.* (1993a,b) and Hickson and Higman (1993). The latter authors also assigned the volcanic rocks in the area an Early Cretaceous age, based on their lithologic similarity to 106 Ma (Albian) volcanics near Mount Alex, about 60 kilometres to the east. Subsequent identification of fossils collected during the 1992 field season suggests that, in addition to Aptian or Albian conglomerates (Vick Lake unit) that might correlate with the Jackass Mountain Group, the area also includes an older sedimentary succession of Hauterivian age (Elkin Creek unit). Limited data suggest that the volcanic rocks in the area may also be of Hauterivian age. The following summary of the geology in this area incorporates these new fossil data, as well as two additional days of fieldwork in 1995, into the database established by the 1992 mapping of Riddell *et al.* (1993a,b).

### *ELKIN CREEK UNIT*

Rocks included in the Elkin Creek unit on Figure 4 consist of sandstone, siltstone, shale and local occurrences of conglomerate. These rocks are locally well exposed on the lower slopes adjacent to Elkin Creek and Elkin Lake, where they are overlain by Miocene - Pliocene plateau basalts of the Chilcotin Group. The unit is also represented by sparse exposures a short distance to the east, on the east side of Big Lake. Sandstone-dominated intervals adjacent to the Taseko River farther to the east

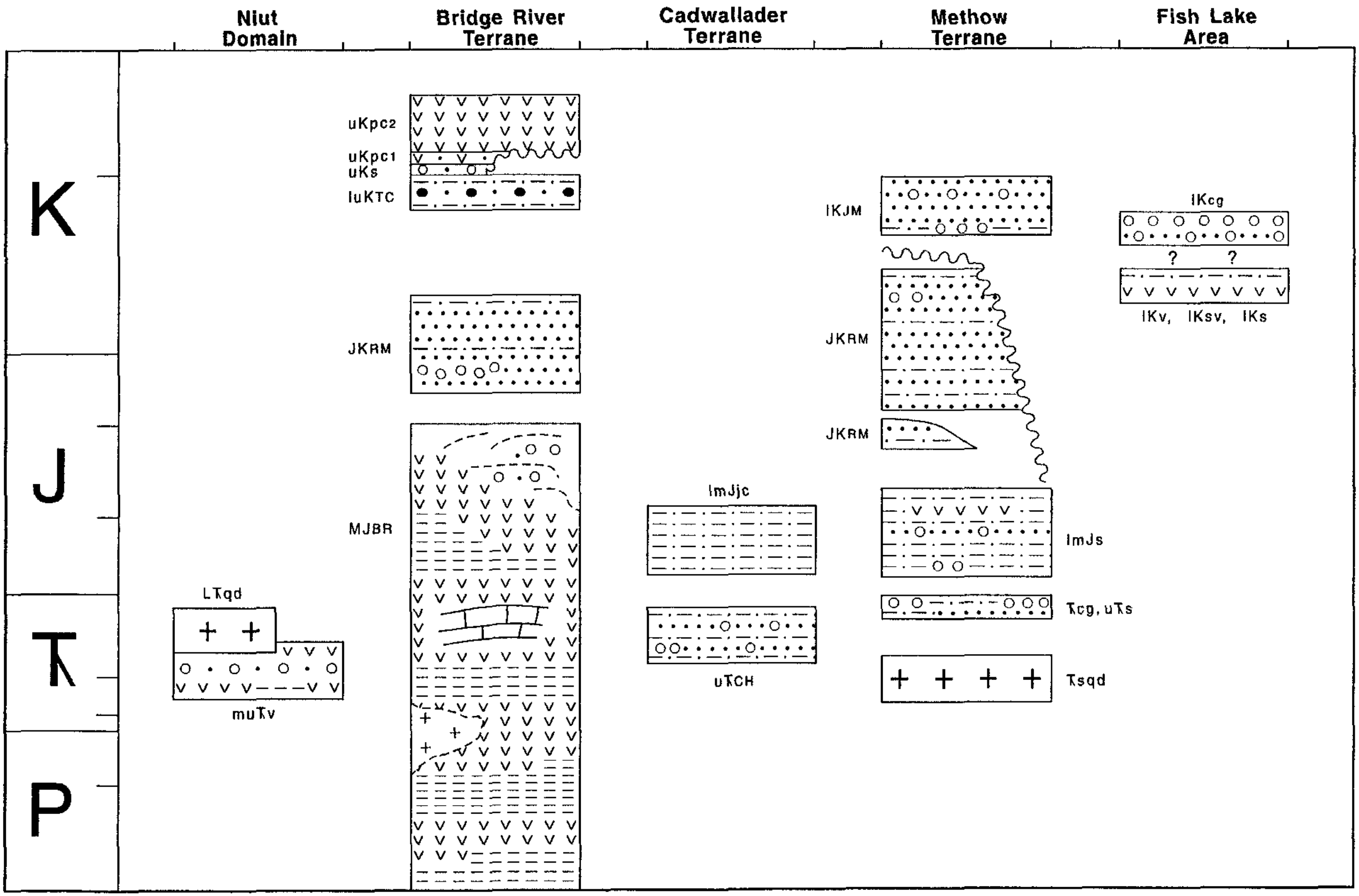


Figure 3. Main tectonostratigraphic assemblages exposed in the Tatlayoko project area. Lithologies are summarized in the legend for Figure 4. Not shown are Lower to Middle Jurassic(?) volcanic rocks of Stikine Terrane that occur northeast of the Yalakom fault in the northern part of the study area.

are also tentatively included in the Elkin Creek unit, although these may actually belong to the younger Vick Lake unit.

The exposures along Elkin Creek and Big Lake are dominated by green to brownish grey, fine to coarse-grained sandstone containing feldspar, volcanic-lithic grains and quartz. The sandstones are typically massive, but locally occur in medium to very thick beds separated by interbeds of friable siltstone or shale. Granule to pebble conglomerate occurs locally and contains rounded clasts of mainly intermediate volcanic rocks, but also includes clasts of granitoid rock. Plant fragments are present in most exposures, and marine fossils occur locally. An ammonite collected from the east bank of Elkin Creek directly northeast of the Yalakom fault has been tentatively identified as *Olcostephanus* sp., which suggests a late Valanginian to early Hauterivian age. A nearby fossil collection includes belemnites, oyster shell fragments, scaphopod shells, and abundant shell fragments of large-valved inoceramids suggestive of the *paraketzovi* group, which also suggests a Hauterivian age (fossil identifications by J.W. Haggart, 1992).

The rocks assigned to the Elkin Creek unit on either side of the Taseko River comprise green lithic-arkosic sandstones with lesser shale and conglomerate. They are lithologically similar to the Hauterivian rocks exposed near Elkin Creek and Big Lake, but have not been dated. Their inclusion in the Elkin Creek unit is tentative, however, because they also resemble sandstones intercalated with Aptian or Albian conglomerates of the Vick Lake unit, which also outcrop in this area. The relationship between the Vick Lake conglomerates and the sandstone-dominated intervals is not exposed, and it is therefore not clear if the sandstones are actually a part of the Vick Lake unit or belong to the older Elkin Creek unit.

The nearest dated Hauterivian rocks that might correlate with the Elkin Creek unit occur in the upper part of the Jura-Cretaceous Relay Mountain Group, which is exposed about 30 kilometres to the east, on the southwest side of the Yalakom fault. The Relay Mountain Group in this area occupies a stratigraphic position between the Lower to Middle Jurassic rocks of the Methow Terrane and the Lower Cretaceous Jackass Mountain Group (Figures 3 and 4). Correlation with the Relay Mountain Group would therefore be consistent with the spatial association of the Elkin Creek unit with the Vick Lake unit, which may correlate with the Jackass Mountain Group (see later section). Alternatively, the Elkin Creek unit may correlate with the Hauterivian Cloud Drifter formation of the Niut domain (informal; Rusmore and Woodsworth, 1993; Mustard and van der Heyden, 1994), which is a lithologically similar succession of sandstones, shales and conglomerates derived from a volcanic and plutonic source area. This correlation is consistent with the 115 kilometres of dextral offset established for the Yalakom fault (Riddell *et al.*, 1993a), as a pre-Yalakom reconstruction based on removal of this offset would place the Elkin Creek exposures opposite the north end of the Niut domain (Figure 2). It is also consistent with the presence of Hauterivian(?) volcanic rocks in the Chaunigan Lake - Fish Lake area, as the Cloud Drifter formation is stratigraphically underlain by volcanic rocks of the Hauterivian (and older?) Ottarasko formation (informal; Rusmore and Woodsworth, 1993; Mustard and van der Heyden, 1994). The relationship between the Ottarasko - Cloud Drifter succession and the Hauterivian part of the Relay Mountain Group is not well established, but the two sequences may represent, respectively, a proximal volcanic facies within a west-facing Hauterivian arc and an adjacent back-arc basinal facies (Umhoefer *et al.*, 1994).

## *VOLCANIC ROCKS*

Volcanic rocks are best exposed on an isolated ridge system northwest of Chaunigan Lake, and on a low hill west of the Taseko River along the northern boundary of the map area (Chaunigan Lake unit of Figure 4). These rocks have not been dated, and their stratigraphic relationships to the Elkin Creek and Vick Lake units have not been established. They consist mainly of andesitic flows and breccias that show varying degrees of chlorite-calcite-epidote alteration. Medium green rusty brown weathering flows include small feldspar and mafic phenocrysts, and locally quartz amygdules within a very fine grained groundmass. Breccias comprise angular to subrounded fragments of green, grey and purple intermediate volcanics, up to 30 centimetres across, in a matrix dominated by smaller volcanic-lithic grains and feldspar crystals. More felsic volcanic rocks occur locally, and dominate the unit at the east end of the ridge, north of Chaunigan Lake. They comprise maroon to mottled green/red-weathering flows containing feldspar and quartz phenocrysts, and associated breccias that contain fragments of similar quartz feldspar porphyry and, locally, a variety of other dacitic to andesitic rock fragments.

Volcanic rocks also outcrop locally along the east side of the Taseko River near the mouth of the creek that drains Fish Lake. These volcanic rocks, together with intercalated sedimentary rocks, are designated the Fish Creek succession (Unit lKsv) on Figure 4, and may correlate with the volcanic and sedimentary package (observed only in drill core) that hosts the Fish Lake porphyry copper-gold deposit a few kilometres to the east. The Fish Creek succession includes hornblende-feldspar-phyric andesite, dacite containing quartz and feldspar phenocrysts, tuffaceous sandstone, well bedded flinty siltstone, dark grey shale, and pebbly sandstone and pebble conglomerate containing volcanic and granitoid clasts. The sedimentary rocks are in part lithologically similar to the those of the Elkin Creek unit, and this correlation is supported by a single fossil collection containing *Inoceramus* bivalves, tentatively identified as *I. colonicus* which is common in Hauterivian to lower Barremian strata of the region (fossil identification by J.W. Haggart, 1992). The associated volcanic rocks are probably the same age, and a sample of columnar jointed

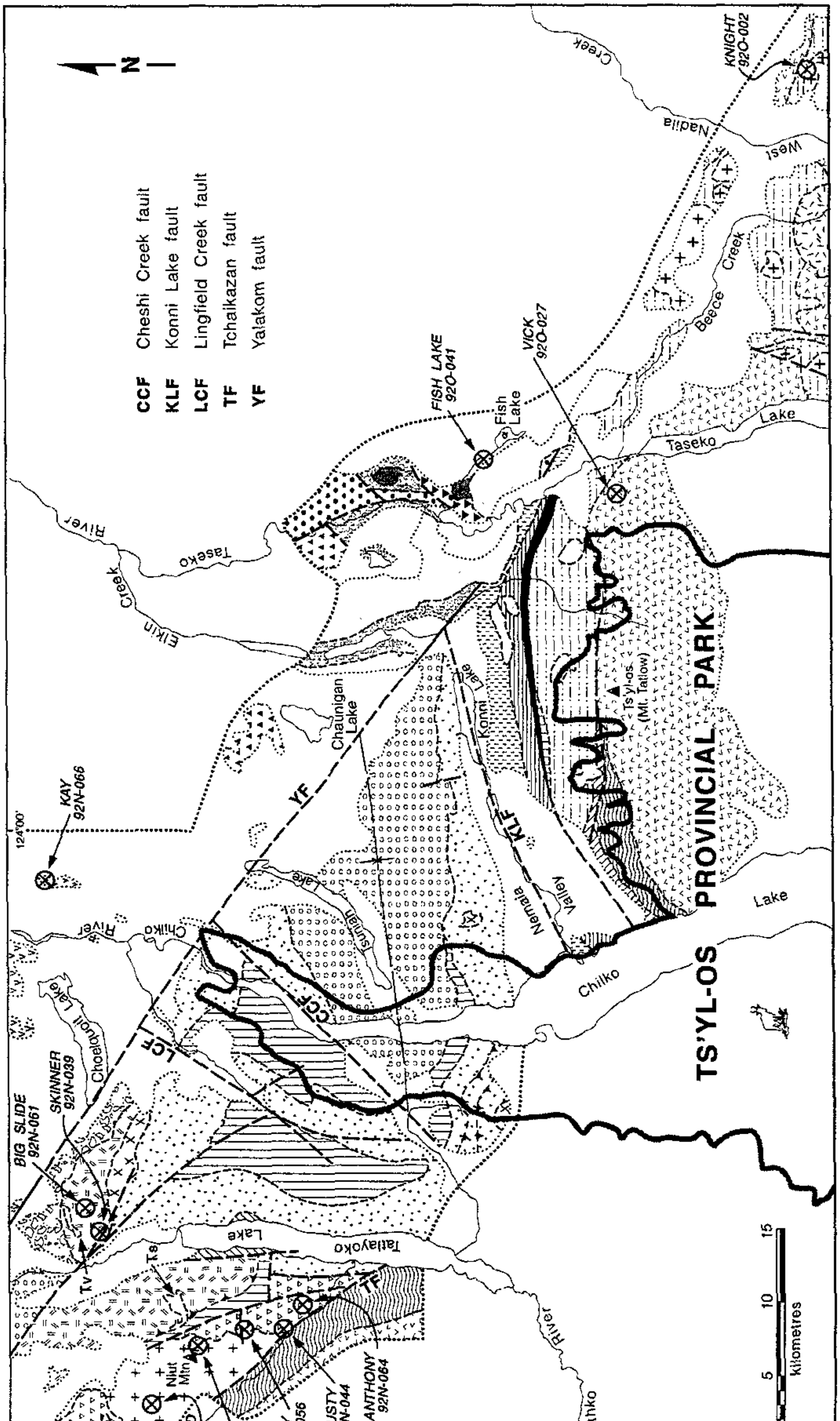


Figure 4. Generalized geology of the Tatlayoko project area, with mineral occurrences identified by name and MINFILE number. The boundary of Ts'yl-os Provincial Park is also shown.

**MIOCENE AND PLIOCENE**
CHILCOTIN GROUP

MPc — *Olivine basalt flows*

## Tyaughton - Methow Basin

**UPPER CRETACEOUS**
POWELL CREEK FORMATION (uKpc2 and uKpc1)

$uKpc_2$ — *Andesitic volcanic breccia, lapilli tuff, ash tuff, laharic breccia, mafic to intermediate volcanic flows; volcanic conglomerate & sandstone*

$uKpc_1$ — *Well stratified volcanic breccia and conglomerate; minor amounts of volcanic sandstone and siltstone*

uKs — *Robertson Creek unit: lithic sandstone, shale, arkosic sandstone, chert-pebble conglomerate*

**LOWER AND/OR UPPER CRETACEOUS**
*Albian and/or Cenomanian*
TAYLOR CREEK GROUP

luKTC — *Shale, siltstone, sandstone, chert-pebble conglomerate*

**LOWER CRETACEOUS**
*Albian*
JACKASS MOUNTAIN GROUP

lKJM — *Conglomerate, arkosic sandstone, gritty sandstone*

**MIDDLE JURASSIC TO LOWER CRETACEOUS**
RELAY MOUNTAIN GROUP

JKRM — *Lithic & arkosic sandstone, siltstone, mudstone, conglomerate, Buchia coquina*

## CRETACEOUS ROCKS NORTHEAST OF YALAKOM FAULT

*Aptian - Albian*

lKcg — *Vick Lake unit: conglomerate; minor amounts of sandstone and shale*

*Hauterivian and(?) younger*

lKv — *Chaunigan Lake unit: andesitic to dacitic breccias, tuffs and flows*

lKsv — *Fish Creek succession: sandstone, shale, conglomerate, tuffaceous sandstone, andesite, dacite*

lKs — *Elkin Creek unit: sandstone, siltstone, shale, conglomerate*

## Niut Domain

**LATE TRIASSIC**

LTrqd — *Quartz diorite, diorite*

**MIDDLE AND UPPER TRIASSIC**

muTrv — *Andesite, pillowed basalt, volcanic breccia, tuff, agglomerate; conglomerate, sandstone, shale*

## Methow Terrane

**LOWER TO MIDDLE JURASSIC**

lmJs — *Huckleberry Formation: siltstone, shale, sandstone, gritty sandstone, pebble conglomerate; minor amounts of silty limestone; locally includes andesitic tuff, volcanic breccia & rare intermediate flows or sills*

**UPPER TRIASSIC**

uTrs — *Lithic sandstone, calcarenite, pebbly calcarenite, fossil hash, siltstone, micritic limestone, arkosic sandstone, pebble conglomerate*

**TRIASSIC (?)**

Trcg — *Pebble to cobble conglomerate; sandstone, siltstone, argillite; micritic limestone*

**MIDDLE TO LATE TRIASSIC**

Trsqd — *Mount Skinner Igneous Complex: quartz diorite, diorite & tonalite intruded by dikes of basalt, diabase, hornblende feldspar porphyry, quartz feldspar porphyry & aplite; also includes masses of fine-grained greenstone that may be dike swarms &/or screens of older volcanic rock; Trv-tuff & welded tuff; Trs-hornfelsed sandstone & siltstone*

## Cadwallader Terrane

**LOWER TO MIDDLE JURASSIC**

lmJjc — *Argillite, cherty argillite, siltstone; minor sandstone*

**UPPER TRIASSIC**
CADWALLADER GROUP

uTrCH — *Hurley Formation: siltstone, shale, sandstone, calcareous sandstone, conglomerate, limestone*

## Bridge River Terrane

**MISSISSIPPIAN TO JURASSIC**
BRIDGE RIVER COMPLEX

MJBR — *Chert, greenstone, argillite, sandstone, conglomerate, serpentinite*

## Jurassic Rocks Northeast of Yalakom Fault

**LOWER TO MIDDLE JURASSIC**

Jv — *Andesite, volcanic breccia, tuff; local sandstone, conglomerate, diorite, gabbro*

## Cretaceous and Tertiary Intrusive Rocks

**EOCENE**

Egd — *Granodiorite, quartz monzonite*

**LATE CRETACEOUS**

LKp — *Hornblende-feldspar-quartz porphyry*

LKd — *Diorite, quartz diorite, hornblende feldspar porphyry*

**CRETACEOUS AND/OR TERTIARY (?)**

KTqd — *Quartz diorite, granodiorite*

Legend to accompany Figure 4

quartz-feldspar-phyric dacite has been submitted for U-Pb dating of zircons in an attempt to test this assertion. A Hauterivian age is also considered most likely for the Chaunigan Lake unit, as it is compositionally similar to the volcanics of the Fish Creek succession and is also spatially associated with the Hauterivian Elkin Creek unit. As noted in the previous section, the volcanic and sedimentary rocks of the Elkin Creek, Chaunigan Lake and Fish Creek successions may correlate with the Ottarasko and Cloud Drifter formations of the Niut belt, which are part of a volcanic-bearing facies that occurs west of coeval sedimentary rocks of the Relay Mountain Group (Umhoefer *et al.*, 1994).

### *VICK LAKE UNIT*

Rocks assigned to the Vick Lake unit outcrop east of the Taseko River, and comprise pebble to boulder conglomerates with only minor amounts of intercalated sandstone and shale. The conglomerates are massive to weakly stratified, with poorly sorted, rounded clasts that commonly range up to 20 centimetres across and locally are as large as 60 centimetres in diameter. The clasts consist mainly of intermediate volcanic rocks, together with a significant proportion of plutonic and mafic volcanic rock fragments; chert and foliated plutonic clasts occur locally. The interstitial sandy matrix is composed of feldspar, lithic grains and quartz. Plant fragments are generally common in the matrix and occur locally as carbonaceous remnants plastered to clast margins. Green coarse-grained sandstone and pebbly sandstone occur as relatively rare intervals up to at least several metres thick within the dominant conglomerates. The sandstones are locally crossbedded, and contain feldspar and lithic grains, in places accompanied by substantial quartz. Woody debris is common, and associated siltstones and shales locally contain moderately well preserved plant fragments. A Cretaceous, probably Aptian to Albian age, has been assigned to plant fossils collected from a locality 600 metres east of the mouth of Fish Creek (E. McIver, written communication, 1993).

The Vick Lake unit is lithologically very similar to parts of the Lower Cretaceous Jackass Mountain Group. In particular, it resembles conglomerates of probable Albian age that are exposed in the Noaxe Creek and Big Bar Creek map areas between 80 and 130 kilometres to the east-southeast (including the French Bar Formation of MacKenzie, 1921; unit lKJMc2 of Schiarizza *et al.*, 1993c; and the polymictic conglomerate unit of Hickson *et al.*, 1994). Correlation of the Vick Lake unit with these Jackass Mountain conglomerates is tentative, however, as no good section of the unit is exposed, and its stratigraphic context is not understood. Furthermore, associated Hauterivian rocks of the Elkin Creek, Chaunigan Lake and Fish Creek successions differ significantly from rocks which stratigraphically underlie the Jackass Mountain Group to the east, although it has not been established that these rocks are in stratigraphic contact with the Vick Lake unit, rather than being entirely in fault juxtaposition.

### *FISH LAKE COPPER - GOLD PORPHYRY DEPOSIT (MINFILE 92O-041)*

The Fish Lake porphyry copper-gold deposit is located in an area of virtually no bedrock exposure about 5 kilometres east of the Taseko River (Figure 4). Recent summaries of the geology of the deposit are provided by Riddell *et al.* (1993a) and Caira *et al.* (1993; in press), who report geological reserves of 1148 million tonnes at an average grade of 0.22 % Cu and 0.41 g/t Au. The Fish Lake deposit is spatially and genetically related to a steeply dipping lenticular body of porphyritic quartz diorite which is surrounded by an east-west elongate complex of steep, southerly dipping, subparallel quartz feldspar porphyry dikes. These rocks, referred to as the Fish Lake Intrusive Complex, cut volcanic and volcaniclastic rocks as well as an older intrusive body of porphyritic diorite, which may be coeval with the volcanics. Mineralization occurs within both the Fish Lake Intrusive Complex and adjacent volcanic, volcaniclastic and plutonic rocks.

A core sample of hornblende-quartz-feldspar porphyry from the Fish Lake Intrusive Complex was collected in 1992 and submitted to the Geochronology Laboratory at the University of British Columbia for U-Pb dating of zircons. Two zircon fractions define a discordia line with a lower intercept of about 80 Ma, which is interpreted as the probable age of the syn-mineralization intrusion (J. E. Gabites, written communication, 1993). This is consistent with a previous whole-rock K-Ar date of 77.2±2.8 Ma obtained from a hornfels containing 40% secondary biotite, which was interpreted as the date of mineralization (Wolfhard, 1976). The volcanic rocks which host the Fish Lake Intrusive Complex and associated mineralization are not dated at the deposit, but are possibly Hauterivian in age, based on correlation with volcanics of the Fish Creek succession just to the west, which are also intruded by small stocks and dikes of hornblende-quartz-feldspar porphyry that may be related to the Fish Lake Intrusive Complex (Fish Lake - Cone Hill intrusive suite of Riddell *et al.*, 1993a,b). This correlation suggests that the host volcanics and syn-mineralization intrusions represent completely different magmatic episodes separated by 40 to 50 million years, in contrast to earlier suspicions that they might be related (Wolfhard, 1976).

## GEOLOGY WEST OF TATLAYOKO LAKE

Most of the effort during the 1995 field season was devoted to mapping within the Niut Range, west of Tatlayoko Lake, in order to tie in with MDA-funded mapping conducted by P. van der Heyden and P. Mustard to the northwest (van der Heyden *et al.*, 1994a; Mustard and van der Heyden, 1994; Mustard *et al.*, 1994). This mapping was concentrated in Triassic volcanic and plutonic rocks of Niut domain, although a few days were also spent within sedimentary and plutonic rocks that bound the Niut domain to the east.

## *NIUT DOMAIN*

The Niut domain is underlain by Middle to Upper Triassic volcanic and sedimentary rocks intruded by Late Triassic quartz diorite of the Niut Mountain pluton. The supracrustal rocks within this belt were assigned to the Lower Cretaceous by Tipper (1969a), and the associated intrusive rocks were consequently thought to be Cretaceous or early Tertiary. Recently, however, sedimentary intervals within volcanic rocks just to the northwest of the present study area were found to contain Triassic fossils (Mustard and van der Heyden, 1994; Mustard *et al.*, 1994), and crosscutting intrusive rocks within and northwest of the study area have yielded Late Triassic U-Pb zircon dates (van der Heyden *et al.*, 1994a; this study). The volcanic and sedimentary rocks correlate mainly with the Middle to Upper Triassic Mount Moore formation (informal; Rusmore and Woodsworth, 1991a; Mustard and van der Heyden, 1994; Mustard *et al.*, 1994), which has been interpreted as a part of the Stikine Terrane.

### VOLCANIC AND SEDIMENTARY ROCKS

Volcanic and sedimentary rocks occur as two separate pendants within the Niut Mountain pluton. The southeastern body consists mainly of massive green, greenish brown to rusty brown weathered andesitic flows, tuffs and breccias. The andesites commonly contain hornblende and feldspar phenocrysts, 1 to 2 millimetres in size, and locally are pyroxene phyric. Associated fragmental rocks typically comprise angular clasts of green to purple hornblende-feldspar and pyroxene-feldspar-phyric andesite within a matrix of smaller lithic grains and feldspar, hornblende and pyroxene crystals. Volcanic rock fragments are typically 1 to 3 centimetres or less in size, but range up to 10 centimetres in some coarse-grained units. Sedimentary intervals associated with the volcanic rocks are dominated by poorly stratified polymictic conglomerates, but also include intercalations of fine to coarse-grained lithic sandstone and shale. The conglomerates contain a wide variety of felsic to mafic volcanic rock fragments, including abundant quartz and quartz feldspar porphyries. They also include recessive weathering fine-grained sedimentary(?) clasts and uncommon medium-grained granitoid fragments. The clasts are typically angular and poorly sorted. They range up to 20 centimetres in size, and grade into a gritty sandstone matrix that includes quartz, feldspar and volcanic-lithic grains.

The rocks of the southeastern pendant are described in more detail by Schiarizza *et al.* (1995a,b), who assigned them a Triassic or Cretaceous age, based on correlation with either the Mount Moore formation (Triassic) or the Ottarasko and Cloud Drifter formations (Early Cretaceous). They are now known to be Triassic at least in part, because the Niut Mountain pluton has yielded a Late Triassic radiometric date where it intrudes the western margin of the succession (*see* next section).

The northwestern pendant of Triassic volcanic rocks was mapped in 1995. It is continuous with Middle to Upper Triassic rocks mapped as Mount Moore formation to the northwest (Mustard *et al.*, 1994), and is intruded by Late Triassic quartz diorite to the west, south and northeast (Figure 4). Within the Tatlayoko project area this pendant consists mainly of fine-grained, medium to dark green, massive to pillowed mafic volcanic rocks that weather to a grey-brown or rusty brown colour. Feldspar and pyroxene phenocrysts are commonly evident, and the phenocryst assemblage hornblende-feldspar occurs locally. Fragmental volcanic rocks appear to be less common, although textures are obscure in many places due to extensive chlorite-epidote alteration. Where observed, they comprise feldspar and mafic crystals, together with lithic fragments to several centimetres in size, within a very fine grained, commonly well indurated groundmass. The lithic fragments are mafic to intermediate volcanic rocks which range from aphyric to porphyritic, the latter containing various combinations of feldspar, pyroxene and hornblende phenocrysts. Light grey felsite, feldspar porphyry and quartz feldspar porphyry occur locally within the mafic volcanic succession. In part they occur as dikes and small irregular intrusive bodies, but some may be extrusive. Sedimentary rocks are a relatively minor component of the northwestern pendant, but narrow intervals of thin-bedded volcaniclastic sandstone and siltstone, or of interbedded chert and siliceous siltstone, were observed locally.

The volcanic and minor sedimentary rocks of the northwestern pendant have not been dated within the present study area, but are clearly intruded by the Late Triassic Niut Mountain pluton. They are continuous with Triassic volcanic and sedimentary rocks to the northwest which have been assigned to the Mount Moore formation (Mustard and van der Heyden, 1994). Corals from thin limestone beds within this succession have been tentatively assigned to the Upper Triassic (van der Heyden *et al.*, 1994a), and chert intercalated with mafic volcanic rocks only 1 kilometre northwest of the present study area has yielded Middle Triassic (Ladinian) radiolarians (F. Cordey and P.S. Mustard, personal communication, 1994). In its type area, about 12 kilometres south of Tatlayoko Lake, a limestone lens intercalated with basaltic breccias of the Mount Moore formation has yielded conodonts of latest Carnian to earliest Norian age (Rusmore and Woodsworth, 1991a).

### NIUT MOUNTAIN PLUTON

The Niut Mountain pluton is a large body of predominantly quartz diorite that underlies most of the Niut domain within the Tatlayoko project area, and clearly intrudes the volcanic and sedimentary rocks within the domain. It consists mainly of massive, equigranular, medium to coarse-grained hornblende ±biotite quartz diorite, locally grading to medium-grained hornblende diorite. The pluton locally includes small bodies of mafic-poor medium-grained granitic rock, and it, together with the volcanic and sedimentary rocks of the domain, is cut by a suite of dikes and small plugs that includes fine-grained diorite, hornblende feldspar porphyry, pyroxene feldspar porphyry and lamprophyre. Most dikes strike northeast and dip steeply, although east, north and northwest strikes are locally predominant.

A sample of quartz diorite collected from the eastern margin of the pluton, 4.25 kilometres south-southeast of Niut Mountain, has yielded a preliminary U-Pb zircon age of 219.5±7.3 Ma (R. Friedman, personal communication, 1995). This compares closely with a U-Pb zircon date of 214.9+8.6/-3.1 Ma from less than 1 kilometre west of the present study area (Mustard *et al.*, 1994), and confirms that the plutonic rocks within Niut domain are a single Late Triassic unit.

## STRUCTURE

Steeply dipping, east-striking faults cut volcanic and sedimentary rocks in the southeastern part of Niut domain, and two northeast-striking faults are mapped within the Niut Mountain pluton to the northwest (Schiarizza *et al.*, 1995a,b). The latter faults are marked by steeply dipping zones of fracturing and brecciation, several tens of metres wide, that are colinear with prominent topographic lineaments. The structure of the northwestern pendant is poorly understood because it contains few bedded rocks and no distinctive markers. Where observed, bedding dips at moderate angles to the north or west, and the strata are right way up, based on graded beds and pillow shapes.

The northwest-striking Tchaikazan fault bounds the Triassic rocks of Niut domain to the southwest, and separates them from Upper Cretaceous volcanic rocks of the Powell Creek formation. Tipper (1969a) interpreted the Tchaikazan fault as a right-lateral transcurrent fault, based on speculative correlation of two faults that were offset by about 30 kilometres along it. More recently Mustard and van der Heyden (1994) have postulated 7 to 8 kilometres of apparent dextral displacement based on offset of a distinctive fossiliferous limestone unit within the Mount Moore formation, a short distance to the northwest of the Tatlayoko Lake map area.

The northeastern limit of plutonic, volcanic and sedimentary rocks of the Niut domain is a system of north to northwest-trending faults that separates them from Jurassic and Cretaceous sedimentary rocks to the northeast. The oldest of these faults is an unexposed north-striking structure that separates a panel of sedimentary and volcanic rocks, tentatively included within Niut domain, from Jurassic rocks of the Methow Terrane a short distance west of Tatlayoko Lake (Figure 4). This fault is truncated by an east-striking fault to the north, which in turn is truncated by a northwest-striking fault to the west. The latter structure forms the northeastern boundary of Niut domain east of Niut Mountain, and juxtaposes it against a narrow lens of Relay Mountain Group (Figure 4). Where exposed, this fault dips steeply east to east-northeast, and is commonly marked by a metre-wide zone of brittle faults and fractures; Niut domain rocks are typically silicified and quartz veined along the fault whereas the adjacent Relay Mountain Group is not. Locally, the rocks on both sides of the main fault are slivered into several parallel fault strands, resulting in a fault zone several hundred metres wide. This fault is truncated by, or merges with, the Tchaikazan fault to the south. It is a relatively young structure because, in addition to the east-striking fault on its east side, it also truncates a northeast-dipping thrust fault within the Relay Mountain Group and east-striking faults within Niut domain to the west (Schiarizza *et al.*, 1995b). It is suspected that it may be a splay from the dextral-slip Tchaikazan fault, which was active mainly in Eocene time (Umhoefer and Kleinspehn, 1995). Neither the age nor the sense of movement are known for the older north-striking fault segment that forms the domain boundary to the south.

## MINERAL OCCURRENCES

The rocks of the Niut domain contain a higher density of mineral occurrences than rocks elsewhere in the Tatlayoko project area (Figure 4). They host five known occurrences that contain disseminated or fracture-controlled pyrite, chalcopyrite and malachite, either within the Niut Mountain pluton or in bordering volcanic and sedimentary rocks. Four other occurrences are within the same belt, 1 to 7 kilometres northwest of the Tatlayoko project area, and other malachite occurrences are scattered throughout the Niut Mountain pluton and bordering volcanic rocks. These showings probably represent a series of porphyry-style mineralizing systems within and adjacent to the Niut Mountain pluton. The Mount Moore formation, which hosts the pluton and much of the mineralization, is correlated by Rusmore and Woodsworth (1991a) with the Upper Triassic Stuhini Group, which comprises part of the Stikine Terrane in northern British Columbia. This correlation is strengthened by the association of the Niut Mountain pluton with the Mount Moore formation, as plutons of similar age intrude the Stuhini Group and are locally responsible for porphyry-style mineralization. This relationship is exemplified by the Hickman batholith, which was emplaced into the Stuhini Group at about 220 Ma, and is genetically related to the Schaft Creek porphyry deposit which is hosted mainly in Stuhini volcanic rocks (Spilsbury, in press). This correlation also sheds a favourable light on the mineral potential of the Niut domain, as Schaft Creek is one of the largest calcalkaline porphyry deposits known within the Canadian Cordillera (McMillan *et al.*, in press).

**TABLE 1. SUMMARY OF MINFILE OCCURRENCES IN THE TATLAYOKO PROJECT AREA.**

| MINFILE No. | NAME | COMMODITY | CAPSULE DESCRIPTION |
|---|---|---|---|
| 092N-020 | Niut Mountain | Cu, Au | A gossanous zone within pyritized volcanic rock of unit muŦv locally contains malachite, chalcopyrite and traces of gold. |
| 092N-039 | Skinner | Au, Cu | Northeast-striking gold-quartz veins, of Eocene age, occur within Trassic diorite and quartz diorite of the Mount Skinner Igneous Complex. A 170-tonne bulk sample extracted from the Victoria vein in 1992 and 1993 produced over 11 000 grams of gold and 8000 grams of silver. |
| 092N-044 | Rusty | Cu | Disseminated chalcopyrite occurs in faulted sedimentary rocks of unit muŦv. |
| 092N-056 | Fly | Cu | Disseminated malachite, azurite, pyrite and chalcopyrite occur within quartz-epidote-carbonate veins and fracture fillings hosted in quartz diorite of unit LŦqd and an associated body of hornblende feldspar porphyry. |
| 092N-061 | Big Slide | Au, Cu | Gold and copper mineralization occurs within a number of subparallel northwest-striking sheeted quartz veins hosted in Triassic quartz diorite of the Mount Skinner Igneous Complex. |
| 092N-064 | Anthony | Cu, Zn, Ag | Malachite, pyrite, chalcopyrite and sphalerite occur in quartz veins and silica-flooded andesite of unit muŦv |
| 092N-065 | Clipboard | Cu | Disseminated malachite occurs in a small stock of granite porphyry that intrudes quartz diorite of unit LŦqd. |
| 092N-066 | Kay | Cu | Disseminated malachite and azurite occur in calcite veinlets within a mafic porphyry of unit lmJv |
| 092O-002 | Knight | Au, Ag | Gold and silver occur within silicified and pyritized sedimentary rocks of the Taylor Creek Group which are intruded by dikes and stocks of Late Cretaceous diorite and hornblende-feldspar porphyry |
| 92O-027 | Vick | Au, Cu, Ag | Pyrite, chalcopyrite, malachite, azurite and iron carbonates occur within quartz veins that follow a northeast-striking shear zone cutting volcanic rocks of the Upper Cretaceous Powell Creek formation. |
| 92O-041 | Fish Lake | Cu, Au, Ag, Mo, Zn | Porphyry Cu-Au mineralization occurs within and adjacent to a Late Cretaceous quartz diorite stock and associated quartz feldspar porphyry dikes, which intrude Lower Cretaceous(?) andesitic volcanic rocks and a pre-mineralization diorite plug. Geological reserves are 1,148 million tonnes averaging 0.22 % Cu and 0.41 g/t Au. |

## *SEDIMENTARY AND PLUTONIC ROCKS EAST OF NIUT DOMAIN*

The geology east of the Niut domain is dominated by a large body of quartz diorite and tonalite that is informally referred to as the Crazy Creek pluton. These plutonic rocks are provisionally included in the Mount Skinner Igneous Complex, which apparently forms the basement to the Methow domain to the east (Figures 3 and 4). Also present in this area are Jura-Cretaceous sedimentary rocks of the Relay Mountain Group, which comprise a narrow, northwest-trending, fault-bounded belt between the Crazy Creek pluton and volcanic and plutonic rocks of the Niut domain to the southwest.

### RELAY MOUNTAIN GROUP

The Relay Mountain Group outcrops as a narrow fault-bounded belt of conglomerates, sandstones and shales that are cut by numerous faults and intruded by abundant sills and plugs of quartz diorite. Where best exposed, about 3.5 kilometres west of Tatlayoko Lake, the relatively wide southern part of the belt comprises two main fault panels. A younger-over-older relationship across the intervening northeast-dipping fault suggests that it accommodated reverse movement, as does a tight syncline within the footwall rocks directly beneath it. The northeastern panel is a coherent, northeast-dipping section that includes two distinct units. The lower unit is about 300 metres thick and consists mainly of arkosic lithic sandstone. Conglomerate dominates about 100 metres in the central part of the unit, and contains rounded pebbles and cobbles of felsic to mafic volcanic rocks together with a smaller proportion of granitoid rock. *Buchia* fossils collected from near the base of the unit, as well as from the upper part of the conglomeratic interval, have been identified as Upper Jurassic (Tithonian) forms (T.P. Poulton, written communication, 1995), confirming an earlier fossil report by Tipper (1969a). The base of the upper unit comprises several tens of metres of a dark grey shale containing *Inoceramus* and belemnite fragments. These rocks abruptly overlie sandstones of the lower unit and pass up-section into about 100 metres of thin to medium-bedded, locally crossbedded arkosic sandstone intercalated with siltstone and friable shale. The upper unit is assumed to be Hauterivian in age, based on the presence of *Inoceramus* fossils and its strong lithologic similarity to the Hauterivian and(?) Barremian rocks of the upper part of the Relay Mountain Group where it is well exposed and dated in the adjacent Potato Range (Tipper, 1969a; Schiarizza *et al.*, 1995a).

The coherent section described above rests structurally above a southwestern fault panel that consists of faulted and folded shale containing intercalations of arkosic and lithic sandstones. The bounding fault was observed in several places and dips between 35° and 75° to the east-northeast. It is generally parallel to bedding in the footwall rocks, and commonly places them against small bodies of quartz diorite that intrude the base of the Jurassic section in the immediate hangingwall. The lower fault panel is, for the most part, lithologically similar to the Hauterivian strata of the Relay Mountain Group, and this correlation is confirmed by the presence of Hauterivian *Inoceramus* fossils in the central part of the panel (fossil identification by T. P. Poulton, 1995). Local fault slivers of chert-pebble conglomerate occur within the upper part of the panel, however, and were probably derived from the mid-Cretaceous Taylor Creek Group, which overlies the Relay Mountain Group south of the Nemaia valley (Figure 4).

The belt of Relay Mountain Group rocks narrows to the northwest, where it becomes a series of fault-bounded slivers of sedimentary rock interleaved with quartz diorite. The sedimentary rocks include conglomerates and sandstones similar to those of the Jurassic section to the south, as well as local shale-dominated lenses that resemble the Hauterivian interval to the south. A single fossil collection from shales in the northern part of the belt contained *Inoceramus* pelecypods of Hauterivian age (identification by T.P. Poulton, 1995).

The intact section of Relay Mountain Group rocks exposed in the upper fault panel in the southern part of the belt differs from sections in the Potato Range, directly east of Tatlayoko Lake, in two main aspects. First of all, the thick interval of Jurassic conglomerates found in this belt does not occur to the east. Secondly, the apparent absence of Berriasian and Valanginian rocks in the Niut Range belt suggests that, here, the disconformity beneath the Hauterivian section represents much more missing stratigraphy than the disconformity beneath Hauterivian rocks in the Potato Range, where there is a thick interval of Berriasian and Valanginian rocks (Tipper, 1969a). These relationships suggest that the Niut Range section originated near the margin of the Relay Mountain basin, as proposed by Jeletzky and Tipper (1968). A further difference relates to the rocks that overlie the Relay Mountain Group. In the Methow domain, east of Tatlayoko Lake, the Relay Mountain Group is stratigraphically overlain by arkosic sandstones and granitoid-bearing conglomerates of the Albian Jackass Mountain Group (Figure 3). The fault-bounded slivers of chert-pebble conglomerate imbricated with Hauterivian rocks of the Relay Mountain Group in the Niut Range, however, suggest that the Relay Mountain Group here was overlain by the Albian Taylor Creek Group. This suggests that the Relay Mountain Group in the Niut Range relates more closely to that part of the group exposed in the south Chilcotin domain, and occurs within the Tyaughton, rather than the Methow sub-basin, as defined by Garver (1989, 1992).

## CRAZY CREEK PLUTON

The Crazy Creek pluton consists mainly of massive, medium to coarse-grained hornblende biotite quartz diorite and tonalite. However, easternmost exposures, adjacent to the Homathko River and northern Tatlayoko Lake, include abundant diorite, as well as tabular to irregular bodies of fine-grained greenstone that may be dike complexes and/or screens of older volcanic or dike rock within the plutonic rock. These eastern exposures strongly resemble the Mount Skinner Igneous Complex, which outcrops in an east-west belt centred near Mount Skinner, east of the Homathko River valley (Schiarizza *et al.*, 1995a,b). Samples of quartz diorite and tonalite from the Mount Skinner Complex have yielded zircon U-Pb radiometric dates of 226.7+8.1/-0.5 and 230±6.0 Ma respectively (R. Friedman, written communication, 1995). Although contact relationships with adjacent rock units are not well defined, the Mount Skinner Complex is interpreted to form the basement to the Upper Triassic and Jurassic sedimentary and volcanic rocks of Methow Terrane that outcrop east of Tatlayoko Lake (Figure 3).

The southwestern margin of the Crazy Creek pluton is a system of faults that juxtaposes the plutonic rocks, together with a pendant of hornfelsed metasedimentary rocks, against unmetamorphosed sedimentary rocks of the Relay Mountain Group. This fault contact was observed locally, where it is vertical to steeply east or northeast dipping. Although no movement sense was established along it, a component of northeast-side-up movement is suspected. The eastern contact of the pluton was not observed, but is suspected to be a northerly striking fault or shear zone, as easternmost exposures of plutonic rock west of the north end of Tatlayoko Lake display a steeply east dipping mylonitic foliation and an associated stretching lineation that plunges 45° to the south-southeast. This fault system is inferred to truncate the belt of Relay Mountain Group to the south and from there extend into Tatlayoko Lake (Figure 4). Its presence there is suggested by a zone of steeply east dipping brittle faults and fractures within Jurassic sedimentary rocks of the Methow Terrane along the lake shoreline. The northern boundary of the Crazy Creek pluton is a northwest-striking fault that places it against unmetamorphosed sedimentary rocks of the Jackass Mountain Group near the northern boundary of the map area. This fault has been traced from near Lingfield Creek, and is thought to be a component of the Yalakom dextral strike-slip fault system.

It is suspected that the entire Crazy Creek pluton correlates with the Mount Skinner Igneous Complex, and is therefore of Middle to Late Triassic age. In this interpretation, a pendant of hornfelsed sandstone and siltstone that occurs within quartz diorite along the southwestern margin of the pluton (Unit Ts of Figure 4) would be Triassic or older. An alternative interpretation, suggested by Schiarizza *et al.* (1995a,b), is that only the eastern, heterogeneous part of the pluton correlates with the Mount Skinner Complex, and most of the pluton is Cretaceous or Tertiary quartz diorite to tonalite related to the Coast Plutonic Complex. In this interpretation, the main part of the pluton might be the same age as the small quartz diorite bodies that intrude the Relay Mountain Group to the west, and the pendant of hornfelsed sedimentary rocks might have been derived from the Relay Mountain Group. A sample of quartz diorite from near the southwestern boundary of the pluton has been submitted for U-Pb dating of zircons in an attempt to discard one or both of these interpretations.

## AGE AND STRUCTURAL CONTROL OF THE SKINNER GOLD-QUARTZ VEIN SYSTEM

The Skinner gold-quartz vein system occurs within early Late Triassic quartz diorite and diorite of the Mount Skinner Igneous Complex, 5 kilometres north of the north end of Tatlayoko Lake (Figure 4). It is a system of en echelon veins within a presumably structurally controlled lineament that trends 070° (Berniolles, 1991). Work to date has been concentrated on the Victoria vein, at the southwest end of the system, which strikes between 050° and 060° and dips steeply to the northwest. A 170-tonne bulk sample extracted from the vein by Ottarasko Mines Limited in 1992 and 1993 produced over 11 000 grams of gold (average grade 65.83 g/t) and 8000 grams of silver (Meyers, 1993, 1994; Schroeter, 1994).

The Victoria vein has been traced for more than 130 metres. It pinches and swells, locally attaining a thickness of 1.4 metres. The vein walls are defined by slickensided faults, and the veins themselves are cut by parallel faults, at least some of which accommodated sinistral movement. Clay gouge commonly occurs along the vein walls, and sericite and chlorite occur locally along fault surfaces. The vein consists almost entirely of quartz, with minor amounts of pyrite, chalcopyrite, malachite and rare visible gold. Gold values are variable, and concentrations as high as 136 grams per tonne across 0.65 metre have been recorded (Berniolles, 1991). Copper shows little relationship to gold, and is locally concentrated in the wallrock adjacent to the vein.

White mica locally lines vugs and open fractures in quartz of the Victoria vein. A sample provided by Louis Berniolles in 1994 was submitted to the Geochronology Laboratory at the University of British Columbia for K-Ar dating of the mica. The mica separate has recently yielded a preliminary Early to Middle Eocene date of 50 to 54 Ma (J. Mortensen, personal communication, September 1995). This provides a minimum age for the vein and most likely dates the late stages of the hydrothermal system responsible for the veining. If this interpretation is true, then the veining was coincident with dextral movement along the Yalakom fault, which is just 5 kilometres northeast of the Skinner occurrence. This suggests that the Skinner vein system formed along an antithetic sinistral fault system related to the Yalakom fault, although its orientation is slightly more easterly than would be expected for antithetic riedel shears in an ideal simple shear model (*e.g.* Wilcox *et al.*, 1973). The Lingfield Creek and Cheshi Creek faults to the southeast may have had a similar origin, but are likewise oriented slightly more easterly than would be expected. These departures may reflect varying degrees of clockwise rotation in the structural blocks southwest of the Yalakom fault, as is suggested by the structural analysis of Umhoefer and Kleinspehn (1995), who relate this block rotation to the area's position between the Tchaikazan and Yalakom faults.

## ACKNOWLEDGMENTS

I would like to thank Roger White for his enthusiastic and very capable assistance during our 1995 fieldwork, and Mike and Audrey King of White Saddle Air Services for their generous hospitality and for safe and reliable helicopter transportation. I also thank J.W. Haggart, T.P. Poulton, H.W. Tipper, M.J. Orchard and F. Cordey for their fossil identifications, and R. Friedman, J. Gabites and J. Mortensen for their radiometric dating. Verna Vilkos prepared the figures for this report, and John Newell and Brian Grant improved the manuscript through their editorial efforts.

## REFERENCES

Bernoilles, L. (1991): Prospecting Report - Skinner Group; *B.C. Ministry of Energy, Mines and Petroleum Resources*, Assessment Report 22007.

Caira, N., Findlay, A. and Riddell, J. (1993): The Fish Lake Porphyry Copper-Gold Deposit; *in* Exploration in British Columbia 1992, *B.C. Ministry of Energy, Mines and Petroleum Resources*, pages 57-67.

Caira, N.M., Findlay, A. and Rebagliati, C.M. (in press): Taseko Mines Limited's Fish Lake Porphyry Copper-Gold Deposit; *in* Porphyry Deposits of the Northwestern Cordillera of North America, Schroeter, T.G., Editor, *Canadian Institute of Mining, Metallurgy and Petroleum*, Special Volume 46.

Friedman, R.M. and Armstrong, R.L. (1988): Tatla Lake Metamorphic Complex: An Eocene Metamorphic Core Complex on the Southwestern Edge of the Intermontane Belt of British Columbia; *Tectonics*, Volume 7, pages 1141-1166.

Garver, J.I. (1989): Basin Evolution and Source Terranes of Albian-Cenomanian Rocks in the Tyaughton Basin, Southern British Columbia: Implications for Mid-Cretaceous Tectonics in the Canadian Cordillera; unpublished Ph.D. thesis, *University of Washington*, 227 pages.

Garver, J.I. (1992): Provenance of Albian-Cenomanian Rocks of the Methow and Tyaughton Basins, Southern British Columbia: a Mid-Cretaceous Link between North America and the Insular Terrane; *Canadian Journal of Earth Sciences*, Volume 29, pages 1274-1295.

Green, K.C. (1990): Structure, Stratigraphy and Alteration of Cretaceous and Tertiary Strata in the Gang Ranch Area, British Columbia; unpublished M.Sc. thesis, *University of Calgary*, 118 pages.

Hickson, C.J. (1992): An Update on the Chilcotin-Nechako Project and Mapping in the Taseko Lakes Area, West-central British Columbia; *in* Current Research, Part A, *Geological Survey of Canada*, Paper 92-1A, pages 129-135.

Hickson, C.J. and Higman, S.(1993): Geology of the Northwest Quadrant, Taseko Lakes Map Area, West-central British Columbia; *in* Current Research, Part A, *Geological Survey of Canada*, Paper 93-1A, pages 63-67.

Hickson, C.J., Mahoney, J.B. and Read, P. (1994): Geology of Big Bar Map Area, British Columbia: Facies Distribution in the Jackass Mountain Group; *in* Current Research 1994-A; *Geological Survey of Canada*, pages 143-150.

Jeletzky, J.A. and Tipper, H.W. (1968): Upper Jurassic and Cretaceous Rocks of Taseko Lakes Map Area and their Bearing on the Geological History of Southwestern British Columbia; *Geological Survey of Canada*, Paper 67-54, 218 pages.

MacKenzie, J.D. (1921): A Reconnaissance between Taseko Lake and Fraser River, British Columbia; *in* Summary Report, 1920, Part A, *Geological Survey of Canada*, pages 70-81.

McLaren, G.P. (1990): A Mineral Resource Assessment of the Chilko Lake Planning Area; *B.C. Ministry of Energy, Mines and Petroleum Resources*, Bulletin 81, 117 pages.

McLaren, G.P. and Rouse, J.N. (1989): Geology and Geochemistry of the Taseko Lakes Area (92O/3,4,5,6); *B.C. Ministry of Energy, Mines and Petroleum Resources*, Open File 1989-25.

McMillan, W.J., Thompson, J.F.H., Hart, C.J.R. and Johnston, S.T. (in press): Regional Geological and Tectonic Setting of Porphyry Deposits in British Columbia and Yukon Territory; *in* Porphyry Deposits of the Northwestern Cordillera of North America, Schroeter, T.G., Editor, *The Canadian Institute of Mining, Metallurgy and Petroleum*, Special Volume 46.

Meyers, R.E. (1993): South-Central District; *in* Exploration in British Columbia 1992, *B.C. Ministry of Energy, Mines and Petroleum Resources*, pages 35-44.

Meyers, R.E. (1994): South-Central Region; *in* Exploration in British Columbia 1993, *B.C. Ministry of Energy, Mines and Petroleum Resources*, pages 43-46.

Monger, J.W.H. and McMillan, W.J. (1989): Geology, Ashcroft, British Columbia (92I); *Geological Survey of Canada*, Map 42-1989, sheet 1, scale 1:250 000.

Mustard, P.S. and van der Heyden, P. (1994): Stratigraphy and Sedimentology of the Tatla Lake - Bussel Creek Map Areas, West-central British Columbia; *in* Current Research 1994-A, *Geological Survey of Canada*, pages 95-104.

Mustard, P.S., van der Heyden, P. and Friedman, R. (1994): Preliminary Geologic Map, Tatla Lake - Bussel Creek (East Half), NTS 92N/15, 92N/14 (East Half); *Geological Survey of Canada*, Open File 2957, 1:50 000 scale.

Riddell, J., Schiarizza, P., Gaba, R.G., Caira, N. and Findlay, A. (1993a): Geology and Mineral Occurrences of the Mount Tatlow Map Area (92O/5, 6, and 12); *in* Geological Fieldwork 1992, Grant, B. and Newell, J.M., Editors, *B.C. Ministry of Energy, Mines and Petroleum Resources*, Paper 1993-1, pages 37-52.

Riddell, J., Schiarizza, P., Gaba, R., McLaren, G. and Rouse, J. (1993b): Geology of the Mount Tatlow Map Area (92O/5, 6, 12); *B.C. Ministry of Energy, Mines and Petroleum Resources*, Open File 1993-8.

Rusmore, M.E. and Woodsworth, G.J. (1991a): Distribution and Tectonic Significance of Upper Triassic Terranes in the Eastern Coast Mountains and adjacent Intermontane Belt, British Columbia; *Canadian Journal of Earth Sciences*, Volume 28, pages 532-541.

Rusmore, M.E. and Woodsworth, G.J. (1991b): Coast Plutonic Complex: A Mid-Cretaceous Contractional Orogen; *Geology*, Volume 19, pages 941-944.

Rusmore, M.E. and Woodsworth, G.J. (1993): Geological Maps of the Mt. Queen Bess (92N/7) and Razorback Mountain (92N/10) Map Areas, Coast Mountains, British Columbia; *Geological Survey of Canada*, Open File 2586, 2 sheets, 1:50 000 scale.

Schiarizza, P. and Garver, J.I. (1995): Guide to the Geology and Tectonic Evolution of the Bridge River Area, Southeastern Coast Belt, Southwestern British Columbia; a guide to accompany days 2 and 3 of Field Trip A5, *Geological Association of Canada - Mineralogical Association of Canada*, Annual Meeting, Victoria, B.C., 87 pages.

Schiarizza, P., Gaba, R.G., Garver, J.I., Glover, J.K., Macdonald, R.W.J., Archibald, D.A., Lynch, T., Safton, K.E., Sajgalik, P.P., Calon, T., Malpas, J. and Umhoefer, P.J. (1993a): Geology of the Bralorne (North Half) and Northeastern Dickson Range Map Areas (92J/14, 15); *B.C. Ministry of Energy, Mines and Petroleum Resources*, Geoscience Map 1993-7.

Schiarizza, P. Gaba, R.G., Coleman, M.E., Glover, J.K., Macdonald, R.W.J., Garver, J.I., Archibald, D.A., Lynch, T. and Safton, K.E. (1993b): Geology of the Bridge River Map Area (92J/16); *B.C. Ministry of Energy, Mines and Petroleum Resources*, Geoscience Map 1993-8.

Schiarizza, P., Glover, J.K., Garver, J.I., Umhoefer, P.J., Gaba, R.G., Riddell, J.M., Payne, D.F., Macdonald, R.W.J., Lynch, T., Safton, K.E. and Sajgalik, P.P. (1993c): Geology of the Noaxe Creek and Southwestern Big Bar Creek Map Areas (92O/1, 2); *B.C. Ministry of Energy, Mines and Petroleum Resources*, Geoscience Map 1993-9.

Schiarizza, P., Glover, J.K., Umhoefer, P.J., Garver, J.I., Handel, D., Rapp, P., Riddell, J.M. and Gaba, R.G., (1993d): Geology and Mineral Occurrences of the Warner Pass Map Area (92O/3); *B.C. Ministry of Energy, Mines and Petroleum Resources*, Geoscience Map 1993-10.

Schiarizza, P., Melville, D.M., Riddell, J., Jennings, B.K., Umhoefer, P.J. and Robinson, M.J. (1995a): Geology and Mineral Occurrences of the Tatlayoko Lake Map Area (92N/8, 9 and 10); *in* Geological Fieldwork 1994, Grant, B. and Newell, J.M., Editors, *B.C. Ministry of Energy, Mines and Petroleum Resources*, Paper 1995-1, pages 297-320.

Schiarizza, P., Melville, D.M. and Jennings, B.K. (1995b): Geology, Mineral Occurrences and Geochemistry of the Tatlayoko Lake Map Area (92N/8, 9, 10); *B.C. Ministry of Energy, Mines and Petroleum Resources*, Open File 1995-7, 2 sheets, 1:50 000 and 1:100 000 scale.

Schroeter, T.G. (1994): British Columbia Mining, Exploration and Development, 1993 Highlights; *in* Exploration in British Columbia 1993, *B.C. Ministry of Energy, Mines and Petroleum Resources*, pages 1-29.

Spilsbury, T.W. (in press): The Schaft Creek Porphyry Copper-Molybdenum-Gold-Silver Deposit, Northwestern British Columbia; *in* Porphyry Deposits of the Northwestern Cordillera of North America, Schroeter, T.G., Editor, *The Canadian Institute of Mining, Metallurgy and Petroleum*, Special Volume 46.

Tipper, H.W. (1969a): Mesozoic and Cenozoic Geology of the Northeastern Part of Mount Waddington Map Area (92N), Coast District, British Columbia; *Geological Survey of Canada*, Paper 68-33.

Tipper, H.W. (1969b): Geology, Anahim Lake; *Geological Survey of Canada*, Map 1202A.

Tipper, H.W. (1978): Taseko Lakes (92O) Map Area; *Geological Survey of Canada*, Open File 534.

Umhoefer, P.J. and Kleinspehn, K.L. (1995): Mesoscale and Regional Kinematics of the Northwestern Yalakom Fault

System: Major Paleogene Dextral Faulting in British Columbia, Canada; *Tectonics*, Volume 14, pages 78-94.

Umhoefer, P.J., Rusmore, M.E. and Woodsworth, G.J. (1994): Contrasting Tectono-stratigraphy and Structure in the Coast Belt near Chilko Lake, British Columbia: Unrelated Terranes or an Arc - Back-arc Transect?; *Canadian Journal of Earth Sciences*, Volume 31, pages 1700-1713.

van der Heyden, P., Mustard, P.S. and Friedman, R. (1994a): Northern Continuation of the Eastern Waddington Thrust Belt and Tyaughton Trough, Tatla Lake - Bussel Creek Map Areas, West-central British Columbia; *in* Current Research 1994-A; *Geological Survey of Canada*, p. 87-94.

van der Heyden, P., Calderwood, A. and Huntley, D.H. (1994b): Preliminary Geologic Map, Charlotte Lake - Junker Lake (East Half), NTS 93C/3, 93C/4 (East Half); *Geological Survey of Canada*, Open File 2919, scale 1:50 000.

Wilcox, R.E., Harding, T.P. and Seely, D.R. (1973): Basic Wrench Tectonics; *American Association of Petroleum Geologists*, Bulletin, Volume 57, pages 74-96.

Wolfhard, M.R. (1976): Fish Lake; *in* Porphyry Deposits of the Canadian Cordillera, Sutherland Brown, A., Editor, *Canadian Institute of Mining and Metallurgy*, Special Volume 15, pages 317-322.

NOTES

# PRELIMINARY PETROGRAPHIC, GEOCHEMICAL AND FLUID INCLUSION STUDIES OF THE FORS DEPOSIT, SOUTHEASTERN BRITISH COLUMBIA (82G/5W)

**Craig H.B. Leitch, Consulting Geologist**

KEYWORDS: Economic geology, sedex deposits, base metals, vein, hydrothermal alteration, Fors, Vine, Sullivan, Purcell Supergroup, Aldridge Formation, Moyie sills.

## INTRODUCTION

At the Fors property, argentiferous lead-zinc sulphide mineralization consisting of pyrrhotite, sphalerite, galena, arsenopyrite, pyrite, chalcopyrite and rare native bismuth occurs in stratiform, semimassive to massive lenses, disseminations and veins at the top of a discordant zone of pebble wacke or fragmental in middle Aldridge sandstone and mudstone (Britton and Pighin, 1995). This preliminary description of the petrography, geochemistry and fluid inclusions is based entirely on examination of drill-core specimens collected by the writer, R.J.W. Turner of the Geological Survey of Canada, J.M. Britton (formerly of the B.C. Geological Survey Branch) and D.L. Pighin of Consolidated Ramrod Gold Corporation. This paper builds on the geological description in Britton and Pighin (1995).

## GEOLOGICAL SETTING

The Fors prospect (MINFILE 082GSW035) is located near Moyie Lake, 17 kilometres southwest of Cranbrook (Figure 1) and 8 kilometres southwest of the Vine prospect, a Middle Proterozoic massive sulphide base and precious metal vein deposit (Höy and Pighin, 1995). Access to the Fors and Vine properties is by paved and gravel roads from Highway 3/95. The exploration history of the Fors property is summarized by Britton and Pighin (1995).

Hostrocks to the Fors and Vine deposits are mainly siliciclastic and lesser carbonate sedimentary rocks of the Aldridge Formation of the Middle Proterozoic Purcell Supergroup, exposed in a major northeasterly plunging anticlinorium cut by high-angle normal and reverse faults (Figure 1; Höy, 1993). The formation comprises in excess of 4000 metres of turbidites probably deposited in an extensional basin in an intracratonic setting (Winston *et al.*, 1984), and consists of three divisions. The lower Aldridge (base not exposed) consists mainly of thin-bedded rusty argillaceous siltstone and is overlain by 3000 metres of thick to thin-bedded turbidites of the middle Aldridge and 500 metres of massive to faintly laminated argillite of the upper Aldridge (Höy, 1993). At the Fors, the top of the lower Aldridge is marked by a concordant pebble wacke or fragmental that is stratigraphically equivalent to the Sullivan horizon (Figure 2; Britton and Pighin, 1995). A number of thick gabbro sills (Moyie sills) intrude the upper part of the lower Aldridge and the middle of the middle Aldridge, with contact features indicating intrusion into wet, partly consolidated sediments (Höy, 1989). Uranium-lead dating of zircons from these sills (1445±11 Ma, Höy, 1989; 1467 Ma, Anderson *et al.*, in preparation) therefore constrain the Proterozoic age of the Purcell basin and its contained mineral deposits.

The Fors area is underlain by gently to moderately north to northeast-dipping strata that mostly show only gentle open folds and are cut by the major northeast-striking Moyie fault and minor northwest-striking high-angle faults (Figure 1). Metamorphic grade, attributed to burial, is middle greenschist facies (McMechan and Price, 1982), with estimates of temperature and pressure for the Sullivan mine area of 440±50 °C and 3±1 kilobars (De Paoli and Pattison, 1993) or 375 °C and 4.5±1 kilobars (Lydon and Reardon, 1993). Regional deformation and metamorphism occurred at about 1350 Ma based on lead-lead dating of sphene from the Sullivan deposit and adjacent rocks (Schandl *et al.*, 1993). Compression and as much as 300 kilometres of eastward translation occurred during the Jura-Cretaceous (Price, 1981), and the area has beeen subjected to Eocene extensional faulting.

Most of the altered rocks described below belong to the middle Aldridge Formation, and consist mainly of detrital quartz and lesser but significant feldspar (up to 20%: Edmunds, 1977), with variable amounts of porphyroblastic biotite, white mica (muscovite and sericite), chlorite, sulphides (pyrrhotite and pyrite), and accessory sphene, allanite, apatite and zircon (Leitch *et al.*, 1991).

## HYDROTHERMAL ALTERATION

Several unusual alteration assemblages are associated with the Fors deposit, either closely or loosely related to the sulphide mineralization. Although these assemblages are all now composed of metamorphic minerals, they presumably developed after distinctive precursor minerals, as has been documented for the Sullivan deposit (Leitch and Turner, 1992; Shaw *et al.*, 1993a,b). The Fors deposit is crudely mushroom shaped (Figure 2; Britton and Pighin, 1995), with the stem consisting of a tourmaline and plagioclase-altered zone within and around the fragmental pipe, and the cap composed of plagioclase-biotite, calcsilicate (actinolite-talc) and mica (biotite-muscovite) alteration assemblages with disseminated to bedded sulphides. Both the stem and the cap are cut by a late-stage, sulphide-rich vein. Following the scheme adopted by and illustrated in hand

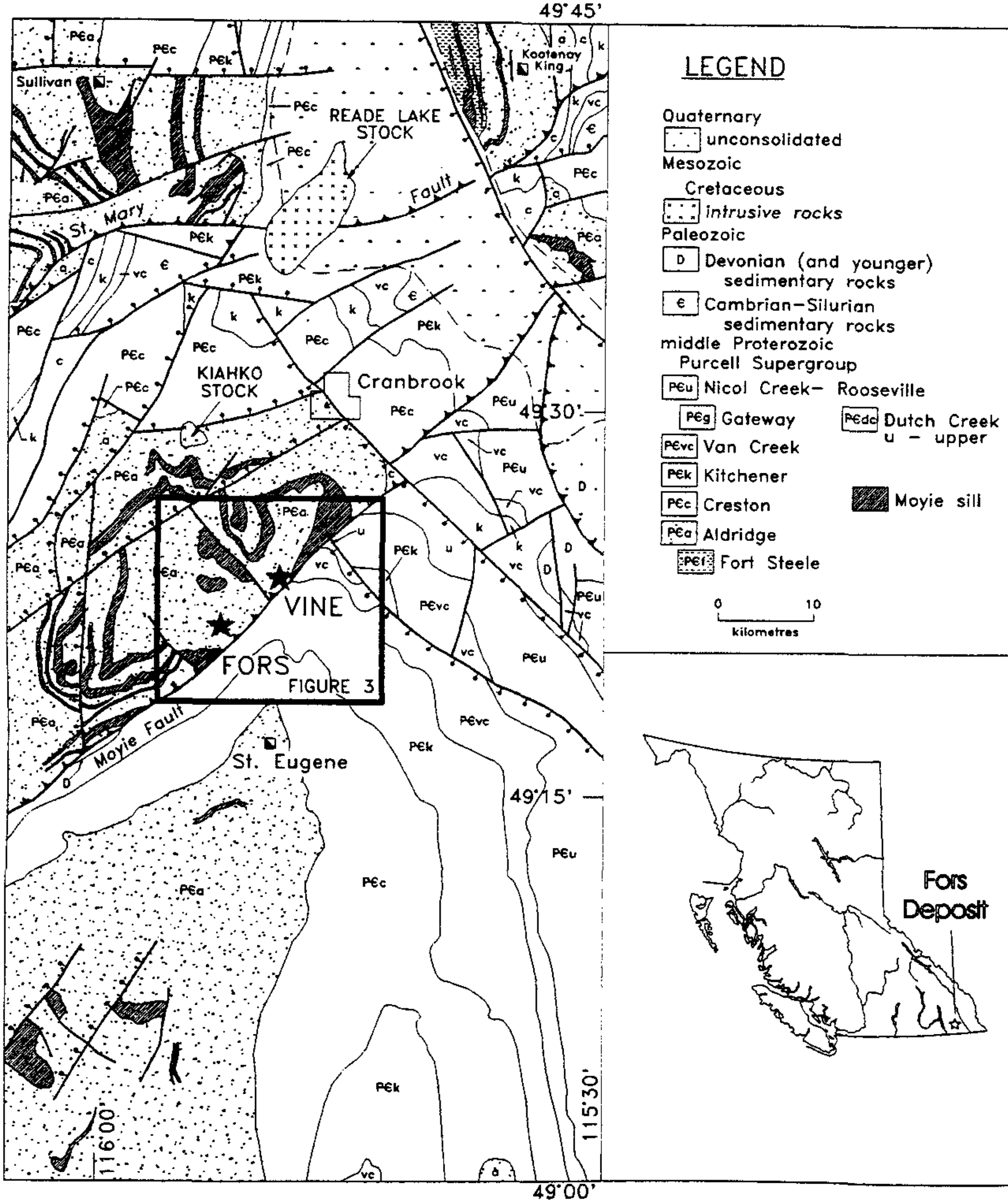


Figure 1. Regional geology and deposit location.

specimen in Britton and Pighin (1995), the alteration types are grouped into five main associations: tourmaline; plagioclase-biotite-garnet; biotite-calcsilicate; sericite; and silica (Figure 2). The petrographic descriptions in this paper are intended to complement the field descriptions in Britton and Pighin.

## *DESCRIPTION OF SAMPLES AND ANALYTICAL PROCEDURE*

The samples selected for this study are mainly from diamond-drill holes 92-1 and 92-2 (located in section on Figure 2), and two from diamond-drill hole 93-10 to examine peripheral alteration. Thin and polished thin sections

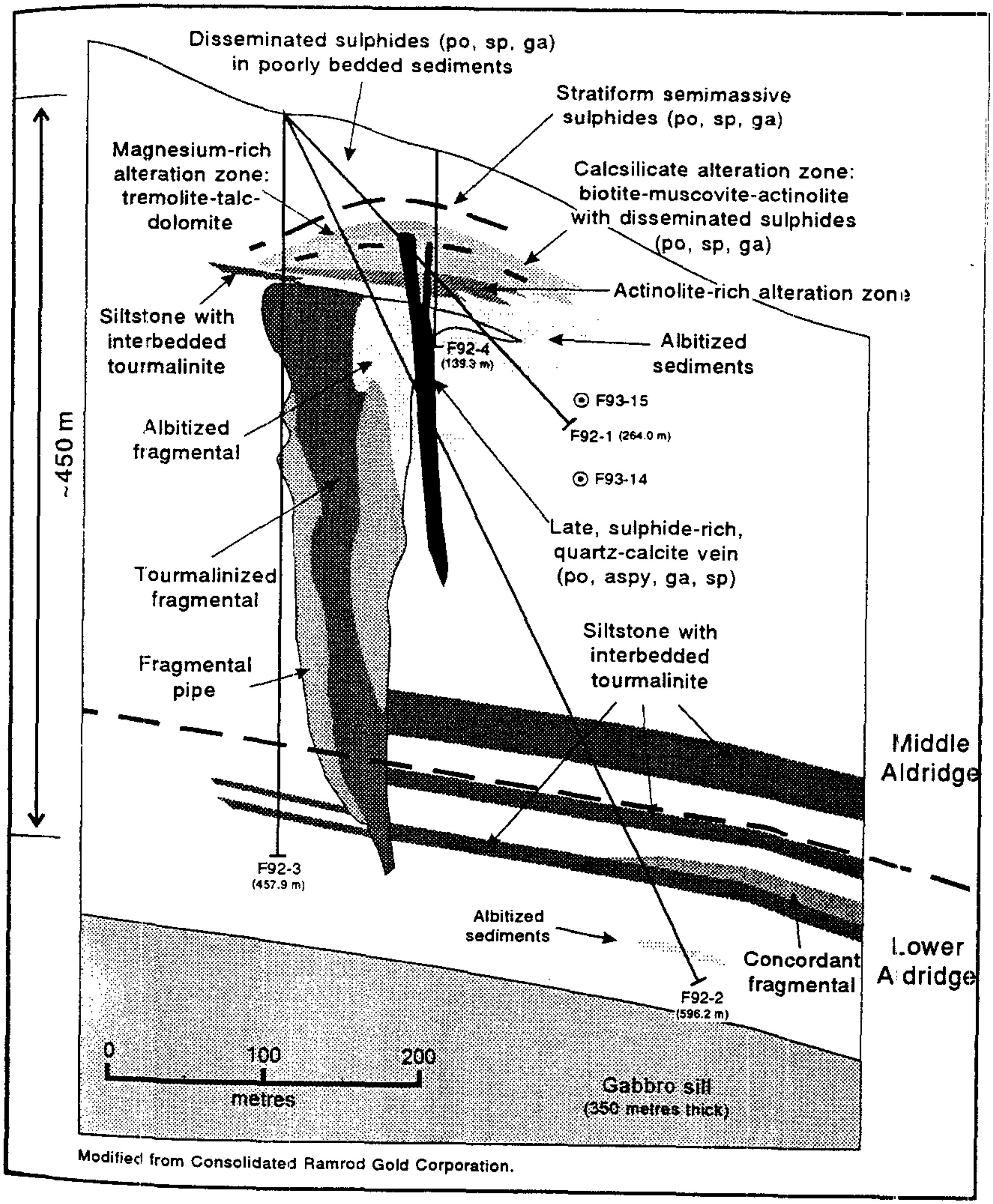


Figure 2. Schematic cross-section, Fors deposit, to show location.

were cut from drill core and examined in transmitted and reflected light and by SEM-EDS (scanning electron microscope - energy dispersive microanalysis). Photographs of hand samples representative of the various alteration types are in Britton and Pighin (1995).

Geochemical analyses on related samples (single offcuts of drill core) were completed for 37 elements [Ag, Al, As, Au, B, Ba, Be, Bi, Ca, Cd, Co, Cr, Cu, Fe, Hg, K, La, Mg, Mn, Mo, Na, Nb, Ni, P, Pb, Sb, Sc, Sn, Sr, Th, Ti, U, V, W, Y, Zn and Zr by HF digestion - ICP (inductively coupled plasma)] at Acme Laboratories, for major oxides $SiO_2$, $Al_2O_3$, $TiO_2$, $Fe_2O_{3t}$, MnO, MgO, CaO, $Na_2O$, $K_2O$, loss on ignition, carbon, sulphur ($S_t$) and barium by fused disk XRF (x-ray fluorescence) and Leco induction furnace at Cominco Exploration Research Laboratory, plus arsenic, antimony and mercury by atomic absorption at Chemex Labs Ltd., and boron by neutron activation by Activation Laboratories Ltd., all under the direction of Ray Lett of the British Columbia Geological Survey Branch.

Following initial petrographic studies, doubly polished sections 50 to 100 microns thick were prepared by standard methods (Holland *et al.*, 1978) for those samples chosen for fluid inclusion microthermometry. A USGS (United States Geological Survey) gas-flow heating and freezing stage, calibrated in accordance with the manufacturer's recommendations, was used to make microthermometric measurements. The accuracy when so calibrated is better than ±0.4°C from -56.6 to +660.4°C (T.J. Reynolds, unpublished manuscript, 1988). Precision was estimated by replicate measurements to be ±1% up to 200°C and ±2% from 200 to 500°C.

## *PETROGRAPHY*

**Tourmalinization** consists of very fine needles of tourmaline replacing feldspar and mica interstitial to the detrital quartz framework in the siltstones. This is characteristic of tourmalinization whether it is of the dark black (bedded) or light brown (discordant fragmental) type. The first type, probably the oldest, is overprinted by most other types of alteration; also, tourmalinized argillite occurs as contorted rip-up clasts in siltstone, and rare dark tourmaline clasts are present in the discordant fragmental (Britton and Pighin, 1995).

An example of the first type (F92-2 422 m) consists of detrital quartz (< 60 µm ) and 10-50% pale greenish brown tourmaline (1-5 by 10-50 µm), with scattered large, euhedral white, to pink garnets to several millimetres in diameter. In contrast to similar fine hydrothermal tourmaline at the Sullivan deposit with Fe/(Fe+Mg), or F/M, ratios about 0.4 to 0.5, Fors tourmaline appears more iron rich (probably schorlitic; Fe:Si peak height ratio of 0.72 sugesting F/M ratio of perhaps 0.6 to 0.7). The garnets are anisotropic and strongly sieved by inclusions of quartz, tourmaline and sphene (the same minerals as in the matrix). The garnet is manganese rich, particularly at the core (Mn:Fe peak height ratio of 1.37). Note that SEM study permits only qualitative analysis, but the garnets from Fors are comparable to garnets from the Sullivan deposit analysed by microprobe which have manganese contents of up to 80 mol % spessartine (Leitch, 1992a). Accessories inlcude sphene (containing minor ilmenite and rutile) and traces of allanite with Ce>Nd>La>Sm, as at Sullivan. The tourmalinite is cut by bedding-parallel veins of quartz-zoisite±muscovite, pyrrhotite, calcite, sphene, arsenopyrite, minor sphalerite and rare galena, and late bedding-perpendicular veins of quartz, Ca-K zeolite, and minor hydrobiotite and pyrite around pyrrhotite, sphalerite, galena and traces of native bismuth.

Examples of the second type are from 277.2 and 281.1 metres in the same hole, in which grey and brown tourmalinite composed of 2x20 micron pale brown tourmaline alternates with 2 to 5 millimetre thick layers of coarser (possibly recrystallized, to 50 µm) deeper brown tourmaline-potassium feldspar-muscovite-garnet and rare 1 to 2-millimetres laminae of reddish brown tourmalinite rich in sphalerite (10 µm, 15%) that also contain up to 15% apatite (to 60 µm), 5% galena (10 µm) and traces of native bismuth (2-5 µm). Detrital quartz is absent in these laminae. The tourmaline appears to be slightly less iron rich (Fe:Si peak height ratio of 0.63) than in the black tourmalinite; garnet is isotropic but pink and similarly manganese rich (Mn:Fe peak height ratio of 1.27). The potassium feldspar appears to be microcline. Bedding-parallel veins consist of pyrrhotite (with minor pyrite in places), sphalerite, chalcopyrite, quartz, zoisite and muscovite and are crosscut by bedding-perpendicular veinlets of green hydrobiotite and calcium (plus minor K and Mg)-bearing zeolite.

Tourmaline also occurs in unusual stylolite-like "veins" with white and pink or pale grey-green envelopes at 155 to 156 metres in hole F92-1. The tourmaline is a pale brown intermediate schorl-dravite with less iron than tourmaline in the fine tourmalinite and lower, variable calcium content compared to tourmalines analysed at Sullivan (Leitch *et al.*, in preparation a). These relationships indicate recrystallization of the tourmaline in the "veins". The white envelopes are composed of feldspar, mainly plagioclase, probably of albite-oligoclase composition (Ca:Na peak heights of about 4:1 to 10:1), significant potassium feldspar or in places secondary quartz, and minor zoisite-clinozoisite (in places containing minor enrichment in rare-earth elements). The plagioclase forms subhedral crystals ranging from fine (0.1 mm) to coarse (0.5-1.0 mm) replacing the original detrital framework of the rock; potassium feldspar is similarly coarse and probably not detrital. Thus white areas can be due to alteration by albite-oligoclase, potassium feldspar or quartz (silicification). The pink coloration is due to fine shreddy biotite (0.1-0.2 mm) and unusually abundant sphene; grey-green colour is due to sericite (50 µm muscovite) that appears to replace fine-grained (but not coarse) albite-oligoclase, with implications for the timing of sericitization (see below).

**Plagioclase (± biotite)** alteration, well exposed in hole F92-1 from 163 to 178 metres, forms a fine sugary white to pink or pale brown rock with significant replacement of the detrital framework by feldspar; the pink to brown colour is due to fine biotite and lesser sphene. Detrital quartz appears to be recrystallized to 0.25-millimetre anhedra. There is generally variable muscovite and minor zoisite present, and accessory pyrrhotite, apatite and zircon. Coarser clots, layers and veins are composed of alkali feldspar (plagioclase and potassium feldspar in variable proportions) and quartz to 1 millimetre diameter, plus minor biotite, muscovite, chlorite, zoisite, pyrrhotite and sphene. White alteration envelopes in these rocks are composed of plagioclase, surrounding fractures filled with zoisite, pyrrhotite, minor muscovite, quartz, sphene with rutile cores, chlorite and rare, pale coloured tourmaline. Carbonate, zoisite and sericite outside the veinlet envelopes may be after former detrital feldspars. "Clots" in the rock consist of zoisite, chlorite, greenish brown tourmaline (probably intermediate schorl-dravite), minor carbonate, sphene and pyrrhotite together with an unidentified bladed mineral with high relief, moderate birefringence and chemistry intermediate between tremolite and zoisite.

These rocks are also cut by narrow, irregular, anastamosing veinlets of sphene, up to 0.3 millimetre thick with traces of allanite and borders of magnesium-rich chlorite (chlorite in these rocks contains significant manganese and has low F/M, about 0.25-0.4, based on optical characteristics and SEM analysis: *cf.* type 0/1 chlorite described at Sullivan by Leitch *et al.* (in preparation a). Sphene veinlets have a dark stylolitic appearance in hand specimen, and are cut by 0.2-millimetre veinlets of a bladed, low relief, low birefringence mineral that is probably zeolite (identified as Ca ± Na, K Al-silicate by SEM).

The composition of plagioclase varies from albite to oligoclase and lesser andesine or even labradorite, based on optical tests (extinction angles where possible, comparison of relief to quartz) supported by SEM analysis which shows Ca:Na peak heights up to 50:1. A sample from the core of a plagioclase-rich zone, 50 metres thick (F92-1 166.5 m, logged as "albitized"), contains major potassium feldspar in addition to plagioclase, with approximate composition ranging from albite-oligoclase to andesine (Ca:Na peak height ratios determined by SEM about 7:1 to 50:1). At the borders of such plagioclase-rich zones, plagioclase in veinlets cutting calcite-rich samples ("skarn" or calcsilicate rocks, *e.g.* F92-2 176.9 m) is very calcic, possibly anorthite with Ca:Na peak height ratios of over 100:1. Above the plagioclase-rich zone in F92-2, similar calcic plagioclase (Ca:Na peak heights over 50:1) is also found in veinlets that cut tremolitic amphibole, but are cut by fractures of zoisite-sulphide-muscovite-calcite (at 70.7 and 98.9 m) or by coarse white quartz (102.4 m).

**Biotite** alteration is distinctive at Fors (it is not known at Sullivan), occurring as envelopes to sulphide-bearing veins and larger zones, generally fringing calcsilicate (tremolite/actinolite-talc) alteration, especially in the cap zone to the deposit (Britton and Pighin, 1995). Biotite forms coarse euhedral flakes to 2 millimetres in diameter that contain inclusions of magnesium-rich (type 0) chlorite and are slightly altered to more iron-rich (type 1/2) chlorite (classifications of chlorite developed at the Sullivan deposit: Leitch *et al.*, in preparation a). Semiquantitative SEM-EDS analysis of the biotites from Fors suggests they are iron, magnesium, and titanium rich. In contrast to macroscopic relations noted by Britton and Pighin (1995), in thin section, tremolite and actinolite appear to be replaced by biotite and quartz, possibly because petrographic observations focus on the results of metamorphic reactions rather than the original hydrothermal relationships. Sphene, zoisite and garnet, and traces of allanite, are also common in the veins with sulphides, which include pyrrhotite, arsenopyrite, sphalerite, galena, chalcopyrite and rare pyrite. As at Sullivan, minerals such as sphene, zoisite, garnet and allanite (or their metamorphic precursors) appear to be closely associated with the hydrothermal mineralizing process.

**Garnetiferous** rocks are mainly found with plagioclase alteration and in sulphide-bearing veins. In the former, garnets form large, rounded to subhedral aggregates or zoned crystals up to 7 millimetres in diameter, with cores more densely sieved than the rims by minute (10-15 μm) inclusions of the same silicates in the rock matrix around them (quartz, plagioclase, sphene). Alternatively, garnet occurs as subhedral skeletal 1 millimetre crystals with biotite, carbonate, quartz, pyrrhotite, tremolite, zoisite, sphene and allanite, in curious orbicular structures up to 1 centimetre across. In veins, garnet occurs as subhedral to euhedral crystals up to 1 millimetre in diameter with the same minerals as in the orbicular structures. Garnet is also present in the major sulphide-rich quartz-calcite vein (Figure 2) and its calcite-rich envelopes (F92-2 221.4 m). The garnet is probably spessartine rich, based on comparison of SEM-EDS analyses (Mn:Fe peak height ratios generally 1 to 1.5) with SEM anlyses of similar garnets from Sullivan subjected to microprobe analysis. Crystal rims are slightly enriched in manganese in some samples. In places, garnet is partly replaced by carbonate (mainly Mn-calcite, but Mn-siderite, found rarely, could be pseudomorphic after garnet).

**Tremolite/actinolite-talc** alteration is concentrated in a cap zone over the deposit that ranges from a core of actinolite-rich rocks to a fringing calcsilicate alteraton zone (biotite-muscovite-tremolite-actinolite-calcite-zoisite, with disseminated sulphides including pyrrhotite, sphalerite, and galena) and an upper magnesium-rich alteration zone consisting of tremolite, talc and dolomite (Figure 2). Amphibole in these alteration zones is generally coarse grained, occurring as ragged subhedral crystals up to 5 millimetres long. Composition varies from a dark green actinolite (Mg:Fe peak height ratio about 1.6) in the core zone to pale green tremolite (Mg:Fe peak height ratio about 2.8) in the fringing zones. Petrographically, amphibole appears to be replaced by carbonate and biotite, and is cut by calcic plagioclase and quartz; in places, it contains inclusions of biotite, sphene and pyrrhotite. However, macroscopically, amphibole is described as replacing biotite (Britton and Pighin, 1995).

**Sericitization** occurs pervasively as a distal aureole around the other alteration assemblages at depth and above the bedded sulphide zone, where it is associated with silicification (Britton and Pighin, 1995). It may be distinguished in the field by its grey-green colour and softness (drill core of sericitic alteration is mostly scratched by steel, unless it occurs in quartz-rich units). In thin section sericite (fine-grained muscovite) occurs as euhedral to subhedral flakes

## TABLE 1
## GEOCHEMISTRY OF ALTERED ROCKS

| Lab.No | Field No. | CaO | $K_2O$ | $P_2O_5$ | $SiO_2$ | $Al_2O_3$ | MgO | $Na_2O$ | $Fe_2O_3$ | $TiO_2$ | MnO | LOI | Total | Ba | As | Hg | Sb | B |
|---|---|---|---|---|---|---|---|---|---|---|---|---|---|---|---|---|---|---|
| | Units | % | % | % | % | % | % | % | % | % | % | % | % | ppm | ppm | ppb | ppm | ppm |
| | Method | XRF | XRF | XRF | XRF | XRF | XRF | XRF | XRF | XRF | XRF | FUS | SUM | XRF | HAA | CAA | EAA | INA |
| | Laboratory | COM | COM | COM | COM | COM | COM | COM | COM | COM | COM | COM | COM | COM | CME | CME | CME | ACT |
| | Detection Limit | 0.01 | 0.01 | 0.01 | 0.01 | 0.01 | 0.01 | 0.01 | 0.01 | 0.01 | 0.01 | 0.01 | 0.01 | 1 | 1 | 10 | 0.2 | 2 |
| 49444 | F92-1 63 | 3.49 | 1.36 | 0.04 | 75.53 | 8.79 | 1.72 | 0.2 | 4.11 | 0.31 | 0.43 | 2.32 | 98.3 | 197 | 1 | 20 | 2.8 | 4 |
| 49445 | F92-1 72.2 | 1.84 | 3.57 | 0.09 | 68.49 | 12.79 | 3.66 | 1.11 | 5.18 | 0.47 | 0.13 | 1.81 | 99.14 | 1605 | 1 | 10 | 0.8 | 430 |
| 49446 | F92-1 76.0 | 13.59 | 0.31 | 0.05 | 50.23 | 2.77 | 17.31 | 0.2 | 8.38 | 0.09 | 0.88 | 3.82 | 97.63 | 21 | 8 | 10 | 10.5 | 9 |
| 49447 | F92-1 141.1 | 5.33 | 3.19 | 0.08 | 68.9 | 16.24 | 0.64 | 2.44 | 1.01 | 0.58 | 0.11 | 0.99 | 99.51 | 680 | 296 | 10 | 1.4 | 35 |
| 49448 | F92-1 166.4 | 6.19 | 0.22 | 0.07 | 64.33 | 21.01 | 0.1 | 6.36 | 0.24 | 0.72 | 0.02 | 0.44 | 99.71 | 57 | 360 | 10 | 1.6 | 19 |
| 49449 | F92-1 173.3 | 2.3 | 1.11 | 0.04 | 84.02 | 7.31 | 0.32 | 1.26 | 2.02 | 0.27 | 0.07 | 0.79 | 99.51 | 259 | 30 | 10 | 0.6 | 46 |
| 49450 | F92-2 105.2 | 1.75 | 2.54 | 0.03 | 83.84 | 7.36 | 0.43 | 0.33 | 0.49 | 0.24 | 0.03 | 0.85 | 97.89 | 1100 | 560 | 10 | 4.4 | 255 |
| 49451 | STD - FER 3 | 2.14 | 0.29 | 0.13 | 49.84 | 1.55 | 1.26 | 0.1 | 40.21 | 0.07 | 0.19 | 3.7 | 99.48 | 59 | 26 | 40 | 3.8 | 83 |
| 49452 | F93-10 39.2 | 1.67 | 3.96 | 0.1 | 66.06 | 13.95 | 4.23 | 1.31 | 5.33 | 0.52 | 0.15 | 2 | 99.28 | 869 | 1 | 10 | 0.8 | 105 |
| 49453 | F93-10 44.1 | 23.63 | 0.21 | 0.05 | 7.06 | 4.82 | 21.48 | 0.05 | 3.93 | 0.2 | 0.86 | 36.81 | 99.1 | 4 | 2 | 40 | 1.4 | 3 |
| 49454 | F93-10 49.3 | 15.25 | 0.04 | 0.04 | 20.83 | 5.88 | 25.42 | 0.02 | 2.91 | 0.2 | 0.4 | 28.41 | 99.4 | 2 | 1 | 20 | 1 | <2 |
| 49455 | F93-10 56.7 | 3.94 | 0.3 | 0.05 | 37.91 | 14.26 | 27.13 | 0.05 | 6.3 | 0.6 | 0.29 | 8.95 | 99.79 | 29 | 1 | 10 | 0.4 | <2 |
| 49456 | F93-10 59.8 | 0.83 | 9.06 | 0.07 | 41.2 | 14.89 | 20.69 | 0.04 | 8.16 | 0.54 | 0.27 | 3.88 | 99.63 | 388 | 2 | 30 | 0.8 | 2 |
| 49457 | F93-10 64.4 | 12.5 | 0.74 | 0.05 | 53.66 | 15.2 | 8.63 | 0.63 | 5.32 | 0.48 | 0.46 | 1.59 | 99.26 | 55 | 1 | 10 | 0.6 | 5 |
| 49458 | F93-10 69.7 | 8.06 | 1.93 | 0.06 | 58.45 | 17.17 | 4.19 | 2.18 | 3.46 | 0.62 | 0.22 | 1.97 | 98.31 | 232 | 64 | 10 | 1.2 | 52 |
| 49459 | F93-10 73.2 | 3.93 | 1.07 | 0.03 | 81.39 | 6.41 | 2.23 | 0.63 | 2.24 | 0.22 | 0.17 | 1.04 | 99.37 | 327 | 1020 | 20 | 2.8 | <2 |

| Lab.No | Field No. | Mo | Cu | Pb | Zn | Ag | Ni | Co | Mn | Fe | As | U | Th | Sr | Cd | Sb | Bi | Sc |
|---|---|---|---|---|---|---|---|---|---|---|---|---|---|---|---|---|---|---|
| | Units | ppm | ppm | ppm | ppm | ppm | ppm | ppm | ppm | % | ppm | ppm | ppm | ppm | ppm | ppm | ppm | ppm |
| | Method | TICP | TICP | TICP | TICP | TICP | TICP | TICP | TICP | TICP | TICP | TICP | TICP | TICP | TICP | TICP | TICP | TICP |
| | Laboratory | ACM | ACM | ACM | ACM | ACM | ACM | ACM | ACM | ACM | ACM | ACM | ACM | ACM | ACM | ACM | ACM | ACM |
| | Detection Limit | 2 | 2 | 5 | 2 | 0.3 | 2 | 2 | 5 | 0.01 | 5 | 10 | 2 | 2 | 0.4 | 5 | 5 | 1 |
| 49444 | F92-1 63 | 2 | 115 | 1331 | 929 | 1.3 | 11 | 3 | 3568 | 2.98 | <4 | <10 | 7 | 178 | 5.4 | 6 | 4 | 9 |
| 49445 | F92-1 72.2 | 2 | 66 | 90 | 204 | <0.3 | 18 | 5 | 915 | 3.65 | <4 | <10 | 7 | 167 | 0.4 | 6 | <5 | 12 |
| 49446 | F92-1 76.0 | 5 | 23 | 6358 | 6215 | 9.1 | 10 | 6 | 5618 | 5.63 | 8 | <10 | <2 | 32 | 46.4 | 16 | 18 | 2 |
| 49447 | F92-1 141.1 | <2 | 4 | 58 | 222 | <0.3 | 15 | 5 | 475 | 0.76 | 45 | <10 | 12 | 264 | 1.9 | <5 | <5 | 12 |
| 49448 | F92-1 166.4 | 2 | <2 | 28 | 11 | <0.3 | 4 | 3 | 86 | 0.15 | 50 | <10 | 11 | 317 | 0.6 | <5 | <5 | 3 |
| 49449 | F92-1 173.3 | 2 | 18 | 21 | 14 | <0.3 | 8 | 2 | 456 | 1.48 | <4 | <10 | 5 | 56 | <0.4 | <5 | <5 | 5 |
| 49450 | F92-2 105.2 | <2 | <2 | 39 | 13 | <0.3 | 9 | 6 | 168 | 0.43 | 174 | <10 | 6 | 49 | <0.4 | 5 | <5 | 5 |
| 49451 | Std. - FER 3 | 14 | 41 | 64 | 216 | 0.5 | 57 | 15 | 934 | 4.99 | 29 | <10 | 12 | 400 | 1.2 | 10 | 6 | 14 |
| 49452 | F93-10 39.2 | 2 | 35 | 64 | 184 | <0.3 | 21 | 8 | 976 | 3.67 | <4 | <10 | 9 | 155 | 0.6 | 9 | <5 | 12 |
| 49453 | F93-10 44.1 | <2 | 16 | 66 | 148 | <0.3 | 11 | 4 | 5414 | 2.76 | <4 | <10 | 5 | 531 | <0.4 | 14 | <5 | 4 |
| 49454 | F93-10 49.3 | <2 | 4 | 15 | 128 | <0.3 | 18 | 4 | 2624 | 1.87 | <4 | <10 | 5 | 719 | 0.5 | 16 | <5 | 5 |
| 49455 | F93-10 56.7 | <2 | 4 | 13 | 254 | <0.3 | 20 | 8 | 1930 | 3.76 | <4 | <10 | 6 | 12 | <0.4 | 11 | <5 | 5 |
| 49456 | F93-10 59.8 | 2 | 4 | 8 | 471 | <0.3 | 29 | 8 | 1765 | 5.3 | <4 | <10 | 11 | 5 | 0.7 | 11 | <5 | 11 |
| 49457 | F93-10 64.4 | 12 | <2 | 196 | 299 | 0.9 | 25 | 2 | 3007 | 3.74 | <4 | <10 | 11 | 303 | 0.4 | <5 | <5 | 10 |
| 49458 | F93-10 69.7 | <2 | <2 | 520 | 383 | 2.5 | 20 | 1 | 1571 | 2.52 | 34 | <10 | 13 | 377 | 2.3 | 8 | 7 | 14 |
| 49459 | F93-10 73.2 | 6 | 6 | 103 | 116 | 0.5 | 8 | 3 | 1032 | 1.66 | 102 | <10 | 6 | 91 | <0.4 | 8 | 4 | 4 |

| Lab.No | Field No. | V | Ca | P | La | Cr | Mg | Ba | Ti | Al | Na | K | W | Zr | Sn | Y | Nb | Be |
|---|---|---|---|---|---|---|---|---|---|---|---|---|---|---|---|---|---|---|
| | Units | ppm | % | % | ppm | ppm | % | ppm | % | % | % | % | ppm | ppm | ppm | ppm | ppm | ppm |
| | Method | TICP | TICP | TICP | TICP | TICP | TICP | TICP | TICP | TICP | TICP | TICP | TICP | TICP | TICP | TICP | TICP | TICP |
| | Laboratory | ACM | ACM | ACM | ACM | ACM | ACM | ACM | ACM | ACM | ACM | ACM | ACM | ACM | ACM | ACM | ACM | ACM |
| | Detection Limit | 2 | 0.01 | 0.01 | 2 | 2 | 0.01 | 1 | 0.01 | 0.01 | 0.01 | 0.01 | 2 | 2 | 2 | 2 | 2 | 1 |
| 49444 | F92-1 63 | 24 | 2.43 | 0.014 | 25 | 198 | 1.12 | 218 | 0.19 | 4.88 | 0.23 | 1.16 | 3 | 24 | 15 | 18 | 9 | 1 |
| 49445 | F92-1 72.2 | 46 | 1.23 | 0.035 | 23 | 101 | 2.21 | 1631 | 0.28 | 6.93 | 0.77 | 2.78 | 5 | 55 | 26 | 19 | 11 | 2 |
| 49446 | F92-1 76.0 | 28 | 8.4 | 0.005 | 7 | 13 | 29.67 | 47 | 0.05 | 1.96 | 0.11 | 0.22 | <2 | 13 | 33 | 8 | 1 | <1 |
| 49447 | F92-1 141.1 | 28 | 3.9 | 0.027 | 18 | 103 | 0.46 | 581 | 0.34 | 9.11 | 1.52 | 1.88 | <2 | 35 | 29 | 27 | 14 | 2 |
| 49448 | F92-1 166.4 | 8 | 4.11 | 0.02 | 7 | 45 | 0.06 | 38 | 0.39 | 10.08 | 3.43 | 0.12 | 10 | 39 | 43 | 35 | 19 | 2 |
| 49449 | F92-1 173.3 | 18 | 1.59 | 0.012 | 22 | 133 | 0.23 | 223 | 0.15 | 3.88 | 0.79 | 0.78 | 2 | 32 | 9 | 15 | 6 | 1 |
| 49450 | F92-2 105.2 | 14 | 1.14 | 0.009 | 16 | 191 | 0.18 | 1034 | 0.12 | 3.63 | 0.22 | 1.98 | 2 | 26 | 24 | 15 | 6 | <1 |
| 49451 | Std. - FER 3 | 75 | 2.76 | 0.124 | 42 | 76 | 2.06 | 530 | 0.36 | 8.86 | 1.03 | 1.51 | 17 | 46 | <2 | 21 | 18 | 4 |
| 49452 | F93-10 39.2 | 46 | 1.13 | 0.043 | 32 | 84 | 2.86 | 813 | 0.29 | 7.65 | 0.74 | 2.69 | 7 | 63 | 11 | 23 | 12 | 2 |
| 49453 | F93-10 44.1 | 14 | 14.84 | 0.007 | 1 | 13 | 40.47 | 19 | 0.04 | 3.69 | 0.01 | 0.21 | 3 | 12 | 2 | 9 | 5 | <1 |
| 49454 | F93-10 49.3 | 16 | 10.58 | 0.01 | 13 | 15 | 44.21 | 5 | 0.01 | 4.26 | 0.01 | 0.01 | 2 | 17 | <2 | 11 | 5 | <1 |
| 49455 | F93-10 56.7 | 37 | 2.73 | 0.019 | 46 | 39 | 33.71 | 12 | 0.05 | 7.96 | 0.04 | 0.19 | 8 | 28 | 2 | 18 | 8 | <1 |
| 49456 | F93-10 59.8 | 47 | 0.38 | 0.026 | 36 | 36 | 29.77 | 418 | 0.31 | 10.25 | 0.03 | 5.6 | 3 | 68 | 6 | 12 | 12 | <1 |
| 49457 | F93-10 64.4 | 36 | 7.87 | 0.01 | 47 | 76 | 14.91 | 64 | 0.27 | 8.94 | 0.32 | 0.48 | 2 | 35 | 23 | 30 | 9 | 2 |
| 49458 | F93-10 69.7 | 52 | 5.29 | 0.017 | 32 | 101 | 3.56 | 230 | 0.32 | 9.41 | 1 | 1.24 | 5 | 51 | 14 | 25 | 14 | 3 |
| 49459 | F93-10 73.2 | 14 | 2.76 | 0.008 | 18 | 181 | 1.44 | 293 | 0.12 | 3.49 | 0.38 | 0.72 | 2 | 19 | 11 | 12 | 7 | <1 |

**NOTES:**

XRF = Fused disc-X-ray fluorescence spectroscopy
FUS = Fusion at 1050°C
SUM = Sum of oxides
HAA = Aqua regia digestion - hydride generation atomic absorption spectroscopy
CAA = Aqua regia digestion-flameless atomic absorption spectroscopy
EAA = HCl-$KClO_3$ digestion - atomic absorption spectroscopy

INA = Thermal neutron activation analysis
TICP = $HClO_4$-$HNO_3$-HCl-HF-Digestion-Inductively Coupled Plasma Emission Spectroscopy
COM = Cominco Research Laboratory
CME = Chemex Laboratories Ltd.
ACM = ACME Analytical Laboratories Ltd.
ACT = Activation Laboratories Ltd.

generally less than 50 microns in diameter, making up to 65% of argillaceous hostrocks but as little as 25% of quartz-rich hostrocks such as siltstones (*e.g.*, hole F93-10, peripheral to the main mineralized zone; not on Figure 2). Sericite-altered layers also occur within the central deposit area, interbedded with tourmalinite and albite-altered rocks. In thin sections from these areas, sericite appears to replace feldspars, including original detrital plagioclase and potassium feldspar, some secondary plagioclase (albitic to calcic in composition), and layers of possibly secondary potassium feldspar.

Minor muscovite, as euhedral flakes up to 0.5 millimetre in diameter, is also found as a probable hydrothermal mineral in many veins with sulphide, zoisite, biotite, tourmaline and sphene, although in places it may possibly be the product of alteration of biotite (with chlorite). Some of these muscovite-bearing veins have plagioclase-biotite envelopes; sericite does not appear to replace albitized rocks. However, pale green sericitic envelopes around sulphide-bearing veins do appear to cut potassium feldspar altered or silicified rocks.

**Silicification** has been described by Britton and Pighin (1995) as occurring in two ways: first, as irregular zones apparently confined to strata overlying the calcsilicate alteration cap, up to the level of the Main showing (Maheux, 1990) or elsewhere in drill core (Klewchuck, 1993), and secondly, as thin envelopes around chalcedonic (?late-stage) quartz veins.

Silicification is difficult to discern reliably in both hand specimen and thin section. Zones of white to pale grey rock, either as envelopes to fractures or veins, or forming pervasive zones, variably identified as silicification or albitization in hand specimen, can turn out on petrographic/SEM examination to be secondary albite, calcic plagioclase, potassium feldspar, or quartz (silicification). In some cases both feldspathic and silicic alteration are present.

In the present study, pervasive secondary (possibly hydrothermal) quartz was identified mainly on the basis of its recrystallized texture, which contrasts with the more rounded outlines of the ubiquitous detrital quartz. This is similar to the textures observed at Sullivan; in contrast to earlier statements (*e.g.* Leitch *et al.*, 1991) that discounted the introduction of quartz due to alteration, it now appears likely that silicification is more widespread at both Fors and Sullivan (Leitch *et al.*, in preparation a). Note that in most of the Fors calcsilicate alteration, the detrital quartz framework is entirely absent; minor quartz occurring with calcsilicate alteration is clearly secondary, and largely appears to replace amphibole.

White alteration envelopes around narrow tourmaline-bearing veins in plagioclase-altered sediments (F92-1 between 150 and 170 m: loosely termed "albitized sediments" in Figure 2) consist of either silicification (euhedral to subhedral crystals of 0.1-0.2 mm diameter) or feldspar alteration (subhedral 0.5-1.0 mm plagioclase mixed in places with anhedral potassium feldspar to 0.5 mm). In thin sections lacking a polished surface (so that SEM studies are not possible), the lack of optical relief between quartz and secondary albite-oligoclase (generally untwinned) makes it impossible to tell silicification and plagioclase alteration apart, even petrographically.

## GEOCHEMISTRY

As part of a preliminary assessment of the geochemistry of alteration, various alteration types were characterized by major oxides ($SiO_2$, $Fe_2O_{3t}$, MnO, MgO, CaO, $Na_2O$, $K_2O$, $H_2O$, C, $S_t$) and trace elements (Ag, As, B, Ba, Bi, Cu, Hg, La, Pb, Sb, Sn, Zn), uncorrected for volume changes, considered most likely to reflect alteration processes. Other oxides ($Al_2O_3$ and $TiO_2$) and trace elements (Nb, Y, Zr) are relatively immobile and may be used to estimate the amount of volume change during alteration, using the average chemistry of unaltered host sediments as a starting point. Geochemical data are in Table 1.

**Actinolite-talc alteration** is represented by samples F92-1 76 (actinolite rich), F93-10 56.7 (tremolite rich) and F93-10 64.4 (silicified, plagioclase altered). This alteration is characterized by high magnesia (to 27%, particularly in those richest in talc) and lime (to 14%). Silica values are low, as low as 7% in rocks made up mainly of carbonate, to 50% in those made up mainly of amphibole or 55% in the silicified example. Alumina and titania vary from extremely low (as low as 3% and 0.1%, respectively) in the samples rich in amphibole and talc, to normal (15% and 0.5%, respectively: Leitch *et al.*, in preparation b) in the samples that include significant muscovite or biotite. This probably indicates significant volume addition in the case of the amphibole or talc-rich samples, and is confirmed by low contents of zirconium, niobium and yttrium. There appears to be a correlation between iron and actinolite content in the amphibole-rich samples, although this is somewhat obscured by the presence of iron and base metal sulphides, as indicated by elevated values for trace elements ($S_t$, Pb, Zn, Sb, Ag, Bi, Cd and Sn) in the actinolite rich sample.

**Carbonate alteration** is represented by samples F93-10 44.1 (dolomite rich) and F93-10 49.3 (talc-sericite-biotite bearing), which are enriched in lime (to 24%) and magnesia (to 25%), and are also distinguished by high loss on ignition to 37%, and carbon up to 10%. As for amphibole-talc-rich samples, low values for the immobile oxides alumina and titania and the immobile elements (Zr, Y and Nb) probably indicate significant volume addition.

**Plagioclase (± biotite) alteration** is represented by samples F92-1 141.1 (with garnet), 166.4 (strong calcic plagioclase), 173.3 (weak, calcic plagioclase), F92-2 105.2 (patchy), and F93-10 69.7 (veinlets). Where most strongly developed, this alteration is characterized by high alumina (up to 21%) and titania (up to 0.72%), probaly due to volume loss during the alteration, which at Sullivan is typified by complete leaching of the original detrital quartz and replacement by plagioclase of albitic composition (Leitch *et al.*, in preparation b). However, at Fors this alteration is more calcic, as evidenced by the lime values being roughly equal or greater than the soda (Table 1). Silica values vary from about 84% in the weakest plagioclase alteration down to 65% in the strongest alteration, correlating with the destruction of detrital quartz and replacement by plagioclase.

Magnesia values are low to very low (0.1% in massive plagioclase alteration) due to the almost complete absence of mafic minerals; potash is also lowest in the strongest plagioclase alteration due to the absence of mica (muscovite and biotite). Manganese tends to be low (0.25%); scattered anomalous values in arsenic (to 560 ppm) and tin (to 43 ppm) or tungsten (to 10 ppm) are not obviously explainable. Both the tin and tungsten analyses are by ICP, and therefore represent minimum values.

**Biotite alteration** is represented by samples F93-10 39.2 (with significant pyrrhotite) and 59.8 (biotite dominant). These samples are characterized by elevated potash values compared to the other samples in the suite (4 to 9%), relatively low soda (1.3 to 0.1%) and lime (1.7 to 0.8%) and moderate to low silica (66 to 41%). Magnesia and iron are elevated, up to 21% and 8%, respectively. Values for the immobile oxides (alumina and titania) and elements (Zr, Y, Nb) are about average for these sediments and thus indicate little or no volume change, in agreement with findings for biotite hornfelsed or granofels altered sediments at the Sullivan deposit (Leitch *et al.*, in preparation b).

**Sericitization** is represented by one sample (F92-1 7.2, rich in muscovite and biotite) which contains somewhat elevated potash (3.6%), iron (5%) and magnesia (3.7%) with normal to slightly depleted silica (68%), immobile oxides alumina and titania, and immobile elements (Zr, Y and Nb). Thus this type of alteration is probably characterized by relatively little volume change, as indicated at Sullivan (Leitch *et al.*, in preparation b).

**Silicification** (samples F92-1 63 and F93-10 73.2) is characterized by moderately high silica (76-81%) and low values for alumina and titania (possibly due to either the protolith being quartzite with low initial values for these oxides, or to volume change during alteration: Leitch *et al.*, in preparation b). All other oxides are also low except CaO (3-4%), possibly due to calcic plagioclase, and $Fe_2O_3$ due to variable sulphide (detected by $S_t$ up to 1.27% and elevated Pb and Zn in the sample from F92-1). Elevated MnO in this sample, which is from massive, silicified quartzite immediately above the stratiform sulphides (Figure 2), is probably due to manganiferous garnet, as noted petrographically from 3 metres deeper in the hole. The other sample, from a silicified zone below a plagioclase-altered zone in F93-10, is not anomalous except for 1000 ppm arsenic.

## FLUID INCLUSIONS

### *PETROGRAPHY*

Although all samples were examined petrographically for fluid inclusions, only two containing fluid inclusions in veins were analysed microthermometrically. All samples examined were from the footwall, below the stratiform semimassive sulphide horizon, and thus could be expected to contain a record of mineralizing solutions that formed the stratiform body. As at the Sullivan deposit (Leitch, in preparation), fluid inclusions are restricted to vein quartz, carbonate and rarely epidote; visible inclusions are not found in the adjacent detrital quartz. This implies that the fluid inclusions are related to the mineralizing episode, and not merely samples of metamorphic fluids. Also as at Sullivan, no primary fluid inclusions were seen in the Fors samples. The majority of inclusions are found along trails, or healed fractures, that do not cross crystal boundaries and therefore are pseudosecondary (*i.e.*, they probably record fluids passing through the rocks during the formation of the deposit). Small (generally 1-2 μm) inclusions along through-going fractures are probably secondary, and were not subjected to further analysis.

The observed fluid inclusions are mostly type 2 (a and b; possibly c) and less commonly type 1 (classification used for the Sullivan deposit in Leitch, 1992b; Leitch, in preparation). The basic distinction between type 1 and 2 is that the former are halite-saturated (over 26 weight % NaCl equivalent, hereafter abbreviated as wt %) whereas the latter are undersaturated. However, both have similar major cations, as indicated by eutectic temperatures.

In quartz veins cutting plagioclase-altered samples (F92-1 166.5 and F92-2 176.9), pseudosecondary type 2a/b inclusions up to 10 microns in diameter, with rounded to irregular outlines, are confined to trails in the quartz and rarely calcite, and do not cross into adjacent plagioclase. Massive carbonate from F92-1 79.5 does not contain visible fluid inclusions.

Laminated tourmalinite with scattered garnet from F92-2 281.1 is cut by pyrrhotite-sphalerite-quartz-minor plagioclase-zoisite-muscovite veins, but none of the silicate minerals contains visible fluid inclusions. Clear to white quartz-calcite-pyrite veins, both bedding parallel and perpendicular, in fine, dark brown, laminated tourmalinite from 422 metres in the same hole contain only very fine (2 μm) secondary fluid inclusions. Black tourmalinite with abundant laminated pyrrhotite from 525 metres in the same hole is cut by quartz-clinozoisite veins. Quartz in these veins contains pseudosecondary type 1 and 2 inclusions with regular or negative crystal shapes up to 7 microns in diameter. The type 1 inclusions contain halite daughter crystals and vapour bubbles roughly equal in size, at 1.5 to 2 microns, indicating vapour to liquid, or V/L, ratios of about 10% by volume and salinities of up to 35 wt%; many also contain one or two other daughter minerals with relief higher than halite, and variable birefringence. These refringent daughter minerals remain unidentified. The clinozoisite crystals contain abundant highly irregular, possibly one-phase (liquid or vapour) inclusions and less common, regular shaped type 2 inclusions to 8 microns in diameter, with vapour bubbles up to 1.5 microns indicating V/L ratios of about 10%.

A quartz-pyrrhotite vein from a major network spanning 20 metres in F92-6 (sampled at 102.6 metres), hosted in biotite-plagioclase-pyrrhotite alteration, contains pseudosecondary type 2 inclusions up to 45 microns long with vapour bubbles up to 8 microns in diameter (rarely to 27 μm , probably indicating necking).

### *MICROTHERMOMETRY*

Microthermometric measurements were only possible on two samples, F92-2 525 and F92-6 102.6. In F92-2 525, most type 1 inclusions froze only with difficulty at about -70 to -90 °C, or froze on warming to about -80 to -90 °C. Eutectic (first melting) temperatures ranged from -63 to -72 °C, indicating significant concentrations of $CaCl_2$ in addition to NaCl (Davis *et al.*, 1990). Magnesium chloride may also be present, but cannot be confirmed from the available data. On further warming, complex melting events observed over the range -45 to -23 °C, with modes near -32 and -24 °C ($Tm_1$ and $Tm_2$), may indicate melting of salt hydrates (see below). Type 2a inclusions displayed similar freezing and eutectic temperatures. In F92-6 102.6 and F92-1 525, type 2b inclusions found along fractures apparently crossing fractures containing type 1 and type 2a inclusions froze around -40 to -47 °C and displayed eutectic temperatures in the same range. In F92-6 102.6, type 2b inclusions froze at about -40 to -47 °C, with eutectic temperatures in the range -37 to -50 °C whereas type 2c inclusions found along separate fractures displayed double freezing at -32 and -45°C, characteristic of fluids containing minor $CO_2$; eutectic temperatures were in the same range as for type 2b. The higher eutectic temperatures for type 2b and c inclusions suggest that although magnesium may be present in these fluids, calcium is not likely.

Salinities of the inclusion fluids were estimated by temperature of dissolution of the halite cube (Ts) for type 1 inclusions, modified by temperature of melting events 1, 2 and final ($Tm_1$, $Tm_2$, $Tm_f$) in type 1 and 2a/b inclusions; for type 2c inclusions, by final melting temperatures modified by clathrate melting ($Tm_c$) where observed. For Ts values in the 220 to 464°C range, salinities of 32-47 wt% NaCl equivalent are indicated (Roedder, 1984). However, due to the "salting out" effect caused by divalent salts, these values may overestimate the salinity (Roedder, 1984). These inclusions can be best understood in the context of ternary NaCl-$CaCl_2$-$H_2O$ and $MgCl_2$-$CaCl_2$-$H_2O$ diagrams (Crawford, 1981). Intermediate melting temperatures $Tm_1$ and $Tm_2$ were difficult to observe in the presence of other solids (ice and/or hydrohalite), but where measured were in the ranges -35 to -45 °C and -24 to -29 °C respectively. The less common event at -35 to -45 °C is interpreted as the melting of a phase such as $CaCl_2.6H_2O$ or $MgCl_2.12H_2O$ (Crawford *et al.*, 1979), and suggests a wide range of the magnesium to calcium ratio in the fluid, possibly due to both elements being present in small amounts in these cases. Melting in the range -24 to -26 °C was much more common; in type 1 (halite-bearing) inclusions, this appeared to be final ice melting, whereas in type 2a/b inclusions, this is interpreted as hydrohalite melting in the presence of ice. In either case, the temperature serves to fix the Na/Ca ratio of the fluid at about 1:1 (or $X_{NaCl}$ of 0.5; less commonly between 0.35 and 0.7).

Salinity estimates can best be made by comparing final ice-melting temperatures to a ternary NaCl-$CaCl_2$-$H_2O$ diagram (Crawford, 1981; *cf.* Peter *et al.*, 1994). Final melting temperatures are between -8.5 and -23 °C for type 2a/b inclusions, giving salinities from 15-20 wt% . For type 2c inclusions, final melting temperatures between -0.2 and -10.6°C indicate relatively low salinities (3 to 13 wt%; Potter *et al.*, 1978). However, these are probably overestimates for the salinities, due to the withdrawal of water into clathrates (Collins, 1979). Clathrate melting is common in type 2c inclusions but rare in type 2a or b; it is not seen in type 1 inclusions. Clathrate melting temperatures mainly in the 6 to 7°C range indicate salinities less than 10 wt%, possibly slightly overestimated by the presence of $CH_4$ in addition to $CO_2$ (Roedder, 1984).

Homogenization temperatures (vapour to liquid) are difficult to measure for these inclusions, due to stretching and decreptitation, but in sample F92-2 525, the range for type 1 and type 2a inclusions is from 125 to 285°C and for type 2b from 98 to 250°C. In sample F92-6 102.6, the range for type 2b is from 260 to 371°C and for type 2c is from 202 to 290°C. As at the Sullivan deposit (Leitch, in preparation) interpretation of seawater depths of 100 to 2000 metres leads to trapping temperatures for type 1 and 2a inclusions of 150 to 300°C. However, type 2b inclusions in quartz-pyrrhotite veins at Fors appear to record higher temperatures of up to 395°C, possibly reflecting late main-stage overprinting in the well developed vent zone, correlative with the second pulse that produced veins enriched in arsenic, tungsten, silver and bismuth (Britton and Pighin, 1995). Although not subjected to microthermometry, fluid inclusions associated with plagioclase alteration at Fors (possibly similar to albitic alteration at Sullivan) may also record similar or lower temperatures than the main-stage alteration (Leitch, in preparation).

# DISCUSSION

One of the key questions at the Fors deposit concerns the setting of the mineralization and whether it differed from that of the Sullivan deposit. Certain features such as the form and distribution of the tourmalinites (black bedded and brown replacing fragmental rocks), and the unusual calcsilicate cap rock, bear on this question.

On the basis of preliminary evidence, tourmaline from the Fors deposit appears to be generally slightly more iron rich than tourmaline at the Sullivan deposit, at least in the black, commonly laminated tourmalinite interbedded with siltstone near the lower to middle Aldridge contact (Figure 2). It is also not clear from the limited analytical work of this study that the tourmaline in brown tourmalinite, commonly observed replacing fragmental rock, is richer in magnesium (as suggested by Britton and Pighin, 1995 and Slack, 1993). Various authors have suggested that increased magnesium content of the hydrothermal tourmaline is favourable for mineralization (*e.g.*, Taylor and Slack, 1984).

It is not clear whether the dark laminated tourmalinite at Fors formed syngenetically on the seafloor, or by replacement of previously formed sediments; although Slack (1993) generally favours the latter, either case is permissive of a brine-pool setting. The absence of detrital quartz, and the presence of anomalous apatite and native bismuth in the sphalerite (±galena)-rich laminae of this tourmalinite, suggests that some of these layers are true chemical precipitates. Although the sieve texture of the garnets in tourmalinite implies that they grew during metamorphism, their high manganese content suggests they grew from a manganese-rich precursor such as carbonate or hydroxide, as at the Sullivan deposit, where such manganese content is taken to indicate the presence of a brine pool.

The calcsilicate caprock is composed of layers rich in amphibole (tremolite to actinolite), talc, carbonate, plagioclase and micas (biotite and muscovite). The magnesium-rich nature of this alteration assemblage suggests it may have formed in response to mixing with downward-welling, magnesium-rich seawater in the footwall, as the system cooled after deposition of the main stratabound sulphide horizon, possibly at the top of the feeder pipe now represented by the tourmalinized fragmental. However, the shape of the calcsilicate cap is suggestive of a mound that could have formed over the top of a vent debouching on the seafloor. In this scenario, stratiform semimassive sulphides would have had to form after the calcsilicate mound.

Absence of the detrital quartz framework in calcsilicate alteration zones suggests they are derived from a different protolith than most of the host clastic sediments, possibly from chemical sediments; alternatively, the original framework may have been totally leached during alteration. Complete leaching of the quartz framework of the hostrocks is well documented at Sullivan, where both chloritized and albitized rocks containing no quartz can be traced into sediments with abundant detrital quartz. At Fors, significant volume addition for samples rich in amphibole, talc and carbonate may indicate swamping of the normal detrital sediment input by a chemical precipitate, either in a hydrothermal mound or a brine-pool setting.

The abundance of calcic plagioclase in the Fors alteration is distinct from the albite so common at Sullivan, and demands an explanation. Possibly there was so much calcium, either derived from the calcsilicate chemical sediment or alteration, floating around in the system that during metamorphism the calcic plagioclase had to form, much as in the metamorphism of a calcsilicate. The timing of plagioclase alteration is also uncertain, but it does not appear to be as late as at the Sullivan, as plagioclase envelopes to tourmalinite veins are seen. Possibly there was more overlap between the tourmalinite and plagioclase alteration phases, or a later pulse of tourmalinite (veining) is present.

As at the Sullivan deposit (Leitch *et al.* in preparation a), sericite alteration appears to form a general envelope to the main mineralized zones at the Fors deposit. Timing of this alteration is difficult to establish, particularly on the basis of petrographic relationships, as at Sullivan. Sericitization of albite-oligoclase envelopes to tourmaline veins does not necessarily suggest sericite is later than albite as only fine (possibly detrital) feldspar is replaced.

Hydrothermal fluids associated with tourmalinite formation, and possibly responsible for the Fors lead-zinc mineralization, appear to have been broadly similar to those at the Sullivan deposit: highly saline (halite saturated to just undersaturated) and containing significant calcium in addition to sodium. Similar fluids are found in the Iron Creek copper-cobalt-gold deposit in Idaho (Leitch and Hall, in preparation) and similar or less saline fluids are found in the Sheep Creek copper-cobalt deposit in Montana (Leitch *et al.*, in preparation c; Zieg and Leitch, 1994). The mineralizing fluids may have been at about 150 to 300°C, similar to temperatures for the Sullivan type 1 - type 2a fluids (Leitch and Turner, 1992; Leitch, in preparation). However, at Fors, there is a suggestion of hotter post-main stage fluids trapped at up to 395 °C in type 2b inclusions in quartz-pyrrhotite veins associated with arsenopyrite, scheelite, and silver-bismuth values. Eutectic temperatures suggest these fluids may have contained magnesium rather than calcium in addition to sodium, inviting the suggestion that they were also associated with the magnesium-rich calcsilicate cap over the deposit. Possibly the magnesium could have been supplied by downward circulation of seawater that mixed with the post-main stage fluids.

By comparison with studies at Sullivan and other localities elsewhere in the Aldridge Formation (Leitch, in preparation), the more dilute fluids containing traces of carbonic fluid (type 2c inclusions) are probably related to Mesozoic metamorphism.

## REFERENCES


Anderson, H.E., Goodfellow, W.D. and Parrish, R.R. (in preparation): U-Pb Geochronology, Petrogenesis and Tectonic Setting of the Middle Proterozoic Moyie Sills, Purcell Basin, B.C.; *Geological Survey of Canada*, Special Volume.

Britton, J.M. and Pighin, D.L. (1995): Fors - a Proterozoic Sedimentary Exhalative Base Metal Deposit, Purcell Supergroup, Southeastern British Columbia (82G/5W); *in* Geological Fieldwork 1994, Grant, B. and Newell, J.M., Editors, *B.C. Ministry of Energy, Mines and Petroleum Resources*, Paper 1995-1, pages 99-109.

Collins, P.L.F. (1979): Gas Hydrates in $CO_2$-bearing Fluid Inclusions and the Use of Freezing Data for Estimation of Salinity; *Economic Geology*, Volume 74, pages 1435-1444.

Crawford, M.L. (1981): Phase Equilibria in Aqueous Fluid Inclusions; *in* Fluid Inclusions: Applications to Petrology, *Mineralogical Association of Canada*, Short Course Handbook Volume 6, pages 75-100.

Crawford, M.L., Kraus, D.W. and Hollister, L.S. (1979): Petrologic and Fluid Inclusion Study of Calc-silicate Rocks, Prince Rupert, British Columbia; *American Journal of Science*, Volume 279, pages 1135-1159.

Davis, D.W., Lowenstein, T.K. and Spencer, R.J. (1990): Melting Behavior of Fluid Inclusions in Laboratory-grown Halite Crystals in the Systems $NaCl-H_2O$, $NaCl-KCl-H_2O$, $NaCl-MgCl_2-H_2O$, and $NaCl-CaCl_2-H_2O$; *Geochimica et Cosmochimica Acta*, Volume 54, pages 591-601.

De Paoli, G.R. and Pattison, R.M.D. (1994): Metamorphic Pressure, Temperature, and Fluid Conditions of the Sullivan Mine, Kimberley, British Columbia, Using Silicate-Carbonate Equilibria (abstract); *in* Minerals Colloquium, Program with Abstracts, Ottawa, Ontario, January 17-19, *Geological Survey of Canada*, unpaginated.

Edmunds, F.R. (1977): The Aldridge Formation, B.C., Canada; unpublished Ph.D. thesis, *Pennsylvania State University*, University Park, Pennsylvania, 368 pages.

Holland, R.A.G., Rey, C.J. and Spooner, E.T.C. (1978): A Method for Preparing Doubly Polished Thin Sections Suitable for Microthermometric Examination of Fluid Inclusions; *Mineralogical Magazine*, Volume 42, pages 407-408.

Höy, T., (1989): The Age, Chemistry, and Tectonic Setting of the Middle Proterozoic Moyie Sills, Purcell Supergroup, Southeastern British Columbia; *Canadian Journal of Earth Sciences*, Volume 26, pages 2305-2317.

Höy, T. (1993): Geology of the Purcell Supergroup in the Fernie West-half Map Area, Southeastern British Columbia; *B.C. Ministry of Energy, Mines and Petroleum Resources*, Bulletin 84, 157 pages.

Höy, T. and Pighin, D.L. (1995): Vine - a Middle Proterozoic Massive Sulphide Vein System, Purcell Supergroup, Southeastern British Columbia (82G/5W); *in* Geological Fieldwork 1994, Grant, B. and Newell, J.M., Editors, *B.C. Ministry of Energy, Mines and Petroleum Resources*, Paper 1995-1, pages 85-98.

Klewchuck, P. (1993): Assessment Report on Two Diamond Drill Holes (F92-2 & 3), Fors Property; *B.C. Ministry of Energy, Mines and Petroleum Resources*, Assessment Report 22817.

Leitch, C.H.B. (1992a): Mineral Chemistry of Selected Silicates, Carbonates, and Sulphides in the Sullivan and North Star Stratiform Zn-Pb Deposits, British Columbia, and in District-scale Altered and Unaltered Sediments; *in* Current Research, Part E, *Geological Survey of Canada*, Paper 92-1E, pages 83-93.

Leitch, C.H.B. (1992b): A Progress Report of Fluid Inclusion Studies of Veins from the Vent Zone, Sullivan Stratiform Sediment-hosted Zn-Pb Deposit, B.C.; *in* Current Research, Part E, *Geological Survey of Canada*, Paper 92-1E, pages 71-82.

Leitch, C.H.B. (in preparation): Fluid Inclusion Studies of the Sullivan Sttratiform Sediment-hosted Zn-Pb Deposit, British Columbia; *Geological Survey of Canada*, Special Volume.

Leitch, C.H.B. and Hall, S.M. (in preparation): Main Copper Zone of the Iron Creek Stratabound Sediment-hosted Cu-Co Deposit, Idaho Cobalt Belt, Lemhi County, Idaho: Fluid Inclusion and Related Studies; *Geological Survey of Canada*, Special Volume.

Leitch, C.H.B. and Turner, R.J.W. (1992): Sulphide-bearing Network Underlying the Western Orebody, Sullivan Stratiform Sediment-hosted Zn-Pb Deposit, B.C.: Preliminary Field, Petrographic and Fluid Inclusion Studies; *in* Current Research, Part E, *Geological Survey of Canada*, Paper 92-1E, pages 61-70.

Leitch, C.H.B., Turner, R.J.W. and Höy, T. (1991): The District-scale Sullivan - North Star Alteration Zone, Sullivan Mine Area, British Columbia: A Preliminary Petrographic Study; *in* Current Research, Part E, *Geological Survey of Canada*, Paper 91-1E, pages 45-57.

Leitch, C.H.B., Turner, R.J.W., Shaw, D.R., Hodgson, C.J. and Brown, T. (in preparation, a): Evolution of the Vent Complex, Sullivan Stratiform Sediment-hosted Zn-Pb-Ag Deposit: Part 2, Wall-rock Alteration and Sulphide Mineralization; *Geological Survey of Canada*, Special Volume.

Leitch, C.H.B., Turner, R.J.W., Ross, K.V., Shaw, D.R. and Höy, T. (in preparation, b): Lithogeochemistry of Altered Wallrocks, Sullivan Stratiform Sediment-hosted Zn-Pb-Ag Deposit; *Geological Survey of Canada*, Special Volume.

Leitch, C.H.B., Zieg, G.A. and Hall, S.M. (in preparation, c): Preliminary Fluid Inclusion and Stable Isotope Studies of the Sheep Creek Stratabound Sediment-hosted Cu-Co Deposit, Meagher County, Montana; *Geological Survey of Canada*, Special Volume.

Lydon, J.W. and Reardon, N. (1994): Sphalerite Compositions of the Sullivan Deposit, British Columbia and their Implications for Timing of Metamorphism (abstract); *in* Minerals Colloquium, Program with Abstracts, Ottawa, Ontario, January 17-19, *Geological Survey of Canada*, unpaginated.

Maheux, P.J. (1990): Geology and Geochemistry Report on the Fors Property, Puma and Cougar Claims; *B.C. Ministry of Energy, Mines and Petroleum Resources*, Assessment Report 19809.

McMechan, M.E. and Price, R.A. (1982): Superimposed Low-grade Metamorphism in the Mount Fisher Area, Southeastern British Columbia—Implications for the East Kootenay Orogeny; *Canadian Journal of Earth Sciences*, Volume 19, pages 476-489.

Peter, J.M., Goodfellow, W.D. and Leybourne, M.I. (1994): Fluid Inclusion Petrography and Microthermometry of the Middle Valley Hydrothermal System, Northern Juan de Fuca Ridge; *in* Proceedings of the Ocean Drilling Program, Scientific Results, Mottl, M.J., Davis, E.E., Fisher, A.T. and Slack, J.F., Editors, Volume 139, pages 411-428

Potter, R.W., Clynne, M.A. and Brown, D.L. (1978): Freezing Point Depression of Aqueous Sodium Chloride Solutions; *Economic Geology*, Volume 73, pages 284-285.

Price, R.A. (1981): The Cordilleran Foreland Thrust and Fold Belt in the Southern Canadian Rocky Mountains; *in* Thrust and Nappe Tectonics, McClay, K.R. and Price, R.A., Editors, *The Geological Society of London*, pages 427-448.

Roedder, E. (1984): Fluid Inclusions; *Mineralogical Society of America*, Reviews in Mineralogy, Volume 12, 644 pages.

Schandl, E.S., Davis, D.W. and Gorton, M.P. (1993): The Pb-Pb Age of Metamorphic Titanite in the Chlorite-Pyrite Altered Footwall of the Sullivan Zn-Pb Sedex Deposit, B. C. and its Relationship to the Ore (abstract); *Geological Association of Canada - Mineralogical Association of Canada*, Program with Abstracts, Volume 18, page A93.

Shaw, D.R., Hodgson, C.J., Leitch, C.H.B. and Turner, R.J.W. (1993a): Geochemistry of Tourmalinite, Muscovite, and Chlorite-Garnet-Biotite Alteration, Sullivan Zn-Pb Deposit, British Columbia; *in* Current Research, Part A, *Geological Survey of Canada*, Paper 93-1A, pages 97-107.

Shaw, D.R., Hodgson, C.J., Leitch, C.H.B. and Turner, R.J.W. (1993b): Geochemistry of Albite-Chlorite-Pyrite and Chlorite-Pyrrhotite Alteration, Sullivan Zn-Pb Deposit, British Columbia; *in* Current Research, Part A, *Geological Survey of Canada*, Paper 93-1A, pages 109-118.

Slack, J.F. (1993): Models for Tourmalinite Formation in the Middle Proterozoic Belt and Purcell Supergroups (Rocky Mountains) and their Exploration Significance; *in* Current Reserarch, Part E; *Geological Survey of Canada*, Paper 93-1E, pages 33-40.

Taylor, B.E. and Slack, J.F. (1984): Tourmalines from Appalachian-Caledonian Massive Sulphide Deposits: Textural, Chemical, and Isotopic Relationships; *Economic Geology*, Volume 79, pages 1703-1726.

Winston, D., Woods, M. and Byer, G.B. (1984): The Case for an Intracratonic Belt-Purcell Basin: Tectonic, Stratigraphic and Stable Isotope Considerations; *Montana Geological Society*, 1984 Field Conference, pages 103-118.

Zieg, G.A. and Leitch, C.H.B. (1993): The Geology of the Sheep Creek Copper Deposits, Meagher County, Montana, Program and Abstracts, Belt Symposium III, August 14-21, *Belt Association Inc.*, Spokane.

NOTES

British Columbia Geological Survey
Geological Fieldwork 1995

# NORTHERN SELKIRK PROJECT, GEOLOGY OF THE DOWNIE CREEK MAP AREA (82M/8)

by J. M. Logan, M. Colpron and B. J. Johnson

KEYWORDS: Downie Creek, Carnes Creek, Columbia River, J&L, Standard, Rain, Keystone, Lardeau Group, Index Formation, Badshot Formation, Hamill Group, volcanogenic massive sulphide, iron-manganese exhalatives.

## INTRODUCTION

Lower Paleozoic rocks of the northern Selkirk Mountains are host to numerous volcanogenic massive sulphide occurrences. These include the Goldstream copper-zinc mine, which has produced 70 000 tonnes of copper and 49 000 tonnes of zinc from 1 738 500 tonnes milled, between April, 1991 and October, 1995 (S. Robertson, personal communication, 1995), and the arsenical gold-rich J&L deposit which has probable and possible reserves in excess of 5 million tonnes averaging 2.71 % Pb, 4.33 % Zn, 7.23 g/t Au and 72 g/t Ag. The stratiform nature of these deposits makes understanding the regional stratigraphic and structural setting fundamental to the assessment of mineral potential and exploration for new deposits. The main objectives of the Northern Selkirk project are to establish the stratigraphic and structural framework of known volcanogenic massive sulphide deposits in the northern Selkirk Mountains, and to assess the potential for similiar deposits in correlative successions elsewhere.

This report presents the results of regional bedrock mapping of the Downie Creek area (NTS 82M/8), completed east of the Columbia River, during the summer of 1995. This program marks the second full season of mapping in the Northern Selkirk Mountains. Reconnaissance mapping and deposit studies were initiated in 1993 (Logan and Drobe, 1994). Mapping of the area around the Goldstream deposit (82M/9 and part of 10) was completed in 1994 (Logan *et al.*, 1995, Colpron *et al.*, 1995). Our 1995 study area ties onto the southern boundary of the Goldstream River area, traces prospective stratigraphy southward (Logan *et al.*, 1996) and builds upon previous compilation of the area by Brown (1991).

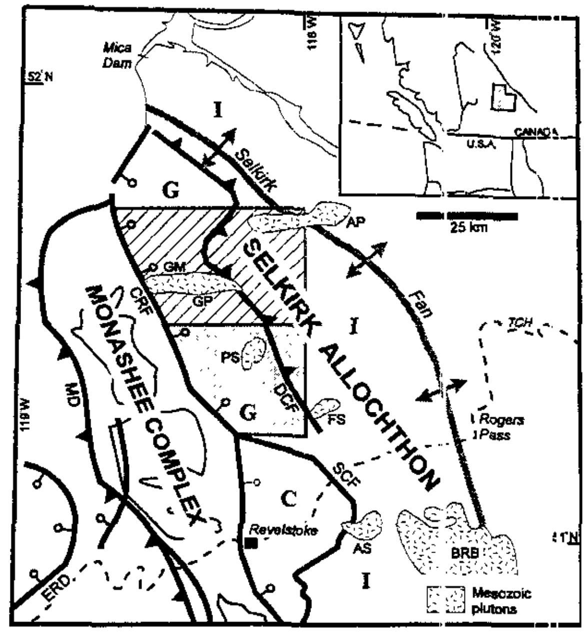


Figure 1: Location of the Downie Creek area (shaded) along the western flank of the Selkirk fan structure, within the Selkirk allochthon; modified after Brown and Lane (1988). Hatched area shows location of the Goldstream River area. I = Illecillewaet slice, G = Goldstream slice, C = Clachnacudainn slice, CRF = Columbia River fault, DCF = Downie Creek fault, SCF = Standfast Creek fault, MD = Monashee décollement, ERD = Eagle River detachment, BRB = Battle Range batholith, AS = Albert stock, FS = Fang stock, PS = Pass Creek pluton, GP = Goldstream pluton, AP = Adamant pluton, GM = Goldstream mine, TCH = Trans-Canada Highway.

## REGIONAL GEOLOGY

The Downie Creek area straddles the boundary between rocks assigned to the North American miogeocline and the pericratonic Kootenay Terrane (Wheeler *et al.*, 1991; Wheeler and McFeely, 1991). It lies along the western flank of the Selkirk fan structure (Wheeler, 1963, 1965; Brown and Tippett, 1978; Price *et al.*, 1979; Price, 1986; Brown and Lane, 1988), a zone of structural divergence that follows the Omineca Belt, and the suture zone between North America and Intermontane Superterrane, from northeastern Washington to east-central Alaska (Eisbacher *et al.*, 1974; Price, 1986). The area is bounded to the west by the Columbia River fault, a major extensional fault of Eocene age along the east flank of the Monashee Complex (Figure 1).

The northern Selkirk Mountains are underlain by a sequence of Neoproterozoic to lower Paleozoic metasedimentary and metavolcanic rocks that form part of the miogeoclinal wedge that accumulated along the western margin of ancestral North America. Wheeler (1963; 1965) has traced the stratigraphic successions defined by Walker (1926), Walker and Bancroft (1929), and Fyles and Eastwood (1962) in the Purcell anticlinorium and the Kootenay Arc, to the south, into the northern Selkirk Mountains. Wheeler assigned the various lithologic units of the northern Selkirk Mountains to the Neoproterozoic Horsethief Creek Group (Windermere Supergroup), the Eocambrian Hamill Group, the Lower Cambrian, *Archeocyathid*-bearing Badshot Formation, and the lower Paleozoic Lardeau Group (Figure 2). To the north and east of Revelstoke, Wheeler also delineated an assemblage of higher grade gneissic and granitic rocks: the Clachnacudainn Complex (Figure 1). Okulitch *et al.* (1975) and Parrish (1992) have shown that orthogneisses of the Clachnacudainn Complex are, in part, Devonian-Mississippian in age.

The northern Selkirk Mountains form part of a large allochthon that was displaced eastward some 200 to 300 kilometres between Late Jurassic and Paleocene time (Price, 1981; Brown *et al.*, 1986, 1992a). As a result, the area is characterized by a complex pattern of superposed folding and faulting. The regional structural style is dominated by the northwest-trending Selkirk fan structure. The eastern flank of this structure is characterized by a northeast-verging imbricate thrust system which is part of the Rocky Mountain fold and thrust belt and is truncated by the Purcell thrust; a major northeast-verging out-of-sequence thrust fault (Simony and Wind, 1970). The western flank is dominated by southwest-verging fold-nappes and thrust faults (Wheeler, 1963, 1966; Raeside and Simony, 1983). Rocks along the western flank of the fan structure are generally metamorphosed to greenschist facies. Amphibolite facies rocks and migmatites occur along a west-northwest-trending metamorphic culmination that approximately follows the northwest trend of the Selkirk fan, extending some 90 kilometres from near Mica dam to Rogers Pass (Figure 1).

The area has also been the locus of intermittent plutonism from Middle Jurassic to Late Cretaceous. Two main suites of granitic plutons intrude the western flank of the Selkirk fan (Gabrielse and Reesor, 1974; Armstrong, 1988): a Middle Jurassic (*ca.* 180-165 Ma)

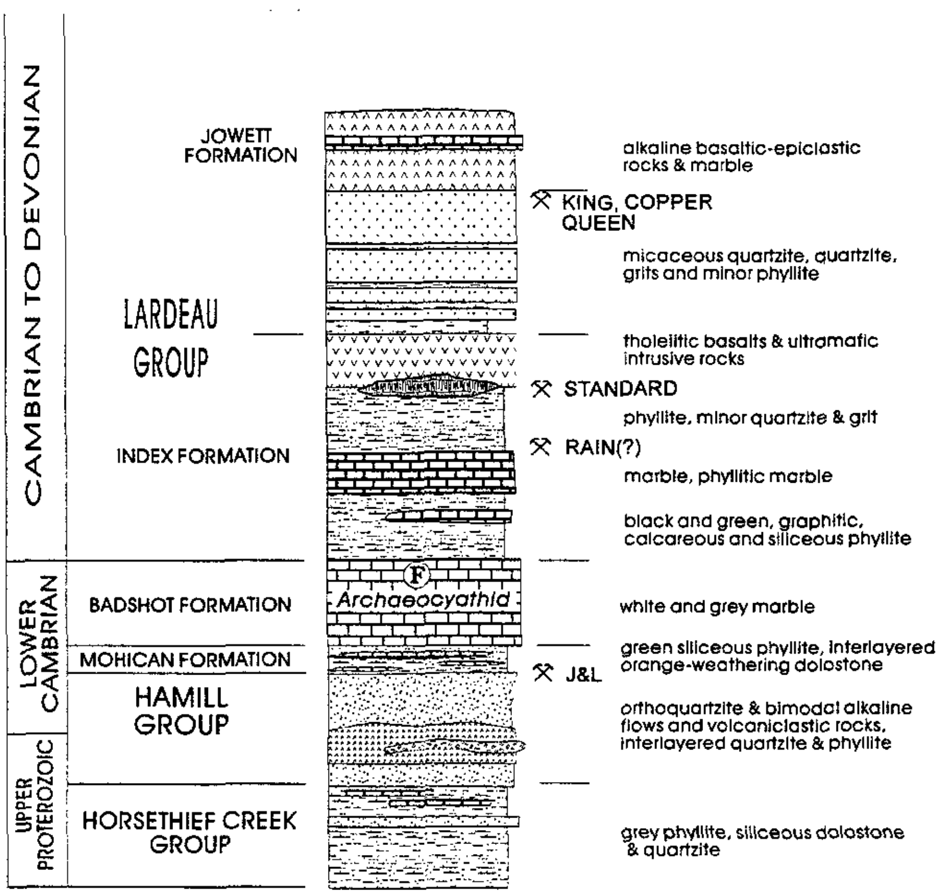


Figure 2: Summary of stratigraphic units mapped in the Downie Creek area.

suite of granodiorite and quartz monzonite that generally cuts the regional structures, but is locally deformed by them; and a mid-Cretaceous (*ca.* 110-90 Ma) suite of quartz monzonite, diorite and two-mica granite that clearly truncates all regional structures. In addition, a less voluminous Late Cretaceous (*ca.* 70 Ma) suite of leucogranites has recently been recognized within the Clachnacudainn Complex (Parrish, 1992).

## STRATIGRAPHY OF THE DOWNIE CREEK AREA

Rocks of the Hamill and Lardeau groups, and the intervening Mohican and Badshot formations, comprise the majority of exposures in the Downie Creek area (Brown, 1991; Wheeler, 1965; Figure 3). Two narrow belts of rock correlated with the Horsethief Creek Group (Wheeler, 1965) are also exposed in the area northeast of Downie Creek (Figure 3).

### *HORSETHIEF CREEK GROUP*

The stratigraphy of the Horsethief Creek Group in the northern Selkirk Mountains has been defined by Brown *et al.*(1978). They have subdivided the Horsethief Creek stratigraphy into lower pelite, middle marble, and upper pelite members. They further suggested that the upper part of the upper pelite member grades westward into a sequence of calcareous pelitic schists with intercalations of marble, impure psammite and quartzite.

In the Downie Creek area, rocks assigned to the Horsethief Creek Group comprise a sequence of soft, tan-weathering, pale green or pinkish grey phyllite, intercalated with pink to light brown siliceous dolostone (5 cm to 2 m thick) and white, pink and light green quartzite. The quartzite beds range from 5 centimetres to 2 metres in thickness and are fine grained and massive. They generally represent less than 30% of the map unit, although micaceous quartzite locally makes up 40-50%.

### *HAMILL GROUP*

Devlin (1989) recognized three stratigraphic divisions within the Hamill Group in the northern Selkirk Mountains: a lower sandstone unit; a greenstone - graded sandstone unit; and an upper sandstone unit. In the Goldstream River area, we mapped the lower two divisions of the Hamill Group (Logan and Colpron, 1995; Colpron *et al.*, 1995). The middle unit of greenstone and volcaniclastic rocks is only locally present in the Downie Creek area, and, as a result, the distinction between lower and upper sandstone units is not easily made.

Most exposures of the Hamill Group are composed of interbedded quartzite and pelite. The quartzite is light green, white or pink, texturally mature, fine to medium grained, and occurs in beds 3 centimetres to 2 metres thick. It is interbedded, in variable proportions, with light green, light grey or dark grey siliceous phyllite in beds a few centimetres to a maximum of 1 metre thick. The quartzite-pelite assemblage is commonly graded, with medium-grained quartzite showing a sharp erosional base and grading into dark siltstone and pelite. The beds are typically characterized by fine, dark, parallel laminations; they locally display tabular crossbeds with well defined mud drapes on the foresets. Locally, small mud chips are present at the base of quartzite beds. Minor buff-weathering sandy dolostone beds are locally interbedded with the quartzite-pelite assemblage. South of Carnes Peak, buff dolostone beds locally represent up to 30-40% of the quartzite-pelite assemblage.

South of Mount Craib, a pure, white to pink orthoquartzite underlies a small peak and extends southeastward for at least 5 kilometres. The orthoquartzite occupies the core of a southwest-verging antiform and has an apparent thickness of less than 100 metres. The quartzite occurs in beds 3 to 4 metres thick, with centimetre-scale interbeds of light grey to light green, rusty weathering siliceous phyllite.

Near its contact with the overlying Mohican and Badshot formations, the Hamill quartzite is typically more massive and thickly bedded (average of 1-2 m) and locally displays large sets (30-50 cm) of trough crossbeds. Its lower contact with the Horsethief Creek Group appears to be gradational; it is marked by an increase in quartzite content and a decrease in dolostone. The Hamill Group has a minimum thickness of about 300 metres in the area northeast of Downie Creek.

Exposures of the greenstone-volcaniclastic assemblage of the Hamill Group are limited to few outcrops along Sorcerer Creek and to alpine exposures of massive greenstone and minor intermediate trachyandesite rocks northeast of Mount Craib (Figure 3).

### *MOHICAN FORMATION*

The Mohican Formation forms a prominent belt of exposures from the west flank of Carnes Peak northward to the confluence of Sorcerer and Downie creeks (Figure 3). Elsewhere, it is represented by only a few metres of section between the Hamill quartzite and the Badshot marble, and locally is absent.

The Mohican Formation consists of light green, light grey, and medium grey siliceous phyllite, commonly intercalated with brown and orange-weathering sandy dolostone beds (1-25 cm thick). Locally, the Mohican also includes light green, fine-grained micaceous quartzite, and beds of light to medium grey marble up to 2 metres thick. East of Roseberry Mountain, a succession of orange-brown weathering dolostone at least 20 metres thick occurs within the Mohican Formation. Near the confluence of Sorcerer and Downie creeks, a light to medium grey pisolitic dolostone can be traced for a few kilometres within the formation. This same dolostone has

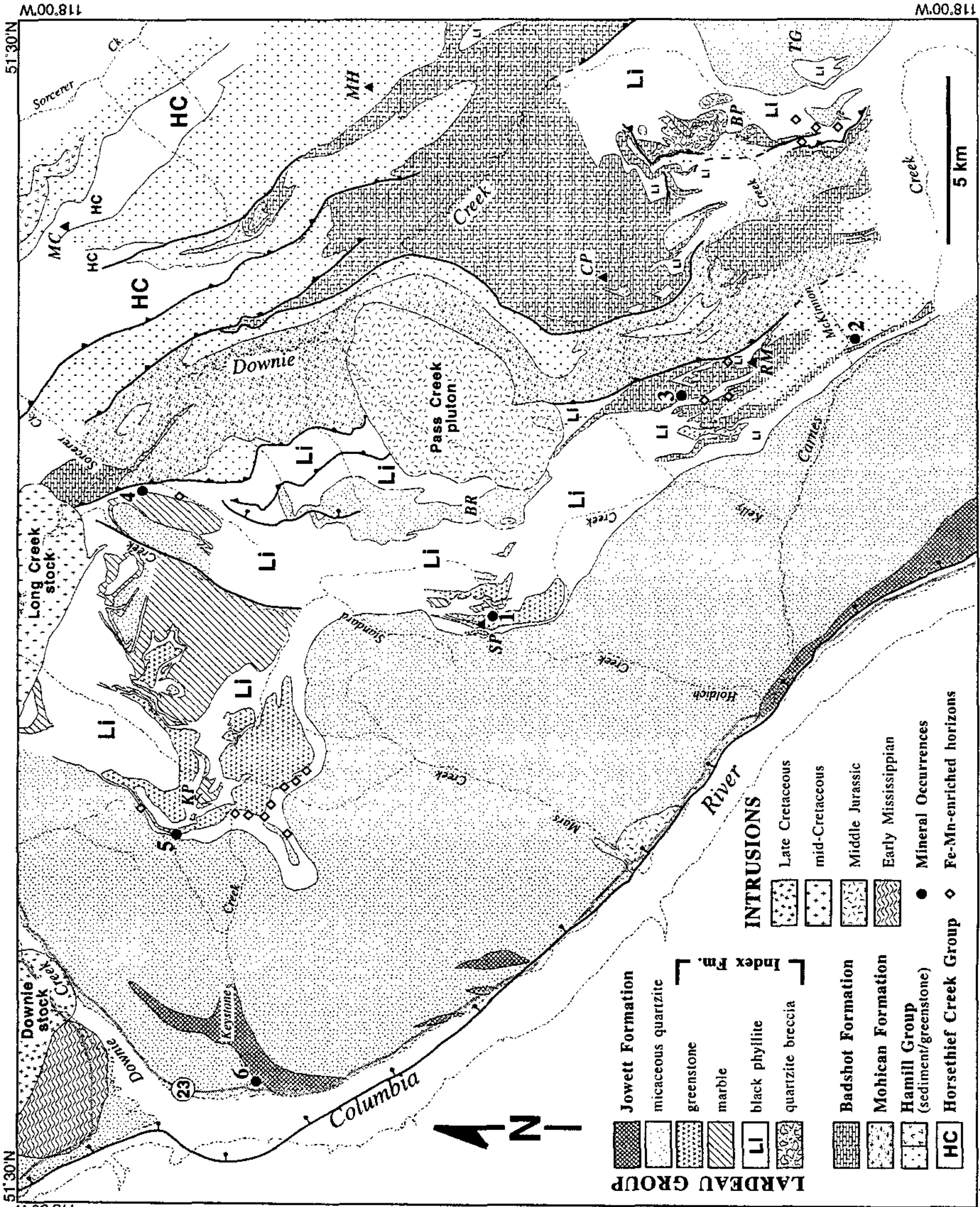

118°00'W
51°30'N
51°15'N
118°30'W
5 km
N
LARDEAU GROUP
Jowett Formation
micaceous quartzite
greenstone
marble
Li black phyllite
quartzite breccia
Index Fm.
Badshot Formation
Mohican Formation
Hamill Group (sediment/greenstone)
HC Horsethief Creek Group
INTRUSIONS
Late Cretaceous
mid-Cretaceous
Middle Jurassic
Early Mississippian
Mineral Occurrences
Fe-Mn-enriched horizons
Columbia
River
Downie stock
Long Creek stock
Pass Creek pluton
Downie Creek
Sorcerer Ck
Standard
Holdich Creek
Mars Creek
Kelly Creek
Carnes
McKinnon
Keystone
Creek
Long Creek
HC
Li
MC
MH
CP
BP
TG
RM
BR
SP
KP
23
1
2
3
4
5
6

been traced northward along the north-side of the Long Creek stock for 5 kilometres (Colpron *et al.*, 1995). White tremolite-bearing marble occurs in scattered exposures along the east side of the Long Creek stock.

## *BADSHOT FORMATION*

Marble of the Badshot Formation forms the prominent peaks of the Carnes Peak massif. It consists of white, light grey, and medium grey marble, locally dolomitic. Near Roseberry Mountain, the Badshot also includes dark grey to black, bioturbated, argillaceous limestone, in which the burrows are filled with brown-weathering sandy dolostone. A few layers of soft, tan phyllite (3-5 m) are also present west of Roseberry Mountain. At Bridgeland Pass, the Badshot includes lenses of dolostone breccia 2 to 3 metres thick. The thickness of the Badshot Formation varies from a few metres to about 300 metres. Rapid changes in thickness are common along the valley of McKinnon Creek. It is uncertain whether they are the result of primary or tectonic processes.

Read and Brown (1979) and Brown (1991) reported the occurrence of *Archeocyathid* in marble of the Badshot Formation at Roseberry Mountain and Bridgeland Pass. In addition to the localities documented by Brown (1991), we have found two new *Archeocyathid* localities, west of Roseberry Mountain and north of Bridgeland Pass. The occurrence of *Archeocyathid* indicates a late Early Cambrian age for marbles of the Badshot Formation.

## *LARDEAU GROUP*

The Lardeau Group (Walker and Bancroft, 1929) conformably overlies the Badshot Formation and is unconformably overlain by the Milford Group (Read and Wheeler, 1976). As defined by Fyles and Eastwood (1962) in the Ferguson area, it includes six formations (Figure 4). In ascending stratigraphic order these are; 1) dark grey and green phyllites, thin limestone and volcanic rocks of the Index Formation, 2) black siliceous argillite of the Triune Formation, 3) grey quartzite of the Ajax Formation, 4) grey siliceous argillite of the Sharon Creek Formation, 5) volcanic rocks of the Jowett Formation, and 6) grey and green quartz-feldspar grit and phyllite of the Broadview Formation. As the Lardeau stratigraphy is traced northward into the Akolkolex River area, the Ajax quartzite pinches out and an intervening unit of grit is exposed between the black phyllites of the Index Formation and the overlying Sharon Creek and Jowett formations (Read and Wheeler, 1976; Sears, 1979). Farther north, in the Illecillewaet synclinorium, the Lardeau Group comprises a lower unit of black graphitic phyllite, a middle unit of green phyllite, quartzite and marble, and an upper unit of grit and black phyllite (Colpron and Price, 1993). Colpron and Price (1993; 1995a) assigned all three units to the Index Formation. A similar three-fold subdivision of the Lardeau Group has been recognized in the Goldstream River map area (Gibson and Höy, 1994; Logan and Drobe, 1994) and was assigned to the Index Formation (Logan and Colpron, 1995).

In the Downie Creek area, the Lardeau Group consists of five lithostratigraphic units which have complex stratigraphic inter-relations (Figure 4). They include, in approximate stratigraphic order; 1) black graphitic, calcareous and/or siliceous phyllite, discontinuous quartzite and limestone; 2) light grey marble; 3) greenstone and metavolcaniclastic rocks; 4) micaceous quartzite, quartzite, quartz grit and grey phyllite; and 5) metavolcaniclastic rocks, greenstone and marble.

### BLACK PHYLLITE

The lower part of the Lardeau Group consists of a 250 to 500-metre succession of dark grey to black calcareous phyllite, brown-weathering phyllitic dolostone and black graphitic phyllite which contains minor dark grey calcitic marble. Locally, dark grey micaceous and dolomitic quartzite beds, light grey marble up to 20 metres thick, quartz grit and chlorite phyllite occur within the black phyllite unit. Black phyllite occurs both below and above the greenstone units exposed in the Keystone and Standard areas (Figures 3 and 4).

South of Keystone Peak, dark grey siliceous phyllite, black cherty quartzite and graphitic phyllite stratigraphically overlie the massive greenstone in the overturned limb of the Keystone antiform. The quartzite and phyllite are rhythmically interbedded, on a centimetre to 10-centimetre scale. Carbonaceous material, pyrite and manganese oxide are ubiquitous throughout the unit in this area. This sequence crops out in the upper drainage basin of Keystone Creek, and can be traced south and east into the upper reaches of Mars Creek.

East of Standard Peak, in the pass between Standard and Kelly creeks and extending up to Belcher Ridge, a sequence of black calcareous and siliceous phyllite, and minor micaceous quartzite and marble, overlies the greenstone unit. The phyllite becomes more siliceous up-section as it gradually passes into the quartzite that underlies Belcher Ridge.

Thin (<3 m) intraformational carbonate conglomerate units are present within black phyllite of the lower Index Formation at Roseberry Mountain and north of Tumbledown glacier. The limestone is typically dark grey or dark brown, contains round and subangular clasts of black and light grey limestone and black phyllite. These units occur stratigraphically above the Badshot-Lardeau

Figure 3: Geological map of the Downie Creek area compiled from our 1995 mapping and from Wild (1990) and Brown (1991). Mineral occurrences: 1 = Standard; 2 = J&L; 3 = A&E; 4 = Rain; 5 = Keystone; 6 = King. Topographical features: MC = Mount Craib; MH = Mount Holway; CP = Carnes Peak; BP = Bridgeland Pass; TG = Tumbledown galcier; RM = Roseberry Mountain; SP = Standard Peak; KP = Keystone Peak.

contact and the basal conglomerate described by Brown *et al.*, (1983).

Southeast of Mount Holway, the base of the black phyllite unit is represented by pale greenish grey sericite phyllite, brown-weathering carbonate and minor pink micaceous quartzite. These rocks are interlayered with, and stratigraphically overlie the Badshot marble. The green phyllite is in sharp contact with the black marble that characterizes the top of the Badshot Formation in the area. It is, in turn, gradationally overlain by dark grey to black, orange-weathering phyllite more typical of the Index Formation. The phyllite consists of thin layers of light green to silver sericite phyllite, and dark brown weathering carbonate, pink micaceous quartzite and grey phyllite. Similar interlayered green phyllite and yellowish brown marble crop out at the contact between light grey marble and black phyllite along the base of Keystone Peak.

## LIGHT GREY MARBLE

A sequence of light grey to white marble, with an apparent thickness of 150 to 300 metres, is exposed in the Keystone area. The marble underlies Keystone Peak and occupies the core of the Keystone antiform; Brown (1991) interpreted it as part of the Index Formation. On Keystone Peak, it is an homogenous light grey to white marble with the bedding outlined by dark grey, wispy laminations.

Light grey and white crystalline marble, thinly foliated buff-weathering phyllitic carbonate and brown-weathering massive dolomitic marble crop out along the ridge-top northeast of Keystone Peak, and down the west slope into Standard Creek. The marble forms the upright limb of the Keystone antiform. It is underlain (in the core of the antiform) by thin-layered black and orange-weathering graphitic phyllite on the slopes overlooking Downie Creek, 5 kilometres to the north. Thinly foliated limonitic-weathering phyllitic carbonate forms the uppermost part of the marble. It is gradational into a thin (<20 m) clastic succession of micaceous quartzite, grey phyllite and feldspathic grit, which in turn are overlain by massive greenstone. Dolomitization affects extensive irregular zones that crosscut bedding within the light grey marble. These zones follow, or terminate abruptly against the foliation, bedding and breccia zones, suggestive of a dolomitizing fluid front.

To the south, in the Standard area, a similar marble occurs in the core of the Standard antiform. However, here the marble appears to be only 5 to 10 metres thick,

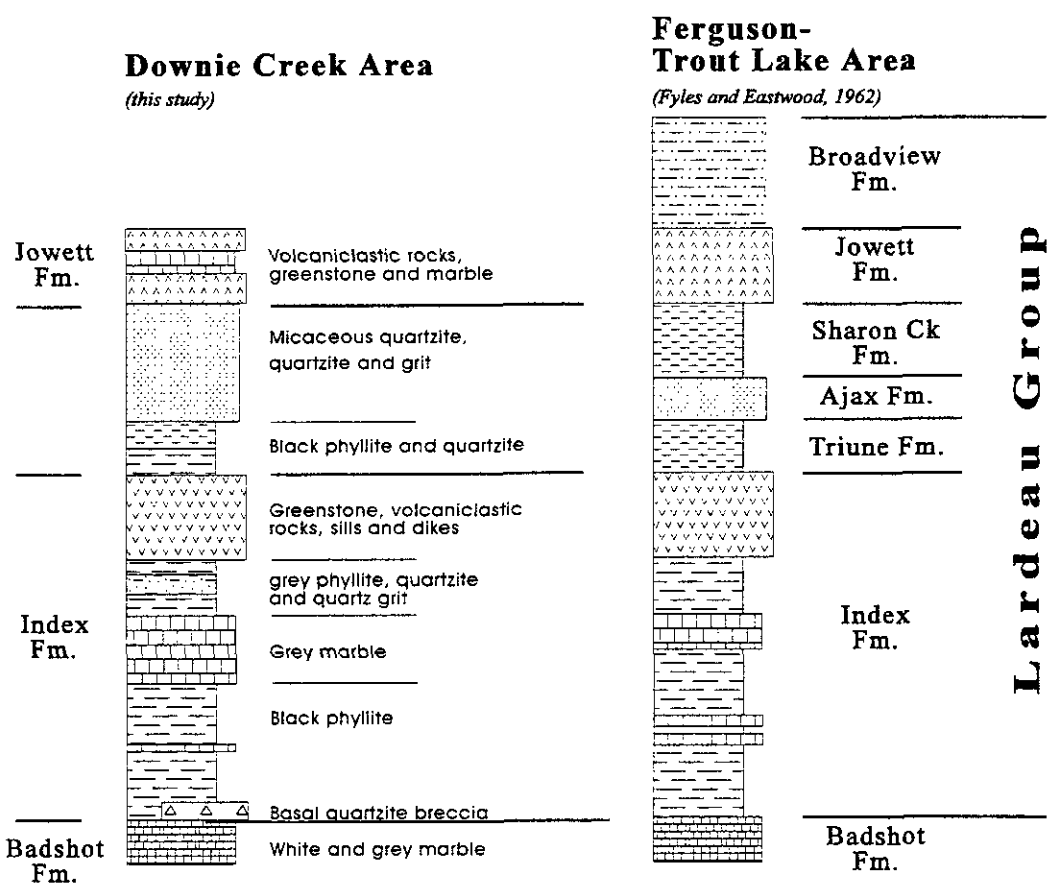


Figure 4: Stratigraphic relations within the Lardeau Group in the Downie Creek area. Ferguson-Trout Lake area stratigraphy after Fyles and Eastwood (1962).

and is underlain by black graphitic and calcareous phyllites. Minor brown-weathering phyllitic dolostone lenses are present within the marble unit at Standard.

## GREENSTONE

Greenstone is present near the top of the black phyllite member in the Keystone and Standard areas. In both areas, black phyllite underlies and overlies the greenstone. The greenstone unit consists of dark khaki-green, massive to weakly foliated metavolcanic rocks. Locally, the massive greenstone is interlayered with thinly foliated phyllite and greenschist of probable tuffaceous origin. In other places, coarser grained, medium grey plagioclase-phyric flows and poorly formed pillowed breccia flows are present. Both lithologies are competent units and typically occur as boudins in more phyllitic greenstone units.

In the Keystone area, the greenstone locally contains epidote pods (*ca.* 30x50 cm). In the Standard Peak area, it is commonly characterized by the presence of abundant, small albite porphyroblasts. In the Keystone area the greenstone unit forms at least two distinct stratigraphic horizons within the black phyllite. Both lower and upper contacts of the greenstone layers are characterized by interdigitations of greenstone, green phyllite and black phyllite on the scale of 10 centimetres to several metres, indicating that the greenstone layers are conformable with the black phyllite unit.

In both the Keystone and Standard areas, ultramafic rocks are common at and near the contact between black phyllite and greenstone. They consist of black, massive antigorite schist; light grey, light green and white talc schist; brown and orange-weathering talc-magnesite schist, serpentine-anthophyllite schist and serpentinite. Small pods and lenses of coarse-grained metadiorite are also commonly associated with ultramafic occurrences in the Standard area. Sills of foliated metadiorite intrude black siliceous phyllite east of the head of Standard Creek. They are 2 to 25 metres thick, concordant with the dominant foliation in the area and composed of medium to very coarse grained, mottled, albite and chlorite. They are typically medium green and white in colour and display a penetrative foliation, outlined by flattened feldspar with chloritic pressure shadows. The thickest sill is medium grained, medium grey in colour and relatively massive, with only a weak fabric outlined by feldspar phenocrysts. The largest intrusion of metadiorite is intruded low in the Lardeau Group stratigraphy, near the contact with the Badshot Formation on the west flank of Roseberry Mountain. These intrusions may be related to similar rocks associated with the greenstone units in the Standard and Keystone areas.

Preliminary geochemistry indicates that the greenstone, green phyllite and the subvolcanic sills in the Standard and Keystone Peak areas, and near the Goldstream River to the north, are tholeiitic basalts of mid-ocean ridge basalt (MORB) affinity.

## MICACEOUS QUARTZITE AND GRIT

Throughout the area, the black phyllite is stratigraphically overlain by a succession of quartzite, micaceous quartzite and grit. These form three northwesterly trending belts in the Downie Creek map area: Tumbledown glacier, Belcher Ridge and the western third of the map area, between Standard, Keystone and Roseberry peaks and the Columbia River (Figure 3).

In the southeastern corner of the map area, between Bridgeland Pass and Tumbledown glacier, the Lardeau Group stratigraphy includes an upright-facing succession of thinly bedded black graphitic, calcareous and locally pyritic phyllite, a mixed package of interlayered green phyllite, quartzite and buff calcareous quartz and feldspathic grits, and an upper package of interbedded rusty phyllite and calcareous quartz-feldspar grit and micaceous quartzite. Graded bedding and flame structures are present in the grit north of Tumbledown glacier.

On Belcher Ridge, the black phyllite unit is gradationally overlain by dark grey and brown quartzite, that locally has a dolomitic cement. The quartzite unit also comprises light grey to pink micaceous quartzite, grey siliceous phyllite and quartz-sericite schist, and subordinate quartz-feldspar grit. A 15 to 20-metre gritty, feldspathic quartzite is locally present at the base of the quartzite unit. The contact with the underlying black phyllites is characterized by intercalated black phyllite and light green micaceous quartzite, with quartzite becoming more abundant up stratigraphic section. Farther north, the contact is sharp and is marked by an intervening unit (up to 20 m thick) of interbedded orange-brown phyllitic dolostone, light green siliceous phyllite, micaceous quartzite and minor grey marble. The quartzites in the Belcher Ridge area are lithologically similar to those exposed along the east side of the Columbia valley, described below.

A thick (?), monotonous package of micaceous quartzite and quartz-muscovite schist stratigraphically overlies the black phyllite and greenstone units of the Lardeau Group along the east flank of the Columbia valley. This quartzite succession occupies the overturned limb of a southwest-verging antiform; it underlies a northwest-trending belt 5 to 10 kilometres wide, east of the Columbia River and extends north into the Goldstream map area (Logan and Colpron, 1995; Colpron *et al.*, 1995; Figure 3).

West of Standard Peak, green siliceous phyllite and micaceous quartzite are in gradational contact with green phyllitic-volcaniclastic rocks, micaceous quartzite, grit and black graphitic phyllite. Graded bedding in the micaceous quartzite indicates that they stratigraphically overlie the black phyllite and greenstone units of the Index Formation.

Adjacent to the contact with the phyllite, the lower sections of this quartzite package are characterized by a resistant medium-bedded white and pale pink or green quartzite and brown micaceous quartzite between Mars and Standard creeks and at Standard Peak. North of Keystone Peak, black phyllite is stratigraphically overlain by green chloritic schist and interlayered buff marble. A covered section separates these schists from green, gritty, chlorite-quartz schist and micaceous quartzite of the quartzite unit, and it is uncertain whether the covered interval contains a transitional facies or a structural break.

Along Carnes Creek, near the mouth of McKinnon Creek, the lower (?) part of the quartzite unit consists of quartzite and light green quartz-sericite schist, interlayered on the scale of a few centimetres and containing abundant white quartz veins and augen of vein quartz. Elsewhere, interbedded micaceous quartzite and green, grey or black phyllite characterize the lower part of the unit. The remainder of the quartzite section is chiefly greenish grey micaceous quartzite and interlayered rusty weathering quartz-muscovite schist. Compositional layering is defined by centimetre-thick, white, fine-grained quartzite layers. Coarse-grained quartzite and local grit layers, contain granules of blue and/or smokey quartz.

### GREENSTONE AND MARBLE

Brown *et al.* (1983) correlated the green metavolcanic rocks and interlayered dolomitic marble exposed along the slopes overlooking the Columbia River with the Jowett Formation. In this area, these rocks are confined to several narrow, north-trending, belts in an inverted stratigraphic panel forming the immediate hangingwall of the Columbia River fault. They consists of a variety of mafic fragmental and epiclastic rocks, including massive to fragmental actinolite schists, dark green calcareous chlorite-albite-muscovite-quartz schist and green chloritic phyllite. They are characterized by a greenschist facies metamorphic assemblage of plagioclase-actinolite-calcite-epidote-chlorite and are interlayered with carbonate. At Holdich Creek, green chlorite-albite-quartz-calcite schist contains 25 metres of white and grey marble. The marble is typically thinly layered, coarsely crystalline, with buff to orange-weathering dolomitic and phyllitic sections at the upper and lower contacts. The contact with the structurally overlying micaceous quartzite and phyllite is gradational.

Preliminary trace element chemistry indicates that the calcareous greenstone exposed along roadcuts at Carnes Creek are alkaline basalts of within-plate affinity and have chemical signatures similar to Jowett Formation volcanic rocks in the Trout Lake area.

## *Contact relations between Badshot Formation and Lardeau Group*

Fyles and Eastwood (1962) interpreted the Lardeau Group to overlie limestones of the Badshot Formation conformably, but describe the contact in the Ferguson area as strongly sheared and the stratigraphic relationship not entirely certain. Reinterpretation of stratigraphic relationships in the Trout Lake area, and regional stratigraphic correlations with the lower Paleozoic rocks in northeastern Washington (Covada Group), has lead Smith and Gehrels (1992a, b and c) to propose that the Lardeau Group has been tectonically juxtaposed over the Badshot Formation and that its present stratigraphic succession may be inverted as a result of thrust imbrications, along layer-parallel faults, of a largely upright sequence. Work in the Illecillewaet synclinorium (Zwanzig, 1973; Colpron and Price, 1993; 1995a) indicates that the Index Formation conformably overlies the Badshot Formation in an upright stratigraphic section.

The contact between the Badshot Formation and the Lardeau Group is exposed at several localities in the Downie Creek area. The basal Lardeau Group displays wide lithological variation; pale green sericite schist, black calcareous and graphitic phyllite, limestone conglomerate and white orthoquartzite breccia are present in different localities. Near Downie Lake (82N/5), marble of the Badshot Formation is overlain by a dolostone-cobble conglomerate (Colpron and Price, 1993). South of Mount Holway, along strike with the Downie Lake section, a green sericite schist abruptly overlies the grey marble of the Badshot Formation. It is in turn overlain by a black phyllite unit. Near Bridgeland Pass, a white orthoquartzite breccia unit is interlayered with minor black phyllite and directly overlies buff-weathering dolomitic limestone conglomerate, phyllitic and massive grey marble of the Badshot Formation. On Roseberry Mountain, the contact is gradational over about 10 metres, and is marked by the presence of dark grey to black argillaceous limestone at the top of the Badshot Formation. The argillaceous limestone gradually becomes more phyllitic up-section and gives way to a sooty graphitic phyllite. Farther west, on Roseberry Mountain, a lensoidal body of white and pale pink quartzite is present along the north-striking contact between massive grey marble of the Badshot Formation and black graphitic phyllite. At its northern end, centimetre-thick quartzite beds are interlayered and continuous with the black phyllite. The orthoquartzite is similar to that comprising the breccia at Bridgeland Pass.

The wide variety of lithologies which overlie the Badshot Formation between Carnes Peak and Downie Lake suggests that the transition from shallow water quartzites and carbonates of the Hamill-Badshot sequence to deeper water facies of the Lardeau Group marks a period of instability along the shelf-margin. This abrupt transition has been interpreted to record the foundering of the sedimentary basin.

## *Stratigraphic relationships of Lardeau Group*

Rocks of the Lardeau Group in the Downie Creek area are broadly similar to the type section in the Ferguson area (Figure 4). In the Downie Creek area, the lower part of the Lardeau Group is characterized by graphitic, calcareous and pyritic black phyllite, green phyllite, phyllitic carbonates and minor quartzite and grit units, typical of deep-water, marginal-basin deposits. Thick accumulations of basaltic flows and volcaniclastic deposits are present near the top of the phyllite package at Keystone and Standard peaks, and are interpreted to reflect local centres of volcanic activity. The greenstones are tholeiitic basalts of mid-ocean ridge (MORB) affinity. This sequence is equivalent to the Index Formation in the Ferguson area, where the Index is subdivided into a lower graphitic phyllite and an upper green phyllite and greenstone units (Figure 4; Fyles and Eastwood, 1962).

The greenstone and black phyllite of the Index Formation are stratigraphically overlain by micaceous quartzite, phyllite and quartz grits in the Downie Creek area. The uppermost stratigraphic unit represented in the area comprises volcaniclastic rocks and interlayered marble; preliminary chemistry indicates that the volcanic rocks are alkaline basalts of within-plate affinities, similar to the Jowett Formation in the Kootenay Arc. On the basis of lithologic and geochemical similarities, the upper volcanic unit of the Downie Creek area is correlated with the Jowett Formation, as suggested by Brown *et al.* (1983).

The micaceous quartzite package has been correlated with: 1) an allochthonous slice of the Neoproterozoic Windermere Supergroup (Wheeler, 1966), 2) the upper Index Formation (Brown *et al.*, 1983; Brown and Lane, 1988), and 3) the Broadview Formation (Brown, 1991; Gibson and Höy, 1994). Our stratigraphic and structural interpretation indicates that it conformably overlies the Index Formation and occurs below the volcaniclastic rocks of the Jowett Formation. Therefore, this unit occupies the same relative stratigraphic position as the Triune, Ajax and Sharon Creek formations in the Ferguson area (Figure 4). These formations comprise a distinctive fine-grained siliceous succession of cherty argillite, phyllite and dark quartzite, bounded below by the volcanic rocks of the upper Index Formation and above by the volcanic rocks of the Jowett Formation. This succession contrasts with the coarser grained sequence of micaceous quartzite and grit present in the Downie Creek area. The Broadview Formation, which overlies the Jowett in the Kootenay Arc, is not present in the Downie Creek Area.

## INTRUSIVE ROCKS

### *DOWNIE CREEK GNEISS*

Lineated granite, quartz monzonite and granodiorite gneiss crops out in the northeastern corner of the map area at Downie Creek (Figure 1). The gneiss extends north into the Goldstream River map area, where it has been included within a mixed package of orthogneiss and paragneiss (Logan and Colpron, 1995). The two-mica granite of the Downie stock intrudes the eastern edge of the gneiss and the Columbia River fault separates it from rocks of the Monashee Complex to the west. Thin sills of orthogneiss intrude paragneiss south of Downie Creek.

The Downie Creek gneiss includes sills and foliated sheets of granitic orthogneiss up to a kilometre thick. The suite is I-type in character and is distinguished by oval aggregates of biotite along the foliation. Locally, fine-grained mafic gneiss occurs as rounded inclusions within more felsic gneiss. It has been affected by the main phases of regional deformation and metamorphism, and overprinted by younger brittle deformation and chlorite alteration associated with the development of the Columbia River fault zone.

Preliminary U-Pb dating on zircon indicates an early Mississippian age for the Downie Creek orthogneiss (R. Friedman, personal communication, 1995). Similar orthogneisses are a major component of the Clachnacudainn Complex, south of the Downie Creek area (Figure 1). Orthogneiss exposed in the CPR quarry, at Albert Canyon, about 28 kilometres east of Revelstoke, has yielded a U-Pb zircon age of 358±6 Ma (Parrish, 1992). West of the Monashee Complex, orthogneiss with similar lithologic characteristics and age are present in the Seymour Range (359±3 Ma; Parrish, 1992) and near Shuswap and Adams lakes (Mount Fowler, 372±6 Ma; Okulitch *et al.*, 1975).

### *PASS CREEK PLUTON*

The Pass Creek pluton is the largest intrusive body in the Downie Creek area (Figure 3). It is a potassium feldspar megacrystic, hornblende-biotite quartz monzonite. Potassium feldspar megacrysts are up to 5 centimetres long and, together with hornblende and biotite, locally define a weak magmatic foliation that parallels the margin of the pluton. Epidote occurs as coatings along fractures and, locally, as fine-grained aggregates within the quartz monzonite. The quartz monzonite phase is cut by dikes of quartz-feldspar porphyry 2 to 3 metres wide. About 1 kilometre west of the Pass Creek pluton, a small body of medium-grained, melanocratic hornblende-biotite monzonite intrudes quartzites of the upper part of the Lardeau Group. Although more mafic in composition, this small intrusion is probably related to the main body of the Pass Creek pluton.

The pluton cuts most of the dominant fold and fault structures in its wallrocks (Figure 3). Along its east side, the trend of structures is apparently deflected around it. Metamorphic minerals (including garnet and andalusite) in the contact aureole appear to postdate the development of the tectonic fabric in the wallrock. These relationships indicate that intrusion of the Pass Creek pluton postdates the development of most of the regional structures, but predates (or is synchronous with) the development of structures along its east side. Brown *et al.* (1992b) report a U-Pb titanite age of 168±3 Ma for the Pass Creek pluton.

East of Carnes Peak, a small body of medium-grained, hornblende-biotite quartz monzodiorite intrudes black phyllites and ultramafic rocks of the lower part of the Lardeau Group. This small intrusion is lithologically similar to both the Pass Creek pluton to the west, and Fang stock to the east, and is, accordingly, probably Middle Jurassic in age.

## *DOWNIE STOCK*

The southern half of the Downie stock is exposed in the northwest corner of the Downie Creek area (Figure 3). Exposures along Highway 23, north of Downie Creek, are of a medium to fine-grained two-mica leucogranite (Logan and Colpron, 1995). The stock has yielded a Rb-Sr date (whole-rock and biotite) of 66±3 Ma (R. L. Armstrong, unpublished data).

## *LONG CREEK STOCK*

The southern half of the Long Creek stock is sparsely exposed along the northern border of the Downie Creek area (Figure 3). It consists of a medium-grained biotite quartz monzonite. Because of its lithologic similarity to the felsic phase of the Goldstream pluton, it is inferred to be mid-Cretaceous in age (Logan and Colpron, 1995).

## *DIKES AND SILLS*

Southeast of Mount Holway, a few dikes (or sills) of light green, foliated plagioclase ± biotite porphyry, 1 to 2 metres wide, intrude rocks of the Hamill and Lardeau groups. The porphyry dikes have a well developed tectonic fabric parallel to the dominant foliation in the area, but intrude the strata at a high angle along the limbs of the main-phase folds. These relationships are interpreted to indicate that the dikes were intruded during the development of the dominant regional structures in the area.

# STRUCTURE

The structure of the Downie Creek area is dominated by northwest-trending, southwest-verging folds and faults that characterize the west flank of the Selkirk fan structure. These structures are superposed upon older isoclinal folds which locally overturned the stratigraphic sequence (Read and Brown, 1979). Both set of structures are deformed by younger east-southeast-trending open folds, and, locally, by another set of northerly trending open folds.

The earliest structures are most readily identified in the area northeast of Downie Creek, where primary sedimentary structures in strata of the Hamill Group provide good control on the stratigraphic facing direction. Here, most of the succession was inverted prior to development of the dominant southwest-verging structures. This panel of inverted stratigraphy extends south into the Carnes Peak and Bridgeland Pass areas; the fault mapped to the west and north of Carnes Peak marks its western limit. At the outcrop scale, the earliest structures are only locally identified by the presence of a bedding-parallel foliation and, rarely, small isoclinal folds that are transected by the dominant foliation. Brown and Lane (1988) interpreted these early isoclinal folds as part of a large-scale west-facing nappe: the Carnes nappe.

The dominant structures are characterized by tight to isoclinal southwest-verging folds. In the area northeast of Downie Creek, moderately dipping, southwest-verging antiforms commonly have sheared overturned limbs. The thrust faults along the overturned limbs of these antiforms may collectively be the northerly continuation of the Downie Creek fault as mapped by Colpron and Price (1993) along strike to the southeast. In general, the fold axes in this area plunge moderately to the northeast, and the large-scale folds have the geometry of reclined folds.

To the west, in the Keystone area, the structural style in rocks of the Lardeau Group is characterized by the southwest-verging, recumbent Keystone antiform (Lane, 1977; Höy, 1979). The core of the antiform is occupied by a thick sequence of marble. Brown (1991) interpreted this marble as part of the Lardeau Group. Lane (1977) and Brown (1991) reported facing directions in grits along the limbs of the Keystone antiform that suggested that the stratigraphic sequence was inverted before the development of the Keystone antiform. However, our mapping in the Keystone area indicates that the stratigraphic sequence was upright prior to formation of the recumbent fold. Thus, the recumbent fold in the Keystone area is an anticline and the marbles in the core of the fold are the oldest rocks in the area.

Farther south, in the Standard Peak area, rocks of the Lardeau Group are folded by a moderately east dipping, tight to isoclinal antiform that Lane (1977) and Brown (1991) correlated with the Keystone antiform. Again, graded beds in quartzite and grits along the northwest flank of Standard Peak indicate that the stratigraphic sequence was upright prior to formation of the antiform.

A thrust fault juxtaposes phyllite and dolostones of the Mohican Formation over black phyllites of the Index Formation, along the east flank of Roseberry Mountain (Figure 3; Brown, 1991). Brown has traced this fault northward to the Pass Creek pluton. It reappears north of the pluton where it juxtaposes the Mohican Formation against a light grey marble that we assign to the Lardeau Group. The fault is truncated again to the north by the Long Creek stock. This fault may be equivalent to the southern segment of the French Creek fault, mapped northeast of the Long Creek stock in the Goldstream River area (Colpron *et al.*, 1995; Logan and Colpron, 1995).

West of Carnes Peak, a fault juxtaposes an overturned panel of the Badshot Formation to the east, over an upright sequence of the Mohican Formation and Hamill Group to the west (Figure 3). To the north, the Mohican is truncated along the fault and the Badshot is juxtaposed against Hamill quartzites that grade westward into siliceous phyllite and dolostone of the Mohican

Formation. The same sequence of rocks extends northward around the east side of the Pass Creek pluton, into the Downie Creek valley and, therefore, the fault can be inferred to extend into the valley, where it appears to be truncated by, or to merge with a southwest-verging thrust fault. There is no direct evidence to constrain the sense of displacement along this fault. Brown (1991) interpreted it as a normal fault, with the possible implication that it is a synthetic extension fault in the hangingwall of the Tertiary Columbia River fault (also Brown and Lane, 1988). The relationships decribed above imply that this fault either predates or is synchronous with the development of the southwest-verging thrust faults, which are elsewhere documented to be Middle Jurassic in age. Alternatively, this fault may be a southwest-verging thrust fault.

The contact between the Index Formation and the assemblage of micaceous quartzite and quartz-muscovite schist to the west, has been interpreted by Brown (1991) as a west-verging thrust fault (the Standard Peak fault). Close inspection of this contact has revealed that, in most locations, the Index Formation is gradational into the structurally underlying quartzite assemblage. In addition, our proposed correlation with similar quartzites in the core of the west-facing synform on Belcher Ridge, east of Standard Creek, limits the displacement that could have occurred along the Standard Peak fault. Although we cannot rule out the existence of the Standard Peak fault, it does not occur along the contact between black phyllite and quartzite at Standard Peak and displacement is therefore apparently not large.

Younger structures which deform the dominant foliation are limited to the development of a crenulation cleavage and small-scale open folds. The most prominent expression of this deformation is seen at Keystone Peak, where the dominant foliation is deformed by an east-southeast-trending open synform. North-northwest-trending open folds are also locally developed. Again the most spectacular example of this episode of folding is seen at Keystone Peak, where the dominant foliation dips toward the peak on either side of the mountain. As a result of the superposition of three phases of folding, the overturned sequence of marble at Keystone Peak occupies the core of a structural basin.

## *COLUMBIA RIVER FAULT*

The Columbia River fault zone separates rocks of the Selkirk allochthon in its hangingwall from rocks of the Monashee Complex in its footwall (Read and Brown, 1981; Figure 1). This ductile-brittle fault of Eocene age is superposed on older, amphibolite-grade mylonites that have been attributed to displacement along the ductile Jurassic to Paleocene Monashee décollment (Lane, 1984; Lane *et al.*, 1989; Brown *et al.*, 1992a). The Columbia River structure is a normal fault which strikes northwesterly and dips 20° to 40° to the east in the Downie Creek map area. Motion is dip slip and of sufficient magnitude to juxtapose greenschist facies rocks of the Goldstream slice against upper amphibolite facies rocks in the footwall (Read and Brown, 1981).

For the most part, the trace of the fault zone lies in the Columbia River and is not exposed. South of Holdich and Carnes creeks the fault is exposed in road cuts along Highway 23. At Carnes Creek, rocks in the footwall are silicified mylonitic gneisses, possibly Devono-Mississippian orthogneiss of the Clachnacudainn Complex (Brown *et al.*, 1993). Mafic plagioclase-actinolite-calcite metavolcaniclastic and interlayered dolomitic marble of the Jowett Formation occupy the hangingwall. Discreet, late-brittle fault zones, less than a metre wide and characterized by ankeritic and clay-altered fault gouge, cut the main fault trace exposed south of the Carnes Creek Road turnoff on Highway 23.

The intensity and variety of alteration varies between rocks in the hangingwall and footwall of the fault zone. Rocks in the footwall, exposed in road cuts south of Carnes Creek, include black amphibolite, interlayered grey, white and brown carbonates, calcsilicate and quartz-rich semipelites of the Monashee Complex. These rocks are intruded by sheeted gneisses of granitic and granodioritic composition that are mylonitic and that are cut by younger foliated and nonfoliated muscovite pegmatites. Footwall rocks are thoroughly fractured, faulted and pervasively altered: as a result, roadcuts south of Carnes Creek are highly unstable. Pervasive silicification of footwall rocks has locally produced pale grey, green and white mottled, homogeneous quartzofeldspathic rocks in which the only texture preserved is the mylonitic fabric. Late-stage, brittle deformation overprints earlier ductile fabrics. Anastomosing brittle fractures, most prevalent in the silicified rocks, are curviplanar, trend northerly and dip steeply to the west. Fluid infiltration along these fractures has resulted in one or all of these alteration processes: sericitization, chloritization, pyrite and late-stage iron carbonate alteration.

Rocks in the hangingwall are less pervasively altered. The Jowett Formation, south of Carnes Creek, is weakly chloritized and iron carbonate altered along discreet fractures and fault zones. Cataclasite and chloritic breccias have developed in competent hangingwall rocks, in particular in the Downie Creek orthogneiss and Downie stock north of Downie Creek.

Additional late-stage, brittle deformation includes east-trending, north-side-down normal faults and, less commonly, north-side-up reverse faults (Lane, 1984). These are generally foliation-parallel shear zones.

## METAMORPHISM

Rocks of the Downie Creek area contain mineral assemblages characteristic of greenschist to amphibolite facies metamorphism. Most of the map area is underlain by assemblages characteristic of the chlorite zone; amphibolite facies rocks are confined to the footwall of the Columbia River fault zone and to the metamorphic culmination at Downie Creek. Relatively narrow metamorphic contact aureoles surround the Downie, Long Creek and Pass Creek plutons.

A metamorphic culmination extends 7 kilometres northeastward up the Downie Creek arm of Lake Revelstoke. It arches over the Downie stock and extends northward into the Goldstream River map area (Colpron *et al.*, 1995). It is bounded to the west by the Columbia River fault. The rocks are garnet-muscovite-biotite-chlorite paragneisses and schists, that are intruded by sills and thick sheet-like bodies of the Downie Creek orthogneiss. The garnet porphyroblasts are synkinematic with respect to the dominant foliation, and the foliation is defined by alignments of biotite and muscovite. The garnets commonly have retrograde rims of fine-grained muscovite, chlorite and quartz. The metamorphic grade decreases progressively eastward, and the gneisses pass structurally upward into biotite and chlorite-zone micaceous quartzite, quartz-muscovite schist and semipelite. It is unclear whether the transition between the gneisses and the micaceous quartzites is defined by a fault or is a result of decreasing metamorphic grade. In roadcuts along Highway 23, at the western end of Keystone Creek, foliation-parallel graphitic shear zones are present within the paragneiss (Gibson, 1989). North of the Downie stock, in the Goldstream River area, the contact between gneiss and micaceous quartzite has been inferred to be a fault, on the basis of scattered exposures of high-strain gneiss near this contact (Logan and Colpron, 1995).

Regional relationships indicate a Middle Jurassic age for southwest-verging deformation and the peak of regional metamorphism (Archibald *et al.*, 1983; Colpron and Price, 1995b). Accordingly, the age of garnet-grade regional metamorphism at Downie Creek is inferred to be Middle Jurassic.

Regional metamorphic assemblages at Downie Creek are, in part, overprinted by the contact aureole of the Late Cretaceous Downie stock. Contact metamorphic assemblages include garnet, biotite, muscovite and, in pelitic and psammitic rocks, muscovite pseudomorphs of andalusite up to 10 centimetres long. Fresh andalusite is present along the northern margin of the Downie stock (Logan and Colpron, 1995). Calcsilicate rocks contain fine radiating clusters of actinolite arranged in a characteristic 'bow-tie' texture along the main foliation surfaces.

The contact aureole along the southern margin of the Pass Creek pluton is less than 250 metres wide and the metamorphic assemblage includes garnet, muscovite, biotite and muscovite pseudomorphs after andalusite. The garnet porphyroblasts are euhedral and devoid of inclusions. They appear to postdate the development of the dominant foliation. Contact aureole assemblages are observed over a distance of about 1 kilometre west of the pluton, where a small monzonite intrusion is exposed. There, muscovite pseudomorphs of andalusite up to 5 centimetres long are randomly oriented along the dominant foliation.

The small, undeformed quartz monzodiorite intrusion east of Carnes Peak has a narrow contact aureole (*ca.* 50 m) in which calcsilicate rocks of the Lardeau Group have the assemblage garnet-biotite-diopside-tremolite-clinozoisite-plagioclase-quartz±muscovite. The assemblage biotite-tremolite-quartz defines the foliation in the country rocks, and the garnet porphyroblasts appear to be synkinematic with respect to developement of the foliation. Although the intrusion itself is undeformed, the textural relations of the calcsilicate minerals suggests that metamorphism was synkinematic with regional deformation.

# MINERAL OCCURRENCES

Stratabound mineral occurrences within the Downie Creek map area can be divided into two main types: stratiform volcanogenic massive sulphide (VMS) and carbonate replacement deposits. Copper-zinc and arsenical lead-zinc-gold-silver mineral assemblages characterize the massive sulphide occurrences. The Standard and Rain copper-zinc prospects are VMS deposits associated with tholeiitic volcanism in the lower Paleozoic Lardeau Group (Index Formation). The King and Copper Queen copper-zinc occurrences are associated with alkaline volcanic rocks of the lower Paleozoic Lardeau Group (Jowett Formation). The J&L gold-rich base metal deposit is hosted in marble and siliciclastic strata of the Eocambrian Hamill Group, which, contains bimodal alkaline volcanic rocks to the north. Lead-zinc-silver assemblages characterize the carbonate replacement occurrences, which include the Yellowjacket zone (J&L), Keystone and A&E(?) (Figure 3).

In addition to these occurrences there are scheelite skarn showings in calcareous rocks of the Index Formation at the southern contact of the Long Creek stock, and disseminated base metal and molybdenum showings in micaceous quartzites in the hangingwall of the Columbia River fault zone.

## *MASSIVE SULPHIDE DEPOSITS*

### STANDARD

The Standard showings comprise a series of discontinuous massive and disseminated sulphide lenses within albite-chlorite-calcite schist, massive greenstone, volcaniclastic sandstone, black phyllite and marble of the Index Formation (Höy, 1979; Höy *et al.*, 1984). Sulphide lenses occur on both limbs of the Standard anticline within the greenstone unit, at contacts between massive greenstone and thinly foliated actinolite-albite-chlorite schist, and between greenstone and ultramafic dikes. Surface trenching has traced the sulphides intermittently for 1500 metres and much of the exploration work has been concentrated in areas where young, easterly trending, upright cross-folds deform the older northerly trending structures, bringing the sulphide-bearing horizon close to the surface.

Sill-like bodies of serpentinite, ultramafic rocks, gabbro and diorite intrude along the contacts between black phyllite and greenstone units and are spatially associated with some of the sulphide occurrences. Sulphides include fine-grained interlayered pyrrhotite, pyrite, arsenopyrite and lesser chalcopyrite and sphalerite. Deformation has produced gneissic textures in the sulphides and remobilized chalcopyrite into pressure shadows around pyrite grains and wallrock inclusions within the massive sulphide layer. Most of the exploration at Standard has been confined to the volcanic package. The sulphide horizon at the Goldstream deposit is hosted by graphitic phyllites adjacent to greenstones. A thick package of black graphitic and calcareous phyllite overlies the greenstone on either side of the Standard anticline; its potential to host base metal sulphide mineralization remains largely untested.

Early reports describe the mineralization as consisting of arsenical iron and copper pyrites with a little bornite, and selected samples returned assays of 10.9 g/t Au, 47.9 g/t Ag and 15 % Cu (Carmichael, 1906). Of note is not the relative amounts but the presence of gold and arsenopyrite, a mineral assemblage found at the J&L and A&E prospects. Lithogeochemical arsenic-gold and copper anomalies occur in pyritic and sericite-altered limestone and quartzose phyllite in the headwaters of Kelly Creek, 2 kilometres south of the Standard showings. These sediments are stratigraphically below the greenstone in the core of the Standard anticline.

## J&L - MAIN ZONE

The J&L property is a stratiform precious and base metal deposit located at the confluence of Carnes and McKinnon creeks, approximately 9 kilometres east of the Columbia River. Considerable underground and surface development has been carried out on the property since it was staked in 1896. In the early to middle 1980s Selco Inc. (subsequently BP Canada Ltd., Selco Division), then Noranda (1986-87), Equinox Resources Ltd. (1988-94) and finally Cheni Gold Mines Inc. (1990-1993) carried out substantial exploration and development work, including underground drilling, bulk sampling and metallurgical testing under option agreements with Pan American Minerals (Meyers and Hubner, 1989; Weicker, 1991). The deposit consists of a Main zone of massive and disseminated sulphides and the Yellowjacket zone, a lead-zinc carbonate replacement (discussed below).

The underground workings were not accessible at the time of our mapping. Höy (1984) described the distribution of mineralization and lithology in a detailed section through the main sulphide layer in the 10+350-metre East crosscut; this, together with McKinlay (1987) and Meyers and Hubner (1989) provide a good description and summary of the geology of the deposit. More recent work is described in B.C. Ministry of Energy, Mines and Petroleum Resources assessment reports by Wright *et al.* (1989) and Weicker (1991).

The Main zone averages 1.6 metres thick (true thickness), developed over 800 metres of strike length underground and traced on surface for over 1.35 kilometres (probable and possible reserves, 5.25 million tonnes averaging 2.71 % Pb, 4.33 % Zn, 7.23 g/t Au and 72 g/t Ag; Canadian Mines Handbook 1995-96, p. 188). Host stratigraphy to the Main zone is the upper part of the Hamill Group, which is composed of interlayered quartzite, micaceous quartzite, quartz-sericite and chlorite schist and grey carbonaceous limestone. The latter forms the footwall of the main sulphide layer. The Main zone is a complex tabular body which follows the limestone-phyllite contact and, in places, branches or splits into multiple parallel layers (Meyers and Hubner, 1989). Sulphide minerals include pyrite, arsenopyrite, sphalerite, galena, and trace amounts of chalcopyrite, pyrrhotite and silver-lead-antimony sulphosalts. The immediate area of the J&L deposit is strongly deformed by west-verging thrust faults and tight to isoclinal folds, it is unclear whether the stratigraphy was inverted prior to the main phase of folding. Pyritized sericite and clay-altered schists in the footwall of the Main zone are crenulated by late southwest-trending cross-folds.

The North zone, possibly an extension of the Main zone, occurs north of McKinnon Creek. It comprises four parallel lenses containing arsenopyrite, pyrite and variable amounts of galena and sphalerite, and extends for a strike length of 1.5 kilometres northwesterly. Together the Main and North zones define a mineralized strike length in excess of 3.3 kilometres. The blind discovery of the Yellowjacket zone in 1990 attests to the high potential for additional mineralized zones in this area, which has not been fully evaluated.

A long-standing controversy regarding the origin of the J&L deposit is based in part on the presence of incompatible mesothermal and epithermal mineral assemblages, finely laminated and crosscutting sulphide textures, mineral zonation and variation in strain along and across the sheet-like massive sulphide body. As a result both the syngenetic massive sulphide (Grant, 1984) and the epigenetic shear-hosted vein (McKinlay, 1987; Wright *et al.*, 1989; Weicker, 1989) classifications have been ascribed to the deposit (see discussion in Meyers and Hubner, 1989). The J&L is a gold-rich base metal deposit with distinct epithermal characteristics; it has all the characteristics of a shallow submarine hydrothermal system (Hannington, 1993) and may be a tectonized exhalative volcanogenic massive sulphide deposit, akin to Eskay Creek.

## RAIN

The Rain property is located between Standard and Murder creeks, south of Downie Creek (Figure 3). Early exploration of the property by Noranda Exploration Company Limited focused on the skarn potential of copper-tungsten mineralization near the confluence of Downie and Sorcerer creeks. Bethlehem Resources Corporation restaked the property in 1989 on the basis of the similiarity between its stratigraphy and that at the

Goldstream mine. Geological mapping, geochemical sampling and diamond drilling confirmed the stratigraphy, and identified anomalous base metal values and the presence of semimassive sulphides associated with manganese-enriched exhalative horizons.

Wild (1990) discovered stratabound banded pyrite in manganese-enriched graphitic phyllites in Murder Creek. He recognized the similiarities to the dark banded phyllites at the Goldstream mine and correlated the graphitic phyllite, sericite schist and carbonate with the Lardeau Group strata. Follow-up geochemical soil sampling traced two base metal anomalies northwesterly from the discovery zone, parallel to the dominant strike of the stratigraphy. Diamond drilling at the northern extension of one of these anomalies intersected several manganese-enriched, garnetiferous and sulphide-bearing horizons correlative with the garnet zone at Goldstream (Cavey and Raven, 1992).

On the Rain, the Index Formation consists of dark calcareous and graphitic phyllite and sericite schist. Massive, light grey, banded marble forms the ridge to the west and structurally underlies the dark phyllites exposed in the creek. Farther west, in Standard Creek, interbedded pale yellow and grey micaceous quartzite and grey, rusty weathering phyllite underlie the grey marble. Thinly interbedded phyllite and carbonate correspond to the calcareous phyllite in the drill holes. Coarse disseminated, stratabound pyrite is common in some graphitic units and Wild (1990) describes a garnet zone within these rocks. The dark phyllite and sericite schist are strongly contorted adjacent to the contact with underlying marble and are overprinted by a quartz-vein stockwork. The contact appears to be faulted. Our mapping (Figure 3) shows that rocks of the lower phyllite member (host to mineralization) are structurally overlain by rusty weathering, typically recessive, pale green, sericite and quartz-sericite schists with interlayered marble of the Mohican Formation. This unit is traceable south along the lower slopes of the Downie Creek valley, across Kelly Crest and then south to Roseberry Mountain.

Much of the lower slopes on the property are covered by thick glacial till and rock exposures are restricted to road and stream cuts. Continuous stratigraphy is rare and interpretation relies on drill core. The stratigraphy of two drill holes (92RN-1 and 92RN-3) is described by Logan and Drobe (1994). Difficulty in correlating stratigraphy from one hole to the next, and the presence of multiple garnet and sulphide horizons intersected by the drilling, are probably the result of structural repetition, possibly by west-verging tight to isoclinal folds and thrust faults similar to those mapped on ridges between Pelkey and Standard creeks, to the south. In addition to the structural complications, mapping by Campbell (1994) indicates that graphitic phyllite (the probable source of the copper, lead, zinc and manganese geochemical anomalies) extends up-slope farther than previously recognized, suggesting that the 1992 drilling may not have extended far enough to intersect the source of the anomaly.

## KING SHOWING

The King showing is a stratabound massive sulphide horizon in micaceous quartzite and quartz-sericite schist exposed in a roadcut along Highway 23, 250 metres south of Keystone Creek. The property has been explored intermittently since 1976, by soil and stream geochemical and geophysical techniques, mapping and limited diamond drilling. Boulders of massive sulphide and anomalous soil geochemistry suggest that mineralization extends for approximately 2 kilometres to the north (Wild, 1988). Sulphides include pyrite, pyrrhotite and small amounts of chalcopyrite and sphalerite. Pyritic quartz-sericite schist exposed on the Key Road, up-slope and farther east, may represent a fold repetition of this same horizon.

The property is underlain by micaceous quartzite, quartz-sericite and chlorite schist, graphitic phyllite and the Downie orthogneiss. Strata are isoclinally folded about north-verging fold axes and are crenulated by younger northeast and southeast-trending cross-folds. Two northeast-trending, layer-parallel graphitic shear zones transect the property. These have been accurately located by electromagnetic surveys, diamond drilling and surface geological mapping, and divide the property into three separate structural slices (Gibson, 1989). The King showing is in the footwall of the westernmost shear, separating the sulphide-bearing micaceous quartzites from chlorite-calcite schists and phyllites in the hangingwall. Drilling in 1986 did not intersect significant mineralization.

Geochemical sampling of mineralized and altered sections along the highway and Key Road in 1993 and 1995 returned low base and precious metal values. Similar mylonitic and pyritic quartzite and sericite schist is exposed 5 kilometres to the south along Highway 23. Analysis of these rocks has also returned low metal values.

## COPPER QUEEN

The Copper Queen showings are located 10 kilometres south of Carnes Creek on the west-facing slope above the Columbia River, at 1500 metres elevation (82M/1). They occur in a thick section of micaceous quartzite, rusty weathering phyllite, interlayered mafic volcanic rocks and carbonate. The showings were not visited this past summer, but are reported to consist of chalcopyrite, sphalerite and pyrite disseminations and lenses located near the base of the Jowett Formation volcanic-carbonate sequence, close to its contact with the structurally overlying micaceous quartzite and sericite schist (Lund and Hajek, 1976).

## *CARBONATE REPLACEMENTS*

### KEYSTONE

The Keystone showings are located at the headwaters of Keystone Creek, less than a kilometre northwest of Keystone Peak (Figure 3). They consist of carbonate replacements in marble, and quartz veins hosted by chlorite-sericite phyllite (Gunning, 1929; Wheeler, 1965). The main showing has been tested by two short adits and surface trenching which expose a medium grey marble, 2 metres thick, within calcareous, rusty weathering and bleached sericite-chlorite schist, dark grey phyllite and micaceous quartzite. Mineralization occurs as foliation-parallel pods of massive and coarsely crystalline intergrowths and crosscutting fracture fillings within or underlying the marble (Höy, 1979). Sulphides, in order of relative abundance, include pyrrhotite, sphalerite, galena, pyrite and minor chalcopyrite. Pyrrhotite occurs as massive lenses enclosing blebs of sphalerite, galena and euhedral grains of pyrite. Deformation has remobilized sphalerite, galena and the trace amounts of chalcopyrite into pressure shadows adjacent to pyrrhotite and into crosscutting fractures.

Sulphide textures suggest that the mineralization predates the main phase of deformation (see Plate XII *in* Höy, 1979). Galena-lead isotopes give a Cretaceous Pb-Pb model age, making it reasonable to correlate at least part of the mineralizing event with intrusion of either the Goldstream pluton or possibly the Long Creek stock, both part of the mid-Cretaceous magmatic suite in the area.

### J&L - YELLOWJACKET ZONE

The Yellowjacket zone is a lead-zinc deposit hosted in siliceous carbonate in the hangingwall of the gold-bearing polymetallic Main sulphide zone at the J&L property. It was discovered in November, 1990, by drilling in the McKinnon Creek valley, north of the 830-metre level portal. Subsequent drilling has outlined probable and possible reserves of 1 003 000 tonnes, grading 7.37 % Zn, 2.59 % Pb and 55.5 g/t Ag (Canadian Mines Handbook 1995-96, p. 188). The Yellowjacket zone strikes generally parallel to the Main zone, but dips more steeply and plunges to the east at 40 to 50° (Weicker, 1991). Mineralization is confined to a carbonate sequence in a succession of sericite and chlorite phyllite, quartzite, carbonate and minor volcanic rocks correlated with the Hamill Group (Weicker, 1991).

The sulphide assemblage is simple, consisting of disseminated pale honey-coloured sphalerite, and silver-bearing galena. The low iron content of the Yellowjacket ore is reflected in the pale sphalerite which contrasts with the dark reddish brown, iron-rich variety in the Main zone. The limestone is variably silicified; gangue minerals include quartz and fluorite.

### A&E AND ROSEBERRY

The A&E showings are located on the northeast slope of Roseberry Mountain. The principal mineralized zone has been explored by two adits, located on opposite sides of a tributary draining north into Burke Creek. Underground maps of the adits by Westars Mines Ltd. (Hope, 1966 *in* Weicker, 1989) show the sulphide zone follows the contact of Badshot marble with sericite schist and phyllite of the Index Formation. Sulphide minerals present at the portal include coarse crystalline intergrowths of arsenopyrite, pyrite, sphalerite and galena, with average base and precious metal grades similiar to the Main zone at the J&L (Weicker, 1989). A second, weakly mineralized zone, approximately 125 metres to the west, occupies the faulted(?) contact between Badshot marble and black graphitic Index phyllite. Sulphide minerals include pyrite and arsenopyrite and minor amounts of sphalerite and galena. The zone is deeply weathered and assay results indicate low metal values (Weicker, 1989).

Mineralization at the A&E occupies two parallel zones, generally less than 1 metre thick, within limestone and schist near the top of the Badshot Formation and in phyllite of the Index Formation. Mineral assemblages are arsenical and gold rich, similar to the Main zone at the J&L, but stratigraphic position correlates with hangingwall strata which host the arsenic-free zinc-lead Yellowjacket zone at the J&L.

The Roseberry showing is on the southwest side of Roseberry Mountain. Its exact location and details of the geology are poorly known. Hostrocks include sericite-chlorite schist and marble of the Badshot Formation. In this area the rocks are intruded by a coarse-grained, foliated metagabbro-diorite intrusion and associated sills. The mineralization is reported to consist of disseminated and podiform massive arsenical sulphides with pyrite, galena and sphalerite. Gold and silver values are reported from underground development on a 1.5-metre vein of massive sulphides within a 15-metre zone of disseminated mineralization (Gunning, 1929).

### CARBONATE-HOSTED MASSIVE SULPHIDE MINERALIZATION, McKINNON CREEK AREA

Fine-grained pyrite, sphalerite, and galena occur in layers up to 5 centimetres thick in the uppermost white to light grey marble of the Badshot Formation, south of McKinnon Creek. Several bedding-parallel mineralized layers are present within 25 centimetres of the contact with underlying laminated, orange-brown and olive-brown carbonates.

## *NEW PROSPECTIVE HORIZONS*

During the course of mapping, several new prospective horizons were discovered in the Downie Creek area. In the McKinnon Creek area, these include laminated pyrrhotite, sphalerite and pyrite horizons and massive lenses of galena-arsenopyrite in black siliceous units within phyllites of the Index Formation, and sphalerite in marble of the Badshot Formation. There are also iron-manganese-silica±copper and zinc-enriched horizons in phyllite of the Index Formation both stratigraphically above and below the greenstone in the Keystone Peak, Roseberry Mountain and Tumbledown glacier areas.

## IRON-MANGANESE-SULPHIDE ENRICHED GRAPHITIC AND SILICEOUS HORIZONS

In the Goldstream area, a distinctive spessartine-bearing, pyrrhotite-rich, thinly laminated graphitic coticule unit, termed the "garnet-zone", is associated with the massive sulphide layer. It is interpreted to be a manganese-iron-rich seafloor hydrothermal precipitate; an exhalite (Höy *et al.*, 1984). The garnet zone also occurs at the Rain property. These garnet zones are important exploration targets and mapping this summer resulted in the discovery of four new iron-manganese-silica-rich horizons in the Index Formation. All of them are characterized by abundant pyrrhotite and/or pyrite and manganese oxide, rhythmic interlaminations of graphitic phyllite and very fine grained, cherty quartzite, but a paucity of spessartine garnets, due to the relatively low grade of metamorphism. Preliminary geochemistry indicates several orders of magnitude above background for manganese, iron and, locally, copper and zinc. These horizons are located south of Keystone Peak, east and west of Roseberry Mountain, and north and west of Tumbledown glacier, between McKinnon and Carnes creeks (Figure 3).

Dark grey siliceous phyllite, black quartzite and graphitic phyllite structurally underlie massive greenstone south of Keystone Peak. The quartzite and phyllite are rhythmically interbedded, on a millimetre to 10-centimetre scale and contain abundant carbonaceous material, pyrite and manganese oxide. Chalcopyrite is present locally in minor amounts. The anomalous manganese and iron content of this siliceous unit makes it readily traceable from the upper reaches of Mars Creek, west and north into the upper drainage basin of Keystone Creek (Figure 3). The Keystone showing lies on strike with this unit, as does a large silicified, pyritized and iron carbonate alteration zone in the structurally overlying green phyllitic volcaniclastic rocks.

Very fine grained, light grey cherty quartzite, finely interlaminated with black carbonaceous phyllite, forms a unit 2 to 3 metres thick in phyllite of the lower Index Formation at Roseberry Mountain. The unit crops out both west and east of the mountain. Weathered surfaces are variably coated with bluish manganese oxide and hematite. Pyrite is abundant, commonly as millimetre-thick, bedding-parallel seams of finely crystalline sulphides. Pyrrhotite and minor chalcopyrite are present locally. Deformed quartz veins up to 10 centimetres wide that cut this unit contain abundant coarse pyrite

Dark grey, very thinly layered graphitic and calcareous phyllite overlie marble of the Badshot Formation, in a structurally upright panel, between Bridgeland Pass and Tumbledown glacier. Within the phyllite, possibly spatially related to a nearby, narrow intrusive greenstone body, is a rusty weathering, siliceous, pyrite and pyrrhotite-rich zone at least 8 metres thick. The gossan consists of fine-grained bedding and foliation-parallel pyrrhotite, crosscut by zones of coarsely recrystallized euhedral pyrite and locally by quartz stockworks. Well rounded, black, mineralized chert clasts occur at several horizons within the gossan. Mineralized clasts contain layers and blebs of sphalerite and/or pyrrhotite. This gossan can be traced south for 1.5 kilometres to the ridge separating Carnes and McKinnon creeks. On the ridge the greenstone unit is not present and the manganiferous unit occurs within the black phyllite unit, a few hundred metres below the sequence of quartzite and grits that core the Illecillewaet synclinorium to the southeast.

An interval of interlaminated, very fine grained quartzite (metachert?) and black graphitic phyllite, at least 15 metres thick and up to about 30 metres in structural thickness where it has been thickened by folding, is exposed to the west, in the headwaters of McKinnon Creek, in a separate panel of black phyllite. Four to five metres of gossan within this siliceous unit contains fine-grained laminated pyrite and sphalerite and massive sulphide lenses up to 30 centimetres thick by about 1 metre long. The massive sulphide lenses contain pyrite, galena, arsenopyrite, possible sphalerite and minor chalcopyrite, and nodular quartz. A 10-centimetre layer of white, fine-grained crystalline barite is present at one locality in the black phyllite unit.

A 2 to 3 metre thick unit of hematite and manganese oxide coated, fine-grained, laminated quartzite with graphitic partings occurs within interlayered phyllitic dolostone, green siliceous phyllite, and black phyllite south of the Rain property, in the Pelkey-Murder creeks area. Massive to foliated greenstone is also exposed within the section, about 20 metres above the laminated siliceous unit. Manganese, iron and base metal values are only slightly elevated above background values. Lithology and stratigraphic position of these rocks correlate well with rocks south of Keystone Peak.

All of these horizons have been sampled. Major and trace element analyses will permit comparisons between those associated with mineralization (Goldstream deposit), metal-poor systems and background phyllites.

# DISCUSSION AND CONCLUSIONS

Stratigraphic relationships established in the Goldstream River area (82M/9) have been traced southeastward into the Downie Creek area. However, the recognition of two distinct volcanic successions (upper part of the Index Formation and the Jowett Formation) in the Downie Creek area, and facing directions within the intervening quartzite package, have resulted in revisions to stratigraphic correlations within the Lardeau Group. The stratigraphic sequence in the Downie Creek area consists of the Index Formation (black phyllite, limestone and greenstone), a micaceous quartzite-grit unit, and the Jowett Formation (greenstone and marble; Figure 4). In the Goldstream River area, the sequence of black phyllite, greenstone and quartzite-grit units was assigned to the lower, middle and upper parts of the Index Formation, respectively. The Index Formation in this area is now thought to comprise only the black phyllite and greenstone units, the quartzite-grit unit being younger and a possible lateral equivalent to the Triune, Ajax and Sharon Creek formations of the Kootenay Arc.

The structural style of the Downie Creek area is dominated by southwest-verging folds and thrust faults. These structures deform earlier recumbent folds. Our mapping has extended the areal extent of these early structures to the northeast in rocks of the Hamill Group. These early folds do not appear to be as significant to the northwest, in the Goldstream River area.

Synkinematic, garnet-grade paragneisses and thick sheet-like bodies of Devono-Mississippian orthogneisses define a metamorphic culmination along the Downie Creek arm of Lake Revelstoke. These gneisses show remarkable similarities to Devono-Mississippian orthogneisses in the Clachnacudainn Igneous Complex. They underlie, in possible fault contact, an inverted stratigraphic panel of micaceous quartzite and Jowett Formation, and are truncated by the Columbia River fault to the west.

Known stratabound/stratiform sulphide occurrences in the area include the copper-zinc deposits at the Standard, Rain, Copper Queen and King showings and the arsenical, gold-silver-zinc J&L deposit. At least two mafic volcanic centres are recognized in the Downie Creek area at Keystone and Standard peaks. Gossan zones, and manganese and silica-enriched iron sulphide horizons, occur along the contacts between black phyllite and mafic volcanic units and within the volcanic units at Standard. This stratigraphy is equivalent to that hosting the Goldstream deposit (Index Formation). The "garnet-zone" at the Goldstream mine may be represented in the Keystone area by a black carbonaceous and manganiferous siliceous phyllite and interbedded quartzite which overlies the volcanic rocks. This unit locally contains sulphides and has been traced laterally for 3 kilometres. A similar horizon crops out east of the J&L deposit in black graphitic and calcareous phyllites of the Index Formation at the southern boundary of the map area. Laminated pyrrhotite, sphalerite and pyrite horizons, massive galena-arsenopyrite-sphalerite lenses, and a layer of white barite are present in black siliceous sections of this phyllite. Exhalative horizons and semimassive sulphides are known on the Rain property; four other horizons have been traced regionally and sampled. The major and trace element geochemistry from these samples provides a substantial database allowing comparisons with the geochemistry from various horizons above and below the mineralization at the Goldstream mine. It is hoped that this will provide a useful exploration tool to differentiate between metalliferous and barren hydrothermal exhalative horizons preserved in the Index Formation in the northern Selkirk Mountains.

Current mapping and regional correlations indicate that the stratiform mineral deposits in the Downie Creek area are hosted by strata ranging in age from Eocambrian to lower Paleozoic. The massive sulphides occur at three stratigraphic levels; 1) the J&L deposit in the middle to upper part of the Lower Cambrian Hamill Group; 2) the Standard and Rain prospects in the upper part of the Index Formation, lower Paleozoic Lardeau Group; and 3) the King and Copper Queen prospects in the Jowett Formation, also lower Paleozoic Lardeau Group. These stratigraphic positions correspond to regionally extensive volcanic episodes, and with the exception of J&L, all are associated with volcanic rocks.

## ACKNOWLEDGEMENTS

We thank Bethlehem Resources Corporation and, specifically, Chris Wild for his stimulating and assertive discussions on the local and regional geology, and for facilitating access to the most recent drill cores. We also thank Dave Lefebure, Ron Smyth and Bill McMillan, of the Geological Survey Branch, and Dick Brown, of Carleton University, for their field visits and discussions. Lee Fortner assisted in the field mapping. Gerry Richard and Eric Crawford of Selkirk Mountain Helicopters are responsible for our safe and enjoyable flying! John Newell reviewed and, as always, improved the manuscript. Additional comments by Dave Lefebure are also appreciated.

## REFERENCES

Archibald, D. A., Glover, J. K., Price, R. A. Farrar, E. and Carmichael, D. M. (1983): Geochronology and Tectonic Implications of Magmatism and Metamorphism, Southern Kootenay Arc and Neighbouring Regions, Southeastern British Columbia. Part I: Jurassic to mid-Cretaceous; *Canadian Journal of Earth Sciences*, Volume 20, pages 1891-1913..

Armstrong, R. L. (1988): Mesozoic and Early Cenozoic Magmatic Evolution of the Canadian Cordillera; *in* Processes in Continental Lithospheric Deformation, Clark, S. P., Jr., Burchfield, B. C. and Suppe, J., Editors, *Geological Society of America*, Special Paper 218, pages 55-91.

Brown, R. L. (1991): Geological Map and Cross Section, Downie Creek Map Area (82M/8); *Geological Survey of Canada*, Open File 2414, 1:50 000 map.

Brown, R. L. and Lane, L. S. (1988): Tectonic Interpretation of West-verging Folds in the Selkirk Allochthon of the Southern Canadian Cordillera; *Canadian Journal of Earth Sciences*, Volume 25, pages 292-300.

Brown, R. L. and Tippett, C. R. (1978): The Selkirk Fan Structure of the Southeastern Canadian Cordillera; *Geological Society of America*, Bulletin, Volume 89, pages 548-558.

Brown, R. L., Carr, S. D., Johnson, B. J., Coleman, V. J., Cook, F. A. and Varsek, J. L. (1992a): The Monashee Décollement of the Southern Canadian Cordillera: A Crustal-scale Shear Zone Linking the Rocky Mountain Foreland Belt to Lower Crust beneath Accreted Terranes; *in* Thrust Tectonics, McClay, K. R., Editor, *Chapman & Hall*, London, pages 357-364. .

Brown, R. L., Journeay, M. J., Lane, L. S., Murphy, D. C. and Rees, C. J. (1986): Obduction, Backfolding and Piggyback Thrusting in the Metamorphic Hinterland of the Southeastern Canadian Cordillera; *Journal of Structural Geology*, Volume 8, pages 255-268.

Brown, R. L., Lane, L. S., Psutka, J. F. and Read, P. B. (1983): Stratigraphy and Structure of the Western Margin of the Northern Selkirk Mountains: Downie Creek Map Area, British Columbia; *in* Current Research, Part A, *Geological Survey of Canada*, Paper 83-1A, pages 203-206.

Brown, R. L., McDonough, M. R., Crowley, J. L., Johnson, B. J., Mountjoy, E. W. and Simony, P. S. (1993): Cordilleran Transect, Rocky Mountain Foreland and Omineca Hinterland, Southeastern British Columbia; *Geological Association of Canada/Mineralogical Association of Canada*, Joint Annual Meeting *1993*, Field Trip Guidebook B-9, 125 pages.

Brown, R. L., McNicoll, V. J., Parrish, R. R. and Scammell, R. J. (1992b): Middle Jurassic Plutonism in the Kootenay Terrane, Northern Selkirk Mountains, British Columbia; *in* Radiogenic Age and Isotopic Studies: Report 5; *Geological Survey of Canada*, Paper 91-2, pages 135-141.

Brown, R. L., Tippett, C. R. and Lane, L. S. (1978): Stratigraphy, Facies Change, and Correlations in the Northern Selkirk Mountains, Southern Canadian Cordillera; *Canadian Journal of Earth Sciences*, Volume 15, pages 1129-1140.

Campbell, I. (1994): Report on Geological and Geochemical Surveys on Murder Creek Project, Rain Property; *B.C. Ministry of Energy, Mines and Petroleum Resources*, Assessment Report 12670.

Carmichael, H. (1906): Big Bend District; in Annual Report of the Minister of Mines for 1905, *B.C. Ministry of Mines and Petroleum Resources*, pages 149-152.

Cavey, G. and Raven, W. (1992): Report of Diamond Drilling on Murder Creek Project, Rain Property; *B.C. Ministry of Energy, Mines and Petroleum Resources*, Assessment Report 22622.

Colpron, M. and Price, R. A. (1993): Geology of the Illecillewaet Synclinorium in the Durrand/Dismal Galciers Area, Western Selkirk Mountains, British Columbia; *in* Current Research, Part A; *Geological Survey of Canada*, Paper 93-1A, pages 191-198.

Colpron, M. and Price, R. A. (1995a): Tectonic Significance of the Kootenay Terrane, Southeastern Canadian Cordillera: An Alternative Model; *Geology*, Volume 23, pages 25-28.

Colpron, M. and Price, R. A. (1995b): Tectonic Significance of Rapid Uplift during SW-verging Deformation along the SW Flank of the Selkirk Fan Structure, SE British Columbia; *Geological Association of Canada /Mineralogical Association of Canada*, Victoria '95, Program and Abstracts, Volume 20, page A-115.

Colpron, M., Logan, J. M., Gibson, G. and Wild, C. J. (1995): Geology and Mineral Occurrences of the Goldstream River Area, Northern Selkirk Mountains (NTS 82M/9 and Part of 10); *B. C. Ministry of Energy, Mines and Petroleum Resources*, Open File 1995-2, 1:50 000.

Devlin, W. J. (1989): Stratigraphy and Sedimentology of the Hamill Group in the Northern Selkirk Mountains, British Columbia: Evidence for Latest Proterozoic - Early Cambrian Extensional Tectonism; *Canadian Journal of Earth Sciences*, Volume 26, pages 515-533.

Eisbacher, G. H., Carrigy, M. A. and Campbell, R. B. (1974): Paleo-drainage Pattern and Late-orogenic Basins of the Canadian Cordillera; *in* Tectonics and Sedimentation, Dickinson, W. R., Editor, *Society of Economic Paleontologists and Mineralogists*, Special Publication 22, pages 143-166.

Fyles, J. T. and Eastwood, G. E. P. (1962): Geology of the Ferguson Area, Lardeau District, British Columbia; *B. C. Ministry of Energy, Mines and Petroleum Resources*, Bulletin 45, 92 pages.

Gabrielse, H. and Reesor, J. E. (1974): The Nature and Setting of Granitic Plutons in the Central and Eastern Parts of the Canadian Cordillera; *Pacific Geology*, Volume 8, pages 109-138.

Gibson, G. (1989): Geological Report on the Key 1 and Key 2 Mineral Claims; *B.C. Ministry of Energy, Mines and Petroleum Resources*, Assessment Report 19393.

Gibson, G. and Höy, T. (1994): Geology of the Columbia River - Big Bend Area, NTS 82M; *B. C. Ministry of Energy, Mines and Petroleum Resources*, Mineral Potential Map 82M.

Grant, B. (1984): The J&L Deposit, *Canadian Institute of Mining and Metallurgy*, District 6 Meeting, Kamloops, Abstract, page 23.

Gunning, H. C. (1929): Geology and Mineral Deposits of the Big Bend Area, B.C.; *Geological Survey of Canada*, Summary Report 1928, Part A, pages 136-193.

Hannington, M. (1993): Shallow Submarine Hydrothermal Systems in Modern Island Arc Settings; *Geological Association of Canada/Mineralogical Association of Canada*, Edmonton '93, Program and Abstracts, Page A-40.

Hope, K. G. (1966): Progress Report on the A&E and J&L Projects of Westairs Mines Ltd.; unpublished report for Westairs Mines Ltd.

Höy, T. (1979): Geology of the Goldstream Area; *B. C. Ministry of Energy, Mines and Petroleum Resources*, Bulletin 71, 49 pages.

Höy, T. (1984): J&L: A Stratabound Gold-Arsenic Deposit, Southeastern British Columbia, (82M/8); *in* Geological Fieldwork 1984, *B.C. Ministry of Energy, Mines and Petroleum Resources*, Paper 1985-1, pages 101-104.

Höy, T., Gibson, G. and Berg, N. W. (1984): Copper-Zinc Deposits Associated with Basic Volcanism, Goldstream Area, Southeastern British Columbia; *Economic Geology*, Volume 79, pages 789-814.

Lane, L. S. (1977): Structure and Stratigraphy, Goldstream River - Downie Creek Area, Selkirk Mountains, British Columbia; unpublished M.Sc. thesis, *Carleton University*, 140 pages.

Lane, L. S. (1984): Deformation History of the Monashee Décollement and Columbia River Fault Zone, British Columbia; unpublished Ph.D. thesis, *Carleton University*, 240 pages.

Lane, L. S., Ghent, E. D., Stout, M. Z. and Brown, R. L. (1989): P-T History and Kinematics of the Monashee Décollement Near Revelstoke, British Columbia; *Canadian Journal of Earth Sciences*, Volume 26, pages 231-243.

Logan, J. M. and Colpron, M. (1995): Northern Selkirk Project - Geology of the Goldstream River Map Area (82M/9 and Parts of 82M/10); *in* Geological Fieldwork 1994, Grant, B. and Newell, J. M., Editors, *B. C. Ministry of Energy, Mines and Petroleum Resources*, Paper 1995-1, pages 215-241.

Logan, J. M. and Drobe, J. R. (1994): Summary of Activities, North Selkirk Project, Goldstream River and Downie Creek Map Areas (82M/8, 9 and parts of 10); *in* Geological Fieldwork 1993, Grant, B. and Newell, J. M., Editors, *B. C. Ministry of Energy, Mines and Petroleum Resources*, Paper 1994-1, pages 153-169.

Logan, J. M., Colpron, M., and Johnson, B. J. (1996): Geology and Mineral Occurrences of the Downie Creek Area, Northern Selkirk Mountains (NTS 82M/8); *B. C. Ministry of Energy, Mines and Petroleum Resources*, Open File 1996-2, 1:50 000.

Logan, J. M., Gibson, G. and Colpron, M. (1995): Geology of the Goldstream Mine Area, Northern Selkirk Mountains (NTS 82M/9); *B. C. Ministry of Energy, Mines and Petroleum Resources*, Open File 1995-3, 1:10 000.

Lund, J. C. and Hajek, J. H. (1976): Report on Big Bend Project, Geological and Geochemical Survey, CC Nos. 1-9; Jack and Jill Mineral Claim, Revelstoke Mining Division; *B.C. Ministry of Energy, Mines and Petroleum Resources*, Assessment Report 6235.

McKinlay, F. T. (1987): Geology and Control of Sulphide Deposition of the J and L Massive Sulphide Deposit, Southeast British Columbia; ; unpublished M.Sc. thesis, *The University of Western Ontario*, XX pages.

Meyers, R. E. and Hubner, T. B. (1989): An Update on the J&L Gold-bearing Polymetallic Sulphide Deposit; *in* Exploration in British Columbia 1989; *B.C. Ministry of Energy, Mines and Petroleum Resources*, pages 81-89.

Okulitch, A. V., Wanless, R. K. and Loveridge, W. D. (1975): Devonian Plutonism in South-central British Columbia; *Canadian Journal of Earth Sciences*, Volume 12, pages 1760-1769.

Parrish, R. R. (1992): Miscellaneous U-Pb Zircon Dates from Southeast British Columbia; *in* Radiogenic Age and Isotopic Studies: Report 5, *Geological Survey of Canada*, Paper 91-2, pages 143-153.

Price, R. A. (1981): The Cordilleran Foreland Thrust and Fold Belt in the Southern Canadian Rocky Mountains; *in* Thrust and Nappe Tectonics, McClay, K. R. and Price, N. J., Editors, *The Geological Society of London*, Special Publication No.9, pages 427-448.

Price, R. A. (1986): The Southeastern Canadian Cordillera: Thrust Faulting, Tectonic Wedging, and Delamination of the Lithosphere; *Journal of Structural Geology*, Volume 8, pages 239-254.

Price, R. A., Brown, R. L. and Tippett, C. R. (1979): The Selkirk Fan Structure of the Southeastern Canadian Cordillera: Discussion and Reply; *Geological Society of America*, Bulletin, Volume 90, pages 695-698.

Raeside, R. P. and Simony, P. S. (1983): Stratigraphy and Deformational History of the Scrip Nappe, Monashee Mountains, British Columbia; *Canadian Journal of Earth Sciences*, Volume 20, pages 639-650.

Read, P. B. and Brown, R. L. (1979): Inverted Stratigraphy and Structures, Downie Creek, British Columbia; *in* Current Research, Part A, *Geological Survey of Canada*, Paper 79-1A, pages 33-34.

Read, P. B. and Brown, R. L. (1981): Columbia River Fault Zone: Southeastern Margin of the Shuswap and Monashee Complexes, Southern British Columbia; *Canadian Journal of Earth Sciences*, Volume 18, pages 1127-1145.

Read, P. B. and Wheeler, J. O. (1976): Geology of Lardeau West-half Map Area; *Geological Survey of Canada*, Open File 432, 1:125 000.

Sears, J. W. (1979): Tectonic Contrasts between the Infrastructure and Suprastructure of the Columbian Orogen, Albert Peak Area, Western Selkirk Mountains, British Columbia; unpublished Ph.D. thesis, *Queen's University*, 154 pages.

Simony, P. S. and Wind, G. (1970): Structure of the Dogtooth Range and adjacent portions of the Rocky Mountain Trench; *in* Structure of the Southern Canadian Cordillera, Wheeler, J. O., Editor, *Geological Association of Canada*, Special Paper No. 6, pages 41-51.

Smith, M. T. and Gehrels, G. E. (1992a): Structural Geology of the Lardeau Group near Trout Lake, British Columbia: Implications for the Structural Evolution of the Kootenay Arc; *Canadian Journal of Earth Sciences*, Volume 29, pages 1305-1319.

Smith, M. T. and Gehrels, G. E. (1992b): Stratigraphic Comparison of the Lardeau and Covada Groups: Implications for the Structural Evolution of the Kootenay Arc; *Canadian Journal of Earth Sciences*, Volume 29, pages 1320-1329.

Smith, M. T. and Gehrels, G. E. (1992c): Stratigraphy and Tectonic Significance of Lower Paleozoic Continental Margin Strata in Northeastern Washington; *Tectonics*, Volume 11, pages 607-620.

Walker, J. F. (1926): Windermere Map-area, British Columbia; *Geological Survey of Canada*, Memoir 148, 69 pages.

Walker, J. F. and Bancroft, M. F. (1929): Lardeau Map-area, British Columbia: General Geology; *in* Lardeau Map-area, British Columbia, Walker, J. F., Bancroft, M. F. and Gunning, H. C., Editors, *Geological Survey of Canada*, Memoir 161, pages 1-16.

Weicker, R. F. (1989): Exploration Report on A&E Showings, J&L Property, Revelstoke Mining Division, British Columbia; *B.C. Ministry of Energy, Mines and Petroleum Resources*, Assessment Report 19454.

Weicker, R. F. (1991): Report on 1991 Summer Exploration Program, J&L Property, Revelstoke, British Columbia; *B.C. Ministry of Energy, Mines and Petroleum Resources*, Assessment Report 22004.

Wheeler, J. O. (1963): Rogers Pass Map-area, British Columbia and Alberta (82N W Half); *Geological Survey of Canada*, Paper 62-32, 32 pages.

Wheeler, J. O. (1965): Big Bend Map-area, British Columbia (82M E Half); *Geological Survey of Canada*, Paper 64-32, 37 pages.

Wheeler, J. O. (1966): Eastern Tectonic Belt of Western Cordillera in British Columbia; *in* Tectonic History and Mineral Deposits of the Western Cordillera, *Canadian Institute of Mining and Metallurgy*, Special Volume 8, pages 27-45.

Wheeler, J. O. and McFeely, P. (1991): Tectonic Assemblage Map of the Canadian Cordillera and adjacent parts of the United States of America; *Geological Survey of Canada*, Map 1712A, 1:2 000 000.

Wheeler, J. O., Brookfield, A. J., Gabrielse, H., Monger, J. W. H., Tipper, H. W. and Woodsworth, G. J. (1991): Terrane Map of the Canadian Cordillera; *Geological Survey of Canada*, Map 1713A, 1:2 000 000.

Wild, C. J. (1988): Geology and Geochemistry on the Key 1-3 Mineral Claims; *B.C. Ministry of Energy, Mines and Petroleum Resources*, Assessment Report 17026.

Wild, C. J. (1990): Geological and Geochemical Report on the Rain 1-17 Mineral Claims; *B.C. Ministry of Energy, Mines and Petroleum Resources*, Assessment Report 20628.

Wright, J. H., Weicker, R. F. and Taal, T. (1989): Report on Diamond Drill Program and Metallurgical Testwork, J&L Property, British Columbia, NTS 82M/8E; *B.C. Ministry of Energy, Mines and Petroleum Resources*, Assessment Report 19469.

Zwanzig, H. V. (1973): Structural Transition Between the Foreland Zone and the Core Zone of the Columbian Orogen, Selkirk Mountains, British Columbia; unpublished Ph.D. thesis, *Queen's University*, 158 pages.

NOTES

# NEW INVESTIGATIONS ON EAGLENEST MOUNTAIN, NORTHERN QUESNEL TERRANE: AN UPPER TRIASSIC REEF FACIES IN THE TAKLA GROUP, CENTRAL BRITISH COLUMBIA (93N/11E)

By George D. Stanley, Jr., The University of Montana
and JoAnne L. Nelson, Geological Survey Branch

KEYWORDS: Regional geology, Upper Triassic, reef complex, carbonate, sedimentology, paleontology, Plughat Mountain Formation, Takla Group.

## INTRODUCTION

A number of carbonate deposits and reefs are known in the Cordillera. Those in Canada are described by Geldsetzer and James (1988). The few examples from the early Mesozoic occur exclusively in Cordilleran displaced terranes. Most show variation in thickness, fossils and facies content. Most of these reef-like carbonate bodies are characterized by a fauna of corals and sponges. They tend to be small, and most lack the thickness and complexity typical of coeval deposits in Tethyan reefs of Europe and Eurasia (Stanley, 1988b). Only two Upper Triassic reef sequences comparable to those of the Tethys are known in the the Americas. These are the Wallowa Terrane of Oregon (Stanley and Senowbari-Daryan, 1986) and an example from the Yukon in the Stikine Terrane (Reid, 1988; Reid and Tempelman-Kluit, 1987). The Yukon example stands alone as the thickest and best developed Triassic reef complex known among Cordilleran terranes. It also reveals close correspondence of fauna and facies with those of distant reefs in the former Tethys region. An example of a Tethyan-type patch reef is known from Lower Jurassic volcanics in Hazelton Group of British Columbia (Stikine Terrane) described by Stanley and McRoberts (1992) and Stanley and Beauvais (1994). All reef examples occur in displaced terranes. According to Stanley (1988a, 1995) they existed during Permian and Triassic time as fringing volcanic islands in the ancient Pacific Ocean. Since that time they have become accreted to the North American craton, as part of allochthonous terranes.

This paper is a preliminary report on a newly recognized Upper Triassic reef complex investigated during the summer of 1995 in the Takla Group of British Columbia. It lies within Quesnellia, a late Paleozoic - early Mesozoic island arc terrane (Figure 1). The site on Eaglenest Mountain in the Kwanika Creek map area was recognized during the course of geological fieldwork (Bailey *et al.*, 1993) and briefly described by Nelson *et al.* (1993). These authors recognized the reefal nature of the massive limestone exposed at this site. It occurs within an augite-phyric, mainly pyroclastic basalt sequence near the assumed top of the Upper Triassic Plughat Mountain succession, which is unconformably overlain by Lower Jurassic volcanic rocks. The Plughat Mountain succession represents a primitive intra-oceanic arc. Its uppermost unit in the Kwanika Creek area is a bright red amygdaloidal to scoreaceous basalt, which overlies darker green pyroclastic and pillow basalt. This stratigraphy suggests that the sequence shallowed upwards and became shallow marine to possibly subaerial by the end of the Triassic.

The Eaglenest site is significant because it provides the first paleontologic and sedimentologic glimpse of carbonate reef rocks within Quesnellia. Data derived from this reef undoubtedly will prove significant by supplying infor-

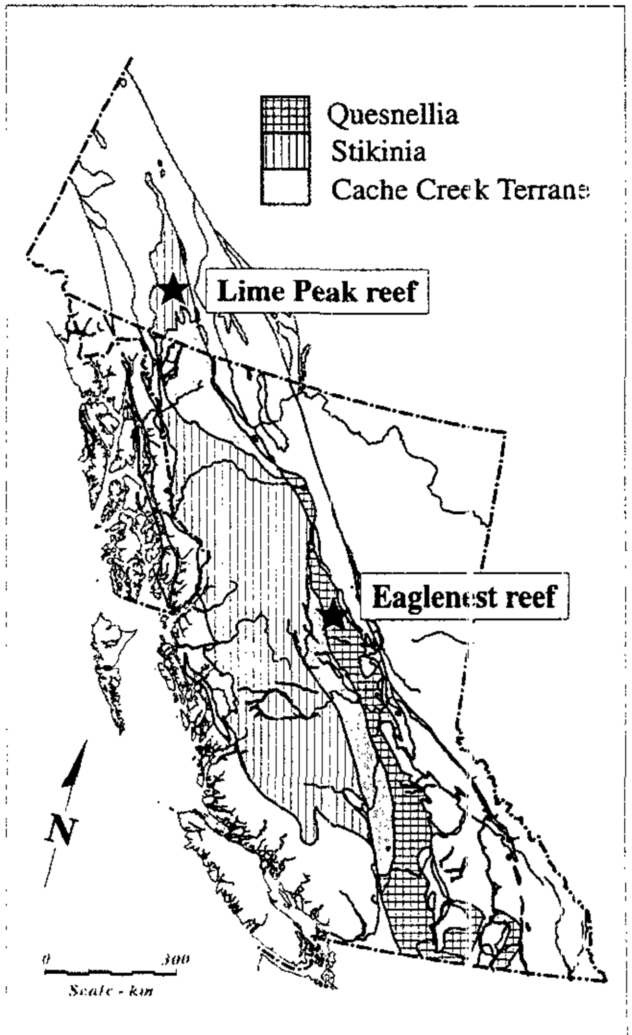


Figure 1. Location of the Eaglenest reef within the Canadian Cordillera.

mation to assess paleogeography and evolution of early Mesozoic reefs and by providing a basis for comparison with the reefs of other terranes. The massive limestone at Eaglenest compares well with the Yukon example previously mentioned. It also has a rich reef fauna, including biostratigraphic fossils which allow dating of the limestone. The Eaglenest complex of reef and reef-associated limestone, its fauna and carbonate lithofacies are currently the subjects of a detailed investigation.

## DESCRIPTION OF THE REEF

Seven rock types (gross lithofacies) were recognized and mapped within the kilometre-wide cliff face at Eaglenest Mountain (Photo 1, Figure 2). The exposure is dominated by limestone lithofacies but volcaniclastic and mixed limestone-volcaniclastic units are also present. The limestone is surrounded by a much thicker volcanic sequence, the Plughat Mountain succession. The thickest exposure of unbroken massive to thick-bedded limestone is at the south end of the outcrop. Here carbonate rocks are juxtaposed against volcaniclastics, with as much as 200 metres of limestone exposed (Photo 1, Figure 2). It is difficult to measure a single representative section because the limestone intervals lie at different attitudes, setting off certain parts of the section from others. These bedded limestone units thicken and thin and are commonly interbedded with adjacent volcaniclastic rocks. At least four isolated blocks are present in the exposed cliff face; they display various bedding attitudes relative to the surrounding rock and to each other. Bedding attitudes in the cliff face are also affected by several normal faults. Dips in the limestone are variable, but most are gentle to northeast. On the other hand, the overall contact between the limestone and the surrounding pyroclastic succession dips moderately to the west. Some of the the sharp contacts between volcaniclastic rocks and limestone are fault controlled but most appear to be depositional. The lithofacies recognized during the field investigation are briefly described below.

### *STRATIGRAPHY AND LITHOFACIES*

The light grey carbonate rock types include: 1) *Heterastridium* conglomerate which overlies the massive limestone at several sites, 2) sponge and coral limestone, 3) massive recrystallized limestone, which forms large bedded sections and also blocks, 4) crinoidal limestone and 5) chaotic breccia and conglomerate. As shown in Photo 1 and Figure 2, these carbonate rock types are associated with noncarbonate rock types consisting of: 1) volcanic sandstone and lime-matrix basalt breccia, 2) bedded bioclas-

Photo 1. Cliff face exposure of limestone on Eaglenest Mountain, view from the southwest.

tic/volcanic sandstone and 3) augite-phyric agglomerate and lapilli tuff. This report focuses primarily on the carbonate rock types and associated fossils.

## HETERASTRIDIUM CONGLOMERATE

The *Heterastridium* conglomerate, at the top of the sequence, is in sharp contact with underlying sponge and coral limestone. This conglomerate ranges in thickness from 8.0 to 10.0 metres and consists almost exclusively of rounded spheres of *Heterastridium conglobatum* 1.5 to 3.0 centimetres in diameter (Photos 2a, 2b). These fossils were deposited in closely packed arrangement in direct contact with each other. *Heterastridium conglobatum* Reuss is a spherical to globular, floating hydrozoan colony which attained global marine distribution during Late Triassic (middle to late Norian) time. For this reason it is a biostratigraphically useful fossil with occurrences in parts of Alaska, western Canada (including the Queen Charlotte Islands) and in western Nevada (Silberling and Tozer, 1968). It is indicative of the upper Norian (Cordilleranus and Amoenum Zones), often occuring with the flat clam *Monotis (Pseudomonotis) subcircularis*. *Heterastridium* has recently been identified in the Antimonio Terrane of Sonora, Mexico (Stanley *et al.*, 1994).

According to Leo Krystyn (written communication 1995), *Heterastridium* in the former Tethys region ranges from at least as low as uppermost middle Norian to upper Norian. Populations of small individuals (2-3 cm diameter) indicate middle Norian (Alaunian 3/II) while larger sizes indicate higher intervals in the upper Norian. This taxon was extinct before the end of the Triassic as no latest Triassic (Rhaetian) occurrences are known. The diameters

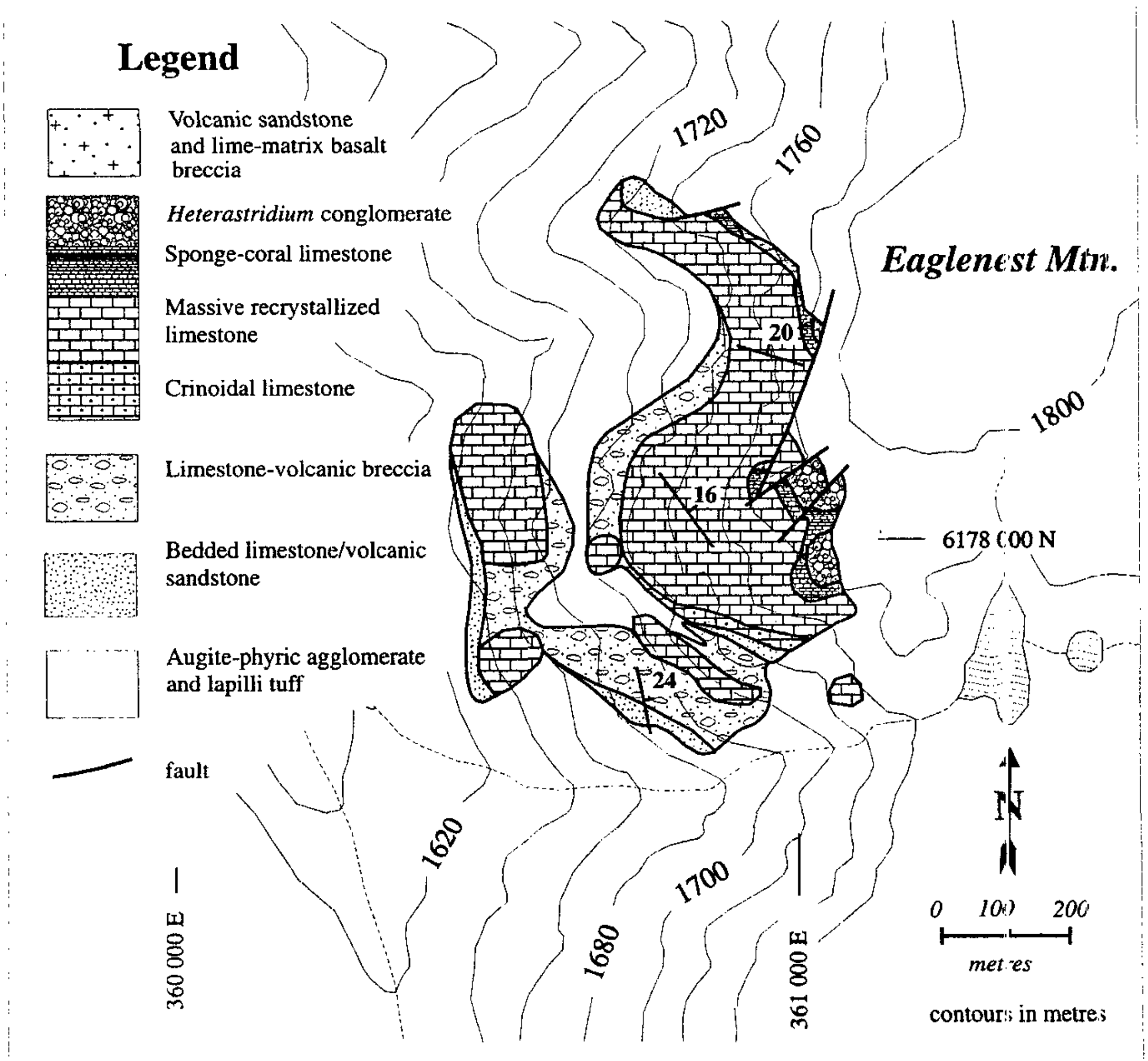


Figure 2. Detailed geologic map of the Eaglenest reef.

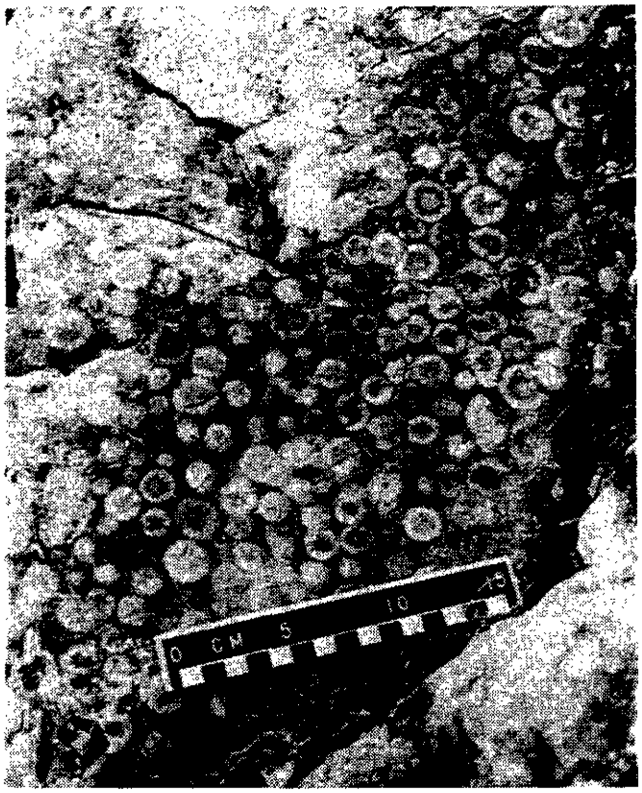

Photo 2a. Outcrop photo of *Heterastridium* conglomerate lithofacies. Note the tightly packed spherical colonies of this floating hydrozoan. Their abundance and the nature of the deposit indicates beaching of thousands of these organisms, or the mass sinking of waterlogged colonies. Scale in centimetres.

Photo 2b. Polished slab of *Heterastridium*, showing the numerous radiating canals of the coenosteum, which were originally filled with air. Most spherical colonies have recrystallized. The void spaces are filled with clear calcite and encrusted by cyanobacteria representing porostomate algae (dark coatings). Scale in centimetres.

found in the Eaglenest indicate middle Norian strata. The voluminous occurrences of *Heterastridium* at Eaglenest are unusual, as these planktonic fossils usually occur fairly dispersed in other North American occurrences and usually indicate deep water. The only other known examples of Heterastridium in concentrations as thick and dense as those at Eaglenest come from the Upper Triassic (Norian) of Karakorum, Timor and New Zealand (Campbell, 1974).

At Eaglenest the basal contact with the Heterastridium conglomerate is unconformable and probably represents a small erosional break. The Het*erastridium* facies appears to fill in local irregularities (probably karst surfaces) on top of the reef limestone. The limestone is also cut by small neptunian? dikes or fractures 10 to 50 centimetres wide. These are infilled with additional reworked? *Heterastridium* but these fissures are filled mostly by coarse-grained, sandy polymict volcaniclastic sediments. The fractures appear to be confined to the top of the reef limestone and do not seem to penetrate very deeply.

## SPONGE-CORAL LIMESTONE

This lithofacies outcrops at several sites in the map area (Figure 2) and is estimated to be 10 to 50 metres thick. It lies directly below the *Heterastridium* conglomerate and is gradational into the underlying massive recrystallized limestone. It consists of abundant upright-growing and encrusting sponges, spongio-morphs, disjectoporoids and corals, mostly in life positions. Such organisms, reef builders at other Triassic reef sites in the Yukon and the Tethys, appear to be an important limestone builder in the Eaglenest limestone. Study of these organisms is currently underway at the University of Montana. Large-chambered thalamid sponges (Photo 3) are volumetrically the most abundant elements. They include the genera *Nevadathalamia* and *Cinnabaria* and possibly other sponges which are already known from the Yukon reef locality and also from nonreef localities in the Luning Formation of western Nevada (Senowbari-Daryan and Reid, 1987, Senowbari-Daryan and Stanley, 1992) and the Antimonio Formation of Sonora (Stanley *et al.*, 1994). Small spar-filled cavities are created by shelter porosity. Other cavities appear to be of solutional origin.

Of less volumetric importance in this lithofacies are moderate to large colonial scleractinian corals (Photo 4). These include *Retiophyllia, ?Kuhnastraea, Chondrocoenia*, indeterminate meandroid corals and large tabular colonies of *Pamiroseris*. Also present are irregularly encrusting yet problematic organisms referred to as disjectoporoids and massively encrusting hydrozoans referrable to the genus *Spongiomorpha*. Spongiostromate crusts, attributable to cyanobacteria, are also present within cavities. Microfossils such as foraminifers and algae have yet to be identified and studied in thin section. Bivalves and gastropods are present, but have not been identified. At one site below the *Heterastridium* conglomerate, a prominent bivalve shell bed charac-terizes the top of the sponge-coral limestone; it may indicate a different paleocommunity that succeeded the reef.

Photo 3. Polished specimen of the chambered sponge *Nevadathalamia* sp. from the sponge-coral lithofacies. The matrix is skeletal debris of corals and molluscs. Scale in centimetres.

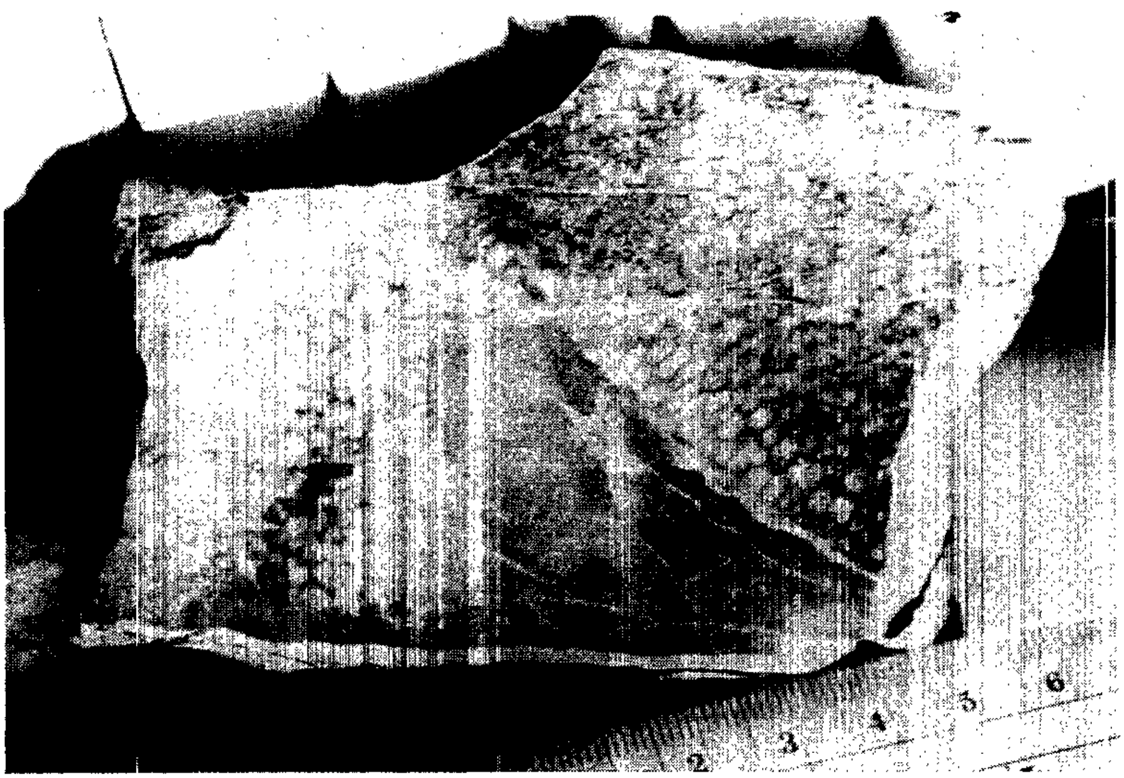

Photo 4. Colonial cerioid coral *Chondrocoenia* sp. Large encrusting colony growing on fine-grained matrix. Sponge-coral lithofacies. Scale in centimetres.

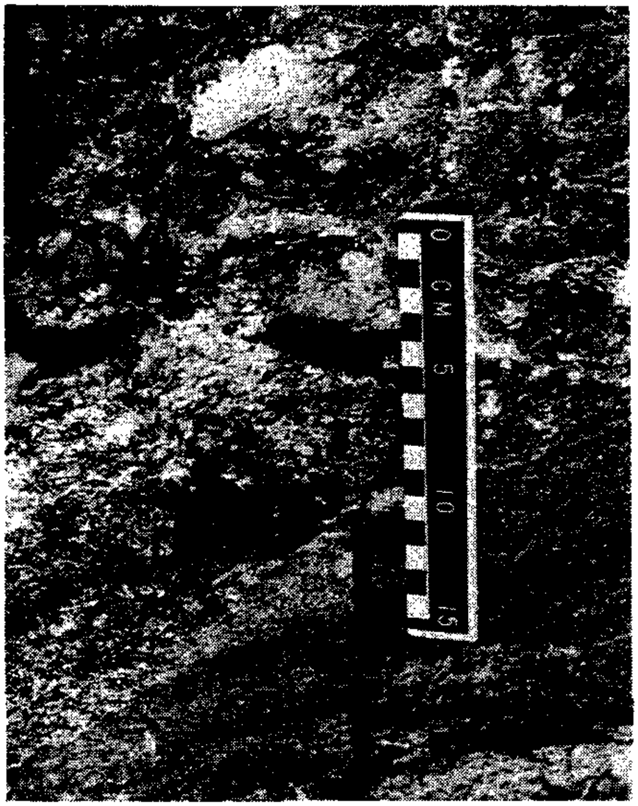


Photo 5. Field photo of crinoidal limestone showing planar and low-angle crossbeds. Scale in centimetres.

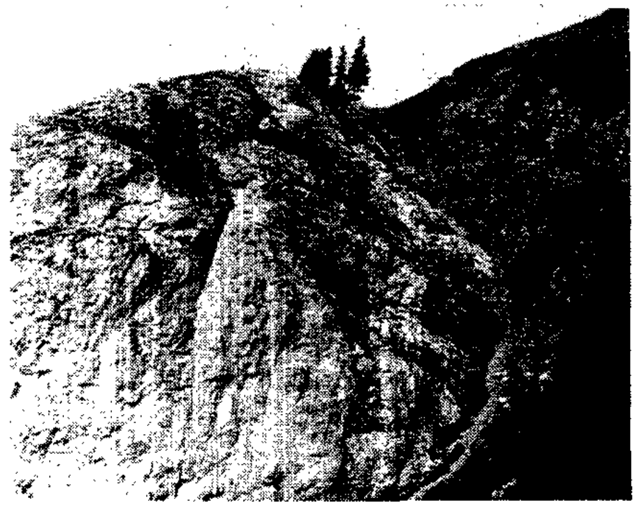

Photo 6. Edge of one of the large blocks of massive recrystallized limestone surrounded by pyroclastic debris and chaotic breccia and conglomerate. The contact is abrupt but unsheared, suggesting that it was emplaced in its matrix by gravity sliding rather than later faulting.

Photo 7. Limestone-volcanic breccia in outcrop, lying above bedded bioclastic/volcanic sandstone (lower left). Outcrop shot shows chaotic breccia composed of large clasts of limestone and volcanic rock up to 4 metres in diameter.


Photo 8. Details of the limestone-volcanic breccia showing clasts of fossils, limestone and volcanic rock fragments. Scale in centimetres.

### MASSIVE RECRYSTALLIZED LIMESTONE

Most of the light-coloured limestone in the cliff face displays a recrystallized texture and is massive to thick bedded. Due to the diagenetic effects of the recrystallization, little is revealed of original lithology, texture or biotic constituents. However some breccia-like textures are present, as well as crinoid columnals, bivalves or brachiopods and some vaguely defined branching coral or sponge-like fossils. We suspect that prior to recrystallization this lithofacies may have contained textures and fossils similar to those of the sponge-coral limestone.

### CRINOIDAL LIMESTONE

This lithofacies (Photo 5) is an impure limestone with laminations and crossbedding. It is mostly a bioclastic limestone characterized by abundant abraded echinoderm debris, predominantly disarticulated and abraded crinoid ossicles (packstone textures) and molluscan shells. Among the crinoid ossicles are scattered five-sided "*Isocrinus*", incorrectly identified as pentamerid corals in Nelson *et al.* (1993). The limestone contains a large admixture of sand-size volcaniclastic grains. Whole cidaroid echinoid spines, test fragments and much molluscan shell debris are present locally. Rare spiriferid brachiopods were also observed. Whole and abraded coarse-ribbed bivalves (including pectinaceans), and reworked corals, sponges and disjectoporoids are common in the upper portions of this lithofacies. The crinoidal limestone is at least 30 metres thick, but thickness varies considerably across the exposed cliff face. Strata are thin to medium bedded, with irregular contacts producing a nodular appearance. Low-angle crossbedding is visible in weathered outcrops.

### LIMESTONE BLOCKS

This lithofacies consists of massive to thick-bedded, light-coloured limestone blocks reaching 100 to 200 metres in length. These are enclosed in a chaotic mixture of breccia and conglomerate described below. At least four such blocks were mapped in the lower parts of the cliff face (Photos 1, 6, Figure 2). The composition of the blocks is pure recrystallized limestone similar to the massive recrystallized limestone lithofacies previously described. Mapping has shown that the large blocks are incorporated within the chaotic breccia and conglomerate described below. Although fossils are difficult to discern due to the recrystallization, typical reef forms of sponges and corals are recognized.

### LIMESTONE-VOLCANIC BRECCIA

This lithofacies consists of a chaotic mixture of poorly sorted, angular to subrounded limestone clasts and rounded volcanic rock fragments set in a matrix of lime mud and/or grain-supported carbonate rock (Photo 7). Individual limestone clasts of various orientations range in size from 2 centimetres to the outcrop-sized blocks described in the previous section. The generally smaller, dark-coloured volcaniclasts are amygdaloidal and augite-phyric basalt (Photos 7, 8). Most limestone clasts are slightly recrystallized. Some contain large coral colonies of *Retiophyllia* as well as sponges and other reef fossils similar to those found in the sponge-coral facies (see above). The chaotic breccia and conglomerate unit occurs within the augite-phyric agglomerate and lapilli tuff beds and is in contact with the crinoidal limestone and the massive recrystallized limestone (Figure 2).

Volcanic sandstone and lime-matrix basalt breccia is found only in one small area in the northeast part of the cliff exposure (Figure 2). This lithology may represent either an incursion of surrounding sediments into the reef or the filling of fissures in the reef. The augite-phyric agglomerate and lapilli tuff surrounding the reef limestone represent volcanic depositional patterns within the inter-arc basin in which the reef developed. The volcanic processes were probably occurring simultaneously with the deposition of the organic reef limestone.

## INTERPRETATIONS

Several of the lithofacies mapped at Eaglenest Mountain - the sponge-coral facies, the massive recrystallized limestone and the crinoid facies - are interpreted to represent part of an Upper Triassic reef complex. These lithofacies are comparable to other Triassic reef sequences, especially those in Oregon and the Yukon. The reef organisms also appear similar to those occurring in other reef complexes and in some nonreef associations such as in western Nevada and Sonora, Mexico but detailed taxonomic study is not yet complete enough to allow meaningful comparisons. Paleontological study currently underway is expected to be completed soon and should yield good comparative data.

We interpret both the sponge-coral facies and the massive recrystallized limestone, comprising the bulk of the carbonate lithofacies, to represent the main reef facies. Further investigations may result in narrower subdivision and recognition of specific environments such as backreef, lagoon etc., but at present, the volumetric abundance of *in situ* framework-building taxa of chambered sponges, corals and other fossils leaves little doubt about a reef origin. The crinoid facies is laterally equivalent and is interpreted to represent a down-slope (forereef) facies.

Eaglenest Mountain is interpreted here as a disrupted reef complex. Unlike reef sequences from some other terranes, the limestone at Eaglenest is disrupted and broken into numerous blocks with variable bedding attitudes relative to each other and to bedding in the surrounding volcaniclastic and volcanic rock lithofacies. At odds with the idea of an *in situ* reef growing on a volcanic edifice (Nelson *et al.*, 1993), we interpret these carbonate rocks to represent an allochthonous series of limestone blocks transported into a deeper water basin or off-shelf (?slope) setting by syndepositional gravity sliding and associated down-slope debris flow. In this interpretation, the limestone bodies now juxtaposed at the Eaglenest site are comparable to olistostromes or olistoliths common on other Triassic island arc settings such as the Eastern Klamath Terrane of California (Eastoe *et al.*, 1987). The blocks were most likely derived from a shallow-water carbonate shelf developing on the fringe of a volcanic island, in an environment of steep constructional slopes and active tectonism. The subrounded to rounded shapes of some limestone and volcaniclasts in the chaotic breccia and conglomerate suggest an episode of recycling and transportation in a shallow shelf setting prior to displacement into deeper water. Subsequent block faulting has slightly modified the original relationships of the limestone.

We base the allochthonous gravity slide hypothesis on the sharp nature of the lower contact of the massive recrystallized limestone with the underlying chaotic breccia and conglomerate - a lithofacies showing classic characteristics of downslope debris flows with small to fairly large size allochthonous blocks (Photos 7, 8). We find that only a few of the observed sharp contacts can be accounted for by faulting. The 200 or more metres of limestone exposed in the cliff face display different inclinations and most likely represent several allochthonous blocks displaced into deeper water by gravity sliding. This would account for the various angles of dip observed in the sequence, the isolated nature of the limestone blocks, the lower contacts of the largest limestone body which rests abruptly on the chaotic breccia and conglomerate lithofacies and the abrupt nature of the contacts between limestone and adjacent volcaniclastic rocks (*e.g.* Photo 6). Olistostromic sliding may have been induced by gravity or triggered by earthquakes in the arc basin. Syndepositional slumping, gravity induced debris flows and general collapse of shelf margins are processes expected within island arc-trench settings. In the case of Eaglenest it appears to have resulted in the disruption and possibly a collapse of a shallow- water, tropical reef.

The *Heterastridium* conglomerate is interpreted to represent a postdepositional event occurring soon after death of the reef and its uplift and karst development, but prior to slumping into deeper water. The irregular contact between the densely packed *Heterastridium* conglomerate and the underlying reef limestone indicate that the original shallow-water reef had been uplifted and subjected to some karst processes. The closely packed *Heterastridium* concentration may represent storm deposits that washed these floating hydrozoan colonies into a shallow water, subtidal (near-shore) environment. Thus interpreted, the *Heterastridium* bank was deposited after waterlogged colonies accumulated in shallow, open shelf water. Comparable accumulations occur in the Hallstätt Beds of Germany and Austria (Zankl, 1969) and in the Norian of New Zealand, where dense *Hetera- stridium* banks are observed (Campbell, 1974). The volcaniclastic fissures filling the top of the limestone most likely represent a subsequent phase which could have coincided with slumping or later faulting.

## *AGE*

Previous conodont collections from the Eaglenest reef complex are broadly Upper Triassic (M. J. Orchard, personal communication to J. Nelson, 1993). The occurrence of the *Heterastridium* conglomerate and the abundance of small-size spherical colonies of *Heterastridium conglobatum* constrain the biostratigraphy to uppermost middle to upper Norian. As we interpret the *Heterastridium* conglomerate lithofacies as a younger post-reef feature of deposition, the underlying reef limestone must be older, probably lower to middle Norian. This age assessment is reasonable considering the similarity of the sponges, corals and other reef organisms with those from lower and middle Norian localities (Senowbari-Daryan and Reid, 1987; Senowbari-Daryan and Stanley, 1992; Stanley *et al.,* 1994). Retrieval of additional conodonts from the Eaglenest rocks could better constrain the age of the reef limestone and associated lithofacies.

## CONCLUSIONS

The limestone lithofacies on Eaglenest Mountain represent the remains of an Upper Triassic reef that was populated by sponges, corals and a variety of reef-building and reef-dwelling organisms. It existed within an island arc setting, preserved in the predominantly volcanic Takla Group. This thick limestone reef in the Takla Group suggests that it lay at tropical to subtropical paleolatitudes. We interpret the limestone lithofacies as sedimentologically allochthonous with respect to the surrounding volcaniclastic rocks. The limestone was displaced as a debris flow with large olistoliths, from an original site on a shallow-water shelf into a basin. This occurred after lithification of the reef, uplift, karst development and the deposition of *Heterastridium* conglomerate.

The Eaglenest limestone is one of the few remnant Upper Triassic reefs in the Cordillera that have yielded well preserved fossils. It offers new insights into reef development and reef fauna in Triassic Quesnellia. Ongoing study of its fossils is expected to provide long needed data for reconstruction of paleogeography and comparisons with other displaced terranes in the Cordillera.

## REFERENCES


Bailey, D., Nelson, J.L., Bellefontaine, D.A. and Mountjoy, K. J. (1993): Geology and Geochemistry of the Kwanika Creek Map Area NTS 93N/11E ; *B.C. Ministry of Energy, Mines and Petroleum Resources*, Open File 1993-4.

Campbell, J.D. (1974): *Heterastridium* (Hydrozoan) from Norian Sequences in New Caledonia and New Zealand; *Journal of the Royal Society of New Zealand*, Volume 4, pages 447-453.

Eastoe, C.J., Gustin, M.M. and Nelson, S.E. (1987): Problems of Recognition of Olistostromes: An Example from the Lower Pit Formation, Eastern Klamath Mountains, California; *Geology,* Volume 15, pages 541- 544.

Geldsetzer, H.J. and James, N.P. (1988): Reefs of Canada and Adjacent Areas; *Canadian Society of Petroleum Geologists,* Memoir 13, 775 pages.

Nelson, J.L., Bellefontaine, K.A., MacLean, M.E. and Mountjoy, K.J. (1993): Geology of the Klawli Lake, Kwanika Creek and Discovery Creek Map Areas, Northern Quesnel Terrane, British Columbia (93N7, 11E, 14E); *in* Geological Fieldwork 1992, Grant, B. and Newell, J.M., Editors, *B.C. Ministry of Energy, Mines and Petroleum Resources,* Paper 1993-1, pages 87-107.

Reid, R.P. ( 1988.): Lime Peak Reef Complex, Norian Age, Yukon; *Canadian Society of Petroleum Geologists,* Memoir 13, pages 114-765.

Reid, R.P. and Tempelman-Kluit, D.J. (1987): Tethyan-type Upper Triassic Reefs in Yukon; *Bulletin of Canadian Petroleum Geology*, Volume 35, pages 316-332.

Senowbari-Daryan, B. and Reid, P. (1987): Upper Triassic Sponges (Spinctozoa) from Southern Yukon, Stikinia Terrane; *Canadian Journal of Earth Sciences*, Volume 24, pages 882-902.

Senowbari-Daryan, B. and Stanley, G.D., Jr. (1992): Late Triassic Thalamid Sponges from Nevada; *Journal of Paleontology*, Volume 66, pages 183-193.

Silberling, N.J. and Tozer, E.T. (1968): Biostratigraphic Classification of the Marine Triassic in North America; *Geological Society of America*, Special Paper 110, 63 pages.

Stanley, G. D., Jr. (1988a): The History of Early Mesozoic Reef Communities: A Three-step Process; Reefs Issue, *Palaios*, Volume 3, pages 170-183.

Stanley, G. D., Jr. (1988b): Reefal Triassic Fossils and their Application to Analysis of Accreted Terranes; *Geological Society of America,* Abstracts with Programs, Volume 20, No.7, page A309.

Stanley, G. D., Jr. (1995): Triassic Reef Ecosystems and Mass Extinctions; *Geological Association of Canada/ Mineralogical Association of Canada,* Annual Meeting, Program with Abstracts, Volume 20, page A100.

Stanley, G.D., Jr. and Beauvais, L. (1994): Corals from an Early Jurassic Coral Reef in British Columbia: Refuge on an Oceanic Island Reef; *Lethaia*, Volume 27, No. 1, pages 35-47.

Stanley, G. D., Jr. and McRoberts, C. A. (1993): A Coral Reef in the Telkwa Range, British Columbia: the Earliest Jurassic Example; *Canadian Journal of Earth Sciences*, Volume 30, pages 819-831.

Stanley, G. D., Jr. and Senowbari-Daryan, B. (1986): Upper Triassic Dachstein-type Reef Limestone from the Wallowa Mountains, Oregon: First Reported Occurrence in the United States; *Palaios*. Volume 1, pages 172- 177.

Stanley, G.D., Jr., González-León, C., Sandy, M.R., Senowbari-Daryan, B., Doyle, P., Tamura, M. and Erwin, D.H. (1994): Upper Triassic Invertebrates from the Antimonio Formation, Sonora, Mexico; *Paleon- tological Society,* Memoir 36, 33 pages.

Zankl, H. (1969): Der Hohe Göll: Aufbau und Lebenbild eines Dachsteinkalk-riffes in der Obertrias der Nördlichen Kalkalpen; *Abhandlungen Senkenbergiana Naturfor- schung Gesellschaft*, Volume 519, pages 1-123.

# NOTES

# GEOLOGY AND MINERALIZATION OF THE GATAGA MOUNTAIN AREA, NORTHERN ROCKY MOUNTAINS (94L/10, 11, 14 AND 15)

**Filippo Ferri, Chris Rees and JoAnne Nelson**

*(Contribution to the Canada - British Columbia Mineral Development Agreement 1991-1995)*

*KEYWORDS*: Northern Rocky Mountains, Gataga River, Kechika Trough, Gog Group, Cambrian, Kechika Group, Road River Group, Earn Group, sedimentary exhalatives, barite, lead, zinc.

## INTRODUCTION

This report summarizes 1995 fieldwork on the Gataga Mapping Project in the central part of the Kechika Trough in northeastern British Columbia (Figures 1, 2). This trough or basin is delineated by Cambrian to Mississippian rocks exposed along the western margin of the northern Rocky Mountains. The basin is host to numerous sedimentary exhalative barite-lead-zinc deposits collectively known as the Gataga mineral district. Deposits occur at various levels, although the most numerous and economically important are Late Devonian, and include the Cirque (Stronsay) and Driftpile deposits.

This mapping program is part of an ongoing cooperative project with the Geological Survey of Canada which began in 1994 and is funded, in part, by the second Mineral Development Agreement between the governments of British Columbia and Canada. The program includes a regional stream sediment and water survey covering the 1994 and 1995 mapping areas (Jackaman *et al.*, 1996, this volume), and detailed studies of major Devono-Mississippian sedimentary exhalative deposits within the Kechika Trough.

The 1995 map area covers the northern termination of the Rocky Mountains along the eastern flank of the Northern Rocky Mountain Trench (Figure 2). Terminus Mountain is the last 'Rocky' Mountain in this chain. The lower relief in this area reflects the disappearance of the thick Cambrian carbonates and coarse siliciclastics which characterize the large thrust stacks in the northern part of the Rocky Mountains to the south. The subdued terrain in the northern part of the map area includes parts of the Rabbit River Plateau and Liard Lowland.

The map area is bounded to the east by the Netson Lake - Netson Creek valleys and to the west by the Northern Rocky Mountain Trench (Figure 3). The southern boundary is roughly delineated by Brownie Mountain and Netson Lake, and the northern limit coincides with the southern part of Horneline Creek. The region between Terminus and Brownie mountains is characterized by rugged, alpine terrain. This becomes more subdued to the north and east where only the very tops of the hills reach timberline and outcrop density is less than 5 percent.

The Kechika Trough represents a long-lived basin of early to middle Paleozoic age. It connects northward with the Selwyn Basin of the Yukon and Northwest Territories, with which it shares similar stratigraphic and tectonic relationships. The Kechika Trough was delineated through time by 'shale-outs' of shelf and platformal successions. Its stratigraphy is characterized by dark, fine-grained siliciclastics and chert, representing quiet, deeper water deposition. This environment of slow sedimentation coupled with tectonism was conducive to the formation of sedimentary exhalative deposits at various times within the basin. Upper Devonian rocks in the Earn Group are the most economically important within the Kechika Trough and are the focus of the present multidisciplinary study. A more detailed description of the regional setting and related references are given in Ferri *et al.* (1995a). A useful regional overview is provided by MacIntyre (1992).

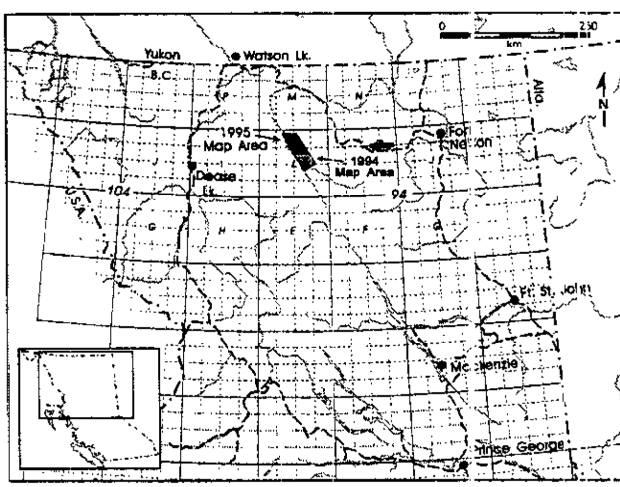


Figure 1: Northeastern British Columbia showing the location of the 1995 and 1994 map areas.

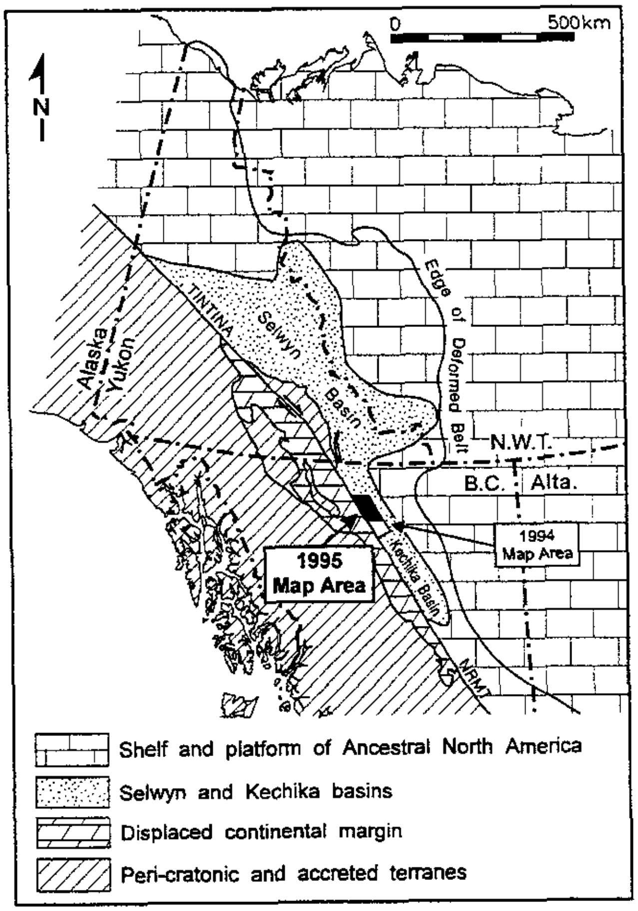


Figure 2: Simplified map of the northern part of the Canadian Cordillera showing the shelf-off-shelf boundary during Ordovician to Silurian time (modified from Cecile and Norford, 1991). NRMT - Northern Rocky Mountain Trench.

## STRATIGRAPHY

The stratigraphy of the map area comprises units ranging in age from Early Cambrian to early Mississippian (Figures 3, 4). These include: Lower to Upper(?) Cambrian siliciclastics, carbonates and volcanics which are, in part, equivalent to the Gog Group; slate, calcareous slate and argillaceous limestone of the Upper Cambrian to Lower Ordovician Kechika Group; siltstone, slate and minor limestone of the Middle Ordovician to Middle Devonian Road River Group, and siltstone and slate of the Middle Devonian to Mississippian Earn Group.

One of the most striking large-scale features in the map area is the lithological and thickness variation exhibited by Cambrian and Ordovician packages. Cambrian thrust panels in the southwest contain thick sequences of shallow-water coarse siliciclastics, carbonates and volcanics which are not present in panels to the northeast, where they are replaced by fine-grained, deep-water siliciclastics. The overlying Kechika Group also changes from thick, calcareous slates and limestone in the southwest to a much thinner package of slates and minor chert in the northeast, which is difficult to distinguish from overlying Road River slates. The coincidence of facies variations in these two units suggests similar stratigraphic and tectonic controls.

## *CAMBRIAN*

Cambrian rocks are exposed in several thrust panels in the map area. By far the thickest and best exposed sections are in the southwest where the rugged range extending from Gataga Mountain to Terminus Mountain consists almost entirely of Cambrian strata (Figures 3,4). Cambrian rocks are also exposed in the east of the map area, on the ridges west of the Netson Creek valley. Thrust panels in the centre of the area consist mainly of younger stratigraphic units, and the Cambrian is present only in relatively narrow zones.

As documented by Ferri *et al.* (1995a, b), the Cambrian in the region is characterized by siliciclastic and carbonate lithological units which interfinger such that the stratigraphy varies within and between thrust panels, making correlation difficult. In the previously mapped area to the southeast, the presence of archaeocyathid fossils in some areas indicates an Early Cambrian age. On this basis these rocks were correlated with the Lower Cambrian Gog Group, the type area of which is in the southern Rocky Mountains, and they were so named. Overlying the Gog Group in many places are either thick carbonates, which were assigned to an unnamed Middle to Upper Cambrian unit, or a thick, coarse polymictic conglomerate which was correlated with very similar deposits in the Rocky Mountains to the east, which have been dated by fossils as Middle Cambrian (Ferri *et al.* 1995a; Fritz, 1991). Where archaeocyathids or these distinctive Middle Cambrian carbonate or conglomerate facies are absent, replaced by ubiquitous sandstone, siltstone and slate, the Cambrian stratigraphy was generally mapped as a composite Cambrian unit, "Gog Group and younger rocks", because the Lower Cambrian could not be differentiated.

The same criteria and terminology are used in the current map area. However, there are two notable features of the Cambrian stratigraphy that differ from that mapped in 1994, the main one being the presence of volcanic and volcaniclastic rocks in the Gataga Mountain area. They occur within a succession, at least 3000 metres thick (base not seen), of fine to coarse-grained, calcareous and noncalcareous siliciclastics, and carbonates (Figure 4, a). The volcanics were recognized by Gabrielse (1962) who tentatively dated them as Devonian to Mississippian, and subsequently revised the age to Middle Ordovician (Gabrielse and Yorath, 1991). However, our work has shown that the volcanics are Cambrian; Early Cambrian

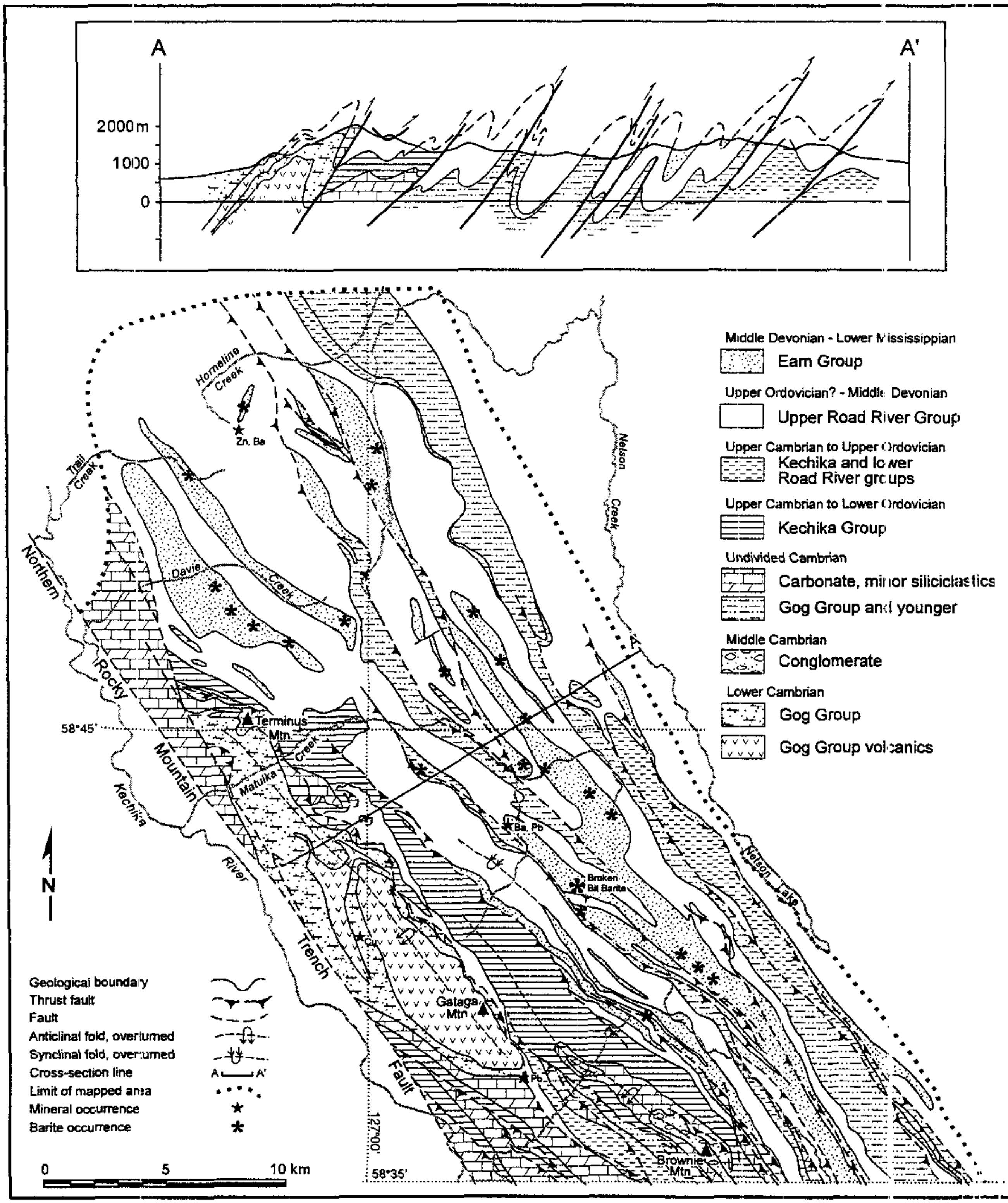


Figure 3: Simplified geological map and cross-section of the study area. The southeastern part of the map, between the south end of Netson Lake and Brownie Mountain, overlaps part of the 1994 field area (Ferri *et al.*, 1995a, b). Note that the cross-section scale is larger than the map scale.

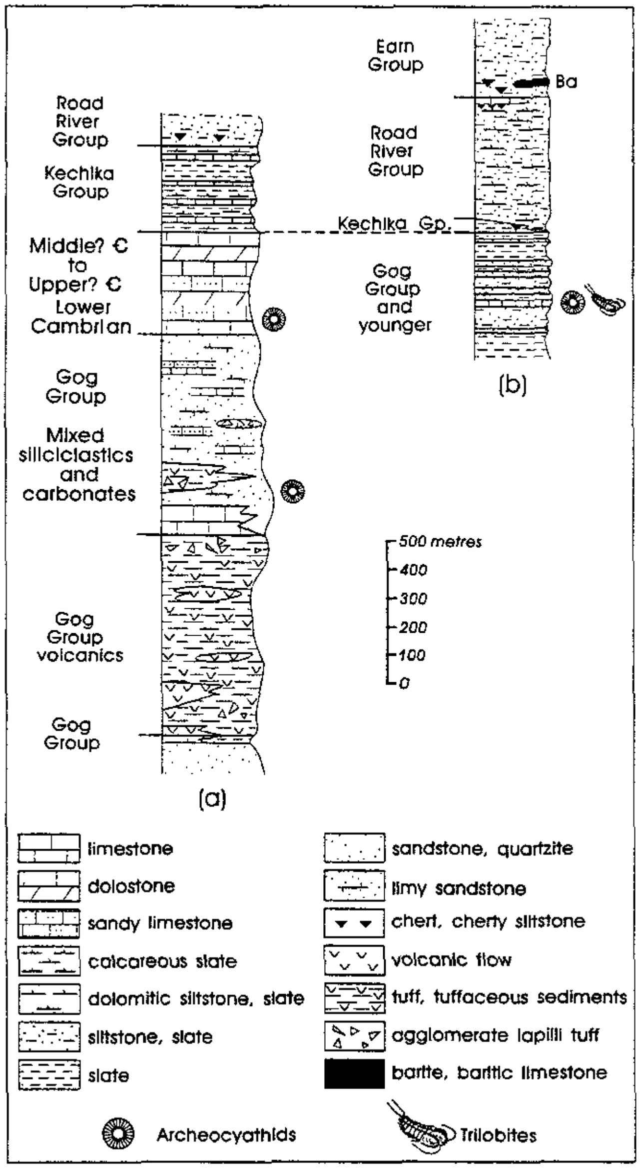


Figure 4: Simplified stratigraphic columns for eastern and western parts of the map area. Section (a) is a composite section of units exposed within the thrust panel in the southwest, containing the Cambrian volcanics. Section (b) represents the eastern and northeastern parts of the map. The two sections show the variation in lithologies and thicknesses of the Cambrian sequence and the Kechika Group. See text for details.

archaeocyathids were found in limestone near the top of the volcanic succession.

Another important difference is that the thick Middle to Upper Cambrian carbonates, mapped to the southeast in 1994, do not appear to continue northwestwards, at least not far beyond the southern edge of the area mapped in 1995. One explanation is that these carbonate build-ups did not accumulate in this part of the miogeocline. Alternatively, they did continue northwards, but are not exposed at the present erosion level, or were eroded in the later Cambrian or Ordovician, before younger rocks were deposited. Evidence for an unconformity at about this time is found in other parts of the map area, where Silurian Road River rocks overlie Lower Cambrian rocks, with little or no intervening Kechika Group or Ordovician Road River (Figure 4, b). More than one of these explanations may apply.

The following sections describe the Cambrian in the map area. The first two deal with the Cambrian stratigraphy in the well exposed Gataga Mountain - Terminus Mountain thrust panel in the southwest, which is dominated by volcanics and relatively coarse grained siliciclastics and carbonates. We believe that this panel is mostly Lower Cambrian, as explained above, with the possibility that the highest limestones may extend into the Middle Cambrian; consequently, it is provisionally assigned to the Gog Group. This is followed by a brief account of Middle and Upper Cambrian conglomerate and carbonates, respectively, which occur in the extreme south of the area. The last section describes the stratigraphy in the central and eastern thrust panels. Some of these rocks contain archaeocyathids locally, and so are partly coeval with the southwestern facies, but they are characterized by slates and siltstones, a paucity of limestone, and the absence of volcanics, indicating that they were deposited in a quite different and probably more basinal environment.

## GOG GROUP: VOLCANIC AND VOLCANICLASTIC ROCKS (LOWER CAMBRIAN)

Volcanic rocks crop out around Gataga Mountain where they form much of a large, complex northeasterly overturned anticline (Photo 1). The core of this fold contains the oldest rocks in the map area, thickly bedded calcareous and noncalcareous quartz sandstones and quartzites. These rocks are overlain by dolostones and limestones followed by slates and siltstones, which grade into the volcanic and volcaniclastic rocks.

Typically, the volcaniclastics comprise pale to mid-green or greenish grey tuffs. Very fine to medium-grained ash tuff and lithic tuff may be massive and homogeneous, or bedded in units up to about 1 metre thick. Some rocks are more thinly bedded or laminated and were mapped as volcanic wacke or tuffaceous siltstone. Grading is not uncommon and crossbedding was tentatively identified in some outcrops. Rarely, lenses of creamy grey chert and calcareous siltstone, or pods of grey limestone, are present within the tuffs. At one locality, the base of the volcanics rests on a dolomitic limestone. Here, the first few metres of tuff are micaceous and pale grey rather than the usual green colour, probably due to carbonate and sericitic alteration at the contact.

Volcanic flows are subordinate, forming about 25% of the volcanic sequence. Some are tens of metres thick. They are usually pale to mid-green and very fine to medium grained. They may be vesicular and

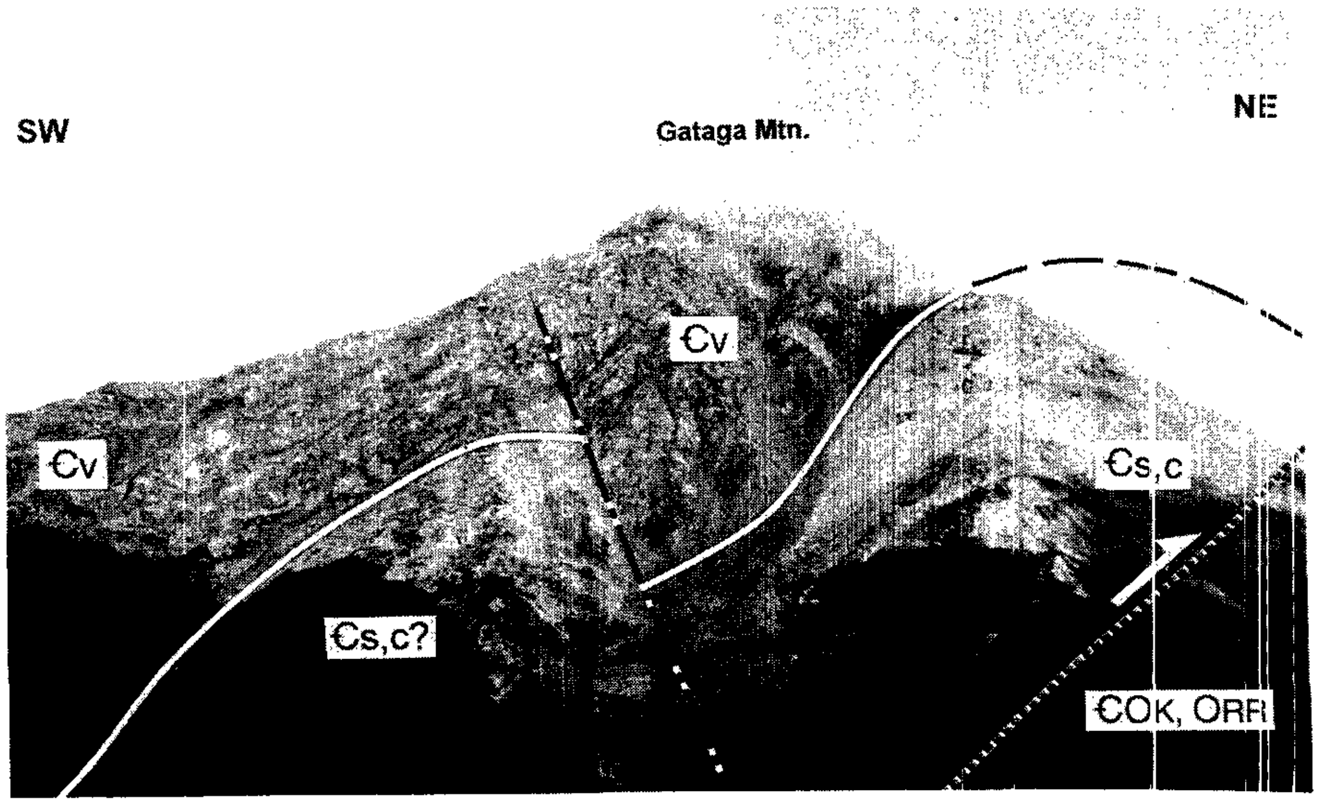


Photo 1: Looking northwest at Gataga Mountain, composed essentially of an anticlinal fold of Lower Cambrian volcanics (Ꞓv) and underlying slate and calcareous and quartzitic rocks (Ꞓs,c). All are correlated with the Gog Group. Thrust at right places the Cambrian on strongly deformed Kechika and Road River group slates (ꞒOK, ORR; *cf.* Photo 9).

amygdaloidal, and some are finely porphyritic. Dark green spots in some volcanic rocks may be chloritized amygdules or pyroxene phenocrysts. Pillows, pillow breccia and flow breccia are fairly common (Photo 2); some pillows are a metre across and many show radiating pipe vesicles and zoning. Preliminary lithogeochemical analysis of the volcanics indicates that they are generally alkalic basalt.

Felsic to intermediate volcanics were mapped in a few localities. The largest body, a few kilometres southeast of Gataga Mountain, consists of pale grey, sericitic and siliceous crystal-lithic dacitic or rhyolitic tuff. It is at least tens of metres thick. A similar but much smaller body on Gataga Mountain itself, is a quartz-feldspar-porphyritic flow or crystal tuff of basaltic andesite composition, with textural features suggesting welding. Both subunits were sampled for radiometric analysis.

One of the most common and distinctive lithologies is a coarse lapilli tuff or agglomerate, which underlies large areas on the slopes west of Gataga Mountain. This rock is generally massive and contains rounded to angular rock fragments in a coarse-grained chloritic or ferro-carbonate clastic matrix (Photo 3). The most common clasts are pale green or buff-grey, and very fine grained, and are thought to be variably altered volcanic rock, possibly carbonatized or sericitized basaltic lava or tuff, although some material may have originally been more felsic. Some are porphyritic. Less commonly, fragments consist of quartzite and siltstone, and rarely limestone. Some clasts are maroon, suggesting partially subaerial sources. The largest clasts are 30 to 40 centimetres across (Photo 4), but most are much smaller. Overall, the deposit is poorly sorted or unsorted. The matrix is grey to green and generally weathers to a grey to rusty orange-brown colour due to the ferroan carbonate. The rock is provisionally interpreted as a volcaniclastic deposit laid

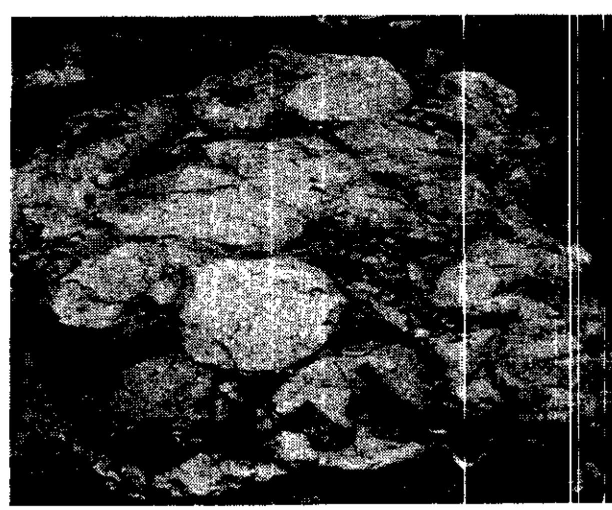

Photo 2: Pillows in the volcanic unit, Lower Cambrian Gog Group, Gataga Mountain.


Photo 3: Lapilli tuff in the volcanic unit, Lower Cambrian Gog Group, northwest of Gataga Mountain. Scale at bottom is 15 centimetres long.

down in a carbonate environment. This is supported by the presence of pods or zones of limestone, orange-brown weathering dolostone, and rusty calcareous siltstone within the agglomerates, as well as in other parts of the volcanic sequence.

Cleavage is variably developed, and is most evident in some of the finer grained, bedded tuffs. A reversal in cleavage-bedding relationships can be mapped across the axial surface of the overturned fold at Gataga Mountain. The matrix of the agglomerates is also well foliated and many clasts are flattened parallel to the fabric.

At least one other lenticular body of volcanics is present slightly higher in this thrust panel. It is similar in composition to the main body, comprising discrete volcanic flows, or possibly sills, up to 4 metres thick, well bedded and laminated tuffaceous wacke and siltstone, and lapilli tuff and agglomerate as described above.

The presence of this volcanic succession in the Cambrian is important. Preliminary observations indicate that the volcanics and their stratigraphic setting are typical of other, rift-related alkalic volcanic sequences documented in the northern Cordilleran miogeocline of British Columbia and Yukon (Goodfellow *et al.*, 1995). These are widespread but sporadically distributed in restricted lenses or piles within the various basinal elements or platform margin of the miogeocline, and range in age from Late Proterozoic to Devonian. Many of the volcanic sequences are characterized by high barium, and are associated with abrupt facies changes in surrounding sedimentary rocks, suggesting "a genetic link between extensional tectonism, magmatism, hydrothermal activity, and the formation of Zn-Pb-barite deposits found in many locations in the Northern Cordillera" (Goodfellow *et al.*, 1995).

## GOG GROUP: SILICICLASTICS AND CARBONATES (LOWER CAMBRIAN)

The volcanic subunits form fairly distinct facies in the Cambrian in the Gataga Mountain area. In contrast, the underlying and overlying Cambrian strata in this thrust panel are typical of the region, being predominantly moderately to well bedded siliceous sediments and carbonates with little or no evidence of volcanism. As mentioned earlier, the oldest rocks, below the lower

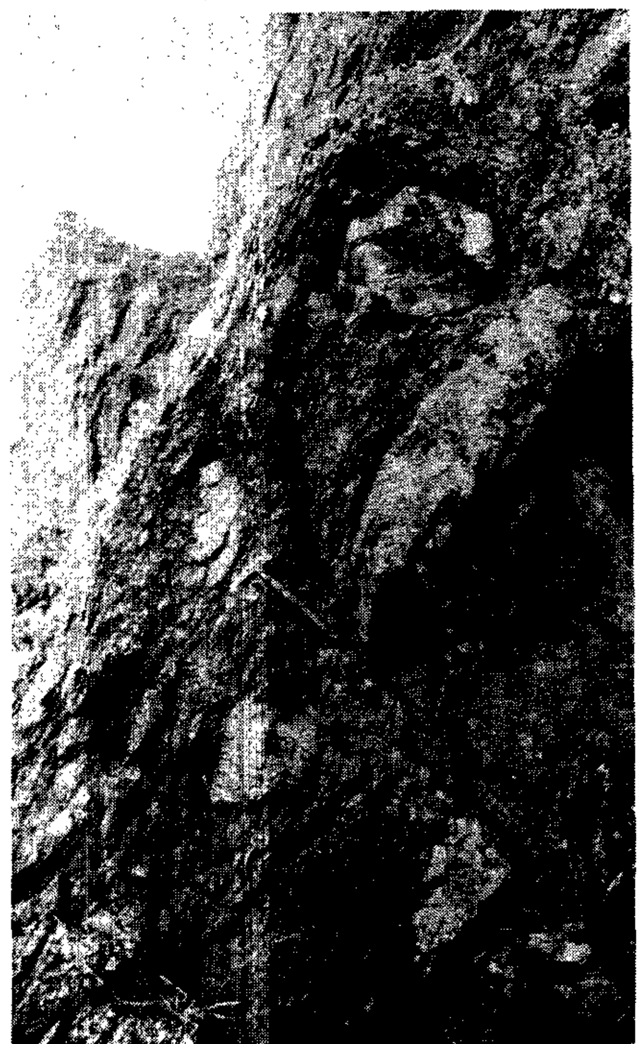
Photo 4: Agglomerate in the volcanic unit, Lower Cambrian Gog Group, northwest of Gataga Mountain. Looking northwest; cleavage dips steeply to southwest.

volcanics, are quartzite, quartz sandstone, dolomitic sandstone, dolostone and limestone. These quartzose rocks are moderately to thickly bedded, and have round sand grains, grading, cross-stratification and ripple laminations. A few metres of grey to greenish slate, cherty slate and siltstone, with minor dolomitic nodules and lenses, are exposed at the top of the section, just below the base of the volcanics.

Above the lower volcanics, the rest of the Cambrian is a mixed succession of sandstone and quartzite (partly limy), limestone and dolostone, and lesser slate and siltstone. The coarser siliciclastics are generally well bedded on a scale of centimetres to decimetres, and some beds show grading, well developed 'herringbone' crossbedding (Photo 5) and, rarely, ripple marks and trace fossils such as worm trails and burrows. Quartzites and quartz sandstones are pale grey to pink or beige, and are more thickly bedded to massive. They are locally calcareous, especially close to limestone. Intervals of platy limestone to limy sandstone are common, forming beds or a series of beds within the siliciclastics. Slate and siltstone are generally subordinate, comprising thin interbeds in the other rocks. Quartz-pebble conglomerate is found interbedded with grey to maroon limestone, sandstone and siltstone at one locality.

A substantial thickness of grey to buff, pale orange-brown weathering dolostone and limestone is exposed just above the lower volcanics on the slopes west of Gataga Mountain. It is fine to medium grained with a sugary crystalline texture, and is somewhat siliceous. These rocks are overlain by a conspicuous unit of well bedded and laminated, maroon siltstone to sandstone, slate and minor tuffaceous interbeds, with a maximum thickness of about 100 metres. The sediments alternate in colour between maroon and a pale yellowish green. The smaller, thinner volcanic unit, referred to in the previous section, overlies these varicoloured siltstones.

This limestone-dolostone, maroon siltstone and thin volcanic sequence appears to pinch out to the northeast within this thrust sheet, replaced by the prevailing mixed siliciclastic and carbonate lithologies, much of which have the striking maroon colour of the previously described siltstones. An unusual conglomerate is mapped at about this stratigraphic level or possibly higher: it is composed almost entirely of well rounded, pebble to cobble-sized clasts of grey or cream-coloured limestone or sandy limestone up to 15 centimetres across, with a few pebbles of maroon siltstone or grey-black chert. It is up to 10 metres thick, well sorted and clast supported, and has a brownish maroon, sandy carbonate matrix.

Lying above all these rocks, the stratigraphically highest rocks in this thrust sheet are thick limestones and lesser dolostones, well exposed north and south of Matulka Creek, particularly at the top of Terminus Mountain. The limestone is generally pale to medium grey and buff-grey, very fine to medium grained and more homogeneous and massive than those lower in the

Photo 5: Herringbone crossbedding in limy quartzite, Lower Cambrian Gog Group, northwest of Gataga Mountain.

stratigraphy which are interbedded with the siliciclastics; however, it is not as uniform as the thick Middle to Upper Cambrian carbonates exposed in the 1994 map area to the southeast. Bedding is generally indistinct, although locally the limestone is sandy and oolitic, or has argillaceous laminae, and bedding is more clearly defined. Dolostone to sandy dolostone is fairly common and weathers pale orange-brown. A few beds of limestone rich in dark grey to black oncolites up to 4 centimetres across were noted. Archaeocyathids were found in limestone near the base of these carbonates, high on the slopes on both sides of Matulka Creek. It is possible that some of the overlying limestones straddle the Lower-Middle Cambrian boundary.

The northeastern boundary of this thrust panel is a thrust fault, placing Cambrian limestone structurally on top of Kechika or Road River Group rocks. The limestone at the contact is locally very well foliated, with a streaky translucent appearance indicative of a very fine grain size produced by a high degree of ductile strain.

## CONGLOMERATE AND LIMESTONE (MIDDLE AND UPPER CAMBRIAN)

The core of an overturned anticlinal fold in the south of the map area consists of conglomerate overlain by thick limestone and dolostone, believed to be of Middle and Late Cambrian age, respectively. Both map units are the same as those mapped on Brownie Mountain in 1994 (Ferri *et al.* 1995a, b). The conglomerate is massive, matrix supported and polymictic, containing well rounded granule to boulder-sized clasts of mainly quartzite, and lesser, subequal amounts of limestone, siltstone and volcanics. Much of the matrix is green and chloritic, and we speculate that much of it is tuffaceous, implying that the conglomerate was derived from the erosion of volcanic as well as sedimentary rocks.

The conglomerate is overlain by pale to medium grey, very fine grained and variably foliated limestone, dolomitic limestone and dolostone. The carbonates are generally massive and fairly 'clean'. Unlike the Lower Cambrian carbonates described earlier, thin beds of sandy limestone or limy sandstone are relatively uncommon. Quartz-carbonate veins with malachite are a feature of these rocks.

## GOG GROUP AND YOUNGER: SLATES AND SILTSTONES, EASTERN FACIES (UNDIVIDED CAMBRIAN)

Cambrian strata outcrop in a continuous belt west of the Netson Creek valley, and in several narrower belts in the centre of the map area, in the cores of anticlinal folds or along the base of thrust panels. These rocks are dominated by noncalcareous slate, slaty siltstone and sandstone, with only minor quartzite and limestone. Slate and slaty siltstone are usually medium to dark grey to olive green, and locally have thin colour laminations. The rocks are fine grained, although laminae of paler grey coarse siltstone or sandstone are quite common. Medium-grained flakes of mica are readily visible on some cleavage surfaces, which weather a rusty brown colour. These micas, the sandy laminae, and worm trails on some surfaces are useful features distinguishing these slates from the slates of other units in the region.

Where sandstone is present it generally forms intervals or interbeds within the slates. It is pale to dark grey, medium grained, micaceous and locally feldspathic, and usually forms well and thinly bedded (1 to 10 cm) outcrops with flaggy to platy partings. Bedding planes are commonly undulose, suggesting rippled surfaces. Locally, larger bodies or beds of white to grey quartzite or feldspathic quartzite are associated with the sandstones and slates. Rarely, thin beds of oolitic or argillaceous limestone are present.

Very locally there are lenses of grey or pale orange weathering, archaeocyathid-rich limestone in the slates. They measure from less than a metre to tens of metres in length, and have a 'rough' or rubbly texture. They represent small biohermal build-ups, and may contain fragments of large trilobites as well as archaeocyathids. One such fauna is identified as late Early Cambrian (B.S. Norford, personal communication, 1995).

Overall, the Cambrian lithologies in the eastern half of the map area are much more pelitic and finer grained, and much less calcareous than those in the major Cambrian thrust panel in the southwest. Restoring the thrust shortening would probably result in a considerable separation between the two depositional environments. A preliminary interpretation of these observations is that the southwestern Cambrian facies represents a relatively shallow marine to intertidal setting, with sedimentation fluctuating between coarse siliciclastic and carbonate deposition, resulting in interfingering lithological units. This may have been due to periodic fault-controlled extension, uplift and subsidence, which was probably related to episodes of submarine alkalic basaltic volcanism. In contrast, the contemporaneous sedimentation represented by the Cambrian rocks farther east probably took place in deeper water and more uniform conditions.

## *KECHIKA GROUP (UPPER CAMBRIAN TO LOWER ORDOVICIAN)*

The Kechika Group exhibits a marked facies change and thinning from southwest to northeast within the map area. This transition is quite abrupt and roughly corresponds to the disappearance of the underlying thick sequences of Lower to Upper(?) Cambrian limestone and quartzite. In the southern part of the map area, the Kechika Group is characterized by interlayered grey to dark grey soft slate, calcareous slate or rare silty slate and grey, buff or orange-weathering, very finely crystalline limestone or dolostone. The carbonate layers are discontinuous to lenticular and typically 0.1 to 2 centimetre thick, although they reach several metres in thickness locally. They comprise up to 50% of the section with an average of 20%. This facies is exposed above thrust panels of Cambrian limestone west of Gataga Mountain and can be traced along the footwall of the thrust carrying the Cambrian volcanic succession from the Brownie Mountain area northward to just northwest of Terminus Mountain. The northernmost outcrop area of this lithology is on the lower slopes of the Rocky Mountain Trench immediately north of Davie Creek and is characterized by banded to mottled, orange to brown-weathering, grey to dark grey calcareous slate to silty slate. This facies of the Kechika Group covers a wide area in its southern trace, reflecting the northward plunge of the large northeast-verging anticline outlined by thick Cambrian carbonates along the ridge containing Brownie Mountain (Figure 3). Kechika rocks also cover a large area along the lower reaches of Matulka Creek. The thickness of Kechika slates and carbonates is difficult to determine due to their strong deformation. Structural sections suggest upwards of 500 metres of Kechika rocks immediately south of Matulka Creek.

The calcareous nature of the Kechika Group is lost up-section and the upper half or one-third is characterized by grey to dark grey or black, blocky to shiny fissile slate, with characteristic faint discontinuous, paler grey laminae (Figure 4, a). Thin, discontinuous or lensoidal beds of finely crystalline limestone are occasionally present in the lower part of this sequence. Sections of dark grey banded slate up to 100 metres thick, within typical calcareous sections of Kechika slates west of the Gataga Mountain, are probably infolded sequences of lower and upper Kechika Group. These upper slates are difficult to differentiate from Ordovician Road River slates and have been grouped with them over most of the map area (see below).

East of the headwaters of Matulka Creek the pale coloured and soft calcareous facies of the Kechika Group is recognized in only a few localities. Interlayered grey to buff-weathering, thin limestone and slate or calcareous slate are found along the top of the first ridge northwest of Netson Lake. These lithologies are exposed near the base of a sequence which passes upward through dark grey to black slate into black graptolitic slates of the Road River Group. This section appears to be several hundred metres thick. Elsewhere in the central and northern parts of the map area, calcareous Kechika rocks are uncommon, replaced by a thin section of dark grey or black slate (Figure 4, b).

No macrofossils were found in the Kechika Group within the map area during the course of the summer. Macrofossils (Ferri *et al., 1995*a, b) and conodonts collected during the 1994 field season suggest a Cambrian to Early Ordovician age (Arenig; B.S. Norford, personal communication, 1994; M. J. Orchard, personal communication, 1995). Fossil collections elsewhere in the Northern Rocky Mountains suggest a latest Cambrian to Early Ordovician age (Cecile and Norford, 1979).

## *KECHIKA - LOWER ROAD RIVER GROUPS (UPPER CAMBRIAN TO MIDDLE ORDOVICIAN)*

In the central and eastern parts of the map area, dolomitic siltstones of the upper Road River Group are sometimes separated from Cambrian siliciclastics by a relatively thin section of blocky to fissile, dark grey to black slate to siliceous slate (Figure 4, b). Structural sections suggest thicknesses of, at the most, 100 metres. In many parts of the map area the proximity of Road River siltstones to Cambrian siliciclastics leaves little room for intervening slates of either the lower Road River or Kechika groups. It is difficult to determine whether the apparent absence of slaty lithologies at this horizon reflects non-deposition or poor exposure of this relatively thin section of recessive slates.

This package of slates has more affinities with the Ordovician Road River Group than with the Kechika Group. It is best developed on the west side of the Netson Creek valley where there are poor creek exposures of grey to brown-weathering, grey to dark grey or black, shiny slates. These slates are locally quite soft and fissile. Faint, paler grey colour banding or laminations are common and sometimes grade into more silty horizons with the characteristic mottling of the overlying Road River siltstones. Some outcrops contain sections of sooty black, slaty siltstone. This unit is sometimes characterized by dark grey to black siliceous argillite or slate with 1 to 3-centimetre beds of grey to black chert.

Dark grey banded slates pass downward into typical soft, light coloured calcareous slates and interlayered limestones of the Kechika Group along the southern part of the ridge immediately west of the north end of Netson Lake. This unit is in excess of several hundred metres thick and is exposed within the core of a northerly plunging anticline. Graptolitic black slates, typical of the Ordovician Road River Group, crop out along the east flank of this anticline just before outcrop is lost towards Netson Lake. These slates are markedly thinner in the next thrust panel to the west where exposures of older and younger units suggest less than 50 metres of section. Extensive exposures of light coloured Kechika slates to the east, across the Netson valley (Gabrielse, 1962), indicate eastward thickening of Kechika and Road River slates.

Only one macrofossil (graptolite) collection was made from this unit, in the southeastern portion of the map area; it is interpreted as Early Ordovician (B.S. Norford, personal communication, 1995).

The lack of identifiable Kechika and Ordovician Road River rocks in the central and northeastern parts of the map area may reflect either negligible thickness or a sub-Silurian Road River unconformity. Underlying Cambrian rocks also undergo a transition within the map area, changing from carbonate and siliciclastics in the south and west, to dominantly pelitic rocks in the north and east. It is not clear if all these stratigraphic features are related, but their coincidence does suggest that this part of the basin was subject to tectonic instability in the Cambrian and Ordovician, leading to marked facies changes and thinning or erosion of stratigraphy. Sub-Lower Silurian erosion or non-deposition has been postulated for the northern Kechika Trough region by Cecile and Norford (1991), and significant lower Paleozoic unconformities have been demonstrated in the Tuchodi Lakes map area immediately to the east (Taylor and Stott, 1973).

## *ROAD RIVER GROUP (ORDOVICIAN TO MIDDLE DEVONIAN)*

Two units of the Road River Group are recognized in the map area: a lower succession of Ordovician black slates with lesser limestone and chert, and a succeeding section of Siluro-Devonian dolomitic siltstone and minor limestone and chert. True sections of Ordovician Road River Group were recognized in only a few localities; elsewhere the group is represented by the dolomitic siltstone unit.

## ORDOVICIAN

Black to blue-grey weathering, black to dark grey shiny slate to siltstone is the dominant lithology of the lower Road River Group. The slate is typically soft and friable although zones of cherty slate or argillite were observed locally. Slaty sections may contain thin, paler grey bands or laminations. Siltstone is graded and intercalated with beds of buff to orange-weathering calcareous slate to silty limestone or dolostone up to 3 centimetres in thickness. These carbonate horizons locally contain tiny (0.1 to 5 mm) authigenic barite crystals. Thin (1 to 2 cm) sandstone beds were observed very locally.

Slates that can be confidently assigned to this unit are known in only a few localities in the east-central part of the map area. Ordovician black slate is structurally interleaved or folded with Road River siltstone and Kechika slate immediately east of Gataga Mountain in the footwall of the thrust carrying Cambrian volcanics and sediments. This structural imbrication becomes less complicated some 5 kilometres to the northwest where 50 to 75 metres of Ordovician black slates, siltstones and carbonates are found between Kechika slates and Road River siltstones in the immediate footwall of this thrust fault. Ordovician slates with interbeds of baritic limestone are found in the centre of the map area, approximately 2 kilometres south of the first big bend in Matulka Creek, along a creek cutting the western overturned limb of a syncline. This section appears to be several hundred metres thick, although this is probably the result of structural thickening.

Elsewhere it is difficult to separate slates of the Ordovician Road River from those of the Kechika Group and they have been grouped together in many cases (see previous section). The weathering characteristics and overall lithology of these slates and siltstones can also be very similar to those of the Earn Group, making it difficult to differentiate between them, especially in isolated outcrops. This is particularly true in the low-relief area east and northeast of Brownie Mountain where a series of tight folds and related faults repeat Road River dolomitic siltstone and Earn Group lithologies. It is quite possible that some of these poorly exposed 'Earn' lithologies could be misrepresented Ordovician Road River Group.

Two graptolite collections were made over the course of the summer's mapping. Both indicate an Early Ordovician age (Tremadoc to Arenig). One collection 2 kilometres west of Terminus Mountain originates from the lowermost part of the Ordovician Road River, approximately 1 metre above its lower contact, and contains early to middle Arenig graptolites (*T. akzharensis* Zone, *P. fruticosus* Zone or possibly lower part of *D. bifudus* Zone; B.S. Norford, personal communication, 1995). Conodont and graptolite collections from the 1994 field season suggest a Middle to Late Ordovician age (Ferri *et al.*, 1995a, b; B.S. Norford, personal communication, 1994; M.J. Orchard, personal communication, 1995).

## SILURO-DEVONIAN ('SILURIAN SILTSTONE')

Buff-brown to orange-weathering, grey to greenish grey siltstone to dolomitic siltstone of the Siluro-Devonian Road River Group is areally the most extensive lithology in the map area. It covers over 60% of the northern half of the map sheet but is largely confined to the central and eastern parts of the southern half, except for narrow zones in the immediate footwall of the thrust carrying the Cambrian volcanics and sediments. It is relatively competent compared to the other basinal facies in the area and tends to form the ridges in the more subdued terrain east and north of Matulka Creek. The transition with the underlying Ordovician slates was not observed within the map area, although upper parts of the Ordovician slate sequence contain paler grey slate to silty slate bands which become thicker and more silty up-section and exhibit a mottling typical of the overlying siltstones. This suggests a transitional contact, as mapped in the Gataga River area to the southeast (Ferri *et al.*, 1995a).

The dominant siltstone lithology is thin to thickly bedded or massive. In many outcrops bedding is discerned by subtle colour variations reflecting changes in argillaceous or dolomite content (Photo 6). It is commonly bioturbated, producing a mottled or wispy texture due to the disruption of laminae, which makes recognition of bedding difficult. Partings are typically blocky, although, in the absence of bioturbation, the relatively planar stratification produces platy to flaggy outcrops. Several trace fossils were observed. The most common type is a series of overlapping, oval, dish-like impressions on bedding surfaces, tentatively identified as *Zoophycus*. They are open at one end, marked by concentric ridges, and up to tens of centimetres wide (Photo 7). Less common are worm casts, 0.5 to 1 centimetre thick, either inclined or perpendicular to bedding. Sediment infills of these tubes or burrows are concave up and are a useful tops indicator where visible in cross-section.

Siltstone is locally quite argillaceous and is grey to dark grey in colour and much more slaty. Sections of grey, nondescript slate to silty slate, over a hundred metres thick, are common within this succession, and are similar to those mapped in 1994 to the south (Ferri *et al.*, 1995a). These slaty lithologies are generally not dolomitic, making identification uncertain. Buff-weathering, grey, wavy laminated to thinly layered limestone locally forms metre-thick sections within this unit in the northern part of the map area.

The top of the siltstone section is locally marked by a limestone-chert couplet from 5 to over 20 metres in

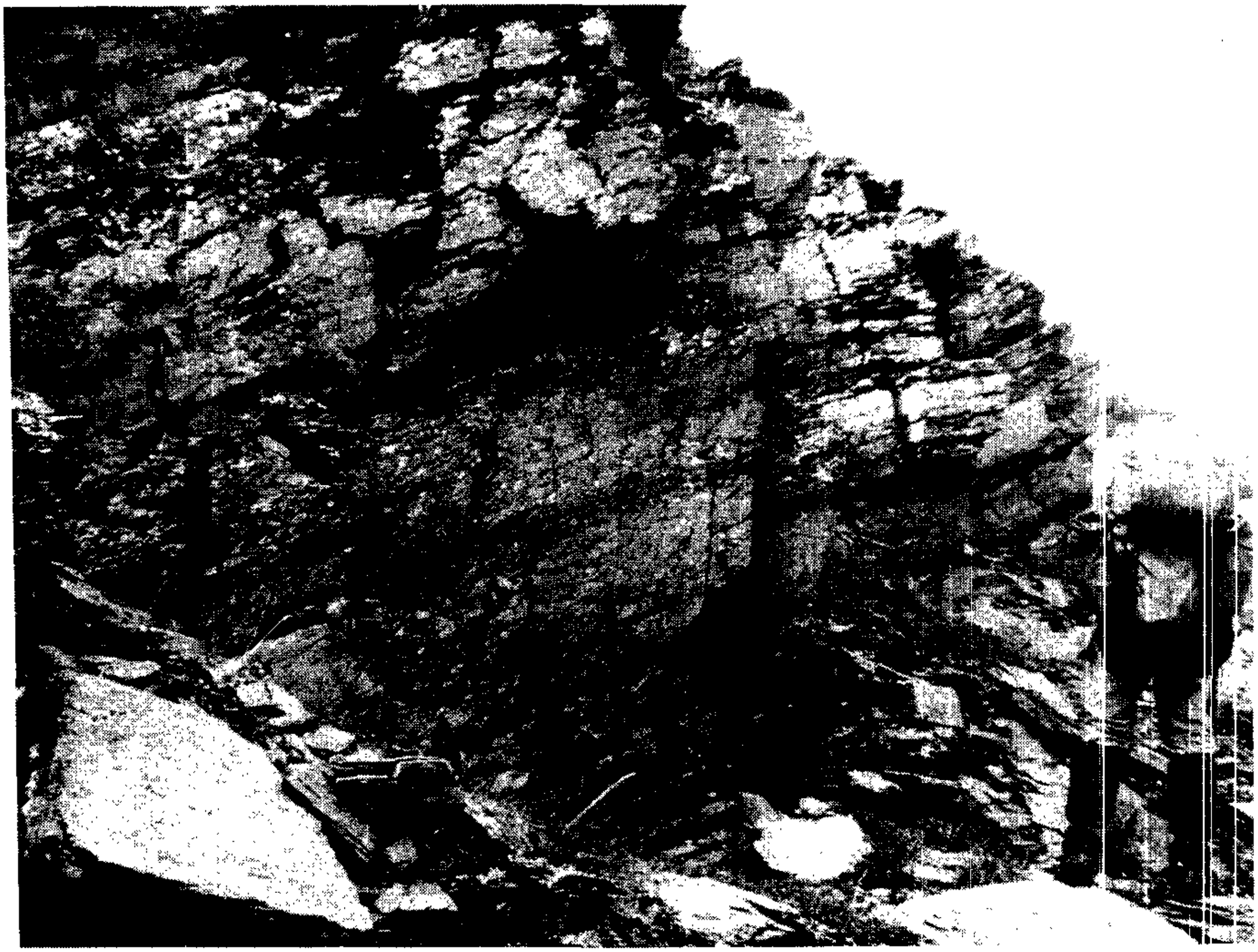

Photo 6: Typical exposure of well cleaved dolomitic siltstone and slate of the Siluro-Devonian Road River Group. Bedding is shown by subtle variations in colour or shade; elsewhere it is often obscure due to bioturbation.

thickness. These subunits are best developed in the northern and eastern parts of the map area. In many localities this unit is overlain immediately by siltstones and slates of the Earn Group. This, together with its distinctive character, makes it an excellent marker unit within the map area.

The limestone is micritic and dolomitic, grey to buff weathering, dark grey to grey-brown, and is up to 20 metres thick. It commonly displays faint laminar bedding traces and breaks into blocky or platy pieces from 1 to 20 centimetres thick. It is locally argillaceous and has a slight fetid odour on breakage. The limestone also contains 1 to 5-centimetre interbeds of argillite to cherty argillite, similar to the overlying chert member.

Chert to argillaceous chert, up to 2 metres thick, is typically found above the limestone, although they are interlayered in some localities. Chert is pale grey to black, orange-brown to maroon in colour. Bedding is planar to very poorly developed, with beds ranging from 1 to 50 centimetres thick. This unit is commonly shot through with tiny quartz veinlets and has blocky to platy partings.

This limestone-chert succession is at the same stratigraphic level and bears some lithologic similarities to a limestone-chert succession described in the Gataga River area (Ferri *et al.*, 1995a) although there, the limestone apparently overlies the chert.

The thickness of the siltstone member of the Road River Group varies significantly over the map area. No sections were measured, but structural interpretations indicate thicknesses ranging from 200 metres in the southeast to possibly 1000 metres in the north. The large expanse of Road River siltstone in the northern half of the map area may reflect this increased thickness, together with the effect of low-amplitude folding and moderate faulting. The stratigraphy may be more complicated in detail, however. At one locality south of Horneline Creek, Earn lithologies rest in apparent disconformity above Cambrian siliciclastics, suggesting either non-deposition of the Road River Group or a substantial pre-Earn unconformity.

No macrofossils were found in this unit during the 1995 field season. Collections made during the 1994 season, together with conodonts recovered in the Gataga River area, suggest a Late Ordovician to Middle Devonian age. Early Silurian graptolites (Wenlock, possibly late Llandovery; B.S. Norford, personal communication, 1994) were collected from the middle of the unit in the Gataga River area (Ferri *et al.*, 1995a). Late

Photo 7: Common type of trace fossil in dolomitic siltstone of Siluro-Devonian Road River Group, found on bedding surfaces. Tentatively identified as *Zoophycus*.

Ordovician to Silurian conodonts were also recovered from nearby dolomitic limestones (M.J. Orchard, personal communication, 1995). Limestone from the limestone-chert couplet, only a few metres below the contact with the Earn Group, just south of Bluff Creek contains late Early Devonian (Emsian) conodonts (M.J. Orchard, personal communication, 1995). Middle Devonian (early? Eifelian) conodonts were collected along the east side of the Kechika River from grey to dark grey, fetid and partly oolitic limestone interlayered with dark grey to black argillite to siliceous argillite originally mapped as Ordovician Road River Group (M.J. Orchard, personal communication, 1995; Ferri *et al.*, 1995b). These rocks may represent deeper water equivalents of Akie and Pesika reefs seen in the southern Kechika Trough (MacIntyre, 1992).

## *EARN GROUP (MIDDLE DEVONIAN TO LOWER MISSISSIPPIAN)*

Earn Group slates, siltstones and minor carbonates are the youngest rocks recognized within the map area. They are primarily confined to the low-relief region along the central axis of the map, although they also outcrop along the northeast-facing slopes overlooking the Netson Creek valley and along the lower parts of Davie Creek. These comparatively recessive lithologies are best exposed along creeks; a particularly good section occurs along a north-flowing tributary of Davie Creek, about 5 kilometres north of Terminus Mountain. Stratigraphic thicknesses are difficult to determine, but structural sections suggest at least several hundred metres are present in thrust panels and folds in the eastern and northwestern parts of the map area. The contact between Road River and Earn rocks was observed in only one locality, along the western limb of an easterly overturned syncline approximately 1 kilometre upstream from the mouth of the large creek flowing west into Matulka Creek. The limestone-chert marker is not developed at this locality, and dolomitic siltstones of the Road River Group are abruptly succeeded by slates and siltstones of the Earn Group.

Most of the Earn Group in the map area is dark grey to blue-grey-weathering, dark grey to black, sooty to siliceous slate, argillite to cherty argillite or chert with lesser silty slate to siltstone or cherty siltstone. Beds in the argillaceous to cherty rock types are from 1 to 20 centimetres thick. Slate is quite fissile to splintery, and very locally contains nodules of radiating barite crystals up to several centimetres in diameter. Grey to dark grey weathering, grey to black argillaceous limestone is rare; it is nodular to well bedded (beds 1 to 30 cm) in sections up to 2 metres thick. Bedded barite up to several metres thick occurs at numerous localities within the Earn Group; it is commonly calcareous and grades into silty baritic

Photo 8: Massive barite with nodules of black chert, in Earn Group.

limestone. The limestone and baritic units sometimes have thin interlayers, lenses or nodules of dark grey to black chert (Photo 8). Barite is also associated with finely laminated, grey to dark grey siltstone or mudstone of possible turbiditic origin, in the southeastern part of the map area.

The predominant, fine-grained and siliceous Earn lithologies are similar to the Gunsteel facies of the Earn Group described in the southern Kechika Trough by MacIntyre (1992). Local, less siliceous slate to silty slate and siltstone in the upper parts of Earn sections may be equivalent to MacIntyre's Akie facies. Coarser siliciclastics were mapped in the Earn Group locally, such as those exposed along a steep-sided, north-flowing tributary of Davie Creek. This section consists of interlayered, finely laminated to crosslaminated brown to buff-weathering, grey siltstone to very fine grained sandstone and dark grey to black fissile slate, up to 10 metres thick. Siltstone/sandstone horizons are 0.1 to 30 centimetres thick and are faintly micaceous on bedding surfaces. These coarser lithologies may be distal tongues of the Warneford facies which, in the southern Kechika Trough, represents westerly derived clastics in the upper part of the Earn (MacIntyre, 1992).

No fossils have been recovered from the Earn Group within the map area. Conodont collections from the southern Kechika Trough indicate that the base of the Earn Group is late Givetian in age (late Middle Devonian) and that syngenetic mineralization is Frasnian to Famennian (Late Devonian; MacIntyre, 1992; Irwin, 1990; S. Paradis and J. Nelson, personal communication, 1995).

## STRUCTURE

The structure of the area is characterized by moderate to very tight, northeasterly overturned folds and northeast-verging thrust faults, typical of the western parts of the Rocky Mountain fold and thrust belt. The thrusts and axial surface traces trend consistently northwest, and most are moderately to steeply dipping. Bedding dips to the southwest in general, but rotates to subhorizontal and northeast dips in fold hinge zones. Cleavage is well developed in argillaceous lithologies and dips moderately to steeply southwest. Folding and thrusting are intimately related; most thrusts carry detached anticlines, generally with overturned strata in the hangingwall.

A few major and numerous minor thrusts control the map pattern. Many of these structures are clearly continuations of those mapped last year (Ferri *et al.* 1995b). One large thrust panel in the southwest of the area is composed of a thick succession of Cambrian rocks, forming a northeasterly overturned anticline, at least 4 kilometres wide (Figure 3). For the most part, it structurally overlies strongly folded Ordovician and Siluro-Devonian Road River rocks, west of an unusually broad belt of Kechika slates and limestone (Photo 9) The anomalous width of the Kechika here is due to structural thickening in the hinge zone of another large, northeast-verging anticlinal fold. Elsewhere, the incompetent Kechika generally outcrops in only narrow zones; in part, this is because of its tendency to be attenuated or form detachment horizons during this style of deformation, but another factor is an apparent thinning of the unit towards the north of the map area.

The structure in the footwall of the thrust sheet in the southwest is particularly complicated southeast of Matulka Creek. Isolated knobs 1 or 2 kilometres east of the thrust are actually klippen of grey to white Cambrian limestone, resting on Silurian Road River siltstone. It is unlikely that they are remnants of the main thrust sheet, as this would require the existence of a large nappe, which was later tightly folded. The preferred explanation is that they are remnants of another thrust panel or horse that formed beneath the main thrust. They both have the same footwall. The limestone in the klippen is more typical of the Middle and Upper Cambrian than of the Lower Cambrian that forms the main thrust sheet.

Most of the rest of the map area, to the north and east, is underlain by Siluro-Devonian Road River siltstone, and Earn slates (Figure 3). The outcrop area of the Road River Group widens northwards. This may simply be due to an increase in thickness, but it may, at least partly, be the effect of more gentle folding and fewer, smaller thrust ramps in this area. Bedding dips are indeed moderate and strikes are variable. If this interpretation is correct, the reason for the change in deformation style northwards may be the conjectured decline in this direction of thick carbonates in the underlying Cambrian; the absence or thinning of the latter might have inhibited the formation of larger fault ramps during thrusting, allowing thrust sheets to develop a more gently undulose form.

The Earn Group is also moderately folded and outcrop belts are generally wider than in the 1994 map area to the southeast. Some outcrop belts of Earn are probably synclinal infolds within a single thrust sheet, rather than separate thrust repetitions. Narrow, alternating belts of Earn and Road River rocks about 7 kilometres east of Gataga Mountain are probably the result of a combination of tight folding and local thrust imbrication.

## ECONOMIC GEOLOGY

The Kechika and Selwyn basins in British Columbia and Yukon Territory, respectively, define a metallogenic province which contains economically significant sedimentary exhalative Pb-Zn-Ba deposits. They occur at several stratigraphic horizons within the basins and

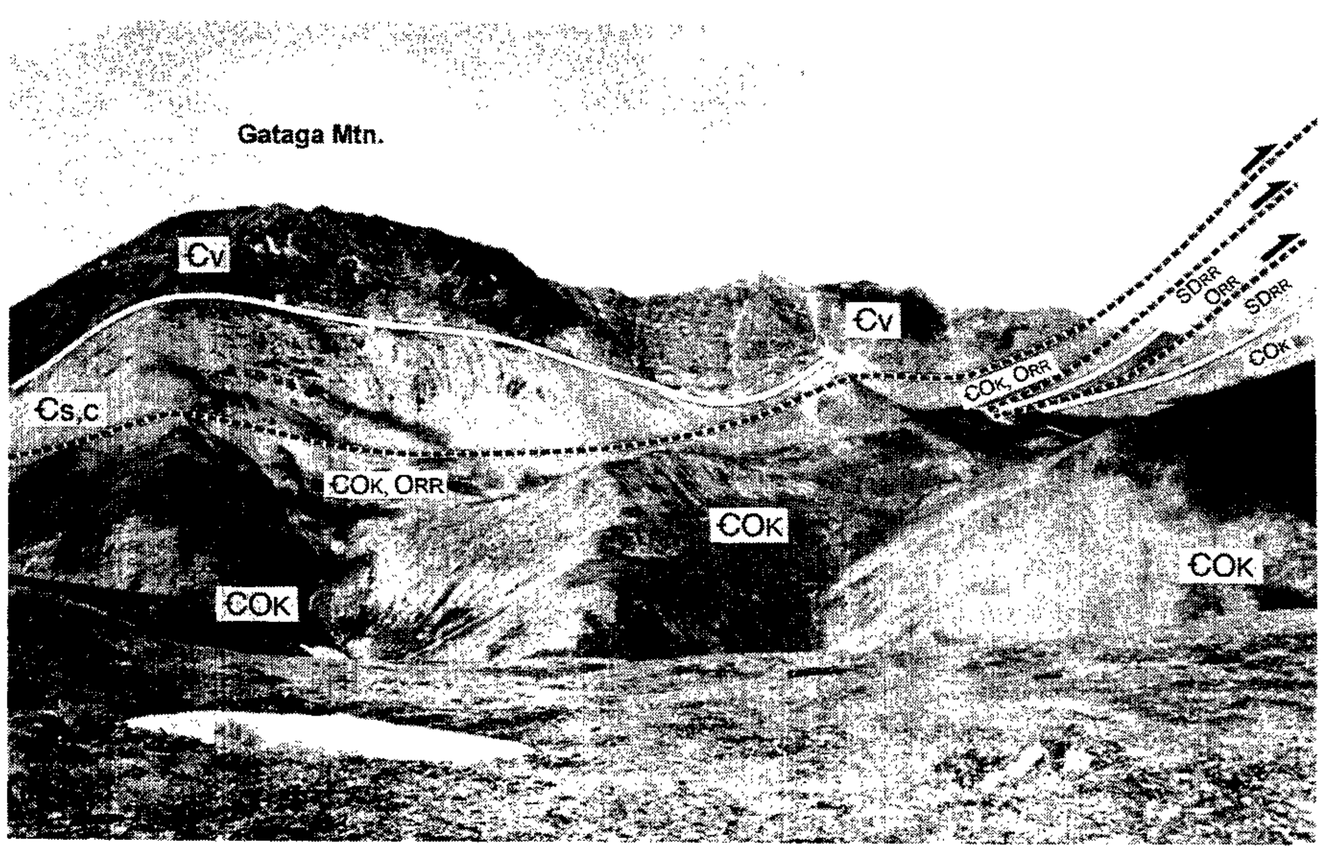


Photo 9: Looking west towards Gataga Mountain, at the leading edge of major Cambrian thrust panel. The hangingwall is a truncated, northeasterly verging anticline (*cf.* Photo 1) comprising volcanics (Ꞓv) overlying quartzites and carbonates (Ꞓs,c) which pinch out northwestwards (to right). Two thin thrust sheets lie in the footwall, in the distance at right, consisting of Kechika (ꞒOK) and Road River (ORR, SDRR) rocks. They appear to die out southeastwards into a zone of highly deformed slates of the Kechika and Ordovician Road River groups (ꞒOK, ORR) at the foot of Gataga Mountain. Tightly folded Kechika Group (ꞒOK) extends from there to the observer.

include the Cambro-Ordovician Anvil mineral district, the Silurian Howard's Pass deposits, and the important Devonian deposits in the MacMillan Pass and Gataga districts (Abbott *et al.*, 1986). Sulphide and barite occurrences of probable sedimentary exhalative origin also occur in the Ordovician (MacIntyre, 1992).

Mapping over the course of the summer located numerous stratiform barite occurrences, nearly all of them in the Devono-Mississippian Earn Group. Other significant mineral occurrences include a zone of lead-rich veinlets in Earn rocks, and a previously known zinc and barite rich, crosscutting breccia in chert and limestone of the uppermost Road River Group. Minor mineral occurrences were noted in Cambrian rocks, including: epigenetic galena in slate; malachite staining in maroon and green siltstones associated with the volcanic unit; and chalcopyrite and tetrahedrite(?)-bearing quartz veins in carbonate rocks.

## *STRATIFORM BARITE*

With one exception, all the stratiform barite in the map area is hosted by the Earn Group. One occurrence was observed within the Ordovician Road River Group.

Eighteen occurrences of barite in the Earn Group were documented over the course of the 1995 field season (Figure 3). Virtually every thrust panel or fold enclosure of Earn rocks contains barite showings along its trace. Most have not been reported in the literature. The showings range from disseminated authigenic barite crystals, or nodules of radiating barite, to massive-bedded barite reaching several metres in thickness, and locally producing 'kill zones' covering tens to thousands of square metres. The most impressive concentration of these occurrences is in the southeastern part of the map area. Here barite showings occur along strike from each other, and in adjacent thrust sheets, suggesting at least one continuous or semi-continuous horizon which has been tectonically disrupted and masked by poor exposure. The most important occurrence in this area we call the 'Broken Bit barite', after a nearby outfitters' camp. This previously unreported barite kill zone is well below timberline, and is approximately 6 kilometres northwest along strike from a horizon of bedded barite, over 2 metres thick, which was traced for several kilometres. Thrust sheets immediately to the west and east also contain bedded barite from 0.5 to 2 metres in thickness. Elsewhere, more than 2 metres of barite is exposed east of the headwaters of Trail Creek (Photo 10), and 1 to 1.5

Photo 10: Calcareous barite layer, 2 metres thick, in Earn Group, north-centre of map area.

metres of barite crops out along a north-flowing tributary of Davie Creek.

Barite tends to occur in the lower part of the Earn Group, although occurrences in the southeast appear to be in the upper part. Metre-scale sections of baritic rock pinch and swell along strike and disappear over tens of metres. Barite beds are sometimes interlayered with slate and siltstone. Due to the lack of exposure, deformation and poor stratigraphic control, it is not known if more than one baritic interval is involved. Enclosing rocks are generally dark grey to black siliceous argillites, slates and lesser siltstone. In the southeast, hostrocks are grey, laminated mudstone to siltstone which appear to be higher in the Earn stratigraphy.

Barite weathers grey and is dark grey to black and forms individual beds from 1 to over 50 centimetres thick (Photo 8). It is medium to coarsely crystalline and invariably calcareous. The most calcareous varieties have a strong fetid odour when broken. Interstitial, orange-weathering iron carbonate may be present, and some bedding surfaces are micaceous. Individual beds sometimes show internal laminations, but commonly are quite massive. Sulphides are conspicuously absent, although in some showings, the baritic layers are associated with sooty black pyritic slate.

The Broken Bit barite kill zone (Figure 3) is the most significant mineral discovery made in this program to date. It is inconspicuous from a distance, as it is not gossanous and looks like a slide in post glacial alluvium. It covers some 3500 square metres, measuring approximately 70 by 50 metres (Photo 11). It consists almost entirely of rubble of massive calcareous barite, some paler grey baritic limestone and a lesser amount of blue-grey-weathering siliceous slate. The largest block of barite is 30 centimetres across and crudely layered. No bedrock is exposed. Little or no sulphides were noted but sporadically the barite is rusty weathering. A sample of calcareous barite assayed 41.46% Ba; more limy material contains about half as much barium. Coarse granular 'sand' below the rubble contains 47.91% Ba, accounting for the lack of vegetation and even lichen. A small creek gully 500 metres along strike to the southeast of the kill zone contains rubble of grey calcareous barite to baritic limestone, suggesting that the barite horizon extends at least this far.

The region east and southeast of the Broken Bit occurrence was prospected in the late 1970s by several companies which were investigating anomalous zinc and copper in stream sediment samples (Stewart, 1980; Boyle, 1978). Subsequent soil sampling confirmed strongly anomalous zinc, lead and copper values, but it was reported that bedrock prospecting around these anomalies did not reveal the presence of significant sulphides, although some barite was found to the south of the area of interest. It was pointedly noted that a number of zinc-rich calcrete deposits occur in the vicinity of the geochemical anomalies (Boyle, 1978).

An overturned panel of Ordovician Road River Group slates, exposed along a creek 2 kilometres south of the first large bend in Matulka Creek, contains thin (1 to 3 cm) beds of orange-weathering baritic silty dolostone with authigenic barite crystals. No barite-bearing carbonates were recognized in other sections of Ordovician Road River slates.

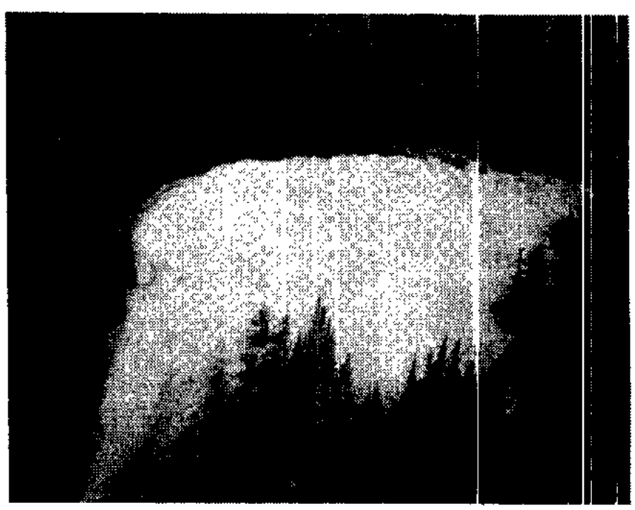

Photo 11: Broken Bit barite 'kill zone', viewed from the air. Zone measures approximately 70 by 50 metres.

## *LEAD AND ZINC SULPHIDES*

Two main occurrences of epigenetic sulphide mineralization were recorded: one in the uppermost Road River Group and the other in the Earn Group.

A sphalerite-barite-rich breccia zone crosscuts chert, cherty argillite and argillaceous limestone of the Road River Group, near the top of a ridge at the head of Horneline Creek (Figure 3). The host-rocks are thought to belong to the chert-limestone couplet which is typically found immediately below the Earn Group. The breccia zone is marked by gossanous weathering of pyrite-rich sections, and loose pieces of rock are noticeably heavy. The zone is about 10 metres long and varies from less than 0.5 metre to over 3 metres in thickness before disappearing below scree. Its geometry is difficult to determine, but it appears to have a pipe-like shape which pinches and swells along its trace. Breccia clasts vary from less than 0.1 centimetre to over 20 centimetres across, and are composed of chert, limestone and argillite. The matrix is predominant, and is part rusty, oxidized material and part carbonate. Pyrite is finely disseminated in the matrix and clasts. No sphalerite is visible, but the breccia reacts strongly to diethylaniline stain ('zinc zap'). Select grab samples from the breccia assay up to 3.4% Zn, 9.1 g/t Ag and 1.0% Ba. More oxidized material contains only 0.2% Zn, 1.1 g/t Ag and only 0.1% Ba. Analysis also shows anomalous concentrations of copper, cadmium and antimony.

The shape of the breccia zone and the absence of shear fractures in it or the host-rocks argues against a tectonic control. One possibility is that the zone represents a hydrothermal conduit or feeder system to overlying Earn group exhalites. About 500 metres to the north of the occurrence is a small area of Earn cherty siltstone and slate with metre-scale lenses of black, baritic limestone.

This showing is documented as the Smoke occurrence (MINFILE 094L 016), and was investigated by Noranda Exploration Company, Limited in 1980 (MacArthur, 1981). Noranda conducted a soil survey in the area around the breccia, but this work did not outline any other targets.

The other sulphide occurrence of note is in Earn Group rocks exposed along Matulka Creek, approximately 5 kilometres downstream from its headwaters. The outcrop consists of slate and siltstone to siliceous siltstone, interbedded with thin, grey to orange-weathering baritic limestone, and is in the same, narrow synclinal fold that contains the Broken Bit barite showing, 4 kilometres to the southeast. A large boulder of fractured, silicified siltstone and slate, almost certainly derived from this exposure, contains galena in quartz veinlets and disseminated in the rock. A selected grab sample assayed over 3% Pb, 15.7 g/t Ag, 0.1% Zn and 0.1% Ba. Comparison of a preliminary Pb/Pb isotopic age obtained from this galena with others from the Selwyn Basin suggests that it is Devonian in age (J.E. Gabites and C.I. Godwin, personal communication, 1995). If correct, this suggests that although the galena and silicification postdate formation of the hostrock, they may be related to a postdepositional feeder system that led to stratiform mineralization in overlying Earn Group sediments, such as might be represented by the nearby Broken Bit barite.

## *MINERAL OCCURRENCES IN CAMBRIAN ROCKS*

Disseminated, patchy galena was found on the southeast side of a ridge some 4 kilometres southeast of Gataga Mountain. It occurs at the base of a sequence of strongly sheared, dark grey to grey-green slates, immediately above grey carbonates. This succession is stratigraphically below the Cambrian volcanic unit. The galena is confined to a zone of silicification in the lowest 5 to 10 centimetres of the sheared slates; its strike length was not determined. A selected grab sample assayed 5% Pb, 30.1 g/t Ag and 0.6% Zn.

A small copper showing is situated approximately 7 kilometres northwest of Gataga Mountain, along the lower slopes of the Northern Rocky Mountain Trench. Malachite staining was observed in interlayered maroon and pale green, micaceous slate to siltstone. Cambrian volcanic rocks lie stratigraphically above and below these sediments, and may interfinger with them locally. A grab sample of mineralized siltstone contains 0.2% Cu together with elevated silver and barium concentrations.

Chalcopyrite and tetrahedrite(?)-bearing quartz veins from 0.01 to 1.5 metres thick cut carbonate rocks along the northern extension of the ridge containing Brownie Mountain. Some of the larger veins are quite conspicuous and can be traced for some distance. The veins are planar to irregular in shape and generally trend 100° to 110°. They can contain wallrock fragments, and vugs lined with tiny quartz crystals are common. Malachite and azurite staining is extensive in copper-rich zones. Similar copper-bearing quartz-carbonate veins were found locally in Cambrian carbonates farther northwest, on the ridges between Gataga Mountain and Terminus Mountain.

## CONCLUSIONS

- Mapping in the Gataga Mountain-Terminus Mountain area has demonstrated that most units and major structures delineated last year in the Gataga River area continue to the north. These include: Cambrian carbonates and siliciclastics which are partly equivalent to the Gog Group; Upper Cambrian to Lower Ordovician Kechika Group; Lower

Ordovician to Middle Devonian Road River Group; and Middle Devonian to lower Mississippian(?) Earn Group.

- Volcanic rocks between Gataga and Terminus mountains are predominantly alkalic basalt, and are believed to be entirely Early Cambrian in age.
- Cambrian rocks exhibit marked facies changes in the map area. Both the volcanics and thick sections of carbonates and coarse siliciclastics and conglomerate disappear northeastward into finer grained siliciclastics and rare carbonate, suggesting basin deepening.
- Kechika Group and lower Road River Group rocks also show a pronounced thinning to the northwest, and are apparently absent in much of the northern part of the map area.
- Many previously undocumented occurrences of bedded barite have been located in the Earn Group. Many of these are 2 metres or more in thickness and are traceable for kilometres. The most substantial deposit is associated with a 'kill zone' 3500 square metres in size.


## ACKNOWLEDGEMENTS

The authors thank Andrew Legun, Carole Augereau and Eric Hou for their capable and cheerful assistance during the summer. Special mention goes to Suzanne Paradis of the Geological Survey of Canada (GSC) for her help at the end of the field season. We are grateful to Dr. Brian Norford and Dr. Mike Orchard (both GSC) for preliminary identifications of our fossil collections. Janet Gabites and Dr. Colin Godwin (both University of British Columbia) provided Pb/Pb analysis. Verna Vilkos' assistance with the diagrams is much appreciated. The two senior authors would like to thank outfitters Andy and JoAnn Knox for their splendid support, guidance and stimulating conversation during the horse packing part of the program. We also thank Gary and Gordon Moore for the use of facilities at their hunting lodge at Terminus Mountain and for their expediting services. Northern Mountain Helicopters and pilot Lee Sexsmith provided excellent service.


## REFERENCES


Abbott, J.G., Gordey, S.P. and Tempelman-Kluit, D.J. (1986): Setting of Stratiform, Sediment-hosted Lead-Zinc Deposits in Yukon and Northeastern British Columbia; *in* Mineral Deposits of Northern Cordillera, Morin, J.A., Editor, *Canadian Institute of Mining and Metallurgy*, Special Volume 37, pages 1-18.

Boyle, P.J.S. (1978): Report on Geological and Geochemical Surveys on the Solo 1 to 4 Mineral Claims; *B.C. Ministry of Energy, Mines and Petroleum Resources*, Assessment Report 7292.

Cecile, M.P. and Norford, B.S. (1979): Basin to Platform Transition, Lower Paleozoic Strata of Ware and Trutch Map Areas, Northeastern British Columbia; *in* Current Research, Part A, *Geological Survey of Canada*, Paper 79-1A, pages 219-226.

Cecile, M.P. and Norford, B.S. (1991): Ordovician and Silurian Assemblages, Chapter 7; *in* Geology of the Cordilleran Orogen in Canada, Gabrielse, H. and Yorath, C.J., Editors, *Geological Survey of Canada*, Geology of Canada, No. 4, pages 184-196.

Ferri, F., Nelson, J. and Rees, C. (1995a): Geology and Mineralization of the Gataga River Area, Northern Rocky Mountains (94L/7, 8, 9 and 10 ; *in* Geological Fieldwork 1994, Grant, B. and Newell, J.M., Editors, *B.C. Ministry of Energy, Mines and Petroleum Resources*, Paper 1995-1, pages 277-298.

Ferri, F., Nelson, J. and Rees, C. (1995b): Preliminary Geology of the Gataga River Area, British Columbia, NTS 94L/7, 8, 9 and 10; *B.C. Ministry of Energy, Mines and Petroleum Resources*, Open File 1995-4.

Fritz, W.H. (1991): Cambrian to Middle Devonian Assemblages, Chapter 7; *in* Geology of the Cordilleran Orogen in Canada, Gabrielse, H. and Yorath, C.J., Editors, *Geological Survey of Canada*, Geology of Canada, No. 4, pages 155-184.

Gabrielse, H. (1962): Geology, Kechika (94L); *Geological Survey of Canada*, Map 42-1962.

Gabrielse, H. and Yorath, C.J. (1991): Tectonic Syntheses, Chapter 18; *in* Geology of the Cordilleran Orogen in Canada, Gabrielse, H. and Yorath, C.J., Editors, *Geological Survey of Canada*, Geology of Canada, No. 4, pages 679-705.

Goodfellow, W.D., Cecile. M.P. and Leybourne, M.I. (1995): Geochemistry, Petrogenesis, and Tectonic Setting of Lower Paleozoic Alkalic and Potassic Volcanic Rocks, Northern Canadian Cordilleran Miogeocline; *Canadian Journal of Earth Sciences*, Volume 32, pages 1236-1254.

Irwin, S.E.B. (1990) Late Devonian Conodont Biostratigraphy of the Earn Group with Age Constraints for Stratiform Mineral Deposits, Selwyn and Kechika Basins, Northern British Columbia and Yukon; unpublished M.Sc. thesis, *The University of British Columbia*, 311 pages.

Jackaman, W. Cook, S., Lett, R., Sibbick, S. and Matysek, P. (1996): 1995 Regional Geochemical Survey Program: Review of Activities; *in* Geological Fieldwork 1995, Grant, B. and Newell, J.M., Editors, *B.C. Ministry of Energy, Mines and Petroleum Resources*, Paper 1996-1, this volume.

MacArthur, R.G. (1981): Geochemical Report on the Smoke Mineral Claim, Liard Mining Division; *B.C. Ministry of Energy, Mines and Petroleum Resources*, Assessment Report 9467.

MacIntyre, D.G. (1992): Geological Setting and Genesis of Sedimentary Exhalative Barite and Barite-Sulfide Deposits, Gataga District, Northeastern British Columbia; *Exploration and Mining Geology*, Volume 1, No. 1, pages 1-20.

Stewart, A. (1980): Geochemical Report on the MAT 1-4 Claims; *B.C. Ministry of Energy, Mines and Petroleum Resources*, Assessment Report 8379.

Taylor, G.C. and Stott, D.F. (1973): Tuchodi Lakes Map Area, Northeastern British Columbia; *Geological Survey of Canada,* Memoir 373, 37 pages.

# GEOLOGY OF THE TODAGIN PLATEAU AND KINASKAN LAKE AREA NORTHWESTERN BRITISH COLUMBIA (104H/12, 104G/9)

**By C.H. Ash and P.K. Stinson, Geological Survey Branch, and R.W.J. Macdonald, Mineral Deposits Research Unit, UBC.**

KEYWORDS: Economic geology, porphyry copper-gold, Tatogga Lake, Stuhini Group, Hazelton Group, Cold Fish Lake volcanics, Lower Jurassic bimodal volcanism, Red-Chris, Groat, Klappan.

## INTRODUCTION

This report presents results from the second year of field mapping, as part of the Tatogga Lake project.

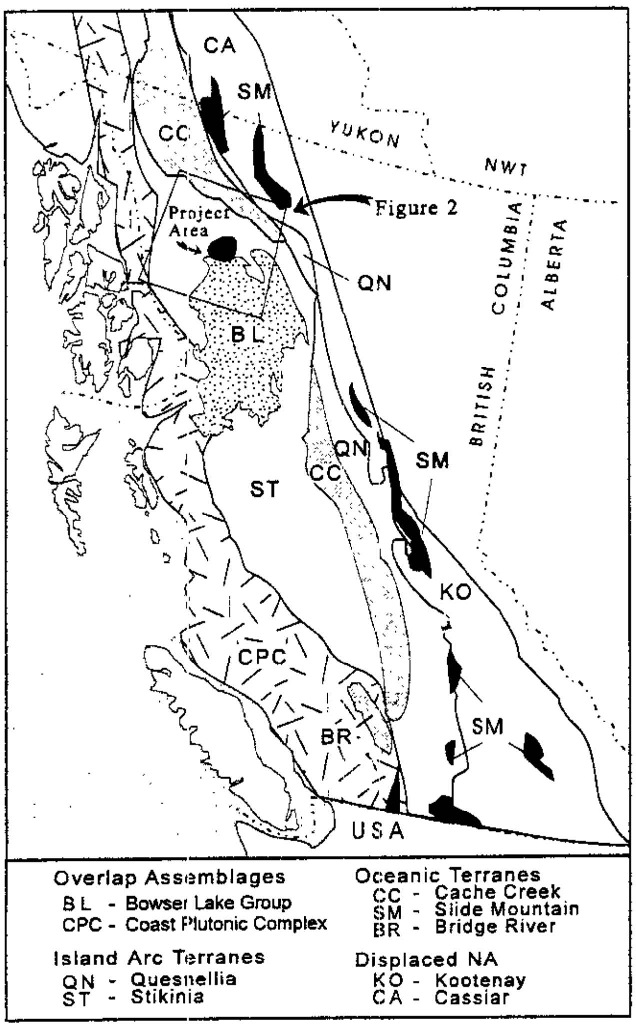


Figure 1. Regional geological setting of the Tatogga Lake project area.

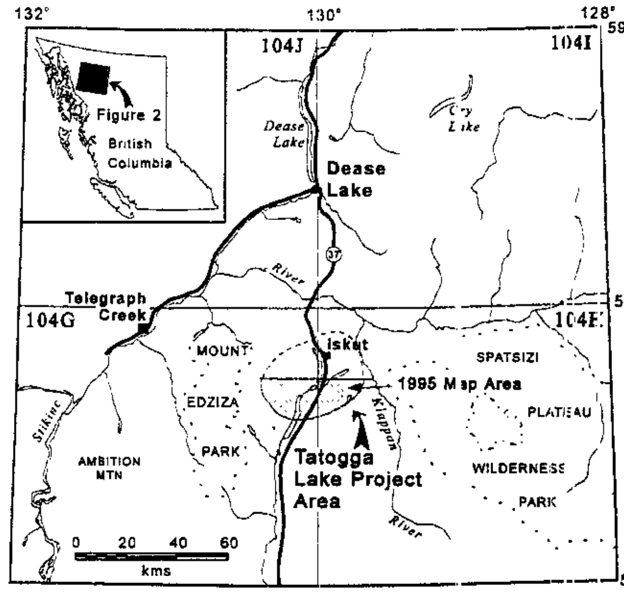


Figure 2. Geographic location of the Tatogga Lake project showing area covered in this report.

This is a geologic and metallogenic mapping program initiated in 1994 to investigate the geology and associated mineral deposits of Stikine Terrane Mesozoic arc-volcanic rocks along the northern margin of the Bowser Basin in northwestern British Columbia (Figure 1; Ash *et al.*, 1995). The project area is located 80 kilometres south of Dease Lake, and is transected by the Stewart-Cassiar Highway (Highway 37), south from the village of Iskut (Figure 2). It includes parts of NTS map sheets 104G/9 and 16, and 104H/12 and 13.

During 1995, fieldwork was conducted from July 6th to September 12th and focused primarily on the southern half of the project area (Figure 2). The 1995 map area encompasses the northwest corner of the Kluea Lake (104H/12) map sheet (Figure 3) and the northeast part of the Kinaskan Lake (104G/9) sheet (Figure 4). The eastern half of the map area (Figure 3) encompases most of the Todagin Plateau and is referred to here as the Todagin map area. A preliminary 1:20 000-scale geology map of the Todagin area, which includes the Red-Chris porphyry copper-gold deposit, has been produced as part of this work (Ash *et al.*, 1996). Mapping of the Kinaskan Lake sheet (104G/9) was only partially completed due to

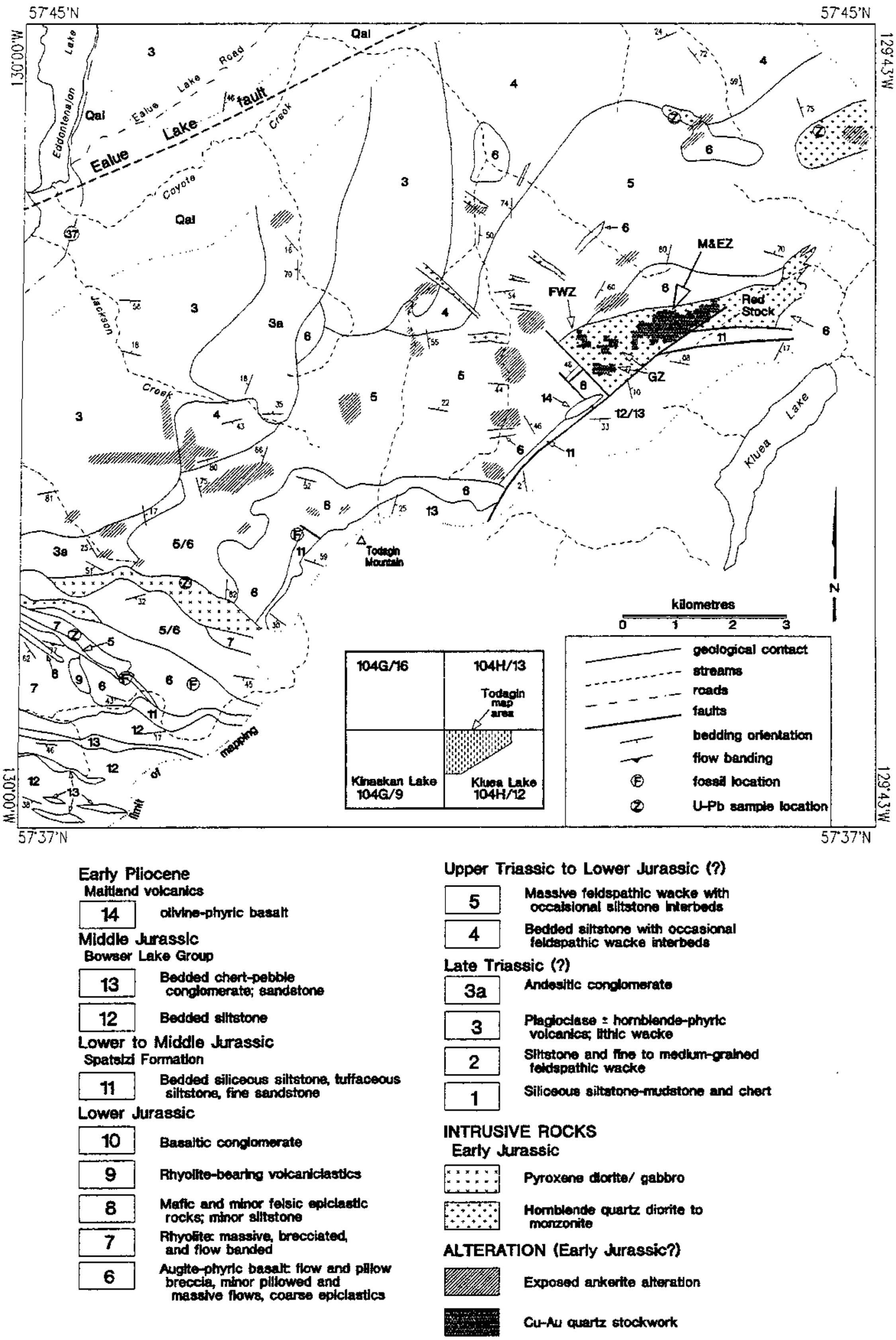


Figure 3. Geology of the Todagin Plateau. E&MZ = East and Main zones, GZ = Gulley zone, and FWZ = Far West zone of the Red-Chris deposit.

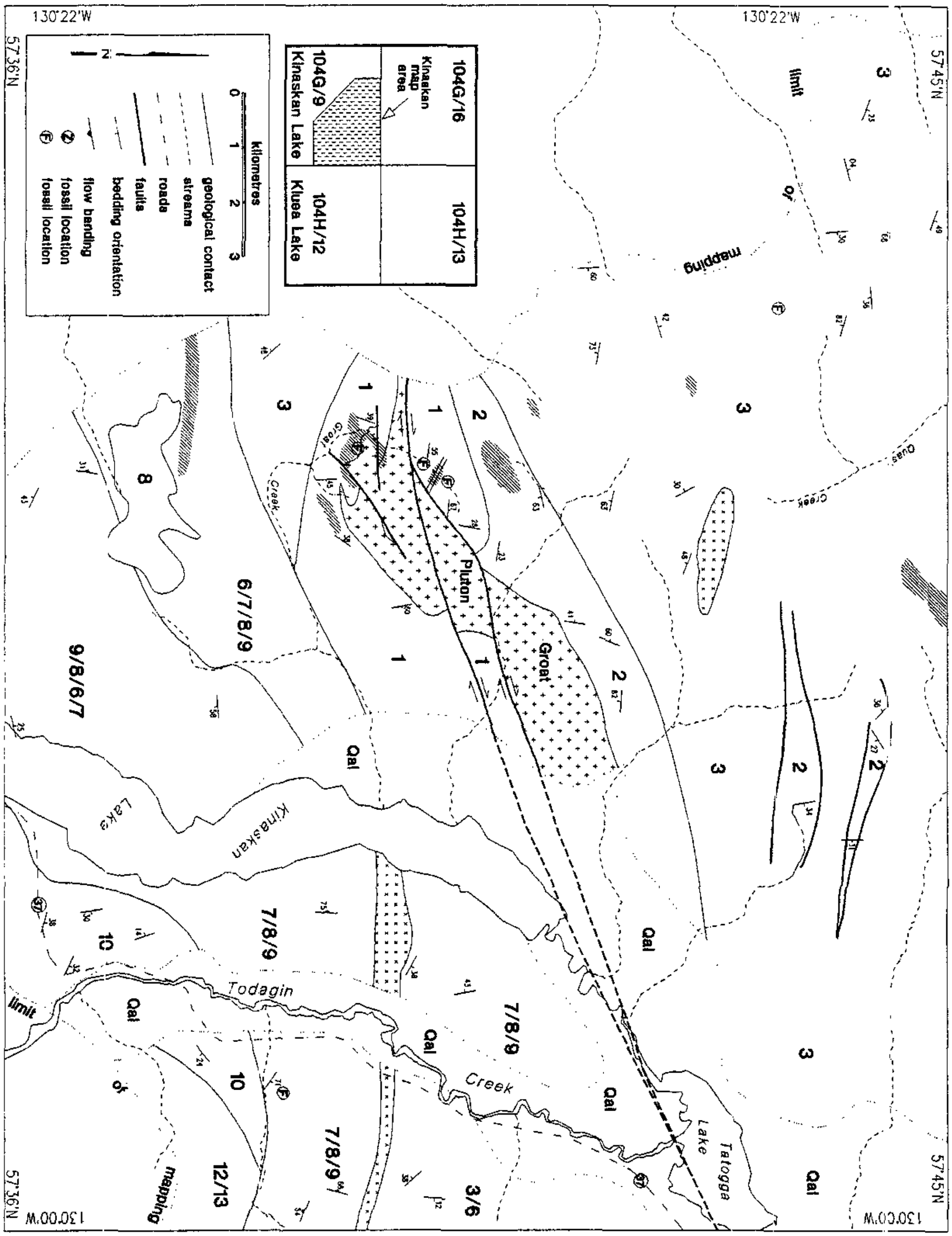


Figure 4. Geology of the Kinaskan Lake area. For legend, see Figure 3.

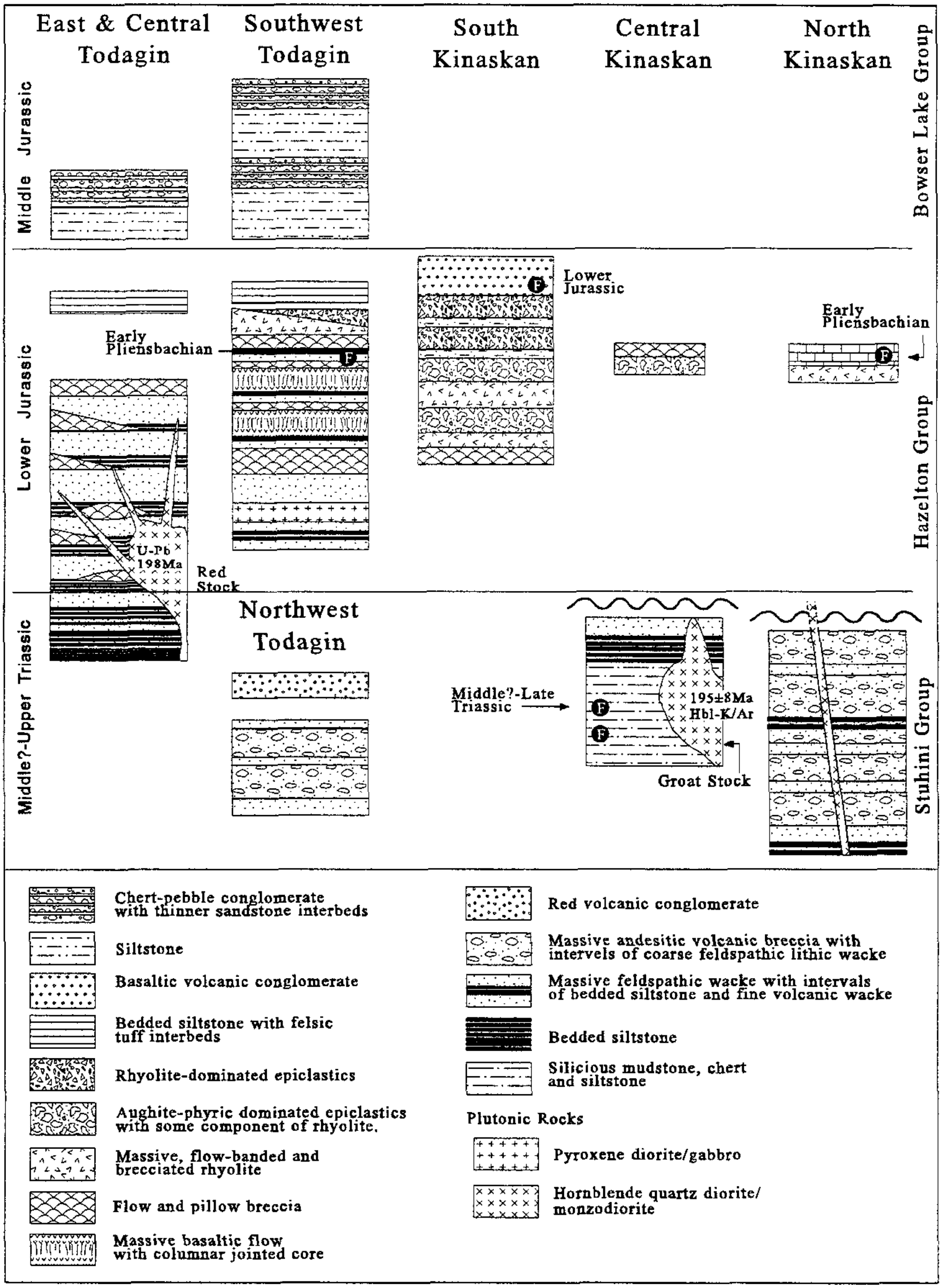


Figure 5. Schematic stratigrasphic sections for the southern half of the Tatogga Lake project area.

extended periods of inclement weather. Accordingly, geological units shown on this sheet remain largely undifferentiated. Results of mapping for this sheet will be released in open file format following completion of mapping, planned for the 1996 field season.

Exploration activity in the area this year was once again dominated by American Bullion Minerals Ltd. which completed its second season of intensive delineation and exploration drilling on the Red-Chris deposit. Drilling was successful in increasing previously defined potential mineable reserves in the East and Main zones and identified two new areas of copper-gold mineralization southwest of the Main zone in the Gully and Far West zones. The latter two zones are collectively referred to as the Yellow Chris. Other exploration activity in the area included a preliminary evaluation of the Klappan group of claims by Homestake Canada Inc. and regional work by Teck Corporation.

For a discussion on aspects of previous work, physiography and regional setting for the project area the reader is referred to Ash *et al.* (1995).

## LOCAL GEOLOGY

The map area is underlain almost entirely by Upper Triassic and Lower Jurassic arc-volcanic rocks that are overlain along their southeastern margin by Middle Jurassic Bowser Lake Group sediments (Figures 3 and 4). These Mesozoic volcanic rocks are divisible into three broad northeast-trending belts. The northwestern belt is dominated by Middle(?) to Upper Triassic andesitic volcaniclastics, mainly massive breccias. The central belt is underlain primarily by Upper Triassic and possibly Lower Jurassic fine to medium-grained epiclastic rocks. Lower Jurassic rocks comprise a bimodal suite of basalts and rhyolites and related subvolcanic rocks that overlie and intrude very fine to medium-grained sedimentary rocks primarily to the southeast. The younger rocks also locally intrude and overlie Triassic rocks throughout the map area.

These rocks have been affected by folding and faulting. Mesoscopic folding is generally only identified within the Lower Jurassic and older, thinly bedded sediments, mainly siltstones, and rarely in limestones. Broad warping of thicker bedded sequences is a characteristic megascopic feature commonly seen in cliff exposures. High-angle brittle faults are abundant throughout the map area and contacts are rarely exposed. As a result it is difficult to establish continuity of contacts between individual Mesozoic volcanic units.

Stratigraphic relationships within individual sections are, however, locally well displayed. The following discussion focuses primarily on local and regional stratigraphic variations. Individual areas with some degree of stratigraphic continuity are separated and their stratigraphy is summarized in a series of generalized sections (Figure 5) keyed to the discussion. Sections are not to scale with respect to thickness or time; the thickness of some sections is exaggerated to show detailed relationships. Most of the Lower Jurassic sections, for example, probably represent a short interval between 200 and 193 Ma (Sinemurian to Pliensbachian).

## *LATE TRIASSIC STRATIGRAPHY*

### NORTH KINASKAN

Upper Triassic rocks represented in this section (Figure 5) underlie the northern half of the Kinaskan map area (Figure 4). The north Kinaskan area comprises a largely undifferentiated sequence of andesitic volcaniclastic rocks with lesser and related coarse to conglomeratic epiclastic sediments. Volcaniclastic rocks are dominated by massive, green, plagioclase±hornblende-porphyritic andesitic breccias, probably lahars or debris-flow deposits. Breccias vary from clast to matrix supported and are generally massive on the outcrop scale (Photo 1). Subangular to subrounded volcanic clasts, usually from 2 to 6 centimetres across, but ranging from one to several tens of centimetres in size, are set in a lithologically similar, fine to medium-grained fragmental matrix. Individual clasts vary in both phenocryst size and

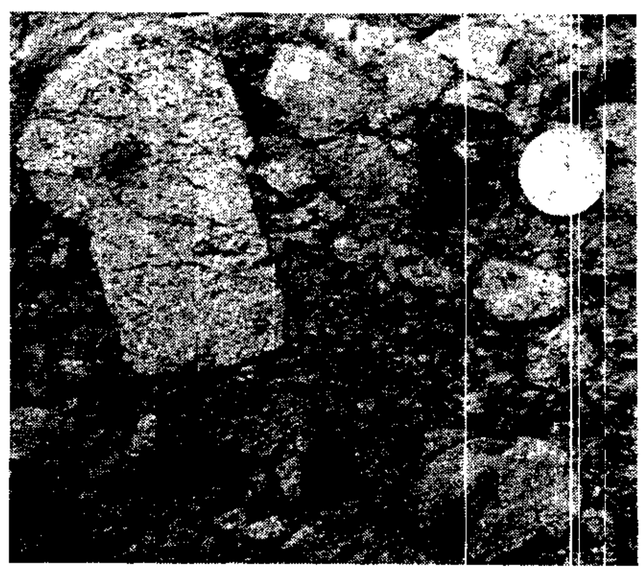

Photo 1. Andesitic volcanic breccia with plagioclase±hornblende-porphyritic clasts, north Kinaskan region.

abundance, containing from 15 to 30%, 1 to 3-millimetre, tabular plagioclase and lesser to trace amounts of hornblende phenocrysts of comparable size, in modal abundances of 3 to 10%. Locally, breccias are more heterolithic, containing aphanitic green volcanic and distinctive red-brown, angular, mudstone clasts in addition to the porphyritic clasts. Matrix material of the heterolithic breccias is more poorly sorted and displays a wider grain size variation than in the other breccia type. The more heterolithic breccias are also typically characterized by a maroon coloured matrix.

Epiclastic sediments include volcanic conglomerates, coarse feldspathic lithic wackes, massive, medium to coarse feldspathic wackes, and bedded siltstones. Volcanic conglomerates and wackes are found primarily as isolated, thickly bedded sequences from several metres to several tens of centimetres thick within the thicker successions of massive volcanic breccias (Photo 2). Bedding in most of this unit typically strikes between west-northwest and west-southwest with moderate dips to the north and south. Several fault blocks near the north edge of the Kinaskan Lake sheet are underlain by much thicker sections of similar lithologies.

Cooper (1978) established a Late Triassic age for this unit several kilometres to the north of the Kluea Lake sheet. This was based on the presence of the pelecypod *Monotis* in limestone interlayered with and overlain by andesitic volcaniclastic rocks in that area. Similarly, Souther (1972) collected *Monotis* fauna

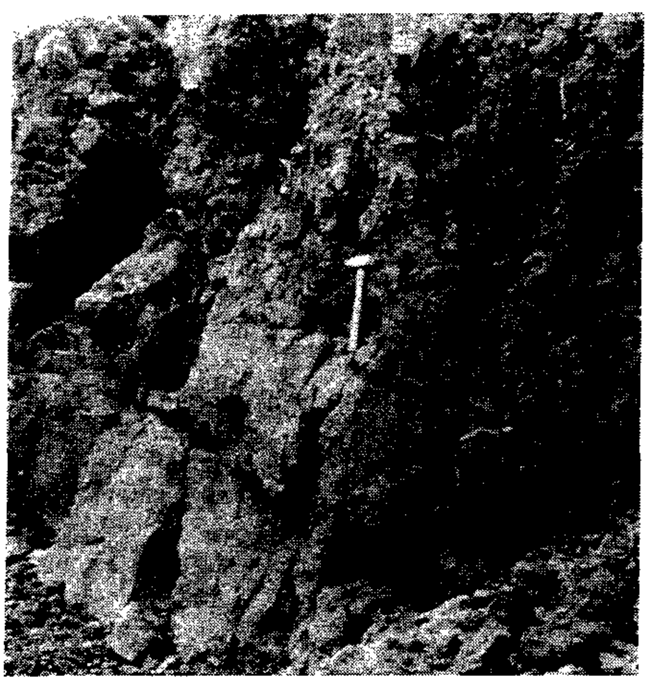

Photo 2. Andesites volcanic breccia overlying thickly bedded, coarse feldpathic lithic wacke,. north Kinaskan region.

from sediments in the northern Kinaskan area lithologically comparable to those described by Cooper. Souther also established that fossiliferous sediments in this area are conformably overlain by the volcaniclastic rocks.

## CENTRAL KINASKAN

Fine-grained clastic and pelagic sedimentary rocks that include fine to medium-grained volcanic wacke, siltstone, siliceous siltstone-mudstone and chert underlie the central part of the Kinaskan sheet (Figures 4 and 5).

Siltstones are dark grey-green and are commonly bedded on the 0.5 to 1-centimetre scale. Rare beds of pebble to cobble conglomerate, less than half a metre thick, containing clasts of plagioclase±hornblende-phyric andesite, occur locally within the siltstone. Siliceous mudstone and chert are dark grey to black and are less commonly bedded.

Three of six samples of siliceous or cherty material collected from near the southwest end of the Groat pluton contain radiolarian fauna indicating that the sequence is Middle(?) to Late Triassic (Ladinian(?)-Carnian-Norian) in age (Cordey, 1995).

A progressive southward increase in the proportion of silicious material in the finer grained clastics may indicate a local facies variation. This facies change is suggestive of a deepening marine environment toward the south and is consistent with the regional variation in Upper Triassic volcanic rocks, from subaerial to submarine in the same direction.

## NORTHWEST TODAGIN

Upper Triassic rocks represented in the northwest Todagin section (Figure 5) underlie the northwest third of the Todagin map area (Figure 3). These are mostly massive green-grey andesitic volcanic breccias similar to those described in the north Kinaskan area. In addition to the breccia unit, a distinctive red-brown weathering conglomerate forms a belt trending northeast from the head of Jackson Creek (Figure 4). Pebble to cobble conglomerates are usually clast supported and beds range from less than 50 centimetres to over a metre in thickness. These are interbedded with thinner, red-brown, massive, coarse feldspathic sandstones similar to the matrix material of the conglomerates. Conglomerate clasts are predominantly rounded to subrounded, plagioclase±hornblende andesite with occasional intrusive clasts.

Conglomerate beds are generally flat lying throughout the belt, however, steeply dipping beds are also present locally. The unit is well exposed in a series of cliffs along the northeastern valley wall above

Jackson Creek where a section 100 to 200 metres thick is exposed. Here the conglomerate appears to overlie both the massive andesitic breccia unit and the feldspathic wacke-siltstone, however, contact relationships between the conglomerate and underlying units are not exposed.

## *LATE TRIASSIC(?) - LOWER JURASSIC STRATIGRAPHY*

### EAST AND CENTRAL TODAGIN

Massive, feldspathic volcanic wackes and bedded black siltstones, locally interbedded with laterally restricted zones of augite-phyric mafic volcanic rocks, underlie the northeastern and central parts of the Todagin map area. Minor amounts of rhyolitic epiclastic sediments are also present. Black to dark brown, bedded siltstone, with occasional thinner intervals of massive, fine to medium-grained feldspathic wacke, dominate the northeastern flank of the plateau. Towards the southwest, massive, medium to coarse-grained feldspathic wackes with occasional thinner intervals of interbedded siltstone and fine sandstone become more common and dominate in the central area. The progession from a siltstone-dominated succession to a wacke-dominated sedimentary sequence towards the south and southwest is suggestive of regional facies variation.

The feldspathic wackes weather tan-brown to buff-grey and are light grey on fresh surfaces. They are characteristically massive and lack obvious sedimentary structures. Typically they are fine to medium grained and equigranular, except for sparse, dark grey to black, angular siltstone fragments from 3 to 15 millimetres in size (Photo 3). The abundance of siltstone fragments is usually from 1 to 2%, but may increase to 20% near bedded siltstone intervals. Massive coarse-grained, poorly sorted varieties of the wacke, with similar siltstone fragments, are also seen locally.

Intervals of dark grey to black, bedded siltstone, ranging from less than a metre to several tens of metres in thickness, occur intermittently throughout the massive wacke sequence. Siltstones are either interbedded with massive volcanic wacke on a scale of several metres, or consist predominantly of continuous intervals of thinly laminated siltstone, and silicious siltstone over distances of several tens of metres. Siltstone beds are laminated to thinly bedded on a 5 to 15-millimetre scale. Siltstone units containing very fine grained volcanic wacke interbeds display well preserved sedimentary structures such as graded bedding, scour marks and load structures (Photo 4). Measurable bedding attitudes in the sedimentary sequence are obtained primarily from these siltstone intervals. As a result, bedding orientation data are

Photo 3. Typical weathering appearance of the massive feldspathic wacke, central Todagin Plateau. Note black siltstone fragments.

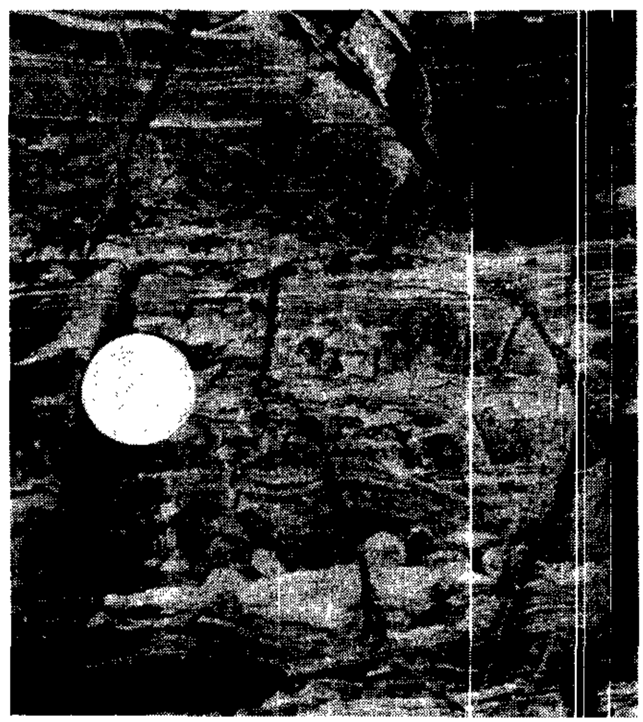

Photo 4. Interbedded siltstone and fine-grained feldspathic sandstone displaying well developed load casts, north central Todagin Plateau.

concentrated in northern and northeastern areas where siltstone is dominant. In the central area, where massive wackes dominate, siltstone intervals are much thinner and less common. In this area, bedding is constrained only locally. In spite of these limitations, a systematic variation in bedding orientation is evident within this sedimentary sequence. Bedding is everywhere moderate to steeply dipping. Along the northeastern flank of the plateau it typically strikes north or slightly east of north and towards the southwest appears to be progressively rotated into a northeast and then east orientation. Sedimentary structures usually indicate that bedding is right way up, but is locally overturned in some steeply dipping beds. This change in the bedding attitude is suggestive of a large-scale regional fold pattern, but this requires confirmation by detailed analysis of structural data.

We suspect that these feldspathic wackes may be in part coeval with, and possibly younger than the Upper Triassic breccia to the north and northwest, from which they are probably derived. A minimum age for this unit is constrained by crosscutting quartz diorite and quartz monzonite dikes and stocks that are dated as Early Jurassic (198 Ma) by U-Pb zircon methods (Friedman, 1995).

Throughout the east Todagin area, mafic volcanic rocks occur as laterally discontinuous, intermittent flow and pillow breccias with occasional coherent flows. Thicker intervals of the unit tend to be concentrated near the contact between Mesozoic volcanics and Bowser Lake sediments. For example, to the north of the Red stock, and northwest of Todagin Mountain, extensive outcrop areas of the unit are characterized by metre-scale flow layering (Photo 5). Volumetrically minor massive basaltic breccias, with clasts of augite-phyric volcanic in a coarse, angular lithic groundmass of similar composition, are also present locally within the thicker basaltic sections (Photo 6).

Basalts are dark olive-green with diagnostic 5 to 15%, black, euhedral augite phenocrysts from 1 to 4 millimetres in size. Rounded, white calcite amygdules, from 2 to 5 millimetres in diameter comprising from 5 to 20% of the rock, are common, though not ubiquitous. Where present, amygdules tend to weather out and impart a vesicular appearance to many exposed surfaces. Calcite veins and veinlets are a common feature of the unit.

Rhyolitic rocks are recognized as medium to coarse-grained bedded epiclastic sediments in a poorly exposed area at the western end of the Red stock. Rhyolitic volcanism is also recorded by thin intervals of felsic tuff within black silicified siltstone along and below Bowser Lake Group sediments at their western margin. In the northeast, this unit occupies steep fault-

Photo 5. Layered massive basaltic flow and flow breccia. Northwest-facing slope of Todagin Mountain.

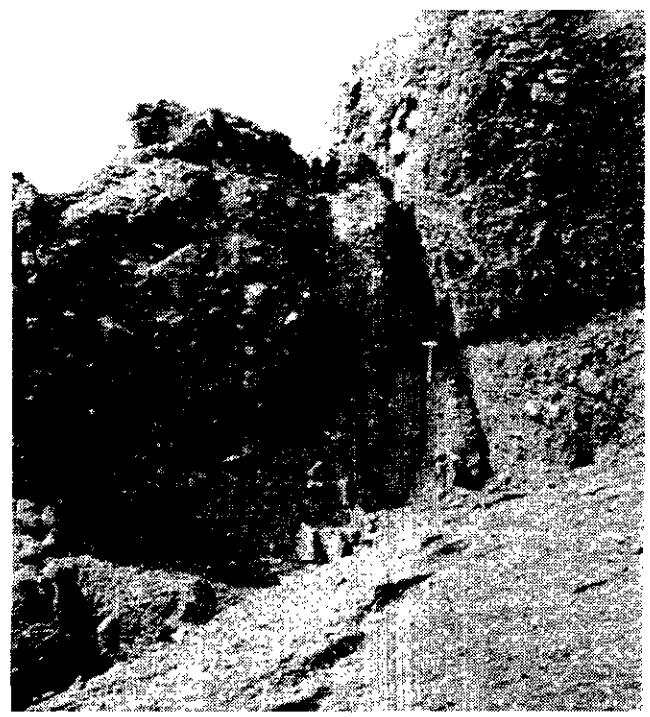

Photo 6. Massive augite-phyric basaltic breccia with clasts of augite-phyric volcanics. Northwest-facing slope of Todagin Mountain.

bounded lenses. To the south it forms an interval, at least several tens of metres thick, between underlying augite-phyric volcanics and overlying Bowser Lake Group chert-pebble conglomerates due west of Todagin Mountain. This unit was assigned to the

Quock Formation of the Spatsizi Group by Evenchick and Green (1990). Although present in many areas along the Bowser contact, the unit appears to be locally faulted out. These rocks are most likely of Pliensbachian age as a potential felsic volcanic source of that age has been mapped to the immediate southwest and is described following.

## LOWER JURASSIC STRATIGRAPHY

### SOUTHWEST TODAGIN

In contrast to the east and central area described above, the southwest part of the Todagin Plateau is dominated by augite-phyric basalts with lesser amounts of siltstone and volcanic wacke (Figure 3). This area also contains a significant component of rhyolitic volcanic and volcaniclastic rocks.

This region has particular significance as it represents an exceptionally well developed section of the Lower Jurassic volcanic stratigraphy. Throughout this area bedding, flow banding and lithologic contacts consistently strike east-southeast, are steeply to moderately inclined and face toward the southwest. Continuous exposures with well preserved volcanic features are found along a number of secondary creeks that flow across strike.

The base of the section is a mixed interval of mafic volcanic flows and medium to coarse-grained volcanic wackes. Above this is an interval of thick mafic flows, locally interlayered with 2 to 6-metre intervals of bedded feldspathic wacke and siltstone. These are overlain by a 10 to 30-metre section of well developed pillow lavas that are succeeded upward by more than 500 metres of bedded rhyolitic volcanic rocks.

Medium to coarse-grained feldspathic wackes with intermittent intervals of black, bedded siltstone are dominant at the base of the section. Coarse to very coarse volcanic wackes, containing 10 to 20% angular pebble-sized siltstone and occasional rhyolite fragments in a matrix of medium to coarse-grained, massive feldspathic wacke, become a recognizable component near the top of the section. Intervals of siltstone or interbedded siltstone and feldspathic sandstone within the mafic volcanic section commonly contain ammonite fauna which have been used to determine the age of the section.

Augite-phyric basalts form a thick interval of layered massive and pillowed flows in the middle of the section. They begin with several tens of metres of pillows and pillow breccias that are overlain by a series of massive flows from 8 to 15 metres thick. Cores of

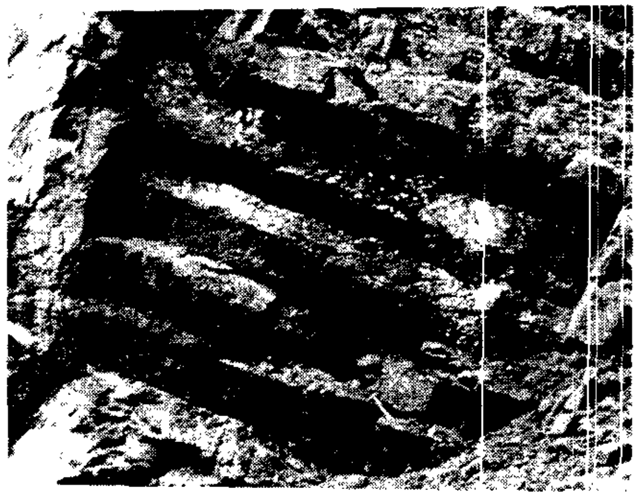

Photo 7. Columnar jointed core in massive augite-phyric volcanic flow within the southwest Todagin section.

many of the flows display well developed columnar joints perpendicular to the flow contacts (Photo 7). Some massive flows are overlain by thinner intervals of pillows and pillow breccias that are overlain, in turn, by 3 to 5-metre intervals of siltstone and sandstone.

Rhyolitic volcanism is first recognized in this section by the appearance of felsic tuff and angular rhyolitic fragments in coarse epiclastic sediments interbedded with the uppermost mafic flows. Coherent rhyolitic volcanic strata first appear as a relatively thick-layered flow above the pillowed mafic volcanic section. Several hundred metres of massive rhyolite at the base of the flow grades upward through a banded zone several metres thick into a 200 to 300-metre

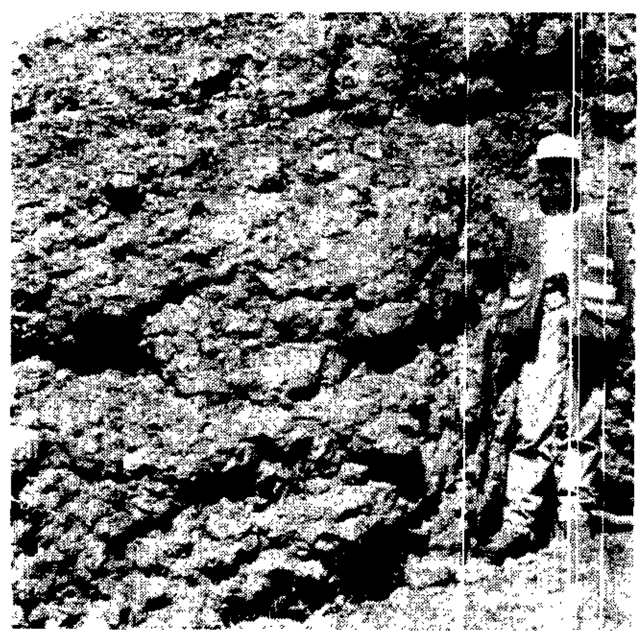

Photo 8. Rhyolite volcanic breccia along the southwestern flank of the Todagin Plateau.

interval of autoclastic breccia (Photo 8). The orientation of flow banding is parallel to the contact between the massive flow and the flow-top breccia and is consistent with that in the underlying mafic volcanic and sedimentary rocks.

Weathered exposures of rhyolite are usually pink in colour, but buff-white to tan-brown varieties are also common. The rocks are aphanitic and usually aphyric, but quartz-porphyritic varieties with 1 to 2-millimetre quartz eyes comprising from 1 to 2% of the unit are locally present, but rare. Sanidine microphenocrysts may also be present. Exposures of the unit vary from massive, to banded to brecciated, with occasional intervals of ash-flow tuff.

## SOUTH KINASKAN

The south Kinaskan area (Figures 4 and 5) is underlain by a largely undifferentiated sequence of Lower Jurassic basaltic and rhyolitic volcaniclastic and epiclastic rocks that are interbedded with coarse, massive feldspathic wackes and siltstones. Relatively homogeneous sections of basaltic volcanic rocks, with alternating intervals of rhyolitic volcanics of comparable thickness, are exposed along the southwest shore of Kinaskan Lake. This stratigraphic interval is interpreted to be the base of the section in this area and correlative with the basalt-rhyolite section in the southwest Todagin area.

Basaltic volcanic rocks include flow breccias and more common epiclastic sediments. Epiclastic sediments comprise bedded sequences of medium to coarse lithic wacke (Photo 9) that form intervals between the more massive breccias. Laharic and autoclastic breccias are both present, but become less prevalent along the southwest shore of Kinaskan Lake where epiclastic sediments dominate. Angular rhyolitic fragments, from several millimetres to several centimetres across, are a minor to locally appreciable component of the epiclastic rocks. The buff-white rhyolite fragments are easily recognized in these typically dark green to black-weathering exposures.

Rhyolitic epiclastic sediments interbedded with siltstone and massive, coarse feldspathic wackes crop out on the plateau west of the southern end of Kinaskan Lake. Beds vary from metres to tens of metres thick. Wackes are in general massive and buff coloured, while siltstones are black and laminated to thinly bedded. Intervals of coarse, buff-white to light grey rhyolite-dominated epiclastic rocks comprise sequences which are bedded on a centimetre scale (Photo 10). Rhyolitic sediments overlying siltstone typically contain 5 to 10% rip-up clasts at their base (Photo 11). These are tabular clasts, oriented parallel to bedding, that decrease in size and frequency upward over distances of 1 to 2 metres. These beds strike east and northeast and face southwards with moderate dips.

Photo 9. Coarse-bedded basaltic lithic wackes, west shoreline of Kinaskan Lake. Note buff white rhyolite fragments.

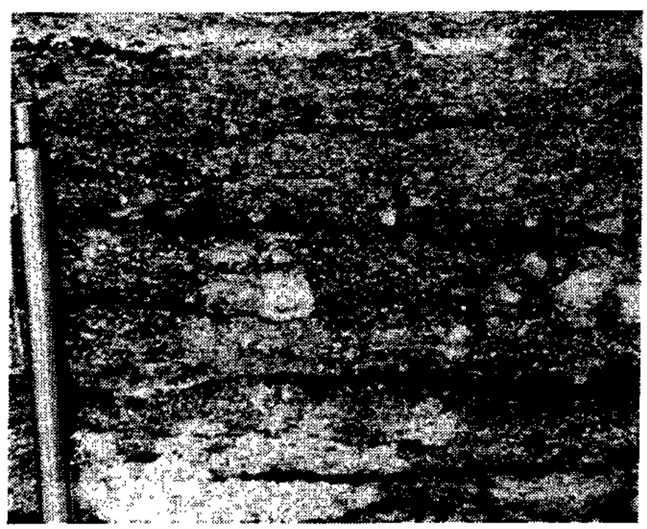

Photo 10. Bedded epiclastic rhyolitic rocks on plateau west of Kinaskan Lake.

Basaltic-pebble conglomerates that underlie Bowser Lake Group sediments form a relatively continuous unit in the southeast corner of the Kinaskan map area. They also occur in isolated

Photo 11. Siltstone rip-up clast at base of rhyolitic epiclastic interval overlying laminated black siltstone, on plateau west of Kinaskan Lake.

Photo 12. Black, thickly bedded basaltic conglomerate, southeast Kinaskan Lake area.

intervals within the undifferentiated sequence to the north. The conglomeratic unit appears to represent the highest stratigraphic interval of the Lower Jurassic volcanic sequence in this area. The unit is dark green to black weathering and locally bedded on a metre scale (Photo 12). Rounded to subrounded lithic fragments of felsic volcaniclastic material are a minor though common constituent of the unit. These are subrounded, pebble to cobble-sized clasts that are more resistant and lighter coloured than the matrix and are concentrated within the bottom 5 to 10 centimetres of individual beds. Graded bedding indicates that this gently dipping sequence is right way up.

## NORTH KINASKAN

Massive, banded and tuffaceous rhyolitic volcanic rocks occur locally in the north Kinaskan area, but are volumetrically minor. Andesitic vocaniclastics are also locally cut by fine-grained quartz-phyric felsic dikes and are probably related to rhyolitic volcanic rocks. These rhyolitic volcanics are locally overlain by bedded sequences of massive fossiliferous limestone, limy grit and lime muds at least several hundred metres thick. Fossils from this unit suggest an early Pliensbachian age (Tipper, 1995; GSC Loc. No. C-208834).

## CENTRAL KINASKAN

Lower Jurassic volcanic rocks in the central Kiniskan area are relatively minor but significant. Several kilometres due north of the centre of the Groat stock an isolated section of basaltic volcanic flows and epiclastic rocks rests unconformably on medium to fine-grained bedded wackes, interpreted to be part of the Upper Triassic sedimentary sequence. Other evidence of Jurassic volcanism in this area includes a 10 metre wide augite-phyric mafic sill in bedded siltstone north of the Groat stock in Groat Creek

## AGE AND CORRELATION OF JURASSIC VOLCANIC ROCKS

The age of this basalt-rhyolite volcanic succession is constrained by both published biostratigraphic data for the area and newly obtained fossil data. Pliensbachian ages have been previously reported for the Lower Jurassic volcanic suite in two separate localities. One of these is near the top of the volcanic succession west of Kinaskan Lake (Evenchick, 1991) and the second is in the southwest Todagin area (Newell and Peatfield, in press).

Two of three macrofossil collections recovered from bedded siltstone-sandstone intervals within the basaltic portion of the southwest Todagin section contained diagnostic fauna (Tipper, 1995). One sample (GSC Loc. No. C-208817) contained several poorly preserved ammonites suggesting several genera indicative of possibly a late Pliensbachian age. Another sample (GSC Loc. No. C-208815) contained well preserved early Pliensbachian fossils. Fossiliferous bedded limestone sequences, locally associated with rhyolitic volcanic rocks in the north Kinaskan area, contain both bivalves and ammonites that are also interpreted to be of early Pliensbachian age (Tipper, 1995; GSC Loc. No. C-208834).

The wider ranging Lower Jurassic *Weyla* bivalve was identified (Tipper, 1995) in two samples collected from limy units at the top of the Lower Jurassic section in both the central Todagin and south Kinaskan areas. The central Todagin sample was from light to dark grey, gritty limestone that forms a laterally restricted interval, possibly 10 to 20 metres thick, between augite-phyric basalt and Spatsizi Group sediments, west of Todagin Mountain (GSC Loc. No. C-208816). The south Kinaskan sample was collected from a limy interval within the basaltic conglomerate unit east of Kinaskan Lake (GSC Loc. No. C-208818).

Isotopic dating of rhyolite from the southwest Todagin map area by U-Pb zircon methods is currently in progress at the University of British Columbia. Processing of the sample recovered some zircons, but they are limited in both size and quantity (R.M. Friedman, written communication, 1995). Analyses are pending.

The early Pliensbachian age of this sequence, combined with the bimodal basalt-rhyolite character of the volcanic rocks and their tectonostratigraphic position immediately below the Bowser Lake Group, suggests that they are correlative with the Cold Fish volcanics (Thorkelson, 1992). The type area of these rocks is along the northeastern margin of the Bowser Basin, 50 kilometres due east of the Todagin map area. Both biostratigraphic and isotopic data constrain Cold Fish volcanics at early Pliensbachian (Thorkelson, 1992). Similar bimodal Lower Jurassic volcanic rocks are also present in the Eskay Creek area to the southwest (Britton *et al.*, 1989; Bartsch, 1992, 1993), indicating that bimodal volcanism was widespread in this part of Stikinia during lower Pliensbachian time.

## *MIDDLE JURASSIC STRATIGRAPHY*

### BOWSER LAKE GROUP, BASAL ASHMAN FORMATION

Middle Jurassic (Bathonian to early Oxfordian) marine clastic sedimentary rocks (Gabrielse and Tipper, 1984; Poulton *et al.*, 1991) of the Bowser Lake Group that crop out along the southern margin of the map area are assigned to the basal Ashman Formation, comprising siltstone, chert-pebble conglomerate and sandstone (Evenchick and Thorkelson, 1993). Sedimentalogical studies indicate that Bowser Lake rocks become progressively younger to the south and that deposition was from the north into the tectonically active northern margin of the Bowser Basin (Ricketts, 1990; Ricketts and Evenchick, 1991; Green, 1991).

### EAST AND CENTRAL TODAGIN

In the east and central Todagin area, interbedded chert-pebble to cobble conglomerates and sandstone form prominent isolated ridges or spurs surrounded by recessive and generally poorly exposed intervals of bedded siltstone. In addition to the prominent east and southeast-trending faults, the area is further dissected by a series of north to northwest-trending, high-angle cross faults that further disrupt the stratigraphy. Chert-pebble and cobble conglomerate with thinner interbeds of sandstone is the dominant lithology in the Todagin Mountain area.

Chert-pebble conglomerates consist of subrounded 0.5 to 3-centimetre, generally light and dark grey or green chert pebbles in a tan-brown to grey sandstone matrix. Massive layers contain 40 to 60% clasts. Bedded exposures comprise layers defined by alternating beds of massive conglomerate tens of centimetres to several metres thick with thinner, massive sandstone interbeds. Bedding in some outcrops is defined by an upward reduction in both size and abundance of chert clasts, repeated over thicknesses of 5 to 15 centimetres.

### SOUTHWEST TODAGIN

Middle Jurassic Bowser Lake Group rocks in the southwest Todagin section are dominated by bedded siltstone with intermittent, thinner intervals of bedded chert-pebble to cobble conglomerate and sandstone (Photo 13). Black, thinly laminated siltstone, with lesser buff-white centimetre-thick sandstone interbeds form homogeneous bedded sections from 600 to 800 metres thick. Conglomerate-sandstone intervals occur as both laterally discontinuous lenses and continuous beds. Lenses are several metres thick and taper laterally over distances of several tens of metres to several hundred metres. Laterally continuous beds are from 100 to 200 metres thick.

Bowser Lake Group rocks in this area form a homoclinal sequence with bedding orientation consistently east-southeast and tops to the southwest. Folding and shearing of Quock Formation sediments immediately below Bowser Lake Group rocks in this area suggest that the basal contact of the Bowser is faulted.

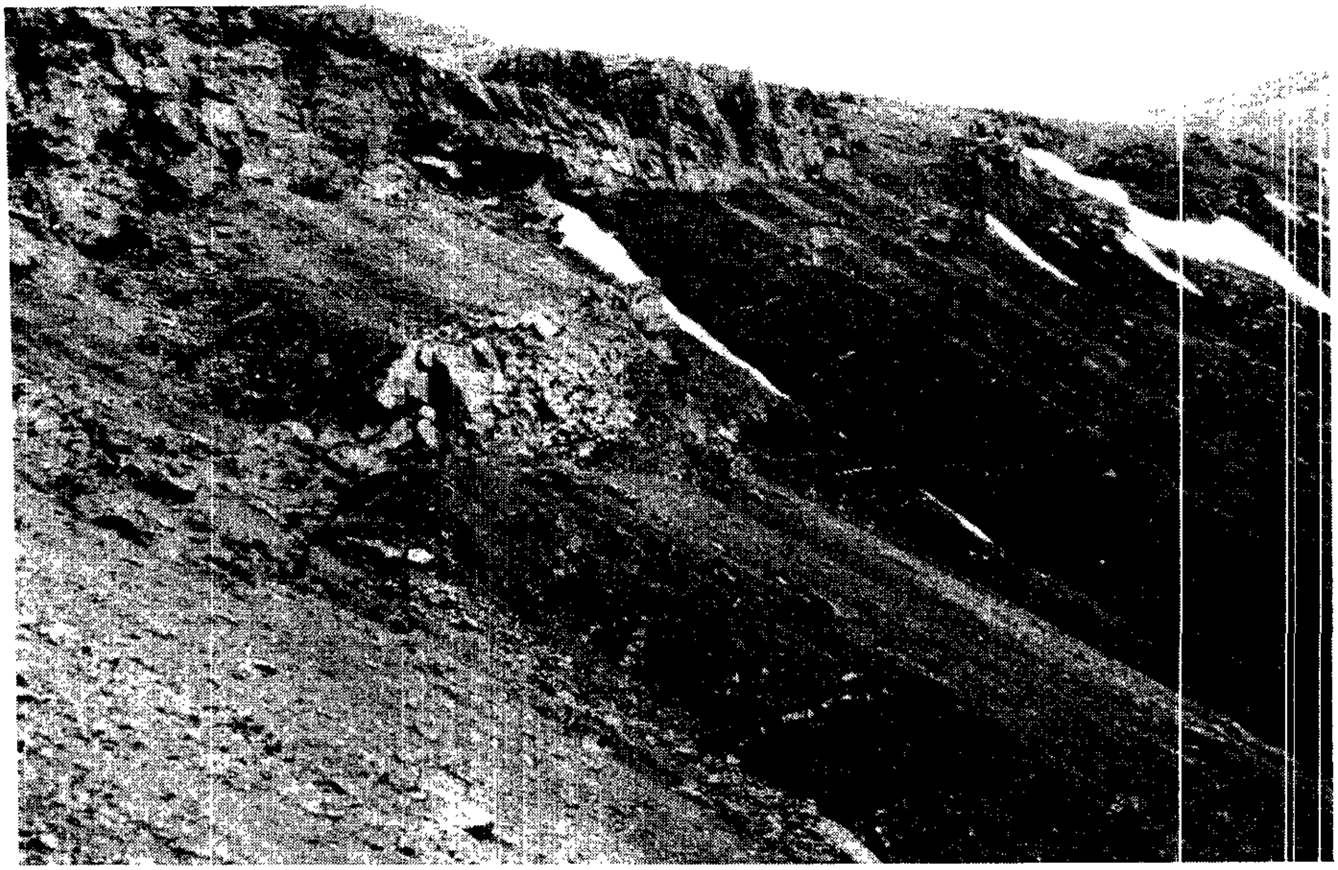

Photo 13. Lenses of interbedded chert-pebble to cobble conglomerate and sandstone in bedded black siltstone. Viewed toward the west along northeast-facing valley wall, southwest Todagin section.

## *MIDDLE JURASSIC INTRUSIVE ROCKS*

### *Hornblende Quartz Diorite to Monzonite*

Hornblende quartz diorite to monzonite occurs as a suite of high-level, elongate stocks and dikes throughout the map area. The largest intrusions of this type include the Red stock and the Groat pluton which are both compositionally variable, equigranular to porphyritic southwest-trending elongate bodies. The Red stock which hosts the Red-Chris deposit, intrudes massive volcanic wackes, siltstone and possibly augite-porphyritic basalt in the southwestern area of the Todagin Plateau (Figure 3 and 4). Abundant related dikes, or possibly plugs, are present north of the Red stock in this area.

The intrusions are compositionally variable, ranging from quartz diorite to quartz monzodiorite. They are characteristically medium grained, equigranular to porphyritic and weather a buff-white to light grey colour. Smaller dikes are usually porphyritic with distinctive medium to coarse-grained hornblende and plagioclase phenocrysts randomly oriented in a light grey, aphanitic groundmass. Plagioclase is the dominant phenocryst phase, occurring as 2 to 5-millimetre subhedral tabular grains comprising from 30 to 45 modal percent of the unit. Hornblende phenocrysts are less abundant, comprising from 6 to 12 modal percent; they are usually of similar grain size, but locally form coarser tabular phenocrysts up to 1 centimetre long and are a diagnostic feature of the unit. The groundmass mineralogy comprises microcrystaline, anhedral, granular quartz and feldspar.

Some dikes, generally on the order of several metres wide, are typically crowded plagioclase porphyries and, in some instances, contain up to 10% quartz as a phenocryst phase. This suggests that they represent slightly more evolved, differentiated phases of the larger stocks.

The Groat pluton intrudes fine-grained clastic and pelagic sedimentary rocks in the central part of Kinaskan Lake area (Figures 4 and 5).

The contacts between the pluton and its country rocks, on surface and in drill core, are characterized by wide sheeted zones of densely packed dikes or sills with screens of country rock, but correlation between holes is poor, as are orientation data (McInnis, 1981; Mehner, 1991). Detailed structural mapping would be needed to determine whether the pluton is a large sill or a discordant plug.

The elongate shape of the Groat pluton does not appear to be primary. Its overall length is increased by dextral offset along two northeast-trending strike-slip faults. These faults are probably a western extension of the regionally significant Ealue Lake fault. The southern fault zone is at least 100 metres wide and is marked by intensely fractured cataclastic zones, with veins of pseudotachylite. Slickenlines (grooves, epidote and chlorite mineral fibres), slickensteps, and the offset of the pluton contact indicate dextral offset along both faults. The mean strike and dip of 25 fracture measurements (mainly from Groat Creek valley, where the two faults seem to merge) is 093°/90° and the mean of 16 slickenline lineations is 06° towards 273°, indicating strike-slip movement. Minor related faults are seen in the 1990 core and marked by small offsets of the pluton contact.

Preliminary U-Pb zircon isotopic data for two intrusions to the north of the Red stock suggest that this suite is Early Jurassic (Friedman, 1995). A small plug or dike of plagioclase-hornblende-quartz-porphyritic quartz diorite on the north flank of the Todagin Plateau (sample CAS94-307; Figure 1) returned an age of 198.6±4.9 Ma. A quartz diorite to monzodiorite stock at the eastern margin of the Todagin Plateau (sample CAS94-215) returned an age 197.9+1.8/-3.2 Ma. An attempt at isotopically dating the Red stock was unsuccessful due to the intensity of alteration affecting the intrusion. Based on the close proximity, comparable geometry and styles of both alteration and mineralization, as well as the obvious textural similarities to less altered, dated rocks, it is assigned a similar age and regarded as an altered equivalent.

Isotopic dating of the Groat stock by hornblende K-Ar analysis (Schmitt, 1977) suggest a cooling age of 195±8 Ma, which is in agreement with the suggested magmatic age of the Red stock and related intrusions. A sample of equigranular hornblende quartz monzonite was collected from the southeastern part of the pluton for radiometric dating. In this sample, euhedral andesine laths are poikilitically enclosed by larger hornblende and orthoclase grains. Initial processing of the sample indicates that it contains sufficient zircon of suitable quality to provide a possible age date (R.M. Friedman, written communication, 1995).

Andesitic volcaniclastic rocks in the north Kinaskan area are locally intruded by several small and widely separated plugs or dikes of medium-grained hornblende diorite. These are interpreted to be coeval with Early Jurassic intrusions to the south and east, which are mineralogically and texturally similar. Intrusive rocks in this area are volumetrically minor, considerably less extensive than those mapped farther to the southwest.

All intrusions coincide to some degree with areas of ankeritic alteration, with or without development of quartz stockwork mineralization. The Red stock is by far the most intensely affected.

### PYROXENE DIORITE

Pyroxene diorite forms a distinct, northwest-trending, elongate pluton, from 0.5 to 1 kilometre wide and over 4 kilometres long, on the southwest end of the Todagin Plateau (Figure 3). It also crops out near the summit of a north-trending ridge between Kinaskan Lake and Highway 37. Continuity of the unit across the Todagin Creek valley is conjectural.

The unit weathers a dull grey to buff white. It is typically medium grained, equigranular and isotropic with plagioclase dominating over pyroxene. Coarse to medium-grained varitextured phases are locally present, but are a minor component.

The age of this unit is not yet defined isotopically. The tabular geometry and orientation of the pluton, concordant with the Lower Jurassic volcanic stratigraphy to the immediate southwest, suggests that it may be a coeval sill-like body related to the augite-phyric basaltic unit. Contact relationships are poorly exposed.

A sample of the medium to coarse-grained varitextured phase of the unit was collected for U-Pb isotopic analysis. Initial processing of the sample reveals that zircon is absent but titanite is present in sufficient quantities to provide a possible date (R.M. Friedman, written communication, 1995).

## ECONOMIC GEOLOGY

Chalcopyrite as disseminations in fracture-controlled quartz vein stockworks is the dominant style of mineralization throughout the map area. It appears to be related to high-level, subvolcanic dikes and stocks which intrude volcanic and sedimentary rocks. In almost all instances copper mineralization is dominant, and associated with elevated concentrations of gold and silver. Two distinct styles of quartz stockwork mineralization are distinguished on the basis of both alteration type and associated lithologies.

The first is characterized by intense quartz-ankerite-sericite alteration in zones of quartz stockwork associated with hornblende quartz diorite to monzonite intrusions. These are dominant in the southern half of the map area and are associated with broad peripheral ankerite alteration halos producing distinctive tan to orange-brown stain zones. Sulphide content in this type is generally low. The Red-Chris deposit is the most significant deposit of this type and has been described previously (Ash *et al.*, 1995). A number of comparable, though smaller showings with similar styles of mineralization are associated with the Groat pluton (Figure 6). These include the GJ/Groat (MINFILE No. 104G-034), Sun (104G-087), Wolf (104G-045) and the Goat Hide (104G-086).

The second type, characterized by finely disseminated pyrite±chalcopyrite in silicified felsic (rhyolitic) dikes and stocks and their immediate hostrocks, is the dominant style of mineralization in the northern half of the project area. It forms impressive, rusty brown, iron oxide stain zones. The felsic rocks generally intrude andesitic breccias and are surrounded by epidote alteration halos with localized patches of pyrite commonly developed. Ankerite alteration or veining has not been identified. Examples include the Edon (104H-004), Coyote (104H-012), Al (104G-044), Castle (104G-076), and possibly much of the Rose of Klappan group of showings (Figure 6). The stain zone associated with the Edon showing (Figure 6) is an excellent example of this type and can be easily seen from Highway 37. The most accessible showing is the Coyote, located at the west end of Ealue Lake along the Ealue Lake road (Figure 6). Rusty brown silicified and pyritized felsite is exposed in a number of roadside outcrops roughly 6 kilometres east of Highway 37.

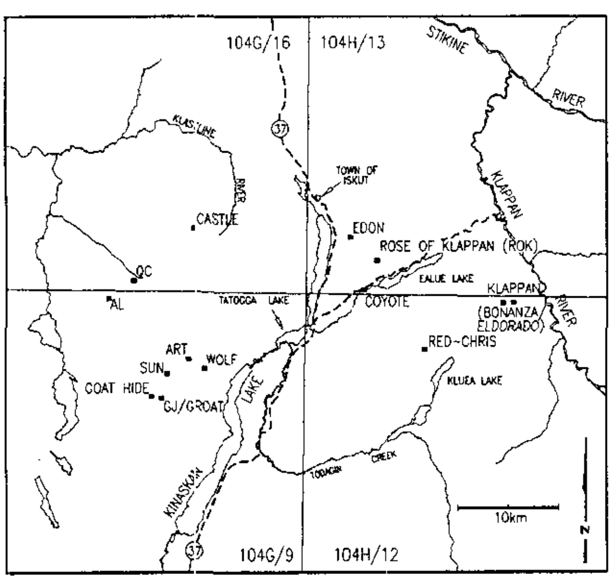


Figure 6. Mineral occurrences in the Tatogga Lake map area.

## *ANKERITE ALTERATION*

Carbonate alteration as ankerite or some variety of iron magnesite is a clearly recognizable feature that is concentrated within and close to Early Jurassic plagioclase-hornblende-phyric intrusions throughout the study area (Figures 3 and 4). The extent and intensity of alteration is, however, highly variable. Zones of iron carbonate alteration range from several tens of metres to over a kilometre in lateral extent. The broadest area of alteration is north of the Red stock which is itself intensely affected. The concentration of hornblende quartz diorite dikes to the north of the Red stock is the likely cause. Areas of ankerite alteration shown to the north and west of the Red stock are surrounded by broad areas of moderate carbonatization. In contrast, areas of alteration in the west central area of the Todagin plateau are usually localized and lack broader haloes of decreasing alteration intensity. Similar alteration is found within and near the Groat pluton, but is much more localized. Alteration does not affect younger, Middle Jurassic Bowser Lake sediments to the south and no ankerite was found associated with the elongate pyroxene diorite, sill-like intrusion in the southwest Todagin area.

The distribution of ankerite alteration as shown on Figures 3 and 4, is indicated where seen in outcrop only. No attempt has been made to correlate between occurrences. Radarsat and other satellite data will be used in an attempt to accurately determine the distribution and extent of ankerite alteration in the area. The Tatogga Lake project area has been selected by the Canadian Space Agency as a site to study the usefulness of satellite data in mountainous terrains. In conjunction with Vern Singhroy of the agency and Eric Grunsky of the British Columbia Geological Survey Branch, landsat thematic mapper and radarsat data will be applied to study spectral responses and structural attributes such as faults.

Ankerite alteration zones are identified by areas of distinctive tan to orange-brown limonitic weathering. They are characterized by discrete veins or broadly fractured zones permeated by ankerite, with associated pervasive carbonatization of surrounding hostrocks. Intense alteration zones are typically cored by carbonate veins 1 to 4 centimetres wide or zones of vein breccia generally from one to several metres wide.

Different lithologies are altered to varying degrees as a function of composition (reactivity with a $CO_2$ rich fluid) and texture (porosity). Mafic volcanic rocks are the most intensely altered and massive wackes to a slightly lesser degree. Siltstones are the least affected lithology, presumably because of their low porosity, maintaining their primary black colour, even in zones of ankerite flooding. This feature is particularly helpful in distinguishing between mafic volcanic rocks and medium-grained massive wackes in areas of intense alteration. Usually where areas of siltstone have been affected by ankerite flooding, breccias are developed with 0.5 to 1-centimetre angular fragments of black siltstone randomly oriented in a tan to orange-brown carbonate matrix.

Concentrations of pyrite as disseminations or clots are occasionally seen within ankerite-altered sediments and volcanics. Assays from these pyritiferous rocks returned no elevated concentrations of precious or base metals. Copper-gold mineralization appears to be preferentially concentrated within and marginal to the intrusive rocks.

A variety of documented mineral occurrences were examined in the course of mapping in the area. Several of these, including the Red-Chris, GJ and Klappan properties are discussed below.

## *RED-CHRIS DEPOSIT*

The Red-Chris is a porphyry copper-gold deposit hosted by the Red stock, an east-northeast elongate intrusive body of pervasively quartz-sericite-ankerite-pyrite (phyllic) altered, plagioclase hornblende porphyry (Panteleyev, 1973, 1975; Leitch and Elliott, 1976; Schink, 1977; Newell and Peatfield, in press). Chalcopyrite and localized concentrations of bornite are associated with zones of quartz stockwork and sheeted quartz veining. The quartz stockwork forms a steeply dipping, high-grade core zone associated with intense and pervasive carbonatization that is surrounded by, and gradational into, barren to weakly mineralized, phyllic (quartz-sericite-ankerite-pyrite) altered host stock. Quartz stockwork zones dip steeply to the north and parallel the long axis of the stock. A detailed description of this deposit, describing styles of alteration and mineralization has been published previously (Ash *et al.*, 1995). Here we summarize significant results from the 1995 drilling program.

In 1994 and 1995 this deposit was the focus of an intensive exploration drilling program by American Bullion Minerals Ltd. During 1994, 21 417 metres was drilled in 58 holes which outlined a potential bulk-tonnage mineable reserve of 157 million tonnes grading 0.5% Cu and 0.4 g/t Au. From early May to mid-November, 1995, a total of 36 830 metres of drilling was completed in 115 holes, focusing primarily on delineating reserves in the Main zone, and to a lesser extent in the East zone. An 800-metre 60° drill hole on the East zone established vertical continuity to over 700 metres. Exploratory drilling to the west of the Main zone, to test induced polarization anomalies in the area of the East and West gullies, was successful in identifying two new zones of stockwork copper-gold mineralization. These are referred to as the Gully and Far West zones or collectively as the Yellow Chris.

Drilling on the Main and East zones was successful in increasing the mineral inventory by close to 30%. Recently released preliminary reserve estimates (George Cross News Letter, November 22, No.224) indicate current geological reserves of 220 million tonnes grading 0.5% Cu and 0.4 g/t Au in the Main and East zones, with potential for an additional 80 million tonnes in the newly discovered Yellow zone. More detailed reserve estimates have not yet been published.

The Gully zone is an east-trending area of quartz stockwork copper-gold mineralization situated between the East and West gullies. A total of 36 holes outlined two parallel, subvertical intervals of copper-gold mineralization to a depth of roughly 300 metres. These zones are separated by an unmineralized interval of gypsum stockwork, most likely along a later fault. Both mineralized intervals have been tested by widely spaced drilling over a strike length of 400 to 500 metres and widths of 200 to 300 metres and they remain open both laterally and vertically.

Roughly two-thirds of the mineralization is hosted by altered Red stock. The remainder is contained within a contact zone of sheeted Red stock with screens of the feldspathic wacke country rock.

Depth to mineralization in this area is variable. The mineralized zone is blanketed by a relatively flat-lying interval of unconsolidated breccia from several metres to several tens of metres thick. The breccia is coarse to pebbly, consisting of 0.3 to 2-centimetre, subangular to angular fragments of altered Red stock. The local occurrence of bornite within the breccia suggest part of this cap may be ore grade. Current theories on the origin of the breccia invoke leaching of gypsum from a pre-existing stockwork by meteoric waters.

Typical assays in the southern part of the Gully zone range from 0.3 % Cu and 0.3 g/t Au over intervals of 15 to 300 metres (J.D. Blanchflower, personal communication, 1995). Occasional high-grade intersections are also encountered; an 18.3-metre interval in hole 95-168 has an average grade of 1.5% Cu and 3.3 g/t Au (including 3 metres grading at 2.47 % Cu and 5.9 g/t Au). Mineralized intervals in the northern part of the Gully zone are narrower,. grades vary from 0.15 to 0.35% copper with corresponding gold values in the range of 0.20 to 0.40 g/t Au.

The Far West zone follows two east-trending vertical structures. Current dimensions, defined by thirteen holes to an average depth of 300 metres, indicate a mineralized zone 300 metres wide by 500

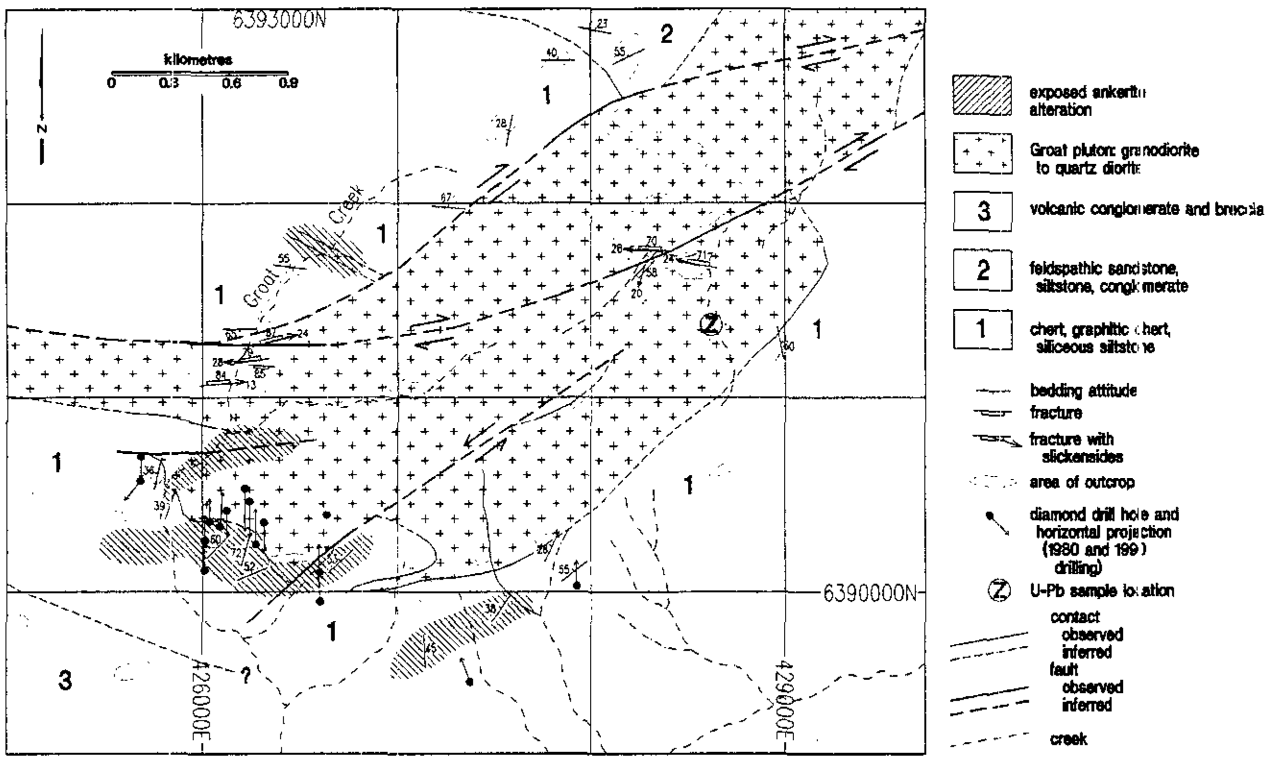


Figure 7. Geology of the Groat property, central Kinaskan Lake map area.

metres long, open both along strike and vertically. As in the Gully zone, mineralization is hosted by both Red stock and volcanic sediments. Grades are from 0.2 to 0.4% Cu with corresponding gold values in the range of 0.2 to greater than 0.4 g/t Au.

## *GJ/GROAT PROPERTY*

The GJ/Groat property is located near the southwestern end of the Groat pluton in the central Kinaskan Lake area (Figures 4 and 7). The pluton underlies a fairly level, grass-covered alpine plateau. Exposure is poor except where the plateau is cut by deep creek drainages. Mineralization and alteration are similar to the Red-Chris deposit but are less extensive. Several companies have explored around the southwestern margin of the pluton since the mid-1960s (Mehner, 1991, provides a summary) with most work centred on the GJ claim. Drilling between 1970 and 1990 totaled 8944 metres; core from 1980 and 1990 is stored on the property. Most of the pluton was mapped as part of the regional mapping project, and a day was spent examining the well preserved 1990 core.

The pluton intrudes Upper Triassic fine-grained clastic and pelagic sedimentary rocks consisting of bedded sandstone, siliceous siltstone, chert and graphitic chert. Volcanic siltstone, sandstone, and conglomerate overlie these siliceous sediments to the north. To the south are coarse andesite and basalt-derived conglomerates. The country rocks are cut by several coarsely augite-phyric mafic sills which, in turn, are cut by Groat dikes.

The Groat deposit is hosted by siliceous sediments and by the southwestern part of the pluton. The most significant mineralized zones (chalcopyrite in quartz stockwork) were drilled by Amoco Canada Petroleum Co. Ltd. in 1970. Five holes were drilled from one set-up at the base of Groat Creek (one vertical and four inclined to the four points of the compass). Intersections in these holes were typically approximately 145 metres averaging 0.25% Cu, 0.5 g/t Au, and 3 g/t Ag (Mehner, 1991). Later drilling by other companies attempted to extend this zone; Texasgulf Canada Ltd. tested alteration and mineralization to the west, on the Goat Hide claim (Forsythe *et al.*, 1977); some holes intersected mineralized intervals, but continuity was not established (J. M. Newell, personal communication, 1995).

The most prominent alteration types on the Groat property are ankerite flooding and silicification. Several zones of intense ankerite alteration and brecciation, 10 to 30 metres wide, cross the deposit

**TABLE 1.**
**METAL ABUNDANCES OF MINERALIZED CORE SAMPLES FROM THE GROAT AND KLAPPAN PROPERTIES**

| Sample Number | Rock Type | *Au | Ag | Cu | *Mo | Pb | Zn | *As | *Sb | *Cs | Ni | *Co | Cd | V | Cr* |
|---|---|---|---|---|---|---|---|---|---|---|---|---|---|---|---|
| | | ppb | ppm | ppm | ppm | ppm | ppm | ppm | ppm | ppm | ppm | ppm | ppm | ppm | ppm |
| | Detection Limit | 2 | 0.3 | 1 | 1 | 3 | 1 | 0.5 | 0.1 | 1 | 1 | 1 | 0.2 | 1 | 1 |
| **Groat Core** | | | | | | | | | | | | | | | |
| GR90-1-22.5 to 25 m | chert, quartz-ankerite-sulphide veined | 54 | 1.1 | 345 | 62 | 19 | 571 | 15 | 3 | <1 | 109 | 7 | 13.8 | 283 | 230 |
| GR90-1-28 to 287.5 m | brecciated & ankerite-flooded chert | 86 | 2.3 | 398 | 18 | 109 | 6205 | 48 | 2.3 | <1 | 31 | 6 | 147 | 45 | 250 |
| GR90-1-45 m | silicified siltstone, pyrite veinlets | 85 | <0.3 | 359 | 5 | 4 | 34 | 3.2 | 0.9 | <1 | 19 | 10 | 0.6 | 25 | 170 |
| GR90-1-67 to 68 m | chert, fracture-filling pyrite | 83 | 0.6 | 662 | 4 | 8 | 53 | 5 | 1.6 | <1 | 13 | 7 | 1.4 | 25 | 180 |
| GR90-1-87 to 88 m | monzodiorite, minor quartz stockwork | 893 | 1.7 | 3536 | 10 | < 3 | 49 | 2.9 | 1.6 | 4 | 11 | 28 | <0.2 | 105 | 44 |
| GR90-2-35 to 35.5 m | monzodiorite, minor chalcopyrite | 110 | 0.4 | 412 | 4 | < 3 | 31 | <0.5 | 1.5 | 2 | 4 | 15 | 0.4 | 121 | 43 |
| GR90-2-57 m | monzodiorite minor qtz veining | 372 | 0.7 | 1581 | 11 | < 3 | 33 | 5.2 | 2.6 | <1 | 5 | 18 | 0.5 | 148 | 35 |
| GR90-2-75 to 77 m | monzodiorite, minor chalcopyrite | 140 | 1.1 | 598 | <1 | < 3 | 49 | 3.5 | 1.8 | 2 | 7 | 17 | 0.7 | 162 | 32 |
| GR90-2-104 to 116 m | recrystalized chert, fracture-filling pyrite | 10 | 1.1 | 218 | 64 | 12 | 48 | 47 | 13 | <1 | 34 | 7 | 0.7 | 134 | 210 |
| **Klappan Core** | | | | | | | | | | | | | | | |
| K80-2-63.6m | quartz vein in altered augite porphyry | 143 | 0.7 | 327 | 10 | 7 | 180 | 13 | 4.4 | <1 | 83 | 25 | 0.9 | 54 | 220 |
| K80-2-94.0m | chlorite-altered augite porphyry | 155 | 1.2 | 478 | 13 | < 3 | 128 | 160 | 6.1 | 5 | 94 | 110 | 0.6 | 99 | 270 |
| K80-2-200.7m | andesitic brx. chlorite+epidote+pyrite | 84 | <0.3 | 27 | <1 | < 3 | 69 | 4.4 | 2 | 3 | 5 | 29 | 0.6 | 135 | 75 |
| K80-3-7.3m | augite porph. basalt : calcite+pyrite | 11 | 0.4 | 60 | <1 | < 3 | 47 | 2.1 | 3.1 | 7 | 45 | 25 | 0.6 | 99 | 240 |
| K80-4-51.6m | augite porph. basalt : calcite+pyrite | 500 | 2.5 | 1361 | <1 | < 3 | 54 | 130 | 11 | 2 | 191 | 42 | 1 | 64 | 570 |

Elements with an asterisk were assayed using instrumental neutron activation (INAA) by ACME Analytical Laboratories Ltd.
Remaining elements were analyzed using inductively coupled plasma emission spectroscopy (ICP) by Activation Laboratories Ltd.

area from east to west (Figure 6). Peripheral to these zones, the pluton and country rock are cut by abundant discrete veins of ankerite and calcite. This carbonate alteration was previously interpreted as pervasive potassium feldspar alteration (McInnis, 1981; Mehner, 1991). Minor quartz stockwork is present throughout the 1991 core and some sedimentary (or volcanic?) units appear to be totally silicified, typically being logged as quartzite. Due to the amount of chert and siliceous siltstone in the Groat country rocks, much of the silica may be locally derived, and "silicified rocks" may be recrystallized chert. Thick zones of quartz stockwork, as described in the Amoco core, were not identified away from the main deposit area. Weak phyllic to argillic alteration appears to be fairly common throughout the intrusive rocks in the deposit area.

Mineralization consists of pyrite and chalcopyrite in stringers, disseminations and quartz and quartz-carbonate veins. Sphalerite and galena are present locally. Results from several assay samples suggest that gold and copper values are higher in the pluton than in its country rocks (Table 1). Mehner (1991) noted a positive correlation between copper, gold, and silver throughout the deposit.

Several similarities between Groat and Red-Chris deposits are evident, despite the apparent difference in their size. These include styles of both alteration (notably ankerite and quartz veining) and mineralization types, as well as their association with coeval and mineralogically similar plutons.

## *KLAPPAN PROPERTY*

The Klappan property is located just off the eastern edge of the study area (Figure 6), west of the Klappan River in a low-lying, tree-covered region with very limited exposure. The claim group, centred on the Eldorado and Bonanza claims, was staked by Texasgulf Canada Ltd. in 1975 in the course of its exploration around the Red-Chris deposit. Esso Minerals Canada optioned the claims and drilled four diamond-drill holes on an induced polarization anomaly (Everett, 1981). In 1995 Homestake Canada Inc. optioned the claims (current property ownership is 55% Homestake Canada Inc. and 45% Falconbridge Ltd.). During August of 1995, Homestake carried out a limited soil and silt sampling program over the property and conducted a brief examination of the 1980 trenches and drill core. The following property description is based on a one-day examination of the drill core, stored on the property, and rare outcrops in the grid area.

Mafic volcanic rocks are exposed in outcrops in the northern part of the claim group and are seen in core with felsic plutonic rocks. The southeastern part of the property is underlain by sediments of the Bowser Lake Group, probably across a fault (as at Red-Chris to the southwest). The most abundant lithology in core and outcrop is augite-phyric basalt. Euhedral augite phenocrysts, 2 to 10 millimetres across, make up 10 to 40% of the rock. They are variably altered to chlorite, often preserving good concentric zoning, and are set in a black to dark green, aphanitic matrix which locally contains calcite or chlorite-filled amygdules.

Massive andesitic breccias crop out in the northwest part of the grid and are below augite basalt in hole K80-2. The breccias consist of angular, feldspar-phyric andesite clasts up to 10 centimetres across, supported in a dark, aphanitic matrix. This unit is similar to breccias described in the northwest Todagin area.

These units are cut by felsic intrusions, seen in drill holes 3 and 4 but not in outcrop. The bottom 17 metres of hole K80-3 is a crowded feldspar porphyry, with 50%, 4 to 8-millimetre feldspar phenocrysts and 10% smaller hornblende phenocrysts. The bottom 30 metres of hole K80-4 intersected fine to medium-grained equigranular granodiorite which appears to be in intrusive contact with augite porphyry.

Alteration and mineralization are intermittent through the core. The volcanic rocks are affected by pervasive but variable chlorite±epidote±pyrite alteration. Locally, epidote and pyrite preferentially replace clasts in the breccia and phenocrysts in the augite porphyry. Spotty potassium feldspar-sericite-calcite alteration was also noted in augite porphyry, in the equigranular granodiorite, and is strong in the crowded feldspar porphyry. Pyrite is disseminated throughout the core and is present in veins, but chalcopyrite is mainly restricted to quartz-pyrite veins. Quartz veins up to 4 centimetres wide are the most common, comprising up to 40% of the core over some 1 to 2-metre intervals. Pyrite and chalcopyrite, where present, are commonly concentrated near the vein walls. White calcite, ankerite, and adularia(?) veins were also observed. Five grab samples were taken from the core and returned 11 to 500 ppb Au and 27 to 1361 ppm Cu (Table 1).

## *SUMMARY OF SAMPLE ASSAY DATA*

During mapping, areas of alteration and mineralization were routinely sampled and assayed for precious and base metal contents. Small areas of gossan, generally on the order of several metres in lateral extent, occur throughout basaltic volcanic rocks in the southwest Todagin area. Disseminated pyrite in trace to minor amounts is the only identifiable sulphide. Assays of five grab samples from individual gossans returned no anomalous metal abundances. Gossanous areas of rhyolitic volcanic rocks with trace, disseminated sulphides were also identified locally, and in some instances chalcedony quartz veins are present. Samples from these areas of alteration also returned no anomalous values.

Locations of the individual samples and their associated assay results are indicated on open file map 1996-4 (Ash *et al.*, 1996).

## CONCLUSIONS

- An early Pliensbachian bimodal basalt-rhyolite volcanic succession is exposed along the northwestern margin of the Bowser Basin in the Tatogga Lake map area.
- On the basis alteration type and lithological association, two distinct styles of porphyry copper-gold mineralization have been recognized in the project area. The first is characterized by intense quartz-ankerite-sericite alteration associated with hornblende quartz diorite to monzonite intrusions surrounded by broad ankerite alteration halos. The second type is confined to the northern half of the project area. It is characterized by pervasive pyritization and silicification associated with rhyolite/felsite dikes and stocks that intrude and epidotize andesite volcaniclastic host rocks. Ankerite is not present in the second type.
- The age of plutonism related to copper-gold mineralization is Early Jurassic (200-198Ma).
- American Bullion Minerals Ltd. has significantly increased potential mineable reserves of copper-gold at the Red-Chris deposit and was also successful in identifying two new zones of copper-gold mineralization.

## ACKNOWLEDGMENTS

Very capable field assistance was provided by Krista Nelson. Many thanks are extended to the staff of American Bullion, including Doug Blanchflower, Theresa Fraser, Brian Thurston, John Deighton and Gordon Allen, for their gracious hospitality and providing information and ideas on the Red-Chris deposit.

Safe and reliable piloting was provided by Mario Chandler and Greg Walz of Vancouver Island Helicopters.

Insights and suggestions provided by Dave Lefebure, Andre Panteleyev, Ron Smyth and Moira Smith during field visits to the area were helpful. The efforts of Howard Tipper and Fabrice Cordey in providing prompt identification of fossil collections is appreciated. This report has been improved by reviews

by John Newell, Derek Brown, Mitch Mihalynuk, Dave Lefebure and Andre Panteleyev.

## REFERENCES


Ash, C.H., Fraser, T.M., Blanchflower, J.D. and Thurston, B.G. (1995): Tatogga Lake Project, Northwestern British Columbia (104H/11, 12); *in* Geological Fieldwork 1994, Grant, B. and Newell, J.M., Editors, *B.C. Ministry of Energy, Mines and Petroleum Resources,* Paper 1995-1, pages 343-358.

Ash, C.H., Stinson, P., Macdonald, R.W.J. and Nelson, K.J. (1996); Geology of the Todagin Plateau (104H/12 NW); *B.C. Ministry of Energy, Mines and Petroleum Resources*, Open File 1996-4. 1:20 000 map.

Bartsch, R.D. (1992): Eskay Creek Area, Stratigraphic Update (104B/9, 10); *in* Geological Fieldwork 1992, Grant, B. and Newell, J.M., Editors, *B.C. Ministry of Energy, Mines and Petroleum Resources,* Paper 1992-1, pages 517-520.

Bartsch, R.D. (1993): A Rhyolite Flow Dome in the Upper Hazelton Group, Eskay Creek Area (104B/9, 10); *in* Geological Fieldwork 1992, Grant, B. and Newell, J.M., Editors, *B.C. Ministry of Energy, Mines and Petroleum Resources,* Paper 1993-1, pages 331-334.

Britton, J.M., Blackwell, J.D. and Schroeter (1989): #21 Zone Deposits, Eskay Creek, Northwestern British Columbia; *in* Exploration in British Columbia 1989, *B.C. Ministry of Energy, Mines and Petroleum Resources,* pages 197-223.

Cooper, M.F. (1978): Geology of the Rose Property Porphyry Copper Occurrence, Northwestern British Columbia; unpublished M.Sc thesis, *Queen's University*, 230 pages.

Cordey, F. (1995): Report on Radiolarians; Report Number FC95-BCGSB-1, *B.C. Ministry of Energy, Mines and Petroleum Resources*, unpublished internal report, 4 pages.

Evenchick, C.A. (1991): Jurassic Stratigraphy of East Telegraph Creek and West Spatsizi Map Area, British Columbia; *in* Current Research, Part A, *Geological Survey of Canada*, Paper 91-1A, pages 155-162.

Evenchick, C.A. and Green, G.M. (1990): Structural Style and Stratigraphy of Southwest Spatsizi Map Area, British Columbia; *in* Current Research, Part F, *Geological Survey of Canada*, Paper 90-1F, pages 135-144.

Evenchick, C.A. and Thorkelson, D.J. (1993): Geology, Spatsizi River, British Columbia (104H); *Geological Survey of Canada*, Open File 2719, scale 1:250 000.

Everett, C.C. (1981): Diamond Drill Hole Report on the Eldorado, Bonanza, Ben, Saloon, Little Joe, Dude and Hoss Mineral Claims; *B.C. Ministry of Energy, Mines and Petroleum Resources*, Assessment Report 9132.

Forsythe, J.R., Peatfield, G.R., Gasteiger, W.A. and Donnelly, D.A. (1977): Report on Geochemical and Geophysical Surveys, Diamond Drilling and Supporting Work; *B.C. Ministry of Energy, Mines and Petroleum Resources,* Assessment Report 6541.

Friedman, R. M. (1995): Current Research at the UBC Geochronology Laboratory: Progress Report of 1994-1995 U-Pb Dating for the British Columbia Geological Survey Branch; *Department of Geological Sciences, University of British Columbia*, in-house report, 17 pages.

Gabrielse, H. and Tipper, H.W. (1984): Bedrock Geology of Spatsizi Map Area (104H); *Geological Survey of Canada*, Open File 1005, Scale 1:125 000.

Green, G.M. (1991): Detailed Sedimentology of the Bowser Lake Group, Northern Bowser Basin, British Columbia; *in* Current Research, Part A, *Geological Survey of Canada*, Paper 91-1A, pages 187-195.

Leitch, C.H.B. and Elliott, T.M. (1976): Geology and Mineralization, Red-Chris Property; unpublished internal report, *Texasgulf Inc*., 28 pages.

McInnis, M.D. (1981) Drilling Report on the GJ & Spike 1 and 2 Claims; B.C. *Ministry of Energy, Mines and Petroleum Resources,* Assessment Report 9773.

Mehner, D.T. (1991) Assessment Report on Diamond Drilling, Contour Soil Sampling and Geophysical Surveys of the GJ Property; *B.C. Ministry of Energy, Mines and Petroleum Resources,* Assessment Report 20933.

Newell, J.M. and Peatfield, G.R. (in press): The Red-Chris Porphyry Copper-Gold Deposit; *in* Porphyry Deposits of the Northwestern Cordillera of North America, Schroeter, T.G., Editor, *Canadian Institute of Mining, Metallurgy and Petroleum*, Special Volume 46.

Panteleyev, A. (1973): Chris; *in* Geology, Exploration and Mining in British Columbia 1972; *B.C. Ministry of Energy, Mines and Petroleum Resources*, pages 535-536.

Panteleyev, A. (1975): Windy, Red, Chris, Sus; *in* Geology, Exploration and Mining in British Columbia 1974; *B.C. Ministry of Energy, Mines and Petroleum Resources*, pages 340-343.

Poulton, T.P., Callomon, J.H. and Hall, R.L. (1991): Bathonian through Oxfordian (Middle and Upper Jurassic) Marine Macrofossil Assemblages and Correlations, Bowser Lake Group, West-central Spatsizi Map Area, Northwestern British Columbia; *in* Current Research, Part A, *Geological Survey of Canada*, Paper 91-1A, pages 59-63.

Ricketts, B.D. (1990): A Preliminary Account of Sedimentation in the Lower Bowser Lake Group, Northern British Columbia; *in* Current Research, Part F, *Geological Survey of Canada*, Paper 90-1F, pages 145-150.

Ricketts, B.D. and Evenchick, C.A. (1991): Analysis of the Middle to Upper Jurassic Bowser Basin, Northern British Columbia; *in* Current Research, Part A, *Geological Survey of Canada*, Paper 91-1A, pages 65-73.

Schmitt, H.R. (1977): A Triassic-Jurassic Granodiorite Monzodiorite Pluton South-east of Telegraph Creek, B.C.; unpublished B.Sc. thesis, *University of British Columbia*, 79 pages.

Schink, E.A. (1977): Geology of the Red-Chris Porphyry Copper Deposit, Northwestern British Columbia; unpublished M.Sc. thesis, *Queen's University*, 211 pages.

Souther, J.G. (1972): Telegraph Creek Map-area, British Columbia; *Geological Survey of Canada*, Paper 71-44, 38 pages and Map 11-1971.

Thorkelson, D.J. (1992): Volcanic and Tectonic Evolution of the Hazelton Group in Spatsizi River (104H) Map Area, North-central British Columbia; unpublished Ph.D. thesis; *Carleton University*, 281 pages.

Tipper, H.W. (1995): Report on Jurassic Fossils from Map Areas 104H/12 and 104/H9 in Northern British Columbia; Report Number J3-1995-HWT, *Geological Survey of Canada*, unpublished internal report, 3 pages.

# AGE OF HOST STRATA VERSUS MINERALIZATION AT ERICKSEN-ASHBY: A SKARN DEPOSIT

By Mitchell G. Mihalynuk, and W. (Bill) J. McMillan, B.C. Geological Survey Branch,
James K. Mortensen and Fiona C. Childe, University of British Columbia
and Michael, J. Orchard, Geological Survey of Canada

*KEYWORDS*: Ericksen-Ashby, skarn, Tulsequah, massive sulphide, zinc, lead, radiogenic isotopes, uranium, geochronology, conodont, biochronology

## INTRODUCTION

The Ericksen-Ashby deposit is located on the sharp northern ridge of Mount Ericksen, about 64 kilometres east of Juneau, Alaska and 130 kilometres south of Atlin in northwestern British Columbia (Figure 1). It is part of a mineralized belt that contains the Tulsequah Chief and Big Bull volcanogenic massive sulphide deposits within 12 kilometres along strike to the north, and was previously interpreted as this type of deposit (e.g. Payne, 1979). Originally discovered in 1929, it has received sporadic assessment work, including surface and underground drilling programs.

Strata hosting the deposit are different from those at both the Tulsequah Chief and Big Bull deposits. However, the Ericksen-Ashby deposit has generally been thought of as correlative, with stratigraphic differences accounted for by rapid facies changes, typical in volcanic arc environments. Most of these strata were originally considered to be Late Triassic in age (Souther, 1971). Late Carboniferous (Moscovian) fossils collected by Nelson and Payne (1984) from a structural high in the Tulsequah camp were the first clear indication that rocks at the Tulsequah Chief must be Paleozoic and not Triassic. It was not until a decade later that the first definitive age of the Tulsequah Chief deposit was obtained by U-Pb dating of zircons in the coarse rhyolite breccia that is included within the orebodies (353 +14 -7 Ma, Sherlock *et al.*, 1994).

In contrast, there were no age data for hostrocks or mineralization at the Ericksen-Ashby deposit prior to this study. Some lead isotope data are reported for the deposit (Godwin *et al.*, 1988), but are interpreted based on a Jurassic age for the host strata, and no description of the sample site or material analyzed is available. Lead isotope data needed to be reevaluated and augmented in light of new age constraints.

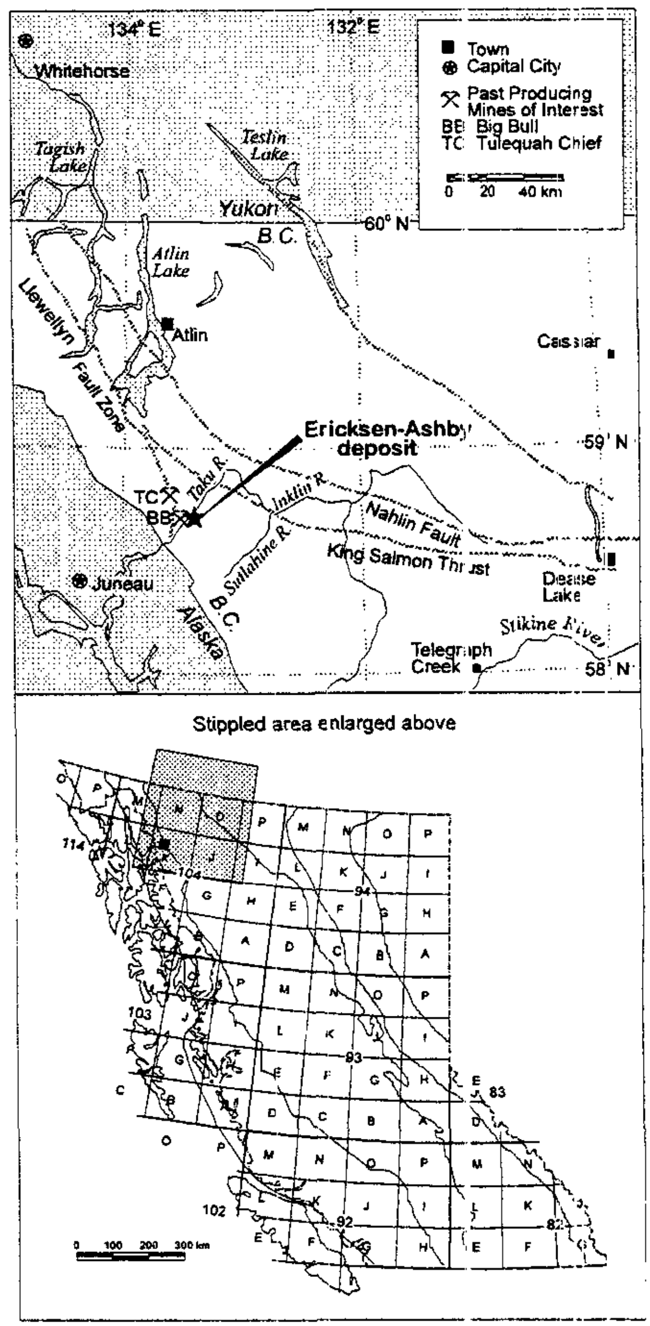


Figure 1. Location of the Ericksen-Ashby deposit in northwestern British Columbia.

## ERICKSEN-ASHBY GEOLOGY

Payne (1979) produced excellent detailed geology and descriptions of mineralization textures at the Ericksen-Ashby deposit during his evaluation of the property. The generalized geology that follows is based primarily on his work as well as brief visits (six man-days in the immediate area, two at the deposit) as part of a BCGS regional mapping program in 1994 (Mihalynuk *et al.*, 1994a, b, 1995a, b).

Strata on Mount Ericksen are dominated by pyroxene-phyric andesite or basaltic andesite and gabbro. Near the north end of the ridge, the volcanic strata are interrupted by two interlayers comprised of chert and carbonate (Figure 2). They are each approximately 100 metres thick, but strong internal deformation by close to isoclinal folds does not permit estimates of original stratigraphic thickness. The structurally highest sedimentary unit bifurcates northward to envelop andesite of approximately the same thickness. It also includes a thin layer of rhyolite. A subjacent, tabular, porphyritic quartz monzonite, 50 to 100 metres thick (but in at least one place up to 350 m thick), known as the Ericksen sill, thermally metamorphoses the entire section on Mount Ericksen.

All massive sulphide mineralization of economic interest occurs in the upper sedimentary division (SED-2 of Payne, 1979). Within SED-2, sulphide layers with high zinc, lead and silver contents occur above a thin, discontinuous rhyolite layer. Some sulphide pods and lenses are discordant, clearly related to late skarn alteration and/or remobilization of the stratiform sulphides.

Field evidence predominantly points to a volcanogenic origin for the deposit. Like the volcanogenic massive sulphides to the immediate north, it is closely associated with a felsic tuff horizon. Mineralization is dominantly stratiform and mainly restricted to the single SED-2 interval (Payne, 1979). Futhermore, a lithologically similar calcareous layer between SED-2 and the Ericksen sill is unmineralized although, given its closer proximity to the intrusion, it would seem a more likely host for skarn mineralization. Thus, Payne interpreted the Ericksen-Ashby as primarily a volcanogenic massive sulphide deposit with partial late remobilization due to the Ericksen sill. While our field observations are consistent with those of Payne and his interpretation, laboratory analytical data from galena from the massive sulphide lenses are incompatible with a volcanogenic origin of the galena

## BIOCHRONOLOGY

Samples were collected for microfossil determination to help clarify the question of correlation between Ericksen-Ashby and massive sulphide stratigraphy of the Tulsequah Chief and Big Bull deposits. Only one sample was productive. It was from a 12-metre section of SED-2, comprised of fine-grained grey limestone with

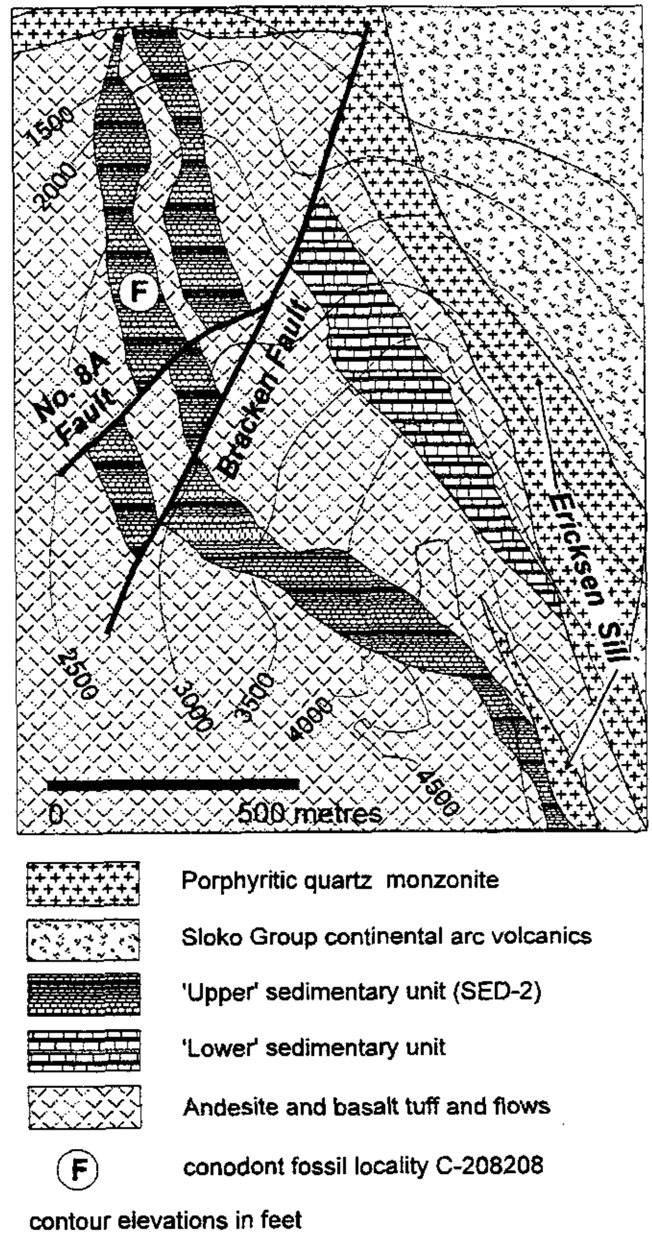


Figure 2. Stylized geology of the Ericksen-Ashby deposit, modified after Payne (1979) and Mihalynuk *et al.* (1995). For more detailed deposit geology see Figure 4 of Payne (1979). The U-Pb isotopic age determination sample site is 1.5 kilometres south of the southeast corner of the figure.

interlayered chert (sample C-208208, see location F, Figure 2). It yielded two deformed conodont fragments with a colour alteration index of 6. These suggest a Late Carboniferous to Permian age, although precise age remains elusive due to poor preservation of the conodonts and intense structural disruption. Nevertheless, the strata are definitely Paleozoic, not Triassic.

## GEOCHRONOLOGY

A sample of pink, blocky to platy weathering, quartz

(15%) - feldspar (20%) porphyry was collected from near the base of the Ericksen sill for U-Pb geochronology (Figure 2). In hand sample the feldspars are zoned, displaying both twinned plagioclase (polysynthetic and simple) as well as untwinned crystals, possibly intergrowths of orthoclase and plagioclase. Mafic phenocrysts include biotite booklets (5%) and hornblende prisms (0.5%). The sample is very fresh and yields good quality zircons.

### *ANALYTICAL TECHNIQUES AND RESULTS*

Sample preparation and U-Pb analyses were carried out at the Geochronology Laboratory of the University of British Columbia. The sample was processed using techniques as described in Mortensen *et al.* (1995). Analytical results are presented in Table 1. Two multigrain zircon fractions were analysed. Both yield concordant analyses (Figure 3), with the best estimate for the crystallization age for the unit given by the total overlap of the two error ellipses with concordia, at 53.5±0.7 Ma. This age is nearly identical to U-Pb age determinations from Sloko Group volcanic strata (Mihalynuk and Friedman, unpublished) which crop out in fault contact with older parts of the succession hosting the Ericksen-Ashby deposit.

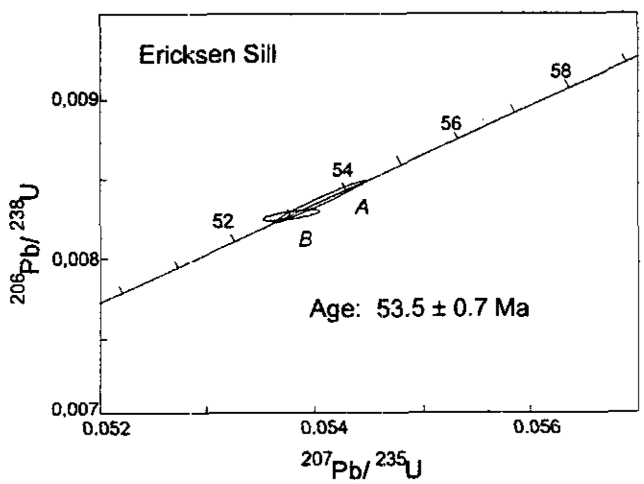


Figure 3. Concordia diagram showing the results of two zircon fractions from the Ericksen sill.

## LEAD ISOTOPE SYSTEMATICS

A sample of mineralized material was collected from SED-2 about 60 metres above the fossil locality. It is fine to medium-grained, massive sphalerite (60%) and galena (20%) with unidentified, fine-grained gangue minerals comprising the remainder of the sample. Galena from this sample was analyzed for its lead isotopic composition. Analytical results of two fractions of galena

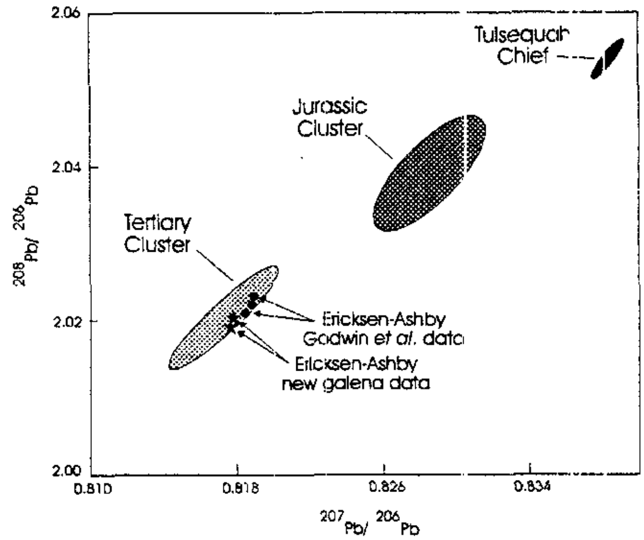


Figure 4. $^{207}Pb/^{206}Pb$ *vs.* $^{208}Pb/^{206}Pb$ diagram for galena from the Erickson-Ashby deposit, references to sources for Tertiary, Jurassic and Tulsequah Chief clusters are given in the text.

from the sample are presented in Table 2, and in a $^{207}Pb/^{206}Pb$ *versus* $^{208}Pb/^{206}Pb$ diagram in Figure 4. The lead isotopic signature of Ericksen-Ashby is compared with the signatures of Jurassic and Tertiary mineralizing epochs in the Stikine Terrane (Alldrick *et al.*, 1987, and UBC Geochronology Laboratory, unpublished data), as well as mineralization at the Devono-Mississippian Tulsequah Chief volcanogenic massive sulphide deposit (Childe, 1994). These data clusters show an increasingly more radiogenic lead signature with time in the Stikine Terrane. Late Carboniferous to Permian syngenetic mineralization in the Stikine Terrane would be expected to have a lead signature intermediate to that of Devono-Mississippian and Jurassic mineralization. However, the lead isotopic signature of galena from the Ericksen-Ashby deposit plots near the centre of the cluster defined by Tertiary mineralization.

## DISCUSSION

Remobilization, metamorphism or skarn alteration of a pre-existing Paleozoic massive sulphide deposit (for example, Höy and Godwin, 1986) would not reset the lead isotopic signature of the galena within this lead-rich deposit. The lead signature is unequivocally Tertiary. In consideration of the 53.5±0.7 Ma age of the Ericksen sill which is responsible for skarn alteration at the deposit it must be concluded that most or all of the lead was deposited during a Tertiary mineralizing event. Thus, Pb-Zn-Ag mineralization at the Ericksen-Ashby deposit is primarily a Tertiary skarn hosted by Late Carboniferous to Permian volcanosedimentary strata. Despite some field evidence to the contrary, it is apparently not a syngenetic deposit.

## TABLE 1. U-PB ANALYTICAL RESULTS FOR SAMPLE MMI-94-18-9

| Fraction[1] | Wt. mg | U ppm | Pb[2] ppm | $^{206}Pb/^{204}Pb$ measured | Pb[3] pg | %$^{208}Pb$ | $^{206}Pb/^{238}U$[4] | $^{207}Pb/^{235}U$[4] | $^{207}Pb/^{206}Pb$[4] | $^{207}Pb/^{206}Pb$ age[5] (Ma) |
|---|---|---|---|---|---|---|---|---|---|---|
| A: n5, +134, a | 0.313 | 810 | 7 | 2009 | 66 | 10.3 | 0.008339±0.73 | 0.05414±0.77 (0.9701) | 0.04709±0.19 | 53.7 ±8.9 |
| B: n5, 74-134, u | 0.246 | 858 | 7 | 537 | 211 | 10.8 | 0.008260±0.18 | 0.05362±0.49 (0.7152) | 0.04708±0.38 | 53.2 ±18.0 |

1 n5 = non-magnetic at 5 degrees side tilt on Frantz isodynamic separator; grain size given in microns; u = unabraded; a = abraded

2 radiogenic Pb; corrected for blank, initial common Pb, and spike

3 common lead corrected for spike and fractionation

4 corrected for blank Pb and U, and common Pb; errors are in percent at a 1σ level; correlation coefficient in parentheses

5 errors are in Ma at a 2σ level

## TABLE 2. COMMON LEAD DATA FOR THE ERICKSEN-ASHBY DEPOSIT

| Sample | Mineral | $^{206}Pb/^{204}Pb$ (% error)[1] | $^{207}Pb/^{204}Pb$ (% error)[1] | $^{208}Pb/^{204}Pb$ (% error)[1] | $^{207}Pb/^{206}Pb$ (% error)[1] | $^{208}Pb/^{206}Pb$ (% error)[1] |
|---|---|---|---|---|---|---|
| EA a | galena | 19.073 (0.010) | 15.594 (0.009) | 38.515 (0.011) | 0.81761 (0.004) | 2.0194 (0.004) |
| EA b | galena | 19.111 (0.007) | 15.627 (0.006) | 38.618 (0.007) | 0.81770 (0.003) | 2.0208 (0.002) |

[1] Errors are quoted at the 2σ (95% confidence) level, values are corrected for instrument fractionation by normalization based on replicate analyses of the NBS-981 standard.

## ACKNOWLEDGMENTS

Sandy Sears helped in mapping and sample collection at the Ericksen-Ashby deposit. Dani Alldrick kindly provided an unsolicited and helpful review of the paper.

## REFERENCES

Alldrick, D.J., Gabites, J.E., and Godwin, C.I. (1987): Lead Isotope Data from the Stewart Mining Camp (104B/1); *in* Geological Fieldwork 1986, *B.C. Ministry of Energy, Mines and Petroleum Resources,* Paper 1987-1, pages 93-102.

Childe, F. (1994): Chronology and Radiogenic Isotope Studies of the Kutcho, Granduc, Anyox and Tulsequah Chief Volcanogenic Massive Sulphide Deposits; *in* Volcanogenic Massive Sulphide Deposits of the Cordillera Project, Second Annual Report, *Mineral Deposit Research Unit,* The University of British Columbia.

Godwin, C.I., Gabites, J.E. and Andrew, A. (1988): Leadtable: A Galena Lead Isotope Data Base for the Canadian Cordillera, with a Guide to its Use by Explorationists; *B.C. Ministry of Energy, Mines and Petroleum Resources*, Paper 1988-4, 188 pages.

Höy, T. and Godwin, C.I. (1986): Significance of a Cambrian Date from Galena Lead-isotope Data for the Stratiform Cottonbelt Deposit in the Monashee Complex, Southeastern British Columbia; *Canadian Journal of Earth Sciences*, Volume 25, pages 1534-1541.

Mihalynuk, M.G., Smith, M.T. Hancock, K.D. and Dudka, S. (1994a): Regional and Economic Geology of the Tulsequah River and Glacier Areas (104K/12 & 13); *in* Geological Fieldwork 1993, Grant, B. and Newell, J.M., Editors, *B.C. Ministry of Energy, Mines and Petroleum Resources*, Paper 1994-1, pages 171-197.

Mihalynuk, M.G., Smith, M.T. Hancock, K.D., Dudka, S. and Payne, J. (1994b): Tulsequah River and Glacier Areas

(104K/12 & 13); *B.C. Ministry of Energy, Mines and Petroleum Resources*, Open File 1994-3.

Mihalynuk, M.G., Meldrum, D., Sears, S. and Johannson, G. (1995a): Geology and Mineralization of the Stuhini Creek Area (104K/11); *in* Geological Fieldwork 1994, Grant, B. and Newell, J.M., Editors, *B.C. Ministry of Energy, Mines and Petroleum Resources*, Paper 1995-1, pages 321-342.

Mihalynuk, M.G., Meldrum, D.G., Sears, W.A., Johannson, G.G., Madu, B.E., Vance, S., Tipper, H.W. and Monger, J.W.H. (1995b): Geology and Lithogeochemistry of the Stuhini Creek Map Area (104K/11); *B.C. Ministry of Energy, Mines and Petroleum Resources*, Open File 1995-1.

Mortensen, J.K., Gosh, D. and Ferri, F. (1995):.U-Pb Geochronology of Intrusions Associated with Cu-Au Porphyry Deposits in the Canadian Cordillera; *in* Canadian Institute of Mining and Metallurgy, Special Volume 46, in press.

Nelson J. and Payne, J.G. (1984): Paleozoic Volcanic Assemblages and Volcanogenic Massive Sulphide Deposits near Tulsequah, British Columbia; *Canadian Journal of Earth Sciences*, Volume 21, pages 379-381.

Payne, J.G. (1979): Geology Report for Semco Mining Corporation on the Ericksen-Ashby Claims; *B.C. Ministry of Energy, Mines and Petroleum Resources*, Assessment Report 7707.

Sherlock, R., Childe, F., Barrett, T.J., Mortensen, J.K., Chandler, T., Lewis, P., McGuigan, P., Dawson, G.L. and Allen, R. (1994): Geological Investigations of the Tulsequah Chief Massive Sulphide Deposit, Northwestern British Columbia; *in* Geological Fieldwork 1993, Grant, B. and Newell, J.M., Editors, *B.C. Ministry of Energy, Mines and Petroleum Resources*, Paper 1994-1, pages 373-379.

Souther, J. G. (1971): Geology and Mineral Deposits of the Tulsequah Map-area, British Columbia; *Geological Survey of Canada*, Memoir 362, 84 pages.

# NOTES

# 1995 REGIONAL GEOCHEMICAL SURVEY PROGRAM: REVIEW OF ACTIVITIES

By Wayne Jackaman, Stephen Cook, Ray Lett, Steve Sibbick and Paul Matysek

*KEYWORDS*: Regional Geochemical Survey, reconnaissance, multi-element, stream sediment, lake sediment, stream water, lake water, Gataga, Nass River, Terrace, Prince Rupert, Cry Lake, Pinchi Lake.

## INTRODUCTION

Work conducted in 1995 as part of the Regional Geochemical Survey Program (RGS) included :

- The publication of previously unreleased instrumental neutron activation stream sediment analytical data from the Terrace (NTS 103I), Prince Rupert (NTS 103J) and Nass River (NTS 103O/P) map sheets.
- A reconnaissance-scale stream sediment and water survey in the Cry Lake map sheet (NTS 104I).
- A reconnaissance-scale stream sediment and water survey over parts of the western margin of the northern Rocky Mountain Trench (NTS 94L).
- The completion of a joint federal-provincial lake sediment and water survey in the northwest corner of the Fort Fraser map sheet (NTS 93K).

## 1995 RGS RELEASE (103I, J, O, P)

On June 2, 1995, RGS open files B.C. RGS 42 and 43 were published for NTS map sheets 103I/J and 103O/P. Originally conducted in 1978, the surveys involved the systematic collection of stream sediments and waters from over 3800 sample sites covering an area of approximately 32 000 square kilometres. The original survey results were published in 1979 and included analytical determinations for 13 metals in stream sediments, and uranium, fluoride and pH in stream waters. In the early 1990s the archived sediment pulps were analyzed using instrumental neutron activation for gold and 25 other metals. This new, previously unreleased information, together with original field and analytical data, was released as open files B.C. RGS 42 and B.C. RGS 43 (Matysek and Jackaman, 1995; Jackaman and Matysek, 1995).

These open file publications incorporated digital information on catchment basins which are used to improve RGS data integration with other polygonal and point databases, as well as enhance geochemical patterns and trends on hard-copy maps. Using results from the surveys, Matysek and Jackaman (1996, this volume) present an example of how catchment basins can be used to identify and evaluate RGS anomalies. Digital data files of the catchment basin polygons have been included as part of each data package.

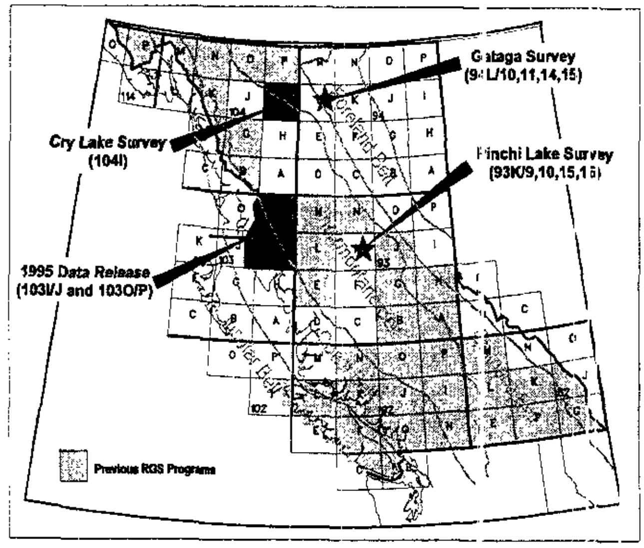


Figure 1. Location map of 1995 RGS projects.

A total of 989 claim units were recorded from June to August 1995 in map sheets 103I, 103J and 103O/P. Although RGS anomalies were staked immediately following the release, numerous areas with anomalous concentrations of base and precious metals remain unstaked as of November 1, 1995.

## CRY LAKE SURVEY (104I)

Located to the east of Dease Lake, the Cry Lake map area (NTS 104I) is relatively unexplored and has significant potential for lode gold, porphyry copper-gold and base metal massive sulphide mineralization. Underlain by the Stikinia, Cache Creek and Slide Mountain terranes, the map area contains 107 recorded mineral occurrences including the Kutcho Creek massive sulphide deposit (MINFILE 104I, 1996).

McElhanney Consulting Limited (Vancouver) was selected by competitive bid to conduct a reconnaissance-scale regional geochemical survey during September, 1995. Stream sediment samples, stream water samples and field observations were systematically collected from 1159 sites over a total area of 13 200 square kilometres. Ministry representation by the senior author was maintained throughout the survey to ensure all aspects of sample collection, data recording, sample drying, packing and shipping were in accordance with standards set by the National Geochemical Reconnaissance Program (Ballantyne, 1991). Stream sediment samples will be analyzed for precious and base metals, pathfinder elements and rare earths (Table 1). Stream water samples will be analyzed for pH, fluoride, uranium and sulphate. Survey results are expected to be released in the spring of 1996.

**TABLE 1. CURRENT RGS ANALYTICAL SUITE FOR STREAM AND LAKE SEDIMENTS**

| Element | Analytical Method | Detection Limit | Unit |
|---|---|---|---|
| Antimony | AAS/INA | 0.2/0.1 | ppm |
| Arsenic | AAS/INA | 0.2/0.5 | ppm |
| Barium | INA | 50 | ppm |
| Bismuth | AAS | 0.2 | ppm |
| Bromine | INA | 0.5 | ppm |
| Cadmium | AAS | 0.2 | ppm |
| Cerium | INA | 3 | ppm |
| Cesium | INA | 1 | ppm |
| Chromium | INA | 5 | ppm |
| Cobalt | AAS/INA | 2/1 | ppm |
| Copper | AAS | 2 | ppm |
| Fluorine | ION | 40 | ppm |
| Gold | INA | 2 | ppb |
| Hafnium | INA | 1 | ppm |
| Iron | AAS/INA | 0.02/0.01 | % |
| Lanthanum | INA | 0.5 | ppm |
| Lead | AAS | 2 | ppm |
| LOI | GRAV | 1.0 | % |
| Lutetium | INA | 0.05 | ppm |
| Manganese | AAS | 5 | ppm |
| Mercury | AAS | 10 | ppb |
| Molybdenum | AAS/INA | 1/1 | ppm |
| Nickel | AAS/INA | 2/20 | ppm |
| Rubidium | INA | 5 | ppm |
| Samarium | INA | 0.1 | ppm |
| Scandium | INA | 0.1 | ppm |
| Silver | AAS | 0.2 | ppm |
| Sodium | INA | 0.01 | % |
| Tantalum | INA | 0.5 | ppm |
| Terbium | INA | 0.5 | ppm |
| Thorium | INA | 0.2 | ppm |
| Tungsten | INA | 1 | ppm |
| Uranium | INA | 0.5 | ppm |
| Vanadium | AAS | 5 | ppm |
| Ytterbium | INA | 0.2 | ppm |
| Zinc | AAS | 2 | ppm |

## GATAGA SURVEY (94L/7, 8, 9, 10, 11, 14, 15)

Located in the Muskwa Ranges of the northern Rocky Mountains, the Gataga regional geochemical survey was conducted as part of a multi-disciplinary examination of this portion of the Kechika Basin (Ferri *et al.*, 1996, this volume), an area which is host to numerous sedimentary exhalitive barite-lead-zinc deposits. Conducted by Ministry personnel, the survey involved the systematic collection of stream sediment and water samples from 186 sites covering an area of 1200 square kilometres. Stream sediment analyses are listed in Table 1. Water samples will also be analyzed for trace and major elements by ICP-MS in addition to pH, fluoride, uranium and sulphate.

As part of a review of geochemical problems faced by mining companies currently exploring for base metal deposits in the Kechika Trough, other geochemical research conducted in the region included a detailed study of spring water chemistry and orientation work on known barite occurrences. These projects were initiated in the Driftpile Creek area of the northern Rocky Mountains during the 1994 field season (Lett and Jackaman, 1994).

## PINCHI LAKE SURVEY (93K/9, 10, 15, 16)

The Pinchi Lake regional lake sediment and water survey was conducted in October, 1995 over four 1:50 000 NTS map areas (93K/9, 10, 15, 16) in the northeast quadrant of the Fort Fraser map area. The survey was carried out jointly by the British Columbia Geological Survey Branch and the Geological Survey of Canada under the auspices of the Mineral Development Agreement (MDA). The survey area straddles a terrane boundary and is bisected by the Pinchi fault zone. To the northeast, early Mesozoic Takla Group rocks of the Quesnel Terrane have potential for porphyry copper-gold targets (Nelson *et al.*, 1991). To the southwest are late Paleozoic to early Mesozoic pelagic sediments, carbonates and ultramafic rocks of the Cache Creek Terrane (Ash and Macdonald, 1993). Felsic intrusive rocks of the Middle Jurassic Shass Mountain pluton (Bellefontaine, 1995) also outcrop in the extreme southwestern corner of the survey area.

Lake sediments and waters were obtained from 413 sites at a sampling density of approximately one site per 9.1 square kilometres. Lake sediment analyses are listed in Table 1. Waters will be analyzed for pH, uranium, fluoride and sulphate. As well, an additional lake water sample was collected at every second site for ICP-MS analysis of trace and major elements.

The Pinchi Lake survey is a contribution to the ongoing Regional Geochemical Survey (RGS) lake sediment coverage of the northern Interior Plateau, providing baseline geochemical data for mineral exploration and environmental studies. Previous surveys in the Nechako River map area (NTS 93F; Cook and Jackaman, 1994) to the south, conducted in 1993, were successful in delineating areas of known mineralization and in revealing locations of new mineralized zones such as the Tsacha gold prospect. In addition, baseline regional data on the distribution of mercury in lake sediments along the Pinchi fault zone should provide valuable information on the natural concentration range of mercury in the environment. The data release is scheduled for summer, 1996.

## REFERENCES


Ash, C.H. and Macdonald, R.W.J. (1993): Geology, Mineralization and Lithogeochemistry of the Stuart Lake Area, Central British Columbia (parts of 93K/7, 8, 10 and 11); *in* Geological Fieldwork 1992, Grant, B. and Newell, J.M., Editors, *B.C. Ministry of Energy, Mines and Petroleum Resources*, Paper 1993-1, pages 69-86.

Ballantyne, S.B., (1991): Stream Geochemistry in the Canadian Cordillera: Conventional and Future Applications for Exploration; *in* Exploration Geochemistry Workshop, *Geological Survey of Canada*, Open File 2390.

Bellefontaine, K. (1995): Geological Complilation of Northeast British Columbia (Vanderhoof to Aiken Lake)-NTS 93F,K,N; 94C; *B.C. Ministry of Energy, Mines and Petroleum Resources*, Open File 1995-24.

Cook, S.J. and Jackaman, W. (1994b): Regional Lake Sediment and Water Geochemistry of part of the Nechako River Map Area (93F/2,3; 93F/6,11,12,13,14); *B.C. Ministry of Energy, Mines and Petroleum Resources*, Open File 1994-19.

Ferri, F., Rees, C. and Nelson, J.L. (1996): Geology and Mineralization of the Gataga Mountain Area, Northern Rocky Mountains; *in* Geological Fieldwork 1995, Grant, B. and Newell, J.M., Editors, *B.C. Ministry of Energy, Mines and Petroleum Resources*, Paper 1996-1, this volume.

Jackaman, W. and Matysek, P.F. (1995): British Columbia Regional Geochemical Survey - Nass River (NTS 103O/P); *B.C. Ministry of Energy, Mines and Petroleum Resources*, BC RGS 43.

Lett R.E., and Jackaman, W. (1994): Application of Spring-water Chemistry to Exploration in the Driftpile Creek Area, Northwestern B.C.; *in* Geological Fieldwork 1994, Grant, B. and Newell, J.M., Editors, *B.C. Ministry of Energy, Mines and Petroleum Resources*, Paper 1995-1, pages 269-275.

Matysek, P.F. and Jackaman, W. (1996): B.C. Regional Geochemical Survey Anomaly Recognition, An Example Using Catchment Basin Analysis; *in* Geological Fieldwork 1995, Grant, B. and Newell, J.M., Editors, *B.C. Ministry of Energy, Mines and Petroleum Resources*, Paper 1996-1, this volume.

Matysek, P.F. and Jackaman, W. (1995): British Columbia Regional Geochemical Survey - Prince Rupert/Terrace (NTS 103I/J); *B.C. Ministry of Energy, Mines and Petroleum Resources*, BC RGS 42.

MINFILE NTS104I (1996): Mineral Occurrence Map; *B.C. Ministry of Energy, Mines and Petroleum Resources*, MINFILE, in print.

Nelson, J.L., Bellefontaine, K.A., Green, K.C. and MacLean, M.E. (1991): Regional Geological Mapping near the Mount Milligan Copper-Gold Deposit (93K/16, 93N/1); *in* Geological Fieldwork 1990, Grant, B. and Newell, J.M., Editors, *B.C. Ministry of Energy, Mines and Petroleum Resources*, Paper 1991-1, pages 89-110.

NOTES

# B.C. REGIONAL GEOCHEMICAL SURVEY ANOMALY RECOGNITION, AN EXAMPLE USING CATCHMENT BASIN ANALYSIS (103I, 103J)

By Paul Matysek and Wayne Jackaman

*KEYWORDS*: Regional Geochemical Survey, geographic information system, catchment basins, stream sediment, stream water, Nass River.

## INTRODUCTION

Since 1976, the Regional Geochemical Survey Program (RGS) has presented stream sediment and water geochemistry data by grouping the data values into distinct percentile ranges and plotting symbols that represent the range. These symbol maps have been useful for the quick appraisal of regional trends and clustering of data. However, they do not account for the considerable variability in trace element concentration encountered with different lithologies. Beginning in 1990, a number of methodologies for integrating bedrock geology with stream sediment geochemistry using a geographic information system (GIS) were examined (Bartier and Keller, 1991; Sibbick, 1994; Jackaman *et al.*, 1995). They concluded that using the catchment basins of each sample site to define its zone of influence (Bonham-Carter and Goodfellow, 1986; Bonham-Carter *et al.*, 1987) provided a logical means for integrating bedrock geology and stream sediment geochemistry. As a result, this method can be used to:

- Reclassify the geological influence on each sample based on its source area.
- Redefine the thresholds which separate anomalous from background populations.
- Define metal concentrations in basins hosting known mineral occurrences.
- Define the actual coverage of a survey.

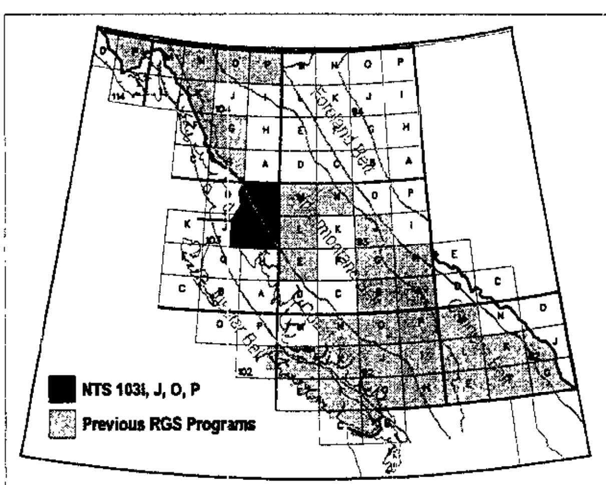


Figure 1. Location map of RGS programs.

RGS open file data packages B.C. RGS 42 (NTS map sheets 103I and 103J) and B.C. RGS 43 (NTS map sheets 103O and 103P) released on June 2, 1995 incorporated catchment basins to improve data integration with other polygonal and point geoscience databases, as well as enhance geochemical patterns and trends on hard-copy maps (Matysek and Jackaman, 1995, Jackaman and Matysek, 1995). Using data from open file B.C. RGS 42 and existing GIS technologies, this paper will present an example of how stream sediment geochemistry can be integrated with digital catchment basins, MINFILE data and bedrock geology to identify and interpret RGS anomalies.

## BACKGROUND

### *SURVEY SUMMARY*

Open file B.C. RGS 42 presents field and analytical data from a 1978 joint federal-provincial stream sediment and water survey conducted in the Terrace (103I) and Prince Rupert (103J) map areas (Figure 1). Stream sediment and water samples were systematically collected from 2128 sites at an average density of one site per 8 square kilometres. The original open file, published in 1979, included analytical determinations for 13 metals in stream sediments and uranium, fluoride and pH in stream waters. In the early 1990s the archived sediment pulps were analyzed using instrumental neutron activation for gold and 25 other metals. This new, previously unreleased information, together with original field and analytical data was released as part of open file B.C. RGS 42 on June 2, 1995. This was the first time that digital catchment basins were included with the release packages.

### *CATCHMENT BASIN DELINEATION*

Catchment basins are defined by the topographic height of land that separates a stream from surrounding streams. The resulting polygons are assumed to represent the metal determination of a single stream sediment or water sample collected at the outlet of the catchment basin. For map sheets 103I and 103J, a total of 2128 catchment basins were delineated from NTS 1:50 000 maps by hand tracing basin polygons onto mylar overlays.

The resulting polygons were digitized, with each polygon labeled to correspond to its unique RGS sample number. On occasion, nested polygons were produced where two samples were taken from successive sites on the same stream; in these cases the downstream polygon was defined to end at the upstream sample site. The corresponding RGS data were joined to each digital polygon record for interpretation. Areas of each polygon, polygon perimeter and percentage coverage of underlying basin formations were calculated using simple GIS subroutines and are included in the data listings of the open file.

This technique is a discrete polygon method and therefore assumes within-polygon uniformity of the geochemistry. However, within a basin, various other physical factors may influence the composition of the stream sediment sample or contribute to within-basin variation. These include variations in bedrock geology, slope, aspect, curvature, vegetation, differential weathering of bedrock, rainfall and wildlife. There are also factors that transcend drainage basin boundaries. Geological material from beyond the catchment boundary may be present due to glacial transport or anthropogenic pollution. These factors should be considered when interpreting catchment basin data.

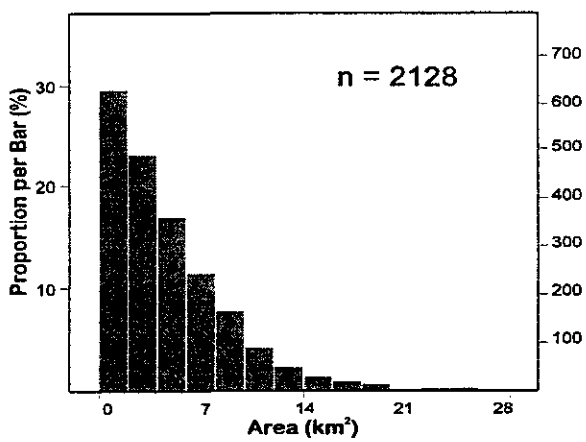


Figure 2. Histogram showing catchment basin areas for map sheets 103I and J.

## CATCHMENT BASINS AND RGS DATA INTEGRATION

### *CATCHMENT BASIN AREAS*

A histogram of catchment basin areas for map sheets 103I and 103J is shown in Figure 2. Catchment basin areas range from less than 1 square kilometre to 40 square kilometres, with a mean area on the order of 5 square kilometres. The modal area of the catchments falls within 1 to 2 square kilometres. Of the 2128 RGS sites, 1327 have drainage basins that cover an area of 5 square kilometres or less. Area coverage of the RGS catchments totals 10 254 square kilometres or 62% of the land area. The remaining unsurveyed 38% represents glaciers, coastal areas lacking well-defined drainage basins, broad valleys or, more importantly, drainages bounded by surveyed catchments that were intentionally excluded from the sampling program. Exclusion of a catchment basin from the survey is a reflection of the intended sampling density of the RGS program. Designed to provide cost efficient regional geochemical data, the RGS program does not define the geochemistry of every first or second order stream within a map area. As a result, mineral occurrences in unsurveyed catchments may be missed. Examination of regional anomalies or subtle geochemical patterns in drainages that bound these unsurveyed areas may help to identify mineralized catchments.

### *GEOCHEMICAL PATTERNS AND CATCHMENT BASINS*

Figures 3 and 4 depict the gold and copper concentrations and associated mineral occurrences recorded in the MINFILE database within sampled catchment areas. These maps illustrate the power of using catchment basins for portraying regional geochemical trends and, in this particular case, identifying and discriminating prospective catchment basins which have high percentile concentrations of gold and copper and contain no recorded mineral occurrences.

### *GEOLOGICAL INFLUENCE*

In previous RGS open files, every RGS sample site was coded on the basis of underlying geology at the sample site. This coding was used to calculate univariate statistics for each element and for the determination of thresholds. Unfortunately, classification of the sample site by its underlying geology may not accurately represent the site and may result in the misidentification of anomalies. This is especially significant where there are two or more geochemically different formations within a catchment basin. As a result, the number and the area of formations within each RGS catchment basin was determined using a geological basemap compiled by MacIntyre *et al.* (1994). Of the 2128 RGS catchments in map sheets 103I and 103J, 51% are underlain entirely by a single formation (*e.g.*, Paleocene granodiorites, N = 142; Paleozoic leucogneiss and migmatites, N = 139; and dacitic pyroclastic rocks of the Telkwa Formation, N = 124), 38% are underlain by two formations and 11% by three or more formations.

### *REFINED THRESHOLD VALUES*

Univariate statistics were calculated on the total dataset and subsets of ten or more catchment basins underlain by a single formation. Percentiles, means, medians and standard deviations have been provided to assist in determining threshold concentrations. For example, mean copper concentration in the 103I and 103J RGS catchment basins is 27 ppm. Possible thresholds using the

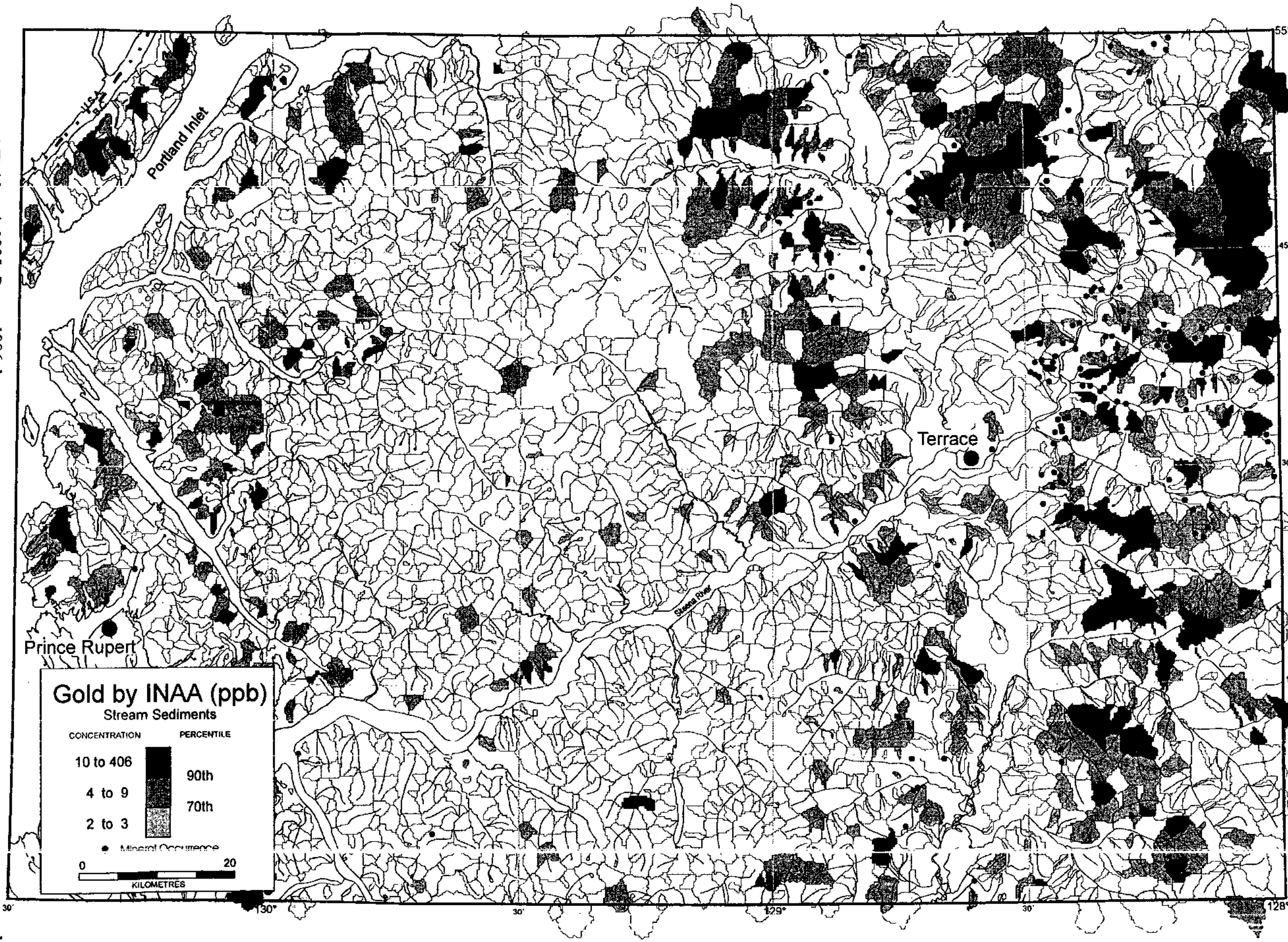


Figure 3. Distribution of gold in stream sediments and the location of known gold occurrences.

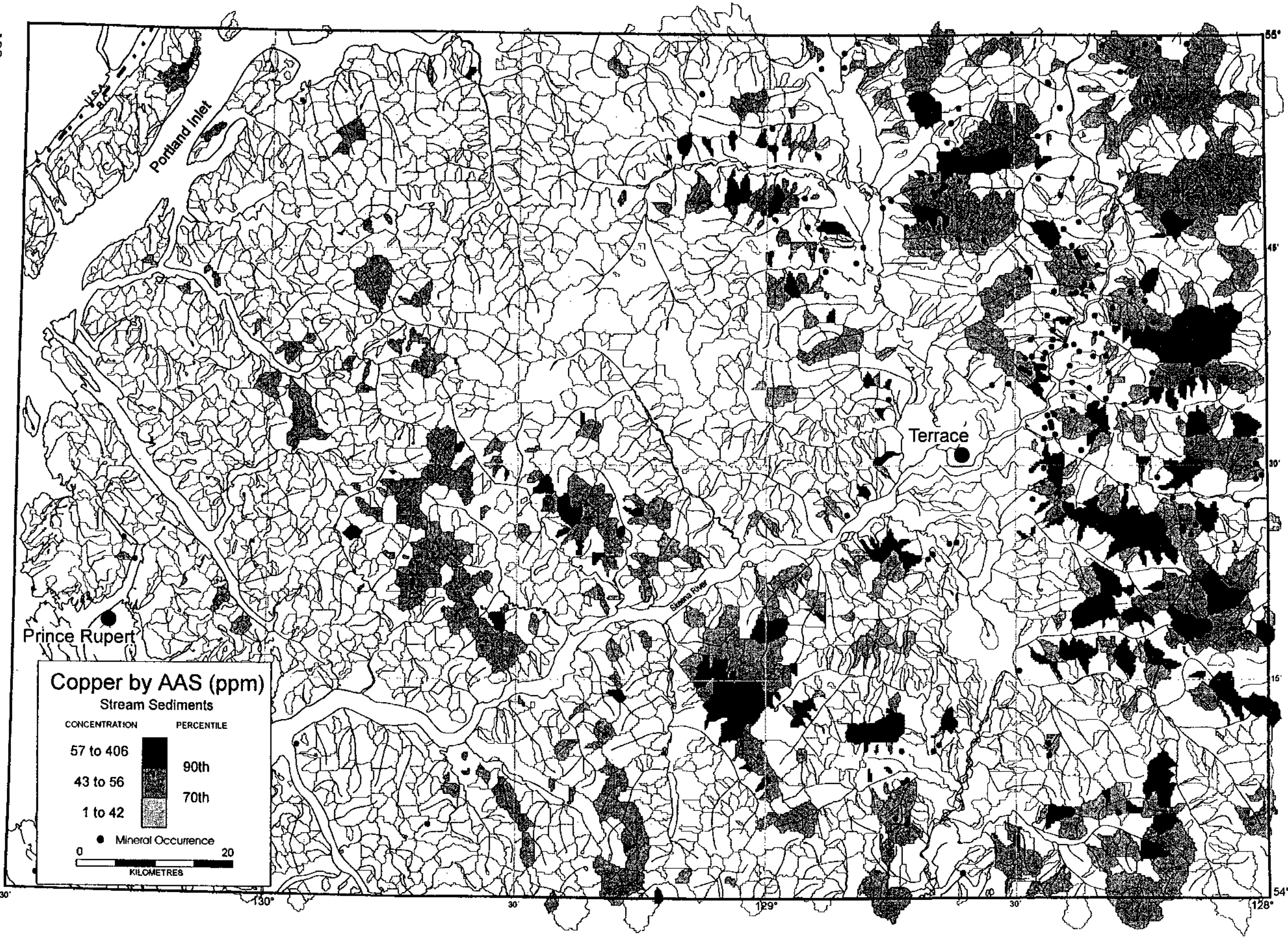


Figure 4. Distribution of copper in stream sediments and the location of known copper occurrences.

mean plus two standard deviations are 81 ppm, or 72 ppm using the 95th percentile concentration. More reliable estimates of background and threshold values can be obtained for basins underlain by a single formation. For example, copper concentrations in homogeneous Paleocene granodiorite catchment basins average 13 ppm while the mean plus two standard deviations concentration is 26 ppm, and 36 ppm at the 95th percentile. In contrast, copper in homogenous Telkwa Formation basins averages 56 ppm with a mean plus two standard deviations concentration of 123 ppm and a concentration of 148 ppm at the 95th percentile concentrations. The presence of multiple formations within a catchment basin presents another challenge for establishing thresholds. Multiple linear regression methods have been used by Bonham-Carter and Goodfellow (1986) and Bonham-Carter *et al.* (1987) to correct for the areal proportions of geologic units within a catchment area.

**TABLE 1. MEDIAN CONCENTRATION OF SELECTED TRACE ELEMENTS IN RGS CATCHMENT BASINS CONTAINING SHOWINGS OR PROSPECTS WITH GOLD (N=60) AND FOR THE TOTAL 103I/J DATASET (N=2120)**

| N | Cu ppm | Pb ppm | Zn ppm | Hg ppb | Au ppb | Sb ppm | As ppm |
|---|---|---|---|---|---|---|---|
| 60 | 44 | 5 | 88 | 20 | 5 | 1.2 | 7.2 |
| 2120 | 20 | 2 | 44 | 20 | 2 | 0.2 | 1.1 |

## *Characterization of Trace Element Concentrations Downstream from Mineral Occurrences*

Of the 137 reported mineral occurrences containing gold, 73, or 53%, fall within RGS catchment basins (MINFILE 103I, 1989; MINFILE 103J, 1989). Ten of these are past producers, three are developed prospects, six are prospects and 54 are showings. Similarly, of the 150 reported occurrences with copper, 111, or 74%, fall within RGS catchment basins. Ten of these are past producers, four are developed prospects, eleven are prospects and 86 are showings.

In order to characterize the stream sediment trace element distributions downstream from mineral occurrences, statistics for RGS basins containing known occurrences were calculated. Basins that contain past producers or developed prospects were not included because of the high probability of contamination due to development work. For example, mean gold values for RGS catchments with occurrences classified as showings *or prospects containing gold are 21 ppb, almost two times* higher than the total dataset mean. Seven catchments returned values greater than 20 ppb, with the highest concentration being 406 ppb gold. However, approximately 28% returned detection limit values (2 ppb), probably reflecting the problems associated with the particle scarcity effect. Similarly, mean copper values for RGS catchments containing showings or prospects with copper are 59 ppm, two times higher than the total dataset mean. Eleven catchments returned values greater than 100 ppm copper, with the highest concentration being 420 ppm.

Median values of associated trace elements in RGS basins can be used to characterize multi-element signatures and identify prospective basins. For example, by applying selected trace element median concentrations obtained from RGS basins containing showings or prospects with gold (Table 1) to the entire database for all the metals, 22 RGS catchment basins were identified (Table 2) that exceeded the listed median values and contained no recorded mineral occurrences. As of November 1, 1995, 16 of the 22 prospective basins were open to staking. Table 1 also lists the medium value concentration of the selected trace elements for the total 103I/J dataset.

**TABLE 2. PROSPECTIVE RGS BASINS**

| Map | ID | Cu ppm | Pb ppm | Zn ppm | Hg ppb | Au ppb | Sb ppm | As ppm | Claim Status |
|---|---|---|---|---|---|---|---|---|---|
| 103I15 | 781115 | 46 | 7 | 116 | 40 | 308 | 1.2 | 13.0 | partial |
| 103I15 | 781133 | 52 | 20 | 114 | 30 | 6 | 1.5 | 19.0 | open |
| 103I15 | 781142 | 64 | 17 | 130 | 70 | 30 | 1.3 | 45.0 | open |
| 103I10 | 783118 | 66 | 7 | 138 | 110 | 12 | 1.5 | 44.0 | open |
| 103I14 | 783126 | 48 | 7 | 98 | 40 | 67 | 1.4 | 33.0 | open |
| 103I15 | 783142 | 48 | 32 | 154 | 40 | 15 | 2.7 | 114.0 | open |
| 103I15 | 783143 | 54 | 17 | 102 | 130 | 38 | 1.4 | 33.0 | open |
| 103I16 | 785036 | 52 | 28 | 194 | 30 | 7 | 2.9 | 75.5 | reserve |
| 103I16 | 785051 | 48 | 10 | 158 | 80 | 6 | 1.5 | 15.0 | reserve |
| 103I09 | 785072 | 56 | 6 | 92 | 70 | 8 | 1.9 | 10.0 | open |
| 103I09 | 785132 | 142 | 14 | 100 | 50 | 6 | 2.6 | 9.0 | open |
| 103I09 | 785137 | 200 | 32 | 186 | 60 | 14 | 2.8 | 23.0 | staked |
| 103I09 | 785146 | 74 | 26 | 102 | 60 | 14 | 2.2 | 8.6 | open |
| 103I10 | 785471 | 68 | 16 | 120 | 30 | 9 | 1.8 | 95.8 | open |
| 103I15 | 785550 | 54 | 10 | 126 | 30 | 24 | 1.6 | 26.0 | open |
| 103I16 | 785560 | 54 | 46 | 196 | 70 | 37 | 4.7 | 65.3 | open |
| 103I09 | 785623 | 88 | 16 | 230 | 30 | 6 | 1.2 | 44.0 | staked |
| 103I16 | 785710 | 84 | 31 | 108 | 50 | 12 | 2.2 | 58.6 | open |
| 103I15 | 785715 | 126 | 60 | 118 | 30 | 18 | 2.1 | 38.0 | partial |
| 103I16 | 785724 | 54 | 10 | 110 | 40 | 46 | 1.5 | 28.0 | open |
| 103I15 | 787790 | 114 | 16 | 310 | 60 | 11 | 2.8 | 60.9 | open |
| 103I15 | 787794 | 58 | 9 | 158 | 40 | 8 | 1.4 | 30.0 | open |

## CONCLUSIONS

Desk-top GIS technologies, combined with an increasing availability of digital geoscience data, have become an extremely powerful mineral exploration tool. The integration of digital catchment basins, MINFILE and bedrock geology with stream sediment geochemistry is a practical example of how this tool can be used to identify and evaluate RGS anomalies which may be worthy of follow-up investigation.

## REFERENCES


Bartier, P.M. and Keller, C.P. (1991): Integrating Bedrock Geology with Stream Sediment Geochemistry in a Geographic Information System (GIS): Case Study NTS 92H; *in* Geological Fieldwork 1991, Grant, B. and Newell, J.M., Editors, B.C. *Ministry of Energy, Mines and Petroleum Resources*, Paper 1991-1, pages 315-321.

Bonham-Carter, G.F. and Goodfellow, W.D. (1986): Background Correction to Stream Geochemical Data Using Digitized Drainage and Geological Maps: Application to Selwyn Basin, Yukon and Northwest Territories; *Journal of Geochemical Exploration*, Volume 25, pages 139-155.

Bonham-Carter, G.F., Rogers, P.J. and Ellwood, D.J. (1987): Catchment Basin Analysis Applied to Surficial Geochemical Data, Cobequid Highlands, Nova Scotia; *Journal of Geochemical Exploration*, Volume 29, pages 259-278.

Jackaman, W. and Matysek, P.F. (1995): British Columbia Regional Geochemical Survey - Nass River (NTS 103O/P); *B.C. Ministry of Energy, Mines and Petroleum Resources*, BC RGS 43.

Jackaman, W., Sibbick, S.J. and Matysek, P.F. (1995): Stream Sediment Geochemistry of the Purcell Supergroup; *B.C. Ministry of Energy, Mines and Petroleum Resources*, Geoscience Map 1995-3.

MacIntyre, D.G., Ash, C.H. and Britton, J.M. (1994): Geological Compilation, Skeena-Nass Area, West-central British Columbia; *B.C. Ministry of Energy, Mines and Petroleum Resources*, Open File 1994-14.

Matysek, P.F. and Jackaman, W. (1995): British Columbia Regional Geochemical Survey - Prince Rupert/Terrace (NTS 103I/J); *B.C. Ministry of Energy, Mines and Petroleum Resources*, BC RGS 42.

MINFILE NTS103I (1989): Mineral Occurrence Map; *B.C. Ministry of Energy, Mines and Petroleum Resources*, MINFILE.

MINFILE NTS103J (1989): Mineral Occurrence Map; *B.C. Ministry of Energy, Mines and Petroleum Resources*, MINFILE.

Sibbick, S.J. (1994): Preliminary Report on the Application of Catchment Basin Analysis to Regional Geochemical Survey Data, Northern Vancouver Island (NTS 92L/03,04,05 and 06); *in* Geological Fieldwork 1993, Grant, B. and Newell, J.M., Editors, *B.C. Ministry of Energy, Mines and Petroleum Resources*, Paper 1994-1, pages 111- 117.

British Columbia Geological Survey
Geological Fieldwork 1995

# SURFICIAL GEOLOGY AND EARTHQUAKE HAZARD MAPPING, CHILLIWACK, BRITISH COLUMBIA (92G/1 & H/4)

**Victor M. Levson, Patrick A. Monahan, Daniel G. Meldrum and Paul F. Matysek,**
**British Columbia Geological Survey Branch**

**Robert F. Gerath,**
**Association of Professional Engineers and Geoscientists of British Columbia**

**Bryan D. Watts, Alex Sy and Li Yan,**
**Klohn-Crippen Consultants Ltd.**

*KEYWORDS:* Chilliwack, earthquakes, geological hazards, liquefaction hazard mapping, seismic microzonation, geotechnical engineering, standard penetration tests, surficial geology, Quaternary

## INTRODUCTION

Earthquake hazard mapping in British Columbia is currently being conducted by the Ministry of Energy, Mines and Petroleum Resources, in cooperation with the B.C. Resource Inventory Committee, the Provincial Emergency Program and Emergency Preparedness Canada. The program is coordinated by the Seismic Microzonation Task Group of the Resource Inventory Committee. To date, the program has included a compilation of earthquake hazard mapping standards and methods (Klohn-Crippen Consultants Ltd., 1994), a conference for land-use and emergency planners (Levson *et al.*, in preparation) and an earthquake hazard mapping pilot project in the Chilliwack area (Levson *et al.*, 1995). The latter project was started in August, 1994 and covers the District of Chilliwack and parts of the Fraser-Cheam Regional District (contained within NTS mapsheet 92H/4W south of the Fraser River and north of 49° 03' N lat.; Figure 1). Earthquake hazards in the Chilliwack area include landslides, liquefaction and amplification hazards, but only liquefaction hazards are discussed in this paper.

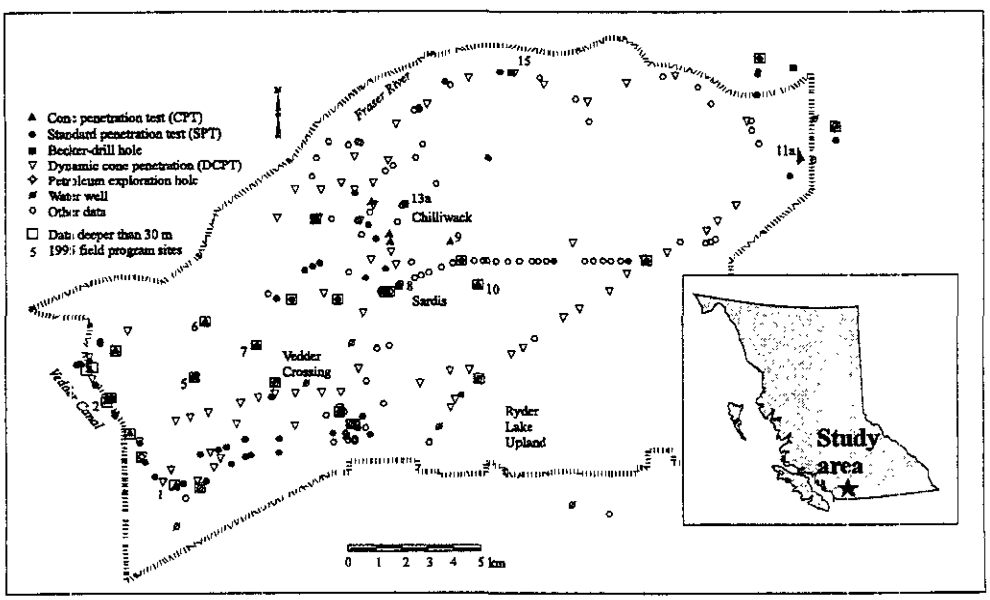


Figure 1. Distribution and type of geotechnical borehole data collected for the study area.

Earthquake hazard maps, or seismic microzonation maps, are detailed (generally 1:20 000 to 1:50 000 scale) maps that identify the relative potential for ground disturbance during an earthquake. Seismic microzonation is defined as "the process of determining absolute or relative seismic hazard at many sites accounting for the effects of geologic and topographic amplification of motion and of soil stability and liquefaction, for the purpose of delineating seismic microzones" (Earthquake Engineering Research Institute, Committee on Seismic Risk, 1984). Earthquake hazard maps are compiled from geologic and geotechnical data and reflect local site conditions, which in addition to earthquake source and magnitude, exert a major control on potential ground disruption. They identify regions that are expected to experience the same relative severity of earthquake hazard and they are used mainly for land-use and emergency planning and prioritizing structural upgrades.

## PREVIOUS WORK

Earthquake hazard mapping has been completed and successfully applied in many countries throughout the world (Levson *et al.*, in preparation). Of particular relevance to British Columbia is recent mapping in Washington and Oregon (Grant *et al.*, 1991; Mabey and Madin, 1993; Mabey *et al.*, 1994; Palmer *et al.*, 1994). Excellent reviews of earthquake hazard mapping methods have been provided by Finn (1991, 1994) and Youd (1991).

Previous related studies in British Columbia include a liquefaction hazard map of the Lower Mainland region focusing on B.C. Hydro's infrastructure (B.C. Hydro, 1992; Watts *et al.*, 1992). A thorough review of earthquake hazards in British Columbia and methods of seismic microzonation mapping for land-use planning purposes was recently completed by Klohn-Crippen Consultants Ltd. (1994). Earthquake hazard mapping and its implications for land-use and emergency planning are discussed by Levson *et al.* (in preparation). A preliminary version of this paper, reporting on the Chilliwack pilot project, was provided by Levson *et al.* (1995). Studies related to microzonation mapping have also been recently conducted in the Lower Mainland by the Geological Survey of Canada (*e.g.* Clague *et al.*, 1992; Hunter *et al.*, 1993; Luternauer *et al.*, 1994). Armstrong (1980, 1984) described and mapped the surficial geology of the Chilliwack study area at a scale of 1:50 000. Groundwater studies have been conducted in the region by Halstead (1986) and Dakin (1994). Other relevant regional reports include a geological investigation of the Sumas Valley based on borehole data (Cameron, 1989) and a soil survey of the Chilliwack region (Comar *et al.*, 1962).

## EARTHQUAKES IN BRITISH COLUMBIA

Southwestern British Columbia is a seismically active area subject to crustal, subcrustal and subduction earthquakes (Rogers, 1992, 1994). The largest earthquake in Canada (M 8.1) occurred near the Queen Charlotte Islands in 1949. The 1946 earthquake (M 7.3) near Courtenay was the most destructive in western Canada. Although a number of damaging earthquakes have occurred in British Columbia and in nearby Washington and Alaska in historic times, most occurred prior to extensive urban development. One of the more recent of these earthquakes, in 1965 in Seattle, caused $12 million in damage. The estimated potential economic impact of a similar (M 6.5) earthquake on the Lower Mainland alone is $14.3 to $32.1 billion (Munich Reinsurance, 1992).

## MITIGATION

Earthquake hazard maps provide fundamental information for seismic hazard mitigation and they are critical tools for effective emergency and land-use planning. Current earthquake hazard mitigation programs in British Columbia are mainly site specific or focused on agency-specific facilities. In contrast, earthquake hazard maps can be used for regional seismic vulnerability assessments and they are a cost-effective way to prioritize mitigation efforts. They do not, however, replace the need for site-specific geotechnical evaluations for new construction. General applications of earthquake hazard maps to land-use and emergency planning include: 1) identification of areas with vulnerable lifeline systems (*e.g.* water, gas and power lines); 2) planning transportation and utility corridors; 3) setting priorities for seismic upgrading or remedial work on schools, hospitals, firehalls and other structures; 4) identifying good areas for new essential facilities (*e.g.* schools, hospitals, bridges, toxic waste containment facilities); 5) identifying areas requiring special study before development, or high-hazard areas with restricted development; 6) property insurance; 7) assessment of risk for financing new projects; 8) providing information on site effects for design of new structures; 9) establishing more stringent design requirements where needed (Klohn-Crippen Consultants Ltd., 1994).

The costs of earthquake hazard map production are relatively low compared to the costs of current seismic vulnerability studies and upgrading programs. For example, the British Columbia Ministry of Education has, in recent years, allocated about $30 million per year to seismic upgrading of schools. Similarly, from 1988 to 1994, B.C. Hydro, a leader in seismic hazard mitigation, spent about $18 million on electric system seismic strengthening (excluding dam safety) and about $4 million on seismic studies and research (Katrichak *et al.*, 1994). In comparison, a liquefaction susceptibility map covering parts of the Lower Mainland, (B.C. Hydro, 1992) cost about $110 000 to produce (Klohn-Crippen Consultants Ltd., 1994).

Earthquake hazards can be mapped at different levels of certainty, with the amount, quality and cost of information required generally increasing with each mapping level. For example, liquefaction hazard maps can be grouped into liquefaction susceptibility, liquefaction potential and liquefaction-induced ground displacement maps (Finn, 1994). Liquefaction susceptibility maps (level 1) are based on surficial geology data such as sediment type, geomorphologic characteristics, relative density, deposit age, water table depth and geologic or historical evidence of liquefaction. Liquefaction potential maps (level 2) indicate the probability of liquefaction actually occurring, by accounting for the expected intensity of seismic shaking (based on past records of earthquakes) as well as soil conditions. Liquefaction-induced ground displacement or lateral displacement maps (level 3) can be produced by accounting for ground movement (lateral spreading) on slopes and towards free faces such as river banks (Youd, 1991).

## METHODOLOGY

The Chilliwack hazard mapping pilot program comprised several phases: 1) collection of existing geotechnical data; 2) surficial geology mapping at a scale of 1:20 000, focusing on the Fraser River valley and Ryder Lake upland area; 3) collection of new cone-penetration data and shear-wave data at several sites selected to fill gaps in the existing database; 4) input of surficial geology and geotechnical data into a geographic information system; 5) development of a three-dimensional geologic model for the area; 6) evaluation of liquefaction and amplification hazards at specific sites within the map area where good quality geotechnical data are available; and 7) integration of surficial geology and geotechnical data to produce an earthquake hazard map. Borehole data were compiled from private and public agencies including the District of Chilliwack, Chilliwack School Board, B.C. Ministry of Transportation and Highways, B.C. Hydro, B.C. Ministry of Environment (Water Management Division and Groundwater Section), Geological Survey of Canada, Department of National Defense, Public Works and Government Services Canada and geotechnical consultants. Further work on the project may include reflection seismic or ground penetrating radar lines in selected areas where borehole data are lacking or where specific problems need to be addressed. The methods used generally follow those recommended by the Seismic Microzonation Task Group (Klohn-Crippen Consultants Ltd., 1994).

The methodology used for the collection of geotechnical data during the field component of the pilot project is described by ConeTec Investigations Ltd. (1995) and is summarized here. Seismic cone penetration test (SCPT) data were obtained using electric cones supplied by ConeTec Investigations Ltd. and deployed with a modified drill rig (MARL-10) operated by Mud Bay Drilling Co. Ltd. (Photo 1). Cone bearing (Qt), sleeve friction (Fs) and dynamic penetration pore pressure (Ut) data were collected at 5-centimetre intervals and recorded digitally. Time-based pore pressure and seismic shear-wave velocity measurements were also recorded every metre. Shear-wave traces were recorded and analyzed according to procedures described by Robertson *et al.* (1986). The spectral analysis of surface waves (SASW) method uses surface waves of the Raleigh type to evaluate the shear-wave velocity and shear modulus profiles of geotechnical sites and to infer soil parameters such as *in situ* density. The method is non-intrusive with both the source (vertical hammer impact) and receivers located on the ground surface. The Becker density test (BDT) uses a diesel hammer to drive a double-walled steel drill-casing into the ground. Blow counts were recorded for each 30.5 centimetres of penetration. The force of each blow was measured, using a pile driving analyzer (PDA), by the British Columbia Ministry of Transportation and Highways.

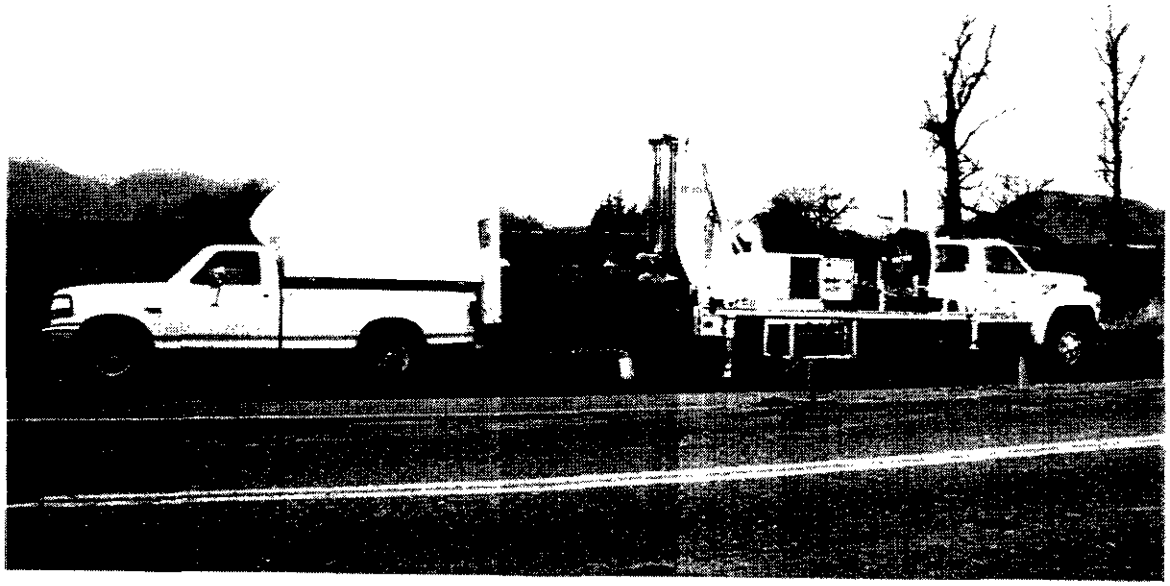

Photo 1. Seismic cone penetration test in progress on Luckakuk Way, south of Chilliwack, showing ConeTec SCPT data-recording truck (left), Mud Bay drill rig (right) and Trans-Canada Highway (background).

## GEOTECHNICAL DATABASE

The geotechnical database for the Chilliwack area consists of over 1700 test holes, including approximately 250 holes with standard penetration test (SPT) data, 50 with cone penetration test (CPT) data, 200 with dynamic cone penetration test (DCPT) data, 60 with Becker penetration test (BPT) data and a few sites with shear-wave data (Figure 1). Drill holes are concentrated along the Trans-Canada Highway, in the Chilliwack, Sardis and Vedder Crossing areas, along the Fraser River and Vedder Canal dikes and along B.C. Hydro's main transmission line (Figure 1). An additional 700+ water-well logs are available for the area; about 70 of the deeper wells were selected to fill in gaps in the data (Figure 2). The geotechnical database includes information on the following: sediment type, grain-size distribution, moisture content, depth to bedrock, stratigraphy, penetration test data, Atterberg (liquid and plastic) limits, shear-wave velocity and other seismic data, shear strength, water table and piezometric pressure. The database also includes accurate location information for each geotechnical hole or data collection site, the agency that collected the data, the client and the date of collection.

## GEOTECHNICAL DRILLING PROGRAM

Seismic cone penetration tests (SCPT) were conducted at eight different locations (Figure 1). A typical example of the results produced from a SCPT test, including cone bearing (Qt), sleeve friction (Fs), friction ratio (Rf) and pore pressure (U) data, is provided in Figure 3, together with an interpretive log of the site. Sands and gravelly sands, fining upwards to silts in the upper 5 metres of the profile, are interpreted to represent alluvial fan deposits. They overlie floodplain silts and clayey silts (at 5-10 m depth) and older Fraser River alluvium (below 10 m depth).

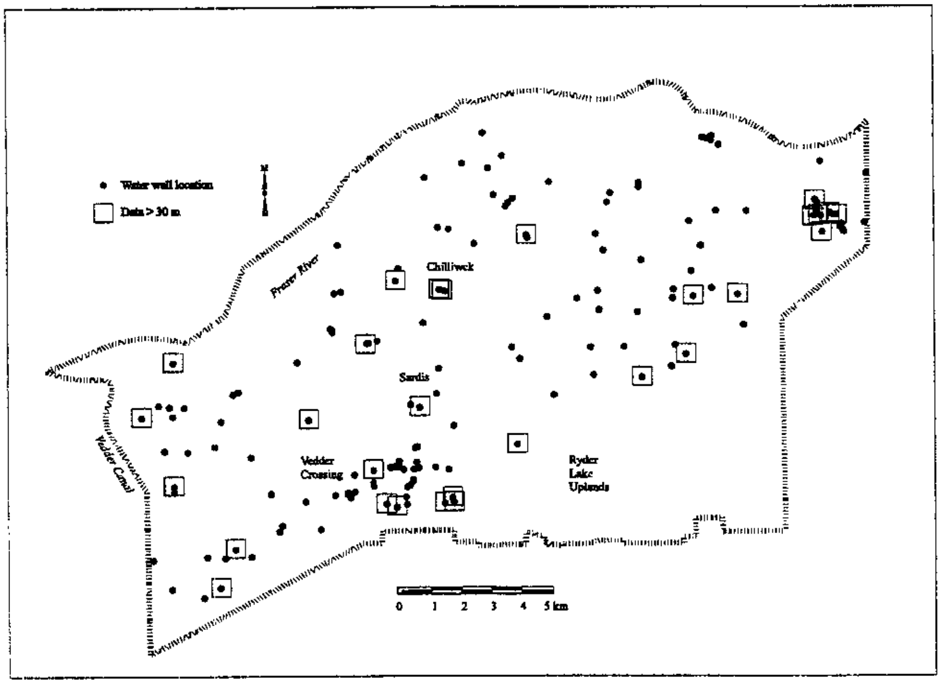


Figure 2. Distribution of water-well boreholes in the study area.

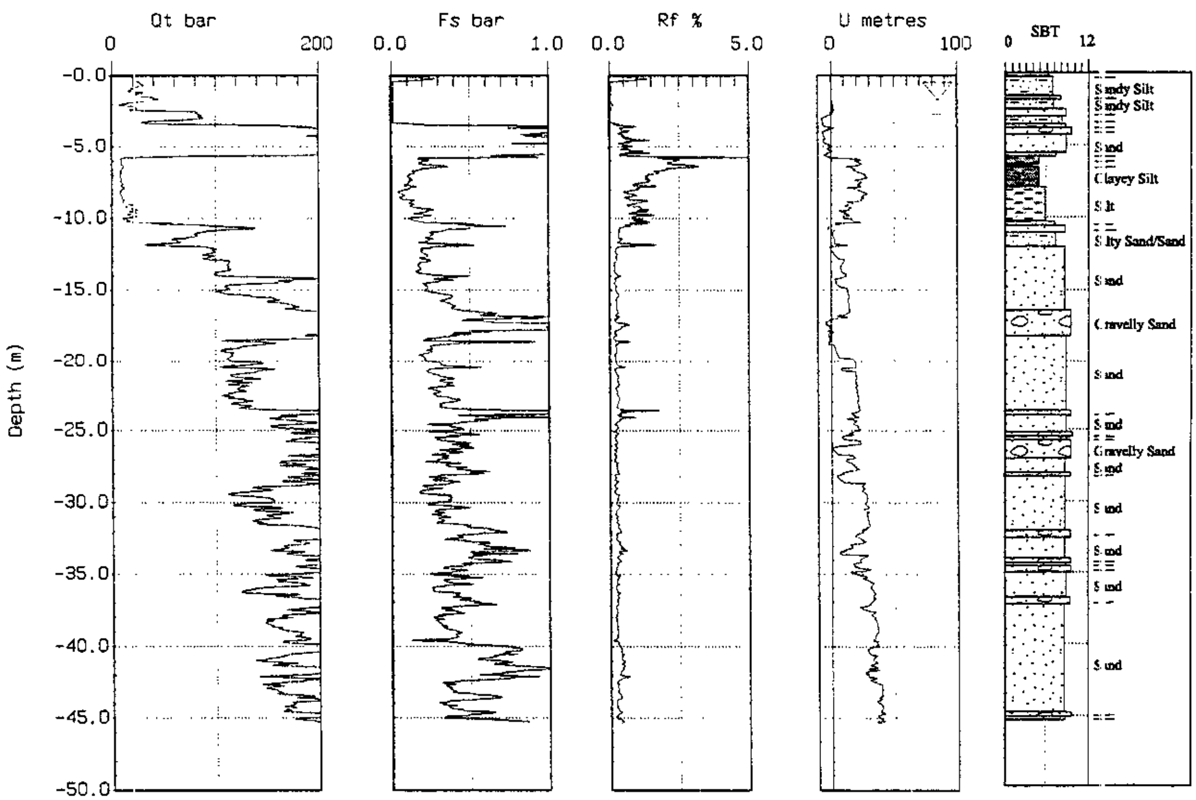


Figure 3. Cone penetration test results from location 7 (Figure 1) showing cone bearing (Qt), sleeve friction (Fs), friction ratio (Rf), pore pressure (U) and soil behavior type (SBT; after Robertson and Campanella, 1988). Alluvial fan sediments in the upper 5 metres of the profile overlie floodplain silts and clayey silts (at 5-10 m depth) and older Fraser River alluvium (below 10 m depth).

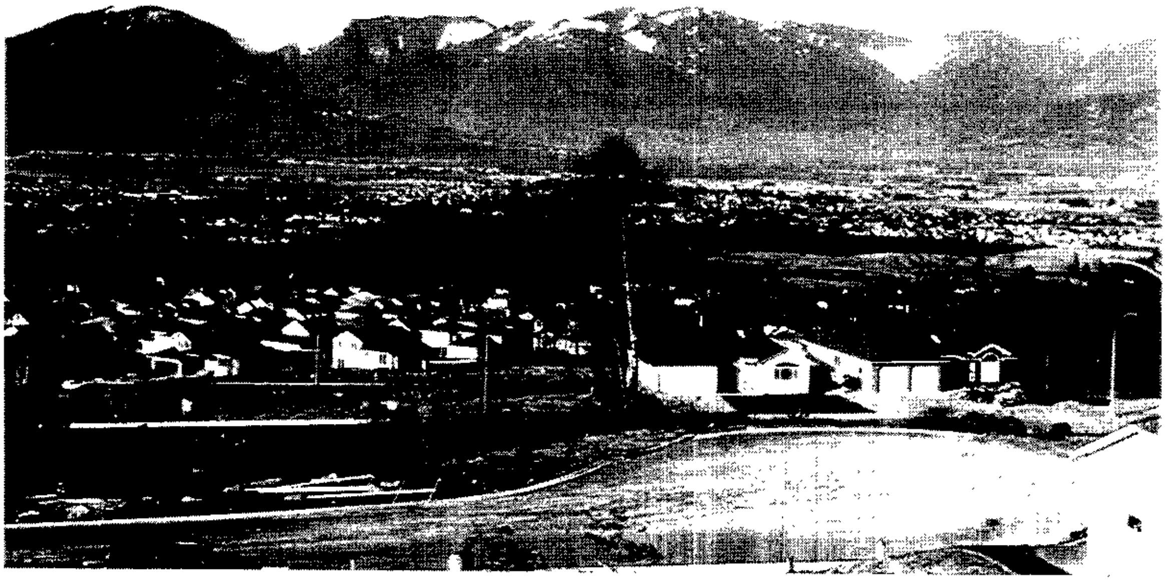

Photo 2. View from the edge of the Vedder Upland northwestward across the Vedder River alluvial fan (foreground) and the Fraser River floodplain (centre). Mountains in background are outside the study area, north of the Fraser River.

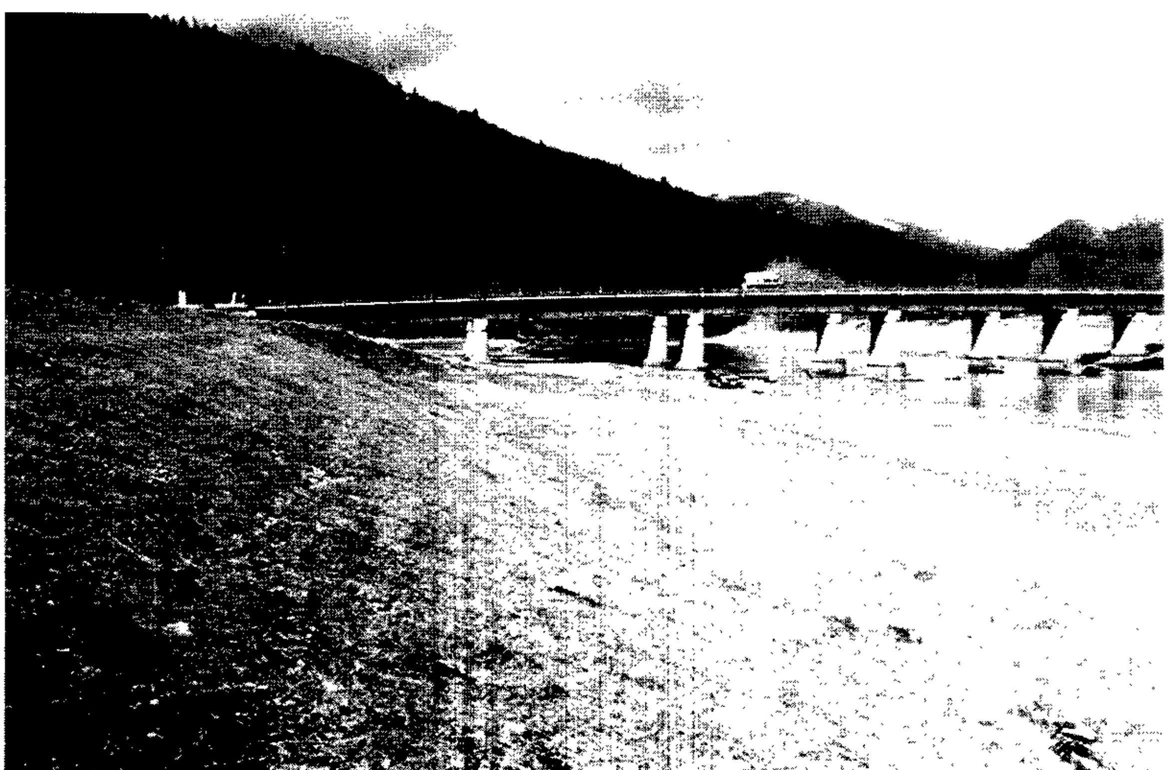

Photo 3. Trans-Canada Highway bridge over the Vedder River canal. Canal dikes (west embankment shown on left) are the highest in British Columbia and protect a large part of the Fraser River valley from flooding.

Spectral analysis of surface waves (SASW) and Becker penetration test (BDT) data were acquired to assess the liquefaction susceptibility of three gravel-rich areas, where conventional CPT or SPT equipment could not be used. Open Becker tests were conducted at two of these sites (8 and 13a) to penetrate the near-surface gravels and allow for deeper SCPTs. Complete results of the program are provided by ConeTec Investigations Ltd. (1995).

## SURFICIAL GEOLOGY

Figure 4 is a chronostratigraphic surficial geology map of the study area, compiled at a 1:20 000 scale using existing information sources, aerial photographic mapping and field confirmation. Data collected for each map unit include: type of sediment, grain-size characteristics, thickness, age, genesis, subsurface stratigraphy and hydrogeologic, geotechnical and geophysical properties. Geological analysis and interpretation of the surficial geology data include an assessment of data quality, description of the relationship of map units with the subsurface stratigraphy and geological interpretation.

The surficial geology of the area is dominated by the Fraser River floodplain which is overlain by a large alluvial fan in the southwestern part of the map area where the Chilliwack-Vedder River enters the Fraser River valley (Photo 2). The alluvial fan deposits become more sandy, less gravelly and thinner towards the fan margins (Figure 3). The Chilliwack-Vedder River system historically has been prone to large floods and has been extensively channelized and diked, the lower canal dikes being the largest in British Columbia (Photo 3). A number of smaller alluvial and colluvial fans and a large landslide deposit (known as the Cheam slide) extend out onto the Fraser Valley from the mountains to the southeast (Figure 4). This large area of landslide debris, overlies glaciogenic deposits and is capped by up to 10 metres of soft silt, peat and marl. The western edge of the study area is dominated by lacustrine silts, sands and clays (Figure 4). Upland areas, such as the Ryder Lake upland, are mantled by glacial deposits and locally are capped by a few metres of loess. Several tens of metres of Pleistocene silt, sand and gravel underlie till, in the upland area southeast of Vedder Crossing, known as Promontory Heights.

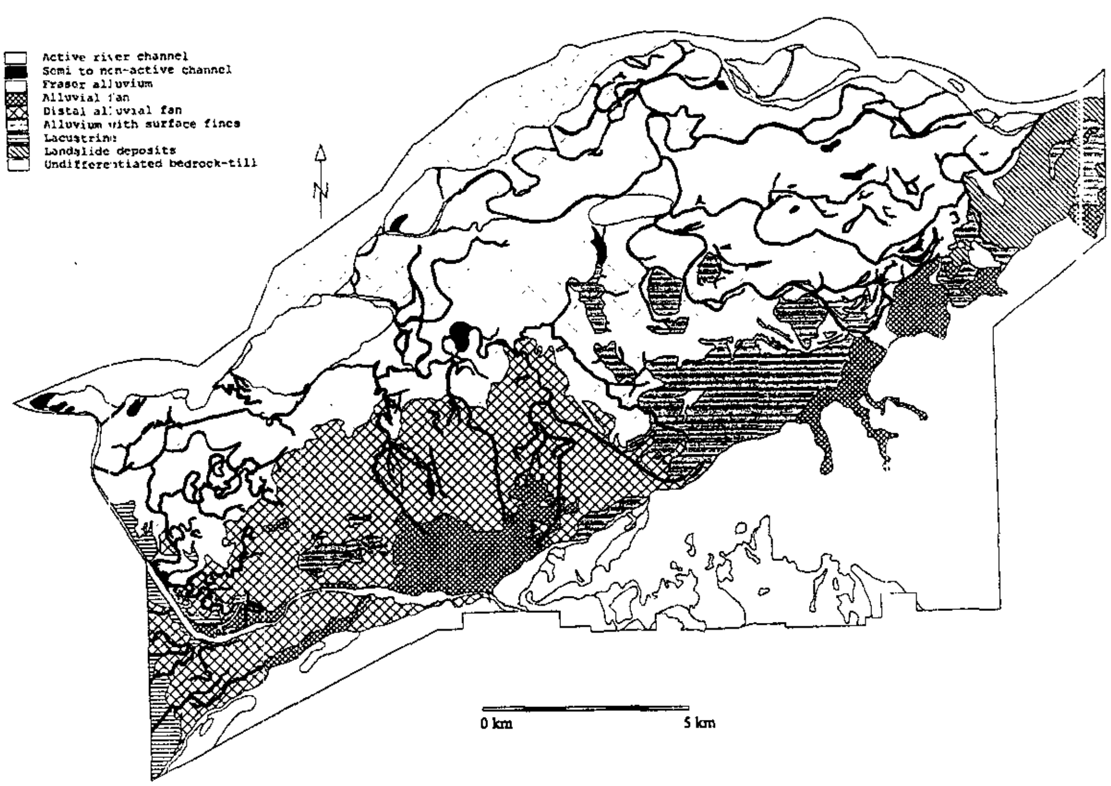


Figure 4. Generalized surficial geology of the study area.

The Fraser River lowland is characterized by numerous semi-active channels and abandoned sloughs. Prior to diking of the river along the northern boundary of the study area, many of these channels were periodically occupied by flood waters. The channels are significant from an liquefaction hazard perspective, not only because they contain loose, unconsolidated sandy sediments, but also because many of them have a significant free-face toward which liquefaction-induced lateral displacements may occur. Elsewhere, Fraser River alluvium is dominated by denser gravels and sands with up to a few metres of overbank silts. Several poorly drained areas with thick surface accumulations of silt, clay and organics are also present on the Fraser Lowland. These include an area southeast of Chilliwack, interpreted as a large paleochannel fill on a relatively old part of the Fraser River floodplain and an area northwest of the Vedder fan, where a number of small, meandering stream channels have incised into the fine sediments.

Geotechnical and geological data compiled for the study area demonstrate that the Fraser River valley is underlain by about 50 metres of sand and gravel interbedded with silt and peat that is interpreted to be a Holocene prograding deltaic and overlying fluvial sequence (Figure 5; Monahan and Levson, in preparation). These deposits are underlain by early Holocene and/or earlier glaciomarine(?) silts, clays and sands that locally extend to depths of over 400 metres. The floodplain deposits pass laterally into the Holocene lacustrine sands, silts and clays that occur in the Sumas Valley (*c.f.* Cameron, 1989). Gravels deposited in the Chilliwack-Vedder River alluvial fan are over 35 metres thick at the mountain front and have prograded over older deposits in the Sumas and Fraser River valleys.

## LIQUEFACTION SUSCEPTIBILITY

As the susceptibility of a soil to liquefaction is dependent on geologic parameters such as grain-size distribution, density, deposit age and water table depth, a first approximation of the liquefaction hazard for an area can be made by an analysis of the surficial geology. The first step in the production of a liquefaction susceptibility map for the Chilliwack area, was the integration of surficial geology data with geotechnical borehole data and other subsurface data such as water-well logs. Three-dimensional geologic models of the area were constructed from this information (*e.g.* Figure 5). Liquefaction susceptibility of each map unit was then estimated based on Youd and Perkins' (1978) correlations between surficial geology and liquefaction, with local modifications introduced by Watts *et al.* (1992). Table 1 is a summary of the estimated liquefaction susceptibility of the main geologic units in the area.

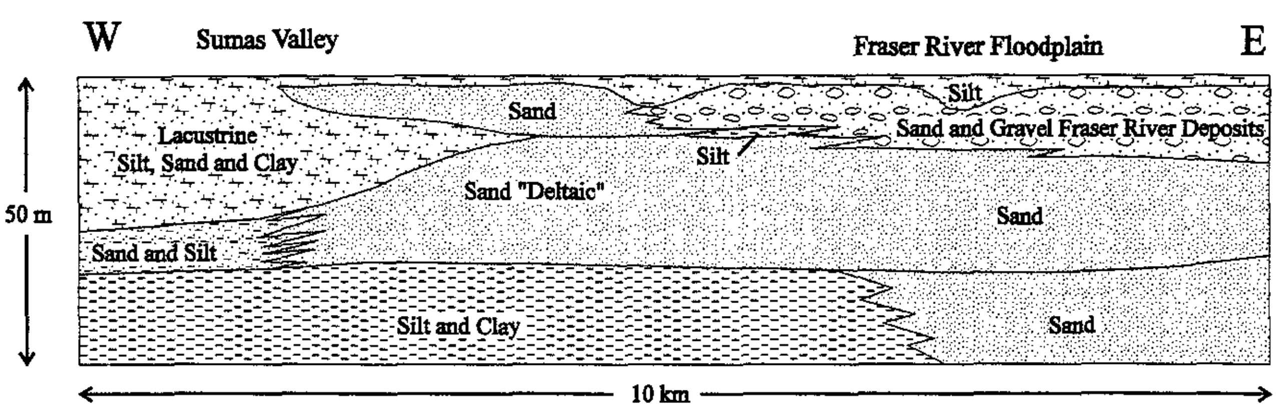


Figure 5. Schematic cross-section illustrating the main Holocene stratigraphic units in the Chilliwack area.

**TABLE 1. ESTIMATED SUSCEPTIBILITY TO LIQUEFACTION OF CHILLIWACK REGION SOILS**

| Surficial Geology | Age | Distribution | Sediment Type | Water Table | Liquefaction Susceptibility |
|---|---|---|---|---|---|
| River channel | Very recent | Along rivers and streams | Sand & gravel | At surface | High to very high |
| Fraser alluvium | Holocene | Widespread on floodplain | Sand, silt & gravel | Near surface | Moderate to high |
| Sandy *alluvial fan* | Holocene | Lower Vedder *River fan* | Sand, silty-sand & *gravelly silty-sand* | Variable | Moderate to high |
| Gravelly alluvial fan | Holocene | At mouth of mountain streams | Gravel, sand & silty-sand | Variable | Low to moderate |
| Alluvium with surface fines | Holocene | Abandoned channels and other lows on floodplain | Silt, clay, & organics over sand & gravel | Near surface | Low to moderate |
| Bog | Holocene | Widespread | Peat & organic silts | At surface | Nil at surface |
| Lacustrine deposits | Holocene / Late Pleistocene | Sumas Valley west of Vedder Canal | Sand, silt and clay | Near surface | Low to high. |
| Till | Pleistocene | Ryder Upland | Diamicton | Variable | Very low |
| Glaciofluvial | Pleistocene | Ryder Upland | Gravel and sand | Variable | Very low |
| Bedrock | Pre-Pleistocene | Mountainous areas | Rock | - | None |

## PROBABILISTIC ASSESSMENT OF LIQUEFACTION POTENTIAL AND SEVERITY

Liquefaction potential was estimated for the Chilliwack area using a modified version of PROLIQ2 (Atkinson *et al.,* 1986) that combines an SPT-based method of liquefaction assessment, developed by Seed (1979), with a probabilistic method of seismic risk assessment (Cornell, 1968). The probability of liquefaction occurring in a 50-year period, at specified depths at a given site, was calculated for 65 test holes at 25 different sites. The assessment was based on the NBCC seismicity model with the mean attenuation curve of Hasegawa *et al.* (1981) and the ground amplification chart of Idriss (1991).

In a liquefaction event, the severity of surface disruption is a function of the depth and thickness of each liquefiable unit, with shallow liquefaction causing more ground disruption and potential structural damage than liquefaction at greater depths. *To account for this, the concept of* 'probability of liquefaction severity' (PLS) was introduced by Klohn-Crippen Consultants Ltd. and is given by:

$$PLS = \frac{\Sigma\,(W_i H_i Pl_i)}{\Sigma\,(W_i H_i)}$$

where $Pl_i$ is the probability of liquefaction at depth $i$, $H_i$ is the layer thickness and $W_i$ is the value of a weighting function. The proposed weighting function has a value of 0.1 at the ground surface and decreases linearly to zero at 20 metres depth, similar to the deterministic calculation introduced by Iwasaki *et al.,* (1981). A simplified example of how PLS reflects the depth of liquefiable units is provided in Figure 6.

Figure 7 illustrates the relationship between surficial geology and liquefaction potential. Sites with similar geology are coded with the same pattern and grouped together with potential liquefaction severity (PLS) plotted on the y-axis. Sequences along semi-active channels or abandoned sloughs on the Fraser River floodplain have the highest PLS, whereas coarse alluvial fan deposits and alluvium overlain by thick sequences of fine sediments and organics have the lowest PLS in the map area. Sandy *alluvial fan deposits and sandy to gravelly alluvium* on the floodplain show intermediate PLS values.

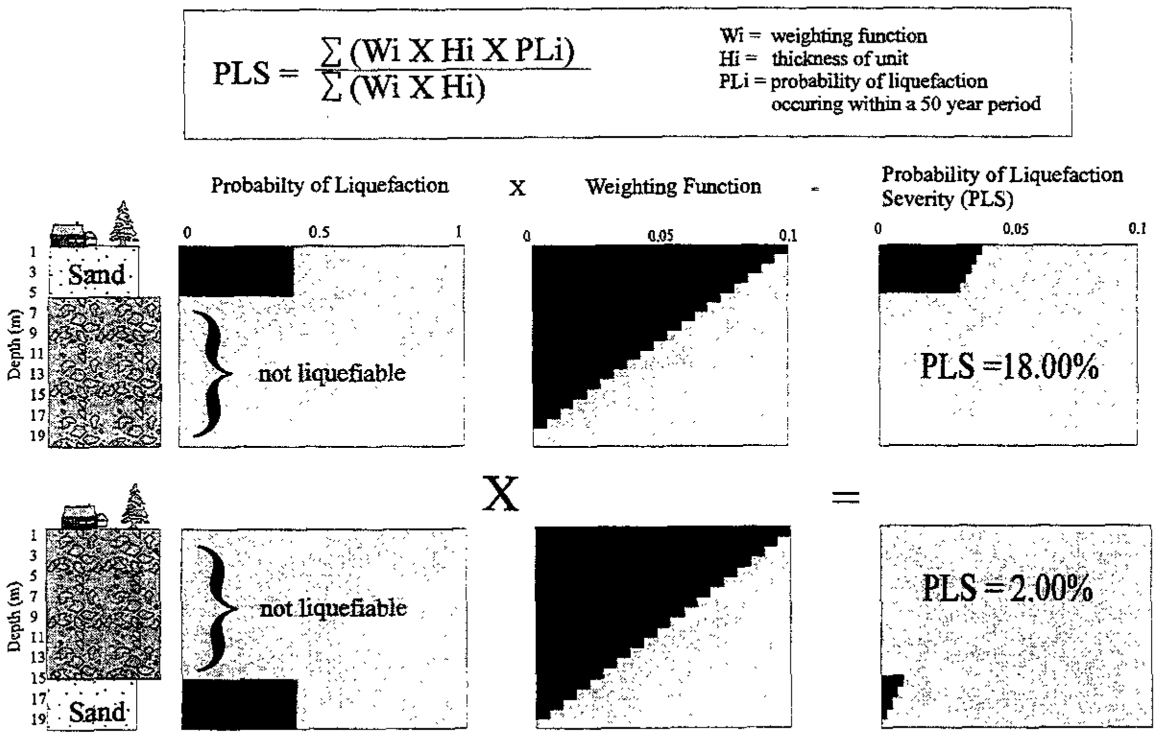


Figure 6. Method of determining probability of liquefaction severity (PLS). The thickness of the sand unit and the probability of liquefaction is the same in both cases, but the PLS is much higher in the first case, reflecting the shallower depth of the liquefiable unit.

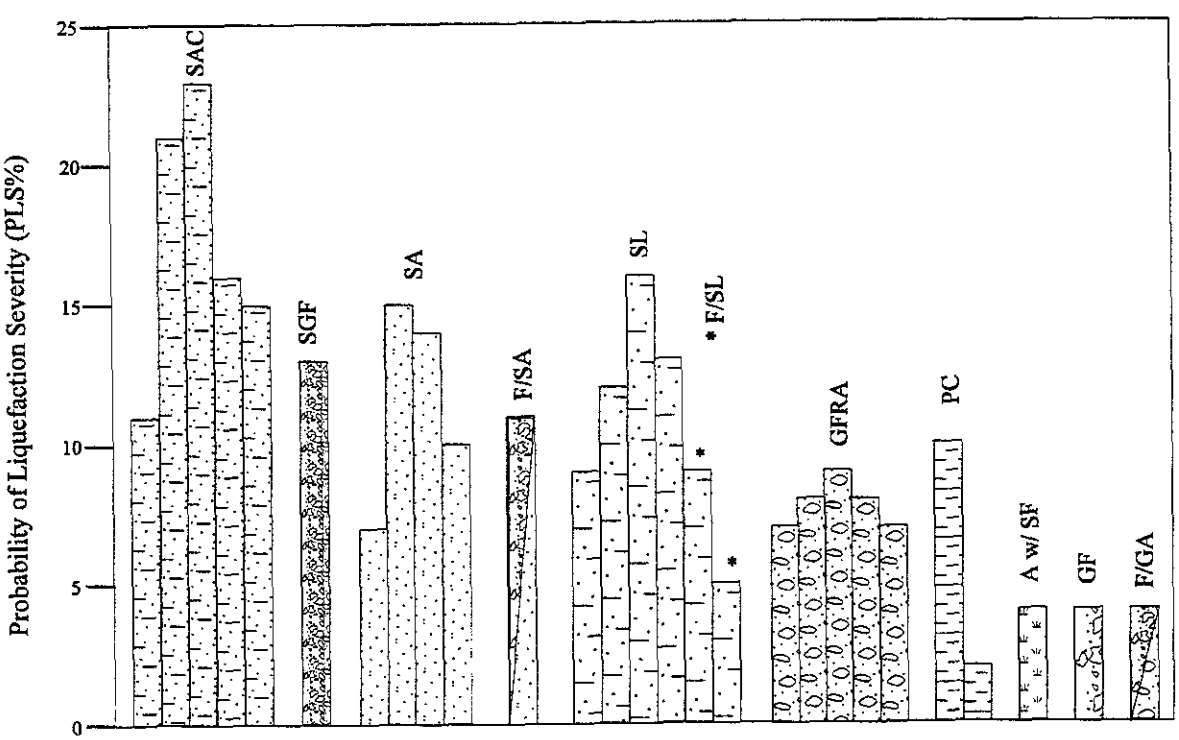


Figure 7. PLS *versus* depositional environment for eleven map units (SAC - semi-active channel, SGF - sand and gravel fan, SA - sandy alluvium, F/SA fan over sandy alluvium, SL - sandy lacustrine, F/SL fan over sandy lacustrine, GFRA - gravelly Fraser alluvium, PC - paleo-channel, A w/SF alluvium with surface fines, GF - gravelly fan and F/GA - fan over gravelly alluvium).

## SUMMARY

The objective of seismic microzonation mapping is to map the relative potential for ground disturbance during an earthquake, based on local geologic, geotechnical and topographic criteria. These site conditions, in addition to earthquake source and magnitude, exert a major control on potential ground disruption. The Chilliwack pilot program has involved: collection of geotechnical data from over 1700 geotechnical test holes; 1:20 000 scale chronostratigraphic, surficial geology mapping; a field program of seismic cone penetration, spectral analysis of surface wave and Becker penetration tests; development of a geologic model; qualitative assessment of liquefaction susceptibility and quantitative assessment of liquefaction potential. This multi-disciplinary program is directed mainly towards land-use and emergency planning applications and to help prioritize funds spent by public agencies on seismic retrofitting.

Relative earthquake hazard maps can be produced from surficial geological data and from the large geotechnical database that exists for most urban areas. A first approximation of the liquefaction hazard is made by integrating surficial geology and geotechnical data to construct a geologic model of the area. Liquefaction susceptibility of each map unit is then estimated using empirical relationships between surficial geology and liquefaction occurrences that have been observed after earthquakes in other areas with similar geologic conditions. Probabilistic assessments of liquefaction that reflect the relative severity of surface ground disruption (PLS) at a number of sites in the study area, further demonstrate the relationship between geology and the liquefaction hazard and provide a more quantitative determination of the hazard in each map unit.

## ACKNOWLEDGMENTS

Fieldwork for this project was funded by the B.C. Resource Inventory Committee. ConeTec Investigations Ltd., Mud Bay Drilling Co. Ltd. and SDS Drilling Ltd. provided contracted assistance for the geotechnical drilling program. Don Gillespie (Ministry of Transportation and Highways) collected pile driving analyzer data at the three Becker penetration test sites. Geotechnical and geologic data were provided by those listed in the text as well as the following: B.C. Buildings Corporation; Canadian National Railway; Fraser-Cheam Regional District; Chilliwack Hospital; University College of Fraser Valley; District of Abbotsford; AGRA Earth and Environmental Ltd.; Cook Pickering and Doyle Ltd.; EKS Engineering Services; GeoPacific Consultants Ltd.; Golder Associates; Macleod Geotechnical Ltd.; Piteau Associates; J.M. Ryder and Associates; Thurber Engineering Ltd.; G.R. Graham Architects; Hemingway Nelson Architects; J.W. Weller and Associates; Rusty's Design Service; KPA Engineering; RKTG Engineering; Southern Railway of British Columbia; Martens Construction; and Peterbern Developments. Special thanks are extended to J. Vickerson, J. Wiley and T. Lewis for their assistance in data collection.

## REFERENCES

Armstrong, J.E. (1980): Surficial Geology, Chilliwack (West Half), British Columbia; *Geological Survey of Canada*, Map 1487A.

Armstrong, J.E. (1984): Environmental and Engineering Applications of the Surficial Geology of the Fraser Lowland, British Columbia; *Geological Survey of Canada*, Paper 83-23.

Atkinson, G.M., Finn, W.D.L. and Charlwood, R.G. (1986): PROLIQ2-A Computer Program for Estimating the Probability of Seismic Induced Liquefaction including both Areal and Fault Sources; *Department of Civil Engineering, University of British Columbia*.

B.C. Hydro (1992): Liquefaction Hazard Assessment for the Lower Mainland Region; Report No. H2477, includes 1:75 000 - scale liquefaction hazard map.

Cameron, V. J. (1989): The Late Quaternary Geomorphic History of the Sumas Valley; unpublished M.A. thesis, *Simon Fraser University*, 154 pages.

Clague, J.J., Naesgaard, E. and Sy, A. (1992): Liquefaction Features on the Fraser River Delta: Evidence for Prehistoric Earthquakes?; *Canadian Journal of Earth Sciences*, Volume 29, pages 1734-1745.

ConeTec Investigations Ltd. (1995): Field Report: Results of SCPT, SASW & BPT Testing in the Chilliwack District; *B.C. Geological Survey*, unpublished report.

Comar, V.K., Sprout, P.N. and Kelley, C.C. (1962): Soil Survey of the Chilliwack Map Area, Lower Fraser Valley; *B.C. Department of Agriculture*, Preliminary Report 4.

Cornell, C.A. (1968): Engineering Seismic Risk Analysis; *Bulletin of the Seismological Society of America*, Volume 58, pages 1583-1606.

Dakin, R.A. (1994): Section 9.1.1 Fraser Lowland; *in* Groundwater Resources of British Columbia, *B.C. Ministry of Environment, Lands and Parks* and *Environment Canada*, pages 9.1-9.30.

Earthquake Engineering Research Institute, Committee on Seismic Risk (1984): Glossary of Terms for

Probabilistic Seismic Risk and Hazard Analysis; *Earthquake Spectra,* Volume 1, Number 1, pages 33-40.

Finn, L.W.D. (1991): Geotechnical Engineering Aspects of Microzonation; Fourth International Conference on Seismic Zonation, *Earthquake Engineering Research Institute,* Volume 1, pages 199-259.

Finn, L.W.D. (1994): Geotechnical Aspects of the Estimation and Mitigation of Earthquake Risk; *in* Issues in Earthquake Risk, Tucker, B.E., Erdik, M. and Hwang, C.N., Editors, *Kluwer Academic Publishers,* pages 35-77.

Grant, W.P., Perkins, W. J. and Youd, T.L. (1991): Evaluation of Liquefaction Potential, Seattle, Washington; *U.S. Geological Survey,* Open File Report 91-441, 44 pages and map.

Halstead, E.C. (1986): Ground Water Supply - Fraser Lowland, British Columbia; *Environment Canada, Inland Waters Directorate,* NHRI Paper 26, IWD Scientific Series 145.

Hasegawa, H.S., Basham, P.W. and Berry, M.J. (1981): Attenuation Relations for Strong Seismic Ground Motions in Canada. *Bulletin of the Seismological Society of America,* Volume 71, pages 1943-1962.

Hunter, J.A., Woeller, D.J., Addo, K.O., Luternauer, J.L. and Pullan, S.E. (1993): Application of Shear-wave Seismic Techniques to Earthquake Hazard Mapping in the Fraser River Delta, British Columbia; *Society of Exploration Geophysicists,* 63rd Annual Meeting Abstracts, pages 501-503.

Idriss, I.M. (1991): Earthquake Ground Motions at Soft Soil Sites; Proceedings, *Second International Conference on Recent Advances in Geotechnical Earthquake Engineering and Soil Dynamics,* St. Louis, Missouri, Volume 1, pages 209-214.

Iwasaki, T., Tokida, K. and Taksuoka, F. (1981): Soil Liquefaction Potential Evaluation with Use of the Simplified Procedure; Proceedings, *First International Conference on Recent Advances in Geotechnical Earthquake Engineering and Soil Dynamics,* St. Louis, Missouri, Volume 3, pages 265-2272.

Katrichak, A.M., Finch, J.F., Little, T.E. and Turner, F.P.P. (1994): A West Coast Utility's Approach to Mitigating Earthquake Hazards. *Earthquake Engineering Research Institute,* Proceedings of the 5th U.S. National Conference on Earthquake Engineering, Volume 4, pages 861-871.

Klohn-Crippen Consultants Ltd. (1994): Preliminary Seismic Microzonation Assessment for British Columbia; *B.C. Resource Inventory Committee,* Report 17, 108 pages.

Levson, V.M., Matysek, P.F., Monahan, P.A. and Watts, B.D. (in preparation): Earthquake Hazard Mapping in British Columbia: Status, Demand and Methodology Development. *B.C. Ministry of Energy, Mines and Petroleum Resources,* Paper.

Levson, V.M., Monahan, P.A., Meldrum, D.G., Matysek, P.F., Watts, B.D., Yan, L. and Sy, A. (1995): Seismic Microzonation Mapping in Southwestern British Columbia: A Pilot Project. *Canadian Geotechnical Society,* Trends in Geotechnique, 48th Canadian Geotechnical Conference, Volume 2, pages 927-936.

Luternauer, J.L., Barrie, J.V., Christian, H.A., Clague, J.J., Evoy, R.W., Hart, B.S., Hunter, J.A., Killeen, P.G., Kostaschuk, R.A., Mathewes, R.W., Monahan, P.A., Moslow, T.F., Mwenifumbo, H.W., Olynyk, H.W., Patterson, R.T., Pullan, S.E., Roberts, M.C., Robertson, P.K., Tarbotton, M.R. and Woeller, D.J. (1994): Fraser River Delta: Geology, Geohazards and Human Impact; *in* Geology and Geological Hazards of the Vancouver Region, Southwestern British Columbia, , J.W.H. Monger, Editor, *Geological Survey of Canada,* Bulletin 481, pages 197-220.

Mabey, M.A. and Madin, I.P. (1993): Relative Earthquake Hazard Map of the Portland, Oregon 7.5 Minute Quadrangle; *Oregon Department of Geology and Mineral Industries* and *Metro,* 10 pages and 1:24 000 map.

Mabey, M.A., Madin, I.P. and Palmer, S.P. (1994): Relative Earthquake Hazard Map for the Vancouver, Washington, Urban Region; *Washington Division of Geology and Earth Resources,* Geologic Map GM-42, 5 pages and 1:24 000 maps.

Monahan, P.A. and Levson. V.M. (in preparation): Chilliwack Seismic Microzonation Project - Data Collection and Geological Overview; *B.C. Ministry of Energy, Mines and Petroleum Resources,* Paper.

Munich Reinsurance Company of Canada. (1992): A Study of the Economic Impact of a Severe Earthquake in the Lower Mainland of British Columbia; 99 pages.

Palmer, S.P., Schasse, H.W. and Norman, D.K. (1994): Liquefaction Susceptibility for the Des Moines and Renton 7.5-minute Quadrangles, Washington; *Washington Division of Geology and Earth Resources,* Geologic Map GM-41, 15 pages and 1:24 000 maps.

Robertson, P.K., Campanella, R.G., Gillespie, D. and Rice, A. (1986): Seismic CPT to Measure In Situ Shear Wave Velocity; *Journal of Geotechnical Engineering,* American Society of Civil Engineers, Volume 112 (GT3), pages 384-403.

Robertson, P.K. and Campanella, R.G. (1988): Guidelines for Using the CPT, CPTU and MARCHETTI DMT for Geotechnical Design; *in* Using CPT and CPTU Data, Washington, D.C., *Federal Highway Administration,* FHWA/PA-87/023+84-24.

Rogers, G.C. (1992): The Earthquake Threat in Southwest British Columbia; *in* Geotechnique and Natural Hazards, *Vancouver Geotechnical Society* and *Canadian Geotechnical Society,* Geohazards '92 Symposium Volume, *BiTech Publishers Ltd.,* pages 63-69.

Rogers, G.C. (1994): Earthquakes in the Vancouver Area; *in* Geology and Geological Hazards of the Vancouver Region, Southwestern British Columbia, Monger, J.W.H., Editor, *Geological Survey of Canada,* Bulletin 481, pages 221-229.

Seed, H.B. (1979): Soil Liquefaction and Cyclic Mobility Evaluation for Level Ground During Earthquakes; *Journal of Geotechnical Engineering,* Volume 105, pages 201-255.

Watts, B. D., Seyers, W.D. and Stewart, R.A. (1992): Liquefaction Susceptibility of Greater Vancouver Area Soils; *in* Geotechnique and Natural Hazards, *Vancouver Geotechnical Society* and *Canadian Geotechnical Society*, Geohazards '92 Symposium Volume, *BiTech Publishers Ltd.*, pages 145-157.

Youd, T.L. (1991): Mapping of Earthquake-induced Liquefaction for Seismic Zonation; Fourth International Conference on Seismic Zonation, *Earthquake Engineering Research Institute*, Volume 1, pages 111-147.

Youd, T.L. and Perkins, J.B. (1978): Mapping of Liquefaction-induced Ground Failure Potential; *Journal of Geotechnical Engineering*, American Society of Civil Engineers, Volume 104 (GT4), pages 433-446.

NOTES

# INDUSTRIAL MINERAL POTENTIAL OF THE TERTIARY ROCKS, VERNON (82L) AND ADJACENT MAP AREAS

**Peter B. Read, Geotex Consultants Limited**

*KEYWORDS*: Industrial minerals, Kamloops Group, Penticton Group, diatomite, precious opal, kadinite.

## INTRODUCTION

This report summarizes the results of 40 days of fieldwork investigating the occurrences of industrial minerals, and some of those aspects of the Tertiary stratigraphy which control their development, in a southeasterly trending area extending 150 kilometres from east of Kamloops (92I) through the Vernon map area (82L) to north of Beaverdell (82E). In this area, the industrial minerals of major interest are kaolinite, diatomaceous earth, swelling clay, zeolites, perlite, precious opal, gypsum and dimension stone, of which the first five are found in Tertiary strata elsewhere in the province. The regional geology of Cockfield (1948) and Monger and McMillan (1989) for the Ashcroft area (92I), Jones (1959) for the Vernon area (82L), Tempelman-Kluit (1989) for the Penticton area (82E), and Okulitch (1979) for the entire region give the geological framework. Mapping by Church (1980) and Christopher (1978), and D. Duba's (1988) unpublished mapping around Whiteman and Bouleau creeks, provided by K. Daughtry, Discovery Consultants Ltd., augment the detailed geological information in some areas of Tertiary rocks. Four major highways and railways effectively link this area to nearby major population centres.

At present, the gypsum quarry at Falkland and a flagstone quarry south of Revelstoke are the main industrial mineral producers in the Vernon map area. The potential for diatomaceous earth, swelling clays, precious opal, kaolinite, zeolites and perlite in the Tertiary strata of the area provide industrial mineral opportunities for the future.

## TERTIARY STRATIGRAPHY

### *KAMLOOPS AND PENTICTON GROUPS*

The volcanic-dominated rocks of the Kamloops and Penticton groups form a continuous sheet stretching 150 kilometres north-northwest from Trepanier on the west side of Okanagan Lake (82E) (Figure 1) to north of the South Thompson River east of Kamloops (92I) (Figure 2). The 25 to 30 kilometre wide belt is broken only where the deeply incised, east or west-flowing drainages of Whiteman Creek, and Salmon and the South Thompson rivers cross it. West of Falkland, Estekwalan and Tuktakamin mountains expose a minimum thickness of 600 metres of mainly volcanic rocks deposited on a paleotopography with a relief of hundreds of metres.

### *KAMLOOPS GROUP*

North of Kamloops, basal sediments along the northeastern edge of the Eocene belt belong to the Chu Chua Formation (Uglow, 1922). In the Kamloops area, the Kamloops Group consists of a lower succession of sediment-tuff±flows of the Tranquille Formation which underlies several members of the 1000 metre thick basalt/andesite Dewdrop Flats Formation. Ewing (1981, p. 74) noted that the basal sediments and intercalated volcanics comprising the Tranquille Formation are laterally restricted because they accumulated in a fault-bounded, northwest-trending basin. Because the typical andesite/basalt rocks of the Dewdrop Flats Formation are extensive east of Kamloops, the formation name has been retained to the east and south.

Ewing's detailed investigation of the Kamloops Group around Kamloops and Church's (1980) mapping of the Eocene rocks west of Vernon resulted in Ewing (1981) proposing a stratigraphy for the Eocene rocks in the area between Vernon and Kamloops where he did no detailed mapping. The informal stratigraphy adopted in this report partly draws on Church's suggestions (1979; 1982) and modifies those suggested by Ewing by replacing the name Tuktakamin breccia with the better exposed Estekwalan tephra on Estekwalan Mountain, and replaces Ewing's suggested Monte Lake basalt with the Dewdrop Flats Formation.

#### CHU CHUA FORMATION (units Esx, Escg, and Essr)

Along the northeastern side of the Eocene belt, the Chu Chua Formation occurs as a few basal lenses of Eocene sediments in Shorts and Bolean creeks, and at the east end of Pinaus Lake, but does not form the numerous lenses shown by Okulitch (1979). In Shorts Creek, tuffaceous shale to grit and rare carbonaceous shale form an unfaulted lens 15 metres thick at the base of the Eocene. Near the valley floor on the north side, the lens thickens to 50 metres of sedimentary breccia comprising angular siltstone and rare granitic clasts up to 40 centimetres on edge. On the southwest side of Bolean Creek, south of Pillar Lake, a few roadcuts expose a lens of sedimentary breccia (**Esx**) 3 kilometres long that reaches a thickness of 125 metres. Angular clasts of grey phyllite, greenstone and granitic rocks up to 1 metre long lie in a crudely bedded matrix of lithic grit. On the north side of Pinaus Lake, within a kilometre of the east end, a few lakeshore outcrops expose a succession of subangular peb-

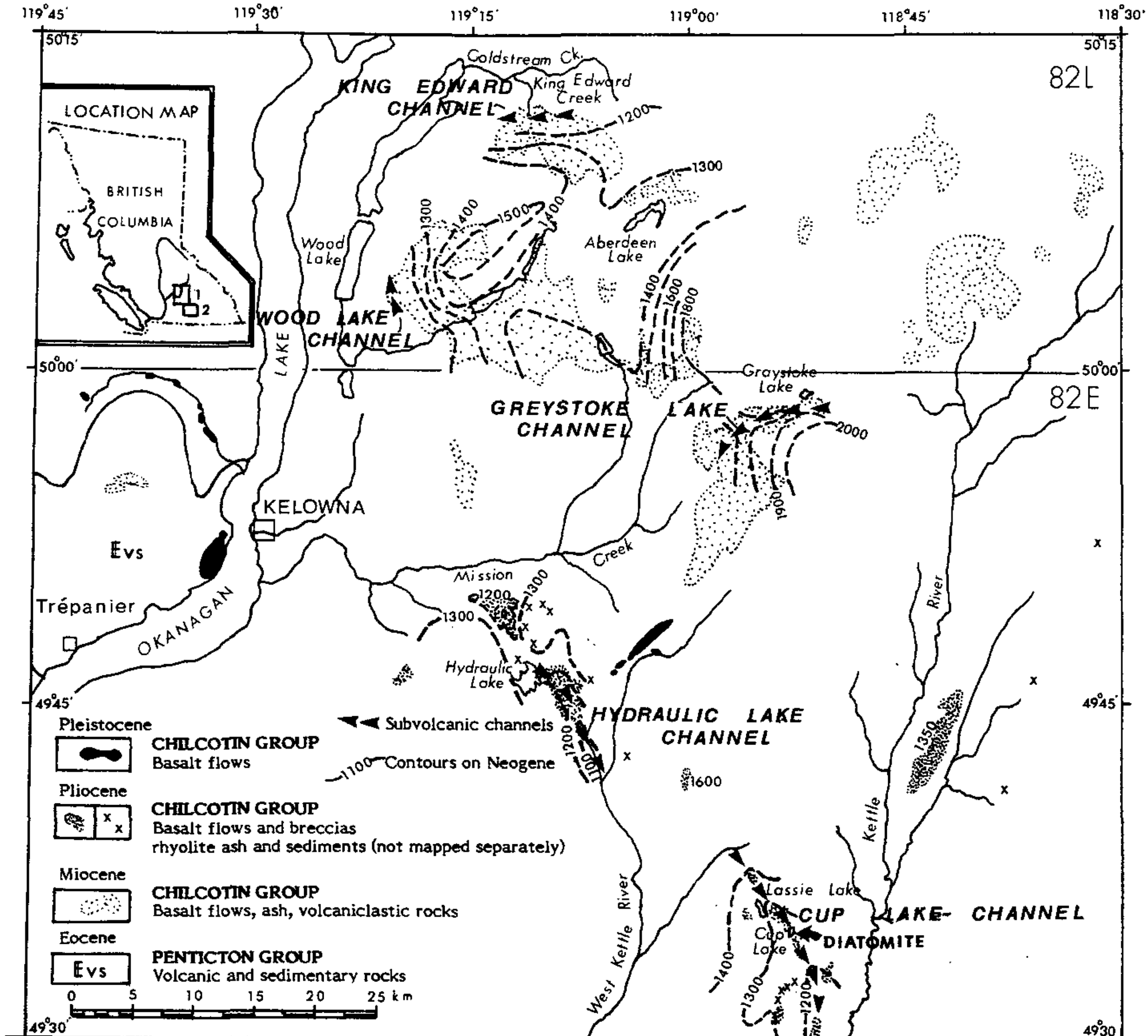


Figure 1. Regional geological map showing the distribution of the sedimentary and volcanic rocks of the Chilcotin Group and subvolcanic drainage channels near Okanagan Lake (82E). Adapted from Mathews (1988).

ble to cobble conglomerate, sandstone and rare carbonaceous shale of unit **Escg**. Outcrops of waterlain rhyolite ash-tuff (**Essr**) form small basal lenses on the south ridge of Siwash Rock Mountain and immediately south of Highway 97 and east of Ingram Creek.

In the basal sedimentary lenses correlated with the Chu Chua Formation, sedimentary breccia and subangular pebble to cobble conglomerate develop almost to the exclusion of fine clastic sediments. Their dominance indicates that the sub-Eocene unconformity either initially had a high paleorelief, or, as favoured by Mathews (1981, p. 1313) for the Enderby area northeast of Vernon, the Eocene basement had a large paleorelief maintained by high-angle growth faulting during deposition. The large size and extreme angularity of the clasts, monomict composition of the breccias and their obvious local derivation support Mathews' interpretation,

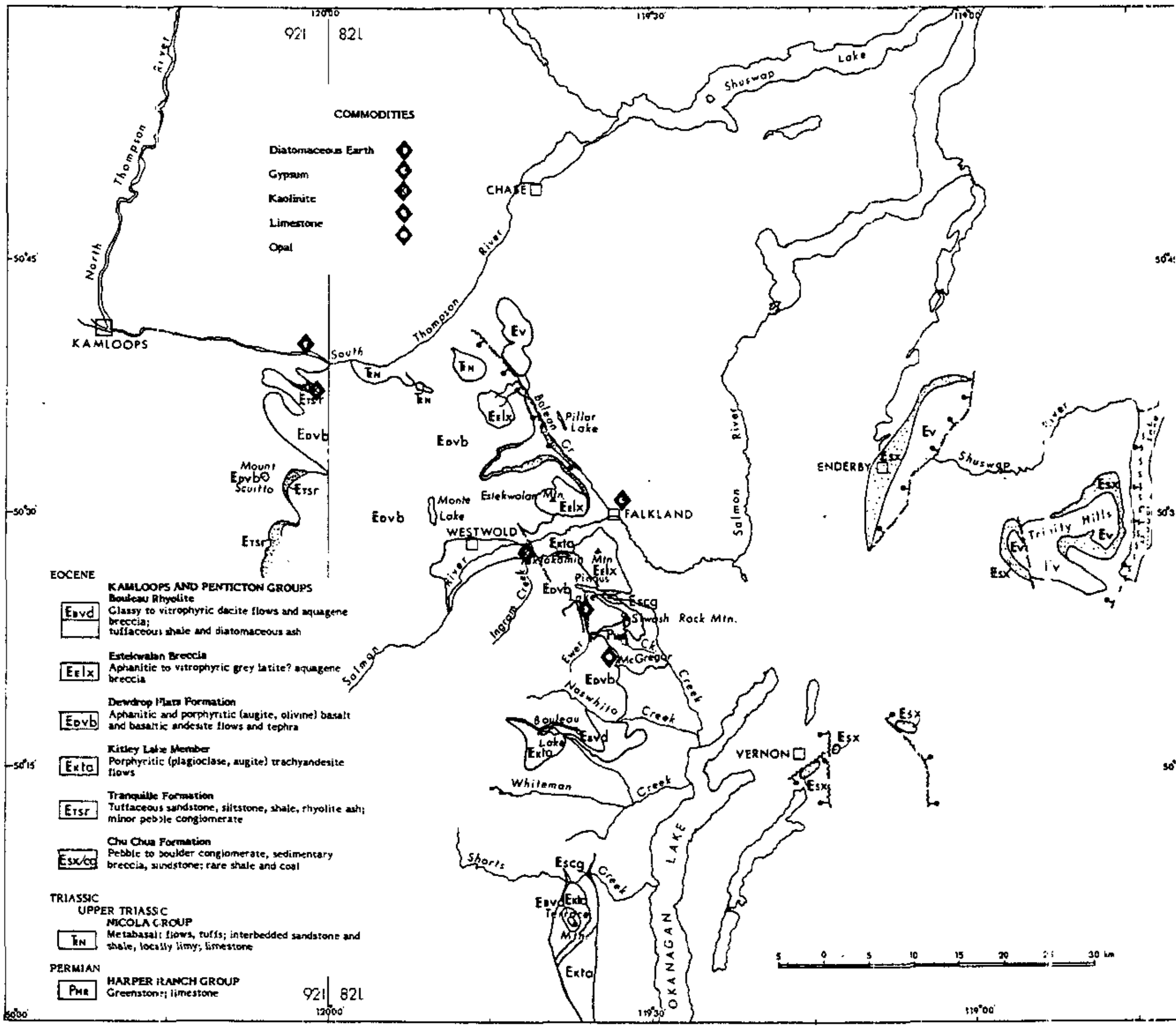


Figure 2. Regional geological map showing the distribution of the sedimentary and volcanic rocks of the Kamloops and Penticton groups of Eocene age.

which may be extended to include the Eocene sediments in the Trinity Hills associated with a north-northeast striking growth fault along Mabel Lake, and, with less certainty, the Eocene sediments in Bolean Creek with a subjacent north-northwest striking growth fault along the creek. By contrast, in the Kamloops Group at Buse Lake and Scuitto Creek, coarse clastic rocks are absent from the basal sedimentary lenses of the Tranquille Formation, which in these two areas probably formed under lacustrine or paludal conditions.

## TRANQUILLE FORMATION (unit ETsr)

Typically tuffaceous sediments locally fill the paleotopographic lows at or near the base of the Eocene succession and form lenses up to 125 metres thick and a few kilometres long. At Buse Lake, on the southwest side of the Eocene belt, a white-weathering airfall and waterlain crystal-vitric rhyolite ash up to 60 metres thick dominates a succession which includes plant-bearing shale and tuffaceous sandstone correlated with the Tranquille Formation (Photo 1). These lenticular sediments and ashes of unit ETsr outcrop at Buse Lake and on the divide between Scuitto and Woodland creeks, but not on the east ridge of Mount Scuitto as indicated by Cockfield (1948).

## DEWDROP FLATS FORMATION (units EDvb and EDbs)

The Dewdrop Flats Formation contains the volcanic-dominated part of the Kamloops Group. Augite-olivine ba-

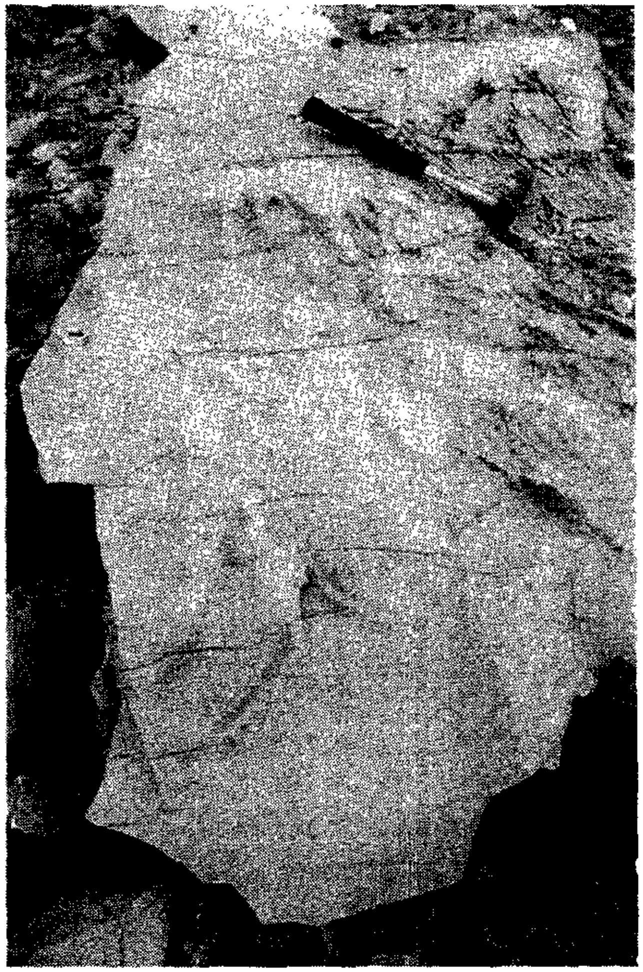

Photo 1. Waterlain rhyolite vitric-crystal tuff of the Tranquille Formation exposed in Buse Lake quarry where it is worked for its kaolinite content.

salt and basaltic andesite flows, interflow breccia and minor basaltic tuff extend from southeast of Kamloops to west of Vernon. Because the rocks in this area cannot be distinguished from those of the Dewdrop Flats Formation, Ewing's suggested name of 'Monte Lake basalt' for these rocks has been discarded. Medium to dark grey, aphanitic to porphyritic (5-15% olivine) basalt flows and interflow breccia of unit **EDvb** extend over 50 kilometres southeasterly from southeast of Kamloops to west of Vernon. Southeast of Kamloops, the mapped area east of Mount Scuitto includes the basal 100 metres of an unknown thickness of basalt flows. Farther to the southeast around Monte Lake, the unit exceeds 300 metres with the top outside the map area, and south of Pinaus Lake it is about 300 metres thick beneath the overlying Bouleau Member. To the southeast on the Klinker property north of McGregor Creek, the member is about 200 metres thick and consists of mostly breccia and lahar with only a few flows. Between McGregor and Naswhito creeks, the formation may end because Church (1979; 1980) mapped a sequence of thin-bedded, fine-grained andesite and dacite lavas immediately under the Bouleau Member.

Well bedded, grey lithic tuff lenses of unit **EDbs** lie within the basalt flows of the Dewdrop Flats Formation. Each tuff lens is less than 2 kilometres long and 100 metres thick, of basalt/andesite composition, and probably of airfall origin. A lens cut by an old logging road at 1450 metres (4750 feet) elevation, on the south side of Siwash Rock Mountain, and another exposed at 1370 metres (4500 feet), on the powerline access road south of the east end of Pinaus Lake, are about 250 metres above the base of the Eocene. Straddling Salmon River valley, another lens outcrops low on the valley sides about half way between Falkland and Westwold. It is less than 100 metres above the base of the Eocene. None of these lenses is locally opalized.

TABLE 1
LOCATION, OPTICS AND X-RAY CHARACTERISTICS OF COMMON AND PRECIOUS OPALS, VERNON MAP AREA

| Unit Sample | Location mE | Location mN | Refractive Indices | X-Ray Diffraction Classification* |
|---|---|---|---|---|
| Bouleau Member | | | | |
| V5M | 314650 | 5583760 | 1.448 ± 0.005 | opal-CT |
| Estekwalan tephra | | | | |
| V33Q | 314520 | 5598530 | 1.545+<D>0.005 | quartz |
| V33AA | 314300 | 5597160 | 1.46-1.47 | opal-CT ± quartz |
| V34E1 | 312730 | 5598050 | 1.430 ± 0.005 | opal-CT ± quartz |
| V35E | 314430 | 5596950 | 1.445 ± 0.005 | opal-CT ± quartz |

Klinker property (data from D. Awram)
317680 5581500

*X-ray diffraction classification of Jones and Segnit (1971)

Ewing's (1981) single whole-rock analysis (Table 1, 27-5) indicates that these rocks lie close to the boundary between basaltic andesite and basalt. The scattered appearance of biotite and hornblende, and sanidine rims on plagioclase suggest that the rocks of this unit may include basaltic trachyandesite and trachybasalt. In thin section, augite phenocrysts are common and olivine is largely pseudomorphed by "iddingsite"±carbonate. A few rocks contain red-brown pleochroic biotite flakes which are resorbed with opaque-rich margins, and partly resorbed basaltic hornblende is rare. Rounded plagioclase phenocrysts ($An_{55-62}$) are sparse and some have sanidine rims. The typical matrix is granular augite and fine plagioclase microlaths with some rocks having fine, pleochroic brown biotite flakes.

## *PENTICTON GROUP*

When Church (1982) proposed the name Penticton Group for the Eocene volcanic and sedimentary rocks of the Okanagan-Boundary region, he did not indicate how to distinguish them from the physically continuous rocks of the long-recognized Kamloops Group (Drysdale, 1914; Rose, 1914) to the northwest. The present map area partly covers the gap between Church's Penticton Group west of Vernon and the type locality of the Kamloops Group. The distinction between the two groups is presently unclear, and upon further study, may disappear because of the priority of the term "Kamloops Group". In the present area, those units which tentatively correlate with members of Church's Penticton Group near Terrace Mountain are assigned to that group. The other units which extend to Kamloops have been placed in the Kamloops Group. In view of the high alkali content of Estekwalan tephra and its restriction to the southeast edge of the Eocene volcanic belt, it is assigned to the Penticton Group.

### ESTEKWALAN TEPHRA (units $E_E$lx and $E_E$vd)

West and south of Falkland, a section of aphanitic to vitrophyric latite (potassic trachyandesite) and trachydacite aquagene breccia at least a 800 metres thick, forms northwesterly trending belt. It underlies the northeastern edge of the Eocene belt and forms the upper parts of Siwash Rock, Tuktakamin and Estekwalen mountains. The east end of the south face of Estekwalan Mountain exposes white-weathering, grey vitric and vitrophyric tephra of unit **$E_E$vd**, containing angular clasts averaging 6 centimetres on edge, and scattered lenses of light grey to white rhyolite ash (Photo 2). Locally the ash is waterlain, zeolitized (heulandite-clinoptilolite), and here and there opalized with opal-CT±quartz

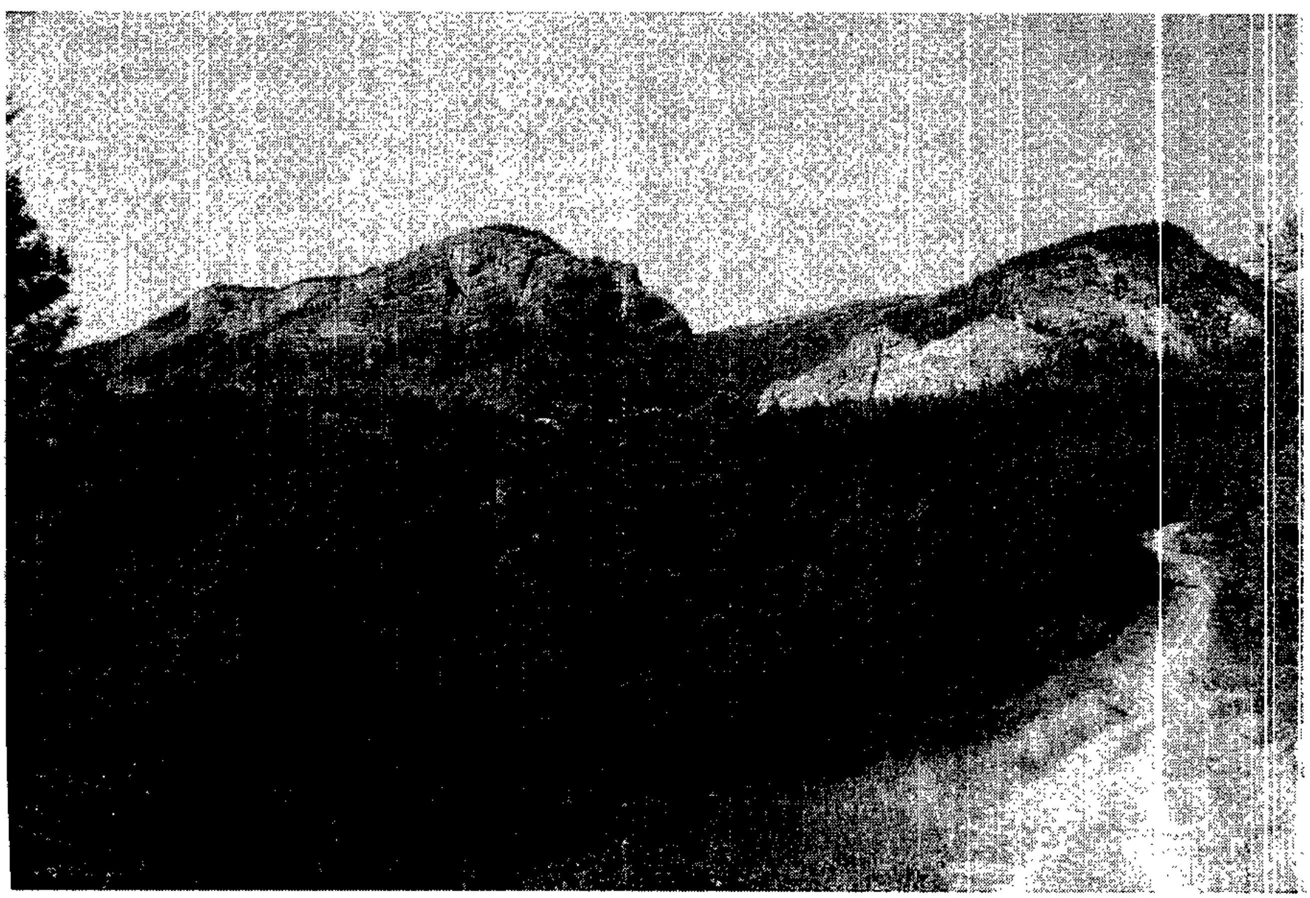

Photo 2. The south face of Mount Estekwalan showing coarsely bedded west-dipping aquagene latite? breccia of Estekwalan tephra ($E_E$lx).

(*see* Precious Opal Potential). Present mapping indicates that the dacite tephra of Estekwalan and Tuktakamin mountains lie on a westward-dipping unconformity. The white-weathering dacite tephra pass upward into buff-brown latite tephra. Because the Estekwalan tephra is particularly prone to rock slides, its basal contact is covered in all but a few localities. The resulting slide debris renders thickness estimates uncertain but they lie between 500 and 1000 metres. On Estekwalan Mountain, the bedding, probably foreset, dips gently westward and indicates, as Ewing noted (1981, p. 70-71), that the Estekwalan tephra forms the western flank of an eruptive centre.

Ochre-brown weathering glassy to vitrophyric (augite, pseudomorphed olivine, rare resorbed plagioclase plated by sanidine, and biotite) latite breccia of unit **EElx** underlies a belt 20 kilometres long extending northwesterly from the east side of Siwash Rock Mountain through the top 300 metres of Tuktakamin Mountain to the north side of Estekwalan Mountain. It may extend a further 15 kilometres northwestward through Mount Martin. The breccia has 2 to 10-centimetre, angular clasts in a soft, ochre-brown weathering palagonite matrix (Photo 3) which is unbedded in outcrop but on some hillsides shows crude bedding with a gentle westward dip (Photo 2). Thin sections show euhedral augite phenocrysts and glomerocrysts with associated coarse apatite prisms, resorbed and euhedral plagioclase laths ($An_{40-45}$) plated by thin sanidine rims, olivine partly replaced to totally pseudomorphed by "iddingsite"±carbonate, and rare resorbed biotite with opaque-rich rims. The matrix consists of feldspar microlaths, granular augite and glass. The unit is at least 300 metres thick, rests on a gently dipping basement and, west of mounts Estekwalan and Tuktakamin, overlies flows of the Dewdrop Flats Formation.

### KITLEY LAKE MEMBER (unit EKLta)

On the south wall of Salmon River valley west of Falkland, a tongue of grey porphyritic trachyandesite flows of unit **EKLta**, 3 kilometres long, contains sanidine-rimmed plagioclase, augite and rare biotite phenocrysts. It lies between the basement and the overlying Dewdrop Flats basalt flows and basalt lithic tuff. The unit is tentatively correlated with the Kitley Lake Member of the Marron Formation. Around 1310 metres (4300 feet) elevation, immediately south of the road to the summit of Tuktakamin Mountain, the outcrop pattern of **EKLta** implies a truncation of the unit and its overlap by Dewdrop Flats basalt flows.

### BOULEAU MEMBER (units EBsr and EBvd)

Within and north of the headwaters of Ewer Creek, a gently west dipping sequence of glassy dacite flows and lapilli tuff of unit **EBvd** overlies a thin tuffaceous (vitric rhyolite) shale and siltstone unit **EBsr** which together exceed 100 metres in thickness. The units are tentatively correlated with Church's (1979) Bouleau rhyolite which extends some 30 kilometres southward to Terrace Mountain where radiometric dating gave a biotite K-Ar age of 52.3±1.8 Ma. The unit rests on the top of the Dewdrop Flats Formation.

Photo 3. Exposures of palagonitic latite? tuff-breccia at the microwave tower on the summit of Mount Tuktakamin.

Cream-weathering, tuffaceous shale and siltstone, containing diatoms, palynomorphs, plant and fish fossils, form a poorly exposed lens of unit **EBsr** which is at least 4 kilometres long and no more than a few tens of metres thick. The presence of diatoms, siliceous sponge spicules and fossil fish indicate the lacustrine setting of this locally opalized unit (*see* Precious Opal Potential) at the base of the Bouleau Member.

Most of the Bouleau Member is a light to dark grey, vitrophyric dacite lapilli tuff of unit **EBvd** with sparse phenocrysts of augite, hypersthene, partly resorbed plagioclase, and rare hornblende and opaque-dusted biotite. Coarse apatite prisms lie in or on the pyroxene phenocrysts which here and there show augite plating rounded hypersthene cores. The plagioclase phenocrysts range from $An_{37-45}$, and in distinction to those of the Estekwalan latite, they lack sanidine rims. The angular clasts range from 2 to 10 centimetres on edge and lie in a white ash matrix. The remainder of the unit is glassy dacite flows. The member is less than 100 metres thick and is capped by a plagiphyric andesite west of the mapped area.

### *CHILCOTIN GROUP*

On the east side of Okanagan Lake, basalts and minor sediments of the Chilcotin Group form residua ranging in area from 0.2 to 140 square kilometres. They lie in a belt up to 50 kilometres wide which extends 90 kilometres from the south side of Coldstream Valley (82L) to the west side of the West Kettle River valley (82E) (Figure 1). Olivine basalt flows, tephra and underlying sediments form the Middle Miocene King Edward Creek Formation and the Late Miocene to Early Pliocene Kallis Formation that compose the Chilcotin Group in the Okanagan Highlands (Mathews, 1988). The Middle Miocene basalt, up to 200 metres in thickness, and Mio-Pliocene basalts, to as much as 100 metres thick, protect underlying and locally intercalated sediments which aggregate to as much as 74 metres in thickness (Christopher, 1983). The sediments comprise fluviatile conglomerate and sandstone, and here and there, overbank swamp deposits of carbonaceous shale, waterlain rhyolite ash and diatomaceous earth. Both the basalts and sediments form scattered remnants of paleo-valley fillings of a formerly extensive drainage system in the Middle and Late Miocene. If one assumes only minor regional tilting since their formation, the systems drained southerly.

Of the diamond-drill core samples collected by Z.D. Hora from several properties in the Cup Lake and Hydraulic Lake paleochannels, core from twelve out of the fourteen holes sampled from Cup Lake contains diatomaceous siltstone and shale sections up to 8 metres thick. An age determination by J.M. White, based on palynomorphs from one of the four most carbonaceous of the diatomaceous samples, yielded a possible Late Miocene to Early Pliocene date which is consistent with the age restriction imposed by the oldest K-Ar age of the overlying basalt flows at 5.9±0.3 Ma (latest Miocene).

## STRUCTURE

Because this study concentrated on the Eocene and younger rocks of the region, only structures in this age range are considered. Although the sub-Eocene unconformity records the type and amount of Eocene and younger deformation, uncertainty concerning the amount of relief of the Eocene paleotopography, and the poor exposure near the base of the Eocene, complicate the reading of this record.

On either side of the Eocene belt stretching from Okanagan Lake to east of Kamloops, inward-dipping bedding attitudes outline a large, upright syncline which extends for more than 150 kilometres to the north-northwest. From south to north, the crossing valleys of Lambly, Shorts, Whiteman, Ewer and Equesis creeks and Salmon River provide glimpses of the inward-dipping limbs of the syncline. High-angle normal faults, with hundreds of metres or less of throw, locally modify the syncline. Near the north end of Okanagan Lake, Thompson and Daughtry (1994) mapped a number of north to northeast-striking high-angle normal faults which are usually west-side down and are consistent in attitude and movement with an Eocene growth fault mapped by Mathews (1981) near Enderby. Midway between Falkland and Westwold a high-angle, west-side-down normal fault traverses the Eocene and offsets an airfall tuff lens to yield a throw of 100 metres. On Bolean Creek, restriction of the Eocene sedimentary breccia to the southwest bank requires either a fault immediately northeast of the breccia outcrops or a steep paleovalley wall. Because minor faults cut the breccia, I prefer a fault. Elsewhere, incomplete mapping of the unconformity shows that elevation differences of up to 600 metres along it probably resulted from Eocene paleotopography rather than faulting.

## INDUSTRIAL MINERAL POTENTIAL

### *DIATOMITE POTENTIAL*

In British Columbia, the fluviatile and lacustrine sediments of the lower part of the Chilcotin Group, that is the Fraser Bend and Deadman River formations, have the greatest diatomite potential. These formations encompass the sediments developed in drainage systems with paludal (swamp) and lacustrine settings that involved silica-charged waters derived from the weathering of a slightly older rhyolite crystal-vitric ash-tuff. Diatoms flourished. Because the deposits are only 5 to 15 Ma old, the diatoms have not recrystallized, lost their porosity and industrial usefulness, as commonly has happened with diatoms found in Eocene rocks in British Columbia (but *see* below). Prior to this investigation, recorded diatomite occurrences clustered along the Fraser River for 175 kilometres from north of Quesnel (93G; Hora and Hancock, 1995) to Gang Ranch (92O) in the south (Read, in press), and from there 125 kilometres southeast to Red Lake east of Deadman River (92I and 92P; Hora, 1986) and Mount Guichon (McMillan, 1978).

The discovery of diatomaceous earth at Cup Lake extends diatomite occurrences a further 220 kilometres to the southeast (Figure 1). Although cursory sampling of the drill core from properties surrounding Cup Lake did not encounter diatoms, it is likely that 15 to 20 years ago the carbonaceous shale which hosts the diatoms was selectively removed for chemical analysis. Present sampling shows that only the sediments of the southerly flowing Cup Lake channel are diatomaceous, but the core from the sediments of a contemporaneous channel through Hydraulic Lake needs close examination as does that from older channels near Graystoke Lake, Wood Lake and King Edward Creek.

In the Vernon map area, several occurrences of Eocene sediments with unrecrystallized diatoms suggest that, locally, Eocene rocks have diatomaceous earth potential. Although diatoms were discovered many years ago in the Eocene rocks of Vermilion Bluffs in the Princeton Basin (Hills 1962, p. 49), widespread zeolite facies regional metamorphism of these diatomaceous rocks has resulted in the recrystallization of the diatoms and a loss in porosity which has rendered them useless as an industrial mineral. Eocene diatomites will survive only in areas with an absence of later recrystallization. A clue that the subsequent recrystallization of the rocks is only slight is the presence of ubiquitous vesicles or fractures, and amygdules filled with agate, opal, chalcedony and strongly hydrated zeolites, such as ferrierite, erionite, mesolite, thomsonite, chabazite and stilbite. These textures or mineral assemblages imply that the rocks have undergone a subsequent alteration involving little silica recrystallization. However, the presence of quartz, prehnite, chlorite, epidote, albite and the common less-hydrated zeolites such as heulandite-clinoptilolite, laumontite and wairakite indicate that the rocks have suffered alteration sufficient to recrystallize the diatoms.

### DESCRIPTIONS OF OCCURRENCES

Diatomaceous tuffs lie at the base of the 100 metre thick Bouleau Member which grades up through tuff and breccia to dacite flows. Although oil-immersion grain mounts show that clay minerals, quartz and feldspar dominate over diatoms, they indicate, more significantly, the occurrence of unrecrystallized diatoms and siliceous sponge spicules in the Eocene of British Columbia.

| | | | | |
|---|---|---|---|---|
| **D1** | **Pinaus** | | MINFILE: | 082LSW159 |
| | STATUS: | Showing | NTS: | S082L/05E |
| | TYPE: | Sedimentary | LAT./LONG.: | 50°23′41″; 119°36′41″ |
| | ELEVATION: | | 1335 m (4375 feet) | |
| | UTM: | LF0313950mE; LF5585550mN | | |

The Pinaus showing is located in a roadcut of cream-weathering, diatomaceous and tuffaceous shale and siltstone with plant fossils and, reportedly, fish fossils. Oil-immersion grain mounts show about 25% unrecrystallized diatoms in a matrix of montmorillonite-altered glass (determined by x-ray diffraction), and minor amounts of quartz and feldspar. The roadcut crosses a few metres of thickness with neither the top or base exposed. Similar appearing, but sparsely diatomaceous sediments with 10% or less unrecrystallized diatoms, form roadcuts and angular blocks of float at LF0313950mE and LF5586600mN at 1335 metres (4375 feet) elevation and under the powerline at LF0313920mE and LF5587120mN at 1365 metres (4475 feet) elevation. In total, the scattered outcrops of diatomaceous earth indicate a strike length of 1.9 kilometres, with both ends open, and a minimum thickness of a few metres.

## *PRECIOUS OPAL POTENTIAL*

Agate[1] is widespread in the Eocene to Pliocene lavas of British Columbia, common opal[2] is sparsely scattered, and precious opal[2] occurs in very few localities. Only one or two chips of precious opal have been found in each of the three British Columbia localities reported by Leaming (1973). With staking of the Klinker claim in 1991 and the Ewer claim in 1992, R.W. Yorke-Hardy recorded the first significant discovery of precious opal in both British Columbia and Canada. The staking of other claims soon followed and covered an area of scattered opal showings which extends past a powerline 6.5 kilometres northwest of the original discovery. Within the staked area, agate is widespread, and a nearby sequence of tuffaceous shale and waterlain rhyolite ash at the base of the Bouleau Member (**EBsr**) is locally altered to a grey vitreous "chert" composed of common opal (Table 1, Sample V5M). Based on an x-ray diffraction identification, the common opal is opal-CT. Similar widespread agate and waterlain rhyolite ash, with locally developed common opal "chert" lenses form in the basal rhyolite ash of the Estekwalan tephra (**EEvd**) between 800 and 1100 metres (2600 and 3600 feet) elevation on the south flank of Estekwalan Mountain (Table 1, Samples V33Q to V35E). These similarities in silica minerals may indicate another area prospective for precious opal.

### DESCRIPTIONS OF OCCURRENCES

| | | | | |
|---|---|---|---|---|
| **O1** | **Klinker Property** | | MINFILE: | 082LSW125 |
| | STATUS: | Producer | NTS: | 082L/05E |
| | TYPE: | Volcanic | LAT./LONG.: | 50°21′49″; 119°33′48″ |
| | ELEVATION: | | 1490 m (4875 feet) | |
| | UTM: | LF0317680mE; LF5581500mN | | |

The Klinker property, consisting of 24 mineral claims, covers several concentrations of precious opal developed in the basal 100 metres of the Dewdrop Flats Formation (EDvb) of the Kamloops Group. The hostrock is a volcanic breccia-lahar mixture composed of angular to rounded

---

[1] **agate** is microcrystalline quartz with a large number of micropores (Deer *et al.*, 1963). It displays a colour variation arranged in planar or concentric zones. Refractive indices fall in the range 1.534 to 1.539. [2] **common opal** is a hydrous cryptocrystalline or colloidal form of silica with a composition of $SiO_2.nH_2O$ with a water content around 6 to 10%. Refractive indices fall in the range 1.44 to 1.47. In **precious opal** a play of delicate colours is observed (Deer *et al.*, 1963).

clasts of basalt, ranging from 0.2 to 0.6 metre in diameter, in a lapilli tuff matrix. In the lahar, the tuff has bedding which swirls around the clasts. Lapilli tuff lenses up to 5 metres thick develop locally and indicate that the volcanic succession dips 20 to 30o to the west. Thin basalt flows and intrusions up to 4 metres thick are scattered throughout. On McGregor Creek Forestry Access Road, about 500 metres east of the Discovery pit (Figure 3), outcrops of grey-green meta-andesite flows and lapilli tuffs of the Harper Ranch Group of probable late Paleozoic age form the basement which dips gently westward and underlies the valley bottom of Ewer Creek north of the property.

On the property, precious opal, agate and common opal fill fractures in the Eocene rocks and permeate podiform rock masses which are up to 0.5 metre in diameter in the lahars. The podiform rock masses are smaller in the lapilli tuffs and absent in the flows or intrusions. Precious opal filled fractures preferentially develop in sets with three preferred strikes: 025±10°, 070±10° and 330±15°; all sets have steep dips. The podiform masses commonly form beside or across opal-filled fractures. Precious opal fills voids developed during the formation of the hostrock, and later openings apparently formed by local dissolution of the host. Here and there the precious opal, agate and common opal have layering which is subhorizontal even in subvertically oriented fracture fillings. The presence of this subhorizontal layering in these materials, which is not subparallel to the orientation of the gently west dipping lapilli tuff, either implies that the precious opal, agate and common opal precipitated after the beds were tilted, or that the beds had a primary dip equal to the difference between the layering in the lahar and in the silica.

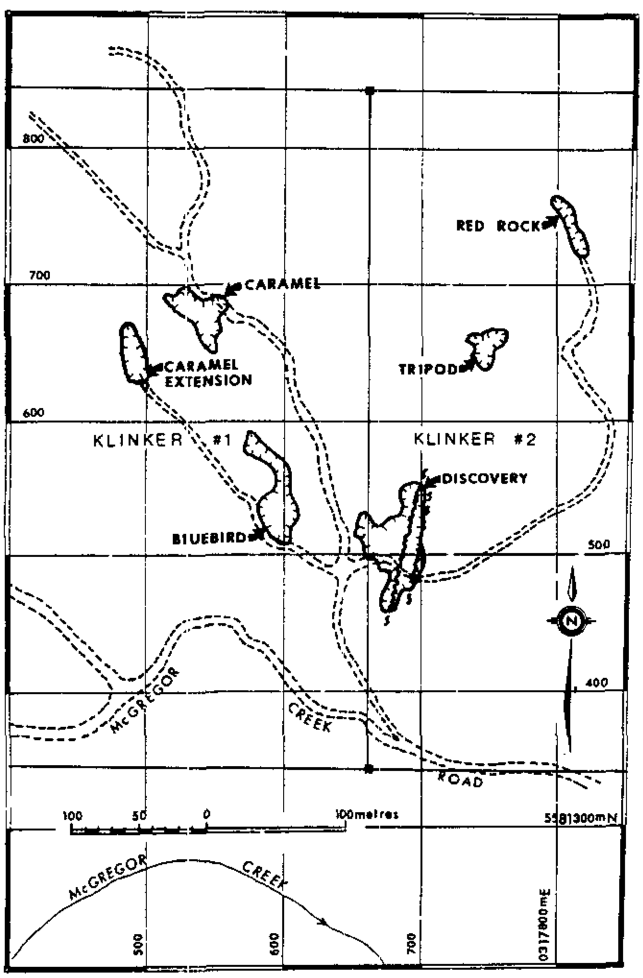


Figure 3. Open pits developed in the basal basalt lahars exposed on the Klinker property of Okanagan Opal Inc.

Of the six shallow pits exposing the precious opal on the Klinker property, the Discovery pit is the largest at 2100 square metres, and together with the smaller Bluebird pit, probably the richest because of subequally developed podiform masses and fracture fillings (Figure 3). A right-lateral strike-slip fault dips 80° northwest (slickensides trend/plunge 195/25S), passes along the eastern side of the pit, and offsets the lahars an indeterminate amount. In the other shallow pits, the Tripod, Red Rock and the Caramel and its extension, podiform masses in the lahars developed at the expense of fracture fillings. A lapilli tuff underlies the eastern side of the Caramel pit. Outside the pit areas, the primary openings in the rock are either mostly empty or less commonly filled with agate, common opal, chabazite - a strongly hydrated zeolite ($CaAl_2Si_4O_{12} \cdot 6H_2O$), and other unidentified zeolites.

## *KAOLINITE POTENTIAL*

In the interior of British Columbia, kaolinite has been reported from Tertiary rocks at Giscome Rapids north of Prince George (Cummings and McCammon, 1952), and at the Fairley prospect west of Princeton (Read, in press). Here and there, felsic volcanism heralded the widespread mid-Eocene volcanism of central British Columbia. Kaolinite deposits may develop where the airfall vitric ashes were deposited in palludal or lacustrine settings under the ambient warm temperate to subtropical climate. Such a combination of conditions probably generated the low-grade kaolinite occurrences at Buse Hill (**K1**) where kaolin has been quarried for more than 25 years, and east of the mouth of Will Creek (**K2**) immediately south of Highway 97, 7 kilometres east of Westwold. Although both of these occurrences are in mid-Eocene strata immediately above the unconformity, not all such ash-tuffs are altered to kaolinite-quartz The mainly airfall, not waterlain, ash-tuff straddling Scuitto Creek remains unaltered

## DESCRIPTIONS OF OCCURRENCES

K1 Buse Lake Quarry — MINFILE: 092INE123
STATUS: Producer — NTS: 92I/09E
TYPE: Sedimentary — LAT./LONG.: 50°37'57"; 12°01'32"

ELEVATION: 520 m (1700 feet)
UTM: GM0710400mE; GM5611790mN

The presently quarried rock was initially staked for its potential use as a building stone (Parks 1917, p. 179-181).

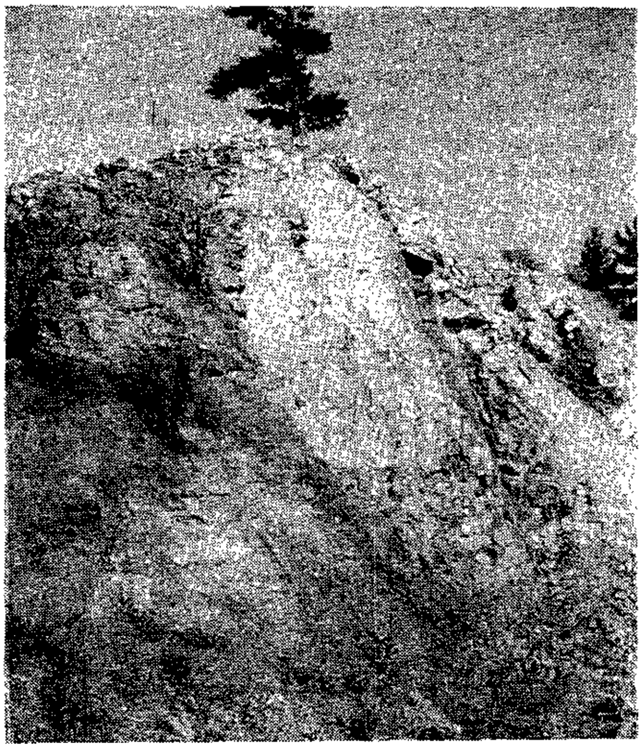

Photo 4. A view to the east in the upper quarry at Buse Lake where the white kaolinite-rich ash-tuff of the Tranquille Formation, exposed under the tree, overlies deeply weathered volcanics of the Nicola Group, exposed above the packsack.

Since 1968, Canada Cement Lafarge Company has operated a quarry at the base of a low hill near the southeast corner of Buse Lake. The company quarries a siliceous tuff of the Tranquille Formation for its high alumina (15.78%) and low alkali contents, and transports it 7.2 kilometres by road to its cement plant on the north side of the Thompson River near the village of Campbell Creek. Although production records are incomplete, the annual production from the quarry is in the range of 9400 (1970) to 26 200 tonnes (1973) with an average of about 20 000 tonnes/year. With an alternate and cheaper source of material, production from the quarry has declined recently to about 10 000 tonnes/year.

Scattered outcrops and two quarries within 300 metres of the southeast shore of Buse Lake expose the basal 100 metres of the Kamloops Group unconformably resting on a basement of metabasalt flows of the Upper Triassic Nicola Group and granitic intrusions. Near the lake, the lower quarry exposes the upper 20 metres of a 30-metre thickness of cream to pale buff rhyolite of unit **ETsr**, and the upper quarry, 300 metres southeast of the lake, exposes the lower 20 metres of Eocene tuff and the underlying flows of the Nicola Group (Photo 4). The rhyolite forms a wispy layered to unbedded succession of mainly airfall vitric-crystal (quartz, biotite) ash with pieces of plant stems but no leaves. In the lower quarry, the upper 6 metres of rhyolite ash is well bedded, with prominent plant stems and tree trunks and intercalated carbonaceous shale layers which yield a palynological age of Eocene. The overlying 2.5 me-

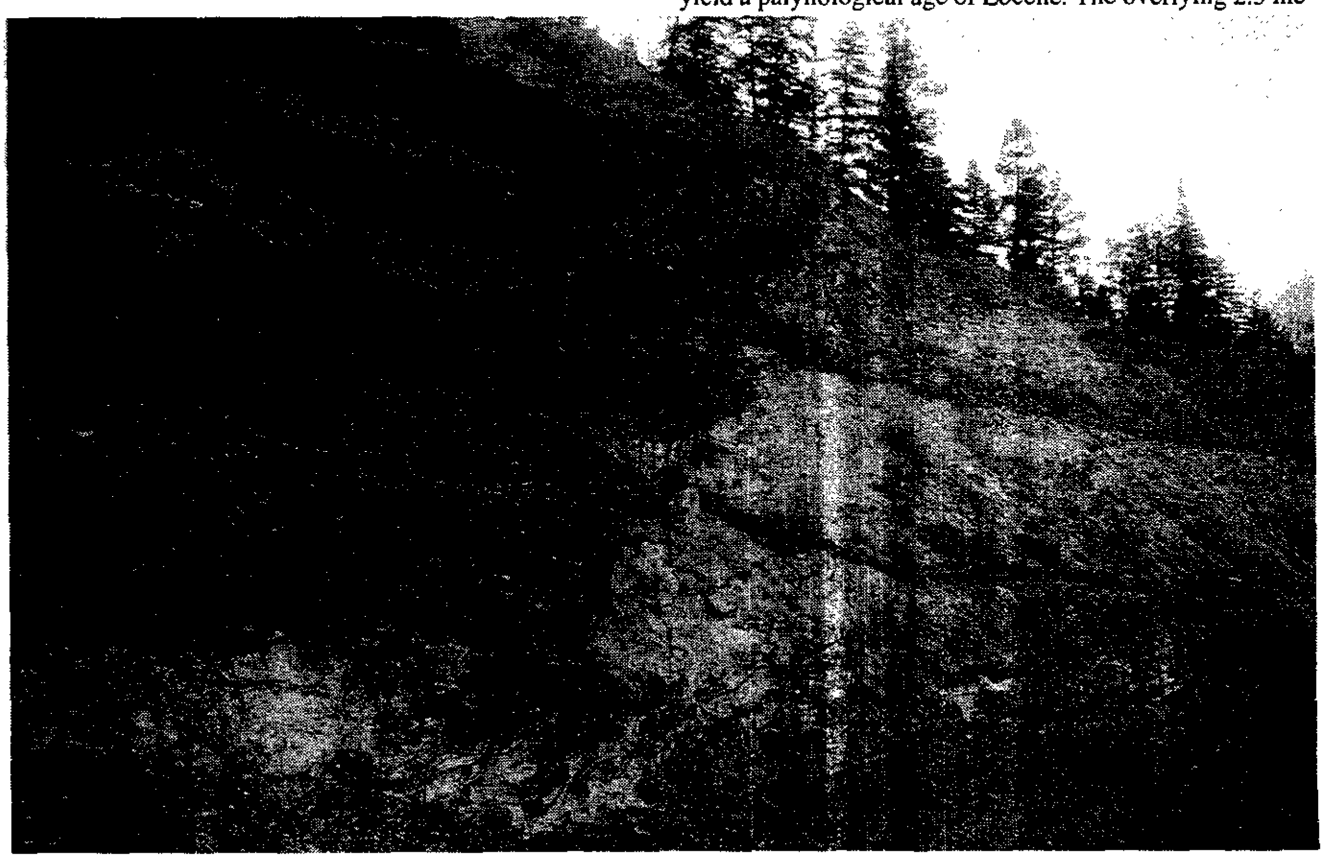

Photo 5. The east wall of the lower quarry at Buse Lake exposes dark columnar basalt flows above white, altered flows, all of the Dewdrop Flats Formation. Lowest outcrops are gently dipping sandstone and carbonaceous shale of the Tranquille Formation.

tre thick andesite flow is amygdaloidal, altered and buff weathering. A thin (0.3 m) carbonaceous shale separates the underlying, altered flow from 16 metres of dark grey, fresh basalt flow with columnar jointing (**Epvb**) capped by 20 metres of porphyritic (pyroxene) andesite flows and tephra (**Epva**) (Photo 5). In agreement with Fulton's interpretation (1975), the rocks and above described section underlying the low hill southeast of Buse Lake are in place and not part of a landslide as suggested by Evans (1983, p. 73-75).

X-ray diffractograms of two samples from the lower quarry and one from the upper show that the Eocene rhyolite tuff is composed of kaolinite and quartz.

References: BCMEMPR (1972, 1986); Evans (1983); Foye (1987); Fulton (1975); Parks (1917); Meyers and Hubner (1991); Sandar (1971, 1974, 1975).

**K2 Will Creek** MINFILE: 082LSW158

STATUS: Showing NTS: 082L/05E

TYPE: Sedimentary LAT./LONG: 50°27′39″; 190°40′55″

ELEVATION: 630 m (2075 feet)

UTM: LF0309670mE; LF5593080mN

The showing is a light grey, unbedded crystal (quartz, biotite) rhyolite ash-tuff exposed in a road ditch immediately uphill from Paleozoic limestone float. Scattered exposures to the east limit any eastward extension of the kaolinite-bearing tuff, and to the west, overburden may limit its economic extension. A single x-ray diffractogram indicates that the material is essentially kaolinite and quartz.

## REFERENCES


British Columbia Ministry of Energy, Mines and Petroleum Resources (1969): Buse Lake Quarry; in Minister of Mines Annual Report 1968, page 297.

British Columbia Ministry of Energy, Mines and Petroleum Resources (1972): Buse Lake Quarry; *in* Geology, Exploration and Mining in British Columbia 1971, pages 478-479.

British Columbia Ministry of Energy, Mines and Petroleum Resources (1973): Buse Lake Quarry; Geology, Exploration and Mining in British Columbia 1972, page 617.

British Columbia Ministry of Energy, Mines and Petroleum Resources (1985): Buse; *in* Exploration in British Columbia 1980, *B.C. Ministry of Energy, Mines and Petroleum Resources,* page 543.

Christopher, P.A. (1978): East Okanagan Uranium Area (Kelowna to Beaverdell) South- central British Columbia; *B.C. Ministry of Energy, Mines and Petroleum Resources,* Preliminary Map No. 29.

Christopher, P.A. (1983): Pb, Kettle, Uranus, Uranium Claims (82E/11E, 14E); *in* Geology in British Columbia 1976, *B.C. Ministry of Energy, Mines and Petroleum Resources,* pages 13-17.

Church, B.N. (1979): Tertiary Stratigraphy and Resources Potential in South-central British Columbia; *in* Geological Fieldwork 1978, *B.C. Ministry of Energy, Mines and Petroleum Resources,* Paper 1979-1, pages 7-15.

Church, B.N. (1980): Geology of the Terrace Mountain Tertiary Outlier; *B.C. Ministry of Energy, Mines and Petroleum Resources,* Revised Preliminary Map 37.

Church, B.N. (1982): Notes on the Penticton Group A Progress Report on a New Stratigraphic Subdivision of the Tertiary South-central British Columbia; *in* Geological Fieldwork 1981, *B.C. Ministry of Energy, Mines and Petroleum Resources,* Paper 1982-1, pages 12-16.

Cockfield, W.E. (1948): Geology and Mineral Deposits of the Nicola Map-area, British Columbia; *Geological Survey of Canada,* Memoir 249, 164 pages.

Cummings, J.M. and McCammon, J.W. (1952): Clay and Shale Deposits of British Columbia; *B.C. Ministry of Energy, Mines and Petroleum Resources,* Bulletin 30, 64 pages.

Deer, W.A., Howie, R.A. and Zussman, J. (1963): Rock-forming Minerals, Volume 4, Framework Silicates; *Longmans, Green and Co. Ltd.,* London, 435 pages.

Drysdale, C.W. (1914): Geology of the Thompson River Valley Below Kamloops Lake, British Columbia; *in* Summary Report 1912, *Geological Survey of Canada,* pages 115-150.

Duba, D. (1988): Notes on Geological Mapping of Whiteman Creek Area; *Discovery Consultants Ltd.,* unpublished report, 3 pages.

Evans, S.G. (1983): Landslides in Layered Volcanic Successions with particular reference to the Tertiary Rocks of South Central British Columbia; unpublished Ph.D. thesis, *The University of Alberta,* 350 pages.

Ewing, T.E. (1981): Geology and Tectonic Setting of the Kamloops Group, South-central British Columbia; unpublished Ph.D. thesis, *The University of British Columbia,* 226 pages.

Foye, G. (1987): Silica Occurrences in British Columbia; *B.C. Ministry of Energy, Mines and Petroleum Resources,* Open File 1987-15, 55 pages.

Fulton, R.J. (1975): Quaternary Geology and Geomorphology, Nicola-Vernon Area, British Columbia; *Geological Survey of Canada,* Memoir 380, 50 pages.

Hills, L.V. (1962): Glaciation, Stratigraphy, Structure and Micropaleobotany of the Princeton Coalfield, British Columbia; unpublished M.Sc. thesis, *The University of British Columbia,* 141 pages.

Hora, Z.D. (1986): New Developments in Industrial Minerals; *in* Geological Fieldwork 1985, *B.C. Ministry of Energy, Mines and Petroleum Resources,* Paper 86-1, pages 239-240.

Hora, Z.D. and Hancock, K.D. (1995): Quesnel Area - Industrial Minerals Assessment; *in* Geological Fieldwork 1994, Grant, B., and Newell, J.M., Editors, *B.C. Ministry of Energy, Mines and Petroleum Resources,* Paper 95-1, pages 395-404.

Jones, A.G. (1959): Vernon Map-area, British Columbia; *Geological Survey of Canada,* Memoir 296, 186 pages.

Jones, J.B. and Segnit, E.R. (1971): The Nature of Opal 1. Nomenclature and Constituent Phases; *Journal of the Geological Society of Australia,* Volume 18, pages 57-68.

Leaming, S. (1973): Rock and Mineral Collecting in British Columbia; *Geological Survey of Canada,* Paper 72-53, 138 pages.

McMillan, W.J. (1978): Geology of the Guichon Creek Batholith; *B.C. Ministry of Energy, Mines and Petroleum Resources,* Preliminary Map 30.

Mathews, W.H. (1981): Early Cenozoic Resetting of Potassium-Argon Dates and Geothermal History of North Okanagan Area, British Columbia; *Canadian Journal of Earth Sciences,* Volume 18, pages 1310-1319.

Mathews, W.H. (1988): Neogene Geology of the Okanagan Highlands, British Columbia; *Canadian Journal of Earth Sciences,* Volume 25, pages 725-731.

Meyers, R.E. and Hubner, T.B. (1991): Industrial Minerals; *in* Exploration in British Columbia, 1990, *B.C. Ministry of Energy, Mines and Petroleum Resources,* page 57.

Monger, J.W.H. and McMillan, W.J. (1989): Geology, Ashcroft, British Columbia; *Geological Survey of Canada,* Map 42-1898, sheet 1, scale 1:250 000.

Okulitch, A.V. (1979): Geology, Thompson-Shuswap-Okanagan, British Columbia; *Geological Survey of Canada,* Open File 637.

Parks, W.A. (1917): Report on the Building and Ornamental Stones of Canada; *Canada Department of Mines, Mines Branch,* Publication No. 452, Volume 5, pages 179-181.

Read, P.B. (in press): Geology and Industrial Minerals of the Tertiary Basins, South-central British Columbia; *B.C. Ministry of Energy, Mines and Petroleum Resources,* Bulletin.

Rose, B. (1914): Savona Map-area, British Columbia; *in* Summary Report 1912, *Geological Survey of Canada,* pages 151-155.

Sadar, E. (1971): Buse Lake Quarry; *in* Geology, Exploration and Mining in British Columbia 1970, *B.C. Ministry of Energy, Mines and Petroleum Resources,* page 513.

Sadar, E. (1974): Buse Lake Quarry; *in* Geology, Exploration and Mining in British Columbia 1973, *B.C. Ministry of Energy, Mines and Petroleum Resources,* page 565.

Sadar, E. (1975): Buse Lake Quarry; *in* Geology, Exploration and Mining in British Columbia 1974, *B.C. Ministry of Energy, Mines and Petroleum Resources,* page 400.

Tempelman-Kluit, D.J. (1989): Geology, Penticton, British Columbia; *Geological Survey of Canada,* Map 1736A, scale 1:250 000.

Thompson, R.I. and Daughtry, K. (1994): A New Regional Mapping Project in Vernon Map Area, British Columbia; *in* Current Research 1994-A; *Geological Survey of Canada,* pages 117-122.

Uglow, W.L. (1922): Geology of the North Thompson Valley Map-area, B.C.; *in* Summary Report 1921, Part A, *Geological Survey of Canada,* pages 72A-99A.

# CLEARCUT PYROXMANGITE/RHODONITE OCCURRENCE, GREENWOOD AREA, SOUTHERN BRITISH COLUMBIA (82/E2)

**by G.J. Simandl and B.N. Church**

*KEYWORDS*: Industrial minerals, pyroxmangite, rhodonite, Mn-garnet, Knob Hill Group, Greenwood camp, quartzite.

## INTRODUCTION

This report describes a new pyroxmangite-rhodonite occurrence visited briefly by the authors as part of a broader study of gemstones in British Columbia. The discovery is on the Clearcut claims, 1.5 kilometres northwest of Mount Roderick Dhu (lat. 49°12', long. 118°37'), 13 kilometres northeast of Greenwood (Figure 1).

Rhodonite is a manganiferous semiprecious stone valued for its pink to deep red colour. After jade, rhodonite is the second most important gemstone found in British Columbia. Lower quality material has ornamental applications such as sculptures, table tops and a variety of decorative items. Other occurrences in the province have been described by Leaming (1966), Danner (1976), Danner and Cowley (1980), Cowley (1979), Hancock (1992), Nelson *et al.* (1990) and others. Other pink manganese silicates that are difficult to distinguish from rhodonite are pyroxmangite and bustamite. It is possible that these minerals also occur in other previously known rhodonite occurrences but were not distinguished from rhodonite.

## GEOLOGICAL SETTING

The northeast part of the Greenwood mining camp, in the vicinity of Mount Roderick Dhu and Jewel Lake (Figure 1), is underlain principally by a metamorphic complex tentatively assigned to the Knob Hill Group (J. Fyles, personal communication, 1995), the Wallace Creek batholith and Coryell intrusions. Mapping in the area has been done by Little (1983), Church (1986) and Fyles (1990).

The Knob Hill Group is an assemblage of pre-Mesozoic rocks forming an east-southeast trending belt extending from the lower course of Clement Creek to Jewel Lake and then to Mount Roderick Dhu. It comprises a variety of volcanic and sedimentary facies converted to amphibolite and quartz-mica schists. The rocks are medium to fine grained and medium to dark coloured. Primary structures, such as bedding, are often difficult to distinguish from foliation and gneissosity. The metasedimentary rocks consist of quartz (15 to 90%), plagioclase, biotite, some garnet and magnetite, and, less commonly, amphibole, chlorite, muscovite and occasionally andalusite (Church and Winsby, 1974).

The protolith of the quartz-rich metasedimentary rocks is difficult to determine because of recrystallization. The amphibolites generally occur as massive lenses, possibly derived from basaltic lava flows and pyroclastic rocks. Typically they consist of 40 to 70% green amphibole, and smaller amounts of plagioclase, quartz, magnetite and titanite. Epidote, calcite and quartz are present in small veins and fissures.

The Late Jurassic Wallace Creek batholith forms two large lobes underlying the area southwest of Jewel Lake and another area at the summit of Mount Roderick Dhu that extends westerly through the headwater basin of Clement Creek. These rocks are medium grained, medium grey and contain xenoliths of the metamorphic complex. Typically the rock consists of approximately 40% plagioclase, smaller amounts of quartz and potassium feldspar, approximately 10% amphibole and epidote, and accessory biotite, chlorite, apatite, titanite and magnetite.

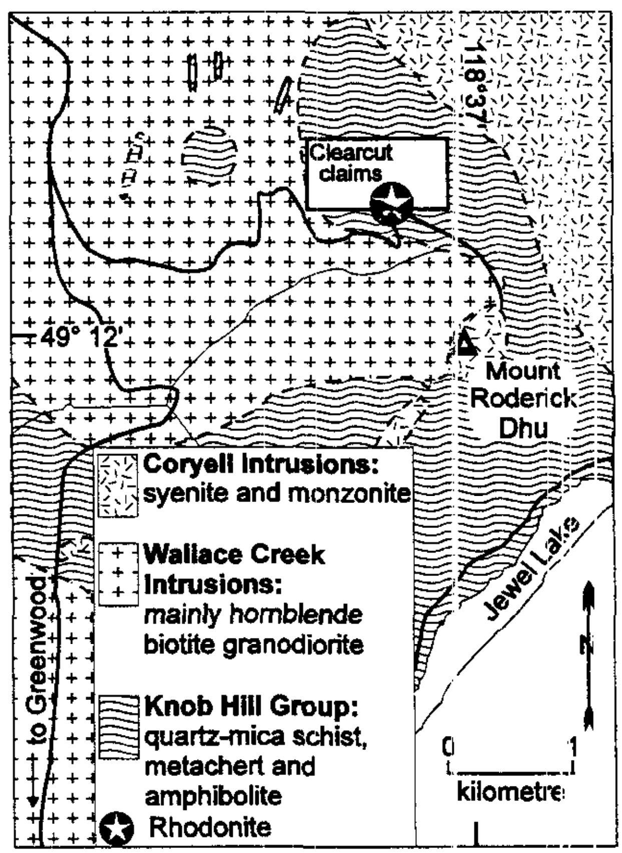


Figure 1: Location and geological setting of the Clearcut pyroxmangite/rhodonite occurrence. (Modified from Little, 1983).

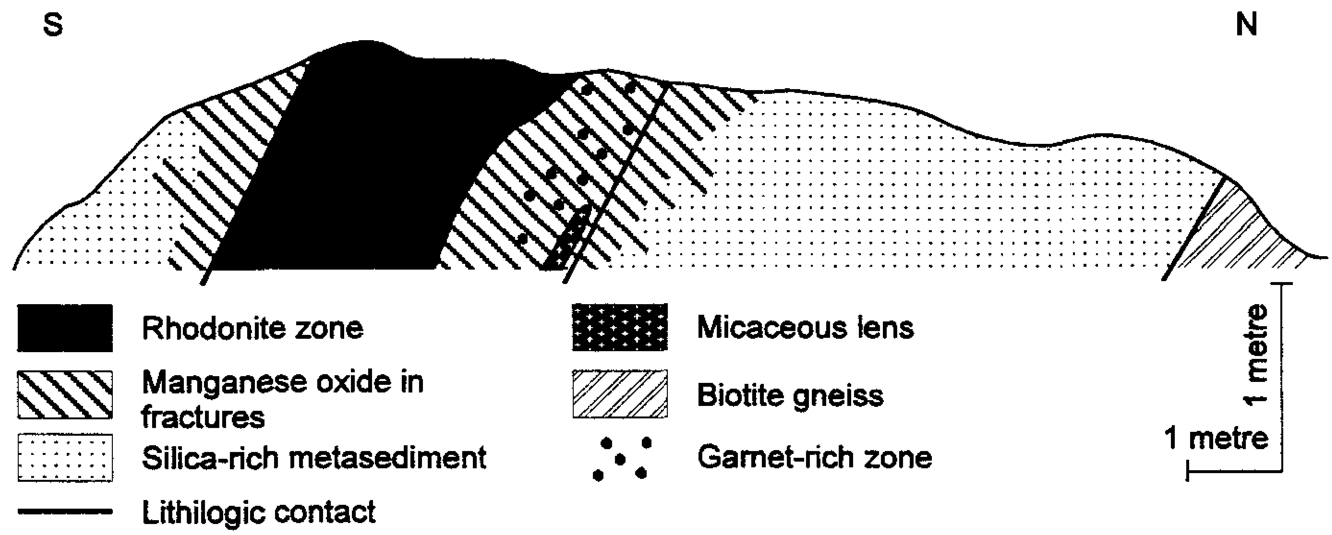


Figure 2: Cross section of the Clearcut pyroxmangite/rhodonite occurrence, looking west.

The Middle Eocene Coryell intrusions consist mostly of quartz-poor syenite and monzonite stocks and dikes occurring throughout the area.

## DEPOSIT DESCRIPTION

The pyroxmangite-rhodonite showing is on the road leading to the microwave tower on Mount Roderick Dhu. The exposure, a road-cut section, is approximately 1 metre high and over 10 metres long. At surface much of the pink manganese silicate is altered and thickly coated with black manganese oxides. Manganese oxides in the proximity of rhodonite follow relatively closely spaced fractures. The section (Figure 2) is approximately perpendicular to the strike of the lithologic contacts. Better exposure is needed to fully document the contact relationships between manganese-bearing lithologies and surrounding rocks. The lithologies shown in the section are described below.

### *SILICA-RICH METASEDIMENT IN THE HANGINGWALL*

Silica-rich metasediments in the hangingwall are light grey to light brown on fresh surfaces and black where weathered, due to a pervasive coating of secondary manganese oxides. The rock is massive, homogeneous and difficult to break. Weak, diffuse layering is observed in some specimens. No primary sedimentary textures, suggesting a clastic protolith, were observed. The rock is nearly monomineralic and consists mainly of quartz (>90%) with aggregates of idiomorphic to subidiomorphic spessartite garnets (<0.5%, <2 mm), accessory green amphibole(?; <0.5%, <1 mm), and slightly chloritized biotite (<0.5%, 2 mm). Boundaries between quartz grains are complex and strongly sutured. Some of the quartz shows wavy extinction. The presence of spessartite makes this rock similar to gondites (spessartite quartzite) they are commonly interpreted as metamorphic equivalents of manganese-bearing metacherts. Accessory minerals include manganese and iron oxides and pink manganese silicate, probably rhodonite and/or pyroxmangite. For simplicity, the term pyroxmangite/rhodonite is used throughout this paper to describe the pink manganese silicate. Approaching the manganese-rich zone, rhodonite becomes more abundant along quartz grain boundaries and microfractures. Along fractures rhodonite is oxidized and some of the garnet appears slightly chloritized. Carbonate minerals, probably manganoan calcite or rhodochrosite, are common in small concentrations, mainly as fracture fillings

### *PYROXMANGITE/RHODONITE-BEARING UNIT*

Manganese silicate is pink and sugary. Locally it shows a variety of textures, ranging from coarse porphyroblasts that are up to several centimetres long enclosed in manganese oxides, to a fine mosaic consisting of quartz and pyroxmangite/rhodonite that appear to be in equilibrium, to nearly pure pyroxmangite/rhodonite characterised by an equigranular granoblastic texture (Photo 1). Pyroxmangite/rhodonite and quartz (<5 mm) are the major constituents of this unit. Their content varies from 30 to 90%.

Euhedral garnets, less than 0.5 millimetre in diameter, are the dominant accessory. Black, amorphous manganese oxides are more abundant in the pyroxmangite/rhodonite unit than in the silica-rich unit and are concentrated along fractures. Graphite flakes, 2 millimetres in cross-section, were observed along one

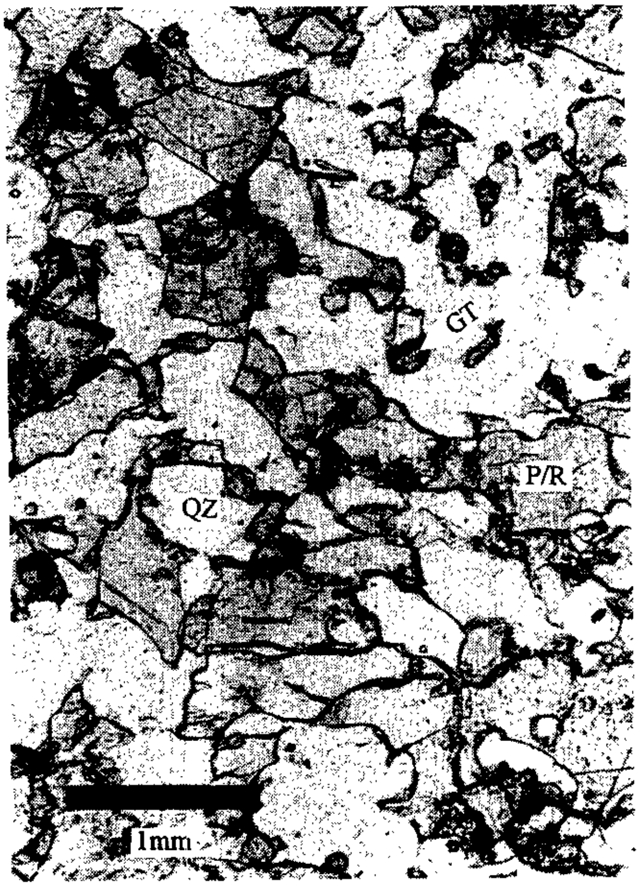


Photo 1: Microphotograph of pyroxmangite/rhodonite rock, Clearcut deposit. P/R = pyroxmangite/rhodonite; QZ = quartz; GT = spessartite.

black, manganese oxide filled fracture. Detailed microscopic, microprobe and geochemical studies that are in progress are needed to characterise this manganese-rich rock.

**A manganese-garnet - quartz zone** consists mainly of quartz (30-60%) and pyroxmangite/rhodonite (30-60%). An orange garnet is coarser and more abundant near the footwall where it forms lenses and streaks, less than 1 centimetre thick, containing up to 70% garnet. Garnet is readily identified on fresh surfaces. Individual garnet grains are subhedral and measure less than 0.5 millimetre in diameter. Overall the garnet represents less than 15% of the rock.

**An amber-coloured micaceous lens**, about 15 centimetres thick, is exposed for 50 centimetres near the base of the outcrop. It probably consists of phlogopite or vermiculite with individual flakes measuring up to 5 millimetres in diameter.

### *SILICA-RICH FOOTWALL ROCK*

The silica-rich footwall unit is massive and consists mainly of interlocking quartz grains with strongly sutured grain boundaries. The quartz grains (up to 6 mm across) form over 90% of the rock, with subhedral garnet grains (<5 mm) forming less than 2%. Other accessory minerals are biotite (<0.5 mm) and iron oxide pseudomorphs after pyrite. As in the silica-rich hangingwall, there is no evidence of a detrital origin for the quartz, and it is probable that this rock was derived from a cherty protolith.

### *BIOTITE GNEISS*

The northern limit of the pyroxmangite/rhodonite showing is strongly weathered gneiss. It probably corresponds to biotite gneiss observed 150 metres from the occurrence. The gneiss is grey on fresh surfaces and weathers brown. It is characterised by quartz-feldspar leucosomes, 2 to 5 millimetres thick, that form over 70% of the rock, separated by biotite-rich melanosomes, less than 1 millimetre thick, locally forming flaser textures. In places, this gneiss also contains some amphibole

## SIGNIFICANCE OF THE CLEARCUT PYROXMANGITE/RHODONITE OCCURRENCE

Relatively poor exposure and the preliminary nature of this study do not permit definitive genetic conclusions. Nevertheless, the Greenwood pyroxmangite/rhodonite occurrence is associated with amphibolite, quartzite and gneiss that are probably metamorphic equivalents of volcanic rocks, siliceous chemical sediments, and pelitic lithologies, respectively. Such lithologies are commonly characteristic of rhodonite occurrences in the Sicker Group (Cowley, 1979) and are known in the Slide Mountain Terrane (Nelson *et al.*, 1990). The absence of primary detrital textures in the silica-rich hostrocks is consistant with a chemical precipitate protolith, either of sedimentary or hydrothermal origin. Many manganese deposits associated with chemical sediments of either volcanic or sedimentary affiliation are known worldwide (Laznicka, 1992) and some are considered distal equivalents of volcanogenic massive sulphide deposits. If this interpretation is correct, then the location of this occurrence farther east than any other in the province, is important from a regoinal point of view. It may be that the Clearcut occurrence formed in a depositional environment similar to manganese silicate occurrences to the west, including those in the Sicker Group on Vancouver Island, and possibly to the north in the Sylvester allochthon.

On the deposit scale, the pyroxmangite/rhodonite and associated quartzite polish well. However, largest pyroxmangite/rhodonite blocks in the exposed portion of the occurrence do not exceed 20 by 20 by 30 centimetres due to closely spaced joints and oxidation. Manganese deposits that originated as chemical precipitates are typicaly stratabound and commonly occur in clusters so adjacent areas may be prospective for rhodonite/pyroxmangite. However, it is not known if the rhodonite showing is related to an exhalative unit.

## OTHER MANGANESE OCCURRENCES

Although manganese is uncommon in the Knob Hill Group, at least one other occurrence is known in the Greenwood area. It is a manganese-stained quartzite with pink manganese silicate (rhodonite?) and garnet, located at the top of the east-facing slope of Boundary Creek at an elevation of 1220 metres (J. Fyles, personal communication, 1995). No detailed prospecting has been recorded in that area.

## ACKNOWLEDGMENTS

The authors are much obliged to George Stewart of Greenwood, owner of the Clearcut claims, for information and access to his property. Thanks are owed to colleagues Joanne Nelson and Kirk Hancock of the B.C. Ministry of Energy, Mines and Petroleum Resources and Suzanne Paradis of the Geological Survey of Canada and Jim Fyles who contributed constructive comments. John Newell's editorial improvements to the manuscript are also acknowledged.

## REFERENCES

Church, B.N. (1986): Geological Setting and Mineralization in the Mount Attwood - Phoenix Area of the Greenwood Mining Camp; *B.C. Ministry of Energy, Mines and Petroleum Resources*, Paper 1986-2, 65 pages.

Church B.N. and Winsby, J. (1975): Denoro Grande, Jewel; *in* Geology, Exploration and Mining in British Columbia 1974, *B.C. Ministry of Energy, Mines and Petroleum Resources*, pages 39-51.

Cowley, P. (1979): Correlation of Rhodonite Deposits on Vancouver Island and Saltspring Island, British Columbia; unpublished B.Sc thesis, *University of British Columbia*, 54 pages.

Danner, W.R. (1976): Gem Materials of British Columbia; Proceedings of Eleventh Forum on the Geology of Industrial Minerals, June 18-20,1975, Kalispell, Montana, *Montana Bureau of Mines and Geology*, Special Publication 74, pages 156-168.

Danner, W.R. and Cowley, P. (1980): Exhalative Manganese Deposits in Sicker Group, Vancouver and Saltspring Islands, Southwestern B.C.; Abstract, *Geological Association of Canada, Cordilleran Section*, Vancouver, January 1980; page 13.

Fyles, J.T. (1990): Geology of the Greenwood - Grand Forks Area, British Columbia; *B.C. Ministry of Energy, Mines and Petroleum Resources*, Open File 1990-25, 19 pages.

Hancock K.D (1992): Arthur Point (Sea Rose) Rhodonite; *in* Exploration in British Columbia 1991, *B.C. Ministry of Energy, Mines and Petroleum Resources*, pages 89-98.

Laznicka, P. (1992): Manganese Deposits in a Global Lithogenetic System: A Quantitative Approach; *Ore Geology Reviews*, Volume 7, pages 279-356.

Leaming, S.F. (1966): Rhodonite in British Columbia; *The Canadian Rockhound*, February 1966, pages 5-11.

Little, H.W. (1983): Geology of the Greenwood Map-area, British Columbia; *Geological Survey of Canada*, Paper 79-29, 37 pages.

Nelson, J. Hora, Z.D. and Harvey-Kelly, F. (1990): A New Rhodonite Occurrence in the Cassiar Area, Northern British Columbia (104P/5); *in* Geological Fieldwork 1989, *B.C. Ministry of Energy, Mines and Petroleum Resources*, Paper 1990-1, pages 347-350.

# "PERLITE" FROM TERRACE MOUNTAIN, VERNON AREA: POSSIBLE INDUSTRIAL APPLICATIONS

By George J. Simandl, B. Neil Church and William Hodgson*
*United States Gypsum Company, Chicago, IL.

*KEYWORDS:* Industrial mineral, perlite, obsidian, Terrace Mountain, acoustic and thermal insulation tiles, non-expanding applications.

## INTRODUCTION

Very little is known about natural hydrated glasses in British Columbia, except perlite. Perlite is defined as natural volcanic glass with a pearly lustre, macroscopic or microscopic onion-skin texture, and rhyolitic composition with 2 to 5% incorporated water ($H_2O^+$). From the industry point of view, however, all hydrated felsic rocks, including rocks with pumiceous and granular textures, are classified as 'perlite' if they expand significantly during heating. Similarly, 'expanded perlite' is defined as a light-weight aggregate produced by rapid thermal expansion of crushed source rocks; the expansion may be as much as 20 times by volume (Breese and Barker, 1994). The key properties of expanded perlite are low density, fire resistance, good thermal and sonic insulation properties and the ability to retain water. Expanded perlite is used extensively in acoustical ceiling tile, concrete, plasters and various horticultural applications. A worldwide survey of minerals in lightweight applications was prepared by Loughbrough (1991), minerals in fibreglass was covered by Russell (1991) and a market study of classical perlite applications was completed by Gunning and McNeal (1994). More than 17 perlite occurrences are currently known in British Columbia (White, 1990; Hora and Hancock, 1994). Unfortunately, volcanic glass that does not expand is usually disregarded by industry. It has potential applications in the production of mineral wool for thermal insulating materials, castings, as a component of sound insulating tiles and as a composite in bituminous roofing sheets. The choice of raw material for these types of applications is based mainly on chemical composition, homogeneity, availability and cost. For example, high sodium content may reduce the need for soda ash and high alumina may reduce the requirements for kaolin addition.

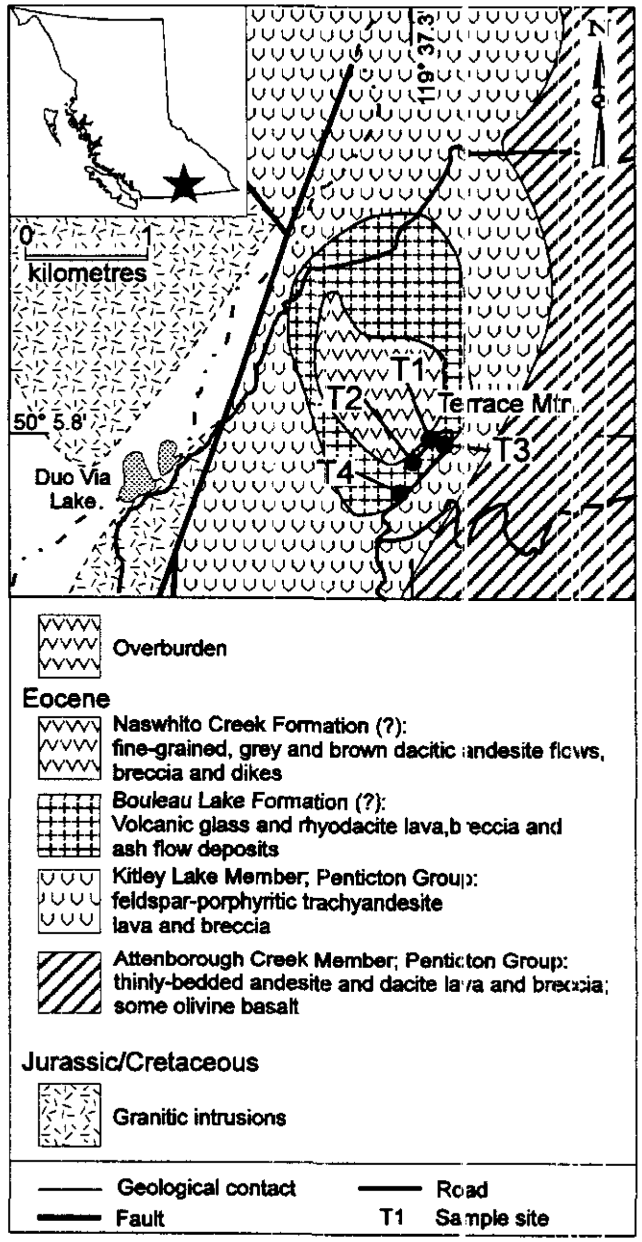


Figure 1. Location and geology of the Terrace Mountain hydrated obsidian deposit (modified from Church, 1980).

## TERRACE MOUNTAIN PERLITE

A large deposit of perlite occurs on Terrace Mountain (lat. 50°06', long. 119°38') 30 kilometres southwest of Vernon and 25 kilometres northwest of Kelowna (Figure 1). Access to the area is by a network of logging roads connected to the paved highway along the west shore of Okanagan Lake.

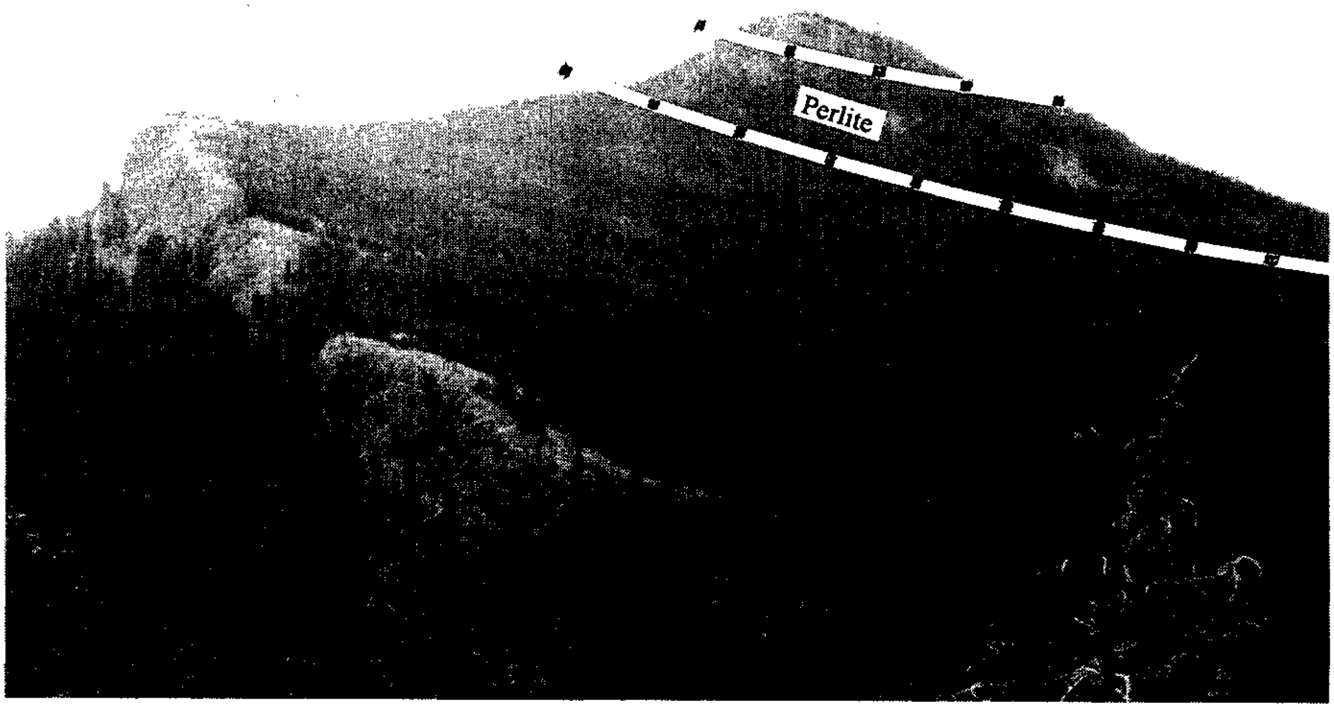


Photo 1. View of Terrace Mountain (looking south) showing the major volcanic units dipping west.

## *GEOLOGICAL SETTING*

Tertiary rocks were first mapped in the Vernon area by Jones (1959) although he made no attempt to describe the structure of the Tertiary outliers or to distinguish the major Miocene and Eocene volcanic units. Detailed mapping of the Tertiary assemblage was completed by Church (1980) at which time a glassy lava unit (perlite) was delineated on the upper slopes of Terrace Mountain.

Terrace Mountain is underlain mainly by relatively fresh volcanic rocks, equivalent to the Penticton and Kamloops Groups (Eocene), in a northerly elongated, westerly dipping half-graben. This structure has been developed on a basement complex consisting of strongly folded and faulted Paleozoic and Mesozoic oceanic cherts, turbidites and greenstones, cut by younger Mesozoic granitic rocks (Church, 1980; 1982). The Tertiary volcanic succession is about 900 metres thick and consists, from top to bottom of: fine-grained dacite, forming a tilted hat, 30 metres thick, on the summit; underlain by 120 metres of perlite containing feldspar and biotitite phenocrysts; underlain in turn by a series of feldspar porphyritic trachyandesite lava flows 180 metres thick, and a series of andesitic lava flows and breccias approximately 550 metres thick at the base (Photo 1). The summit dacite is tentatively correlated with similar rocks near Naswhito Creek, 20 kilometres to the north; the volcanic glass unit that contains feldspar and biotite phenocrysts may be equivalent to the Bouleau Lake ash-flow deposit that occurs below the Naswhito Creek unit. The trachyandesites and andesitic units exposed on the lower slopes of Terrace Mountain are tentatively correlated with the Kitley Lake and Attenborough Creek members, respectively, of the Penticton Group (Church, 1982).

The age of the volcanic glass unit, determined from K-Ar analysis of the biotite phenocrysts, is 52.3±1.8 Ma (Church, 1980). This is similar to the age of the Marron Formation of the Penticton Group (Church, 1973; 1982).

## *PERLITE DEPOSIT*

Perlitic rock covers several square kilometres on the upper slopes of Terrace Mountain. It is grey on fresh surfaces, alters to light brown and is characterized by fractured, unaltered plagioclase phenocrysts (2 to 7 mm in diameter), comprising about 15% of the rock. Accessory biotite, usually less than 3 millimetres in size is also set in a greenish grey glassy matrix. Anhedral olivine crystals less than 0.5 millimetre across, iron oxide (0.5 mm) and pyrite (0.5 mm) are trace components disseminated through the glass matrix. Perlitic onion skin and arcuate fractures are visible throughout the glass (Photo 2), which is, in places, partially converted to palagonite. The degree of palagonitization varies through the deposit, but is generaly minor.

The chemical composition of the rock resembles alkali-rich dacite (Table 1), differing somewhat from the rhyolite compositions that are typical of world-class perlite deposits and well known British Columbia occurrences, such as the Frenier perlite. The Terrace Mountain perlite has lower $SiO_2$, and higher $Al_2O_3$, CaO and $TiO_2$ contents than other major perlite occurrences. Nevertheless, the $H_2O^+$ content is in the range characteristic of most perlites. The rock has very low $SO_2$ content, minimizing the potential of sulphur release to the atmosphere during processing.


Photo 2. Microphotograph of the perlite showing feldspar phenocrysts in glassy matrix. PE = perlite; PL = plagioclase; BT = biotite; MT = magnetite.

**TABLE 1. CHEMICAL COMPOSITION OF TERRACE MOUNTAIN PERLITE COMPARED WITH ANALYSES OF SAMPLES FROM SOME WELL KNOWN PERLITE DEPOSITS.**

| | Terrace Mt BC | No Agua NM | Superior AZ | Big Pine CA | Akita Japan | Argentina |
|---|---|---|---|---|---|---|
| $SiO_2$ | 66.65 | 72.10 | 73.60 | 73.60 | 74.20 | 72.30 |
| $TiO_2$ | 0.47 | 0.06 | 0.10 | 0.07 | 0.06 | 0.08 |
| $Al_2O_3$ | 15.59 | 13.50 | 12.70 | 13.20 | 12.90 | 13.40 |
| $Fe_2O_3$ | 1.25 | 0.80 | 0.70 | 0.80 | 0.68 | 1.00 |
| FeO | 0.68 | | | | | |
| MgO | 0.42 | 0.50 | 0.20 | 0.10 | 0.05 | 0.30 |
| CaO | 1.46 | 0.89 | 0.60 | 0.60 | 0.45 | 0.59 |
| $Na_2O$ | 4.42 | 4.60 | 3.20 | 4.10 | 4.10 | 3.40 |
| $K_2O$ | 4.85 | 4.40 | 5.00 | 4.10 | 4.00 | 4.70 |
| $H_2O^+$ | 3.37 | 3.00 | 3.80 | 3.30 | 3.30 | 3.70 |
| $H_2O^-$ | 0.67 | | | | | |
| $CO_2$ | 0.11 | | | | | |
| $SO_2$ | <0.05 | | | | | |

## *IMPORTANCE OF THIS OCCURRENCE*

The possibility of producing insulating fibre or tiles and castings from the melted rock should be further investigated. A plant located at Stara Voda near Lazne Kynzvart in the Czech Republic provides an example of an operation where volcanic rock is melted and cast into a variety of shapes (Hruska, 1991). Traditional melting material for such a plant is basalt. An industrial insulation plant in Grand Forks, British Columbia, owned by Bradford Enercon Inc., manufactured mineral wool insulation for industrial products until 1991. The melting technology employed at this operation was electric melting and coke-fired cupola. The plant was melting locally available copper slags blended with imported basalt rock. A similar plant, owned by United States Gypsum Company, is located near Tacoma, Washington. These two cupola, coke-fired operation use a combination of local basalt and slag to produce a variety of industrial and commercial insulation products.

The advantages of the Terrace Mountain occurrence are its size and favorable location in southern British Columbia, close to both the Okanagan area and American markets. Assuming no problems related to the porphyritic texture, the high water content of the rock could contribute towards lowering the temperature of fusion, relative to unhydrated but otherwise chemically equivalent rocks, resulting in substantial energy savings. The low iron and relatively high alumina provide an interesting alternative source of fibre-forming chemistry that could displace the much more energy-intensive basalt additive currently in use. Further detailed studies are needed to determine if such a rock would meet specifications for batch formulations required by the industry for non-expanding applications.

The degree of expansion is not expected to match that of perlites currently on the market or potentially available from the Frenier deposit or other British Columbia occurrences. On the other hand, preservation of water in the Terrace Mounain occurrence is an important indicator of exploration potential to find "true perlite" deposits in the area. Rhyolitic rocks were reported by Church (1980 ) in the Bouleau Lake area, however these rock have low water contents.

## ACKNOWLEDGEMENTS

The authors are much obliged to Suzanne Paradis of the Geological Survey of Canada, David B. Lefebure and Kirk D. Hancock of the B.C. Ministry of Energy, Mines and Petroleum Resources, Don Gunning from the British Columbia Trade Development Corporation and Gregory G. Cork of United States Gypsum Company for their constructive comments. Figures were drafted by Kirk D. Hancock.

## REFERENCES


Breese, R.O.Y. and Barker, J.M. (1994): Perlite; *in* Industrial Minerals and Rocks; 6th Edition, Carr, D.D., Editor, *Society for Mining, Metallurgy and Exploration, Inc.*, pages 735-749.

Church, B.N. (1973): Geology of the White Lake Basin; *B.C. Ministry of Energy, Mines and Petroleum Resources;* Bulletin 61, 120 pages.

Church, B.N. (1980): Geological Map of the Terrace Mountain Outlier (parts of 82L4, 5); *B.C. Ministry of Energy, Mines and Petroleum Resources,* Preliminary Map No. 37.

Church, B.N. (1982): Notes on the Penticton Group, A Progress Report on a New Stratigraphic Subdivision of the Tertiary, South-central British Columbia; *in* Geological Fieldwork 1981, *B.C. Ministry of Energy, Mines and Petroleum Resources,* Paper 1982-1, pages 12-16.

Gunning, D. and McNeal & Associates Consultants Ltd. (1994): Perlite Market Study for British Columbia; *B.C. Ministry of Energy, Mines and Petroleum Resources*; Open File 1994-21.

Hora, Z.D. and Hancock, K.D. (1994): Nazko Cinder Cone and New Perlite Ocurrence; *in* Geological Fieldwork 1994, Grant B. and Newell, J.M., Editors, *B.C. Ministry of Energy, Mines and Petroleum Resources,* Paper 1995-1, pages 405-407.

Hruska, J. (1991): Czechoslovakia's Minerals, Production Reserves and Exploration; *Industrial Minerals*; No. 289, pages 49-53.

Jones, A.G. (1959): Vernon Map-area, British Columbia; *Geological Survey of Canada,* Memoir 296, 186 pages.

Loughborough, R. (1991): Minerals in Lightweight Insulation; *Industrial Minerals*; No. 289, pages 31-35.

Russell, A. (1991): Minerals in Fibreglass; *Industrial Minerals*; No. 290, pages 27-41.

White, G.V. (1990): Perlite and Vermiculite Occurrences in British Columbia; *in* Geological Fieldwork 1989, *B.C. Ministry of Energy, Mines and Petroleum Resources;* Paper 1990-1, pages 481-487.

# THE GEOLOGY AND GEOCHEMISTRY OF THE MINERAL HILL - WORMY LAKE WOLLASTONITE SKARNS, SOUTHERN BRITISH COLUMBIA (92G/12W)

By G.E. Ray and C.E. Kilby

*KEYWORDS:* Economic geology, skarn, industrial minerals, wollastonite, garnet, pyroxene, petrochemistry

## INTRODUCTION

The Mineral Hill - Wormy Lake area is located on the Sechelt Peninsula approximately 60 kilometres west-northwest of Vancouver and 5 kilometres north of Sechelt (Figure 1). It lies at the southern end of the Coast Plutonic Belt and the wollastonite-bearing skarns are hosted by elongate and deformed roof pendants of calcareous rocks that possibly form part of the Upper Triassic Quatsino Formation. These pendants are surrounded by a variety of Jurassic plutonic rocks that range in composition from gabbro to granodiorite.

Publications relevant to the regional geology include those by Roddick (1970, 1979, 1983), Price *et al.* (1985) and Friedman *et al.* (1990). In 1987 and 1988, Tri-Sil Minerals Inc. conducted an exploration program on the property which is described by Goldsmith and Logan (1987) and Goldsmith and Kallock (1988). Later, brief examinations of the property were conducted by staff of the British Columbia Geological Survey; these observations are described by White (1989) and Fischl (1991).

This paper presents the results of a four-week mapping and sampling program conducted in the summer of 1995. An 18 square kilometre area between Wormy Lake and Mineral Hill was geologically mapped (Ray and Kilby, 1995). Major and trace element geochemical data from the intrusive rocks, and assay data from mineralized occurrences, are reported here. The results of microprobe analysis of skarn minerals such as wollastonite, garnet and pyroxene are also presented.

## METASEDIMENTARY ROCKS

Skarn-altered and deformed remnants of calcareous sedimentary rocks form narrow, discontinuous units that lie close to, and are partially controlled by the Wormy Lake fault zone, a linear zone of ductile and brittle deformation (Figure 2). Both the metasedimentary units and the fault zone extend from Snake Creek, northwestwards to Wormy Lake. Beyond Wormy Lake, the metasediments and the fault are believed to extend northwards beyond the mapped area. However, south of Snake Creek, the metasediments and the fault zone terminate against gabbroic rocks of the Crowston Lake pluton along the easterly striking Snake Creek fault (Figure 2).

In the Wormy Lake area, and northeast of the Wormy Lake fault, the metasedimentary package reaches its maximum outcrop width of approximately 400 metres. Less than 800 metres southeast of the lake, it quickly thins or disappears and is only seen as very narrow units (some less than 20 m thick) that form discontinuous fault-bound slices within the Crowston Lake pluton. Further south, however, and southwest of the Wormy Lake fault, the skarn-altered package again thickens until, at its southern extremity southeast of Mineral Hill, it reaches 250 metres in outcrop width.


Figure 1: Location of the Mineral Hill - Wormy Lake area, southern British Columbia.

The calcareous units have been intruded by swarms of gabbroic sills and dikes from the adjoining Crowston Lake pluton. The metasediments have been deformed and overprinted by varying degrees of exoskarn alteration so that, in many instances, the character of the protolith is uncertain. Originally, however, they are believed to have mainly comprised relatively pure, massive to bedded limestone and calcareous siltstone. Some of the original limestones now form discontinuous but extensive marble units which are marked by karst topography. The marbles are coarse-grained, white to grey rocks that vary from massive to well foliated and layered. The layering probably represents transposed bedding; many marbles

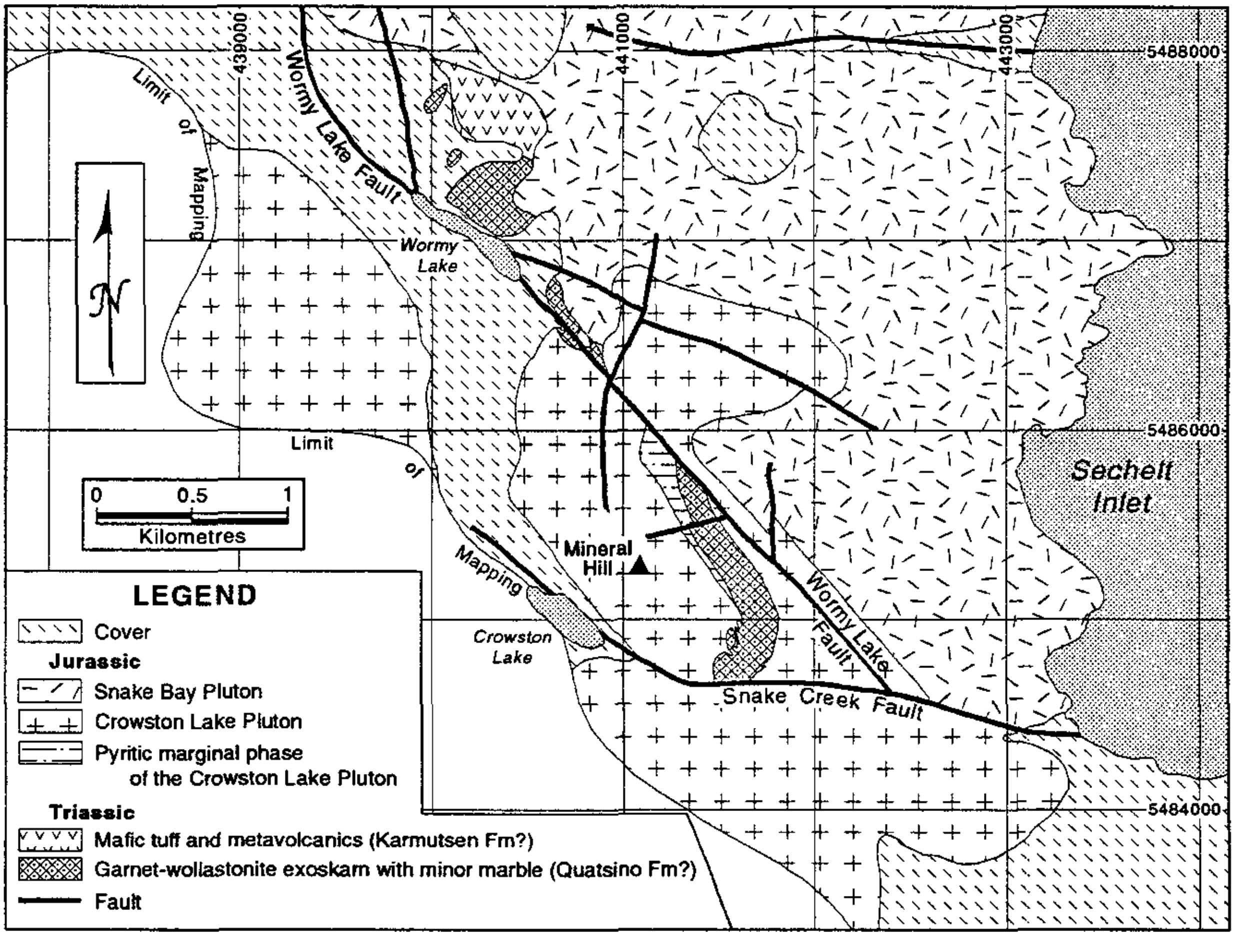


Figure 2: Geology of the Mineral Hill - Wormy Lake area (adapted from Ray and Kilby, 1995).

show evidence of intense ductile and flow folding as well as boudinage structures.

Apart from some marble remnants, most of the calcareous sedimentary rocks have been converted to skarn containing various quantities of garnet, wollastonite, epidote, clinopyroxene and, less commonly, vesuvianite. Adjacent to the Crowston Lake pluton, much of the original limestone has been replaced by massive garnetite. However, well layered garnet-wollastonite-pyroxene-epidote skarns are common and this layering is also believed to mark transposed bedding.

## METAVOLCANICS AND TUFFS

An unusual unit of mafic rocks outcrops approximately 500 to 800 metres north of Wormy Lake. It probably represents metamorphosed and skarn-altered volcanics and bedded calcareous tuffs of either the Triassic Karmutsen Formation or the Lower to Middle Jurassic Bowen Island Group, as defined by Friedman *et al.* (1990). In appearance and texture these rocks vary from fine to medium grained and from massive to well layered. The layering, which generally ranges from 1 to 10 centimetres in thickness, often consists of alternating units of mafic-rich and felsic-rich material; we believe it represents original bedding. Where skarn alteration is intense, some layers have been almost entirely replaced by brown garnet with minor pyroxene. Crosscutting garnet veinlets are also present but no wollastonite has been seen in these rocks. The more massive exposures are generally highly mafic and are believed to be altered volcanics.

In thin section, the mafic layers are seen to consist of between 30 and 50% dark green hornblende crystals that reach 0.3 millimetre in length and which have a subparallel alignment. Freshly recrystallized plagioclase and strained quartz make up most of the groundmass. The amphibole is intergrown with small brown-coloured and isotropic garnets. Minor constituents include clinopyroxene, biotite, chlorite, epidote, zircon, sphene and opaque minerals.

## INTRUSIVE ROCKS

The geology of the area is dominated by parts of two major Jurassic intrusive bodies that, for this study, are informally named the Crowston Lake and Snake Bay plutons. No conclusive field evidence was seen to determine their age relationships: it is possible that they form part of a single, compositionally zoned intrusion, although the mafic Crowston Lake body probably predates the more felsic Snake Bay pluton.

The skarn-altered metasediments are cut by numerous gabbroic sills and dikes that are genetically and temporally related to the Crowston Lake pluton. In addition, both the plutons, and the exoskarn packages, are cut by two compositionally distinct suites of minor intrusions that form narrow sills and dikes.

## *CROWSTON LAKE PLUTON*

The Crowston Lake pluton occupies the western and southern parts of the mapped area (Figure 2). Its full extent is unknown but our mapping indicates that it outcrops over an area of 6 square kilometres. The pluton comprises medium to very coarse grained, massive to weakly foliated mafic rocks. Hornblende, lesser pyroxene and rare olivine are the dominant mafic minerals; they total between 10 and 60% by volume.

Whole-rock analyses (Table 1) and plots (Figure 3A and B) indicate that the Crowston Lake pluton is calcalkaline and subalkaline, and that it varies compositionally from gabbro to quartz diorite (Figure 3C). Trace element plots (Figure 3D) indicate that the pluton represents a volcanic arc granitoid as defined by Pearce *et al.* (1984). Small mafic xenoliths occur rarely, and locally the body is cut by narrow dikes of highly mafic microgabbro as well as by veins and irregular patches of mafic pegmatitic material containing hornblende and plagioclase crystals up to 2 centimetres long. Both the microgabbro dikes and pegmatitic segregations probably represent late phases of the pluton. Where the pluton is intersected by fault fractures, or overprinted by endoskarn alteration, it tends to be extensively epidotized, and carries minor garnet. Immediately northeast of Mineral Hill, the margin of the pluton adjacent to its contact with exoskarn is marked by a zone of fine to medium-grained mafic rocks, 100 metres thick, that carries disseminated pyrite and minor magnetite. It is uncertain whether this zone represents a unit of (?Karmutsen Formation) metabasalt or a strongly altered marginal phase of the pluton, however, the latter interpretation is preferred.

In thin section the more mafic gabbroic rocks are seen to contain between 40 and 60% unaltered plagioclase that forms crystals up to 2 millimetres in length in the groundmass and up to 5 millimetres long as phenocrysts. Twinning indicates that the plagioclase is of labradorite composition ($An_{50-58}$). Most of the plagioclase is fresh but the cores of some crystals are cloudy and altered and some labradorite phenocrysts display optical zoning in plane polarized light.

Pyroxene makes up to 20% by volume in some mafic gabbroic samples, and both clinopyroxene and orthopyroxene are present. The latter forms prismatic crystals up to 3 millimetres long that are characterized by low birefringence and lamellar twinning. Clinopyroxene tends to be more common and widespread than orthopyroxene.

Most pyroxenes are partially rimmed by, or completely altered to, brown or pale green hornblende which can comprise over 25% of the rock. Locally, the pyroxene and hornblende are partially altered to tremolite-actinolite and pale green chlorite which also occurs in late, crosscutting veins. In addition, light brown biotite crystals occur as aggregates, as rims around opaque minerals or as a partial replacement of hornblende and pyroxene. Generally, however, the biotite content of the gabbro is less than 1%.

Olivine-bearing gabbros are exposed in some localities, such as the eastern shore of Crowston Lake. The olivine is commonly strongly corroded and rimmed with pyroxene, amphibole and opaque iron minerals. The olivine-bearing rocks are often characterized by abundant laths of plagioclase with subparallel orientation due to igneous flow.

Accessory minerals include apatite, magnetite, ilmenite and leucoxene. In addition, some of the gabbros contain trace quantities of pyrrhotite, chalcopyrite, pyrite and hematite.

Calcareous metasediments close to the pluton are intruded by swarms of gabbroic sills and dikes. Areas of intense endoskarn development, either in the main pluton or in these smaller bodies, are commonly bleached and variably altered to epidote, plagioclase and minor garnet.

## *SNAKE BAY PLUTON*

Part of Snake Bay pluton occupies the eastern and northeastern portions of the mapped area (Figure 2) and its coarse-grained, massive to weakly foliated rocks are well exposed along the western shore of Sechelt Inlet from Carlson Point to Snake Bay. Along the shore of the inlet, the rocks are leucocratic, containing between 4 and 8% mafic minerals, and biotite tends to be more common than hornblende. Westwards from the shore however, the pluton becomes more mafic; compared to the rocks along Sechelt Inlet they contain less potassium feldspar and biotite and more hornblende, which can comprise between 8 and 15%.

Whole-rock analyses (Table 1) and plots (Figure 3A and B) indicate that the rocks in the Snake Bay pluton are calcalkaline and subalkaline and that they vary compositionally from quartz diorite to granodiorite (Figure 3C). Trace element plots (Figure 3D) indicate that the pluton represents a volcanic arc granitoid as defined by Pearce *et al.* (1984).

Immediately adjacent to its contact with the Crowston Lake gabbro, the Snake Bay body becomes noticeably more mafic (up to 20% hornblende) and it tends to contain less quartz. Xenoliths are relatively rare in the pluton, but shoreline exposures along Sechelt Inlet and rocks close to the pluton margins commonly contain small (<0.3 m wide), rounded fragments of microgabbro, amphibolite and silicified metasediments. However, no xenoliths of exoskarn have been identified in the Snake Bay body, even in areas such as southeast of Wormy Lake, where the xenolith-bearing pluton outcrops less than 15 metres from garnet-wollastonite exoskarn.

# TABLE 1. COMPARATIVE MAJOR AND TRACE ELEMENT ANALYSES OF VARIOUS INTRUSIVE ROCKS, MINERAL HILL - WORMY LAKE AREA

| | Crowston Lake Pluton | | | | | | Snake Bay Pluton | | | |
|---|---|---|---|---|---|---|---|---|---|---|
| | GR94-84 | GR94-85 | GR95-12 | GR95-14 | GR95-60 | GR95-92 | GR95-16 | GR95-17 | GR95-45 | GR95-47 |
| CaO | 6.85 | 6.83 | 11.20 | 10.27 | 8.93 | 11.45 | 4.96 | 3.87 | 2.31 | 7.05 |
| $K_2O$ | 1.10 | 1.19 | 0.13 | 0.20 | 0.60 | 0.61 | 1.80 | 2.44 | 3.39 | 1.36 |
| $P_2O_5$ | 0.15 | 0.20 | 0.24 | 0.10 | 0.58 | 0.18 | 0.12 | 0.09 | 0.05 | 0.34 |
| $SiO_2$ | 58.20 | 58.08 | 49.34 | 50.94 | 51.08 | 44.72 | 64.81 | 67.12 | 72.62 | 55.66 |
| $Fe_2O_3$* | 6.63 | 6.60 | 9.36 | 8.76 | 10.10 | 12.95 | 4.46 | 3.46 | 1.81 | 8.37 |
| $Al_2O_3$ | 17.73 | 17.62 | 19.00 | 18.94 | 17.08 | 16.44 | 15.86 | 15.07 | 14.10 | 16.99 |
| MgO | 3.41 | 3.41 | 6.06 | 5.75 | 5.11 | 7.80 | 2.18 | 1.46 | 0.67 | 3.99 |
| $Na_2O$ | 3.77 | 3.70 | 3.04 | 3.09 | 3.59 | 2.33 | 3.64 | 3.64 | 3.42 | 3.35 |
| $TiO_2$ | 0.63 | 0.62 | 0.91 | 0.86 | 1.49 | 1.78 | 0.48 | 0.39 | 0.20 | 1.12 |
| MnO | 0.12 | 0.14 | 0.15 | 0.16 | 0.17 | 0.15 | 0.11 | 0.08 | 0.05 | 0.14 |
| $Cr_2O_3$ | 0.01 | 0.01 | 0.01 | 0.01 | 0.01 | 0.02 | 0.01 | 0.01 | 0.01 | 0.01 |
| LOI | 0.90 | 0.93 | 1.17 | 0.89 | 1.46 | 2.09 | 0.85 | 0.84 | 0.54 | 1.22 |
| SUM | 99.50 | 99.33 | 100.61 | 99.97 | 100.20 | 100.52 | 99.28 | 98.47 | 99.17 | 99.60 |
| $Fe_2O_3$ | ND | ND | 3.36 | 2.93 | 2.57 | 4.54 | 1.89 | 2.14 | 0.67 | 2.75 |
| FeO | 3.07 | 4.16 | 5.40 | 5.25 | 6.78 | 7.57 | 2.31 | 1.19 | 1.03 | 5.06 |
| Ba | 474 | 479 | 119 | 148 | 317 | 157 | 656 | 943 | 1722 | 427 |
| Rb | 23 | 25 | <5 | <5 | 12 | 5 | 38 | 48 | 66 | 28 |
| Sr | 502 | 503 | 733 | 707 | 557 | 575 | 409 | 360 | 273 | 543 |
| Y | 32 | 33 | 14 | 15 | 32 | 41 | 37 | 23 | 18 | 38 |
| Zr | 119 | 126 | 14 | 12 | 59 | 77 | 164 | 161 | 104 | 157 |
| Nb | 5 | <5 | 6 | <5 | 10 | 17 | 6 | 5 | <5 | 20 |
| V | 133 | 135 | 259 | 192 | 125 | 376 | 106 | 67 | <5 | 188 |
| Sn | <5 | <5 | <5 | <5 | 5 | 13 | 9 | <5 | 6 | <5 |

| | 1st generation minor intrusions | | | | | 2nd generation minor intrusions | | | | | |
|---|---|---|---|---|---|---|---|---|---|---|---|
| | GR95-37 | GR95-40 | R95-42A | GR95-51 | GR95-54 | GR95-29 | GR95-38 | GR95-42 | GR95-43 | GR95-53 | GR95-59 |
| CaO | 4.48 | 4.81 | 4.6 | 4.64 | 4.71 | 10.95 | 7.47 | 10.84 | 11.13 | 10.02 | 7.38 |
| $K_2O$ | 1.75 | 1.42 | 0.97 | 1.53 | 1.77 | 1.63 | 0.72 | 1.61 | 0.60 | 0.57 | 0.58 |
| $P_2O_5$ | 0.22 | 0.22 | 0.21 | 0.22 | 0.22 | 0.18 | 0.17 | 0.18 | 0.19 | 0.18 | 0.22 |
| $SiO_2$ | 65.12 | 65.35 | 65.31 | 64.93 | 64.42 | 51.83 | 50.36 | 51.80 | 49.56 | 50.57 | 56.37 |
| $Fe_2O_3$* | 3.45 | 3.37 | 3.67 | 3.18 | 3.41 | 7.12 | 8.45 | 7.25 | 7.49 | 7.02 | 7.64 |
| $Al_2O_3$ | 17.52 | 17.02 | 17.39 | 17.48 | 17.36 | 17.07 | 18.32 | 17.04 | 18.26 | 17.87 | 18.37 |
| MgO | 1.12 | 1.11 | 1.14 | 1.08 | 1.23 | 5.91 | 5.76 | 5.91 | 6.29 | 6.21 | 3.24 |
| $Na_2O$ | 4.78 | 4.90 | 4.84 | 4.73 | 4.71 | 2.76 | 3.94 | 2.82 | 3.02 | 3.08 | 3.57 |
| $TiO_2$ | 0.28 | 0.25 | 0.28 | 0.25 | 0.26 | 0.67 | 0.76 | 0.66 | 0.68 | 0.65 | 0.65 |
| MnO | 0.05 | 0.11 | 0.14 | 0.10 | 0.12 | 0.13 | 0.16 | 0.12 | 0.16 | 0.13 | 0.10 |
| $Cr_2O_3$ | 0.01 | 0.01 | 0.01 | 0.01 | 0.01 | 0.01 | 0.01 | 0.01 | 0.01 | 0.02 | 0.01 |
| LOI | 0.98 | 1.20 | 1.30 | 1.08 | 0.97 | 1.78 | 3.79 | 1.97 | 2.86 | 2.35 | 1.53 |
| SUM | 99.76 | 99.77 | 99.86 | 99.23 | 99.19 | 100.04 | 99.91 | 100.21 | 100.25 | 98.67 | 99.66 |
| $Fe_2O_3$ | 2.34 | 1.20 | 1.05 | 1.22 | 0.88 | 2.35 | 2.42 | 2.42 | 1.30 | 1.32 | 3.41 |
| FeO | 1.00 | 1.95 | 2.36 | 1.76 | 2.28 | 4.29 | 5.43 | 4.35 | 5.57 | 5.13 | 3.81 |
| Ba | 941 | 742 | 623 | 792 | 843 | 986 | 179 | 981 | 430 | 402 | 257 |
| Rb | 32 | 24 | 18 | 24 | 26 | 28 | 21 | 31 | 11 | 12 | 12 |
| Sr | 664 | 630 | 611 | 663 | 636 | 831 | 571 | 820 | 693 | 644 | 567 |
| Y | 17 | 20 | 22 | 18 | 19 | 21 | 26 | 20 | 25 | 20 | 25 |
| Zr | 131 | 130 | 135 | 124 | 128 | 58 | 64 | 65 | 54 | 49 | 93 |
| Nb | 15 | 9 | 10 | 7 | 9 | 10 | 12 | 7 | 12 | 7 | 13 |
| V | 24 | 19 | 25 | 35 | 21 | 144 | 168 | 140 | 172 | 133 | 246 |
| Sn | <5 | <5 | 6 | 8 | 6 | 20 | 14 | 15 | <5 | 5 | 18 |

$Fe_2O_3$* = Total iron as $Fe_2O_3$. Major elements in weight %; trace elements in ppm. ND = sample not analysed.

Analytical Methods

CaO, $K_2O$, $P_2O_5$, $SiO_2$, $Fe_2O_3$*, $Al_2O_3$, MgO, $Na_2O$, $TiO_2$, MnO, $Cr_2O_3$ and $Fe_2O_3$ = Fused disc - X-ray fluorescence.

FeO = Titration.

Ba, Rb, Sr, Y, Zr, Nb, V and Sn = Pressed pellet - x-ray fluorescence.

Analyses completed at Cominco laboratory, Vancouver, B.C.

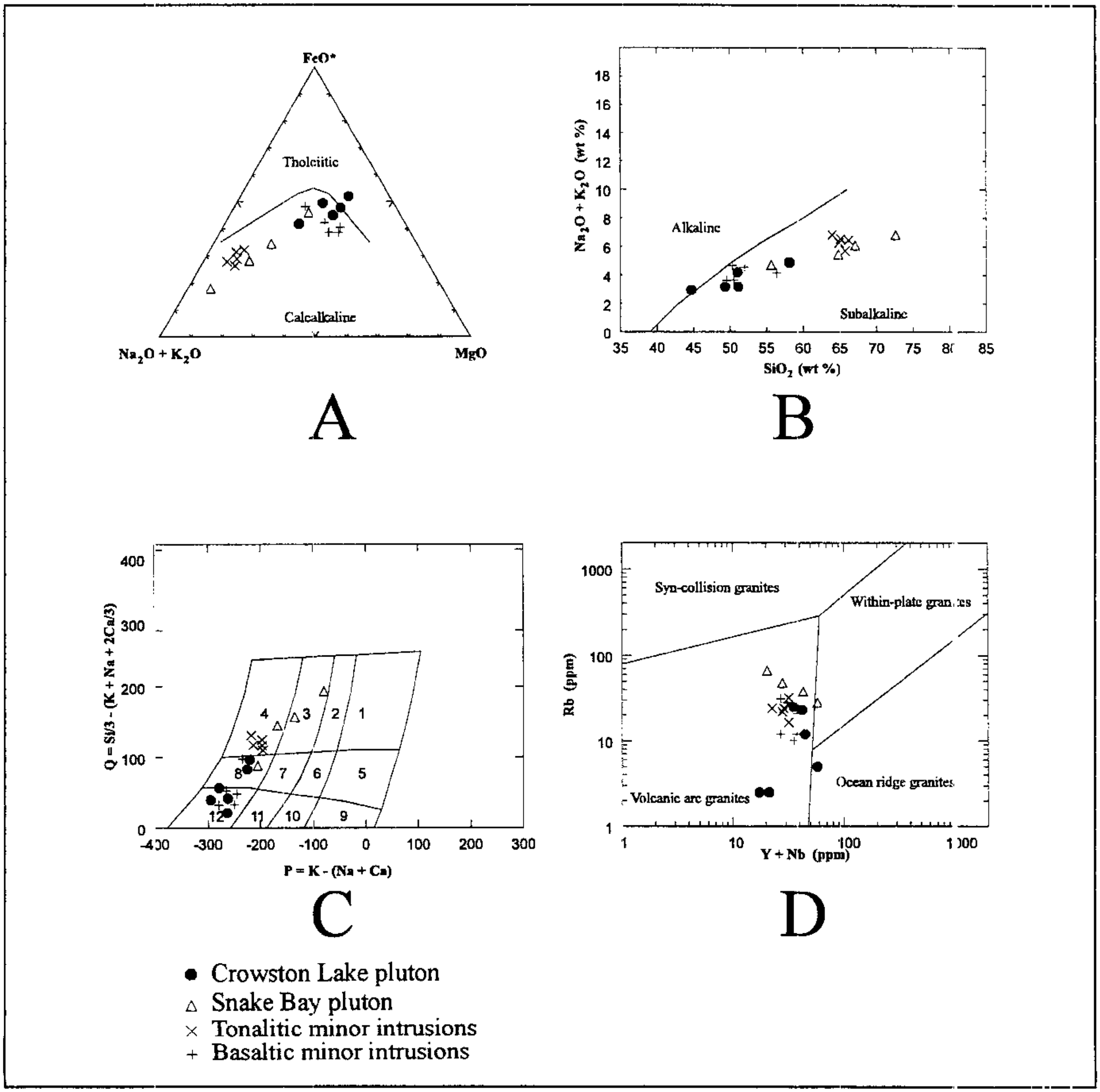


Figure 3. Plots comparing the geochemistry of the various intrusive rocks in the Mineral Hill - Wormy Lake area. A. AFM plot. B. Alkali-silica plot. C. Plot (after Debon and Le Fort, 1983) showing the compositions of the intrusive rocks. Rock compositions are as follows: 1. granite, 2. adamellite, 3. granodiorite, 4. tonalite, 5. quartz syenite, 6. quartz monzonite, 7. quartz monzodiorite, 8. quartz diorite, 9. syenite, 10. monzonite, 11. monzogabbro, 12. gabbro. D. Trace element discrimination plot (after Pearce *et al.*, 1984).

## *MINOR INTRUSIVE ROCKS*

Several generations of minor intrusions are seen throughout the area. The oldest are gabbroic sills and dikes related to the Crowston Lake pluton. This suite commonly forms swarms of sills and dikes that, where they intrude the calcareous metasediments, are spatially associated with the development of extensive garnet-wollastonite-pyroxene skarn assemblages. They are medium to coarse-grained rocks that vary from mafic to highly mafic. In thin section, many are seen to be variably altered to epidote, particularly where they have been deformed by boudinage structures or overprinted by garnet-bearing endoskarn alteration.

The next recognized phase of minor intrusions is narrow sills and dikes which are most commonly seen intruding the garnet-wollastonite-bearing exoskarns east of Mineral Hill. Chemical plots indicate they are subalkaline and that they have a tonalitic composition (Figure 3B and C). They are fine-grained porphyritic to equigranular dark-coloured rocks that are commonly altered, siliceous and locally crosscut by veins of garnet and epidote; no wollastonite has been identified in these veins.

In thin section the less altered samples are seen to contain phenocrysts of hornblende and potassic feldspar up to 3 millimetres in length. The latter have fine optical zoning and are variably altered; the corroded and ragged amphibole phenocrysts are extensively chloritized. The very fine grained groundmass comprises abundant altered plagioclase lathes up to 0.2 millimetre in length with lesser amounts of quartz, chlorite, epidote and opaque minerals.

A subsequent phase of minor intrusion resulted in swarms of easterly striking sills and dikes. They tend to occupy fractures related to the east-trending Snake Bay fault and are most abundant east of Mineral Hill. They are seen cutting both the Snake Bay and Crowston Lake plutons as well as the exoskarns and marbles. Where they intrude marble their margins are commonly marked by thin zones of exoskarn containing garnet and wollastonite. Geochemical plots indicate this youngest generation of minor intrusions has a basaltic composition (Figure 3C); it is believed to be related to the Cretaceous Gambier Group volcanic and extensional event.

In thin section these fine-grained rocks are seen to be moderately to strongly altered. Elongate and altered phenocrysts of plagioclase, hornblende and augite reach 2 millimetres in length; the clinopyroxene is commonly rimmed by amphibole. The fine-grained groundmass consists largely of subparallel aligned plagioclase laths up to 0.2 millimetre long. Other minerals in the groundmass include crystals of altered, pale coloured hornblende with variable epidote, chlorite, biotite and opaques. Many of these rocks are extensively epidotised.

## SKARN

Elongate bodies of exoskarn outcrop discontinuously along a 4.5 kilometre strike length of the Wormy Lake fault zone between Wormy Lake in the north and Mineral Hill in the south (Figure 2). Endoskarn, by contrast, is far less extensive, although it is locally important along the margins of the Crowston Lake pluton and in gabbroic dikes and sills that intrude calcareous metasediments.

The intensity of exoskarn development varies from weak in the marbles, where minor amounts of garnet, clinopyroxene and epidote are seen, to intense where the original impure calcareous metasediments are entirely replaced by skarn minerals. The principal exoskarn minerals are: garnet, wollastonite, epidote, clinopyroxene, plagioclase, quartz and calcite. Accessory minerals include vesuvianite, rhodonite and prehnite as well as the local and rare development of sulphides such as pyrite, sphalerite and chalcopyrite.

Generally, exoskarns throughout the area are characterized by high garnet:pyroxene ratios (approximately 10:1 to 2:1) although thin layers of pyroxene-dominant skarn are locally present. Exoskarns vary texturally from massive to very well layered. Massive garnetite is locally developed, particularly in limestone protoliths or close to the Crowston Lake plutonic rocks. It consists of between 50 and 100% garnet that is generally pale to medium brown in colour. However, dark reddish brown, green, amber and black garnets are also seen. Layered exoskarn comprises alternating layers up to 1 metre thick that are either white, brown or pale green in colour. Colour variations are related to individual layers being rich in either wollastonite, garnet, pyroxene, epidote or quartz-calcite-plagioclase assemblages.

Three episodes of exoskarn formation are recognised, all of which resulted in garnet-epidote assemblages; wollastonite, however, was only developed in the first and third of these skarn episodes.

The first episode was the dominant skarn-forming event. It was spatially and genetically related to the syntectonic emplacement of the Crowston Lake pluton and its gabbroic sill-dike swarm. It resulted in the pervasive and widespread wollastonite-garnet-pyroxene-vesuvianite assemblages that are of economic industrial mineral interest. Accompanying movements along the precursor structure of the Wormy Lake fault zone generated ductile deformation fabrics in the exoskarns as well as boudin structures in the gabbro sills and dikes.

At least two phases of garnet and wollastonite growth took place during the first skarn-forming event. The earliest phase resulted in the coeval development of garnet and wollastonite-rich layers that have selectively replaced original lithologies. Most of the wollastonite formed during this first phase occurs as crystals less than 0.5 centimetre long. They occur either as disseminations with garnet, pyroxene and carbonate, or in massive layers of up to 80% wollastonite. Microprobe analyses of garnets, pyroxene and wollastonite are presented in Tables 2 to 4. The garnets are grossularitic (Figure 4A) with an average composition of $Gr^{67}$-$Ad^{29}$-$Pyral^{4}$ (Table 2) and the diopsidic pyroxenes (Figure 4B) average $Di^{85}$-$Hd^{12}$-$Jo^{3}$ (Table 3).

A second phase of garnet and wollastonite generally occurs in crosscutting veins, although some late porphyroblasts of wollastonite, which locally overgrow sphalerite, also formed at this time. The garnet and wollastonite veins seldom exceed 12 centimetres in thickness. Vein garnet is generally lighter brown in colour than the earlier garnet, which varies from medium to very dark brown to black. The second phase wollastonite, in both veins and porphyroblasts, is much coarser grained; individual crystals reach 3 centimetres in length.

Subsequently, a second and minor skarn-forming event accompanied the intrusion of early tonalitic dikes. Both the dikes and the immediately adjacent calcareous hostrocks are cut by narrow, fracture-filled veins of garnet-epidote skarn. No wollastonite was produced during this second skarn-forming event.

The third skarn episode was related to subsequent intrusion of a swarm of basaltic dikes and sills, and is developed immediately adjacent to these bodies where, they intrude marbles. Exoskarn alteration seldom exceeds 15 centimetres in thickness but a well defined mineralogical zoning is apparent. From dike to marble, this skarn zoning consists of: (1) proximal garnet-rich skarn; (2) distal wollastonite-rich

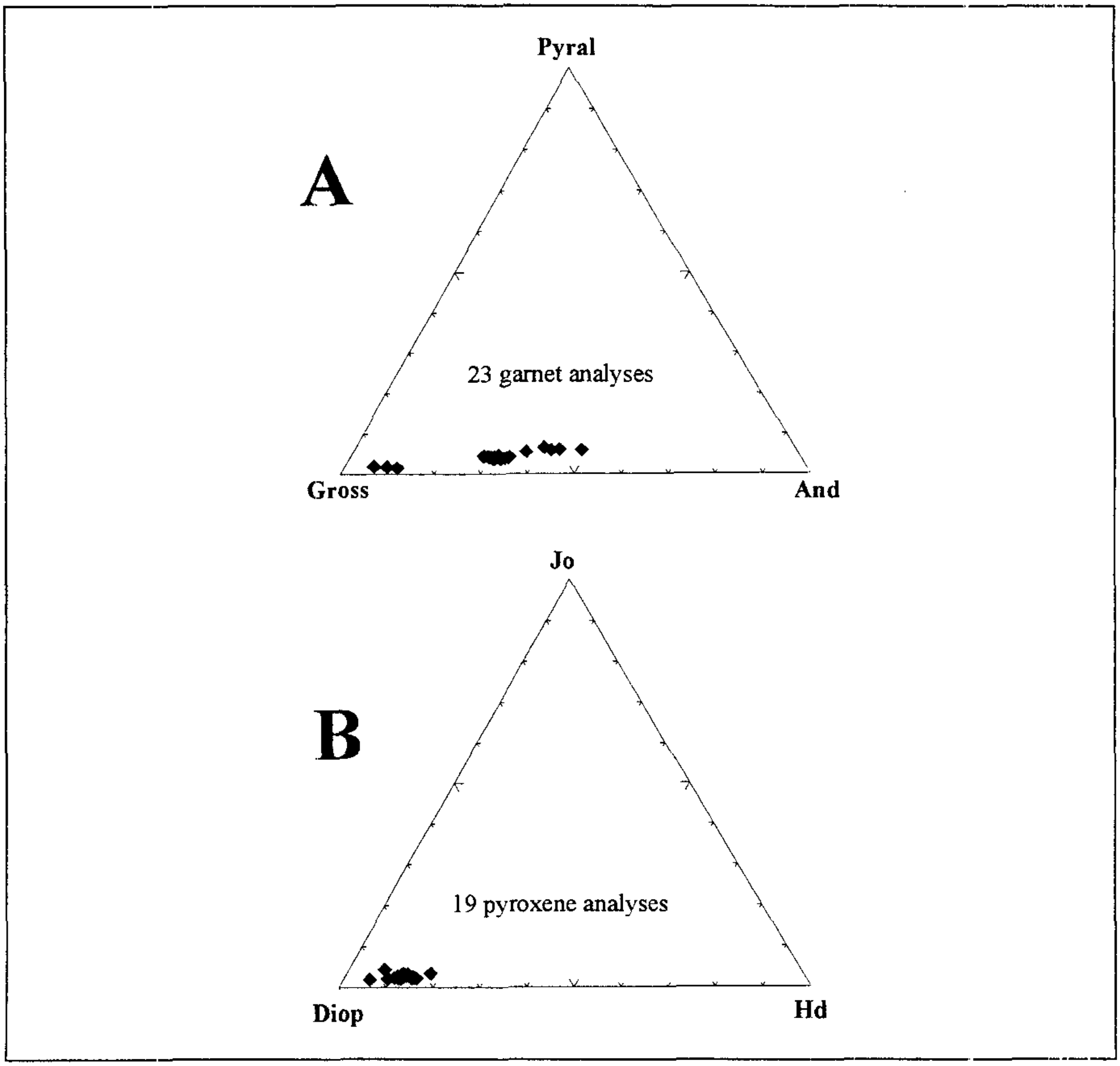


Figure 4. Composition of garnets (A) and pyroxene (B) at the Mineral Hill skarn, Sechelt, B.C.

skarn; (3) strongly bleached marble with pyrite cubes; and (4) grey to white marble without sulphides. Each mineralogical zone seldom exceeds 5 centimetres in thickness. The proximal garnet-rich zone locally includes an inner layer of yellow, amber or green garnet and an outer layer of dark red garnet. The dark red garnet crystals are often elongate, suggesting that they may have pseudomorphed early wollastonite.

Endoskarn alteration throughout the area occurs mainly in the Crowston Lake pluton and its gabbroic dikes and sills. To a far lesser extent, it is also present in extensional and boudin-related fractures developed in the early tonalitic dikes, but it has not been identified in the later basaltic dikes. Endoskarn in the Crowston Lake pluton and its related minor intrusions is commonly characterized by epidote occurring pervasively or in veins, and by plagioclase and rhodonite. Garnet in endoskarn is relatively uncommon; it tends to form in veins and is usually darker than the typically light brown garnet developed in exoskarn.

## WOLLASTONITE MINERALIZATION

The wollastonite-rich skarns at Mineral Hill have been the focus of work since their wollastonite content was recognised in 1986 by prospector Rudy Riepe. Wollastonite, a member of the pyroxenoid mineral group, is a calcium metasilicate ($CaSiO_3$). It is the only naturally occurring, nonmetallic, white acicular mineral. Its acicularity, together with other physical properties, has

## TABLE 2. REPRESENTATIVE MICROPROBE ANALYSES OF EXOSKARN GARNETS AT MINERAL HILL

| Spot | 3a | 4a | 3 | 6 | 7 | 54 | 56 | 57 | 60 | 62 | | | |
|---|---|---|---|---|---|---|---|---|---|---|---|---|---|
| Sample | R94-74 | R94-74 | R94-74 | R94-74 | R94-74 | R94-75 | R94-75 | R94-75 | R94-75 | R94-75 | Avg** | Max** | Min** |
| $Na_2O$ | 0.02 | 0.04 | 0.02 | 0.00 | 0.06 | 0.00 | 0.02 | 0.06 | 0.00 | 0.00 | 0.02 | 0.06 | 0.00 |
| FeO | 9.72 | 8.89 | 9.41 | 9.03 | 8.56 | 10.84 | 3.41 | 2.82 | 13.00 | 11.88 | 8.76 | 13.00 | 2.82 |
| $K_2O$ | 0.00 | 0.00 | 0.00 | 0.00 | 0.00 | 0.00 | 0.01 | 0.00 | 0.00 | 0.00 | 0.00 | 0.01 | 0.00 |
| $SiO_2$ | 37.98 | 38.10 | 37.72 | 38.02 | 38.17 | 37.07 | 38.52 | 39.16 | 36.43 | 36.76 | 37.79 | 39.16 | 36.43 |
| CaO | 35.26 | 34.74 | 34.33 | 34.78 | 34.54 | 32.84 | 36.34 | 36.49 | 32.14 | 32.66 | 34.41 | 36.49 | 32.14 |
| $Al_2O_3$ | 14.37 | 15.05 | 14.85 | 14.48 | 15.23 | 13.09 | 18.81 | 19.92 | 11.82 | 12.49 | 15.01 | 19.92 | 11.82 |
| $TiO_2$ | 0.63 | 0.64 | 0.71 | 0.88 | 0.82 | 1.54 | 0.97 | 0.26 | 1.30 | 1.01 | 0.88 | 1.54 | 0.26 |
| MgO | 0.33 | 0.52 | 0.43 | 0.40 | 0.49 | 0.36 | 0.02 | 0.05 | 0.37 | 0.40 | 0.34 | 0.52 | 0.02 |
| MnO | 1.05 | 0.96 | 0.97 | 0.94 | 1.11 | 1.74 | 0.66 | 0.72 | 2.02 | 2.17 | 1.23 | 2.17 | 0.66 |
| TOTAL | 99.35 | 98.94 | 98.44 | 98.53 | 98.98 | 97.48 | 98.77 | 99.50 | 97.08 | 97.38 | 98.44 | 99.50 | 97.08 |
| Na | 0.003 | 0.007 | 0.003 | 0.000 | 0.009 | 0.000 | 0.003 | 0.009 | 0.000 | 0.000 | 0.00 | 0.01 | 0.00 |
| Fe | 0.635 | 0.580 | 0.618 | 0.593 | 0.558 | 0.723 | 0.220 | 0.180 | 0.877 | 0.798 | 0.58 | 0.88 | 0.18 |
| K | 0.000 | 0.000 | 0.000 | 0.000 | 0.000 | 0.000 | 0.001 | 0.000 | 0.000 | 0.000 | 0.00 | 0.00 | 0.00 |
| Si | 2.965 | 2.973 | 2.962 | 2.983 | 2.975 | 2.958 | 2.970 | 2.987 | 2.939 | 2.951 | 2.97 | 2.99 | 2.94 |
| Ca | 2.950 | 2.904 | 2.888 | 2.924 | 2.884 | 2.807 | 3.003 | 2.982 | 2.779 | 2.810 | 2.89 | 3.00 | 2.78 |
| Al | 1.322 | 1.385 | 1.374 | 1.339 | 1.399 | 1.231 | 1.711 | 1.791 | 1.124 | 1.182 | 1.39 | 1.79 | 1.12 |
| Ti | 0.037 | 0.038 | 0.042 | 0.052 | 0.048 | 0.092 | 0.056 | 0.015 | 0.079 | 0.061 | 0.05 | 0.09 | 0.02 |
| Mg | 0.039 | 0.061 | 0.050 | 0.047 | 0.057 | 0.043 | 0.002 | 0.006 | 0.044 | 0.048 | 0.04 | 0.06 | 0.00 |
| Mn | 0.069 | 0.063 | 0.064 | 0.062 | 0.073 | 0.117 | 0.043 | 0.046 | 0.138 | 0.148 | 0.08 | 0.15 | 0.04 |
| Sum | 8.02 | 8.01 | 8.00 | 8.00 | 8.00 | 7.97 | 8.01 | 8.02 | 7.98 | 8.00 | 8.00 | 8.02 | 7.97 |
| Mole % | | | | | | | | | | | | | |
| Pyral | 3.68 | 4.20 | 3.83 | 3.77 | 4.44 | 5.48 | 1.57 | 1.77 | 6.07 | 6.60 | 4.14 | 6.60 | 1.57 |
| Grossularit | 63.89 | 66.27 | 65.17 | 65.55 | 67.05 | 57.52 | 87.03 | 89.10 | 50.11 | 53.11 | 66.48 | 89.10 | 50.11 |
| Andradite | 32.43 | 29.53 | 31.00 | 30.68 | 28.51 | 37.00 | 11.40 | 9.14 | 43.83 | 40.29 | 29.38 | 43.83 | 9.14 |

Avg**, Max** and Min** = average, maximum and minimum of 23 analyses

made it an industrial mineral with expanding uses and increasing demand.

Within the study area, wollastonite-bearing skarn alteration is located in two main zones; (1) south of the Wormy Lake fault, along the southeastern slope of Mineral Hill (Figures 2 and 5; MINFILE 092GNW052), and (2) north of the Wormy Lake fault, where it occurs in a zone trending at approximately 335°, which is irregularly exposed and open to the north (Figure 2; MINFILE 092GNW053). The southern zone is up to 250 metres in outcrop width, and the northern zone reaches a maximum outcrop width of approximately 400 metres.

In 1987 and 1988, Tri-Sil Minerals Inc. conducted an exploration program on the southern half of zone 1 (Figure 5). Twenty-four drill holes, totaling 1719 metres in length, were put down to test the grade and continuity of the wollastonite-rich skarns southeast of Mineral Hill. This work, which included geological mapping at a scale of 1:1250, has been described by Goldsmith and Logan (1987) and Goldsmith and Kallock (1988).

A program of road building and trenching was undertaken on the skarn (zone 2) north of the Wormy Lake fault during the period 1989 to 1990 by Performance Minerals of Canada Ltd. During mapping, we identified a new area of wollastonite skarn 500 metres north of the northern tip of Wormy Lake. Well layered wollastonite-garnet skarn is exposed along the crest of a prominent hill for over 15 metres and consists of light brown garnet and fine to coarse (5 mm) wollastonite, in parts up to 80%.

Wollastonite is widespread throughout the skarn rocks in both zones. Grain size and mode of occurrence vary widely between outcrops and as reported in drill holes. Visually estimated grades in outcrops range from less than 0.5% up to 80% wollastonite. Wollastonite crystals are generally white to buff in colour. Massive 2 to 3-centimetre layers of wollastonite fibres up to 0.5 centimetre in length are common, or wollastonite may occur closely intergrown with grossular garnet and pyroxene over greater widths. In veins and porphyroblasts, wollastonite is much coarser grained and fibrous, reaching 3 centimetres in length. In rare instances garnet-wollastonite-pyroxene skarn float with light to dark brown garnet carries wollastonite crystals up to 11 centimetres long. Comparative analyses of wollastonite from Mineral Hill and from elsewhere are given in Table 4. These indicate that the Mineral Hill wollastonite has a very low iron content but is enriched in manganese (up to 1.13% MnO).

Goldsmith and Logan (1987) and Goldsmith and Kallock (1988) report visual estimates of wollastonite grade in drill-hole intersections from zone 1. These vary

TABLE 3. REPRESENTATIVE MICROPROBE ANALYSES OF EXOSKARN PYROXENES AT MINERAL HILL

| Spot | 1 | 9 | 10 | 12 | 13 | 66 | 67 | 68 | 70 | 73 | | | |
|---|---|---|---|---|---|---|---|---|---|---|---|---|---|
| Sample | GR94-74 | GR94-74 | GR94-74 | GR94-74 | GR94-74 | GR94-75 | GR94-75 | GR94-75 | GR94-75 | GR94-75 | Avg** | Max** | Min** |
| $Na_2O$ | 0.00 | 0.07 | 0.00 | 0.03 | 0.00 | 0.22 | 0.07 | 0.00 | 0.04 | 0.07 | 0.04 | 0.22 | 0.00 |
| FeO | 3.79 | 4.21 | 3.74 | 4.42 | 3.50 | 5.55 | 1.99 | 2.45 | 4.12 | 3.78 | 3.80 | 5.55 | 1.99 |
| $K_2O$ | 0.01 | 0.00 | 0.00 | 0.00 | 0.00 | 0.01 | 0.00 | 0.00 | 0.00 | 0.02 | 0.01 | 0.02 | 0.00 |
| $SiO_2$ | 52.07 | 50.54 | 52.14 | 50.35 | 53.13 | 52.98 | 54.78 | 54.52 | 54.28 | 54.47 | 52.76 | 54.78 | 49.65 |
| CaO | 25.38 | 25.24 | 25.60 | 25.00 | 25.63 | 24.86 | 25.79 | 25.81 | 25.72 | 25.77 | 25.50 | 25.96 | 24.86 |
| $Al_2O_3$ | 2.41 | 4.08 | 2.03 | 4.43 | 1.68 | 0.99 | 0.18 | 0.05 | 0.10 | 0.19 | 1.72 | 5.05 | 0.05 |
| $TiO_2$ | 0.32 | 0.53 | 0.13 | 0.41 | 0.17 | 0.07 | 0.00 | 0.01 | 0.02 | 0.01 | 0.16 | 0.53 | 0.00 |
| MgO | 14.57 | 13.50 | 14.70 | 13.74 | 14.94 | 13.71 | 16.85 | 15.75 | 15.14 | 15.38 | 14.71 | 16.85 | 13.29 |
| MnO | 0.84 | 0.75 | 0.66 | 0.72 | 0.83 | 1.06 | 0.33 | 1.37 | 0.94 | 0.91 | 0.82 | 1.37 | 0.33 |
| TOTAL | 99.40 | 98.92 | 99.01 | 99.11 | 99.88 | 99.48 | 99.99 | 99.96 | 100.36 | 100.60 | 99.52 | 100.85 | 97.85 |
| | | | | | | | | | | | | | |
| Na | 0.000 | 0.005 | 0.000 | 0.002 | 0.000 | 0.016 | 0.005 | 0.000 | 0.003 | 0.005 | 0.00 | 0.02 | 0.00 |
| Fe | 0.118 | 0.132 | 0.117 | 0.138 | 0.108 | 0.173 | 0.061 | 0.075 | 0.127 | 0.116 | 0.12 | 0.17 | 0.06 |
| K | 0.001 | 0.000 | 0.000 | 0.000 | 0.000 | 0.001 | 0.000 | 0.000 | 0.000 | 0.001 | 0.00 | 0.00 | 0.00 |
| Si | 1.932 | 1.890 | 1.942 | 1.879 | 1.958 | 1.978 | 1.996 | 2.001 | 1.996 | 1.995 | 1.95 | 2.00 | 1.86 |
| Ca | 1.009 | 1.011 | 1.022 | 1.000 | 1.012 | 0.995 | 1.007 | 1.015 | 1.013 | 1.011 | 1.01 | 1.03 | 0.99 |
| Al | 0.105 | 0.180 | 0.089 | 0.195 | 0.073 | 0.044 | 0.008 | 0.002 | 0.004 | 0.008 | 0.08 | 0.22 | 0.00 |
| Ti | 0.009 | 0.015 | 0.004 | 0.012 | 0.005 | 0.002 | 0.000 | 0.000 | 0.000 | 0.000 | 0.00 | 0.01 | 0.00 |
| Mg | 0.806 | 0.752 | 0.816 | 0.764 | 0.820 | 0.763 | 0.915 | 0.862 | 0.830 | 0.839 | 0.81 | 0.92 | 0.74 |
| MN | 0.026 | 0.024 | 0.021 | 0.023 | 0.026 | 0.034 | 0.010 | 0.043 | 0.029 | 0.028 | 0.03 | 0.04 | 0.01 |
| Sum | 4.01 | 4.01 | 4.01 | 4.01 | 4.00 | 4.01 | 4.00 | 4.00 | 4.00 | 4.00 | 4.01 | 4.02 | 4.00 |
| Mole % | | | | | | | | | | | | | |
| Jo | 2.78 | 2.61 | 2.18 | 2.47 | 2.73 | 3.46 | 1.05 | 4.36 | 2.96 | 2.86 | 2.69 | 4.36 | 1.05 |
| Dp | 84.83 | 82.87 | 85.59 | 82.61 | 85.96 | 78.66 | 92.81 | 87.97 | 84.19 | 85.36 | 84.93 | 92.81 | 78.66 |
| Hd | 12.39 | 14.52 | 12.23 | 14.92 | 11.31 | 17.88 | 6.14 | 7.67 | 12.85 | 11.78 | 12.38 | 17.88 | 6.14 |

Avg**, Max** and Min** = average, maximum and minimum of 19 analyses

significantly from hole to hole and within holes. For example, hole 88-8(B) has a total length of 63.7 metres. Visual estimates of wollastonite between 9.8 to 17.0 metres depth (7.2 m length) can be summarized as follows: 1.9 metres garnet+wollastonite grading 65% wollastonite; followed by 0.7 metre quartz and epidote, grading less than 5% wollastonite; followed by 2.5 metres wollastonite+garnet, grading 75% wollastonite; followed by 2.2 metres limestone grading 5% wollastonite.

Goldsmith and Kallock made preliminary estimates of drill-indicated possible and probable reserves for their "central" section (Figure 5; approximately 125 metres north and south of 5 485 000 N) of the skarn (zone 1) southeast of Mineral Hill. These estimates total approximately 196 000 cubic metres of material grading 52% wollastonite; equivalent to 291 000 tonnes of wollastonite. There are other significant drill intersections outside this central section; for example, a 14.6-metre intercept in hole 88-2 with a visual estimate of 85% wollastonite, which is part of a 39.8-metre interval visually estimated to average 52% wollastonite.

During 1991-1992 Tri-Sil quarried nearly 30 000 tonnes and shipped approximately 20 000 tonnes of run-of-mine crushed rock to the Tilbury cement plant in Delta, British Columbia. This wollastonite-garnet mix was used as a cement additive (R. Riepe, personal communication, 1995).

## SULPHIDE MINERALIZATION

Minor amounts of sulphide are locally present in the area. Four styles of mineralization are recognized on the basis of sulphide content and hostrock lithology:

- Pyrite±chalcopyrite veinlets in fractures cutting the Snake Bay pluton,
- Pyrite±magnetite±chalcopyrite as disseminations or veinlets in the Crowston Lake pluton.
- Disseminations, layers and deformed pods and lenses of pyrite±sphalerite±chalcopyrite hosted by garnet-wollastonite exoskarn.
- Pyrite±pyrrhotite pods and lenses in marble.

Assays of mineralized grab samples representative of all four types of mineralization are presented in Table 5.

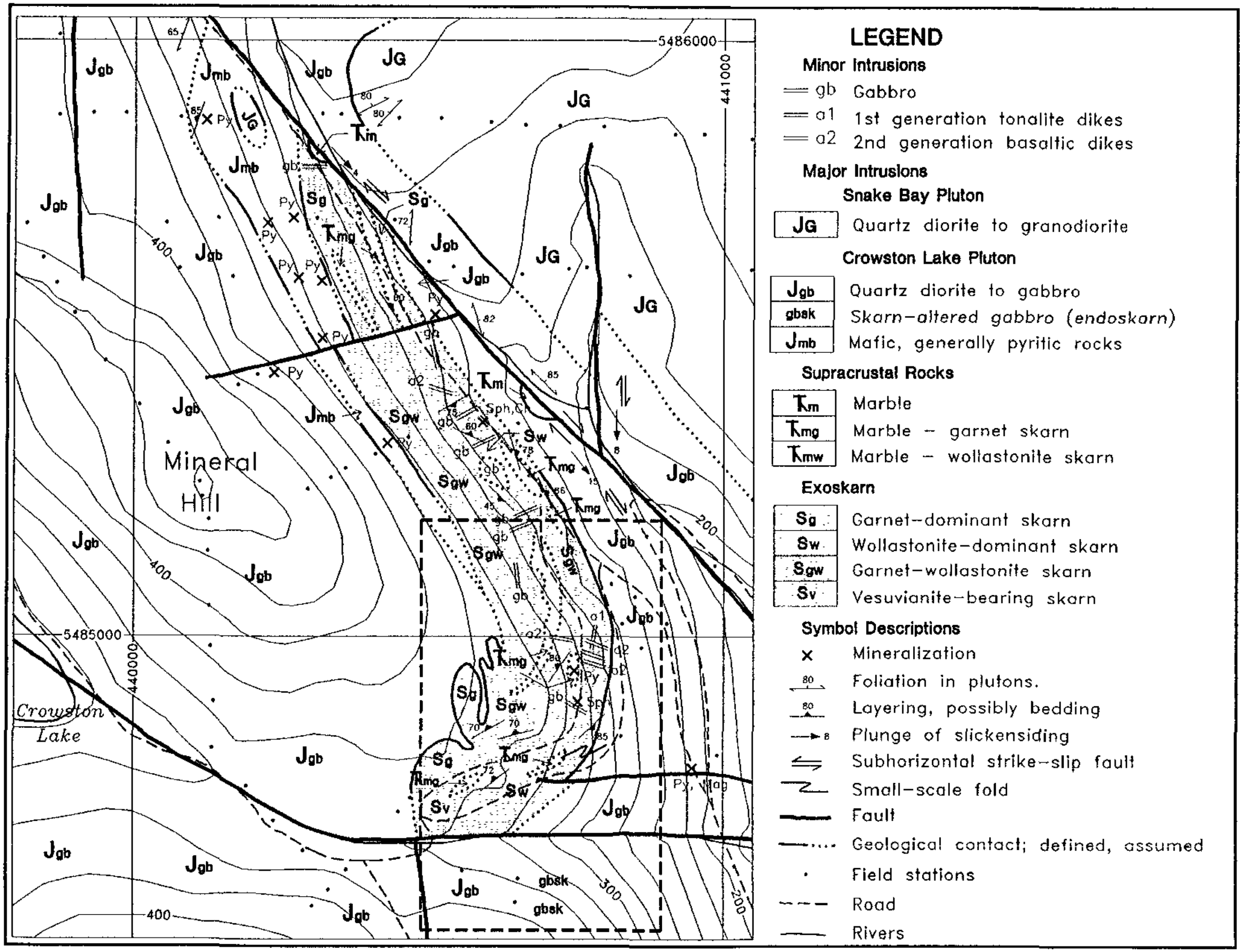

Figure 5. Map of the wollastonite skarn (zone 1) southeast of Mineral Hill (adapted from Ray and Kilby, 1995). Dashed box in lower right-hand corner is approximate boundary of mapping and drilling reported on by Goldsmith and Logan (1987) and Goldsmith and Kallock (1988). Mineralization includes; Py = pyrite, Sph = sphalerite, Ch = chalcopyrite, and Mag = magnetite.

## TABLE 4. COMPARATIVE ANALYSES OF WOLLASTONITE CRYSTALS FROM THE MINERAL HILL SKARN AND ELSEWHERE

**MINERAL HILL WOLLASTONITE (Samples GR94-74 & 75)**

| Crystal | 5a | 6a | 7a | 12a | 13a | 5.00 | 15 | 16 | 17 | 18 | 19 | 74 | Avg |
|---|---|---|---|---|---|---|---|---|---|---|---|---|---|
| $Na_2O$ | 0.00 | 0.00 | 0.00 | 0.00 | 0.00 | 0.02 | 0.03 | 0.01 | 0.00 | 0.02 | 0.00 | 0.0[illegible] | 0.01 |
| $SiO_2$ | 51.49 | 51.60 | 51.55 | 51.30 | 50.93 | 51.33 | 51.25 | 51.11 | 51.67 | 51.44 | 51.54 | 51.2[illegible] | 51.37 |
| $Al_2O_3$ | 0.01 | 0.01 | 0.04 | 0.09 | 0.02 | 0.08 | 0.05 | 0.03 | 0.03 | 0.03 | 0.03 | 0.0[illegible] | 0.04 |
| MgO | 0.07 | 0.05 | 0.14 | 0.16 | 0.10 | 0.05 | 0.06 | 0.07 | 0.11 | 0.07 | 0.12 | 0.0[illegible] | 0.09 |
| FeO | 0.14 | 0.12 | 0.14 | 0.17 | 0.12 | 0.22 | 0.21 | 0.19 | 0.22 | 0.09 | 0.14 | 0.2[illegible] | 0.17 |
| MnO | 0.54 | 0.49 | 0.50 | 0.53 | 0.48 | 0.53 | 0.49 | 0.52 | 0.53 | 0.55 | 0.54 | 1.1[illegible] | 0.57 |
| $K_2O$ | 0.00 | 0.00 | 0.02 | 0.00 | 0.01 | 0.00 | 0.00 | 0.01 | 0.00 | 0.00 | 0.00 | 0.0[illegible] | 0.00 |
| CaO | 48.16 | 47.44 | 47.83 | 47.43 | 47.54 | 47.52 | 47.86 | 47.45 | 47.43 | 47.69 | 47.60 | 47.1[illegible] | 47.59 |
| $TiO_2$ | 0.02 | 0.00 | 0.01 | 0.02 | 0.01 | 0.01 | 0.02 | 0.00 | 0.04 | 0.00 | 0.02 | 0.0[illegible] | 0.01 |
| $Cr_2O_3$ | 0.00 | 0.00 | 0.00 | 0.00 | 0.00 | 0.00 | 0.00 | 0.00 | 0.03 | 0.00 | 0.00 | 0.0 | 0.00 |
| **Total** | 100.43 | 99.72 | 100.22 | 99.70 | 99.22 | 99.76 | 99.97 | 99.38 | 100.06 | 99.89 | 100.00 | 99.9[illegible] | 99.86 |

**OTHER WOLLASTONITE**

| Sample | EMT1* | DHZ1* | DHZ3* | DHZ5* | W-3* | IW-2* |
|---|---|---|---|---|---|---|
| $Na_2O$ | 0.02 | 0.00 | 0.24 | 0.00 | 0.08 | 0.10 |
| $SiO_2$ | 51.26 | 51.10 | 50.53 | 50.00 | 51.32 | 48.69 |
| $Al_2O_3$ | 0.02 | 0.12 | 0.67 | ND | 0.07 | 0.71 |
| MgO | 0.07 | ND | 0.61 | ND | 0.10 | 0.57 |
| FeO | 0.28 | 0.64 | 0.51 | 10.32 | 1.11 | 9.54 |
| MnO | 0.28 | 0.13 | 0.02 | 1.22 | 0.10 | 1.92 |
| $K_2O$ | 0.00 | ND | 0.12 | ND | 0.12 | 0.03 |
| CaO | 47.67 | 47.86 | 47.01 | 38.86 | 46.22 | 38.04 |
| $TiO_2$ | 0.01 | ND | ND | ND | 0.05 | 0.06 |
| $Cr_2O_3$ | 0.00 | ND | ND | ND | ND | ND |
| **Total** | 99.61 | 99.85 | 99.71 | 100.40 | 99.17 | 99.66 |

ND = element not analysed. FeO = Total iron as FeO.

Microprobe analyses of wollastonite from Mineral Hill and Emerald Tungsten by S. Cornelius @ Dept. of Geology, Washington State University, Pullman, WA 99164

EMT1* = average of eleven wollastonite analyses from Emerald Tungsten Mine, Salmo, B.C.

DHZ1* = Pale green wollastonite, Willsboro, New York (Deer, Howie and Zussman, 1963).

DHZ3* = Wollastonite from a limestone-granodiorite contact, Adamello, Italy (Deer, Howie and Zussman, 1963).

DHZ5* = White iron-wollastonite, around chert nodules in meta-dololomite, Skye, Scotland (Deer, Howie and Zussman, 1963).

W-3* = Wollastonite, Sampo mine, Japan (Matsueda, 1973).

IW-2* = Iron-wollastonite, Sampo mine, Japan (Matsueda, 1973).

Gold values are generally low in all samples. The highest gold (423 ppb) occurs in thin (<2 cm) veinlets that cut the Snake Bay pluton (Table 5); these veinlets contain minor chalcopyrite, pyrite, quartz, carbonate and sericite. Generally, however, no significant metal enrichment is seen in any of the plutonic rocks.

The third type of sulphide mineralization, hosted in layered garnet-wollastonite exoskarn, can be separated into two subtypes. The first is characterized by silicification and fine-grained disseminated pyrite. Assays on two samples (GR95-23 and 24) indicate no significant metal enrichment (Table 5).

The other subtype occurs as thin layers or small tectonized pods and lenses of black sphalerite with lesser pyrite and chalcopyrite. This style of mineralization is seen in drill-road exposures southeast of Mineral Hill, at several localities farther north along the Wormy Lake fault zone, and in an old exploration pit approximately 200 metres southeast of the southern end of Wormy Lake. At this pit, a zone 1 to 5 metres thick is marked by extensive, black secondary manganese oxides and sphalerite. Individual sphalerite-bearing layers are generally only 1 to 6 centimetres thick and are separated by layers of barren skarn dominated either by wollastonite, dark brown garnet, clinopyroxene or carbonate.

In drill-road exposures east of Mineral Hill, this type of mineralization occurs either as weak disseminations of sphalerite in skarn or as discontinuous and narrow (1 m by 10 cm) tectonized lenses in layered, boudinaged garnet skarn. Assays of four grab samples of sphalerite-bearing rock are presented in Table 5. Most samples

## TABLE 5. ASSAYS OF MINERALIZED GRAB SAMPLES FROM THE MINERAL HILL-WORMY LAKE AREA

| | | Sulphides in Snake Bay pluton | | | | Sulphides in Crowston Lake pluton | | |
|---|---|---|---|---|---|---|---|---|
| Sample | | GR95-18 | GR95-19 | GR95-35 | GR95-68 | GR95-20 | GR95-61 | GR95-62 |
| UTM | North | 5487695 | 5488099 | 5486790 | 5487577 | 5484526 | 5485599 | 5485604 |
| UTM | East | 440865 | 438766 | 439694 | 438639 | 440980 | 440318 | 440277 |
| Mo | ppm | 4 | < 2 | 5 | < 2 | < 2 | < 2 | 3 |
| Cu | ppm | 16943 | 198 | 55 | 419 | 77 | 258 | 388 |
| Pb | ppm | < 5 | < 5 | 10 | 10 | 9 | 7 | 10 |
| Zn | ppm | 103 | 58 | 22 | 39 | 76 | 35 | 49 |
| Ni | ppm | 30 | 26 | 11 | 53 | 50 | 63 | 79 |
| Mn | ppm | 112 | 1119 | 515 | 1264 | 1111 | 1322 | 1670 |
| Sr | ppm | 2 | 144 | 385 | 305 | 631 | 326 | 412 |
| Cd | ppm | 3.2 | 1.2 | 0.5 | 1 | 2.1 | 0.8 | 1 |
| Bi | ppm | 14 | < 5 | < 5 | < 5 | < 5 | < 5 | < 5 |
| V | ppm | 4 | 75 | 116 | 151 | 192 | 175 | 185 |
| P | % | 0.01 | 0.05 | 0.11 | 0.05 | 0.35 | 0.04 | 0.04 |
| Ba | ppm | 40 | 39 | 148 | 111 | 65 | 41 | 75 |
| Zr | ppm | 3 | 24 | 4 | 14 | 33 | 18 | 35 |
| Sn | ppm | < 2 | < 2 | < 2 | 3 | < 2 | < 2 | < 2 |
| Y | ppm | 3 | 11 | 6 | 12 | 28 | 17 | 17 |
| Nb | ppm | < 2 | < 2 | < 2 | < 2 | 2 | < 2 | < 2 |
| Be | ppm | < 1 | < 1 | < 1 | < 1 | < 1 | < 1 | < 1 |
| Hg | ppb | 95 | 5 | 5 | <5 | 15 | <5 | <5 |
| S | % | 7.94 | 2.94 | 4.17 | 2.42 | 3.95 | 2.51 | 2.88 |
| Se | ppm | ND | ND | 0.2 | 0.6 | ND | 4.2 | 3.2 |
| Te | ppm | ND | ND | <0.1 | 1.2 | ND | <0.1 | 0.1 |
| Au | ppb | 423 | <2 | <2 | 24 | 6 | <2 | <2 |
| Ag | ppm | <5 | <5 | <5 | <5 | <5 | <5 | <5 |
| As | ppm | 130 | 42 | 5.6 | 5.6 | 16 | 5.8 | 11 |
| Br | ppm | <0.5 | <0.5 | <0.5 | <0.5 | <0.5 | <0.5 | <0.5 |
| Co | ppm | 330 | 79 | 59 | 85 | 51 | 86 | 110 |
| Cr | ppm | 8 | 91 | 16 | 140 | 220 | 140 | 150 |
| Cs | ppm | <1 | <1 | 2 | <1 | <1 | <1 | <1 |
| Hf | ppm | <1 | <1 | 3 | <1 | 2 | <1 | <1 |
| Ir | ppb | <5 | <5 | <5 | <5 | <5 | <5 | <5 |
| Rb | ppm | 22 | <15 | 35 | <15 | <15 | <15 | <15 |
| Sb | ppm | <0.1 | 1.6 | <0.1 | 0.6 | 1.1 | 1.6 | 2.6 |
| Sc | ppm | 0.9 | 25 | 16 | 41 | 18 | 40 | 38 |
| Th | ppm | 1.1 | <0.2 | 2.7 | 0.9 | 2.8 | <0.2 | 1.4 |
| U | ppm | <0.5 | 1.5 | 2.3 | <0.5 | 21 | <0.5 | <0.5 |
| La | ppm | 2.5 | 5 | 21 | 4.5 | 18 | 4.3 | 6.2 |
| Ce | ppm | 6 | 10 | 44 | 12 | 25 | 11 | 17 |
| Nd | ppm | 7 | <5 | 24 | <5 | 11 | <5 | 7 |
| Sm | ppm | 0.6 | 1.4 | 4.1 | 1.6 | 3.3 | 1.6 | 1.9 |
| Eu | ppm | <0.2 | 0.7 | 1.3 | 0.7 | 1.7 | 0.8 | 0.7 |
| Tb | ppm | <0.5 | <0.5 | <0.5 | <0.5 | 1 | 0.8 | 0.8 |
| Yb | ppm | 0.8 | 2.4 | 2.8 | 2 | 3.5 | 3.3 | 3.1 |
| Lu | ppm | 0.011 | 0.35 | 0.42 | 0.26 | 0.54 | 0.52 | 0.53 |
| F | ppm | 180 | 70 | 480 | 920 | 410 | 540 | 400 |

TABLE 5. Continued

| | | Sulphides in garnet-wollastonite skarn | | | | | | Sulphides in marble | |
|---|---|---|---|---|---|---|---|---|---|
| Sample | | GR95-23 | GR95-24 | GR95-30 | GR94-82 | GR94-70 | GR94-73 | GR95-85 | GR95-86 |
| UTM | North | 5486252 | 5486204 | 5485362 | 5486694 | 5484890 | 5484890 | 5484942 | 5484942 |
| UTM | East | 439684 | 439866 | 440590 | 439623 | 440751 | 440751 | 440745 | 440745 |
| Mo | ppm | 8 | < 2 | < 2 | <2 | <2 | <2 | 43 | 38 |
| Cu | ppm | 28 | 245 | 2864 | 65 | 5223 | 3770 | 79 | 34 |
| Pb | ppm | 10 | 10 | < 5 | 4 | 7 | 7 | < 5 | 10 |
| Zn | ppm | 40 | 23 | 6756 | 6604 | 99999 | 88617 | 160 | 89 |
| Ni | ppm | 6 | 16 | 321 | 24 | 236 | 318 | 75 | 30 |
| Mn | ppm | 412 | 396 | 1849 | 51212 | 4546 | 4170 | 4685 | 1704 |
| Sr | ppm | 191 | 1211 | 57 | 27 | 16 | 118 | 35 | 183 |
| Cd | ppm | 0.8 | 1.1 | 47.5 | 49.5 | 1104.2 | 758 | 2.4 | 1.9 |
| Bi | ppm | < 5 | < 5 | 5 | <5 | <5 | <5 | < 5 | < 5 |
| V | ppm | 20 | 103 | 38 | 98 | 49 | 49 | 338 | 170 |
| P | % | 0.05 | 0.11 | 0.29 | 0.13 | 0.10 | 0.08 | 0.29 | 0.52 |
| Ba | ppm | 263 | 13 | 124 | <10 | <10 | <10 | 12 | 230 |
| Zr | ppm | 43 | 31 | 54 | 12 | 18 | 13 | 35 | 29 |
| Sn | ppm | < 2 | < 2 | < 2 | <2 | <2 | <2 | < 2 | < 2 |
| Y | ppm | 23 | 16 | 10 | 13 | 7 | 8 | 15 | 22 |
| Nb | ppm | 21 | < 2 | 2 | 3 | 3 | 3 | 6 | 8 |
| Be | ppm | 1 | < 1 | < 1 | 1 | 1 | 1 | < 1 | < 1 |
| Hg | ppb | 10 | 15 | 15 | 80 | 5410 | 8135 | 10 | 10 |
| S | % | 0.7 | 3.74 | 10.11 | 0.68 | 12.62 | 8.32 | 10.5 | 4.51 |
| Se | ppm | ND | ND | 3 | 4 | 2.6 | 5 | 2.8 | 10.4 |
| Te | ppm | ND | ND | 0.3 | <0.1 | <0.1 | <0.1 | <0.1 | <0.1 |
| Au | ppb | <2 | <2 | 160 | 102 | 60 | 2 | 43 | 67 |
| Ag | ppm | <5 | <5 | <5 | 4.1 | 12.7 | 14.2 | <5 | <5 |
| As | ppm | 60 | 10 | 150 | 32 | 87 | 110 | 54 | 30 |
| Br | ppm | <0.5 | <0.5 | <0.5 | 0.25 | 0.5 | 0.6 | <0.5 | <0.5 |
| Co | ppm | 37 | 64 | 540 | 6 | 820 | 760 | 41 | 15 |
| Cr | ppm | 28 | 22 | 69 | 50 | 95 | 83 | 82 | 61 |
| Cs | ppm | 3 | <1 | 2 | <1 | <1 | <1 | <1 | <1 |
| Hf | ppm | 11 | 3 | 2 | <1 | <1 | <1 | <1 | <1 |
| Ir | ppb | <5 | <5 | <5 | <5 | <5 | <5 | <5 | <5 |
| Rb | ppm | 99 | <15 | <15 | <5 | <5 | <5 | <15 | 17 |
| Sb | ppm | 2.5 | <0.1 | 4.1 | 0.5 | 1.1 | 0.2 | 2.5 | 8.6 |
| Sc | ppm | 14 | 16 | 8.8 | 3 | 3.8 | 4.2 | 2.6 | 3.3 |
| Th | ppm | 14 | 3.5 | <0.2 | 0.5 | 0.2 | 1.5 | 1.4 | 1.4 |
| U | ppm | 3.9 | 1.8 | <0.5 | 6.1 | 0.7 | 7.8 | 41 | 38 |
| La | ppm | 51 | 32 | 8.4 | 6 | 5.4 | 8.3 | 7.6 | 18 |
| Ce | ppm | 98 | 59 | 13 | 8 | 10 | 14 | 14 | 24 |
| Nd | ppm | 40 | 24 | 9 | 7 | 8 | 2.5 | 11 | 10 |
| Sm | ppm | 6.9 | 5.4 | 1.3 | 1.2 | 0.7 | 0.8 | 1.8 | 2.5 |
| Eu | ppm | 1.4 | 1.6 | <0.2 | 0.5 | 0.5 | 0.4 | 0.8 | 1 |
| Tb | ppm | 1.4 | 0.9 | <0.5 | <0.5 | <0.5 | <0.5 | <0,5 | 0.7 |
| Yb | ppm | 5.2 | 3 | 0.9 | 1.1 | 0.1 | 0.1 | 1 | 1.6 |
| Lu | ppm | 0.76 | 0.4 | 0.16 | ND | ND | ND | 0.17 | 0.24 |
| F | ppm | 420 | 480 | 1500 | 380 | 400 | 330 | 1700 | 2200 |

Analytical methods:

Mo, Cu, Pb, Zn, Ni, Mn, Sr, Cd, Bi, V, P, Ba, Zr, Sn, Y, Nb and Be by mixed acid digest - ICP @ Acme Analytical Labs. Ltd., Vancouver, B.C.

Fluorine by specific ion electrode @ Actvation Labs. Ltd., @ Ancaster, Ontario.

Au, Ag, As, Br, Co, Cr, Cs, Hf, Ir, Rb, Sb, Sc, Th, U, La, Ce, Nd, Sm, Eu, Tb, Yb and Lu by thermal neutron activation @ Activation Labs. Ltd., Ancaster, Ontario.

Hg by cold vapour AAS and sulphur by Leco analyser @ Acme Analytical Labs. Ltd., Vancouver, B.C

Se and Te by flame AAS @ Chemex Labs Ltd., Vancouver, B.C.

ND = sample not analysed

contain anomalous quantities of zinc, cadmium, copper and cobalt; the two samples collected from the drill-road exposures east of Mineral Hill carry the highest silver values (up to 14 ppm). These samples are also strongly anomalous in mercury (5410 and 8135 ppb Hg) which is most unusual for skarn and suggests that the zinc mineralization is not related to the skarn-forming hydrothermal event.

The fourth type of mineralization occurs as disseminations, clusters and pods of coarse pyrite±pyrrhotite hosted by strongly deformed marbles. The sulphide pods seldom exceed 15 centimetres in diameter; they occasionally contain crystalline masses of a glassy, brilliant green mineral which x-ray defraction analysis indicates is diopside (M.A. Chaudhry, personal communication, 1995). Assays of two sulphide-rich samples collected from the marbles show no significant metal enrichment although anomalous quantities of fluorine are present (Table 5).

## GEOLOGICAL HISTORY OF THE AREA

Due to deformation and skarn alteration and the consequent lack of fossils, the precise age of the narrow unit of metasedimetary rocks along the Wormy Lake fault zone is unknown. A supracrustal succession assigned to the Lower to Middle Jurassic Bowen Island Group by Friedman *et al.* (1990) crops out immediately north of the mapped area, and on strike with the fault zone. However, this central part of the Sechelt Peninsula, north of the mapped area, also contains pendants of strongly foliated marble that have been correlated with the Upper Triassic Quatsino Formation (Roddick and Woodsworth, 1979). Thus, on the basis of lithology, the marbles and other skarn-altered metasediments along the Wormy Lake fault zone probably belong to the Quatsino Formation rather than Bowen Island Group.

At least three structural episodes have been recognised on the Sechelt Peninsula and in the surrounding Coast Range area (J.W.H. Monger, personal communication, 1995). These are:

1. A post-180 Ma, pre-155 Ma (Middle to Late Jurassic) event that affected the Bowen Island Group and older rocks, and produced isoclinal folding.
2. Extensional movements that accompanied the Early Cretaceous Gambier Group volcanism, and
3. An Early to Late Cretaceous contractional event that produced shear zones such as those near the Brittania massive sulphide deposit on Howe Sound.

This suggests that the structural and intrusive history of the Mineral Hill - Wormy Lake area includes the following five stages:

1. The Late Jurassic, syntectonic emplacement of the Crowston Lake pluton into Quatsino limestones, accompanied by development of the main garnet-wollastonite-pyroxene skarn assemblages at Mineral Hill and Wormy Lake. Deformation included tight folding with development of axial planar penetrative fabrics. Flattening was accompanied by boudinage of the gabbro sills, skarn and marble horizons, as well as sinistral ductile transcurrent movements along incompetent carbonate horizons within the Wormy Lake fault zone. This deformation probably coincided with the regionally developed post-180 Ma, pre-155 Ma structural event described by J.W.H. Monger (personal communication, 1995).
2. Syntectonic intrusion of the Snake Bay pluton which, like the Mineral Hill gabbro, is weakly foliated locally. It is uncertain whether the Snake Bay body was emplaced immediately after the Crowston Lake pluton, in which case the two intrusions may represent part of the same magmatic episode and therefore be related, or whether the two bodies are separated by a considerable time break.
3. Brittle, subhorizontal and dextral movement along the Wormy Lake fault.
4. Extensional tectonism producing easterly striking normal faults that are downthrown to the south. This faulting was accompanied by, and controlled, an early set of porphyritic tonalitic sills and dikes which were themselves fractured and partially altered to garnet-epidote endoskarn.
5. Continued extensional tectonism and easterly trending faulting coincided with the emplacement of narrow basaltic dikes.

The deformation continuing throughout stages 4 and 5 is probably correlative with Early Cretaceous extensional movements related to the Gambier Group. It is likely that the early tonalitic and later basaltic dikes are feeders for some of the Gambier volcanics which have presumably been removed by erosion in the Mineral Hill - Wormy Lake area.

## CONCLUSIONS

The following conclusions are drawn with respect to the Mineral Hill - Wormy Lake area:

1. Significant thicknesses of high-grade (>50%) wollastonite are present not only at Mineral Hill but also east and north of Wormy Lake where new wollastonite-rich outcrops were discovered.
2. The wollastonite-garnet-pyroxene skarns are concentrated in elongate and deformed roof pendants that probably represent altered calcareous sediments of the Triassic Quatsino Formation.
3. Massive to well layered mafic rocks in the area are interpreted to represent altered tuffs and volcanics of either the Triassic Karmutsen Formation or the Jurassic Bowen Island Group.
4. The skarn-altered roof pendants are partly controlled by the northwesterly trending Wormy Lake fault.
5. Slickenslides and offset measurements suggest that the Wormy Lake fault underwent an early period of ductile and sinistral movement. This was followed by brittle, dextral subhorizontal displacement, and later brittle vertical movements. Similar episodes of early sinistral and later dextral horizontal movements have

been recognized on Texada Island (Webster and Ray, 1990) and in the Yalakom River area (Schiarizza *et al.*, 1990).

6. Several generations of intrusive-related skarn are recognized. However, the dominant garnet-wollastonite skarn-forming event was related to the emplacement of the gabbroic Crowston Lake pluton and its coeval dike-sill swarm.

7. Major and minor element analyses indicate all the major and minor intrusions in the area are subalkaline and calcalkaline, and represent "volcanic arc" granitoids. They vary compositionally from gabbro to quartz diorite to tonalite to granodiorite.

8. Microprobe analyses on skarn assemblages indicate the presence of grossularitic garnets, diopsidic pyroxenes and wollastonites with a very low iron content (avg. 0.17% total iron as FeO).

9. The sulphide content of the skarns and intrusive rocks is generally low. Assay results indicate the area offers little gold or base metal potential. Minor quantities of sphalerite-bearing skarn have sporadically high mercury values (up to 8135 ppb Hg) which suggests that the sulphides are not related to a skarn hydrothermal system.

## ACKNOWLEDGMENTS

We thank Rudy Riepe, of Performance Minerals of Canada Ltd., for the help and hospitality he gave to us during this field project. Appreciation is also given to the management and staff of Tri-Sil Minerals Inc. Informative talks with J.W.H. Monger of the Geological Survey of Canada, D.V. Lefebure of the B.C. Geological Survey Branch, and with E. Fernandez were of great value. R.E. Lett and M.A. Chaudhry assisted with the geochemical samples, and the microprobe analyses were completed by S. Cornelius at the Geoanalytical Labs., Washington State University, Pullman, Washington. The paper was improved by the editing of J.M. Newell and B. Grant.

## REFERENCES

Debon, F. and Le Fort, P. (1983): A Chemical-Mineralogical Classification of Common Plutonic Rocks and Associations; *Royal Society of Edinburgh Transactions*, Earth Sciences, Volume 73 (for 1982), pages 135-149.

Deer, W.A., Howie, R.A. and Zussman, J. (1963): An Introduction to the Rock-forming Minerals; Volume 2, *Longman*, London, U.K., pages 167-175.

Fischl, P. (1991): Wollastonite and Tremolite Occurrences in British Columbia; *B.C. Ministry of Energy, Mines and Petroleum Resources*, Open File 1991-17 48 pages.

Friedman, R.M., Monger, J.W.H. and Tipper, H.W. (1990): Age of the Bowen Island Group, Southwestern Coast Mountains, British Columbia; *Canadian Journal of Earth Sciences*, Volume 27, pages 1456-1461.

Goldsmith, L.B. and Logan, J.M. (1987): Geological Mapping and Diamond Drilling of Wollastonite Occurrence, Mineral Hill Claim Group, Sechelt Area, British Columbia; unpublished report for *Tri-Sil Minerals Inc.*, 18 pages.

Goldsmith, L.B. and Kallock, P. (1988): Geological Mapping and Diamond Drilling of Wollastonite Occurrence, Mineral Hill Claim Group, Sechelt Area, British Columbia; unpublished report for *Tri-Sil Minerals Inc.*, 25 pages.

Pearce, J.A., Harris, N.B.W. and Tindle, A.G (1984): Trace Element Discrimination Diagrams for the Tectonic Interpretation of Granitic Rocks; *Journal of Petrology*, Volume 25, pages 956-983.

Matsueda, H. (1973): Iron-Wollastonite from the Sampo Mine Showing Properties Distinct from those of Wollastonite. *Mineralogical Journal*, Volume 7, Number 2, p. 180-201.

Price, R.A., Monger, J.W.H. and Roddick, J.A. (1985): Cordilleran Cross-section, Calgary to Vancouver; *in* Field Guides to Geology and Mineral Deposits in the Southern Canadian Cordillera, *Geological Association of Canada*, Cordilleran Section Meeting, pages 3-1 to 3-85.

Ray, G.E. and Kilby, C.E. (1995): Geology of the Mineral Hill - Wormy Lake Skarns, B.C. (92G/12W); *B.C. Ministry of Energy, Mines and Petroleum Resources*, Open File 1996-6, 1:10 000 scale.

Roddick, J.A. (1970): Douglas Channel - Hecate Strait Map Area, British Columbia; *Geological Survey of Canada*, Paper 70-41.

Roddick, J.A. (1979): Vancouver West Half; *Geological Survey of Canada*, Open File 611.

Roddick, J.A. (1983): Geophysical Review and Composition of the Coast Plutonic Complex, South of Latitude 55° N; *Geological Association of America*, Memoir 159, pages 195-211.

Roddick, J.A. and Woodsworth, G.J. (1979): Geology of Vancouver, West Half, and Mainland Parts of Alberni; *Geological Survey of Canada*, Open File 511.

Schiarizza, P., Gaba, R.G., Coleman, M., Garver, J.I. and Glover, J.K. (1990): Geology and Mineral Occurrences of the Yalakom River Area (92O/1, 2 92J/15,16); in Geological Fieldwork 1989, *B.C. Ministry of Energy, Mines and Petroleum Resources*, Paper 1990-1, pages 53-72.

Webster, I.C.L. and Ray, G.E. (1990): Geology and Mineral Deposits of Northern Texada Island (92F/9, 10, and 15); *in* Geological Fieldwork 1989, *B.C. Ministry of Energy, Mines and Petroleum Resources*, , Paper 1990-1, pages 257-265.

White, G.V. (1989): Wollastonite Occurrences in British Columbia; *in* Geological Fieldwork 1988, *B.C. Ministry of Energy, Mines and Petroleum Resources*, Paper 1989-1, pages 489-496.

NOTES

# ZIPPA MOUNTAIN WOLLASTONITE SKARNS, ISKUT RIVER MAP AREA (104B/11)

By Bart J. Jaworski and Gregory M. Dipple
The University of British Columbia

*KEYWORDS*: Economic geology, wollastonite, skarn, Iskut River, contact metamorphism.

## INTRODUCTION

Skarns associated with the Zippa Mountain Igneous Complex of the Iskut River area are unusual for their high wollastonite contents. They are the focus of British Columbia's only active wollastonite exploration venture. Wollastonite is increasingly sought as an industrial mineral for the ceramics, paint, steel and automobile industries. Much recent demand stems from its utility as a replacement for asbestos and as a strength additive in industrial plastics. This report summarizes results of recent mapping of two wollastonite skarn deposits on the east flank of the syenitic Zippa Mountain pluton. We argue that the skarns resulted from extensive fluid infiltration into marble xenoliths in the pyroxenite border phase of the intrusion. The final stages of infiltration and skarn formation postdate the incorporation of the xenoliths into the intrusion. The apparent lack of wollastonite skarn around the other two intrusive phases of the Zippa Mountain Igneous Complex may stem from their lower heat contents.

## ZIPPA MOUNTAIN IGNEOUS COMPLEX AND ASSOCIATED ROCKS

The Zippa Mountain Igneous Complex is located in the Iskut River map area of northwest British Columbia (inset in Figure 1), 5 kilometres south of the Iskut River and 32 kilometres upstream from its confluence with the Stikine River. It is composed of three Late Triassic intrusions, the Zippa Mountain, Mount Raven and Seraphim Mountain plutons, closely associated in space and time (Figure 1).

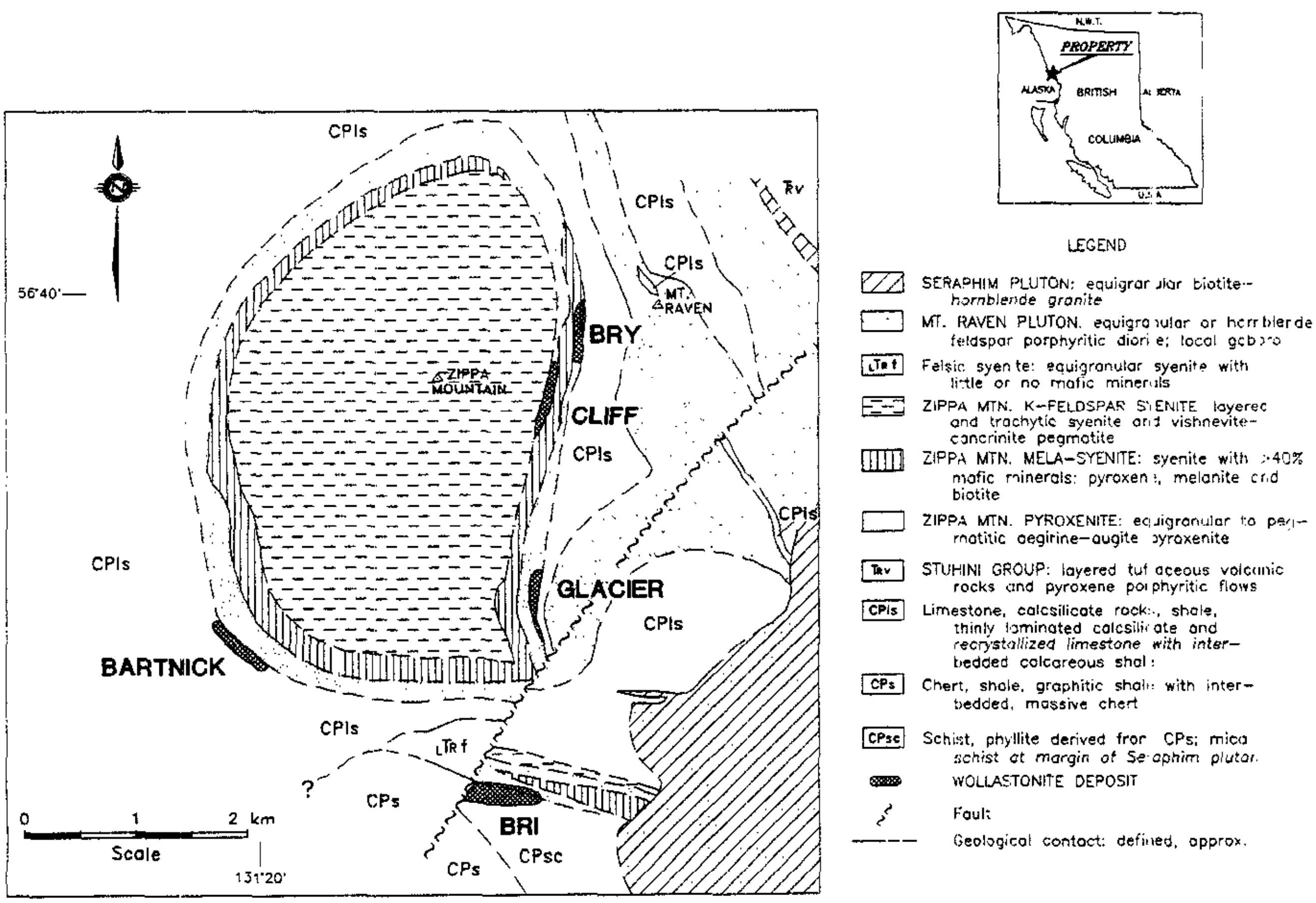


Fig. 1. Geology of the Zippa Mountain pluton and wollastonite skarns, after Lueck and Russell (1994).

The complex intrudes Paleozoic metasediments of the Stikine assemblage and Triassic volcanics of the Stuhini Group (Lueck and Russell, 1994). The Paleozoic strata are intensely folded, faulted and metamorphosed and display isoclinal, overturned and recumbent folds (Anderson, 1989). Regional metamorphic grade in the vicinity of Zippa Mountain is lower greenschist (Anderson, 1989).

The three plutons of the Zippa Mountain complex exhibit a diversity of chemical compositions despite their close spatial and temporal association. The following description of the complex derives from Lueck and Russell (1994). The Zippa Mountain pluton is a 3.5 by 5 kilometre elliptical laccolith consisting of a syenite core with border phases of mela-syenite and pyroxenite. The pluton is alkaline and strongly silica-undersaturated and is characterized by well developed planar mineral fabrics. The Mount Raven pluton is a fine-grained, equigranular hornblende diorite. It outcrops immediately east of the Zippa Mountain pluton and is characterized by the presence of pervasive gossan derived from the weathering of abundant pyrite. The Seraphim Mountain pluton is exposed southeast of the Mount Raven pluton and is a homogenous, equigranular hornblende biotite granite. Field relationships indicate that the Zippa Mountain pluton is the oldest of the three intrusions and the Seraphim Mountain pluton is the youngest. However, the earliest phases of the Mount Raven pluton predate the latest phases of the Zippa Mountain pluton. The close temporal relationship of the three plutons is also indicated by radiometric dating: an age of approximately 210 Ma is recorded by U-Pb in zircon from the Zippa Mountain pluton (M.L. Bevier, unpublished data cited in Lueck and Russell, 1994; Anderson *et al.*, 1993) and 213 ±4 Ma is recorded by K-Ar in hornblende from the Seraphim Mountain pluton (analysis GSC 90-40; R.G. Anderson in Hunt and Roddick, 1991).

Although all three plutons intrude limestone (the probable host of the skarns, Figure 1), the wollastonite skarns are restricted to the margins of the Zippa Mountain pluton. Five wollastonite localities have been identified to date. Two of these, the Cliff and Glacier deposits, were the focus of investigation during the 1995 field season; both lie within the pyroxenite border phase of the Zippa Mountain pluton. The Cliff deposit outcrops on the east margin of the pluton as a prominent west-facing, white cliff about 160 metres long and 100 metres high. The Glacier deposit is located approximately 1.6 kilometres south of the Cliff deposit and outcrops on a north-facing slope as a 300 by 50 metre exposure.

Igneous and metamorphic rocks are displaced by a fault which trends northeast and extends over 8 kilometres within the wollastonite property (Figure 1). This fault is significant because it truncates the southeast corner of the Zippa Mountain pluton and may offset wollastonite occurrences in that area.

## WOLLASTONITE SKARN LOCALITIES

The Glacier and Cliff wollastonite occurrences are both composed of metasedimentary and skarn rocks enclosed in pyroxenite of the Zippa Mountain pluton. The two showings are lithologically similar and both appear to have formed by incorporation of marble and calcsilicate into pyroxenite. They differ, however, in that the Cliff occurrence consists of a single large screen while the Glacier outcrop contains many xenoliths that are highly dissected by pyroxenite dikes, veins and dikelets. Detailed maps of the Cliff and Glacier deposits are presented in Figures 2 and 3. The map units are described below.

## *IGNEOUS ROCKS*

### PYROXENITE

The pyroxenite border phase of the Zippa Mountain pluton weathers dark green and consists of fine-grained, dark green aegirine-augite (90%) and interstitial apatite (10%) with trace amounts of euhedral titanite and biotite (Lueck and Russell, 1994). Biotite usually occurs as millimetre-scale mica books within an aegirine-augite groundmass, and less commonly, as inclusions within poikilolitic pyroxene. Within the Glacier deposit, a biotite-rich pyroxenite unit can be mapped as a discrete irregular zone within the pyroxenite (Figure 2). It consists largely of biotite and pyroxene with minor amounts of interstitial potassium feldspar. Numerous pyroxenite dikes and dikelets, as narrow as 1 centimetre, cut virtually all skarn and metasedimentary units at the Glacier locality.

### DIORITE

A diorite porphyry dike, 15 metres wide, crosscuts the skarn and Zippa Mountain plutonic phases in the Glacier deposit. It contains between 15 and 25% plagioclase phenocrysts up to 4 millimetres in diameter, set in an aphanitic groundmass. The phenocrysts and groundmass are strongly altered. The main phase of the dike weathers brown to orange and is represented by the rusty diorite unit on Figure 2. The origin of the diorite dike is uncertain, but it may be related to the Mount Raven pluton.

## *METASEDIMENTS*

### CALCSILICATE

Fine-grained green calcsilicate contains diopside and grossular garnet with varying amounts of biotite, melanite garnet, potassium feldspar and wollastonite. Grossular is concentrated in layers and pods 2 to 5 centimetres thick. These layers may be veins or sedimentary features. Biotite occurs within subparallel layers 0.5 to 4 millimetres thick and in pockets. The thin, parallel nature of these biotite layers suggests that they represent argillaceous beds within the original sediment.

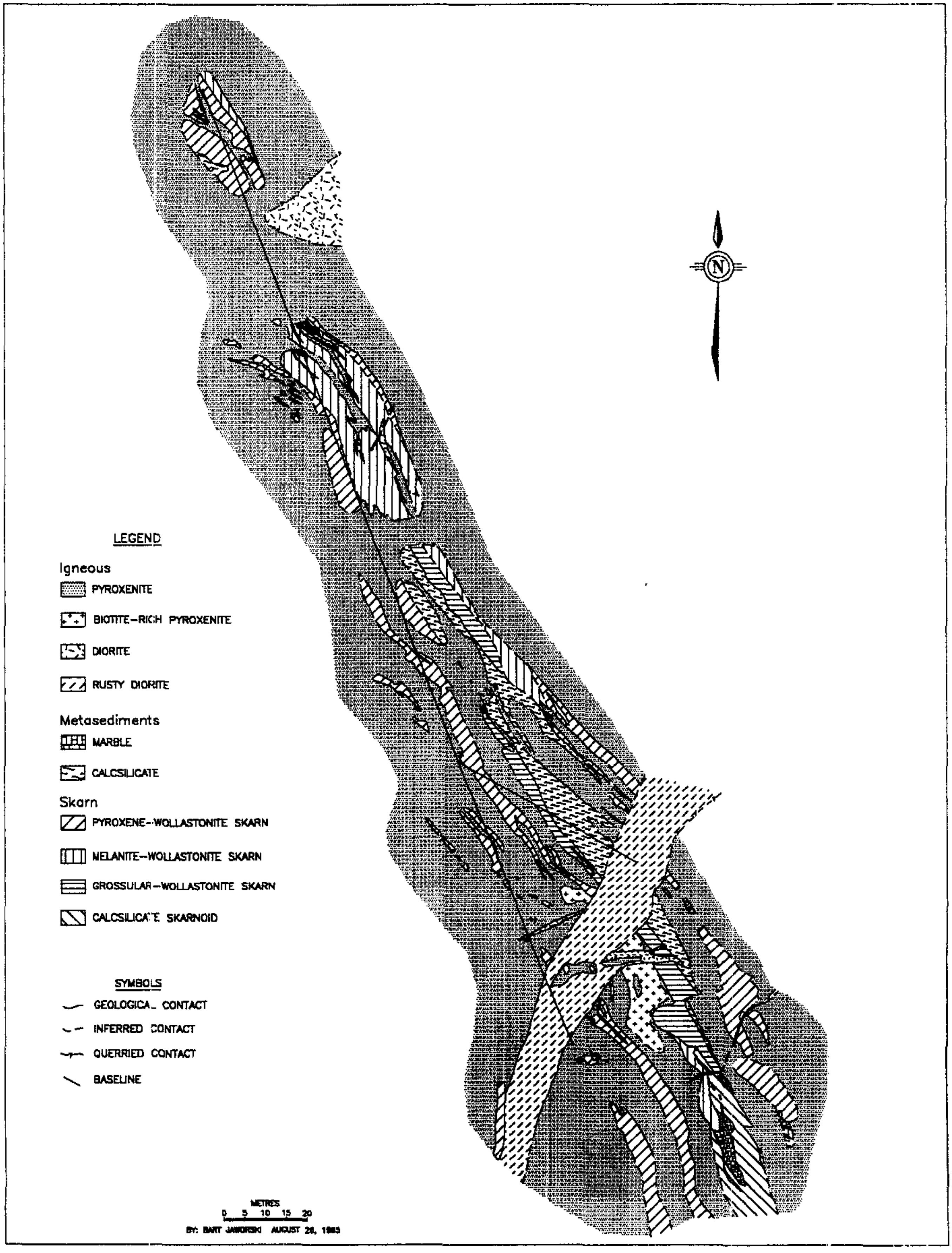


Fig. 2. Detailed geology of the Glacier wollastonite deposit.

### MARBLE

Light green to grey marble outcrops in the southeastern end of the Glacier deposit. It is composed predominantly of recrystallized calcite, 1 to 2 millimetres in diameter, and probably represents a clean limestone protolith that was unreactive during metamorphism. It is locally characterized by millimetre-scale dark green laminations that probably contain fine-grained diopside.

## *WOLLASTONITE SKARN UNITS*

Five map units are identified within the wollastonite skarn of the Cliff and Glacier localities, on the basis of texture and the relative abundances of accessory minerals. All units except the calcsilicate skarnoid contain between 50 and 95% wollastonite by volume. Pyroxene, melanite, and grossular-wollastonite skarn units are defined by the relative abundances of pyroxene, melanite garnet and grossular garnet. Two texturally distinct units were further distinguished in the field, based on grain size: the coarse wollastonite unit and the fine-grained calcsilicate skarnoid. The average grain size of skarn minerals is about 3 millimetres, but varies considerably between less than a millimetre in the calcsilicate skarnoid to 4 centimetres in the coarse wollastonite skarn.

### PYROXENE-WOLLASTONITE SKARN

Light grey to cream-weathering pyroxene wollastonite skarn is the most abundant skarn unit in the Cliff and the Glacier localities. It contains abundant pyroxene (up to 45 volume % and on average 10%) with no visible garnet. Pyroxene occurs as fine-grained disseminated diopside within the wollastonite matrix and as wispy, light green layers of diopside. The fine, parallel-laminated nature of these layers and their consistent orientation, suggests they may reflect bedding within a protolith limestone such as is observed in the marble described above. The pyroxene-

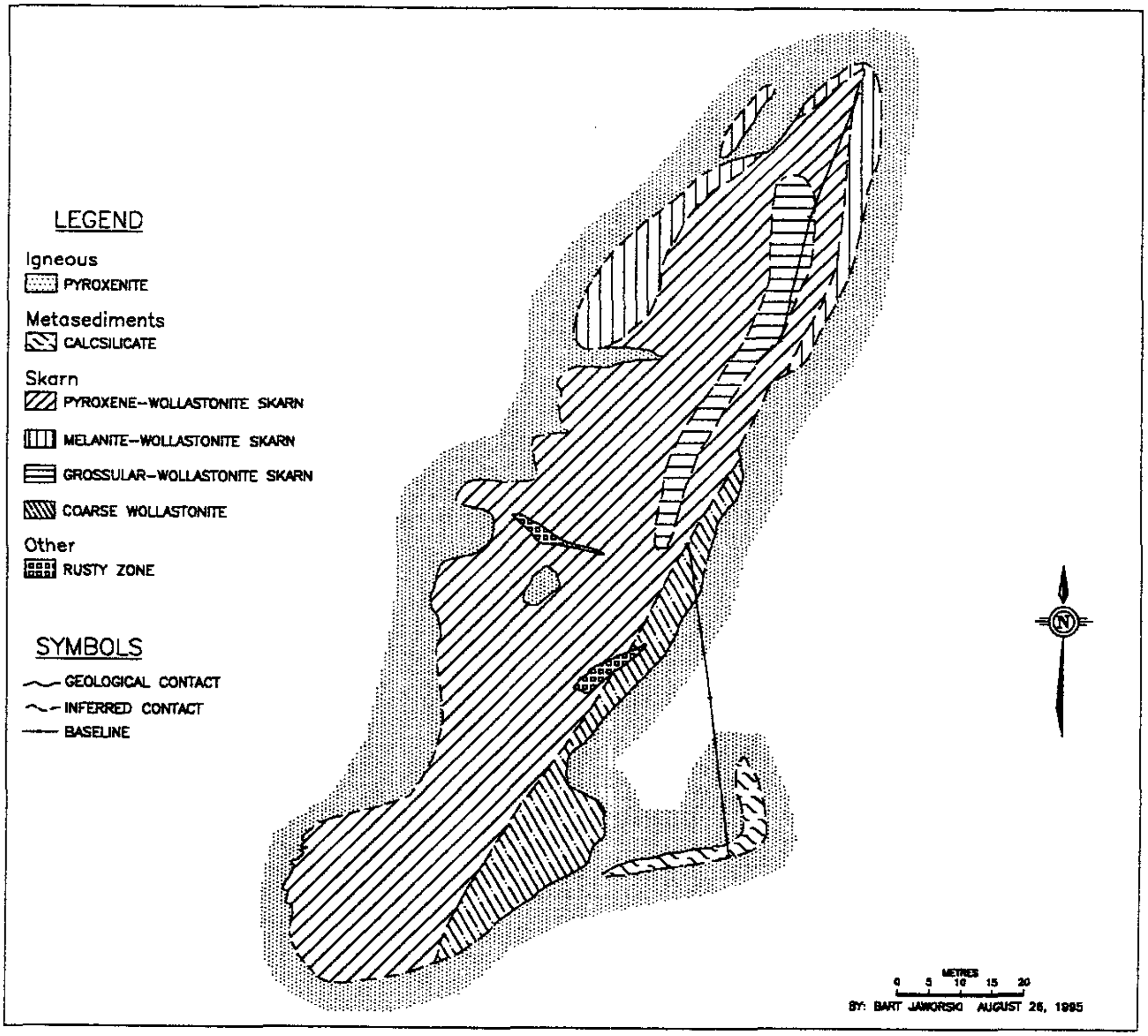


Fig. 3. Detailed geology of the Cliff wollastonite deposit.

wollastonite skarn is commonly dissected by pyroxenite dikelets. In places it becomes difficult to distinguish between diopside stringers of probable sedimentary origin and pyroxenite dikelets of igneous origin.

### MELANITE-WOLLASTONITE SKARN

Melanite-wollastonite skarn contains up to 20% black, fine to coarse-grained melanite garnet, with or without pyroxene. Typical skarn contains about 10% melanite, 3% pyroxene and 87% wollastonite. Locally, pyroxene abundance approaches 15%. Preferential weathering of wollastonite gives the rock a warty, light to dark grey appearance. Melanite garnet occurs as disseminated crystals within the wollastonite and as irregular millimetre-scale stringers. The skarn is locally brecciated; fragments of melanite-poor skarn are surrounded by wollastonite containing abundant disseminated melanite. Melanite commonly contains microscopic inclusions of calcite and diopside.

### GROSSULAR-WOLLASTONITE SKARN

This cream to pink-weathering unit is characterized by the presence of 5 to 10% grossular garnet in a wollastonite matrix and the absence of pyroxene. Grossular occurs in centimetre-scale layers and disseminated throughout. It locally contains up to 15% melanite.

### COARSE WOLLASTONITE SKARN

Massive, white outcrops of coarse wollastonite skarn consist predominantly of coarse-grained, randomly oriented wollastonite. The rock typically contains less than 5% of the accessory phases pyroxene, grossular and/or melanite. Titanite is locally present in haloes around potassium feldspar veins.

### CALCSILICATE SKARNOID

A greenish white, fine-grained unit that outcrops at the south end of the Glacier deposit is distinguished from other skarn units by its fine grain size and from calcsilicate metasediment by its skarn mineralogy. Thin section examination reveals that it contains 5 to 10% coarse melanitic garnet in a fine-grained matrix of potassium feldspar, garnet (andradite?) and apatite, with or without diopside and wollastonite. Apatite is locally abundant, up to 20%. Calcite is common but appears to be related to fracturing and retrograde alteration.

## *VEINS*

Metasediments, wollastonite skarn and pyroxenite are cut by several generations of veins that cannot be depicted at map scale. The oldest veins appear to be associated with latest stages of crystallization of the pyroxenite while the youngest veins crosscut all lithologies. They are described below in chronological order, as determined from crosscutting relationships.

### POTASSIUM FELDSPAR VEINS

Irregular, centimetre-scale potassium feldspar veins cut metasediments and wollastonite skarn. They commonly contain euhedral, medium to coarse-grained titanite, melanite and pyroxene, with minor amounts of apatite (5%); however, they are highly variable and are locally composed of pure potassium feldspar. Melanite locally displays oscillatory zoning that overgrows cores of grossular garnet. These veins are crosscut by melanite-apatite veins.

### MELANITE-APATITE VEINS

Melanite-garnet commonly occurs with apatite and less commonly with pyroxene in centimetre-scale irregular veins. Melanite is usually medium to coarse-grained and is surrounded by fine-grained apatite. These veins commonly cut skarn and calcsilicate, and usually occur within cores of pyroxenite dikes or spatially associated with pyroxenite.

### QUARTZ AND CALCITE VEINS

Two sets of randomly oriented, monomineralic veins, one containing calcite, the other quartz, cut metasedimentary, igneous, and skarn units. The planar veins are 0.5 to 3.5 centimetres wide. Their relative age is unknown because crosscutting relationships between the two vein sets were not observed.

## ZONING

Despite the complex pattern of skarn types in the two deposits, there is a consistent zoning in skarn mineralogy between outcrops and at different scales. Map-scale zonation (tens of metres) is generally parallel to the long dimension of the xenoliths, and may reflect control of alteration and/or fluid flow by sedimentary composition (Figures 2 and 3). Both deposits are cored by grossular-wollastonite skarn, and pyroxene-wollastonite skarn is generally found surrounding this core. At the Glacier deposit, pyroxenite-wollastonite skarn lies along the edges of many of the largest xenoliths and occurs as trains of isolated xenoliths on the margins of the deposit. Most of the screen at the Cliff deposit is composed of pyroxene-wollastonite skarn which completely surrounds the grossular-wollastonite unit. However, some zoning appears to crosscut lithologic boundaries. For example, melanite-wollastonite skarn wraps around the north end of the Cliff deposit (Figure 3) although there is no evidence for isoclinal folding within the screen. Individual xenoliths are also rimmed by melanite-rich zones that appear, at least in part, to be replacements (Photo 1). The complex skarn zoning in the Glacier deposit also suggests that it is not entirely controlled by sedimentary lithology. In the centre of the deposit, grossular and melanite-wollastonite skarn are truncated by calcsilicate. Similarly, the complex zoning of marble, calcsilicate skarnoid and grossular and melanite-wollastonite skarn at the south end of the Glacier deposit is probably controlled, in part, by infiltration. This is corroborated by field observations that skarn zonation cuts across bedding inferred from centimetre-scale laminations.

## PROCESSES OF SKARN FORMATION

Our observations suggest that the wollastonite skarns formed by fluid infiltration into carbonate xenoliths in the margin of the Zippa Mountain pluton. The close spatial association of skarn and pluton, and the similarities between skarn and igneous mineral assemblages, suggest that the infiltrating fluids derived from the pluton. However, the sedimentary composition of xenoliths undoubtedly influenced skarn formation. Below we list the evidence for infiltration and lithologic control of skarn formation and briefly discuss the relative timing of skarn-forming processes.

Perhaps the most striking evidence for an infiltration origin for the wollastonite skarn is the exceptional wollastonite purity. Most skarn contains greater than 70% wollastonite by volume and no calcite or quartz. Without fluid infiltration, formation of wollastonite from calcite marble by the reaction calcite + quartz -> wollastonite + $CO_2$ is limited by quartz content. Thermally driven wollastonite formation should therefore produce calcite-wollastonite marbles with generally low wollastonite abundances. The presence of almost pure wollastonite skarn requires either that the protolith was a 1:1 molar mixture of calcite and quartz, or that some chemical components were introduced into the skarn by fluid infiltration. The purity of wollastonite and general lack of calcite at Zippa Mountain suggests that skarn formation resulted, at least in part, from reaction of calcite with metasomatically introduced $SiO_2$ to produce wollastonite.

An infiltration origin for the skarns is also supported by the zonation and overprinting relationships of melanite-bearing skarns. At the north end of the Cliff deposit, melanite-wollastonite skarn wraps around the screen. Melanite-rich alteration is also observed around individual small xenoliths at the Glacier deposit (Photo 1). Melanite-wollastonite skarn at the south end of the Glacier deposit appears to grade into marble and/or grossular-wollastonite skarn. Overprinting relationships also support a replacement origin for melanite: individual melanite crystals are cored by diopside or grossular.

There is also significant evidence for some lithologic control of skarn formation. Skarn zoning at the two deposits is generally elongate parallel to bedding and the long axes of the xenoliths. For example, the distribution of coarse wollastonite skarn at the Cliff deposit may be controlled by the original extent of a very pure calcite marble. Similarly, the distribution of calcsilicate, calcsilicate skarnoid, grossular-wollastonite skarn, and melanite-wollastonite skarn at the Glacier deposit may reflect original sedimentary features. Together they define a continuous band that strikes north-northwest across the entire deposit. The complex zoning in the Glacier deposit probably resulted from local control by heterogeneous metasediments on fluid flow and resulting metasomatism.

Both wollastonite skarn deposits examined to date at Zippa Mountain are contained in xenoliths of carbonate

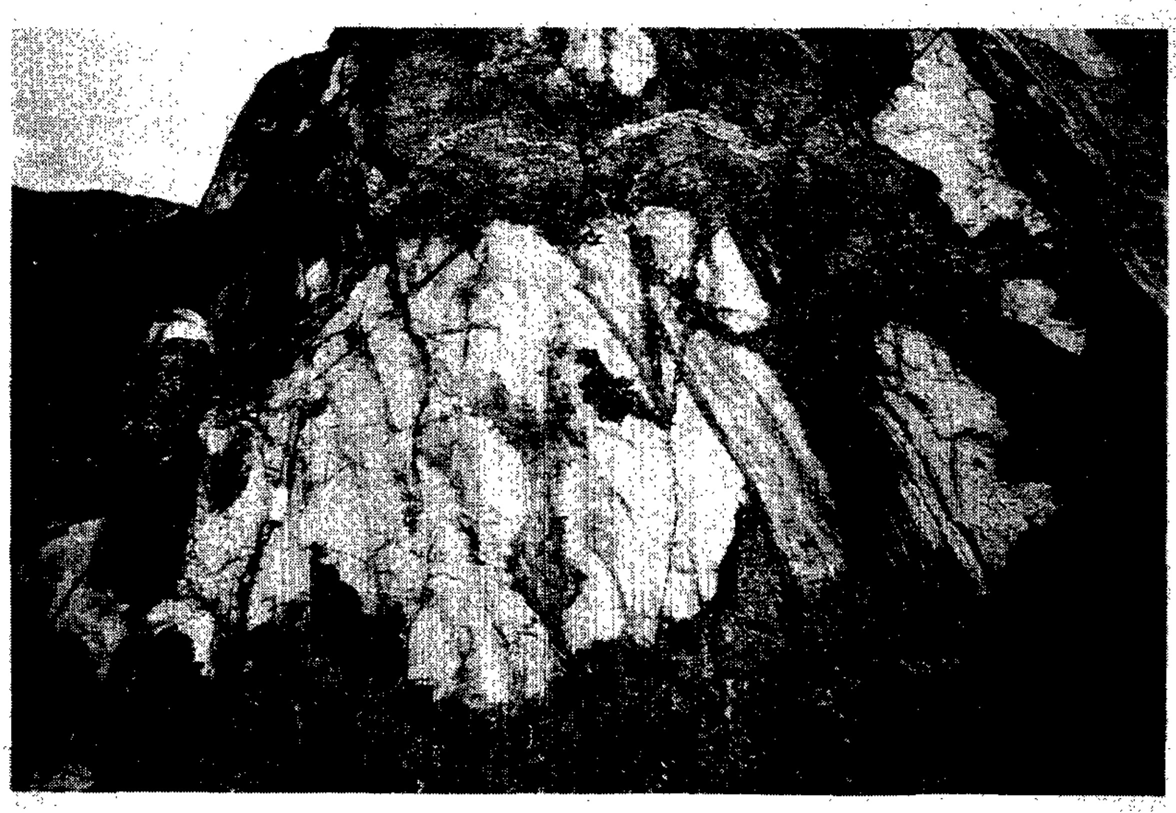

Photo 1. Outcrop of wollastonite skarn xenoliths in the Glacier deposit. Pencil flare for scale; view is to the east. Note the dark rinds of melanite alteration ringing the xenoliths and melanite alteration along fractures in the large xenolith.

metasediments within the pyroxenite border phase of the pluton. It is likely that at least some fluid infiltration postdated the incorporation of xenoliths into the pluton. Complete enclosure of xenoliths by melanite alteration requires that the alteration postdate dismembering of the sedimentary rocks (Photo 1). The large-scale zonation of melanite-wollastonite skarn at the Cliff deposit also suggests that skarn formation postdated incorporation of the screen into the pluton. Xenoliths continued to disintegrate after incorporation, as evidenced by fracture-related melanite alteration in the interior of the xenolith pictured in Photo 1. In fact, the lack of concentric zoning in xenoliths at the Glacier deposit probably resulted from continued fracturing, diking, and assimilation.

## IMPLICATIONS

Wollastonite skarns have not been found associated with the Mount Raven and Seraphim Mountain plutons. Identification of the factors critical to skarn formation at Zippa Mountain therefore may aid future exploration for wollastonite in British Columbia. Wollastonite skarn formation requires: a calcite-rich protolith and a high $SiO_2$ content (either inherited from the protolith or introduced by fluid infiltration), and one or both of high temperature and low $CO_2$ activity (*e.g.*, Greenwood, 1967). Wollastonite can form at low temperatures if the $CO_2$ activity is very low, or at high $CO_2$ activities if the temperature is very high. All three plutons of the Zippa Mountain igneous complex meet the first two criteria. They intrude limestones and probably exsolved silica-bearing aqueous fluids. The Mount Raven and Seraphim Mountain plutons contain magmatic biotite and/or hornblende and are quartz normative. The Zippa Mountain pluton contains magmatic biotite and is silica undersaturated (Lueck and Russell, 1994). Despite this, fluids from the Zippa Mountain pluton carried sufficient dissolved silica to drive wollastonite skarn formation. However, syenite and pyroxenite of the Zippa Mountain pluton were probably emplaced at higher temperatures than granite and diorite of the other plutons. Incorporation of marble xenoliths into the margin of the intrusion would also raise their temperature relative to intact wallrocks outside the intrusion. A critical factor for wollastonite skarn formation at Zippa Mountain may have been the unusually high temperatures resulting from emplacement of syenite coupled with the incorporation of marble xenoliths into the pyroxenite border phase.

## ACKNOWLEDGMENTS

This project was funded by grants from Super Twins Resources Ltd. of Vancouver and the Geological Survey Branch of the British Columbia Ministry of Energy, Mines and Petroleum Resources. We thank Brian Lueck for introducing us to the Zippa Mountain skarns. Some of our samples were collected during a bulk sampling program organized by Bryan Slim and implemented by Tim Bissett and Craig Lynes. Constructive comments by John Newell are appreciated.

## REFERENCES

Anderson, R.G. (1989): A Stratigraphic, Plutonic, and Structural Framework for the Iskut River Map Area, Northwestern British Columbia; *in* Current Research, Part E, *Geological Survey of Canada*, Paper 89-1E, pages 145-154.

Anderson, R.G., Bevier, M.L., Nadaraju, G., Lewis, P. and MacDonald, J. (1993): Jurassic Arc Setting for Stikinia's "Golden Triangle" (abstract); *Geological Association of Canada - Mineralogical Association of Canada*, Program with Abstracts, Volume 18, page A3.

Greenwood, H.J. (1967): Wollastonite: Stability in $H_2O$-$CO_2$ Mixtures and Occurrence in a Contact-metamorphic Aureole near Salmo, British Columbia, Canada; *American Mineralogist*, Volume 52, pages 1669-1680.

Hunt, P.A. and Roddick, J.C. (1991): A Compilation of K-Ar Ages: Report 20; *in* Radiogenic Age and Isotopic Studies: Report 4; *Geological Survey of Canada*, Paper 90-2, page 122.

Lueck, B.A. and Russell, J.K. (1994): Geology and Origins of the Zippa Mountain Igneous Complex with Emphasis on the Zippa Mountain Pluton, Northwestern British Columbia; *in* Current Research 1994-A; *Geological Survey of Canada*, pages 77-85.

NOTES

British Columbia Geological Survey
Geological Fieldwork 1995

# KYANITE AT PRINCE RUPERT AND KITIMAT (103H, J)

By K.D. Hancock and G.J. Simandl

*KEYWORDS:* Industrial minerals, kyanite, staurolite, garnet, high-alumina amphibolite, refractory minerals, Prince Rupert, Dudevoir Passage, Trail Bay, Hawkesbury Island, Coast Belt.

## INTRODUCTION

There are more than 45 kyanite occurrences reported in British Columbia (Figure 1). They are generally restricted to high-alumina, high-grade metasedimentary rocks in the Coast and Omineca tectonic belts. Two small occurrences near the coast were examined as part of a reconnaissance program for refractory minerals in the province.

Kyanite is the high-pressure polymorph of the aluminosilicate, $Al_2SiO_5$. Sister polymorphs are andalusite and sillimanite. When calcined these minerals are converted to mullite, a highly refractory material. Kyanite converts to mullite at 1370°C and the conversion is accompanied by a nonreversible volume expansion of 18% (Skillen, 1993). Because of the significant volume change, calcination is often required before manufacturing refractory shapes. Kyanite is used primarily in refractories, about half for steel making, a quarter for nonferrous metals processing and the rest in glassmaking and ceramics. In North America, kyanite is the most widely used $Al_2SiO_5$ polymorph, because it is abundant, found close to markets and relatively

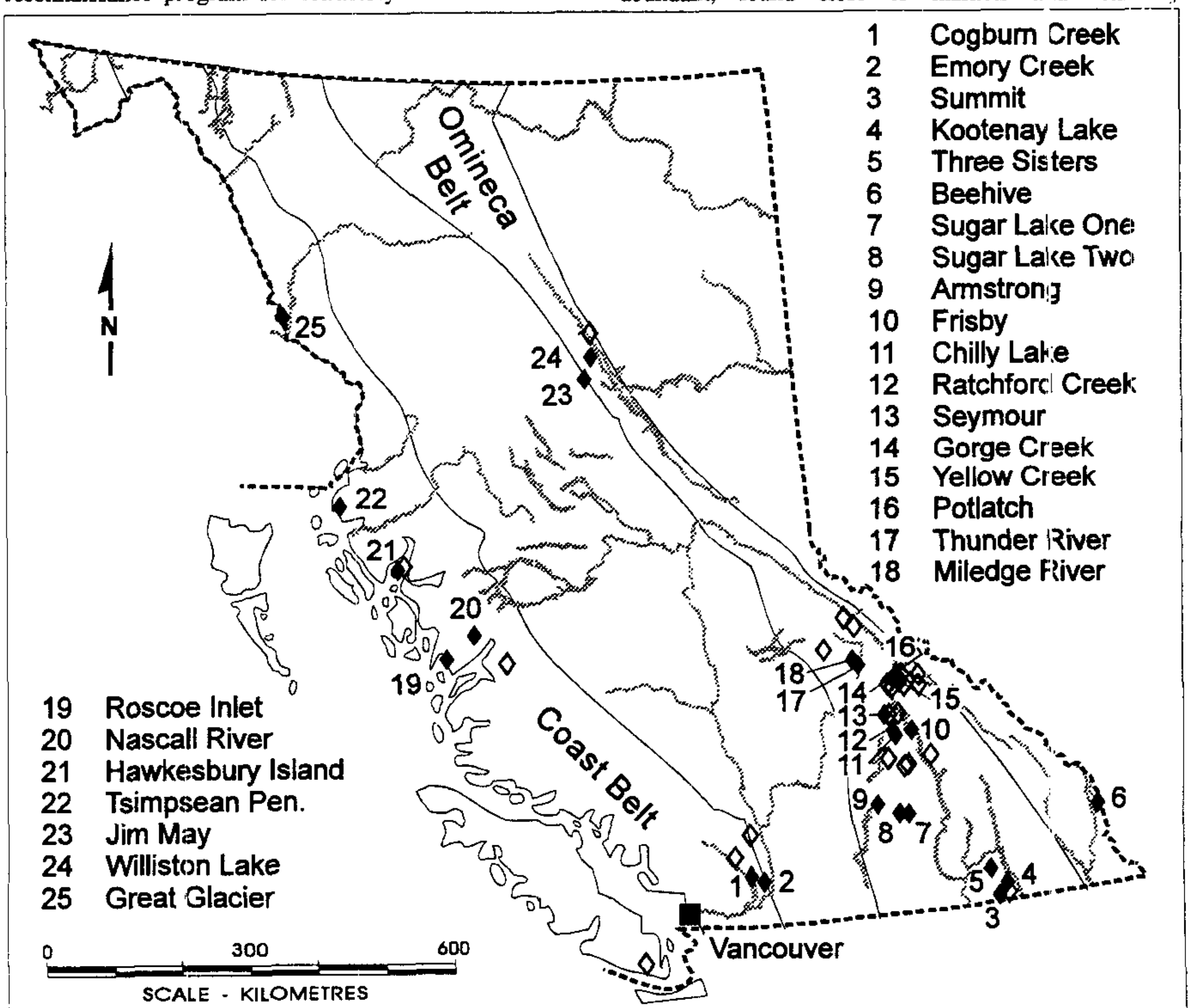


Figure 1: Location of significant kyanite occurrences in British Columbia. Major showings are named.

inexpensive energy is available. In British Columbia, a deposit with an acceptable product, located near tidewater and natural gas service, would have commercial potential. Previous work on andalusite occurrences is reported by Simandl *et al.* (1995).

At the time of writing (November, 1995), United States kyanite prices are US$116-146 for raw kyanite and US$210-240 for calcined product, both with 54 to 60% $Al_2O_3$ in 18-ton lots, ex-plant (Industrial Minerals, Number 337, October, 1995). The sizes of typical US kyanite products are 35, 48, 100, 200 and 325 mesh. Concentrates are about 91% kyanite, less than 1% iron oxides and the rest quartz (Sweet, 1994). The composition of this product is listed in Table 1.

**TABLE 1: COMPOSITION OF TYPICAL US KYANITE PRODUCT (SWEET, 1994)**

| | |
|---|---|
| $Al_2O_3$ | 54 to 60.06% |
| $SiO_2$ | 37.64 to 43.70% |
| $Fe_2O_3$ | 0.40 to 1.16% |
| $TiO_2$ | 0.67% |

## LOCATION

During 1995, kyanite occurrences were examined at Dudevoir Passage and Trail Bay, 36 and 31 kilometres respectively, north of Prince Rupert on Tsimpsean Peninsula, and at the central height of land on Hawkesbury Island, 40 kilometres south of Kitimat. Access to the showings is by boat and helicopter, respectively.

An important note is that occurrences on Hawkesbury Island are at the southern limit of the Foch-Miskatla-Kitsaway protected area, which is currently under review. Part of the described showings are within a no-staking reserve but the kyanite zones extend downslope, to the east and away from the protected area. The authors' objective was to characterize and describe high-grade metamorphic kyanite occurrences in the Coast Belt.

## DUDEVOIR PASSAGE AND TRAIL BAY

### *GEOLOGICAL SETTING*

The Dudevoir Passage and Trail Bay kyanite

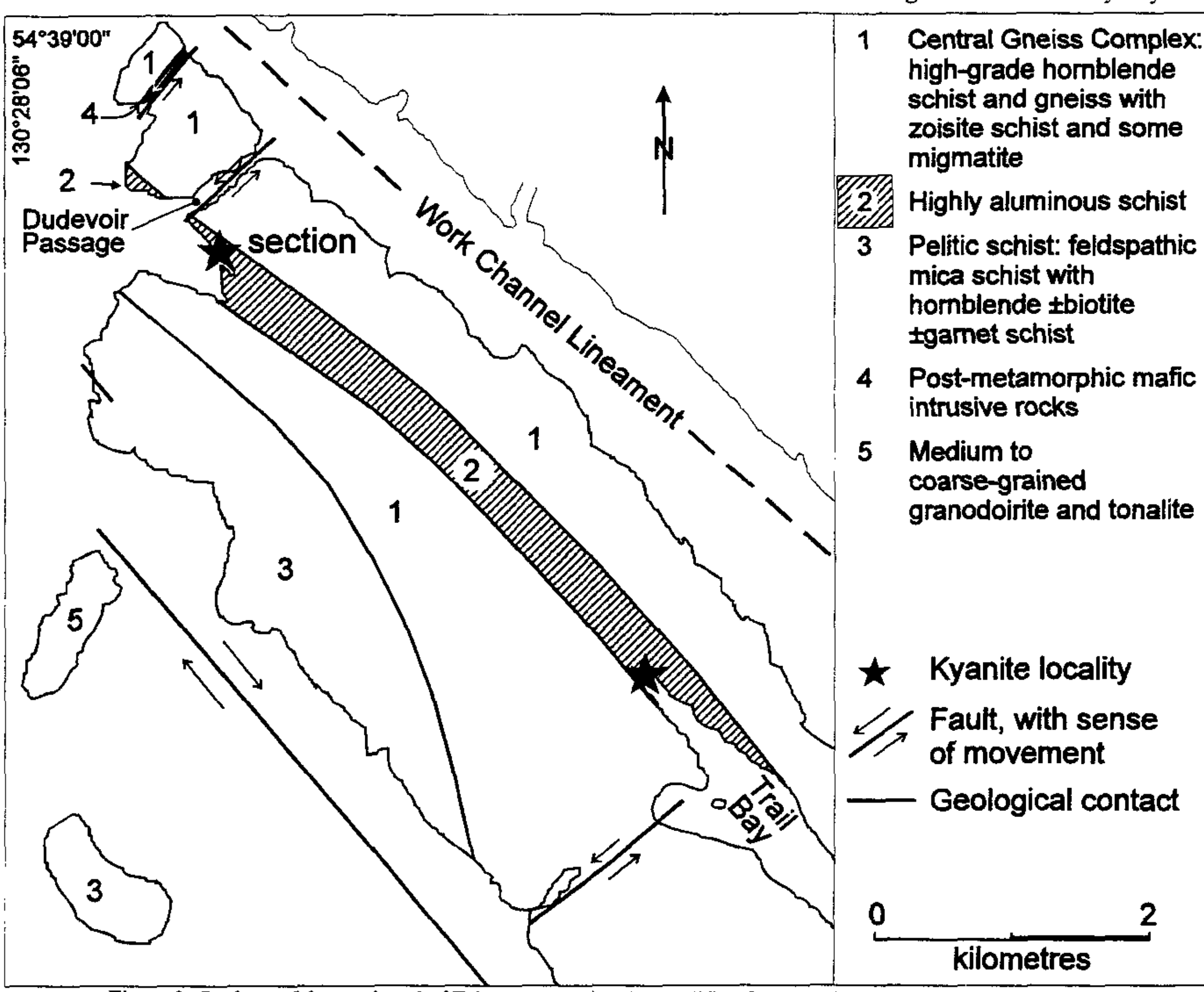


Figure 2: Geology of the north end of Tsimpsean Peninsula (modified from Snyder, 1980 and Hutchison, 1982)

occurrences are on the Tsimpsean Peninsula within the Coast Belt. The geology of the area is summarized from Hutchison (1982) and Snyder (1980). Two regional-scale units and two intrusive rock types are mapped in the area: high-grade hornblende schist and gneiss, pelitic schist, weakly metamorphosed mafic intrusions and granodiorite (Figure 2).

The high-grade hornblende schist and gneiss, with zoisite schist and some migmatite, are part of Hutchison's Central Gneiss Complex.

The amphibolite-grade pelitic schist is predominantly calcareous with some feldspathic mica schist, dark greenish grey hornblende±biotite±garnet schist, and some interlayers of metabasite. A strongly aluminous pelitic schist (unit 2, Figure 2) is part of this package and hosts the Dudevoir Passage and Trail Bay kyanite-garnet occurrences. In outcrop, kyanite-bearing rocks are indistinguishable from the surrounding host. However, on close inspection of the weathered surface, kyanite appears as small rectagular knobs and bumps. In the "high-grade" zones the kyanite forms crystal "mats" and is very distinctive. Weathering and wave action have also created kyanite and garnet placer concentrations in the shoreline debris of rock and gravel. This has proven to be a useful prospecting tool where beaches have developed at the toe of the rock bluffs.

Other units present in the area examined include postmetamorphic mafic intrusive rocks and later, medium to coarse-grained granodiorite and tonalite intrusions (Snyder, 1980).

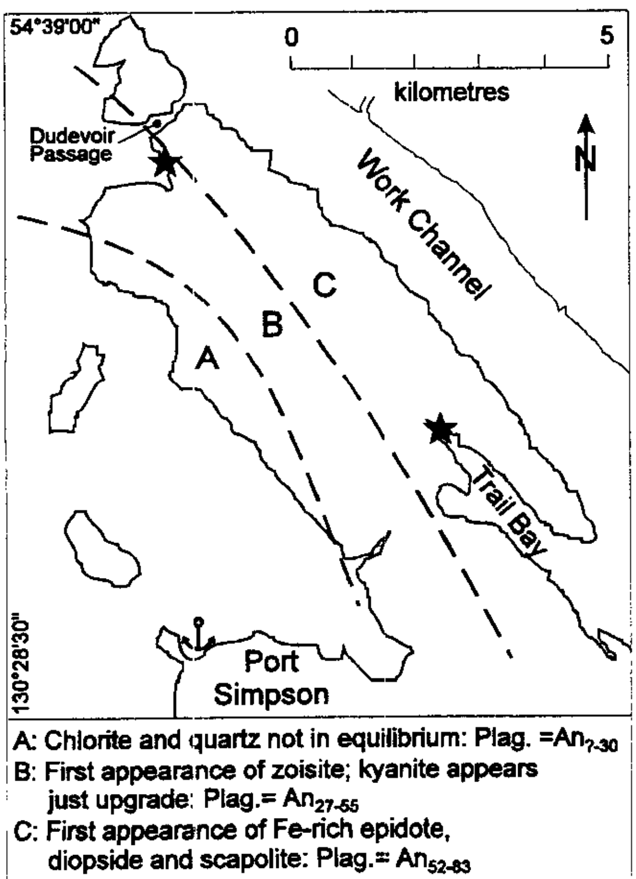


Figure 3: Metamorphic zones at the north end of Tsimpsean Peninsula (from Snyder, 1980)

Rocks on the Tsimpsean Peninsula have a well developed planar structural fabric that strikes northwest and dips moderately to gently to the southwest. At the northern end of the peninsula, along the Work Channel lineament, the fabric is subvertical. Small-scale folds appear to have a generally random orientation.

Metamorphic grade increases from west to east, from greenschist to amphibolite facies. The metamorphic mineral assemblages have been examined by Snyder (*ibid.*) and are shown in Figure 3. The lower boundary of zone A is defined by the final disappearance of chlorite in the presence of quartz. Zone B is defined by the first appeareance of anhedral zoisite prophyroblasts that crosscut foliation. Kyanite appears just above this boundary. Zone C is defined by the first appearance of iron-rich epidote, diopside and scapolite Most of the alumina-rich zone that hosts the kyanite occurrences is in zone C.

## *KYANITE OCCURRENCES*

### DUDEVOIR PASSAGE

Dudevoir Passage is at the northern end of the peninsula. The kyanite outcrops are small bluffs at the waters edge, approximately 450 metres south of the western mouth of the passage. Thick coastal rainforest covers the bedrock and makes travel on foot from the coastline very difficult.

A section was measured across the Dudevoir Passage showing from west to east (Figure 4). The layers are oriented 130°/80° SW. The section begins in dark grey to purplish brown and medium to coarse-grained kyanite schist. The schist comprises mainly quartz and plagioclase with 10 to 15% each of biotite and muscovite flakes less than 3 millimetres across. Pyrite and magnetite are minor constituents (< 1% each).The dark grey rocks contain up to 0.5% graphite. Kyanite content is variable, about 10 to 25% in the schist and 20 to 25% in the graphitic layers, with crystal lengths from a few millimetres to about 2 centimetres. Kyanite crystals contain some microscopic quartz inclusions.

Porphyroblastic coarse-grained amphibole-garnet gneiss (metabasite) is garnet rich near its contacts and rich in feldspar and mafic minerals towards the centre of the unit. The garnets are porphyroblastic and masses can be up to 5 centimetres across. The mafic-rich centre consists of amphibole and possibly pyroxene and makes up 30 to 60% of the rock mass; crystals are from 1 to 5 centimetres long, some partially chloritized. Iron oxides and pyrite make up less than 1% of the rock.

The kyanite-garnet schist contains kyanite (10-25%), thin layers of very dark red garnets (5-7%), muscovite (>10%), graphite (2%) and quartz (50%). The garnets contain abundant quartz inclusions. The graphite occurs as very fine interstitial flakes and intergrowths with biotite. Magnetite and pyrite form less than 0.5% of the rock.

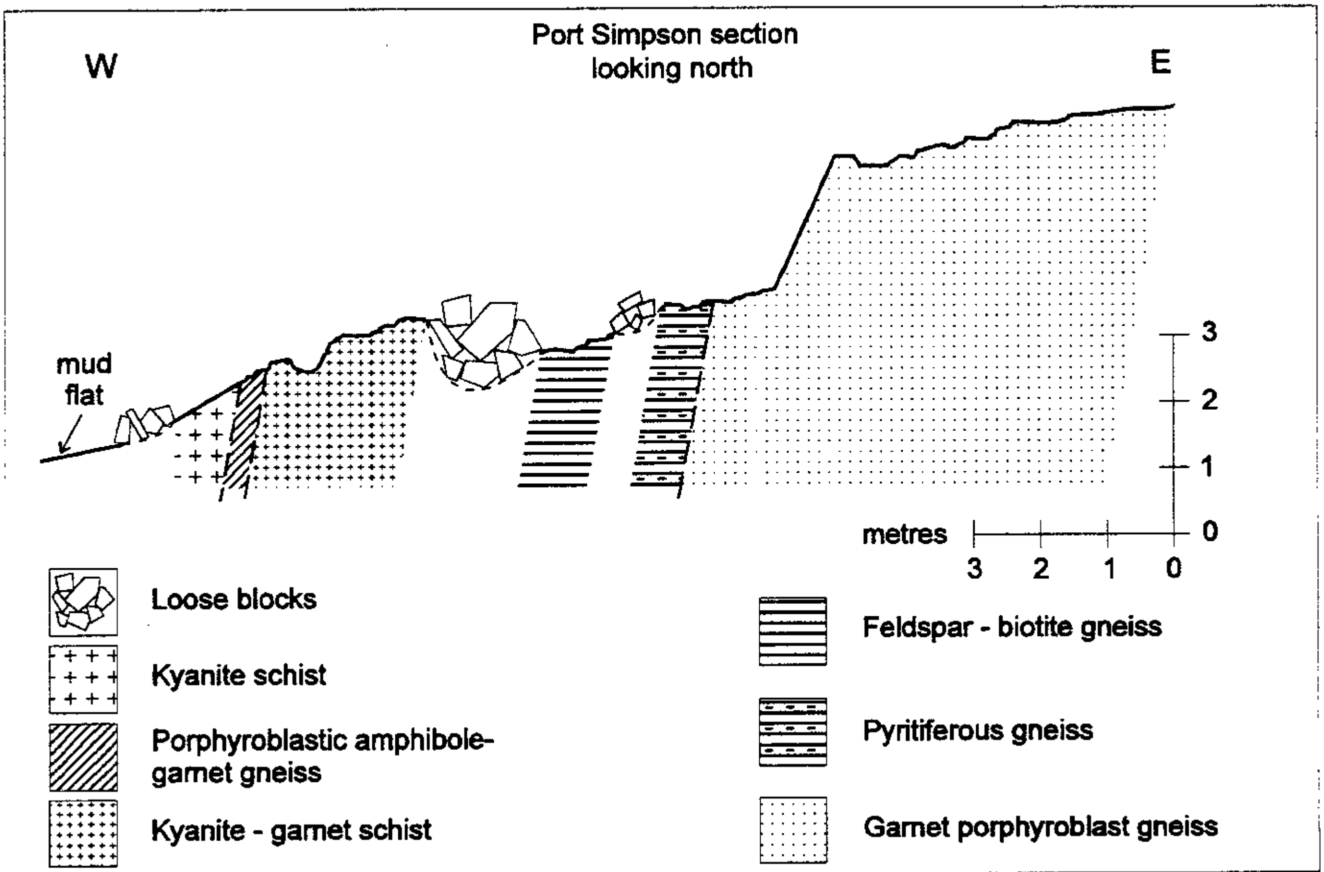


Figure 4: Section across the Dudevoir Passage kyanite showing.

Feldspar-biotite gneiss is rusty brown, medium to coarse grained and contains less than 1% fine-grained, disseminated pyrite. The fresh surface is greenish grey. The gneiss comprises mostly feldspar and quartz with about 10% biotite and less than 1% pyrite. There is less than 1% disseminated garnet, with grains less than 1 millimetre in diameter.

The pyritiferous gneiss has a notable reddish patina on the seawashed surface: it is medium grained and contains 8% pyrite. Disseminated pyrite grains are less than 3 millimetres long but have been stretched along the fabric of the gneiss forming "smears". Iron oxides form less than 1% of the rock. Calcite is a minor accessory mineral.

Garnet gneiss is distinctive by virtue of its large garnet porphyroblasts. These are up to several centimetres across and form up to 15% of the rock. The porphyroblasts are partly altered to chlorite and contain abundant clear white to colorless, acicular quartz inclusions. Biotite forms "smears", suggesting it may be a retrograde product of pyroxene or amphibole.

## TRAIL BAY

The best kyanite outcrops in Trail Bay are at the head of the bay. Kyanite also occurs along the western shore in discontinuous outcrops over approximately 600 metres (Figure 2). The outcrops are best exposed at low tide but caution is necessary as the mud beach is very flat and the tide changes are ±8 metres. The outcrops are small bluffs along the shore, similar to those at Dudevoir Passage to the north.

The kyanite-bearing gneiss comprises roughly 35 to 40% kyanite, 40% quartz, 10% biotite (<6 mm), 5% feldspar, less than 5% staurolite (1-2 mm), 2% garnet (<2 mm) and trace pyrite. Kyanite contains a few inclusions of iron oxides and some graphitic material. The graphitic material is almost amorphous. A single kyanite zone is well exposed in many outcrops at the head of the bay but, towards the southern limit of the exposures, the strike is quite variable and more than one zone may be present. The kyanite-bearing gneiss is interlayered with medium-grained biotite gneiss.

The kyanite-bearing gneiss is about 3 metres wide and is exposed for nearly 50 metres along strike. It is bronze-grey on weathered surfaces and steel grey when broken. Kyanite crystals often appear to be steel grey rather than the more typical blueish hue. Very coarse kyanite crystals, up to 5 centimetres long, form between 20 and 40% of the gneiss. In a few places, kyanite makes up 80% of the rock. Other minerals include quartz (±40%), biotite (±10%), feldspar (±5%), staurolite(?) (<1%) and trace graphite.

A section across the zone was not mapped in detail due to a rising tide. A quick overview indicates it comprises, from west to east: the kyanite gneiss, 3 metres wide with the western margin not exposed; a band of interlayered biotite gneiss and porphyroblastic amphibolite or pyroxenite less than 50 centimetres wide; a massive, black, coarse-grained porphyroblastic amphibolite or pyroxenite 4 to 5 metres wide; 7 metres of biotite gneiss followed by about 7 metres of biotite gneiss with foliation-parallel, massive white feldspar pegmatite layers/veins(?), from 0.1 to 2 metres wide that end in a cover of saltwater grasses. The pyroxenite was not seen elsewhere in the bay and the feldspar pegmatite is confined to the eastern shore.

Individual kyanite-bearing outcrops along the west side of the bay typically contain 5% kyanite, 2 to 5 centimetres long; about 1% garnet, 2 to 5 millimetres in diameter and, sporadically, up to 5% fine-grained graphite. The trend of the gneissosity is between 140°/75° and 340°/80°.

In a general sense, all these showings, and other locations reported by Hutchison (*ibid.*) on the shore below Basil Lump and opposite the mouth of Quottoon Inlet, are on strike with each other and probably part of a single alumina-rich zone, parallel to Work Channel.

## HAWKESBURY ISLAND

### *GEOLOGICAL SETTING*

The geological setting of Hawkesbury Island is summarized from Roddick (1970).

Eight major units are mapped on the island (Figure 5). They are, from north to south: hornblende biotite granodiorite (1), granitiod gneiss (2), a complex agmatite (3), hornblende-plagioclase-amphibolite schist (4), hornblende-biotite quartz diorite (5), biotite quartz diorite (6), gneissic diorite migmatite complex (7) and hornblende diorite (8). Hornblende-plagioclase amphibolite schist underlies the centre of the island with granitiod gneiss and agmatite exposed at the northern end and the other lithologies to the south.

The hornblende-plagioclase-amphibolite schist contains alumina-rich metapelite that carries kyanite. The schist is part of a regional suite of metasedimentary rocks, largely hornblende-plagioclase schist with lesser quartzite, crystalline limestone, migmatite and some granitiod rocks. It appears to grade into the adjacent units but contact relationships are not clear. It has poorly developed layering and weakly developed foliation, especially where there is little biotite. The unit is also shot through with irregular masses of quartz-feldspar gneiss, *lit-par-lit* gneiss, agmatite and quartz diorite or granodiorite.

Metamorphism on the island has reached amphibolite facies and the staurolite-quartz and kyanite-muscovite-quartz grades. Sillimanite has been found in stream sediments in a few small areas at the north end of the island, suggesting some slightly higher metamorphic grades may occur locally.

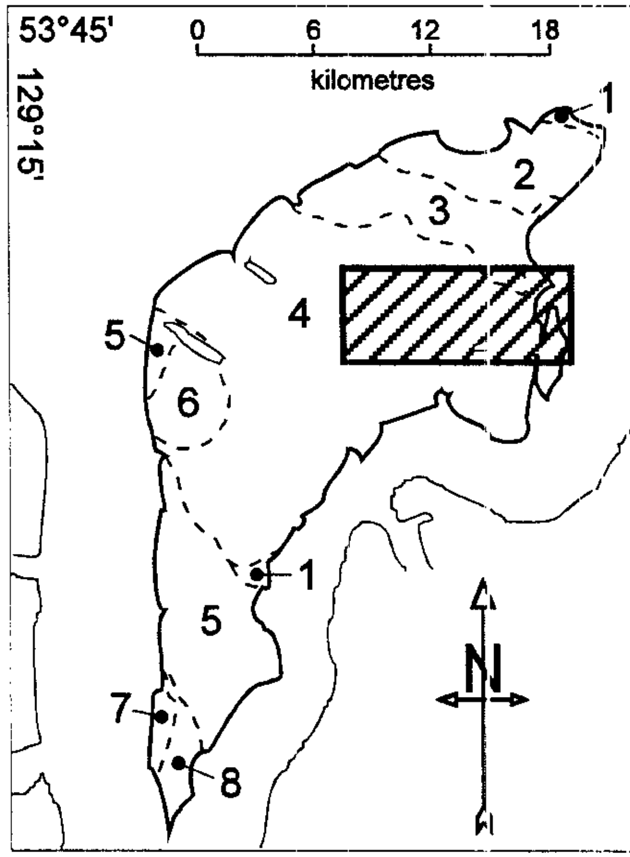


Figure 5: Geology of Hawkesbury Island (modified from Hutchison, 1982; see text for unit names; inset is location of Figure 6).

### *KYANITE OCCURRENCES*

Kyanite was first noted on Hawkesbury Island by Money (1959) while mapping the geology of the island for Texas Gulf Sulphur Company as part of a regional exploration program for volcanogenic massive sulphides in the Ecstall River pendant. Kyanite occurs in a number of discrete zones of high-grade metapelitic gneiss that are part of Roddick's feldspar-hornblende schist unit. Only two of the zones were examined and a detailed section was mapped across one of them (zone 1, Figure 6).

#### ZONE 1

The first kyanite-bearing zone, in a quartz-feldspar-biotite gneiss, was traced for 900 metres along strike and varies from 3 to 25 metres across. It has an easterly trend and a subvertical northerly dip (280°/70°). Individual gneissic layers pinch and swell by an order of magnitude, from 0.1 to 1 metre, and are complexly folded. Quartz-feldspar pegmatite layers/veins/sweats exhibit ptygmatic folding. Significant minerals include kyanite, garnet and staurolite.

Individual subunits are difficult to trace for more than several tens of metres. In general, larger subunits, like the kyanite zone, can be traced out, but it too has

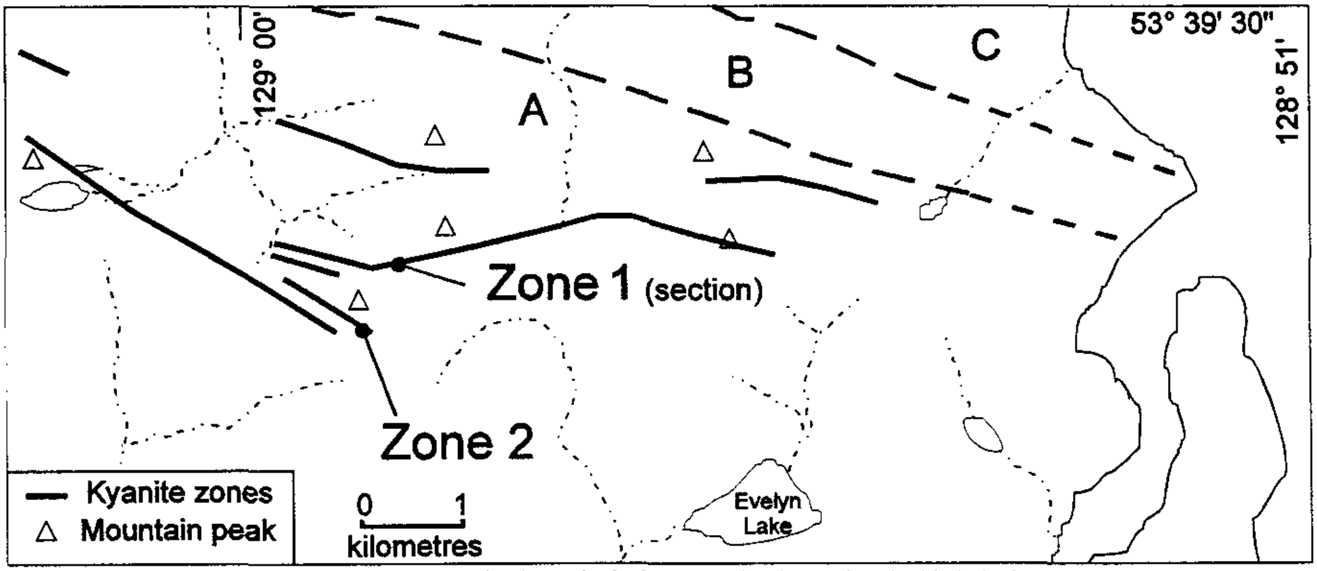

Figure 6: Kyanite occurrences on Hawkesbury Island. A: plagioclase amphibolite; B: interbedded plagioclase amphibolite and quartz-potassium-feldspar-plagioclase gneiss; C: quartz-potassium-feldspar-plagioclase gneiss (from Money, 1959).

significant thickness variations. The mapped section is on one of the widest zones, exposed across 25 metres. The many kyanite zones exposed in the area appear to be distinct stratigraphic units, but may well be part of a structurally repeated sequence. Rock units exposed in the section are described below, from north to south.

Quartz-feldspar-biotite gneiss is light grey and fine grained with well developed centimetre-scale layering. Massive quartz lenses with order of magnitude variations in thickness and length are scattered across this unit.

Large lenses or sweats of quartz-feldspar pegmatite are common throughout the section. They are usually subparallel to layering, massive to coarse grained and often contorted. Staurolite, muscovite and garnet are often concentrated at their edges and form masses of very coarse crystals, especially muscovite.

Crenulated feldspar-quartz-biotite-garnet gneiss bounds the alumina-rich zone. It is medium grey in colour and well layered with massive quartz lenses and layers scattered through it. It is strongly crenulated in parts, but not across the whole unit. Disseminated garnet occurs as small grains (<1 mm) comprising about 1% of the rock; disseminated staurolite forms up to 5% of the rock, especially on the south side of the subunit.

Staurolite-garnet-muscovite gneiss, the first unit in the alumina-rich zone, is mottled brown on weathered surfaces and is strongly crenulated. In places, staurolite makes up to 70% of the rock. Small disseminated garnets are fairly uniformly distributed across the unit. Large lenses and sweats of quartz-feldspar pegmatite are subparallel to layering. Staurolite forms dense masses along pegmatite contacts and large muscovite books form prominent pockets in the pegmatites.

Kyanite±staurolite gneiss layers vary from 0.1 to 7 metres wide. Kyanite content is variable, reaching 60%, with crystals from 0.2 to 4 centimetres long. The crystals contain inclusions of quartz and are almost free of iron oxides. Layers with high kyanite concentrations (>10%) have a distinctive grey-blue colour. In the wider layers, kyanite-rich rock is interlayered with discontinuous quartz-feldspar-muscovite lenses, about 5 centimetres thick and a few metres long. Staurolite is commonly disseminated in concentrations of up to 5%, but up to 40% in some layers. Up to 5% garnet, several millimetres in diameter, is disseminated throughout these layers. In a few places garnet forms small, massive lenses. The gneiss is also muscovite rich and biotite content is only a few percent, with quartz and feldspar making up the balance of the rock.

Staurolite-kyanite-muscovite gneiss contains up to 65% staurolite and kyanite but averages about 7% overall. Staurolite and kyanite crystals are coarse, from 2 to 10 millimetres in diameter and 5 to 20 millimetres long. Garnet grains are up to 1 centimetre in diameter but comprise less than 5% of the rock. Muscovite books are scattered and are less than 5 millimetres across. The groundmass is feldspar and quartz.

Staurolite-garnet gneiss is about 5% staurolite, 3% garnet and less than 10% biotite with the balance feldspar and quartz. Feldspar-quartz pegmatite layers are common. Staurolite and garnet grains are typically less than 3 millimetres in diameter. Garnets are partly retrograded to chlorite.

Fine-grained staurolite-garnet-kyanite gneiss is shot through with feldspar-quartz pegmatite layers. It contains 10% staurolite, 5% garnet and 5% kyanite with the remainder feldspar and quartz.

Coarse-grained staurolite-garnet-kyanite gneiss is distinct from the previous unit in that the high-grade metamorphic minerals are much coarser and more abundant. Staurolite forms about 40% of the rock with crystals 4 to 20 millimetres in diameter. There is about 10% garnet, from 5 to 30 millimetres in diameter and less than 10% kyanite. Quartz-rich layers, 5 to 50 millimetres wide, make up about 30% of this unit.

Kyanite-muscovite gneiss is distinctive because of the 15% muscovite content. Coarse kyanite crystals

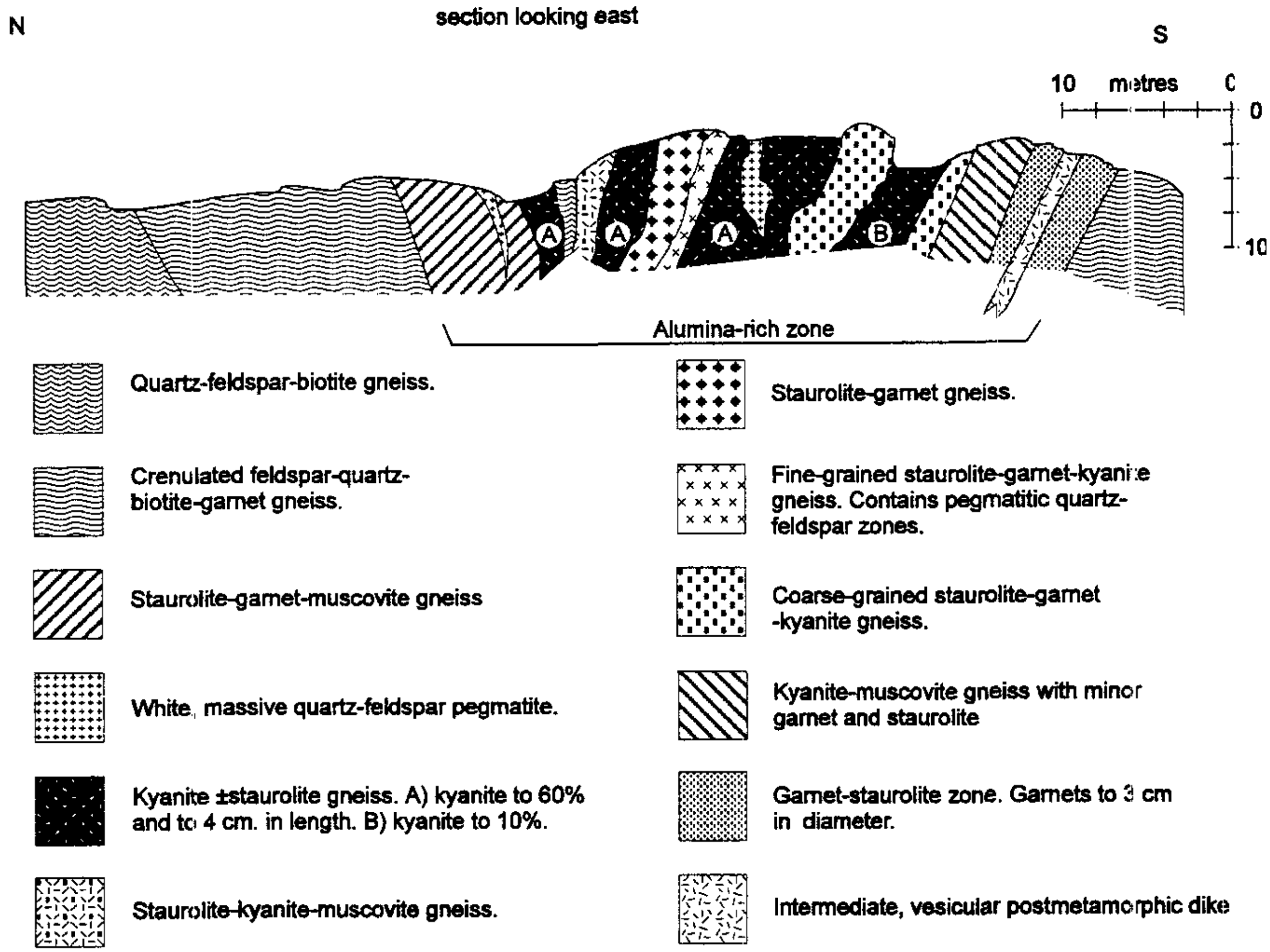


Figure 7: Section across the zone 1 kyanite showing on Hawkesbury Island (see Figure 6 for location).

comprise 20% of the rock with garnet at 1 to 5% and staurolite scattered and variable from 0 to 20%.

The garnet-staurolite gneiss is spectacular as the garnets are large, up to 3 centimetres in diameter, and form about 30% of the rock. Staurolite is present as an accessory mineral.

A slightly altered, postmetamorphic intermediate dike crosscuts the section. It is fine grained and vesicular with about 30% amphibole, more than 60% feldspar and 10% quartz, in the vesicles.

## ZONE 2

The second zone, located 450 metres south of zone 1, at the crest of a ridge, was traced for 225 metres along strike and is about 10 metres wide (Figure 6). It is similar in character to the first zone. It too is complexly folded on outcrop scale and along strike. Individual concentrations of kyanite, garnet, staurolite and muscovite vary greatly from one layer to the next. Typically kyanite occurs in concentrations of 10% in layers less than 25 centimetres thick with grains 1 to 2 centimetres long. Staurolite averages less than 5%; grains are up to 2 centimetres long, nearly black and often forms dense masses adjacent to coarse-grained quartz-feldspar lenses. Garnets are almost ubiquitous as disseminated grains 0.5 to 2 centimetres in diameter with concentrations in the 1 to 10% range. In or immediately adjacent to quartz-feldspar lenses, garnets form masses about a metre long, with euhedral crystals up to 7 centimetres in diameter. Garnets in pegmatites and felsic layers are much less resorbed than those in the surrounding schist or gneiss. Layers rich in kyanite, garnet or staurolite tend to have a few percent muscovite and low concentrations of biotite. Magnetite crystals, less than 10 millimetres in diameter, are scattered through some of the pegmatites.

# ECONOMIC CONSIDERATIONS

### *TSIMPSEAN PENINSULA*

At Dudevoir Passage and Trail Bay, the kyanite occurrences are probably part of the same alumina-rich zone. It is possible that kyanite reported on the shore 13 and 29 kilometres southeast of Trail Bay (Hutchison, *ibid.*) may be part of this same zone. Where measured, the zone is about 3 metres wide but may be thicker in fold hinges. The kyanite crystals are coarse, up to 2 centimetres long, with relatively few, coarse inclusions of quartz. Graphitic material present in the kyanite layers could probably be removed by calcination.

### *HAWKESBURY ISLAND*

There are at least seven major kyanite zones on Hawkesbury Island. They vary in size from a few metres to several tens of metres wide and some have been traced for up to 5 kilometres. Individual zones contain 10 to 70% kyanite, 0.2 to 4 centimetres long. It is unlikely that kyanite alone could be economically recovered, but mining for kyanite, garnet, staurolite and possibly muscovite may be feasible.

## REFERENCES


Hutchison, W.W. (1982): Geology of the Prince Rupert - Skeena Map Area, British Columbia; *Geological Survey of Canada*, Memoir 394, 116 pages.

Money, P.L. (1959): Geology of Hawkesbury Island; unpublished M.Sc. thesis, *University of British Columbia*, 159 pages.

Roddick, J.A. (1970): Douglas Channel - Hecate Strait Map-area; *Geological Survey of Canada*, Paper 70-41, 56 pages.

Simandl, G.J., Hancock, K.D., Church, B.N. and Woodsworth, G.J. (1995): Andalusite in British Columbia - New Exploration Targets: *in* Geological Fieldwork 1994, Grant, B. and Newell, J.M., Editors, *B.C. Ministry of Energy, Mines and Petroleum Resources*, Paper 1995-1, pages 385-394.

Skillen, A. (1993): Sillimanite Minerals; *in* Raw Materials for the Refractory Industry, Consumer Survey, 3rd. Edition, O'Driscoll, M. and Griffiths, J.B., Editors, *Industrial Minerals*, pages 49-63.

Snyder, J.G. (1980): A Metamorphic and Structural Study of the Port Simpson Area, British Columbia; unpublished M.A. thesis, *Bryn Mawr College*, 88 pages.

Sweet, P.C. (1994): Sillimanite Group - Kyanite and Related Minerals; *in* Industrial Minerals and Rocks, 6th Edition, Carr, D.D., Senior Editor, *Society for Mining, Metallurgy, and Exploration, Inc.*, pages 921-927.

# CONTROLS ON COAL WASHING DIFFICULTY

# (82G/15 93L/11)

By Barry D. Ryan

*KEYWORDS*: Coal washing, washing difficulty, dispersed mineral matter, lithotypes, detrital macerals, coal-forming environments.

## INTRODUCTION

Coal seams are a mixture of pure coal and rock. The coal scientist may be interested in the relationship between the coal-rock mixture and the environment in which the coal formed. The mining engineer is more interested in how easy it will be to separate the coal from the rock and how much coal will be lost in the process. A number of papers (Sanders and Brookes, 1986; Sarkar and Das, 1974) have attempted to bridge the gap between the interests of the scientist and the engineer by looking at the linkage between environmental controls on coal formation and washing difficulty. These papers may be of some interest to the engineer, but he or she is more interested in predicting the washing characteristics of a particular coal seam than in finding a genetic explanation for the characteristics.

The first part of this paper looks at some possible environmental controls of washing difficulty of British Columbia coals. Lithotype and maceral evidence are obtained from a number of published papers and the relationship between these data and the amount of dispersed mineral matter is discussed. It is generally considered that it is the amount and distribution of the finely dispersed mineral matter that most effects washing difficulty. If the coal contains a higher than normal amount of finely dispersed mineral matter then it will be difficult to wash. There is no universal definition of this material. It is probably present in the coal as fine particles associated with the different coal macerals, as fillings in the coal macerals and as chemically bound components in the coal molecular structure. Changes in washability are caused by changes in the amount and distribution of this material.

The dispersed mineral matter has a number of origins:

- wind blown;
- water transport;
- original component of the vegetation;
- introduced subsequent to the start of coalification (syngenetic or epigenetic emplacement)

The source and amount of the dispersed mineral matter and the environment in which the coal formed are related and therefore there will be some relationship between washing difficulty of the coal and the depositional environment in the coal swamp.

The second part of the paper examines a way of estimating washing difficulty, using small samples. New data from the Elkview and Quintette mines are introduced and data from the Corbin, Quinsam and Telkwa properties are re-interpreted.

Washing difficulty is not the same as plant recovery, which is the main concern of the plant engineer. Plant recovery is dependent on:

- the type of wash plant used;
- the size-consist of the run-of-mine coal (ROM coal);
- the amount of rock mixed into the coal by the mining process (in-seam and out-of-seam dilution);
- the washing difficulty of the coal.

The first three elements are largely under the control of the operator the last is largely an inherent property of the coal seam.

The difficulty of washing coal is related to the degree of liberation of rock from coal in the size-consist (range of particle sizes) that enters the plant. If there is incomplete liberation of rock from coal then whatever the washing process in the plant, some rock will be misplaced in the clean product and some coal will escape with the reject material. Rock splits are generally easy to liberate from the coal and an increase in their amount in the ROM coal decreases plant recovery but does not make the coal more difficult to wash. It is the amount of dispersed mineral matter that most influences washing difficulty.

A wash plant can respond to changing washing characteristics of ROM coal by making process adjustments or by blending different seams with different washing difficulty. The key is foreknowledge of changes in the washing characteristics of the seams to be mined. The method of predicting washing difficulty proposed in this paper helps in this respect.

## PART 1 ENVIRONMENTAL CONTROLS ON WASHING DIFFICUILTY

### *RELATIONSHIP BETWEEN LITHOTYPES AND DISPERSED MINERAL MATTER*

Coal seams can be subdivided into lithotypes which are, outcrop mappable zones of coal within the seam, distinguished by brightness, banding and general appearance. Terms such as bright, banded or banded dull are used. Lithotype mapping is a somewhat tedious and subjective process, however the results may correlate with washing difficulty if there is a relationship between lithotypes and dispersed mineral matter. There may also be an underlying relationship between macerals, that make up the lithotypes, and the dispersed mineral matter.

A number of studies provide information on the maceral composition of various lithotypes and the amount of mineral matter associated with each. The mineral matter that is reported as part of a lithotype analysis is finely dispersed because the lithotype mapping excludes obvious rock bands. This will be the mineral matter that controls washing difficulty.

It is apparent from the maceral composition of lithotypes that there is some correlation of vitrinite content with lithotype brightness (Lamberson and Bustin, 1993; Holuszko, 1993) but in other studies there is little correlation (Cathyl-Bickford, 1993). Cathyl-Bickford concluded that the main control on lithotype appearance is the amount of finely dispersed mineral matter. Dull or banded lithotypes contain more finely dispersed mineral matter than the brighter lithotypes.

Kalkreuth *et al.* (1991) found that there are two types of dull lithotypes, one formed in a dry environment and is inertinite rich, whereas the other formed in a wetter, tidally influenced environment, is inertodetrinite rich and contains more dispersed mineral matter. Similar conclusions were reached by Davis (1992). These two dull lithotypes will probably have different washing difficulties because they contain different concentrations of dispersed mineral matter.

It appears that lithotype appearance may give some indication of washing difficulty but there will be exceptions. A seam with a lot of dull lithotypes may not always be difficult to wash. Seams with a high proportion of the bright lithotypes are more likely to be easy to wash. Only if lithotype appearance is a good indicator of the amount of dispersed mineral matter will lithotype mapping provide useful information on washing difficulty.

Holuszko (1993) studied the washing characteristics by lithotype of seam 16 (Greenhills mine, Figure 1) from the Mist Mountain Formation. She used the optimum washability number introduced by Sarkar and Das (1974) as a measure of washing difficulty and found that, on average, the brighter lithotypes contained less mineral matter and are easier to wash. The optimum washability number correlated with the amount of mineral matter in the lithotypes.

## *RELATIONSHIP BETWEEN MACERALS AND DISPERSED MINERAL MATTER*

If lithotype mapping is not a useful indicator of washing difficulty, then it might be worth looking on a more detailed scale to investigate the relationship between macerals and washing difficulty. This may lead to an understanding of conditions in the original peat swamp that effect washing difficulty. Two studies of coal from the Gates Formation in northeast British Columbia and two studies of coal from the Mist Mountain Formation in southeast British Columbia are discussed.

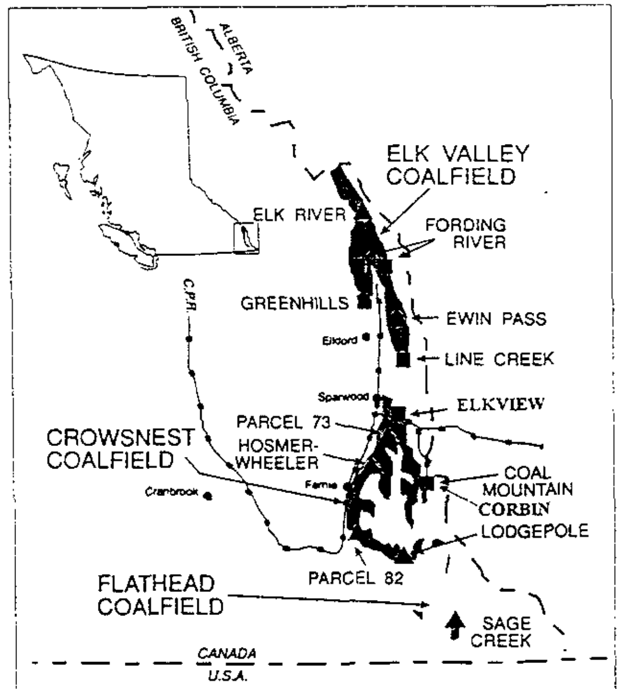


Figure 1. Location of mines in southeast British Columbia.

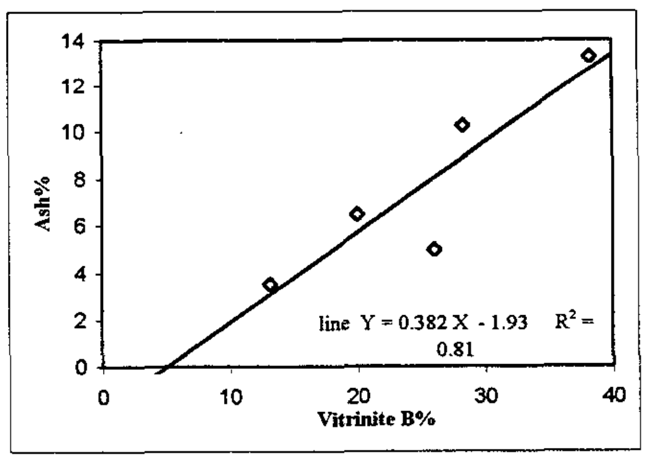


Figure 2. Vitrinite B *versus* ash in lithotypes from the Mist Mountain Formation ( data from Holuszko, 1993)

Data from Holuszko (1993) indicate a good correlation of vitrinite B with the amount of mineral matter (Figure 2). Above a threshold of 5%, there is about 0.4% mineral matter for each 1% of vitrinite B. This could be interpreted as meaning that vitrinite B is associated with a potential 40% porosity in the coal seam.

Vitrinite B (equivalent to desmocollinite) is structureless vitrinite of lower reflectance than vitrinite A.. It is formed from the gel components of the degraded vegetation and, based on its present form, may in part have a detritial origin (Stach *et al.*, 1975). When vitrinite is subdivided into vitrinite A and B it is

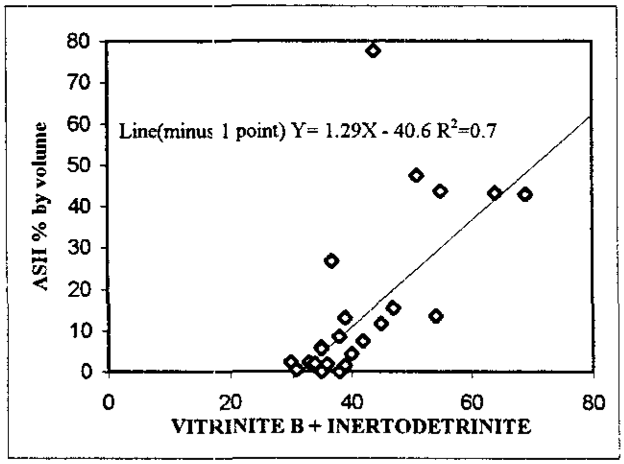


Figure 3. Vitrinite B plus inertodetrinite *versus* ash, southeast British Columbia samples (data from Dawson *et al.*,1994)

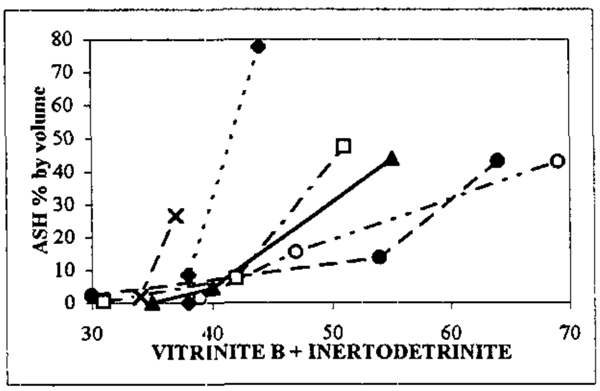


Figure 4. Vitrinite B plus inertodetrinite *versus* ash for samples at different specific gravity (data from Dawson *et al.*, 1994). Lines represent different SG splits of the same sample.

probable that the true detrital vitrinite (vitrodetrinite) is counted with the vitrinite B. Vitrodetrinite is composed of vitrinite fragments produced either by turbulence in the peat swamp or because the swamp was dry and contained a high proportion of reeds easily broken into small fragments.

Detailed petrography for a number of Mist Mountain seams is contained in Dawson *et al.* (1994). Mineral matter was correlated with all individual maceral types and with the sum of vitrinite B plus inertodetrinite. Inertodetrinite is composed of detrital fragments of fusinite and therefore represents the inert maceral contribution to the detrital macerals in the coal. The best correlation was between mineral matter and the sum of detrital macerals, which has an $R^2$ value of 0.70, excluding one high-ash point (Figure 3). It appears that below about 30% detrital maceral content there is no relationship of mineral matter with detrital maceral content. It is possible that a minimum amount of detrital maceral material is required before water movement through the vegetation mat can introduce finely dispersed mineral matter. The data suite plotted in Figure 3 includes samples that were split into three density fractions ( 1-1.3 specific gravity (SG), 1.3 -1.6 SG and 1.6 - 2.5 SG). These data also clearly indicate a correlation of vitrinite B plus inertodetrinite with mineral matter, both of which are concentrated in the denser fractions (Figure 4). The three density fractions of each sample are joined by lines in Figure 4; as the ash increases, the remaining organic material contains a higher proportion of the detrital macerals. The slope of the bestfit lines in Figures 3 and 4 indicates that more than 0.5% ash is added to the coal for each 1% increase in the content of detrital macerals. This could imply a porosity of greater than 50%.

General data from Line Creek mine (southeast British Columbia, Figure 1) tend to indicate that variations in washability are not related to over-all maceral content. Seam 8, which has a higher inert maceral content than 10 seam, washes better than 10 seam yet, within 10 seam, the sub-seam with higher vitrinite content washes better than the rest of the seam.

Lamberson and Bustin (1993) report petrography for a number of coals from the Gates Formation in northeast British Columbia. Their data also indicate a correlation of vitrinite B plus inertodetrinite with mineral matter (Figure 5). Data from Kalkreuth and Leckie (1989) appear to indicate that as mineral matter increases, the ratio of fusinite+semifusinite to inertodetrinite+macrinite+micrinite decreases. This may be because of an increase in inertodetrinite in the sample which would indicate a correlation between dispersed mineral matter and inertodetrinite.

The positive correlation of vitrinite B plus inertodetrinite with mineral matter indicates that it may be intermixed with these macerals in Mist Mountain and Gates coals. It has also been suggested that mineral matter is negatively correlated with total vitrinite content (Renton and Cecil, 1979). They proposed that some seams are thinner because the vegetation experienced more biological degradation, leaving a coal seam with a higher ash residue and a greater content of inert macerals. This may imply that an increase in inertinite is accompanied by an increase in dispersed mineral matter, or that there is just an increase in the total mineral matter, much of it occurring as discrete bands.

Gamson *et al.* (1993) suggest that mineral matter may fill in the cell (phyteral) porosity in fusinite and semifusinite. This would imply a correlation of dispersed mineral matter with inertinite content. It is probable that the cell porosity available from the inert macerals is more limited than the coarser porosity made available by the presence of detrital maceral fragments. It is also possible that the cell porosity will not always be filled with finely dispersed mineral matter. Syngenetic mineral matter may well concentrate in the cell structure in the inert macerals, but other, possibly more abundant, types of dispersed mineral matter will be intermixed with the detrital macerals.

In general, there does not appear to be a consensus on the relationship between dispersed mineral matter and coal macerals. However, in the Mist Mountain and Gates formations there is evidence to suggest a

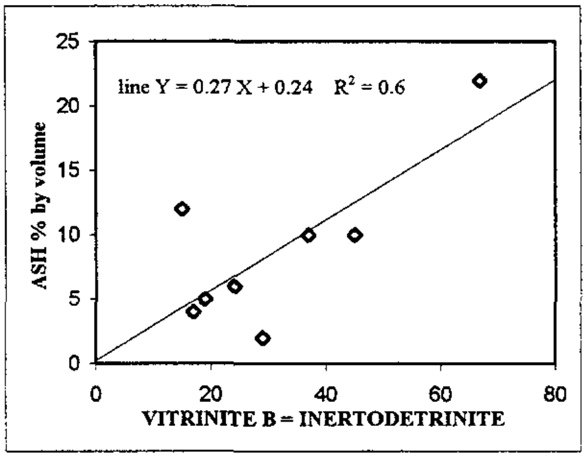


Figure 5. Plot of vitrinite + inertodetrinite *versus* ash for samples from Gates Formation (data from Lamberson and Bustin, 1993).

correlation of dispersed mineral matter with the detrital coal macerals from both the vitrinite and the inertinite groups. This permits some discussion of the connection between coal swamp environment and washing difficulty.

## *RELATIONSHIP BETWEEN ENVIRONMENT AND WASHING DIFFICULTY*

Regional variations in washing difficulty of seams in the Mist Mountain and Gates formations are probably related to changes in the amount of the detrital coal macerals, inertodetrinite and vitrinite B, generated in the coal swamp. A dry environment favours a decrease in the amount of vitrinite and an increase in the ratio of vitrinite B to vitrinite A. Tidal influence, and more agitation and transportation of organic material in the swamp, favours the formation of inertodetrinite and also vitrinite B. The association of inertodetrinite with vitrinite B has been interpreted to represent a reed-type raised bog environment (Diessel, 1982). An increase in the amount of detrital macerals not only indicates drier conditions, but also more degradation and transportation of organic material in the peat swamp. This provides the opportunity for the inclusion of small mineral particles in the organic debris.

Kalkreuth and Leckie (1989) suggest that high contents of inertodetrinite and vitrinite B in the Gates Formation are caused by flooding and turbulence in the swamp, related to off-shore storms. This would explain why there is generally more consistency in washing characteristics laterally within seams than from seam to seam. Seams higher in the Mist Mountain Formation formed in a delta environment, removed from the shore line, and based on this model, should therefore generally have better washing characteristics.

In general, Lower Cretaceous coals of North America are characterized by high contents of inert and detrital macerals (Kalkreuth and Leckie, 1989) and this is considered to be characteristic of coals formed in a strandplain environment. Despite different climate and vegetation types, Permian coals from India, Australia and South Africa, which are often difficult to wash, probably formed in similar environments and are also characterized by high levels of inert and detrital macerals.

Coal seams at the Telkwa property and Quinsam mine (Figure 6) formed in estuarine conditions that were probably fairly tranquil compared to the strandplain environment represented by seams in the lower parts of the Mist Mountain and Gates formations. Petrography for both these properties is presented in Matheson *et al.* (1994).

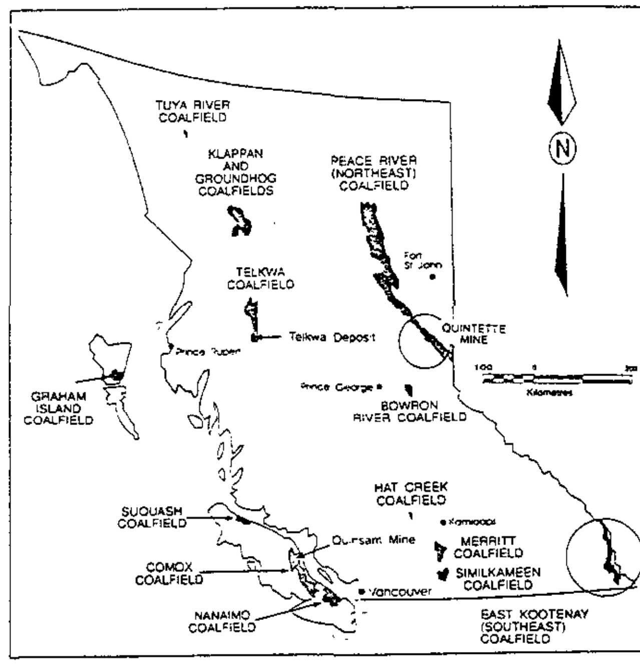


Figure 6. Location map for coal properties in British Columbia.

Data for the number 1 seam at Quinsam reveal a negative correlation of mineral matter with vitrinite B plus inertodetrinite and a positive correlation with vitrinite A (Figure 7). Much of the dispersed mineral matter was possibly introduced after coalification and therefore its location was controlled by cleating developed most extensively in bands rich in vitrinite A. Quinsam coal is characterized by calcite that occurs on cleats, predominately in the brighter vitrinite-rich lithotypes (Ryan, 1994). The data are from samples collected in the 2-north area where the first underground mine was developed. The seam has poorer washing characteristics to the south of this development.

At Telkwa, samples were collected from the upper and lower coal units. The mineral matter contents of the samples are generally high, which indicates the presence of rock splits. There is no correlation of mineral matter with any of the macerals, which implies that it will be difficult to find any relationship between peat swamp environment and washing difficulty. The lower seam (seam 1), which is more difficult to wash (Ryan, 1992), contains more total vitrinite and less vitrinite B plus inertodetrinite than the upper seams. This implies that washing difficulty may increase as the amount of vitrinite A increases, which is similar to the situation at Quinsam. It appears that seams formed in an estuarine environment wash easily, except for seams formed around the margins of the basin or over uneven basement surfaces.

The difficulty of washing can be related, in broad terms, to depositional environment. The Lower Cretaceous coals of eastern British Columbia have more dispersed mineral matter than Appalachian coals, probably because of a more turbulent environment in the swamps. It is probable that younger coals, such as Telkwa, Quinsam and some of the Tertiary coals, formed in more quiescent estuarine or lacustrine environments. They generally have less dispersed mineral matter and are easier to wash. Any variations in ease of washing for these coals may correlate with the vitrinite A content and derive from the fact that this maceral is brittle, cleats easily, and is therefore a host for minerals deposited on cleat surfaces and micro-fractures.

This discussion provides some insight into possible relationships between coal-forming environments and washing difficulty. It is obvious that neither lithoptype mapping nor maceral analysis will provide a reliable way of predicting washing difficulty.

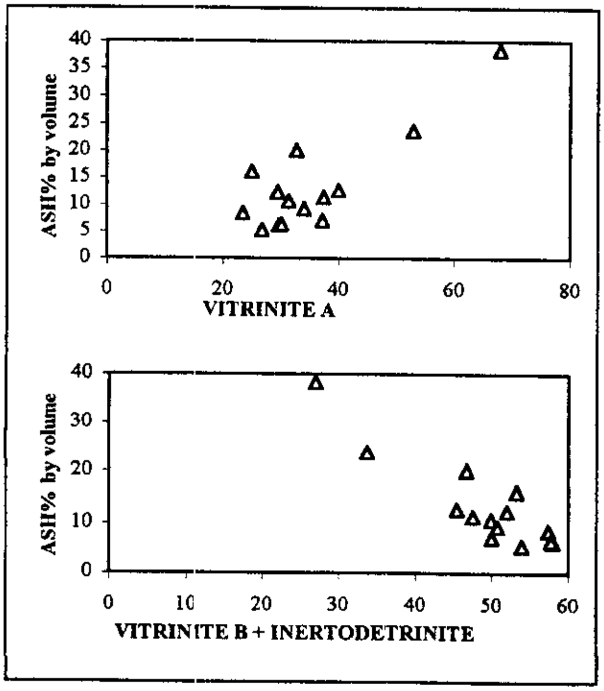


Figure 7. Vitrinite A and vitrinite B *versus* ash for Quinsam samples (data from Matheson *et al.*, 1994).

# PART 2 METHODS OF PREDICTING WASHING DIFFICULTY

## *COAL QUALITY PARAMETERS USED FOR ESTIMATING WASHING DIFFICULTY*

Plant engineers need to have some information on the washing difficulty of coal being delivered to the plant. Plant recovery cannot be predicted accurately without knowing details of the equipment in the plant, but it is possible, without knowing plant details, to rank coals in terms of washing difficulty. This is often done using results from pilot plant runs or washability tests on bulk samples.

Changes in washing difficulty can be illustrated using washability data in a number of ways; all attempt to reduce the large amount of data acquired in a full washability analysis to a single number. This number purports to represent washing difficulty. It should be treated with caution because it will, in part, represent inherent properties of the coal and, in part, the degree of crushing and liberation resulting from sample preparation.

Sanders and Brookes (1986) discuss the use of the degree of washing number and the optimum washability number first introduced by Sarkar and Das (1974). The degree of washing number is defined as:

$$N = yld \times (Ra-Wa)/Ra$$

where yld = yield, Ra = raw ash, Wa = wash ash and the optimum washability number is defined as:

$$Wn = 10 \times (Nopt/Wa)$$

where Nopt = maximum value for N determined by calculating all possible N values for a range of specific gravities and Wa is corresponding wash ash.

The optimum washability number varies depending on the size-consist of the samples. A smaller size-consist improves mineral-matter liberation and results in a higher optimum washability number. Because of this, washability numbers from different seams or areas should not be compared with each other, unless the size-consists of the samples used in the washability analyses are the same.

The addition of rock dilution to a seam should not effect washing difficulty. The effect of adding rock to a seam on the degree of washing number and optimum washability numbers was checked by mathematically adding nearly pure rock to a pre-existing washability curve (Figure 8). The dotted line represents the coal and the solid line coal plus 20% rock. The degree of washing number is changed by the addition of the rock, but the calculated optimum washability number is similar. The specific gravity at which the maximum degree of washing number occurs decreases with the addition of the rock.

It is possible to calculate a washability number at each specific gravity using the appropriate degree of washing number. If this is done, the optimum washability number derived is different from that calculated by taking the maximum degree of washing

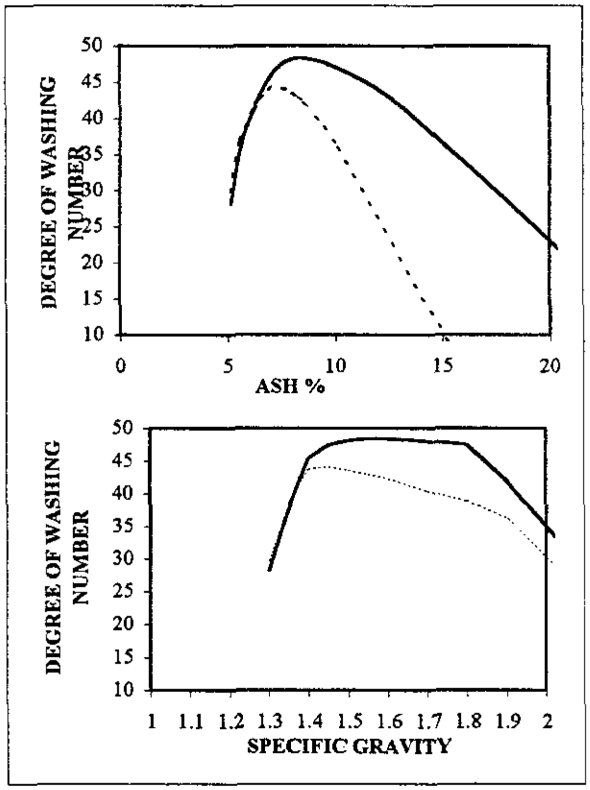


Figure 8. Effect on degree of washing number of adding 20% rock dilution to a sample.

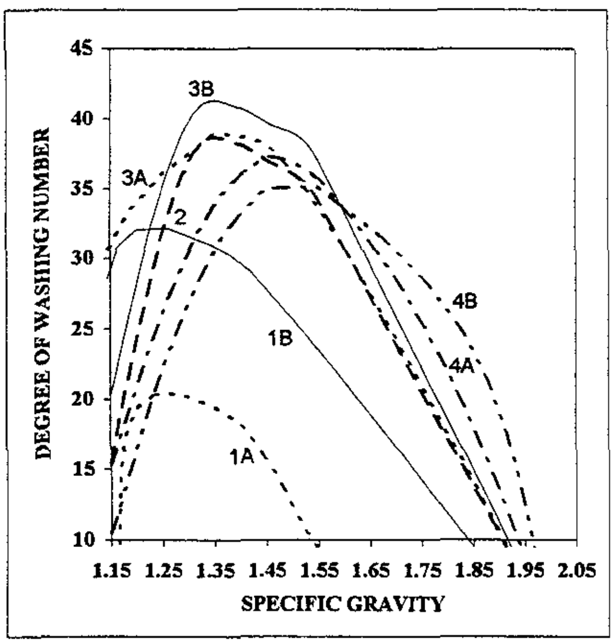


Figure 9. Degree of washing numbers *versus* specific gravity for seams from Line Creek mine (data from Ryan, 1992).

number and its corresponding wash ash. The maximum degree of washing number, divided by its corresponding ash, does not necessarily provide the highest value for the optimum washability number.

When looked at in detail, there are some inconsistencies in optimum washability numbers. They are a useful way of reducing a lot of washability data to a single number which is a relative indication of washing difficulty. However, they are not an absolute measure of washing difficulty. They are sensitive to the size-consist of the samples and the amount of out-of-seam dilution included in them.

Washability data, obtained for a number of seams in the lower part of the Mist Mountain Formation (Ryan, 1992), illustrate the changes in degree of washing numbers with SG for each seam (Figure 9). The seams are numbered from 1 at the bottom of the section. The maximum degree of washing occurs at specific gravities ranging from 1.26 to 1.5. Sanders and Brookes found that seams more difficult to wash had optimum washability numbers occurring at higher specific gravities, with higher clean ash concentrations. In a wash plant, seams may be washed as blends at a fixed SG to achieve a constant wash ash. This means that comparing optimum washability numbers may be deceptive. Degree of washing numbers should be compared at either a fixed wash ash or a fixed SG. The specific gravities at optimum washabilities for the Mist Mountain data do not correlate with the optimum washability number, illustrating the extreme variability of the washing characteristics of these seams.

Other methods of predicting washing difficulty from full washability data (Ryan (1992) involve calculation of the amount of near-gravity material. The amount of material in the SG range from about 1.4 to 1.6 is compared to the amount of material with an SG less than 2.1. This technique is a fairly accurate way of calculating directly the amount of dispersed mineral matter.

All these methods require a complete washability analysis, which is time consuming and expensive. In situations where multiple seams, from numerous locations, are being mined, it is not always possible to have sufficient bulk sample results and it is therefore useful to be able to predict changes in washability using, quicker, less expensive tests on small samples

## *DATA FROM THE ELKVIEW AND QUINTETTE MINES*

Seven samples from Elkview mine and three samples from the Quintette mine were collected for this study, with the intention of extending the conclusions reached in Ryan (1992).

The Quintette mine (Figure 6) is located in the Peace River coalfield in northeast British Columbia and mines coal from the Gates Formation. At this mine, seams E and G generally wash well, whereas the J seam is more difficult to wash. Two samples of J seam were collected from the Shikano North and P1 Mesa pits and a single sample of G2 seam from the Wolverine pit. The Elkview mine (Figure 1) is located in the Elk River coalfield in southeast British Columbia and mines coal from the Mist Mountain Formation. Hangingwall and footwall samples were collected from the basal Number 10 seam (Elk 2 pit). Two duplicate samples were collected from the overlying 8UX seam (Baldy pit) and an additional sample from 8LG seam in the Elk 2 pit.

TABLE 1

QUALITY AND SCREEN DATA FOR WASHABILITY SAMPLES

| SAMPLE | PIT | SCREEN DATA 10-0.5 mm | SCREEN DATA < 0.5 mm | RAW DATA >0.5 mm $H_2O$ ad | RAW DATA >0.5 mm ASH% | RAW DATA >0.5 mm VM% | RAW DATA >0.5 mm FC% | 1.4 SG FLOAT > 0.5 mm yield | 1.4 SG FLOAT > 0.5 mm $H_2O$ ad | 1.4 SG FLOAT > 0.5 mm ASH% | 1.4 SG FLOAT > 0.5 mm carb rec |
|---|---|---|---|---|---|---|---|---|---|---|---|
| ELKVIEW | | | | | | | | | | | |
| 7R1/A | Baldy East | 78.42 | 21.58 | 0.55 | 35.20 | 16.41 | 47.84 | 50.35 | 0.45 | 7.51 | 70.99 |
| 7R1/B | Baldy West | 83.00 | 17.00 | 0.64 | 32.25 | 17.22 | 49.89 | 43.75 | 0.38 | 7.21 | 59.22 |
| 8LG | Elk 2 | 80.59 | 19.41 | 0.65 | 21.14 | 19.00 | 59.21 | 61.62 | 0.61 | 5.52 | 73.18 |
| 8UX/A | Baldy | 67.65 | 32.35 | 0.58 | 20.29 | 21.11 | 58.02 | 52.51 | 0.58 | 6.64 | 60.85 |
| 8UX/B | Baldy | 78.14 | 21.86 | 0.59 | 32.97 | 16.97 | 49.47 | 38.98 | 0.30 | 6.96 | 53.50 |
| 10FW | Elk 2 | 62.30 | 37.70 | 0.70 | 17.56 | 18.47 | 63.27 | 56.14 | 0.86 | 6.16 | 63.27 |
| 10HW | Elk 2 | 53.66 | 46.34 | 0.65 | 10.89 | 19.52 | 68.94 | 68.53 | 0.62 | 5.88 | 71.70 |
| QUINTETTE | | | | | | | | | | | |
| J | Shikano North | 75.60 | 24.40 | 0.62 | 18.27 | 17.03 | 64.08 | 67.26 | 0.51 | 6.46 | 76.18 |
| J | Mesa P1 | 80.92 | 19.08 | 0.66 | 10.16 | 22.99 | 66.19 | 83.94 | 0.57 | 5.73 | 87.28 |
| G2 | Wolverine | 79.68 | 20.32 | 0.73 | 12.01 | 21.17 | 66.09 | 70.90 | 0.39 | 4.95 | 75.99 |

carb rec = carbon recovery ad = air dried

TABLE 2

WASHABILITY DATA FOR SAMPLES FROM QUINTETTE AND ELKVIEW

7R1A ELKVIEW

| SG | INC W | CUM WT | INC ASH | CUM ASH |
|---|---|---|---|---|
| 1.3 FLOAT | 10.55 | 10.55 | 2.75 | 2.75 |
| 1.3 - 1.35 | 10.06 | 20.61 | 6.23 | 4.45 |
| 1.35 - 1.4 | 20.14 | 40.75 | 10.36 | 7.37 |
| 1.4 - 1.45 | 6.96 | 47.71 | 15.78 | 8.60 |
| 1.45 - 1.5 | 3.51 | 51.22 | 21.59 | 9.49 |
| 1.5 - 1.6 | 2.98 | 54.20 | 29.03 | 10.56 |
| 1.6 - 1.7 | 2.55 | 56.75 | 39.84 | 11.88 |
| 1.7 SINK | 43.26 | 100.01 | 81.71 | 42.08 |

7R1B ELKVIEW

| SG | INC W | CUM WT | INC ASH | CUM ASH |
|---|---|---|---|---|
| 1.3 FLOAT | 8.81 | 8.81 | 2.66 | 2.66 |
| 1.3 - 1.35 | 11.62 | 20.43 | 6.28 | 4.72 |
| 1.35 - 1.4 | 18.33 | 38.76 | 10.07 | 7.25 |
| 1.4 - 1.45 | 7.14 | 45.90 | 15.16 | 8.48 |
| 1.45 - 1.5 | 5.70 | 51.60 | 19.79 | 9.73 |
| 1.5 - 1.6 | 5.17 | 56.77 | 28.19 | 11.41 |
| 1.6 - 1.7 | 5.63 | 62.40 | 37.31 | 13.75 |
| 1.7 SINK | 37.62 | 100.02 | 73.94 | 36.39 |

8LG ELKVIEW

| SG | INC W | CUM WT | INC ASH | CUM ASH |
|---|---|---|---|---|
| 1.3 FLOAT | 22.06 | 22.06 | 3.26 | 3.26 |
| 1.3 - 1.35 | 25.92 | 47.98 | 6.58 | 5.05 |
| 1.35 - 1.4 | 11.70 | 59.68 | 11.00 | 6.22 |
| 1.4 - 1.45 | 4.17 | 63.85 | 16.06 | 6.86 |
| 1.45 - 1.5 | 3.16 | 67.01 | 20.43 | 7.50 |
| 1.5 - 1.6 | 3.45 | 70.46 | 27.54 | 8.48 |
| 1.6 - 1.7 | 4.40 | 74.86 | 37.21 | 10.17 |
| 1.7 SINK | 25.14 | 100.00 | 60.13 | 22.73 |

10 FW ELKVIEW

| SG | INC W | CUM WT | INC ASH | CUM ASH |
|---|---|---|---|---|
| 1.3 FLOAT | 7.93 | 7.93 | 2.05 | 2.05 |
| 1.3-1.35 | 13.36 | 21.29 | 5.29 | 4.08 |
| 1.35-1.4 | 13.78 | 35.07 | 7.71 | 5.51 |
| 1.4-1.45 | 11.34 | 46.41 | 10.61 | 6.75 |
| 1.45-1.5 | 10.30 | 56.71 | 14.45 | 8.15 |
| 1.5-1.6 | 10.41 | 67.12 | 21.57 | 10.23 |
| 1.6-1.7 | 10.89 | 78.01 | 32.47 | 13.34 |
| 1.7 SINK | 21.99 | 100.00 | 51.04 | 21.63 |

8UXA ELKVIEW

| SG | INC W | CUM WT | INC ASH | CUM ASH |
|---|---|---|---|---|
| 1.3 FLOAT | 20.06 | 20.06 | 2.75 | 2.75 |
| 1.3-1.35 | 13.02 | 33.08 | 7.87 | 4.77 |
| 1.35-1.4 | 15.96 | 49.04 | 13.07 | 7.47 |
| 1.4-1.45 | 5.33 | 54.37 | 21.76 | 8.87 |
| 1.45-1.5 | 11.02 | 65.39 | 26.09 | 11.77 |
| 1.5-1.6 | 15.90 | 81.29 | 32.42 | 15.81 |
| 1.6-1.7 | 6.14 | 87.43 | 40.83 | 17.57 |
| 1.7 SINK | 12.55 | 99.98 | 61.27 | 23.05 |

J SHIKANO NORTH PIT QUINTETTE

| SG | INC WT | CUM WT | INC ASH | CUM ASH |
|---|---|---|---|---|
| 1.3 FLOAT | 8.73 | 8.73 | 2.91 | 2.05 |
| 1.3-1.35 | 17.04 | 25.77 | 5.18 | 4.12 |
| 1.35-1.4 | 36.36 | 62.13 | 9.36 | 7.19 |
| 1.4-1.45 | 8.54 | 70.67 | 15.21 | 8.16 |
| 1.45-1.5 | 4.87 | 75.54 | 20.02 | 8.92 |
| 1.5-1.6 | 2.98 | 78.52 | 24.58 | 9.52 |
| 1.6-1.7 | 2.48 | 81.00 | 28.44 | 10.09 |
| 1.7 SINK | 18.99 | 99.99 | 77.51 | 22.90 |

J MESA PIT QUINTETTE

| SG | INC WT | CUM WT | INC ASH | CUM ASH |
|---|---|---|---|---|
| 1.3 FLOAT | 19.71 | 19.71 | 2.50 | 2.05 |
| 1.3-1.35 | 33.09 | 52.80 | 5.92 | 4.48 |
| 1.35-1.4 | 30.32 | 83.12 | 9.42 | 6.28 |
| 1.4-1.45 | 4.72 | 87.84 | 14.75 | 6.73 |
| 1.45-1.5 | 2.76 | 90.60 | 18.35 | 7.09 |
| 1.5-1.6 | 2.58 | 93.18 | 21.83 | 7.50 |
| 1.6-1.7 | 1.65 | 94.83 | 29.46 | 7.83 |
| 1.7 SINK | 5.18 | 100.01 | 59.76 | 10.57 |

G2 WOLVERINE PIT QUINTETTE

| SG | INC WT | CUM WT | INC ASH | CUM ASH |
|---|---|---|---|---|
| 1.3 FLOAT | 18.41 | 18.41 | 2.69 | 2.03 |
| 1.3-1.35 | 33.46 | 51.87 | 4.37 | 3.55 |
| 1.35-1.4 | 18.99 | 70.86 | 8.55 | 4.89 |
| 1.4-1.45 | 6.34 | 77.20 | 15.00 | 5.73 |
| 1.45-1.5 | 6.33 | 83.53 | 19.89 | 6.79 |
| 1.5-1.6 | 6.89 | 90.42 | 27.37 | 8.36 |
| 1.6-1.7 | 3.58 | 94.00 | 36.34 | 9.43 |
| 1.7 SINK | 6.00 | 100.00 | 66.28 | 12.84 |

10 HW ELKVIEW

| SG | INC WT | CUM WT | INC ASH | CUM ASH |
|---|---|---|---|---|
| 1-1.3 | 12.82 | 12.82 | 1.82 | 2.05 |
| 1.3-1.35 | 17.37 | 30.19 | 5.56 | 4.07 |
| 1.35-1.4 | 26.79 | 56.98 | 9.60 | 6.67 |
| 1.4-1.45 | 20.56 | 77.54 | 13.90 | 8.59 |
| 1.45-1.5 | 10.50 | 88.04 | 18.65 | 9.79 |
| 1.5-1.6 | 6.93 | 94.97 | 24.87 | 10.89 |
| 1.6-1.7 | 2.23 | 97.20 | 34.49 | 11.43 |
| 1.7-2.5 | 2.81 | 100.01 | 63.52 | 12.89 |

8UXB ELKVIEW

| SG | INC WT | CUM WT | INC ASH | CUM ASH |
|---|---|---|---|---|
| 1.3 FLOAT | 7.46 | 7.46 | 3.26 | 2.75 |
| 1.3-1.35 | 10.91 | 18.37 | 6.72 | 5.11 |
| 1.35-1.4 | 15.37 | 33.74 | 11.03 | 7.81 |
| 1.4-1.45 | 7.29 | 41.03 | 16.61 | 9.37 |
| 1.45-1.5 | 7.20 | 48.23 | 21.94 | 11.25 |
| 1.5-1.6 | 5.71 | 53.94 | 29.44 | 13.17 |
| 1.6-1.7 | 4.90 | 58.84 | 39.71 | 15.38 |
| 1.7 SINK | 41.16 | 100.00 | 77.48 | 40.94 |

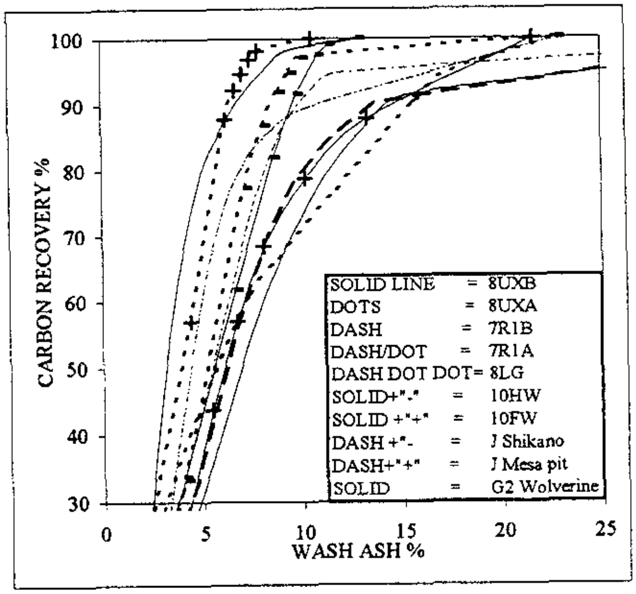


Figure 10. Plot of carbon recovery *versus* wash ash for data from this study.

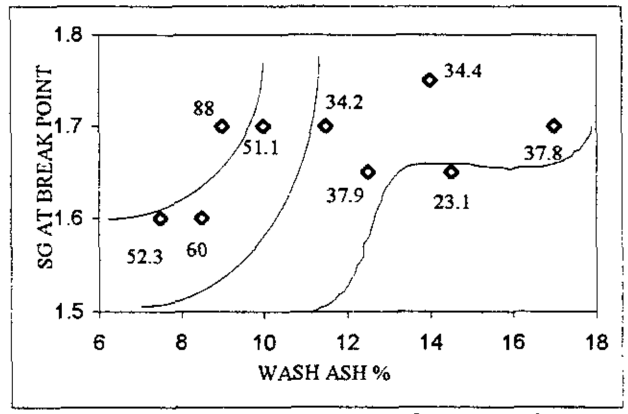


Figure 11. Plot of wash ash *versus* $SG_b$ for samples from this study.

Two samples of 7R1 seam were collected from different areas in the Baldy pit. Samples were subjected to proximate analysis and screened in sizes 10 to 0.5-millimetres and less than 0.5 millimetres.(Table 1). A full washability analysis was performed on the 10 to 0.5-millimetre fraction (Table 2).

## *THE WASH ASH VS CARBON RECOVERY PLOT AND WASHING DIFFICULTY*

The optimum washability number of Sarker and Das (1974), derived from full washability data, can also be predicted with moderate accuracy from a single float-sink analysis using the wash ash and carbon recovery (Ryan, 1992). This means that calculated optimum washability numbers, or estimates of washing difficulty, can be derived from small samples and useful initial estimates made of changes in washing difficulty. Often small drill-core or channel samples are subjected to a standardized float-sink analysis. in which the samples are crushed to minus 9.5 millimetres and all floated at the same specific gravity This provides a good database for illustrating changes in washability

The amount of dispersed mineral matter in a sample is proportional to the wash ash. At any specific gravity, the ash of the float sample may vary from zero to the value corresponding to the ash of a rock-plus-coal mixture with the same density as that of the separating liquid. Higher concentrations of wash ash indicate higher concentrations of dispersed mineral matter. It is also possible to calculate the amount of coal lost in the sink material, providing another estimate of the efficiency of liberation. This term is referred to here as the carbon recovery and is calculated as follows:

$$CR = yld \times (100 - Wa \times K)/(100 - Ra \times K)$$

where K = (weight of mineral matter)/(weight of resultant ash)

Carbon recovery is therefore the ratio of coal in the wash sample to coal in the original sample. The calculation is insensitive to changes in the amount of rock dilution, but sensitive to the amount of dispersed mineral matter which will tend to reduce the carbon recovery. Samples with low contents of dispersed mineral matter will have low wash ash and high carbon recovery values.

Using the full washability data from Table 2, it is possible to construct plots of carbon recovery *versus* wash ash (Figure 10). The curves for individual seams tend to have break points above which carbon recovery is insensitive to increases in wash ash. These break points occur at slightly different ash values, and if carbon recovery is plotted against specific gravity, similar break points are apparent at specific gravities ranging from 1.6 to 1.75. Obviously the concentration of dispersed mineral matter in individual coal particles does not exceed a value fixed by the specific gravity of the break point ($SG_b$). The value $SG_b$ is the optimum SG at which to wash the coal for best carbon recovery and low ash content; unfortunately this does not necessarily mean that the wash ash will meet market specifications. The wash ash values on the x-axis tend to indicate the number of particles contaminated with mineral matter and the value of $SG_b$ tends to indicate the concentration of ash in these particles. Difficult to wash coals will plot in the lower right of the diagram and easy to wash samples in the top left. The data from Elkview and Quintette are presented on this type of plot (Figure 11) which may be useful in demonstrating relative washing difficulty. The plot, however, is still derived using full washability analyses.

The $SG_b$ values are not sensitive to increases in the amount of rock dilution and correspond to the point where particles composed mainly of rock are first incorporated in the wash product. This specific gravity is higher than that corresponding to the optimum washability number. Above the $SG_b$ value, carbon recovery *versus* specific gravity plots for different seams tend to converge; below this value, which varies from about 1.6 to 1.75 SG, the curves tend to follow parallel but different trends. Obviously carbon recovery values for a particular coal seam are more distinct if measured on a sample floated at an SG less than 1.6.

A plot that combines wash ash and carbon recovery measured at a specific gravity of less than 1.6 should provide a good way of separating coals of the same rank based on their washing difficulty. Both parameters are independent of rock dilution and, because they are obtained from a standard proximate analysis, samples have been prepared to a standard size-consist.

This approach was used by Ryan (1992) with moderate success, based upon comparing the carbon recovery *versus* ash plot to previously calculated optimum washability numbers. There was a distinct trend for samples with high washability numbers to plot in the top left of the diagram and those with low values to plot in the bottom right. These samples were analyzed at an SG of 1.5. In the present study, the wash ash *versus* carbon recovery diagram was constructed for data at 1.5, 1.45 1.4 and 1.35 SG. On each diagram the optimum washability numbers were posted next to the appropriate data points. It was found that the best relationship between position of point and optimum washability number was obtained for data plotted at 1.4 SG.

## *INTERPRETATION OF ELKVIEW AND QUINTETTE DATA*

The carbon recovery *versus* wash ash data for the Elkview and Quintette mines measured at a 1.4 SG are plotted on Figure 12. The optimum washability numbers derived from the full washability, are posted next to the points. The positions of the points correspond well with the values of the optimum washability numbers. Contours for optimum

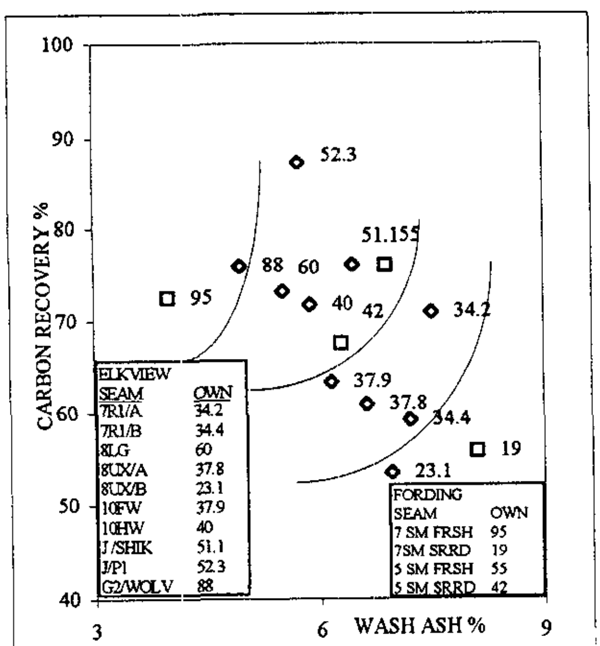


Figure 12. Wash ash *versus* carbon recovery at 1.4 SG for samples from Quintette, Elkview and Fording mines.

washability numbers are sketched onto the figure to illustrate the general trend of increasing optimum washability numbers to the top left of the diagram

There is no reason to assume a perfect correspondence between the position of a point in the figure and the optimum washability number. The two may not correspond exactly and the diagram may be giving a better estimate of washing difficulty than the optimum washability number. For the Quintette data, the diagram separates the more easily washed G seam from the two J-seam samples which plot some distance apart. The Elkview data scatters widely. The seam-10 footwall sample, which is reported to wash better than the hangingwall coal, plots some distance from the 10-seam hangingwall sample. The two duplicate 8UX samples plot quite close to each other, despite the fact that the calculated washability numbers differ. The sample of 8LG collected from the Elk 2 pit washes better than the 8UX samples from Baldy pit. The two samples of 7 seam from the Baldy pit do not appear to have very different washing difficulties and the increase in ash to the west must result mainly from the addition of rock splits which will effect the plant recovery, but not the washing difficulty.

## *EXAMPLES OF VARYING WASHING DIFFICULTY*

Bustin (1982) provides washability data for seams from the Fording mine (Figure 1). The data are used to calculate washability numbers, carbon recovery and wash ash values at 1.4 SG. The data are plotted in Figure 12. The four samples are from two seams, and represent sheared and unsheared coal from each seam. The 7-seam samples, which have optimum washability numbers of 95 and 19, illustrate a significant increase in washing difficulty with shearing. On the other hand ,the washing difficulty of 5 seam (optimum washability numbers 55 and 42) is not much increased by shearing.

Development on the Telkwa property, in northwest British Columbia, has reached an advanced stage and in 1986 Crowsnest Resources Limited submitted a

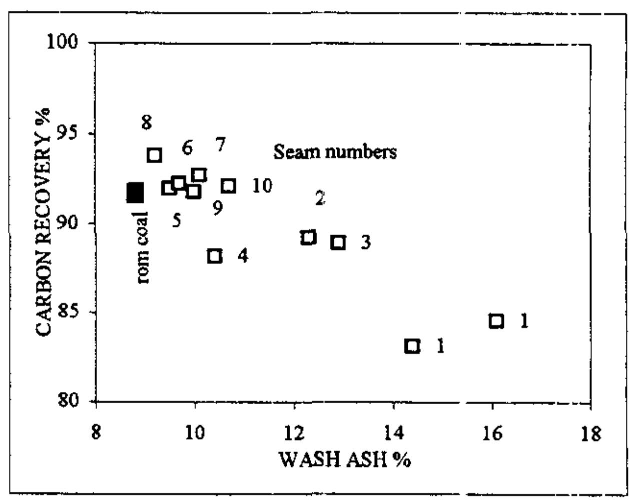


Figure 13. Carbon recovery *versus* wash ash, average data for seams from the Telkwa property, northwest British Columbia.

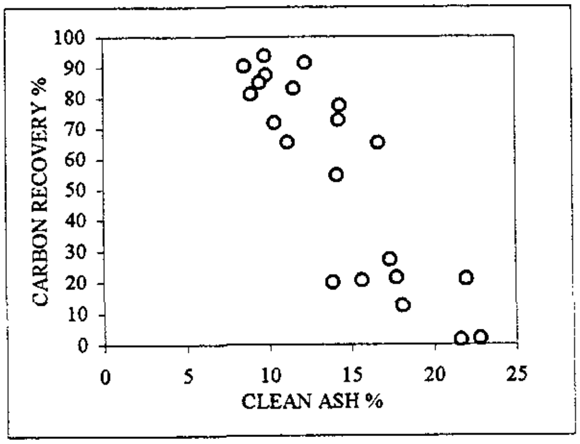


Figure 14. Carbon recovery *versus* wash ash for samples from the Corbin property, southeast British Columbia.

Stage Two Application document describing the geology and proposed mining activities for the area south of the Telkwa River. Averaged raw and wash proximate data for the ten seams in this area were included in the report. A plot of carbon recovery *versus* wash ash indicates that the seams probably have a wide range of washing difficulties (Figure 13). The data plot into clusters with increasing washing difficulty; ( cluster 1 = seams 5,6,7,8, 9, 10; cluster 2 = seams 2, 3, 4; and cluster 3 = seam 1 ). This information should be considered when blending seams for ROM coal.

Data from the Corbin property, adjacent to and south of the Coal Mountain mine in southeast British Columbia (Figure 1), indicate that the coal has a wide range of washing difficulty with high-ash coal being very difficult to wash (Figure 14).

The Quinsam coal mine is located in the Comox coal basin on Vancouver island. Data for the number 1 seam in the 2-north area (Gardner, 1992) can be used to construct a carbon recovery *versus* wash ash plot at 1.4 SG (Figure 15) which has the same axes as Figure 14 for comparison purposes. The number 1 seam in this area washes very easily in comparison to coal from Quintette or Elkview. In the area to the south, the number 1 seam does not wash as well (S.L. Gardner, personnel communication 1995). No comparison can be made with the Telkwa or Corbin data because they were analysed at 1.5 SG in contrast to Quinsam, Quintette, Fording and Elkview data which were analysed at 1.4 SG.

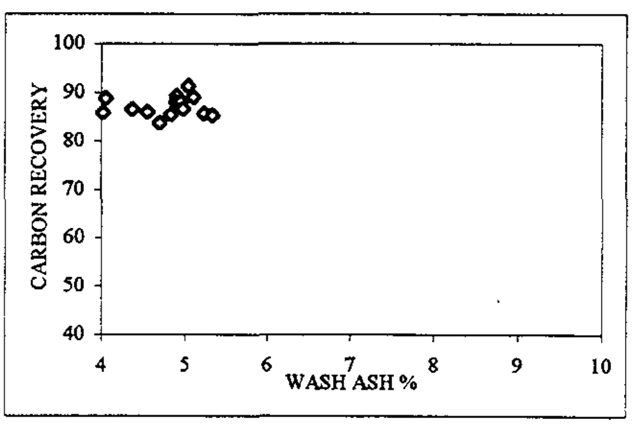


Figure 15. Carbon recovery *versus* wash ash for samples of number 1 seam, Quinsam mine; same scales as Figure 14 for comparison.

## SUMMARY

Washing difficulty is related to the amount of dispersed mineral matter in the coal. There appears to be a correlation between detrital maceral content and the amount of dispersed mineral matter in Cretaceous coals from southeast and northeast British Columbia. Increases in both dispersed mineral matter and detrital mineral abundance may be caused by increased turbulence in coal swamps as a result of off-shore storms. Alternatively increase in detrital vitrinite may result from a change to more reedy vegetation in a dryer swamp. This also may provide a porosity into which dispersed mineral matter can be deposited.

Based upon these observations, there is some correlation between washing difficulty and swamp environment; but this will not be of use to a coal wash plant engineer seeking an easy way to obtain information on the probable washing difficulty of coal from new areas in a mine. This type of information is available from full washability analysis of bulk samples; for convenience, the data may be expressed as a single number such as the optimum washability number of Sarkar and Das (1974). There are some concerns with the optimum washability number and, if a full washability analysis is available, then it might be more useful to calculate the amount of near-gravity material.

In the absence of a full washability analysis, a plot of carbon recovery *versus* wash ash provides reasonable estimates of relative washing difficulty. This information can be cheaply obtained using small samples analysed at a single specific gravity. A more detailed examination of the relationship between carbon recovery and wash ash over a range of specific gravities indicates that data obtained at an SG of 1.4 provide the most accurate assessment of washing difficulty.

The plot is used to illustrate the wide variation in washing difficulty of some Lower Cretaceous coals from British Columbia. Washing difficulty varies on all scales, from mine to mine or within a single seam.

Cretaceous coals, such as those at Telkwa and Quinsam, formed, in an estuarine environment generally wash better. There appears to be more variation of washing difficulty in Telkwa coals than Quinsam coals. The washing difficulty for these coals correlates with the amount of vitrinite A. Possibly mineral matter is post-depositional and is deposited on cleats and microfractures in the vitrinite.

Maximum recovery is achieved when a plant operates under constant conditions and the run of mine coal maintains a constant quality. Frequent adjustments to the operating density in the plant will result in a decrease in recovery. The washing difficulty of seams can vary widely and this information is essential if consistent run of mine blends are to be maintained and plant recovery maximized.

## REFERENCES


Bustin, R.M. (1982): The Effect of Shearing on the Quality of some Coals in the Southeastern Canadian Cordillera; *Canadian Institute of Mining and Metallurgy*, Bulletin, Volume 75, pages 76-83.

Cathyl-Bickford, C.C. (1993): Geology and Petrography of the Wellington Seam, Nanaimo Coalfield Vancouver Island; unpublished M. Sc. thesis, *University of British Columbia*.

Davis, A (1992): Coal Under the Microscope, Deciphering the Influence of Depositional Environment; *Energiia*, Volume 3, Number 6, *University of Kentucky*, Centre of Applied Energy Research.

Dawson, F.M., Ryan, B.D., Pratt, K. and Clow, J.C. (1994): Coalbed Methane Micropermeability Project, Final Report; *Institute of Sedimentary and Petroleum Geology*, IIP publication.

Diessel, C.F.K. (1982): An Appraisal of Coal Facies based on Maceral Characteristics; *Journal of Australian Coal Geology*, Volume 4, pages 474-484.

Gamson, P.D., Beamish, B.B. and Johnson, D.P. (1993): Coal Microstructure and Micropermeability and their Effects on Natural Gas Recovery; *Fuel*, Volume 73, pages 87-99.

Gardner, S.L. (1992): Quinsam Coal Exploration Report; *B.C. Ministry of Energy, Mines and Petroleum Resources*, Coal Assessment Report 815.

Holuszko, M.E. (1993): Washability of Lithotypes from a Selected Seam in the East Kootenay Coalfield, Southeast British Columbia (85J/2); *in* Geological Fieldwork 1992, Grant, B. and Newell, J.M., Editors, *B.C. Ministry of Energy, Mines and Petroleum Resources*, Paper 1993-1, pages 517-525

Kalkreuth, W.D. and Leckie, D.A. (1989): Sedimentological and Petrographical Characteristics of Cretaceous Strandplain Coals: A Model for Coal Accumulation from the North American Western Interior Seaway; *International Journal of Coal Geology*, Volume 12, pages 381-424.

Kalkreuth, W.D., Marchoni, D.L., Calder, J.H., Lamberson, M.N, Naylor, R.D. and Paul, J. (1991): The Relationship Between Coal Petrography and Depositional Environments from Selected Coal Basins in Canada; *International Journal of Coal Geology*, Volume 19, pages 21-76.

Lamberson, M.N. and Bustin, R.M. (1993): Coalbed Methane Characteristics of Gates Formation Coals, Northeastern British Columbia: Effect of Maceral Composition; *American Association of Petroleum Geologists*, Bulletin, Volume 77, pages 2062-2076.

Matheson, A., Grieve, D.A., Holuszko, M.E and Goodarzi, F. (1994): Selected Thermal Coal Basins of British Columbia; *B.C. Ministry of Energy, Mines and Petroleum Resources*, Paper 1994-3.

Renton, J.J. and Cecil, C.B. (1979): Coal Compositional Relationships in Support of the Chemical Coal Model; Carboniferous Coal Guidebook, , Donaldson, A., Presley M.W. and Renton J.J., Editors, *University of West Virginia*.

Ryan, B.D. (1992): Estimation of Coal Washability Using Small Samples; *Journal of Coal Quality*, Volume 11, pages 13-19.

Ryan, B.D. (1994): Calcite in Coal from the Quinsam Mine, British Columbia, Canada; Its Origin, Distribution and Effects on Coal Utilization; *in* Geological Fieldwork 1992, Grant, B. and Newell, J.M. Editors, *B.C. Ministry of Energy, Mines and Petroleum Resources*, Paper 1995-1, pages 243-260.

Sanders, G. J. and Brookes, G. F. (1986): Preparation of the Gondwana Coals; 1. Washability Characteristics; *Coal Preparation*, Volume 3, pages 105-132.

Sarkar,G.G. and Das, H.P. (1974): A World Pattern of the Optimum Ash Levels on Cleans from Washability Data of Typical Coal Seams; *Fuel*, Volume 53, page 74.

Stach, E. Mackowsky, M.-TH., Teichmuller, M., Taylor, G.H., Chandra, D, and Teichmuller, R. (1975): Coal Petrography; *Gebruder Borntraeger*, Berlin.

NOTES

# LIGNITE OCCURRENCES ON THE COAL RIVER, NORTHERN BRITISH COLUMBIA (94M/10)

By Barry D. Ryan

KEYWORDS: Coal River, lignite, coal, peat, clay, energy resource, leonardite.

## INTRODUCTION

Coal River flows south to join the Liard River approximately 150 kilometres east of Watson Lake and 40 kilometres south of the Yukon border (Figure 1). The area has subdued topography and elevations range from about 550 to 600 metres. The river crosses the Alaska Highway at kilometre 858. Coal was first reported in the area by McConnell (1891). At the mouth of Coal River, he found lignite boulders which he describes as being of inferior quality, and spent part of a day traversing up the river to try and find the source. A walk of several miles failed to locate it. He describes Coal River as a "small clear stream about 100 feet wide". The author prefers to describe it as a fast-flowing river, 100 metres wide, which he traversed in a jet boat. McConnell also mentions lignite in an unnamed creek which enters the Liard from the south and is 11 kilometres beyond (west?) of Hyland River. McConnell's account is repeated by Dowling (1915) who did not visit the location and provides no additional data.

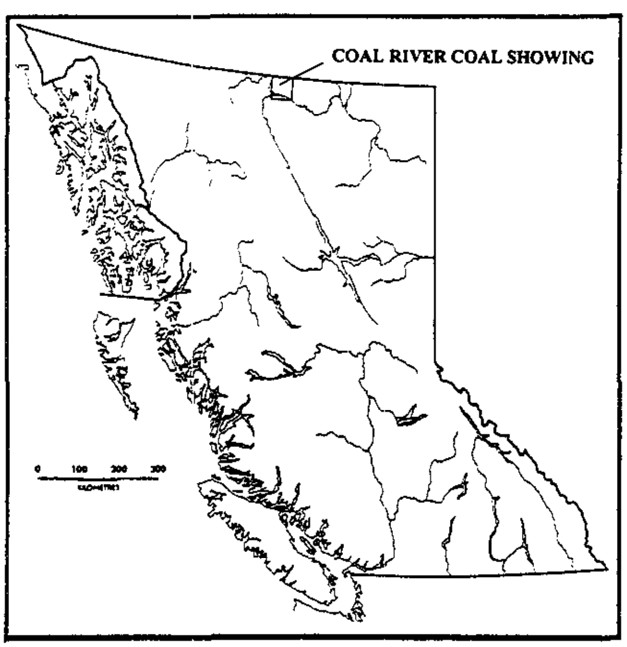


Figure 1. Location map for Coal River.

The source of the lignite was located by Williams and DeLeen prior to 1944 (Williams, 1944) about 10 kilometres (6 miles) as the crow flies up river from the Alaska Highway. At about the same time, crews building the Alaska Highway were using lignite boulders, washed down from the outcrop, for heating in an army camp. Williams found an outcrop of fifteen feet (4.6 metres) of lignite dipping to the southwest at about 25° on the west bank of the river. He states that "the footwall is not visible". Part of the seam was on fire and he describes foul smelling gases and the presence of tar at the surface. The burning area is described as small. He quoted local reports that led him to believe that the lignite extended for several kilometres up river to a falls, but he gave no estimate of the resource. He analyzed a sample of the lignite and also mentioned the extensive deposits of white clay that outcrop on the west side of the river (Photo 1). A test of the clay indicated a cream to grey colour after firing, but no mineral analysis was made.

MacKay (1947) mentions Coal River in a table and assigns it a possible mineable tonnage of 5 million tonnes based on an assumed aereal extent of 0.5 square miles. This assumption is very conservative when compared to the present mapping.

A partial map of the area published by McLearn and Kindle (1950) who outlined an area of about 50 square kilometres possibly underlain by Tertiary lignite-bearing sediments. The area was mapped in 1958 and 1960 by Hugh Gabrielse (1962) who mapped a small area of Tertiary lignite-bearing sediments on Coal River but found no other occurrences in the general vicinity. The area to the north, in the Yukon, was mapped by Douglas and MacLean (1963). According to Campbell (1967) there is the potential for coal in the Watson Lake - Hyland River area but no potential along Coal River in the Yukon. Since 1962 there has been little mapping activity in the area.

No map has been found which locates McConnell's second lignite outcrop near Hyland River to the west. There is a mention of coal in Tatsino Creek 10 kilometres east of Hyland River in Hughes and Long (1979). They also mention Coal River in a discussion of Early Tertiary coal deposits in the Tintina Trench.

## GEOLOGY

The author visited the area in 1989 for half a day and collected samples of lignite float. When dry the lignite has a density not much greater than that of water, and forms tough, matted blocks that are easily transported down river and deposited high on sand banks. In 1990 two days were spent mapping the showing. Generally, Tertiary outcrops are restricted to the river banks and the rest of the area is covered by trees, swamp and a burn zone. The area adjacent to the river is characterized by large crescent-shaped slumps, presumably where younger sediments have slid on the clay layer (Photo 2).

A number of lignite outcrops were located along the river (Figure 2) and are described briefly in Table 1. The main outcrop is on the west bank where the hangingwall section of the seam is exposed with a shallow apparent dip to the south for a length of over 100 metres (Photo 3). Exposure away from the river banks is effectively zero. The full thickness of the seam was not observed in any of the outcrops and the thickness exposed ranges up to over 8 metres at outcrop 46 (Table 2). Generally 3 to 4 metres of lignite are exposed in the outcrops on the west bank. On the east bank the topography is flatter and outcrops less well developed. The operator of the Coal River Lodge said that his water well, drilled near his buildings, intersected 15 metres of coal at a depth of 15 metres. This may or may not be the same seam that outcrops 10 kilometres up Coal River.

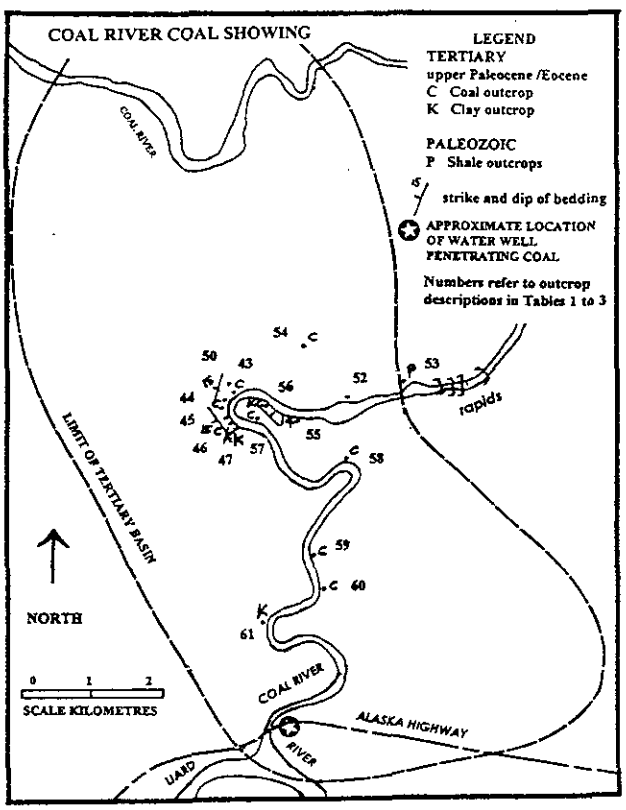


Figure 2. Sketch map of the Coal River lignite showings.

When saturated with water, the lignite has a blocky appearance and is dull, dark brown to black in colour. Resin blebs are visible in some samples. In some outcrops the lignite appears to have dried out and remnants of branches and trunks are visible (Photo 4). These fragments are often aligned and trend 120° to 180°. This orientation may originate with the way the vegetation accumulated in the swamp and is generally quite consistent within a single outcrop.

The lignite is cleated with two sets generally developed. The better developed set scatters but averages an 80° dip to 110°. The second set maintains a very consistent orientation and dips 68° to 033°. Bedding is generally obscure but where visible has a zero to 15° dip, rotating about a northwest-trending axis.

The lignite burning-zone mentioned by Williams is no longer burning and is located on the west bank of the river, near outcrop 44 where lignite is partially coked and overlain by at least 8 metres of baked clay and clinker. In places the ash has melted to form a dark glassy material. The topography in the area is marked by collapse structures were the ground has caved in over the burnt out seam.

On the west bank of the river the lignite is overlain by about 10 metres of white to light grey clay which contains occasional iron-stained surfaces, but otherwise appears to be quite pure. On the east side of the river lignite outcrops are not well exposed and no thickness estimates were made. Here the lignite is underlain by a grey clay. It is assumed, but not proved, that the lignite outcrops on both sides of the river are of the same seam.

Lignite was also located in a borrow pit 0.6 kilometre north of Hyland River on the Alaska Highway. Boulders of lignite up to 1 x 2 metres in size are scattered in a fluvial gravel. Small-sized float was found in the Hyland River below the Alaska Highway

TABLE 2
LITHOLOGICAL SECTION
OUCTROP 46 WEST BANK OF COAL RIVER

| fro | to | thick | Description |
|---|---|---|---|
| 0 | 1 | 0.69 | hanging wall, flaky, brown, dull fusain with 1-2 mm resin blebs |
| 1 | 1.6 | 0.41 | blocky brown dull fusain some resin and plant fragments |
| 1.6 | 2.1 | 0.34 | as above |
| 2.1 | 2.3 | 0.14 | striated bark layer |
| 2.3 | 5 | 1.86 | blocky fusain |
| 5 | 9.5 | 3.09 | patchy outcrop patially covered by soil |
| 9.5 | 10 | 0.34 | bark layer |
| 10 | 12 | 1.38 | blocky fusain, footwall not exposed |
| total thick = 8.2 metres | | | thick = true thickness metres |
| From to measurements are oblique to true thickness section | | | |

TABLE 3
COAL QUALITY DATA: COAL RIVER LIGNITE

| OUTCROP | COMMENTS | $H_2O$% ar | $H_2O$% ad | VM% ad | Ash% ad | FC% ad | CV ad | TS% | PS% | SS% | OS% | |
|---|---|---|---|---|---|---|---|---|---|---|---|---|
| 91-44 | close to burn zone | 42.98 | 14.27 | 48.39 | 4.76 | 32.58 | 5301 | | | | | |
| | | | 0 | 56.44 | 5.55 | 38 | 6183 | | | | | |
| 91-44 | mdst band in lignite | 8.27 | 4.42 | 23.13 | 62.16 | 10.29 | | | | | | |
| | | | 0 | 24.2 | 65.03 | 10.77 | | | | | | |
| 91-46 | lignite with resin | 42.51 | 24.66 | 41.97 | 5.05 | 28.32 | | 0.12 | 0.01 | 0.02 | 0.09 | |
| | | | 0 | 55.71 | 6.7 | 37.59 | | | | | | |
| 91-46 | lignite with bark | 10.92 | 5.81 | 64.16 | 2.33 | 27.7 | | | | | | |
| | | | 0 | 68.12 | 2.47 | 29.41 | | | | | | |
| 91-46 | blocky lignite | 21.13 | 10.43 | 51.21 | 7.2 | 31.16 | 5436 | | | | | |
| | | | 0 | 57.17 | 8.04 | 34.79 | 6069 | | | | | |
| 90-14 | float sample | ND | 10.67 | 47.39 | 9.99 | 31.95 | | 0.19 | | | | |
| | | | 0 | 53.06 | 11.18 | 35.76 | | | | | | |
| 90-15 | float sample | ND | 5.53 | 59.4 | 3.45 | 31.62 | | 0.48 | | | | |
| | | | 0 | 62.88 | 3.65 | 33.47 | | | | | | |
| | | | 0 | 53.9 | 7.4 | 38.7 | 5889 | | | | | |
| GSC | Williams (1944) | softening temperature of ash | | | 1366°C | | | | | | | |
| sample | Ash oxide analysis | $SiO_2$ | $Al_2O_3$ | TiO | $Fe_2O_3$ | CaO | MgO | $Na_2O$ | $K_2O$ | $P_2O_5$ | $SO_3$ | UD |
| 91-46 | lignite with resin | 10.81 | 19.27 | 0.24 | 7.95 | 46.36 | 8.32 | 0.3 | 0.24 | 1.49 | 3.27 | 1.75 |
| ar | Moisture as-received basis | TS% | total sulphur | | SS% | sulphate sulphur | | | | | | |
| ad | moisture air-dried basis | PS% | pyritic sulphur | | OS% | organic sulphur | | | | | | |
| CV | heat value in calories /gram | | | | | | | | | | | |

bridge. There are therefore three possible occurrences of lignite in the general area of Hyland River, these being the locations mentioned by McConnell (1889), Hughes and Long (1979) and the one described above.

## COAL QUALITY

Samples of the lignite were analyzed by Williams in 1944 and by the Geological Survey Branch in 1990 and 1991. The data are presented in Tables 3 and 4. Vitrinite reflectance measurements were difficult to make because of the very low rank. The average of the five mean maximum reflectance measurements obtained is 0.2%, which classifies the material as a peat and not lignite. This is supported by the average volatile matter on a dry ash-free basis which is 75% (Figure 3) but is not supported by the heat value or the as-received moisture measurements, both of which are characteristic of a coal with higher rank. Hughes and Long (1979) classify the coal occurrences in the Watson Lake area to the northwest as peat, based on reflectance measurements of 0.21% and less, but on the basis of proximate data they classify the coal as sub-bituminous C to lignite A. The Coal River data plot within the Watson Lake cluster outlined on their carbon (daf) *versus* reflectance plot (Figure 4). Other Tertiary deposits in the Tintina Trench are of higher rank.

The calorific value averages about 25.12 megajoules per kilogram (6000 calories/gram) for 7% ash on a dry basis, which is high for a peat or lignite. This contradicts the original comment of McConnell that the lignite is of inferior quality. The heat value of the Coal River samples (average reflectance 0.20%) compares favourably with data from other British

TABLE 4
VITRINITE REFLECTANCE: COAL RIVER LIGNITE

| Outcrop | Description | east | north | Elev | Rmax% |
|---|---|---|---|---|---|
| 91-44 | close to burn zone | 614875 | 6619700 | 512 | 0.19 |
| 91-45 | woody fragments | 614600 | 6619475 | 503 | 0.2 |
| 91-46 | blocky lignite | 614575 | 6619375 | 500 | 0.21 |
| 91-51 | blocky lignite | 614900 | 6619800 | 518 | 0.16 |
| 91-54 | lignite | 615800 | 6620300 | 512 | 0.22 |

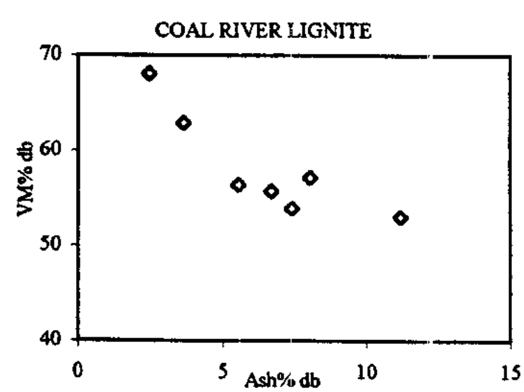


Figure 3. Plot of ash *versus* volatile matter, dry basis, for Coal River lignite data.

Columbian Tertiary deposits such as Tuya River (average reflectance 0.50%, Ryan, 1991), Hat Creek (average reflectance 0.36%; Church *et al.*, 1979) and Rapid River (average reflectance 0.33%, unpublished data, Figure 5). The net calorific value of a Coal River product at 7% ash (dry basis) and 20% moisture would be about 18.6 megajoules per kilogram (4440 calories/gram).

The ash is generally less than 10% on a dry basis, which would be equivalent to less than 15% for a bituminous coal with lower volatile matter. The lignite can therefore be considered to be low in ash. The sulphur averages 0.3% on a dry basis. A single sulphur-forms analysis indicates that about 75% of the sulphur is organic. If all the sulphur is released as $SO_2$ then this amounts to about 5.5 lbs $SO_2/10^6$ BTU (2.4 kilograms per gigajoule) or, if only the pyrite is responsible for $SO_2$ release, this reduces to about 1.4 lbs $SO_2/10^6$ BTU (0.6 kilogram per gigajoule).

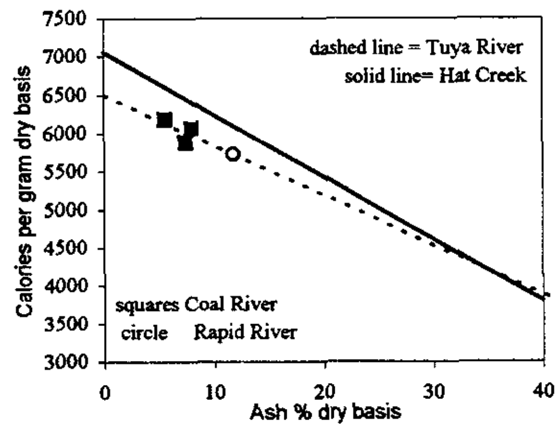


Figure 5. Plot of heat value *versus* ash, dry basis, for a number of Tertiary lignites from British Columbia.

## COAL RESOURCE

The Tertiary basin has a possible area of about 35 square kilometres, as outlined on Figure 2. Most of the lignite outcrops are concentrated in one area on the west side of Coal River but there is a report of a 15-metre intersection of coal in a water well drilled near the mouth of the river. It is possible that the Tertiary basin extends north to cross Coal River above the rapids and outcrop of Paleozoic rocks (Figure 2). This area was not traversed and it should be noted that there are no lignite boulders in the river north of the main outcrops on the west bank. It seems reasonable, based on the thickness data recorded and the possible extent of the basin, to calculate a potential resource by multiplying half the basin area by a lignite thickness of 5 metres. This provides a preliminary resource estimate of about 100 million tonnes of peat/lignite. The indications are that this resource is at shallow depth.

Because of the low calorific value, the lignite would have to be used at source for power generation. Modern integrated gasification combined cycle (IGCC) plants can generate electricity from a wide range of coals (Richards, 1994) with minimum environmental impact.

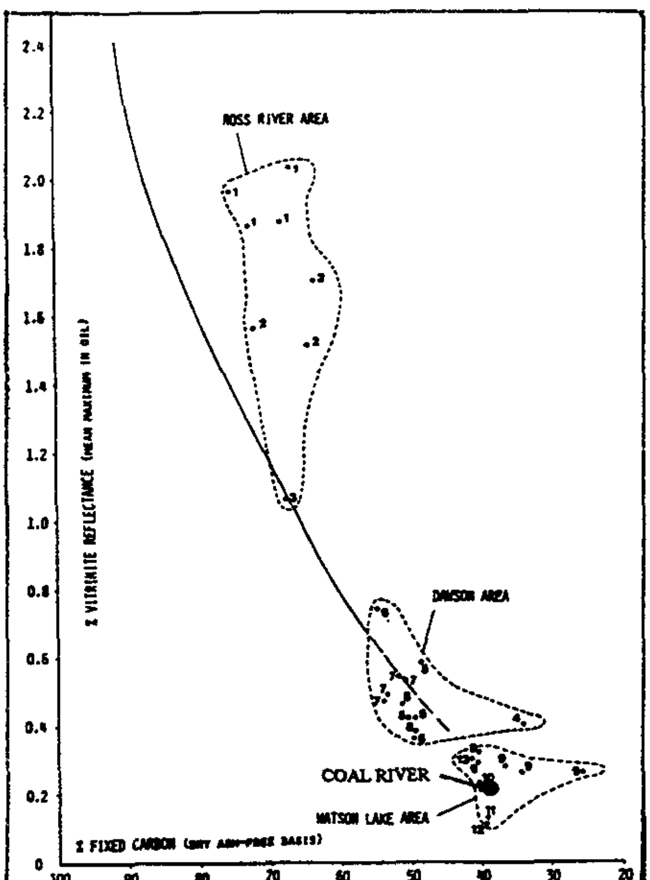


Figure 4. Plot of vitrinite reflectance *versus* fixed carbon from Hughes and Long (1979). Solid line is from McCartney and Teichmuller (1972).

## OTHER POSSIBLE RESOURCES

The lignite is overlain by clay which is at least 10 metres thick in two locations and is a near white, plastic clay with occasional iron-stained surfaces. The clay that underlies the lignite is darker, but still plastic. Table 5 presents XRD and oxide analysis results. It appears that the clay at outcrop 61 is composed mostly of quartz and illite with minor amounts of chlorite, feldspars and carbonates. Iron is present in all analyses, ranging from 2% to 6%. Generally, for industrial uses, iron oxide has to be reduced to less than 1%, which might be difficult in this case because the iron is probably present in the mineral chlorite. If used as a pottery clay and fired, the high iron will produce a dark colour, but otherwise will not effect its properties.

No resource estimate is made for the clay above or below the lignite, but based on the size of the basin and the thickness of the bed,a resource of over 10 million of tonnes is possible.

It is possible that a resource of leonardite exists but in the absence of exploration and testing this remains unproved.

## REFERENCES


Campbell, J.D. (1967): Guide to Coal Deposits, Yukon and MacKenzie District NWT: A Compilation; *Research Council of Alberta*, Edmonton, Alberta, Report 66-6.

Church, B.N., Matheson, A. and Hora, Z.D, (1979): Combustion Metamorphism in the Hat Creek Area, British Columbia; *Canadian Journal of Earth Sciences*, Volume 16, pages 1882-1887.

Douglas, R.J.W. and MacLean, B.C. (1963): Geology of the Yukon and Northwest Territories; *Geological Survey of Canada*, Map 30-1963.

Dowling, D.B. (1915): Coal Fields of British Columbia; *Geological Survey of Canada*, Memoir 69.

Gabrielse, H. (1962): Rabbit River; *Geological Survey of Canada*, Preliminary Map 2-1961.

Hoffman, G.L., Nikols, D.J., Stuhec, S. and Wilson, R.A. (1993): Evaluation of Leonardite and Humalite Resources of Alberta; *Energy, Mines and Resources Canada*, Contract #23403-2-0031/01-XSF.

Hughes, J.D. and Long, D.G.F. (1979): Geology and Coal Resource Potential of Early Tertiary Strata along Tintina Trench, Yukon Territory; *Geological Survey of Canada*, Paper 79-32.

MacKay, B.R. (1947): Coal Reserves of Canada; *Geological Survey of Canada*, Report of the Royal Commission on Coal 1946.

McCartney J.T. and Teichmuller M. (1972): Classification of Coals According to Degree of Coalification by Reflectance of Vitrinite Components; *Fuel*, Volume 51, pages 6-68.

McConnell, R.G. (1891): Report on Exploration in the Yukon and Mackenzie Basins; *Geological Survey of Canada*, Annual Report 1888, 1889, Volume IV, Part D.

McLearn, F.H. and Kindle, E.D. (1950): Geology of Northern British Columbia; *Geological Survey of Canada*, Memoir 259.

Richards, P.C. (1994): Gasification: The Route to Clean and Efficient Power Generation with Coal; *Canadian Institute of Mining Mmetallurgy and Petroleum Bulletin*, Volume 87, pages 135-140.

Ryan, B.D. (1991): Geology and Potential Coal and Coalbed Methane Resource of the Tuya River Coal Basin; *in* Geological Fieldwork 1990, B.C. *Ministry of Energy, Mines and Petroleum Resources*, Paper 1991-1, pages 419-427

Williams, M.Y. (1944): Geological Reconnaissance along the Alaska Highway from Fort Nelson, British Columbia to Watson Lake, Yukon; *Geological Survey of Canada*, Paper 44-28.

NOTES

# SOURCE AND DISTRIBUTION OF PHOSPHORUS IN BRITISH COLUMBIA COAL SEAMS

By Barry D. Ryan and D.A. Grieve

KEYWORDS: Phosphorus, coal, steel, macerals, maceral porosity, phosphorus strip-logs.

## INTRODUCTION

Phosphorus contents of coal from around the world vary although there is a tendency for Permian coals from India and Australia, and Cretaceous coals from Western Canada to have more phosphorus than Carboniferous coals from Europe and USA (Table 1). This may be because of the evolution of vegetation type over geological time or because of the conditions in the coal swamps. Data presented here suggest that most of the phosphorus in coal derives from the original vegetation and, in fact, the amount of phosphorus in coal may be less than expected based on its concentration in vegetation. How the phosphorus is removed from the coal is less clear although a number of possible methods are suggested that infer broad distribution patterns of phosphorus in various lithotypes and macerals. In some cases there is evidence to indicate that phosphorus is concentrated in the inert macerals, but in other cases the evidence is contradictory or ambiguous.

Phosphorus is generally considered an undesirable element in steel, which it makes brittle. It can be removed from the hot metal used to make the steel, but companies generally prefer to control the amount entering the steel-making process. Phosphorus originates in the iron ore, sinter pellets and in the coal used to make blast furnace coke. Steel mills have limited sources of supply of iron ore but can buy coal from a number of suppliers. They therefore sometimes give preference to coals with lower phosphorus contents, and the phosphorus content can have implications on the marketability of coal for coke making. This is generally not the case for thermal coal in which phosphorus contents ranging from 0.1 to 1.5% $P_2O_5$ in ash may be acceptable (Skorupska, 1993).

Limited data indicate that phosphorus is difficult to remove from coal by conventional washing techniques. It is therefore important, in metallurgical coal mines, to understand the distribution of phosphorus in the coal seams, because blending of the run of mine (ROM) coal, rather than washing, may be the best way of controlling the amount in clean coals.

Data collected during this study are not identified with respect to any particular mine and seams are identified by letter, starting with A at the base of the Mist Mountain Formation. The lettering system does not correspond with the seam numbering in any particular mine, but does retain the relative statigraphic positions of all the data discussed in this paper. Samples were collected from the Fording, Greenhills, Elkview and Line Creek mines (Figure 1). At some mines, incremental channel samples were collected across seams. In addition samples of run-of-mine (ROM) and plant-product coal were collected. Coal samples were analyzed for phosphorus, sulphur, sulphur forms, as well as a number of other properties. Samples of hangingwall and footwall rock, and possible tonstein bands, were also collected and subjected to x-ray diffraction and oxide analysis.

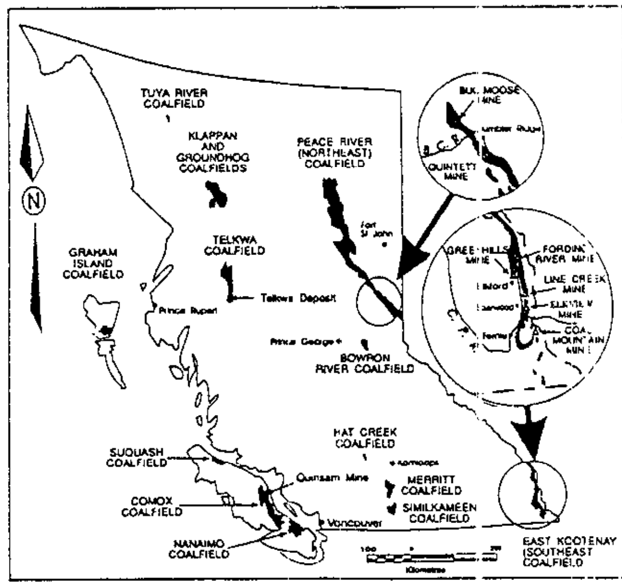


Figure 1. Location map for coal mines and properties in British Columbia.

## PREVIOUS WORK

There is abundant literature on major oxides, minor and trace elements in coal. Unfortunately phosphorus is often neglected in these studies, apparently sometimes not being considered either a trace element, important major oxide or minor element. Also, when data are located, it is often not clear if they are for raw or washed samples. Sometimes the data are expressed as $P_2O_5$ in ash without providing the concentration of ash in the sample, making it impossible to calculate the concentration of phosphorus in the total sample. In short, there is deceptively little useful published phosphorus data.

There have been a number of studies on the occurrence of minor and trace elements in coal, conducted with the goal of classifying the elements into

**TABLE 1**
**PHOSPHORUS CONTENT IN MAJOR COAL BASINS**

| COAL BASIN | COUNT | P ppm | TYPE | AGE | SOURCE |
|---|---|---|---|---|---|
| **World** | ? | 500 | coal | variable | Valkovic (1983) |
| **USA** | | | | | |
| US coals | 32 | 185 | coal | variable | Abernathy & Gibson (1963) |
| Appalachia | 754 | 182 | coal | Carboniferous | Finkleman (1980) |
| Pennsylvania | 31 | 191 | coal | Carboniferous | Abernathy *et al.* (1969) |
| Illinois | 11 | 260 | coal | Carboniferous | Abernathy *et al.* (1969) |
| Arkansas | 10 | 8 | coal | Carboniferous | Haley (1978) |
| Washington | 6 | 763 | coal | Tertiary | Abernathy *et al.* (1969) |
| **Britain** | | | | | |
| Northumberland, England | 33 | 610(122)* | coal | Carboniferous | Asuen (1987) |
| **Australia** | | | | | |
| New South Wales | ? | 310 | coal | Permian | Swaine (1977) |
| Queensland | 11 | 700 | coal | Permian | Queensland Coal Board, (1975) |
| **South Africa** | | | | | |
| Whitbank | 41 | 920 | coal | Permian | Cairncross *et al.* (1990) |
| **India** | 5 | 5640 | coal | Permian | Pareek and Bardhan, (1985) |
| **Japan** | 13 | 400 | coal | Tertiary | Gmelin (1965) |
| **U.S.S.R.** | 427 | 570 | peat | Tertiary | Gmelin (1965) |
| **Canada** | | | | | |
| Nova Scotia | 16 | 63 | coal | Carboniferous | Faurschou *et al.* (1982) |
| Saskatchewan | 9 | 226 | coal | Tertiary | Faurschou *et al.* (1982) |
| **British Columbia** | | | | | |
| Klappan | 16 | 1020 | coal | Cretaceous | Coal Assessment Reports |
| Gething Formation | ? | 630 | coal | Cretaceous | Grieve (1992) |
| Gates Formation | ? | 420 | coal | Cretaceous | Grieve (1992) |
| Mist Mountain Formation | ? | 760 | coal | Cretaceous | Grieve (1992) |
| Telkwa prospect | 66 | 520 | coal | Cretaceous | Matheson *et al.* (1994) |
| Quinsam mine | 14 | 128 | coal | Cretaceous | Matheson *et al.* (1994) |
| Hat Creek prospect | 43 | 176 | lignite | Tertiary | Hill (1990) |
| Tuya River prospect | 2 | 136 | lignite | Tertiary | Ryan (1991) |
| Rapid River prospect | 1 | 65 | lignite | Tertiary | unpublished data |
| Coal River prospect | 1 | 436 | peat | Tertiary | unpublished data |

* data converted to coal basis. P% (coal) = P%(ash) x ash% / 100 assuming 20% ash

those having organic or inorganic affinity. In the classic sense, organic affinity means that the element is part of the organic molecules that make up the coal. In practice, elements that are difficult to remove by conventional washing methods, and tend to remain with the coal, are described as having an organic affinity. These elements may occur in very small mineral grains dispersed in the coal in a way unrelated to the ash content. Consequently the term organic affinity may be somewhat misleading and a better way of describing the occurrence of elements may be to simply to refer to them as elements that follow the coal or the ash during washing. Those following the coal will be difficult to remove and may be a problem for the coal user. Those removed by washing may provide problems for the coal producer when disposing of the tails and coarse reject material.

A number of papers have investigated the distribution of phosphorus in coal. Two of the key papers are by Finkleman (1980) and Gluskoter *et al.* (1977). There is no clear agreement in these papers as to whether phosphorus has organic or inorganic affinities and they suggest a number of possible sources for the phosphorus. The comprehensive paper by Gluskoter *et al.* used washability analysis to assign elements a coal or ash affinity. They found that phosphorus sometimes has an inorganic affinity but in a majority of the cases, follows the coal. Finkleman reviewed existing literature and used x-ray diffraction and scanning electron microscope techniques to identify the modes of occurrence of many elements, including phosphorus, in coal. Powell (1987) suggested that ionic potential can be used to separate elements in organic or inorganic affinities and that, based on this, $P^{3+}$ should have organic affinity and $P^{5+}$ should be inorganic.

Studies of phosphorus in British Columbia coals include Van Den Bussche and Grieve (1990), Grieve and Holuszko (1991) and Grieve (1992). This paper builds on the work of Grieve (1992).

A number of researchers investigated the distribution of elements, including phosphorus, in seam sections. These include Karner *et al.* (1986) who studied the distribution of elements in a North Dakota lignite of Paleocene age and described phosphorus as having an uncertain or inorganic association. Other papers include Harris *et al.* (1981) who studied coals in eastern Tennessee, and Hill (1990) who studied the Hat Creek deposit in British Columbia.

## PHOSPHORUS IN STEEL MAKING

Phosphorus can make some grades of steel brittle, in part because it remains as an oxide impurity. Low phosphorus contents are essential in high-quality construction steels, though it is not always harmful and is added to certain steels to improve machineability or fluidity of castings (Stubbles, 1986).

Phosphorus enters the steel from the iron ore, sinter pellets, coke and in the coal used in pulverized coal injection. Other sources that are sometimes important are recycled sinter from steel making and scrap iron, both of which are added to the blast furnace and concentrate and recycle phosphorus back into the furnace. The phosphorus content of iron ore depends on its origin. Sedimentary hematite ores generally contain less than 0.1% whereas limonite or siderite ores contain up to 1.5%. Magmatic magnetite ores contain the most, ranging up to 2%. Most of the iron ore now mined in the Great Lakes area of North America contains less than 0.05%. The sensitivity of steel mills to phosphorus from sources other than the iron ore depends on the content in the iron ore they use and on what technology they have for removing phosphorus from hot metal. It is generally assumed that all the phosphorus reporting to the blast furnace will end up in the hot metal. Steel mills therefore have two choices, either limit the phosphorus load to the blast furnaces, or remove it from the hot metal later. North American steel mills have limited technology for removing phosphorus and therefore attempt to minimize the load to the blast furnace and attempt to keep the concentration in the hot metal to less than 0.05%. This effectively puts pressure on the coal suppliers to maintain a low concentration of phosphorus in the coal, and some steel mills require concentrations in the coal to be less than 0.03% phosphorus.

In Japan, hot metal is produced with as much as 0.1% phosphorous, but it also has a low silicon content which makes it possible to use various basic fluxes to reduce the phosphorus content of the hot metal to less than 0.01% and sometimes down to 10 ppm. In the U.S., phosphorus contents in the hot metal are kept below 0.05% and less aggressive dephosphorization techniques used to remove it. Stubbles (1986) provides a comprehensive discussion of the sources of phosphorus in steel and different dephosphorization techniques.

It is possible to estimate the contribution that phosphorus from coal makes to the total in the hot metal, because it is all retained in the coke (Mahony *et al.*, 1981). It is therefore possible to calculate the content in the coke by using an estimate of the coke yield, which is often about 78% for western Canadian coals. Coke to hot metal ratios in blast furnaces are dropping with the introduction of pulverized coal injection (PCI) technology. If a coke rate of 350 kilograms per tonne hot metal (THM) is assumed, then it is possible to calculate the amount of phosphorus added from the coke. There is an additional complication in that most geological literature expresses the phosphorus content in coal as percent $P_2O_5$ in the ash. Figure 2 provides a set of curves that estimate the coal-derived phosphorus in the hot metal given the ash content of the coal and the $P_2O_5$ content of the ash. The diagram assumes a 78% coke yield, a 350 kg/THM ratio, and that all the phosphorus from the coke enters the hot metal. As an example, a sample with 0.6% $P_2O_5$ and 9% ash has a phosphorus content in coal of 0.0285% and in the resultant coke of 0.03%. If this phosphorus is added to the hot metal (assuming 350 kg coke/THM) then it will account for 0.0105% phosphorus in the metal. This amount will be added to that already present in the iron ore and the total

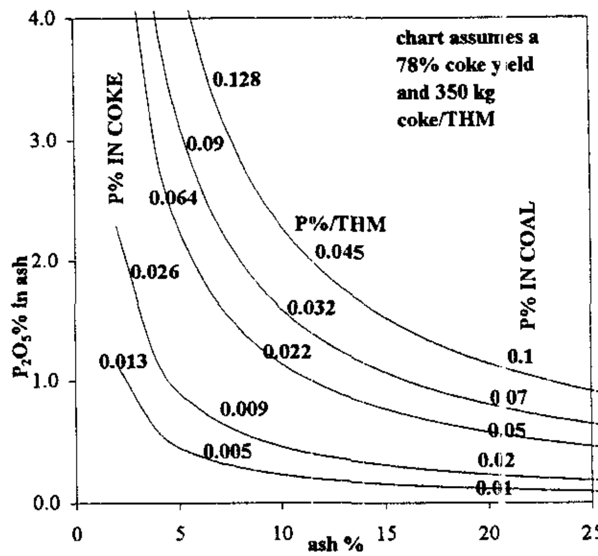


Figure 2. Relationship of $P_2O_5$% in ash to phosphorus in coal, coke and hot metal.

must not exceed the hot metal concentrations acceptable to the steel mills, which are in the range of 0.03%.

## PHOSPHORUS MINERALS FOUND IN COAL

There are a limited number of phosphorus minerals that have been identified in coal; the important ones are described in Table 2. They fall into three major groups: the apatites; the crandallite (plubogummite) group characterized by the presence of aluminum; and the monazites, characterized by the presence of rare earths. Apatite has been reported in a number of western Canadian coals (Grieve, 1992) and is often present as fluorapatite. Apatite averages 17.3% phosphorus and flourapatite contains, on average, 3.5% fluorine. The ratio of fluorine to phosphorus in the apatite can range from 0.0 to 0.2 and for fluorapatite averages about 0.2. This means that a plot of phosphorus *versus* fluorine cannot be used to identify the presence of fluorapatite unless a slope of 0.2 is derived, especially as fluorine has other possible hosts in coal. Plots of phosphorus *versus* fluorine data in Grieve (1992) have slopes ranging from 0.4 to 0.86, indicating a considerable excess of fluorine above that required to make fluorapatite The ratio of $P_2O_5$ /CaO in apatite is more constant than the F/P ratio and averages 0.755. If the $P_2O_5$/CaO ratio exceeds this, then it is very unlikely that the phosphorus is present as apatite and it may be truly organic, present in crandallite group minerals, or in monazite.

The crandallite group includes the minerals gorceixite, goyazite and crandallite. Gorceixite is a barium-aluminum phosphate containing on average, about 10% phosphorus, 20% barium oxide and variable but small amounts of calcium oxide. It is sometimes reported as the phosphorus mineral in coal and has been reported in tonsteins (Grieve, 1983). Strontium is often associated with barium, and the strontium mineral

TABLE 2
PHOSPHORUS MINERAL ANALYSES
from Dana's System of Mineralogy, Palache *et al.* (1951)

| NAME | count | CaO | MnO | $P_2O_5$ | F | Cl | $H_2O$ | $CO_2$ | F/P | P | $P_2O_5$/CaO |
|---|---|---|---|---|---|---|---|---|---|---|---|
| APATITE | 15 | 52.62 | 0.98 | 39.48 | 2.05 | 0.69 | 1.18 | 1.29 | 0.12 | 17.23 | 0.76 |
| formula | | $Ca_5(PO_4)_2(OH,F,Cl)$ | | | | | | | | | |
| | | CaO | $Al_2O_3$ | $P_2O_5$ | BaO | $H_2O$ | CeO | P | Ba/P | | |
| GORCEIXITE | 5 | 1.16 | 34.54 | 23.69 | 19.72 | 14.40 | 2.18 | 10.34 | 1.68 | | |
| formula | $Ba,Al_3(PO_4)_2(OH)_5,H_2O$ | | | | | | | | | | |
| | | SrO | $Al_2O_3$ | $P_2O_5$ | BaO | $H_2O$ | P | Sr/P | | | |
| GOYAZITE | 4 | 19.50 | 37.92 | 24.84 | 2.08 | 14.51 | 10.84 | 1.61 | | | |
| formula | $Sr,Al_3(PO_4)_2(OH)_5,H_2O$ | | | | | | | | | | |
| | | $Ce_2O_3$ | $(LaNd)_2O_3$ | | $Y_2O_3$ | $ThO_2$ | $Fe_2O_3$ | $P_2O_5$ | P | Th/P | |
| MONAZITE | 4 | 28.06 | 30.57 | | 2.77 | 8.24 | 0.70 | 28.18 | 12.30 | 0.63 | |
| formula | (Ce,La,Th)$PO_4$ | | | | | | | | | | |

**TABLE 3**
**CORRELATION COEFFICIENTS OF PHOSPHORUS VERSUS OTHER ELEMENTS**

| REFERENCE | DESCRIPTION | COUNT | Ca | Ba | Sr | F | Th |
|---|---|---|---|---|---|---|---|
| Gluskoter *et al.* (1977) | Illinois | 114 | -0.22 | -0.13 | 0.64 | 0.38 | 0.02 |
| Harris *et al.* (1981) | Eastern Tennesse | 20 | 0.52 | ND | 0.97 | ND | ND |
| | | 44 | 0.22 | ND | 0.93 | ND | ND |
| Hill (1990) | Hat Creek, B.C. | 64 | 0.17 | 0.64 | 0.89 | ND | ND |
| Asuen (1987) | Northumberland, England | 33 | -.042 | ND | -0.128 | ND | 0.177 |

equivalent of gorceixite is goyazite. Crandallite is the calcium end-member. High barium and strontium and low fluorine contents in the ash, probably indicate the presence of gorceixite or goyazite rather than apatite. The strontium and barium in gorceixite and goyazite may originate from interstitial waters, vegetation or weathering of carbonates. Initially the barium and strontium were probably adsorbed onto clays or organic material, but during early diagenesis they were incorporated into phosphate minerals. Gluskoter *et al.* (1977) performed oxide analyses on ashes from a number of coals and produced a correlation matrix which indicates that phosphorus generally has a poor correlation with other elements except for strontium. Harris *et al.* (1981) also found a good correlation of phosphorus with strontium (Table 3). Their incremental samples indicate a wide variation in phosphorus concentrations, but there is a good correlation with the strontium concentrations of the samples, indicating the possible presence of goyazite. Goyazite, on average, has a Sr/P ratio of 1.61 (Table 2) whereas the two seams studied have Sr/P ratios of 0.405 and 0.27. Unfortunately the authors did not measure barium which, if it had also correlated with phosphorus, would have suggested the presence of gorceixite. The correlation of phosphorus to calcium is poor, indicating it is probably not present as apatite.

Phosphorus concentrations in Carboniferous coals from England (Asuen, 1987), are low, averaging 0.06%, and do not correlate with either calcium or strontium concentrations. The phosphorus may be present as gorceixite or monazite, or may be organically bound. Finkelman (1980) reports that monazite occurs in about 50% of the samples he studied and apatites in about 10%. Brown and Swaine (1964) state that phosphorus usually occurs as fluorapatite in Australian coals.

## SOURCES OF PHOSPHORUS IN COALS

Phosphorus in coal originates from four sources; the first three are inorganic and the fourth organic. They are:

As a component of the sediment introduced into the swamp.

As a component of volcanic ash bands (tonstein bands).

As a component of the original vegetation.

From animals or as isolated grains of phosphorus-rich minerals derived from volcanic activity or basement erosion and introduced separately from normal ash material.

After coalification, the phosphorus may be present:

Bound to the coal structure.

As very small disseminated phosphatic mineral grains in the microporosity of the coal.

As a component of ash or tonstein bands.

As coatings on cleat surfaces.

As occasional detrital fragments of phosphorus-rich minerals of extraneous origin.

Figure 3 illustrates the possible inter-relationships between source and location of phosphorus in coal after diagenesis has permitted mobility and recrystallization. The figure also indicates relative ease of removal and whether the amount of phosphorus is likely to correlate with ash, reactive macerals or inert macerals in the coal.

A sediment source implies a correlation with the amount of ash in the seam and an underlying control which relates back to the basement rocks for the coal-bearing stratigraphy. Any phosphorus-rich grains in the ash must be very small so that they are completely mixed with the ash material and are introduced into the swamp in a constant proportion with the ash. If the phosphorus is introduced as a component of tonstein bands, then the coal adjacent to them may also be high in phosphorus. It

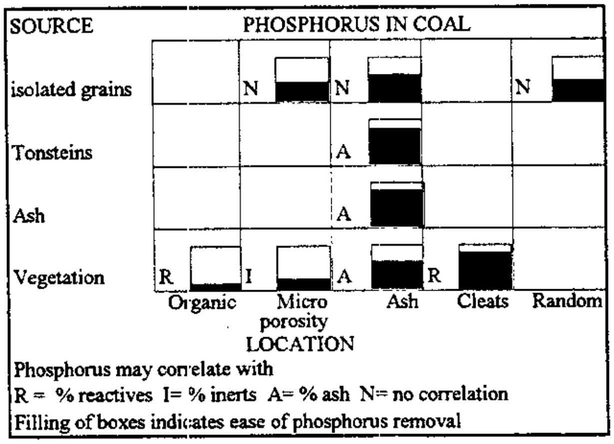


Figure 3. Source *versus* location of phosphorus in coal.

does not seem reasonable that a thin tonstein band can have a marked effect on the phosphorus content of a coal seam 1 to 5 metres thick. Phosphorus introduced as isolated grains will not correlate with either the ash or coal content of the seam. Phosphorus minerals generally have densities 20% to 50% greater than common ash-forming minerals. It is therefore possible to visualize different methods of introducing them into the swamp. The vegetation source may be the most important and it implies a relationship of phosphorus content to the total amount of organic material and probably some sort of underlying maceral control.

In general, it may not be realistic to attempt to distinguish between an extraneous or organic source for the phosphorus by the washing characteristics of the coal or by whether it is now present as identifiable phosphorus minerals.

## *SEDIMENT SOURCE*

The sediment transported into the coal swamp can best be described as a shale and it is therefore important to investigate the phosphorus contents of shales. Wedepohl (1978, Table 15-K-1) provide phosphorus data from a number of sources. The table lists average $P_2O_5$ contents of a variety of rocks and the data for shale are reproduced here in Table 4. The data are remarkably consistent and average 0.15% $P_2O_5$ (or 0.065% P). A number of other papers quote oxide analyses for shales that include $P_2O_5$ contents and average values range from 0.07% (Turekian and Wedepohl, 1961) to 0 18% (Blatt *et al.*, 1980) and 0.26% (Huang, 1962). The data indicate that average $P_2O_5$ contents range from less than 0.1% to 0.3%. This compares to the Clarke number of 0.1050% (Clarke and Washington, 1924). The concentration of $P_2O_5$ in coal ashes is often higher than 0.3%. This is probably because some, maybe most, of the phosphorus reporting as $P_2O_5$ in the ash is actually derived from the coal part of the sample. It certainly appears that the phosphorus in a coal seam can not all be attributed to the ash in the coal if the ash has an average shale content of phosphorus (0.065% or 650 ppm P). This would account for 130 ppm in a coal seam with 20% ash which is low compared to the data in Table 1.

TABLE 4

AVERAGE PHOSPHORUS CONTENTS OF SHALES

| Location | count | av $P_2O_5$ | range |
|---|---|---|---|
| Carboniferous coalfield, Wales | 63 | 0.16 | 0.07-1.24 |
| As above <0.5μ size | 63 | 0.28 | 0.07-1.26 |
| Shale | 78 | 0.17 | |
| Shale | 277 | 0.16 | |
| Paleozoic, Europe | 36 | 0.117 | |
| Paleozoic, Japan | 14 | 0.047 | |
| Mesozoic, Japan | 10 | 0.105 | |
| AVERAGE $P_2O_5$ % | total count 541 | 0.148 | |
| AVERAGE P % | | 0.0646 or 646 ppm | |
| Data from table 15-K-1 in Wedepohl (1978) | | | |

## *TONSTEIN SOURCE*

Tonsteins have been studied as potential stratigraphic markers in coal seams. It is generally believed that most of them are of volcanic origin and that they therefore represent ideal time lines preserved in the coal seams. They could also be ash layers derived from forest fires (B.N. Church, personal communication, 1995). In this case they still provide time lines in the coal seam, but will probably be less extensive than a volcanic ash. In rocks adjacent to the coal seams, the more turbulent and rapid conditions of deposition result in mixing of the ash with other sediments and discrete tonstein bands do not survive. Some tonsteins contain phosphatic minerals and could be a source of phosphorus in coal seams.

A number of authors report oxide analyses on tonsteins from around the world (Table 5).

Generally the $P_2O_5$% concentrations are low except for one tonstein in southeast British Columbia (Grieve, 1983) and four from the Hat Creek deposit in central British Columbia (Hill, 1988) which will be discussed later. Phosphorus in the tonsteins averages 0.09% or 900 ppm, ignoring the Hat Creek data. Based on this average concentration, it is unlikely that tonstein bands that are a minor constituent of coal seams can have much effect on

TABLE 5

PHOSPHORUS CONCENTRATIONS IN TONSTEINS

| Location | Count | Av $P_2O_5$ | Range | Reference |
|---|---|---|---|---|
| NE BC | 43 | 0.19 | 0.02 - 0.96 | Kilby (1984) |
| China | 17 | 0.0164 | 003 - 0.104 | Burger *et al.* (1990) |
| SE BC | 7 | 0.0457 | 0.02 - 0.1 | Ryan and Grieve, this study |
| SE BC | 1 | 4.5 | | Grieve (1983) |
| Spain | 1 | 0.091 | | Bieg and Burger (1992) |
| South Africa | 1 | 1.97 | | Spears *et al.* (1988) |
| Hat Creek | 4 | 11.53 | .49 - 15.58 | Hill (1988) |
| WEIGHTED AVERAGE 0.083 % $P_2O_5$ | | | | |
| AVERAGE P% 0.365 or 3620 ppm | | | | |
| Average minus Hat Creek data is 0.22% P | | | | |

TABLE 6
PHOSPHORUS LEVELS IN VEGETATION

| | Pine | Loblolly Pine | Spruce | Beech | White Oak | Red Oak | Hickory | P ppm in coal |
|---|---|---|---|---|---|---|---|---|
| Phosphorous in ppm | | | | | | | | |
| STEM | | 130 | | | 130 | 130 | 130 | 230 |
| ROOT | | | | | | | | |
| wood | 77 | | | 170 | | | | 220 |
| bark | 330 | | | 220 | | | | 490 |
| TRUNK | | | | | | | | |
| wood | 47 | | 49 | 110 | | | | 125 |
| bark | 300 | | 350 | 650 | | | | 775 |
| BRANCHES | | 220 | | | 280 | 320 | 380 | 535 |
| wood | 50 | | | 220 | | | | 240 |
| bark | 620 | | 140 | 700 | | | | 870 |
| TWIGS | | | | | 390 | 490 | 580 | 870 |
| wood | 240 | | | 700 | | | | 840 |
| bark | 620 | | | | | | | 1110 |
| needles | 11000 | | 1300 | | | | | 2140 |
| leaves | | 1080 | | 1300 | 132 | 1080 | 1400 | 2760 |
| buds | | | | 2300 | | | | 4110 |
| AVERAGE VEGETATION | | | | 2000 | | | | 3570 |

Phosphorus data for vegetation is converted to concentrations in coal assuming
1 No loss of phosphorus.
2 Average carbon in vegetation is 48%.
3 Average carbon in coal is 85%.

the phosphorus content of the whole seam. Spears *et al.* (1988) analyzed a Permian tonstein from West Waterberg, South Africa which has a concentration of 1.97% $P_2O_5$. They suggested that the phosphorus may have originated outside the volcanic ash, in the adjacent organic matter. The anion $PO_4^-$ is precipitated in the ash with cations such as $Ca^{++}$, $Sr^{++}$ and $Ba^{++}$ because of lack of competition from other anions such as $SO_4^-$ which, if present, would have used up the available supply of cations. The same suggestion is made by Spears and Kanaris-Sotiriou (1979) to explain why the phosphorus content of ten out of thirty-one European tonsteins averaged 4.36% $P_2O_5$. Triplehorn (1990) states that aluminum phosphate minerals of the crandallite group (crandallite, gorceixite and goyazite) have been recognized replacing kaolinite in tonsteins. Hill (1988) discusses the possible mobilization of phosphorus into the tonsteins and suggests obliquely that it might come from guano deposits. Based on the high concentrations of barium and strontium in the Hat Creek tonsteins, he identified crandallite and goyazite, often in association with either siderite or ankerite. The suggestion that phosphorus in tonsteins comes from the coal is important because it implies the existence of a mechanism for extracting it from the vegetation before it is turned into coal.

Kilby (1984) studied tonstiens from Lower Cretaceous coals in northeast British Columbia and reports 58 analyses which average 0.19% $P_2O_5$ (0.083% P). Apatite was reported in about 20 samples and gorceixite in seven of the samples (Kilby, 1983). The $P_2O_5$ /CaO ratio indicates that there is excess CaO in the rocks over that required to make apatite. Analyses of 20 tonsteins and ash bands collected during this study average 0.09% $P_2O_5$ (0.039% P). The $P_2O_5$ /CaO ratio indicates that, in most cases, there is sufficient CaO to account for all the phosphorus as apatite. This does not mean that the mineral is present, in fact x-ray diffraction work did not identify any phosphorus minerals. Of the twenty samples, five are specifically identified as tonsteins and they average 0.058% phosphorus, a value not noticeably higher than that expected for average shales.

It appears that tonsteins and ash bands in the Cretaceous coals in British Columbia generally have low concentrations of phosphorus, often lower than the surrounding coal. Exceptions are found in the southeast where Grieve (1983) reports an analysis on a single tonstein with 4.5% $P_2O_5$, BaO >0.5% and SrO >0.5%, indicating the presence of gorceixite. At Hat Creek, Hill (1988) reports four tonstein samples which average 11.53 % $P_2O_5$ and contain crandallite; despite this, Hat Creek lignite is generally not enriched in phosphorus.

## *VEGETATION SOURCE*

Phosphorus occurs in vegetation in low concentrations and is an essential nutrient. Salisbury and Ross (1969) state that higher plants require about 0.2%. Data from this and other sources are compiled in Table 6. The carbon content of the vegetation must also be known before phosphorus contents in vegetation can be compared to contents in coal. Based on data from Ledig and Botkin (1974), the carbon content of dry conifers is about 49.6% and for hardwoods varies from 50% to 53% on a dry basis (Shah *et al.*, 1992). This implies a phosphorus to carbon ratio of about 0.004. Medium-volatile bituminous coals have over 85% carbon on a dry ash-free basis so, if all the phosphorus stays in the coal and the same P/C ratio is maintained, 0.2% phosphorus in vegetation will be equivalent to about 0.36% phosphorus in a coal free of extraneous ash.

Grasses probably have a higher P/C ratio than trees (Marschner, 1986) and this implies possible phosphorus contents in coal averaging over 0.5% (5000 ppm). Contents in dry samples of wheat range from 0.3% to 0.5%, and Wedepohl (1978) provides a table (Table 15-L-7) which lists concentrations for a number of small plants that range from 0.1% to 0.645% on a dry basis.

The phosphorus concentrations in vegetation and the predicted concentrations in coal based upon these levels, assuming no loss of phosphorus, are higher than average concentrations seen in British Columbia coals which are generally less than 0.1% (Grieve, 1992). It appears that there may be a process at work that removes phosphorus during coalification.

Generally there is more phosphorus in deciduous trees than pines and it is not uniformly distributed within a single species. In trees it is concentrated in bark and leaves of a number of different species (Table 6, Kramer and Kozlowski, 1979). This is because the element is an essential plant nutrient and is usually found in those parts of the plant that grow most rapidly. It is also probable that plants growing in difficult climates require more to survive. Plants extract the phosphorus from the soils as orthophosphate derived from minerals such as apatite which is soluble in acid soils.

In a swamp environment, the phosphorus could be recycled upwards from the dead vegetation into the overlying growing vegetation, effectively migrating upwards through the swamp. This may influence its distribution within the coal seam. The concentration of phosphorus in different parts of plants will also influence its distribution in macerals in the coal and any process that separates the macerals may also separate the phosphorus.

## *OTHER SOURCES*

Other sources of phosphorus include guano or animal remains and extraneous grains of phosphatic minerals which may be of volcanic origin or originate from basement rocks. Isolated grains of phosphatic minerals, such as monazite, or animal-derived material, will cause an erratic distribution of phosphorus *versus* ash in the coal seam. This type of phosphorus is probably responsible for the occasional very high values for some samples, irrespective of their ash content. Bones and guano generally have more than 10% $P_2O_5$. Inorganic phosphorus may be introduced as single isolated grains of minerals such as apatite (17% P) or monazite (12.4% P). In this case, phosphorus may correlate with the presence of fluorine, calcium or thorium. The presence of monazite probably indicates an inorganic origin for the phosphorus. Monazite derived from basement rocks often survives as a detrital mineral in sands, eventually being deposited in the coal swamp. Finkleman (1980) states that monazite is generally inorganic, but that if it is authogenic it is characterized by low thorium contents. Apatite, on the other hand, is more often authogenic and the phosphorus may have originated in the vegetation.

If phosphorus is concentrated in apatite, then a single grain of apatite embedded in the coal may noticeably increase the phosphorus content of the sample while having very little effect on the overall ash content. For example, if 0.1% apatite dispersed as discrete grains is added to coal which has a phosphorus content of 0.05% then this will contribute an additional 0.017% phosphorus to the 0.05% already present, increasing the concentration by 36%.

## MOBILIZATION AND REDEPOSITION OF PHOSPHORUS

The amount of phosphorus in coal probably depends, in large part, on the amount in the original vegetation, and on how much of this was mobilized and removed from the coal swamp during early diagenesis. The phosphorus removed from the organic material in the swamp may well be deposited in footwall or hangingwall material, or in ash bands (tonsteins) within the coal. High levels in these materials, or in coal adjacent to them, may be evidence of removal of phosphorus from the rest of the seam rather than contamination of the seam with phosphorus from the surrounding rocks, which generally have low concentrations.

Two basic ways of removing phosphorus from vegetation in a swamp environment are discussed. One invokes mobilizing it by inorganic means at depth in the swamp and the other by using bacteria or fungi at or near the surface.

The removal of phosphorus at depth by inorganic processes probably takes place when the leaf, bark and twig material that contains most of the phosphorus is reduced to a gel in anaerobic and possibly acid conditions. The gel later becomes the maceral vitrinite Under these conditions, Swain (1970) suggests that the phosphorus breaks down to orthophosphate ($HPO_4^-$) and is removed from the rotting vegetation. Organic and inorganic phosphorus can also be dissolved by humic acids generated by the decay of vegetation in anaerobic and acid conditions. Solubility increases in acidified water, especially if concentrations of ferric iron are low, because it tends to form insoluble compounds with phosphorus (Patrick and Khalid, 1974). It appears that phosphorus can be dissolved from organic or inorganic sources in acid or non-acid environments, but it is probably more mobile in acid environments low in ferric iron and calcium-rich clays which can fix phosphorus.

Phosphorus in vegetation can be removed (mineralized) by the action of fungus and bacteria which both generally prefer higher pH conditions that exist near the surface of the swamp. The oxidizing action of bacteria and fungi are responsible, in part, for forming the inert macerals in the coal.

Phosphorus can be fixed organically or inorganically in peat or lignite. Powell (1987) suggests that ionic potential (cation charge/ionic radius) can be used to separate elements into organic and inorganic affinities. He states that $P^{3+}$ is organically bound whereas $P^{5+}$ is more likely to be bound in a phosphate mineral. Thus the trend from acid swamp conditions to less acid, early coal seam environments will be accompanied by a tendency for organic phosphorus to form phosphate minerals.

Inert macerals, in which the vegetation is reduced to a carbon skeleton, are formed by bacterial or fungal attack, or by forest fires. The macerals obviously form in aerobic conditions at the expense of material that would otherwise form vitrinite. The resultant carbonized material retains the original cell structure and probably most of the phosphorus, because it is not volatilized during burning. The maceral will therefore, initially, always have a better mesoporosity (phyteral porosity) than the vitrinite maceral. Phyteral porosity often forms long cylinder-like cavities which are the remains of the cell structures (cell lumen, Gamson *et al.*, 1993). Porosity is maintained in the inert macerals while the vitrinite material is going through a jellification process and has limited porosity. The inert macerals will therefore offer a ready site for the redeposition of phosphorus, as a mineral, at a time when it is most mobile in the pre-coal material. Phosphorus in Australian coals is common as a cell infilling (Cook, 1962; Kemezys and Taylor, 1964) and may therefore concentrate in the inert macerals. Mobilized phosphorus may well crystallize as crandallite group minerals, such as goyazite, based on the good correlation with strontium in coals studied by Gluskoter *et al.* (1977), Harris *et al.* (1981) and Hill (1990) (Table 3).

It is possible that some mobilized phosphorus does not find a home in the inert maceral porosity and it is not clear where it goes. One possibility is that it is recycled upwards, through the decaying vegetation, and continuously reused by the living plants. It may therefore be enriched in hangingwall coal or rock. This has not been seen in this study but is apparent in some of the seam profiles of Gluskoter *et al.* (1977). Spears *et al.* (1988) have suggested a process by which phosphorus can precipitate as a phosphate in adjacent tonstein or ash bands.

The amount of phosphorus in a seam will depend, in part, on the composition of the original vegetation and on how effectively it is mobilized out of the vegetation (proto-vitrinite) and deposited in inert macerals or removed from the swamp. In the absence of a process that forms inert macerals, coals derived from a high proportion of bark, leaves and small plants will be characterized by high contents of formless vitrinite and high contents of organically bound phosphorus that will be very difficult to wash out. Local variations of phosphorus concentrations within the seam may correlate with the inert maceral content in the coal. High contents may be found in fusinite which has the best developed phyteral porosity. Other inert macerals probably lost some of their organic phosphorus by bacterial or fungal activity, but have had secondary phosphorus deposited in the phyteral porosity and may now contain more than the adjacent vitrinite macerals.

It is unlikely that phosphorus is introduced into the coal seam after diagenesis. As the rank increases from lignite to low-volatile bituminous there is a decrease in mass of at least 20% because of the loss of volatile matter. This results in an equivalent increase in concentration of phosphorus from low to high rank coals. In most low rank coals, organic derived phosphorus may show an organic affinity and specifically be concentrated in the inertinite macerals as finely dispersed phosphatic minerals. Over time, as conditions become less reducing, phosphorus may be mobilized and, unable to find porosity in the coal, move out into ash bands, roof or floor rock. There is some indication that phosphorus as carbonate-apitite can deposit on cleats in the latter stages of their formation (Spears and Caswell, 1986). In this study there is a tendency for phosphorus to be associated with siderite which Spears and Caswell consider to be an early diagenetic mineral. The phosphorus associated with oollitic or banded siderite may be mobilized during early biogenic coalification, indicating a diagenetic mobility of phosphorus in association with iron. In acidic conditions, high concentrations of $Fe^{++}$ help to keep the phosphorus in solution. If these solutions move into higher pH environments then siderite and phosphate minerals may precipitate.

## THEORETICAL PHOSPHORUS VERSUS ASH DISTRIBUTIONS

A phosphorus (y axis) *versus* ash (x axis) plot can be used to illustrate various associations of phosphorus in coal, such as the four locations illustrated in Figure 3. If the phosphorus is uniformly distributed in the ash or coal part of the sample, then a plot of the data will scatter along a line with positive slope if it is in the ash and a negative slope if it is in the coal.

The amount of compaction experienced by coal depends on the amount of ash in it. This means that, if phosphorus is introduced into the coal swamp as random extraneous grains, as distinct from ash, then the concentration will increase in the low-ash coal because of increased compaction. Coal compacts at least five times more than adjacent rock and therefore the concentration will be increased by a similar factor in low-ash coal compared to ash bands. In this case phosphorus *versus* ash plots will imply that the phosphorus originates in the coal, which it did not.

Cleats are preferentially developed in low-ash coal and in bright vitrinite-rich lithotypes. Consequently if phosphorus is concentrated on cleats (Spears and Caswell, 1986) then concentrations will increase markedly as ash contents decrease and as the amount of vitrinite in the sample increases.

With the introduction of the possibility of inhomogeneous distribution of phosphorus in porosity in the organic part of the sample, more complicated plots are possible, especially as there is often a correlation between the ash content and the reactives/inerts maceral ratio in the coal, which tends to increase as the ash content decreases. This is illustrated in Figure 4, using data from a number of sources (Gates Formation, northeast British Columbia, Lamberson and Bustin, 1993; Greenhills mine, Holuszko, 1993 and Lower Mist Mountain Formation, Dawson *et al.*, 1994). All the plots show a tendency for the reactives/inerts ratio to increase as the ash decreases below about 10%. If phosphorus is concentrated in the inert macerals, and the reactives/inert

TABLE 7
PHOSPHORUS CONTENTS IN COAL LITHOTYPES

| Coal type | count | P ppm | Location |
|---|---|---|---|
| Durite | 5 | 140 | Ruhr Area, West Germany |
| Vitrite | ? | 200 | Upper Silesia, Poland |
| Vitrite | 6 | 110 | Ruhr Area, West Germany |
| Chanel Coal | 3 | 600 | as above |
| Boghead coal | 1 | 600 | as above |
| Fusite | 3 | 1 100 | as above |
| Fusite | 3 | 99 000* | Upper Silesia, Poland |
| Fusite | 20 | 5 700 | Central England |

* concentration in ash, concentration in coal probably 5 to 10 times lower.

*Data from Table 15-L-10 in Wedepohl (1978). References are listed in the same publication.*

TABLE 8

DULL AND BRIGHT LITHOTYPES HAND PICKED FROM SEAMS G AND J

| Sample | Yield | $H_2O$ | VM% | Ash% | FC% | P% | TS | PS | SS | OS |
|---|---|---|---|---|---|---|---|---|---|---|
| G dull raw | 100 | 0.60 | 22.8 | 16.48 | 60.12 | 0.92 | 0.30 | 0.03 | 0.01 | 0.26 |
| G dull wash | 92.29 | 0.62 | 22.9 | 15.10 | 61.34 | 0.24 | | | | |
| G dull sink | 7.71 | | | 33.00 | | 9.06 | | | | |
| G bright raw | 100 | 0.84 | 24.5 | 5.26 | 69.42 | 0.06 | 0.36 | 0.01 | 0.01 | 0.35 |
| G bright wash | 99.2 | 0.6 | 22.8 | 5.22 | 71.35 | 0.07 | | | | |
| G bright sink | 0.8 | | | 10.2 | | 0 | | | | |
| J dull raw | 100 | 0.68 | 24.9 | 23.25 | 51.53 | 0.15 | 0.50 | 0.02 | 0.01 | 0.48 |
| J dull wash | 79.16 | 0.60 | 26.3 | 20.25 | 52.89 | 0.16 | | | | |
| J dull sink | 20.84 | | | 34.65 | | 0.11 | | | | |
| J bright raw | 100 | 0.69 | 28.4 | 9.28 | 61.66 | 0.16 | 0.52 | 0.01 | 0.01 | 0.51 |
| J bright wash | 91.88 | 1.81 | 29.8 | 5.8 | 62.57 | 0.13 | | | | |
| J bright sink | 8.12 | | | 48.7 | | 0.5 | | | | |

sink data calculated TS = total sulphur PS = pyritic sulphur SS = sulphate sulphur OS = organic sulphur

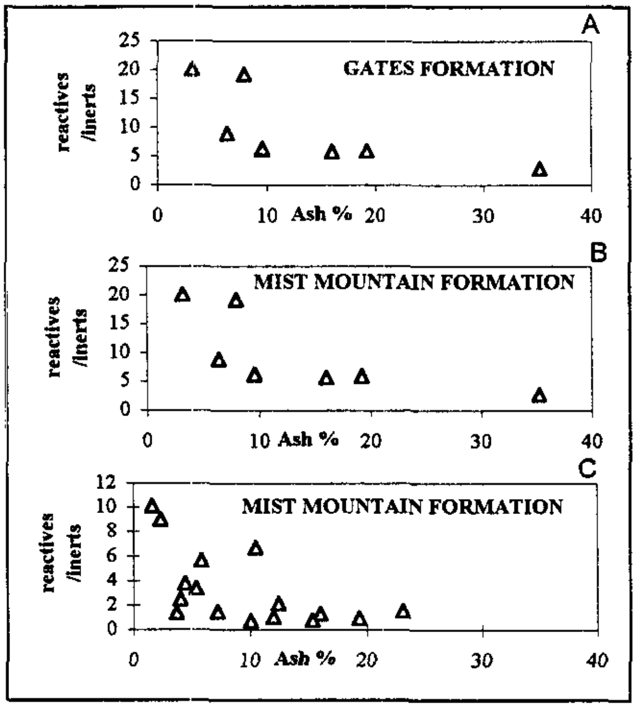


Figure 4. Plots of reactives/inerts ratio *versus* ash content for some British Columbian coals. Data from Lamberson and Bustin (1993)(A), Holuszko (1993)(B) and Dawson *et al.* (1994)(C).

ratio increases as ash content decreases, then the phosphorus concentration reaches a maximum at intermediate ash contents. This is an important distinction from the other plot patterns.

## EVIDENCE FOR A LITHOTYPE AND MACERAL CONTROL ON PHOSPHORUS DISTRIBUTION

There is some evidence in the literature for a lithotype control on the distribution of phosphorus in coal, but it is by no means unambiguous. A number of references are mentioned by Wedpohl (1978), many of which were previously cited by Gmelin (1965). The data (Table 7) indicate that the phosphorus is concentrated in fusite by a factor of five to ten times compared to vitrite. Berger (1958) studied some Russian coals and noted that the concentration of phosphorus in bright coals was eight to ten times less than in dull coals, which are usually ash or inert-maceral rich.

Harris *et al.* (1981) studied the distribution of elements in channel samples through two high-volatile coal seams of Middle Pennsylvanian age in eastern Tennessee. Their paper provides lithotype and petrographic data on an incremental basis though the two seams. There is a tendency for high phosphorus concentrations to correlate with high contents of dull lithotypes and inert macerals, and low contents to correlate with high ash contents. There is a strong correlation of phosphorus with strontium which has been seen in a number of datasets and is interpreted to indicate that much of the phosphorus is occurring as goyazite, which is probably an early diagenic mineral.

During the channel sampling at one of the mines, samples of dull and bright lithotypes were collected from seams G and J (Table 8). In seam G the phosphorus content is high and strongly concentrated in the dull lithotype ( 0.92% P) which contains three times as much ash as the bright lithotype. A 1.5 specific gravity float of the dull lithotype reduced the phosphorus to 0.24% but had little effect on the ash. The calculated composition of the sink material is 9.06% phosphorus and 33 % ash. At this phosphorus concentration, the sink material must contain a high percentage of phosphatic minerals. The dull lithotype from seam J contains much less phosphorus (0.15% P) and about the same amount as the bright lithotype from the seam. Neither the ash nor phosphorus were removed by washing at 1.5 SG. More data are required, but it appears that high phosphorus concentrations are associated with the dull lithotypes and not with the ash in the dull lithotypes.

Run-of-mine and product coal samples from G seam were collected during this study. Samples were screened to various sizes and analysed for phosphorus. In addition, the size fractions of the ROM coal were washed at 1.5 SG and also analysed (Table 9, Figure 5). The ROM coal has ash and phosphorus concentrations of 22% and 0.17%, which are reduced to 8.8% and 0.16% by washing in the plant. Obviously the plant is effective at removing ash, *but not phosphorus, which does not follow the ash.* This could be surprising because there is a strong correlation between phosphorus *versus* ash for the raw size fractions (Figure 5A). This must be an artifact of the data because,

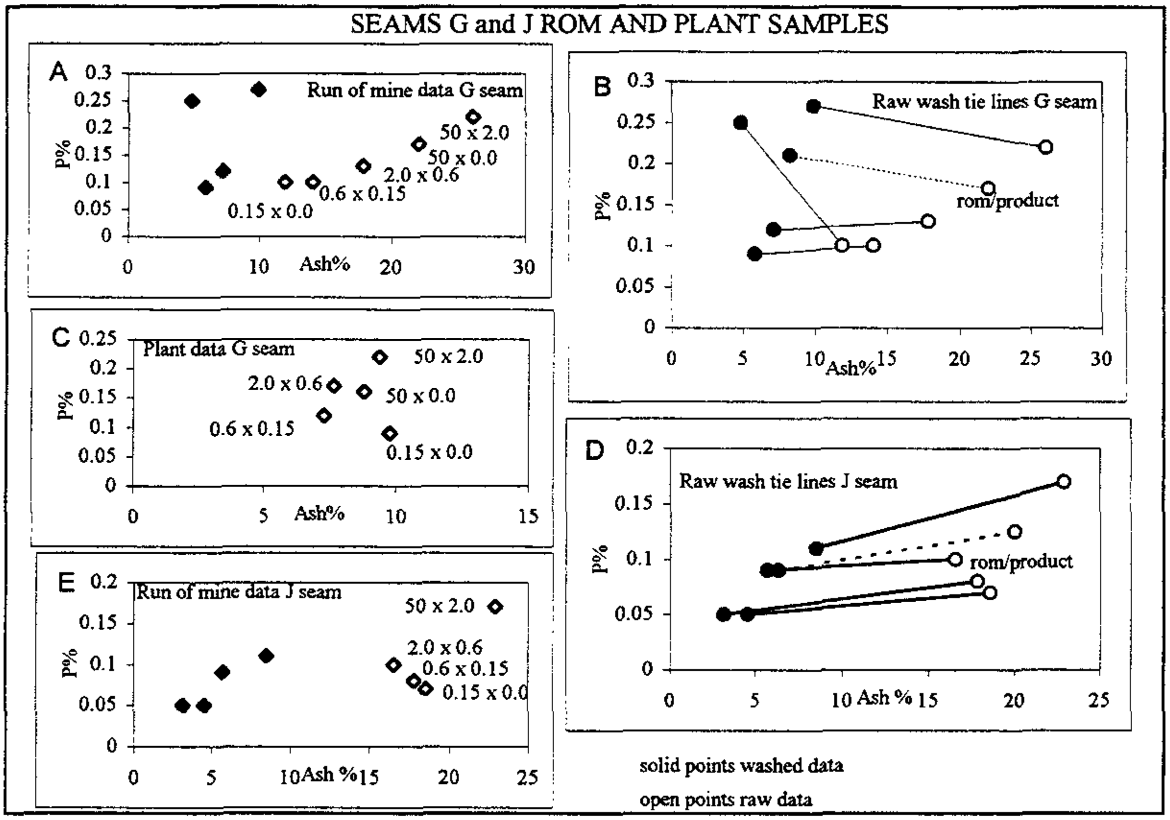


Figure 5. Plots of phosphorus *versus* ash for G and J seam washability data.

TABLE 9
SEAMS G AND J WASHABILITY DATA
All data air-dried basis

| Sample | Weight | float | Yield | $H_2O$% | VM% | Ash% | FC% | P% |
|---|---|---|---|---|---|---|---|---|
| Run of mine G seam | | | | | | | | |
| raw coal | 100 | | 100 | 0.83 | 20.08 | 22.01 | 57.1 | 0.17 |
| 50 x 2.0mm | 59.55 | | 100 | 0.78 | | 18.03 | | 0.22 |
| 50 x 2.0mm | | 1.5 S | 65.42 | 0.75 | | 9.94 | | 0.27 |
| 2.0 x 0.6mm | 17.15 | | 100 | 0.87 | | 17.87 | | 0.13 |
| 2.0 x 0.6mm | | 1.5 S | 79.75 | 1.19 | | 7.22 | | 0.12 |
| 0.6 x 0.15m | 13.27 | | 100 | 1 | | 14.08 | | 0.1 |
| 0.6 x 0.15mm | | 1.5 S | 83.57 | 2.12 | | 5.92 | | 0.09 |
| 0.15 x 0mm | 10.03 | | 100 | 1 | | 11.96 | | 0.1 |
| 0.15 x 0mm | | 1.5 S | 66.33 | 3 | | 4.89 | | 0.25 |
| Plant Product G seam | | | | | | | | |
| Sample | Weight | float | Yield | $H_2O$% | VM% | Ash% | FC% | P% |
| wash coal | 100 | | 100 | 0.99 | 21.16 | 8.83 | 69 | 0.16 |
| 50 x 2.0mm | 37.06 | | 100 | 0.98 | | 9.39 | | 0.22 |
| 2.0 x 0.6mm | 19.29 | | 100 | 1 | | 7.7 | | 0.17 |
| 0.6 x 0.15m | 20.81 | | 100 | 1.07 | | 7.31 | | 0.12 |
| 0.15 x 0mm | 22.84 | | 100 | 1.15 | | 9.79 | | 0.09 |
| Run of mine J seam | | | | | | | | |
| Sample | Weight | float | Yield | $H_2O$% | VM% | Ash% | FC% | P% |
| raw coal | 100 | | 100 | 0.92 | 27.17 | 20.43 | 51.5 | 0.08 |
| 50 x 2.0mm | 46.15 | | 100 | 0.9 | | 22.93 | | 0.17 |
| 50 x 2.0mm | | 1.5 S | 71.85 | 0.6 | | 8.53 | | 0.11 |
| 2.0 x 0.6mm | 22.33 | | 100 | 0.88 | | 16.55 | | 0.1 |
| 2.0 x 0.6mm | | 1.5 S | 81.34 | 0.74 | | 5.73 | | 0.09 |
| 0.6 x 0.15m | 18.61 | | 100 | 0.92 | | 17.83 | | 0.08 |
| 0.6 x 0.15mm | | 1.5 S | 76.22 | 0.87 | | 3.21 | | 0.05 |
| 0.15 x 0mm | 12.9 | | 100 | 1.05 | | 18.57 | | 0.07 |
| 0.15 x 0mm | | 1.5 S | 62.97 | 0.77 | | 4.59 | | 0.05 |

when the product coal is plotted in Figure 5C, there is a wide variation of phosphorus contents but little change in ash content.

The underlying control on phosphorus content is not the ash but the inert maceral content of the coal which increases in the coarse size fractions in both the ROM and washed coal. The vitrinite maceral is more brittle and always fractures into smaller fragments and concentrates in the finer sizes when a sample is crushed and screened. Both the ash and the phosphorus tend to locate in the phyteral porosity in the inert macerals, but it is more difficult to dislodge phosphorus than ash. Consequently the ROM data appear to indicate an ash affinity for the phosphorus when, in fact, both the ash and phosphorus have an affinity for the porosity in the inert macerals which concentrate in the coarser sized coal once it is crushed and screened.

The maceral compositions of the G seam samples described in Table 9 were determined (Table 10). The results are preliminary, are based on 500 point counts per sample and are expressed on a mineral-matter-free basis. Inert macerals are concentrated in the coarser size fractions and the inert maceral content correlates with phosphorus in the samples. Mineral infilling in the cells preserved in the fusinite and semifusinite is clearly visible and based on the correlation in Figure 6 must consist largely of a phosphorus mineral.

The petrography for samples from southeast British Columbia was determined in Dawson *et al.* (1994). These samples were analysed for phosphorus during this study, to make use of the existing petrographic information. The samples (Table 11, Figure 7) are from seams A lower, A upper, P and Y. Individual samples were separated into a number of SG splits; raw(r), 1.4 SG float(f), 1.4-1.6 SG middlings(m) and 1.6 SG sink(s).

TABLE 10
PETROGRAPHY FOR G SEAM, WASHABILITY DATA

| | mineral matter free maceral percentages | | | | | |
|---|---|---|---|---|---|---|
| | Vitrinite | | Semi | | Total | Total |
| sample | A | B | Fusinite | fusite | reactives | inerts |
| run-of-mine G seam | | | | | | |
| 50 x 0.0mm R | 52.4 | 20.9 | 21.8 | 4.5 | 73.3 | 26.3 |
| 50 x 2.0mm R | 47.1 | 23.3 | 19.4 | 10 | 70.4 | 29.4 |
| 50 x 2.0 F | 31.1 | 31.9 | 24.8 | 12.1 | 63 | 36.9 |
| 2.0 x 0.6m R | 52 | 21 | 21.2 | 5.6 | 73 | 26.8 |
| 2.0 x 0.6m F | 46.1 | 28.8 | 18.7 | 6.3 | 74.9 | 25 |
| 0.6 x 0.15m R | 55.3 | 24.6 | 15.5 | 3.3 | 79.9 | 18.8 |
| 0.6 x 0.15m F | 46.7 | 34.7 | 14 | 3.3 | 81.4 | 17.3 |
| plant product G seam | | | | | | |
| 50 x 2.0mm W | 25 | 51.3 | 17.4 | 6.4 | 76.3 | 23.8 |
| 2.0 x 0.6m W | 44.3 | 25.8 | 25.8 | 3.1 | 70.1 | 28.9 |
| 0.6 x 0.15m W | 46.9 | 41.5 | 6.3 | 5.3 | 88.4 | 11.6 |
| R = raw sample F= 1.5 SG float sample | | | | | | |
| W= plant washed sample | | | | | | |

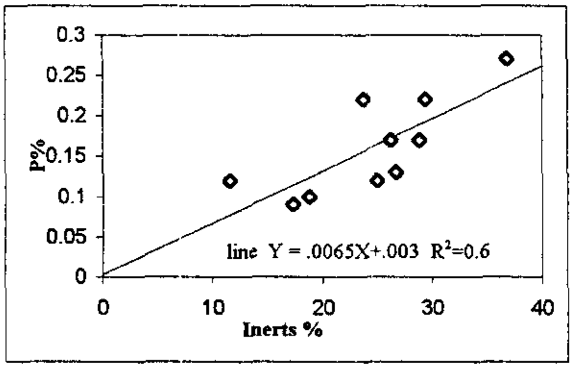


Figure 6. Plot of phosphorus *versus* inerts for G seam, washability samples.

The middling splits are enriched in the inert macerals relative to other splits from the same seam and consequently there is a range of maceral composition for the splits from each seam. Attempts were made, using the four splits from each seam, to predict the phosphorus content of each split by assigning phosphorus concentrations to the ash, reactive and inert components of each split. In sample A lower, the phosphorus is uniformly distributed, whereas in seams P and Y it is concentrated in the inerts. A plot of predicted *versus* measured phosphorus (Figure 7) indicates that apart from one split, a good match is achieved. Split Y(sink) obviously contains phosphorus liberated from the other Y seam splits. The data appear to indicate that phosphorus is preferentially concentrated in the inert macerals in each seam, although in some cases it is coarse enough to be liberated and its original association is not known. It is interesting to note that if all the data are examined on a phosphorus *versus* inert maceral plot, there is no apparent relationship because of the wide range of concentrations in the inert macerals from the different seams.

The data of Gluskoter *et al.* (1977) can be interpreted to indicate a maceral control on the phosphorus concentrations in the samples they considered to have organic affinity. They studied the organic *versus* inorganic affinity of phosphorus in eight

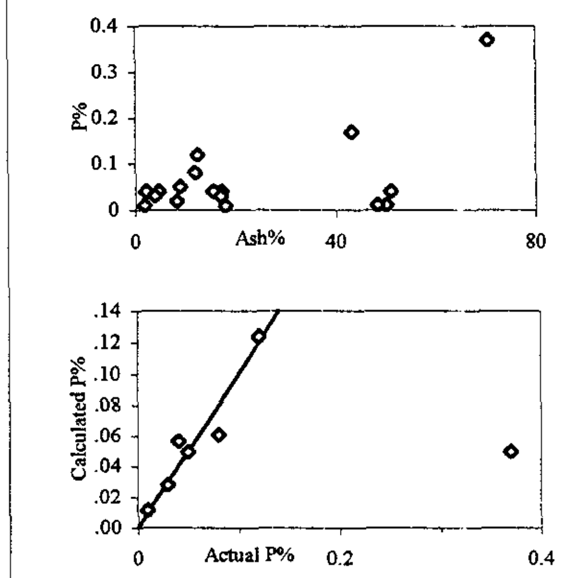


Figure 7. Phosphorus and ash data for different specific gravity splits of samples. Data from Dawson *et al.* (1994).

samples, by measuring the concentration in different density splits. Obviously the ash increases as the density increases and, if the concentration of phosphorus also increases with specific gravity then this indicates an ash affinity and the reverse indicates an organic affinity. Of the eight samples analyzed, Gluskoter assigned five samples organic affinity, one intermediate and two inorganic affinity. It is interesting to plot the phosphorus contents *versus* specific gravity for each sample (Figure 8). Two plots show a trend of continuously increasing phosphorus concentration as the specific gravity increases. Some of the other plots actually show a maximum phosphorus concentration at intermediate values. This indicates an organic affinity, but it is surprising that the maximum phosphorus concentration does not occur in the lowest density sample with the lowest ash.

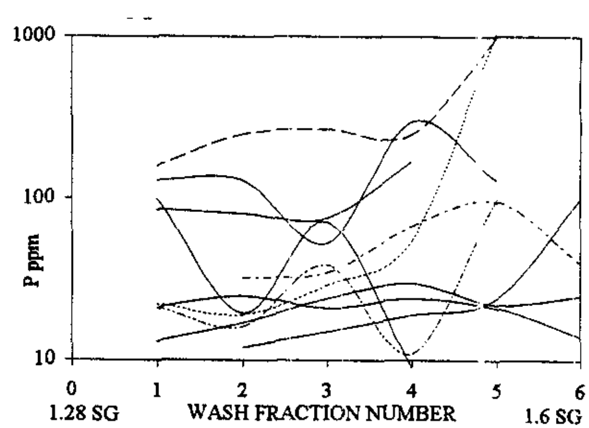


Figure 8. Phosphorus *versus* specific gravity plots for data from Gluskoter *et al.* (1977).

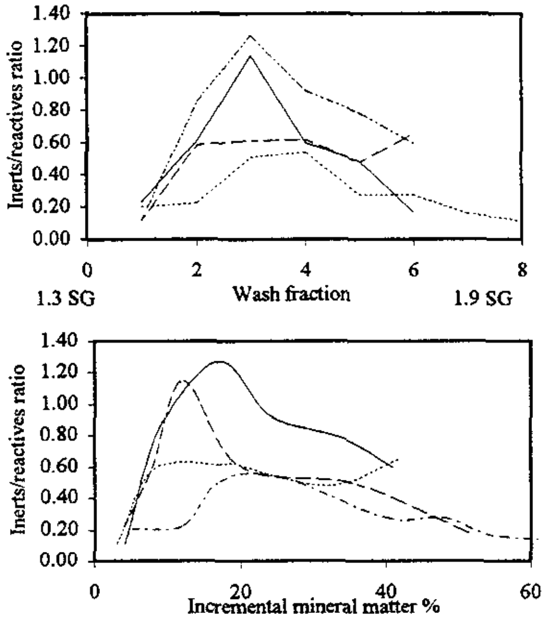


Figure 9. Plot of inerts/vitrinite ratio *versus* specific gravity and incremental ash. Data from Bustin (1982).

Washing a coal at different specific gravities produces maceral fractionation in which the inerts/vitrinite ratio reaches a maximum at intermediate values, as illustrated by data in Table 11 and from Bustin (1982; Figure 9). If the phosphorus is concentrated in the inert macerals then this explains the phosphorus-ash relationships obtained by Gluskoter *et al*. It appears that in a group of samples with a range of ash contents, either naturally occurring (Figure 4) or produced by washing the samples (Figure 9), the inert /reactives ratio will be at a maximum at intermediate ash concentrations. In both cases, if phosphorus is concentrated in the inert macerals then a maximum will occur in samples of intermediate ash concentration.

Many phosphorus *versus* ash and phosphorus *versus* specific gravity distributions can be explained by an inhomegeous distribution of phosphorus between the coal macerals. Because of the preference for both phosphorus and ash to locate in the inert macerals, phosphorus sometimes appears to have an ash association, but only in samples containing low and intermediate ash concentrations. Also because, the concentration of phosphorus in inerts in different seams varies widely, a phosphorus *versus* inerts relationship may only be apparent in closely related samples.

## ASH-PHOSPHORUS DISTRIBUTIONS IN BRITISH COLUMBIAN COALS

There are a number of datasets for coals from British Columbia that can be used to illustrate data patterns in phosphorus *versus* ash plots (Figure 10). Data for Tertiary lignites from Hat Creek (Hill, 1990) form a scatter with maximum phosphorus at about 25% ash and less in samples with more or less ash. Data for high-volatile coals comes from the Cretaceous Telkwa and

TABLE 11
PETROGRAPHY AND PHOSPHORUS DATA

| Sample | yield | ash | P% | T R | T I | ratio I/R | SR | SI | P%[1] |
|---|---|---|---|---|---|---|---|---|---|
| best fit P concentrations | | | | ash= | .040 | reacts= | .040 | inerts= | .040 |
| A-1/r | 100.0 | 17.12 | .040 | 57 | 43 | 0.75 | 47.24 | 35.64 | .040 |
| *A-1/f* | *41.6* | *4.61* | *.040* | *79* | *21* | *0.27* | 75.36 | 20.03 | .040 |
| A-1/m | 41.8 | 15.38 | .040 | 44 | 56 | 1.27 | 37.23 | 47.39 | .040 |
| A-1/s | 16.6 | 50.92 | .040 | 48 | 52 | 1.08 | 23.56 | 25.52 | .040 |
| A-2/r | 100.0 | 16.98 | .030 | 47 | 53 | 1.13 | 39.02 | 44.00 | .042 |
| A-2/f | 28.9 | 8.19 | .020 | NA | NA | | | | |
| A-2/m | 60.5 | 17.88 | .010 | NA | NA | | | | |
| A-2/s | 10.6 | 43.24 | .170 | calc | NA | | | | |
| best fit P concentrations | | | | ash= | .006 | react= | 0 | inerts= | 0.09 |
| P/r | 100.0 | 3.90 | .030 | 71 | 29 | 0.41 | 68.23 | 27.87 | .028 |
| P/f | 76.2 | 1.80 | .010 | 91 | 9 | 0.10 | 89.36 | 8.84 | .012 |
| P/m | 21.8 | 8.87 | .050 | 42 | 58 | 1.38 | 38.27 | 52.86 | .050 |
| P/s | 2.0 | 48.20 | .011 | calc | | | | | .003 |
| best fit P concentrations | | | | ash= | .000 | react= | 0 | inerts= | 0.40 |
| Y/r | 100.0 | 12.02 | .080 | 87 | 13 | 0.15 | 76.54 | 11.44 | .061 |
| Y/f | 77.9 | 2.12 | .040 | 90 | 10 | 0.11 | 88.09 | 9.79 | .057 |
| Y/m | 11.6 | 12.50 | .120 | 68 | 32 | 0.47 | 59.50 | 28.00 | .124 |
| Y/s | *10.5* | 70.46 | *.370* | *61* | 39 | *0.64* | *18.02* | *11.52* | *.050* |

calc = data calculated P%[1] = calculated P — r = raw data
TR = total reactives mineral-matter-free basis — f = float data
TI = total inerts mineral-matter-free basis — m = middlings data
SR = reactives in sample — s = sink data
*SI = inerts in sample*

Quinsam properties (Matheson *et al*., 1994) which are of similar age and depositional environment, although Telkwa samples, which contain more inert macerals, have the higher phosphorus concentrations. Data for medium-volatile coals are from the present study and Grieve (1992). Most of the data plot in triangular distributions with maximum phosphorus occurring at intermediate ash concentrations. The Klappan property provides data for high-rank coals (Coal Assessment Reports 110, 111 and 748). These data indicate a weak tendency for phosphorus content to increase as ash content increases. In most of the plots, there is no indication of phosphorus concentrating in the pure coal or ash components of the samples.

The predominance of the triangular scatter pattern is probably caused by a combination of two factors. The phosphorus tends to concentrate in the inert macerals and the reactives/inerts ratio tends to decrease with increasing ash. The combined effect of these two variables is to produce maximum phosphorus concentrations at intermediate ash concentrations as hypothesized by the model developed above.

## IN-SEAM PHOSPHORUS VARIATION

As part of this study, incremental seam samples were collected from five sites at one mine and three sites at another. The distribution of phosphorus within a seam may provide clues to its origin, and the information may also be useful if selective mining is considered. Additional data have been collected from a number of sources to provide a database of phosphorus distribution within seams. Samples collected as part of this study were analyzed for raw proximate, sulphur and phosphorus.

TABLE 12

AVERAGE QUALITY FROM INCREMENTAL AND GRAB SAMPLE TRENCH DATA

length weighted average data

| seam | count | $H_2O$ ad | Ash% | VM% | FC% | TS | PS | SS | OS | P% | Yield | $H_2O$ ad | Ash% | VM% | FC% | P% |
|---|---|---|---|---|---|---|---|---|---|---|---|---|---|---|---|---|
| A fw | 1 | 0.7 | 17.56 | 18.47 | 63.3 | | | | | 0.07 | 56.14 | 0.76 | 6.28 | 22.29 | 70.67 | 0.04 |
| A hw | 1 | 0.65 | 10.89 | 19.52 | 68.9 | | | | | 0.01 | 68.53 | 0.72 | 5.94 | 22.26 | 71.08 | 0.01 |
| C-1 | 1 | 0.58 | 20.29 | 21.11 | 58 | | | | | 0.08 | 52.51 | 0.7 | 6.7 | 25.52 | 67.08 | 0.08 |
| C-2 | 1 | 0.59 | 32.97 | 16.97 | 49.5 | | | | | 0.15 | 38.98 | 0.68 | 7.13 | 21.69 | 70.5 | 0.13 |
| D-1 | 1 | 0.55 | 35.2 | 16.41 | 47.8 | | | | | 0.17 | 50.35 | 0.75 | 7.44 | 21.87 | 69.94 | 0.2 |
| D-2 | 1 | 0.64 | 32.25 | 17.22 | 49.9 | | | | | 0.07 | 43.75 | 0.7 | 7.28 | 21.55 | 70.47 | 0.07 |
| D-3 | 1 | 0.65 | 21.14 | 19 | 59.2 | | | | | 0.12 | 61.62 | 0.74 | 5.64 | 23.49 | 70.13 | 0.1 |
| E | 10 | 0.77 | 14.2 | 20.95 | 62.4 | 0.27 | 0.013 | 0.01 | 0.25 | 0.15 | 81.11 | 0.53 | 8.81 | 22.02 | 66.94 | 0.103 |
| G-1 | 12 | 0.52 | 17.94 | 22 | 59.5 | 0.5 | 0.013 | 0.01 | 0.49 | 0.04 | 75.79 | 0.41 | 9.73 | 22.76 | 67.1 | 0.029 |
| G-2 | 8 | 0.59 | 17.78 | 23.04 | 58.59 | | | | | 0.20 | 81.22 | 0.68 | 8.76 | 25.17 | 65.40 | 0.18 |
| G[1] | 1 | dry | 13.74 | 23.29 | 63 | | | | | 0 | | | | | | |
| I | 13 | 0.94 | 11 | 21.06 | 64.1 | 0.31 | 0.01 | 0.01 | 0.3 | 0.08 | 85.17 | 0.43 | 5.34 | 22.76 | 68.61 | 0.086 |
| J-1 | 3 | 0.66 | 31.12 | 21.92 | 46.3 | | | | | 0.05 | 62.92 | 1.01 | 7.09 | 28.21 | 63.69 | 0.09 |
| J-2 | 4 | 0.55 | 19.15 | 22.56 | 57.75 | | | | | 0.06 | 76.58 | 0.52 | 8.92 | 24.69 | 65.88 | 0.10 |
| L | 11 | 0.9 | 6.94 | 24.7 | 57.4 | 0.6 | 0.02 | 0.01 | 0.57 | 0.03 | 82.85 | 0.78 | 4.37 | 26.14 | 58.56 | 0.024 |
| L[1] | 1 | dry | 46.17 | 16.6 | 37.2 | | | | | 0.081 | | | | | | |
| O | 17 | 1.16 | 9.14 | 31.06 | 58.6 | 0.43 | 0.073 | 0.02 | 0.34 | 0.05 | 92.85 | 0.63 | 5.11 | 34.22 | 65.39 | 0.043 |

G[1] = Data from Bonnell *et al.* (1984) TS = total; PS = pyitic; SS = sulphate and OS = organic sulphur

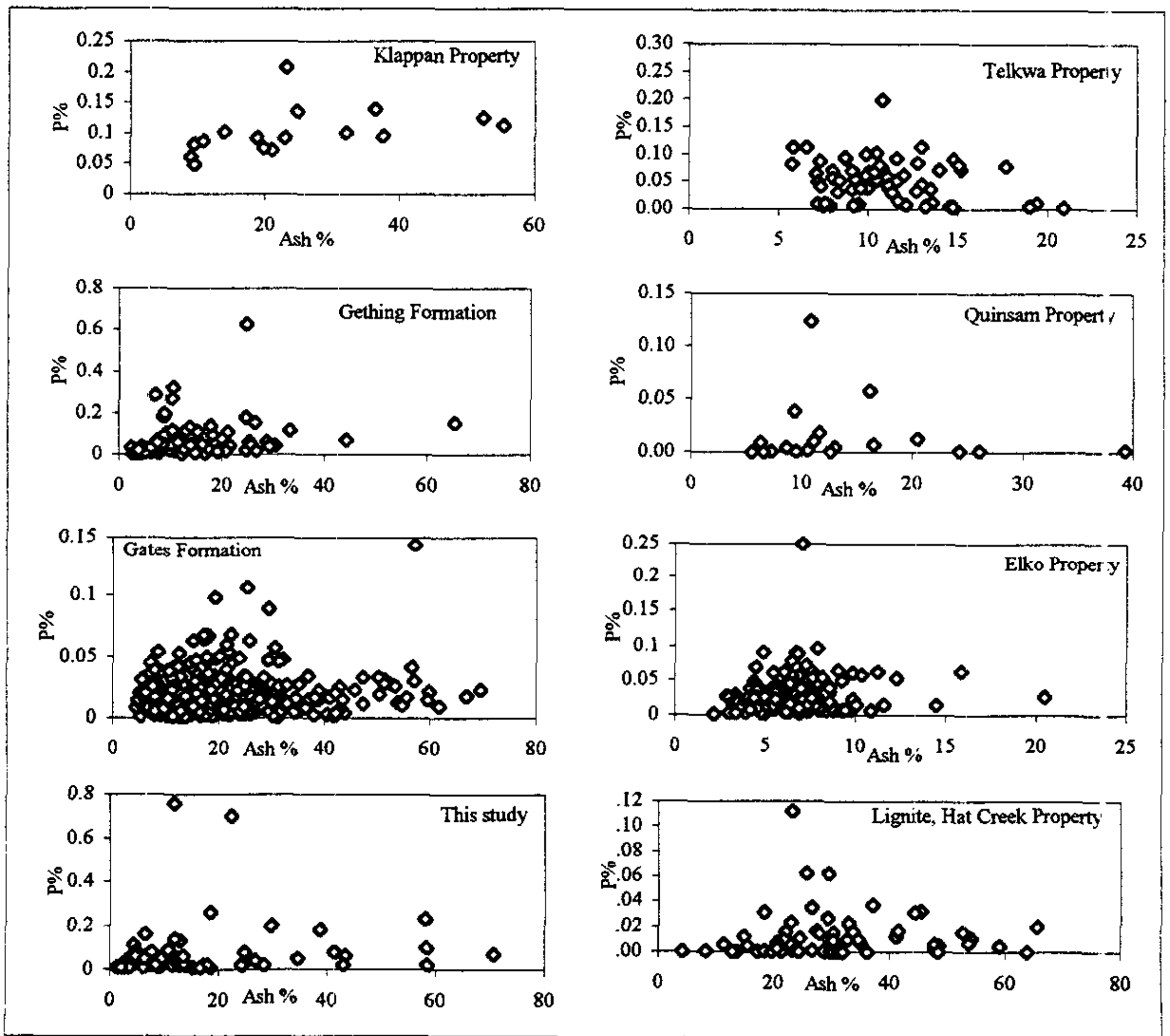


Figure 10. Phosphorus *versus* ash distributions for British Columbia coals of different ranks (sources specified in text).

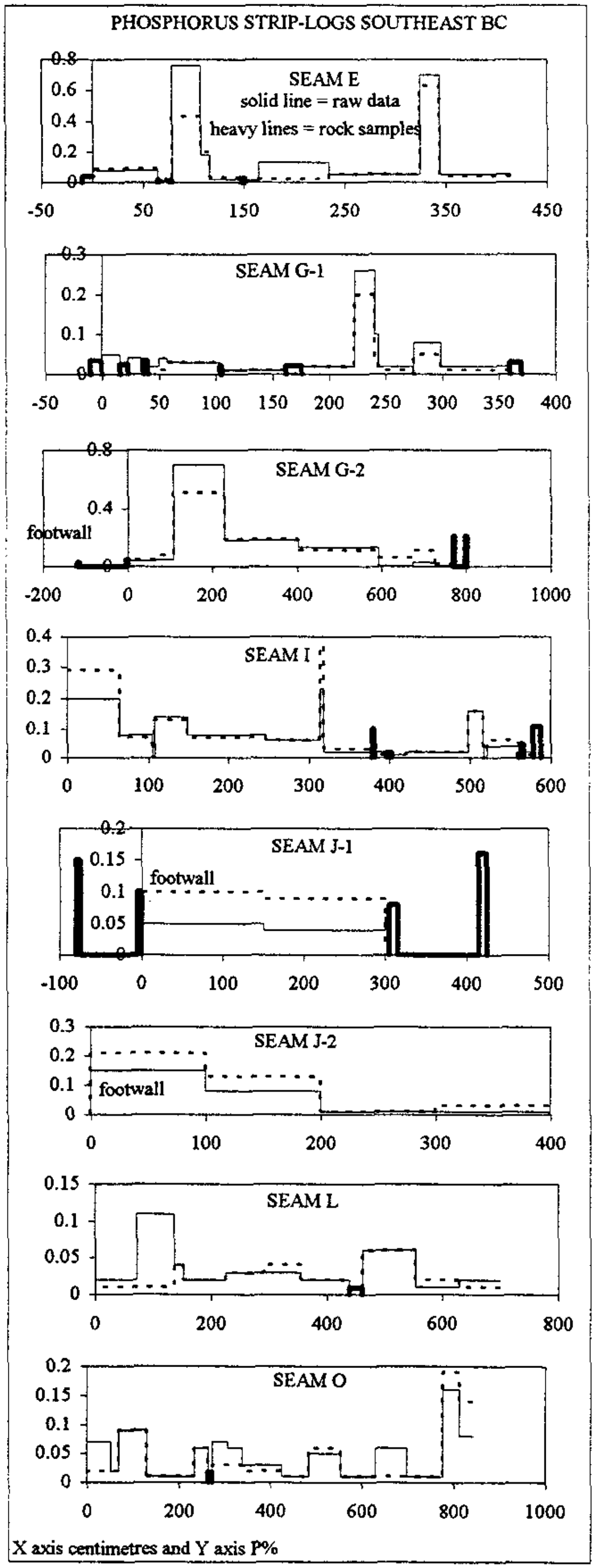


Figure 11. Strip-logs of raw and wash phosphorus for data collected during this study.

Samples collected as part of this study were analyzed for raw proximate, sulphur and phosphorus. Samples were then washed at 1.5 SG and analysed for ash and phosphorus. The incremental seam data are summarized in Table 12. Seams sampled include seams E, G, I, J, L and O. Hangingwall rock, footwall rock, ash and tonstein bands were analysed for a full suite of oxides and for mineral identification using x-ray diffraction. The phosphorus and ash data for these seams are displayed as strip-logs in Figure 11, in which the dotted lines represent the wash data and the solid lines the raw data. Rock partings, hangingwall or footwall material are identified by heavy lines. In addition to the data generated during this study, strip-logs for ash and phosphorus are constructed from data from Grieve (1992; Figure 12) in which the samples represent constant increments.

The incremental samples collected as part of this study were delineated based on lithotype, amount of shearing, or obvious ash or tonstein bands. There is a tendency for phosphorus concentrations to increase if:

- The predominant lithotype is dull.
- In the presence of siderite.
- If the coal is sheared.

The lithotype association is in agreement with the data in Table 8 and is best developed in seam G-2 (Figure 11) where the pronounced phosphorus high in the seam corresponds with an outcrop of dull lithotypes. In many of the strip-logs phosphorus has a negative correlation with ash (Figure 12).

There is a tendency seen in some data for phosphorus to increase toward the footwall and hangingwall. There is no evidence in the data collected during this study that the rocks enclosing the seams have a halo of high phosphorus; nor are ash or tonsteins bands within the seams enriched in phosphorus compared to the adjacent coal. In fact, the concentrations in the rocks are similar to those in the whole coal and consequently can only account for about one-fifth of the phosphorus in the coal, assuming 20% ash in the coal. The rest is probably from the vegetation, or possibly from phosphorus-rich fragments, air or water transported into the swamp.

The ash oxide data indicate that there is not enough

TABLE 13
RAW PHOSPHORUS IN THE BASAL SEAM
MIST MOUNTAIN FORMATION

| Location | Seam | Ash | $P_2O_5$ | P in coal |
|---|---|---|---|---|
| Elkview | Balmer[1] | 14.47 | 1.16 | 0.073 |
| Elkview | Balmer[1] | 15.57 | 0.74 | 0.050 |
| Elkview | Balmer[2] | 16.8 | 0.52 | 0.038 |
| Greenhills | 1 seam[1] | 26.54 | 0.04 | 0.005 |
| Corbin | Mammoth[1] | 18.68 | 0.06 | 0.005 |
| Corbin | Mammoth[1] | 15.82 | 0 | 0.000 |
| Byron Creek | Mammoth[3] | 21.71 | 1.16 | 0.031 |
| Byron Creek | Mammoth[3] | 21.32 | 0.74 | 0.035 |
| Byron Creek | Mammoth[3] | 21.5 | 0.52 | 0.013 |
| Line Creek | 10 seam[3] | 21.1 | 0.04 | 0.027 |

1 = Bonnell *et al.* (1985) 2 = Goodarzi *et al.* (1985)
3 = Grieve (1992)

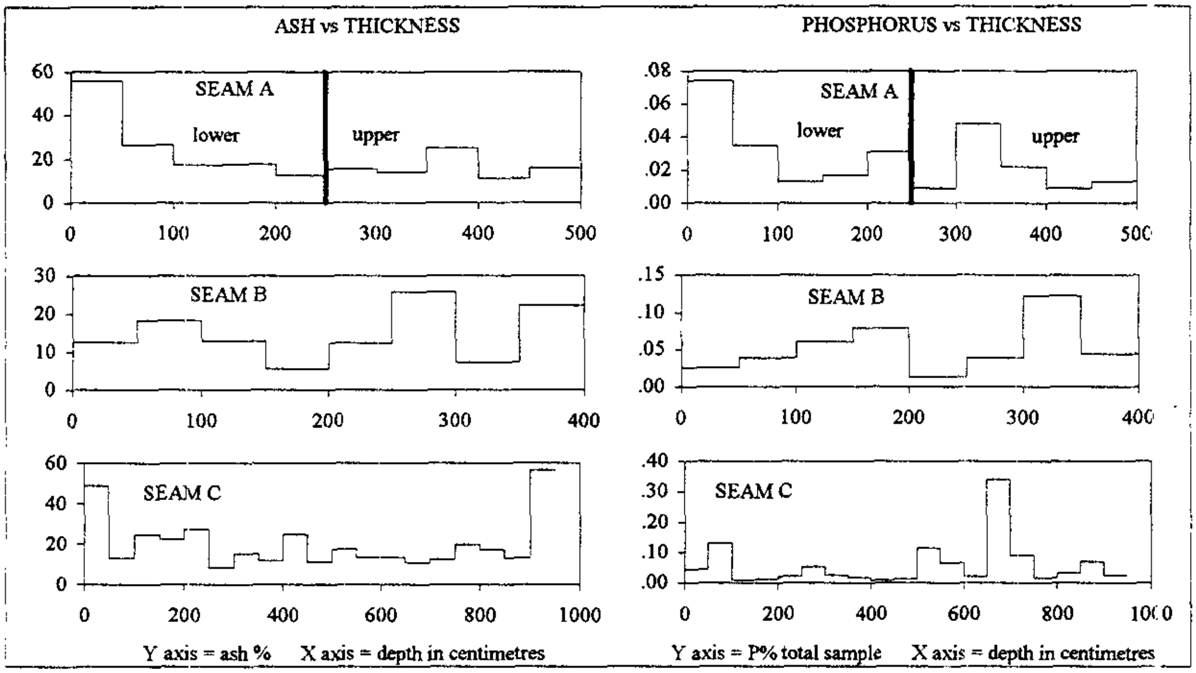


Figure 12. Strip-logs for raw phosphorus and ash. Constructed from data in Grieve (1992).

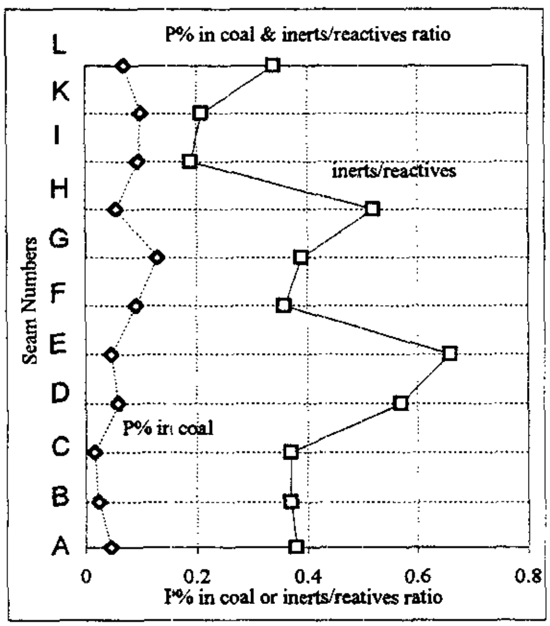


Figure 13. Average P% *versus* inerts/reactives ratio for seams in the lower part of the Mist Mountain Formation.

barium to use all the phosphorus to make gorciexite, but that there is excess CaO over that required to make apatite with all the phosphorus present. Strontium was not analysed for, so it is not known if the phosphorus is present in the mineral goyazite. The x-ray diffraction data did not identify any phosphatic minerals and a majority of the samples contained mainly quartz and kaolinite with anatase (TiO oxide) as a frequent minor mineral.

## REGIONAL DISTRIBUTION OF PHOSPHORUS IN MIST MOUNTAIN COALS

Within a single seam, the phosphorus may be concentrated in the inert macerals, but this does not mean that, from seam to seam, there has to be a correlation between concentrations of inert macerals and phosphorus. In fact, the lowest seam in the Mist Mountain section (Mammoth seam) at Coal Mountain (Figure 1) is one of the most inert rich seams in the Mist Mountain Formation, but is not characterized by high phosphorus (Table 13). There is no database of phosphorus and petrographic analyses on a seam by seam basis through the Mist Mountain Formation. It is possible, however, to extract some information from Coal Assessment Reports. Often the phosphorus and petrographic data were obtained from different samples of the same seam, but it is hoped that by averaging the data, simple trends may be apparent. A plot of average phosphorus concentrations *versus* average inert/reactives ratio produces a moderately good negative correlation (Figure 13). Seam numbering is schematic, starts at the base of the Mist Mountain Formation, and does not correspond to nomenclature used at any particular mine. Data were obtained for the lower third of the formation. The high-inert seams are not characterized by high phosphorus.

If the above correlation is real, then it implies that the initial phosphorus loading of a seam is related to vegetation type or conditions outside the coal swamp. The initial development of inert macerals provides porosity and limited permeability for moving the phosphorus, which is strongly concentrated in inert

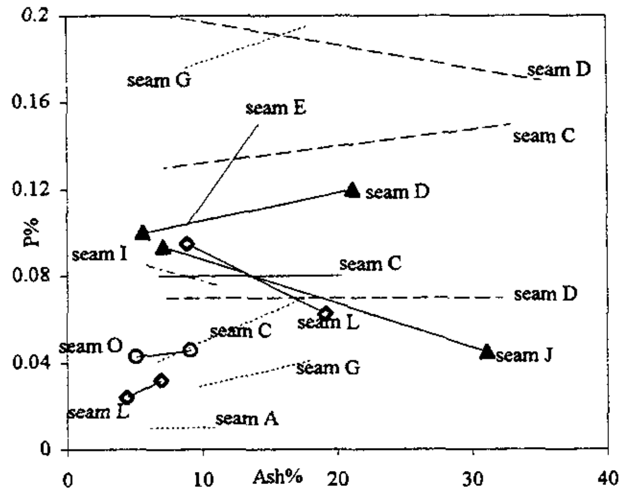


Figure 14 Tie-line plots for average raw and wash phosphorus data from seams studied in this paper.

macerals with respect to reactive macerals, but the overall phosphorus content in the seam remains high. As more inerts are generated, permeability improves and phosphorus moves out of the seam. Consequently, although it is still concentrated in the inerts, the overall concentration in the coal decreases. The petrographic data in Table 11 support this hypothesis. The seam with the highest reactives content also has the most phosphorus and it appears to be strongly concentrated in the inert macerals.

There seems to be a high-phosphorus seam in the lower part of the section in most of the mines in southeast British Columbia. It is approximately the fourth major seam up-section at the mines and the second up-section at the Elko property at the northern end of the Elk Valley coalfield (Grieve, 1992). At present it is not known if the seams represent the same stratigraphic horizon and no reason for the increased phosphorus is postulated. There are some data to suggest that the phosphorus in the lowest seam in the Mist Mountain Formation is consistently low, as illustrated by analyses for coal from Coal Mountain in the south to Greenhills in the north (Table 13).

## WASHING CHARACTERISTICS OF PHOSPHORUS AND METHODS OF CONTROL

The washing characteristics of phosphorus are illustrated using a tie-line plot in which raw and wash data, plotted on the same ash *versus* phosphorus plot, are joined by a line (Figure 14). Lines with positive slopes indicate removal of phosphorus during washing and lines with negative slopes indicate that the phosphorus is concentrating in the clean coal.

The incremental data from the eight sampling sites are averaged, based on the length represented by each sample. In addition, grab samples from seams were analysed for raw and wash ash and phosphorus (Table 12). All the data are plotted in Figure 14 with the seam numbers identified. It is apparent that phosphorus behaves inconsistently when washed. Washing concentrates phosphorus in some seams and reduces it slightly in others. The average raw phosphorus contents of the seams range from 0.032% to 0.2% (Table 12) and the wash contents from 0.024% to 0.18%. The ratios of wash to raw phosphorus range from 69% to 167%. In general, washing did not reduce the phosphorus concentration by more than 30%. It is clear that even if phosphorus tends to be associated with ash in the raw samples, it does not follow the ash during washing and is in general more difficult to remove.

Samples for full washability analysis were collected from one of the mine wash plants during a time when a single seam, was being processed. A comparison of the phosphorus in the ROM and product coal ( Figures 5 B and D) indicates that the plant was not able to remove much phosphorus. It is also apparent from Figure 5 that phosphorus is concentrated in the coarser size fractions and is very difficult to remove. Even in the finest size, phosphorus is concentrated in the clean coal, indicating that there is little liberation.

The best way of controlling phosphorus in the clean coal may be by blending ROM coal. Another possibility is to wash the coarser size at a lower cut point, but this will divert coal to the reject stream and may not reduce the phosphorus by much in the clean coal. Some of the clean coarse-fraction coal, which contains the highest phosphorus concentration, could be diverted as a thermal product in which phosphorus content is not as much of a concern; the result would be a lower concentration in the metallurgical product.

## CONCLUSIONS

It is proposed that much of the phosphorus in coal originates in the parent vegetation, in which there is ample to account for all that is found in coal. In fact, there may be more than enough and the problem is not one of how to get the phosphorus into coal, but one of how and where has it gone. It is suggested that the formation of inert macerals by the action of fires or bacteria in the pre-coal swamp environment produces a maceral with a robust and plentiful porosity. Shortly thereafter, the remaining vegetation goes through a gellification stage in an anaerobic, possibly acidic environment. During this stage, phosphorus is mobilized, largely from the vegetation, and redeposited in the cell porosity in the inert macerals. It forms minerals such as the calcium phosphate, apatite, the barium phosphate, goriexite and the strontium phosphate, goyazite. Many computerized x-ray diffraction systems will identify apatite, but the identification of the barium and strontium phosphates may be more difficult. This is important because, whereas x-ray diffraction work records the presence of apatite and gorciexite, oxide data implies that the phosphorus is often present as goyazite. Once redeposited in phyteral porosity in the inert macerals, the phosphorus is difficult to liberate by conventional washing techniques.

Based on this, phosphorus content should correlate with the amount of inerts in adjacent samples from a single seam. The concentration in the inert macerals may be much higher than that in the reactive macerals or in ash bands. Because inherent ash also often resides in the phyteral porosity, there may be a correlation between phosphorus and ash, but this will not hold at higher ash concentrations when a larger component of the ash is derived from elsewhere. There will not necessarily be a correlation of phosphorus concentration with inerts content of samples from different seams because of the wide range of phosphorus concentrations in inerts. The phosphorus concentration of separate seams may correlate with vegetation type or other regional parameters.

Much of the phosphorus is present in phosphatic minerals in the coal and it may be possible to liberate and remove it during washing, as indicated by some seam data. However, it may be so finely dispersed in the phyteral porosity in inert macerals, that it will be difficult to remove. The best way of reducing phosphorus in clean coal may be by blending with ROM coal. This will require building good advanced knowledge of phosphorus concentrations in seams into long range mine plans.

## ACKNOWLEDGMENTS

Sampling at the mines was facilitated by senior mine geologists Ken Komenac, Martin Zral, Pat Gilmar and Ted Hannah. Projects such as this develop out of discussions with mine employees and are successful because of their continuing cooperation.

## REFERENCES

Abernathy R.E. and Gibson F.H. (1963): Rare Elements in Coal; *U.S. Bureau of Mines*, Information Circular, No. 8163.

Abernathy, R.F., Peterson M.J. and Gibson F.H. (1969): Major Ash Constituents in U.S. Coals; *U. S. Bureau of Mines*, Report of Investigations, 7240.

Asuen, G.O. (1987): Assessment of Major and Minor Elements in the Northumberland Coalfield England; *International Journal of Coal Geology*, Volume 9, pages 171-186.

Blatt, H., Middleton, G. and Murray, R. (1980): Origin of Sedimentary Rocks; *Prentice-Hall*, New Jersey.

Berger, I.A. (1958): Geochemistry of Coal; *Economic Geology*, Volume 53, pages 823-841.

Bieg, G. and Burger, K. (1992): Preliminary Study of Tonsteins of the Pastora Formation (Stephanian B) of the Cinera-Maltallana Coalfield, Northwestern Spain; *International Journal of Coal Geology*, Volume 21, pages 139-160.

Bonnell, G.W., Janke, L.C. and Romaniuk, A.S. (1984): Analysis Directory of Canadian Commercial Coals, Supplement No. 5; *Canada Centre for Mineral and Energy Technology*, Report 84-1E.

Brown, H.R. and Swaine, D.J. (1964): Inorganic Constituents of Australian Coals, Part 1, Nature and Mode of Occurrence; *Journal of the Institute of Fuel*, Volume 37, pages 422-440.

Burger, K., Zhou, Y. and Tang, D. (1990): Synsedimentary Volcanic-ash-derived Illite Tonsteins in Late Permian Coal-bearing Formations of Southeast China, *International Journal of Coal Geology*, Volume 15, pages 341-356.

Bustin, R.M. (1982): The Effect of Shearing on the Quality of some Coals in the Southeastern Canadian Cordillera, *Canadian Institute of Mining and Metallury*, Bulletin, Volume 75, pages 76-83.

Cairncross, B., Hart, R.J. and Willis, J.P. (1990): Geochemistry and Sedimentology of Coal Seams from the Permian Witbank Coalfield, South Africa; A Means of Identification; *International Journal of Coal Geology*, Volume 16, pages 309-325.

Clarke, F.W. and Washington, H.S. (1924): The Composition of the Earths Crust; *U.S. Geological Survey*, Professional Paper 127, page 117.

Coal Assessment Reports: Reports organized by number and available to the general public at B.C. *Ministry of Energy, Mines and Petroleum Resources*, 1810 Blanshard Street Victoria British Columbia.

Cook, A.C. (1962): Fluorapatite Petrifications in a Queensland Coal; *Australian Journal of Science*, Volume 25, page 94.

Dawson, F.M., Ryan, B.D., Pratt, K. and Clow, J.C. (1994): Coalbed Methane Micropermeability Project; Industrial Partners Project, *Institute of Sedimentary and Petroleum Geology*, Calgary.

Faurschou, D.K., Bonnell, G.W. and Janke, L.C. (1982): Analysis Directory of Canadian Commercial Coals; Supplement No 4; *Energy, Mines and Resources Canada*, CANMET Report 82-13E.

Finkelman, R.B. (1980): Modes of Occurrence of Trace Elements in Coal; unpublished Ph.D. thesis, *University of Maryland*, 301 pages.

Gamson, P.D., Beamish, B.B. and Johnson, D.P. (1993): Coal Microstructure and Micropermeability and their Effects on Natural Gas Recovery; *Fuel*, Volume 72, pages 87-99.

Gluskoter, J.J., Ruch, R.R., Miller, W.G., Cahill, R.A., Dreher, G.B. and Kuhn, J.K. (1977): Trace Elements in Coal: Occurrence and Distribution; *Illinois State Geological Survey*, Circular 499.

Goodarzi, F., Foscolos, A.E. and Cameron, A.R. (1985): Mineral Matter and Elemental Concentrations in Selected Western Canadian Coals; *Fuel*, Volume 64, pages 1599-1604.

Grieve, D.A. (1983): Tonsteins: Possible Statigraphic Correlation Aids in East Kootenay Coalfields; *in* Geological Fieldwork 1982, *B.C. Ministry of Energy, Mines and Petroleum Resources*, Paper 1983-1, pages 36-41.

Grieve D.A. (1992): Phosphorus in British Columbia Coking Coals; *B.C. Ministry of Energy, Mines and Petroleum Resources*, Open File 1992-20.

Grieve, D.A. and Holuszko, M.E. (1991): Trace Elements, Mineral Matter and Phosphorus in British Columbia Coals; *in* Geological Fieldwork 1990, *B C. Ministry of Energy, Mines and Petroleum Resources* Paper 1991-1, pages 361-370.

Gmelin, L. (1965): Handbuch der Anorgaanischem Chemie. Phosphor; *Teil A. Weinheim, Verlag Chemie*.

Haley, B.R. (1978): Resources of Low-volatile Bituminous Coal and Semianthracite in West-central Arkansas; *U.S. Geological Survey*, Bulletin 1632.

Harris, L.A., Barrett, H.E. and Kopp, O.C. (1981): Element Concentrations and their Distribution in Two Bituminous Coals of Different Paleoenvironments; *International Journal of Coal Geology*, Volume 1, pages 175-193.

Hill, P.A. (1988): Tonsteins of Hat Creek, British Columbia: A Preliminary Study; *International Journal Of Coal Geology*, Volume 10, pages 155-175.

Hill, P.A. (1990): Vertical Distribution of Elements in Deposit No. 1, Hat Creek, British Columbia: A Preliminary Study; *International Journal of Coal Geology*, Volume 15, pages 77-111.

Holuszko, M.E. (1993): Washability of Lithotypes from a Selected Seam in the East Kootenay Coalfield, Southeast British Columbia; *in* Geological Fieldwork 1992, Grant, B. and Newell, J.M., Editors, *B.C. Ministry of Energy, Mines and Petroleum Resources*, Paper 1993-1, pages 517-525.

Huang, W.T. (1962): Petrology; *McGraw Hill*, New York.

Karner, F.R., Schobert, H.H., Falcone, S.K. and Benson, S.A. (1986): Elemental Distribution and Association with Inorganic and Organic Components in North Dakota Lignites; In, Mineral Matter and Ash in Coal, *Comstock*, M.J., Editor, *American Chemical Society, Symposium*, Series 301, pages 70-89.

Kemezys, M. and Taylor, G.H.(1964): Occurrence and Distribution of Minerals in some Australian Coals; *Fuel*, Volume 37, pages 389-397.

Kilby, W. (1983): Tonsteins and Bentonites in Northeast British Columbia; *in* Geological Fieldwork 1982, *B.C. Ministry of Energy, Mines and Petroleum Resources*, Paper 1983-1, pages 95-107.

Kilby, W. (1984): Tonstein and Bentonite Correlations in Northeast British Columbia; *in* Geological Fieldwork 1983, *B.C. Ministry of Energy, Mines and Petroleum Resources*, Paper 1984-1, pages 257-277.

Kramer, P.J. and Kozlowski, T.T. (1979): Physiology of Woody Plants; *Academic Press, Harcourt Brace Jovanovich*, London, Table 10-2.

Lamberson, M.N. and Bustin, R.M. (1993): Coalbed Methane Characteristics of Gates Formation Coals, Northeastern British Columbia: Effect of Maceral Composition; *American Association of Petroleum Geologists*, Bulletin, pages 2062-2076.

Ledig, F.G. and Botkin, D.B. (1974): Photosynthetic $CO_2$-uptake and the Distribution of Photosynthate as Related to Growth of Larch and Sycamore Progenies; *Silvae Genetica*, Volume 23, pages 188-192.

Mahony, B., Moulson, I. and Wilkinson, H.C. (1981): Study of the Relation between the Phosphorus Content of Coal and Coke; *Fuel*, Volume 60, pages 355-358.

Marschner, H. (1986): Mineral Nutrition of Higher Plants; *Academic Press, Harcourt Brace Jovanovich*, London, Table 12-4.

Matheson, A., Grieve, D.A., Holuszko, M.E. and Goodarzi, F. (1994): Selected Thermal Coal Basins of British Columbia (1994): *B.C. Ministry of Energy, Mines and Petroleum Resources*, Paper 1994-3.

Palache, C., Bergman, H. and Frondel, C. (1951): Dana's System of Mineralogy; Volume II, *John Wiley and Sons*.

Pareek, H.S. and Bardhan, B. (1985): Trace Elements and their Variation Along Seam Profiles of Certain Coal Seams of Middle and Upper Barakar Formations (Lower Permian) in East Bokaro Coalfield, District Hazarigh, Bihar, India; *International Journal of Coal Geology*, Volume 5, pages 281-314.

Patrick, W.H. and Khalid, R.A. (1974): Phosphate Release and Sorption by Soils and Sediments: Effect of Aerobic and Anaerobic Conditions; *Science*, Volume 186, pages 53-55.

Powell, M.A. (1987): The Inorganic Geochemistry of Two Western U.S. Coals: Emery Coal Field, Utah and Powder River Coal Field, Wyoming; unpublished Ph.D thesis, *University of Western Ontario*, London, Ontario.

Queensland Coal Board. (1975): Physical and Chemical Properties and Classification; 5th Edition, Queensland Coal Board, Brisbane, Australia.

Ryan B.D. (1991): Geology and Potential Coal and Coalbed Methane Resource of the Tuya River Coal Basin, (104J/2,7); *in* Geological Fieldwork 1990, *B.C. Ministry of Energy, Mines and Petroleum Resources*, Paper 1991-1, pages 419-429.

Salisbury, B.F. and Ross, C. (1969): Plant Physysiology; *Wadsworth Publishing Company Inc.*, Belmont, California, Table 10-2.

Shah, N., Girard, P., Mezerette, C. and Vergnet, A.M. (1992): Wood to Charcoal Conversion in a Partial Combustion Kiln: An Experimental Study to Understand and Upgrade the Process; *Fuel*, Volume 71, pages 105-115.

Skorupska, N.M. (1993): Coal Specifications; Impact on Power Station Performance; *IEA Coal Research*.

Spears, D.A. and Caswell, S.A. (1986): Mineral Matter in Coals: Cleat Minerals and their Origin in some Coals from the English Midlands; *International Journal of Coal Geology*, Volume 6, pages 107-125.

Spears, D.A. and Kanaris-Sotiriou, R. (1979): A Geochemical and Mineralogical Investigation of some British and other European Tonsteins; *Sedimentology*, Volume 26, pages 407-425.

Spears, D.A., McL.D.Duff, P. and Caine, P.M. *et al.* (1988): The West Waterberg Tonstein, South Africa; *International Journal of Coal Geology*, Volume 9, pages 221-233.

Stubbles, J.R. (1986): Phosphorus and Sulphur in Steel Making; *Iron and Steel Making Journal*; Three part Series in issues from March 1986 to March 1987

Swain, F.M. (1970): Non Marine Organic Geochemistry; Cambridge University Press, Cambridge.

Swaine, D.J. (1977): Trace Elements in Coal; *in* Trace Substances in Environmental Health XI, Hemphill, D.D., Editor, *University of Missouri*, pages 129-134.

Triplehorn, D.D. (1990): Applications of Tonsteins to Coal Geology: Some Examples from Western United States; *International Journal of Coal Geology*, Volume 16, pages 157-160.

Turekian, K.K. and Wedepohl, K.H. (1961): Distribution of Elements in some Major Units of the Earths Crust; *Geological Society of America*, Bulletin, Volume 72, page 172

Valcovik (1983): Trace Elements in Coal; Boca Raton; *CRC Press*, Volume 1, page 210, Volume II page 251.

Van Den Busche, B.G. and Grieve, D.A. (1990): Phosphorus in British Columbia Coking Coals, *in* Geological Fieldwork 1989, *B.C. Ministry of Energy, Mines and Petroleum Resources*, Paper 1990-1, pages 427-430.

Wedepohl, K.H. (1978): Handbook of Geochemistry, Volume II, Part 5; *Springer-Verlag*, Berlin.

# BRITISH COLUMBIA AGGREGATE INVENTORY PROJECT

By Peter Bobrowsky, Nick Massey, Alex Matheson and Paul Matysek

*KEYWORDS:* aggregate, digital database, inventory, potential mapping, sand and gravel

## INTRODUCTION

In 1994, the Geological Survey Branch launched an initiative focused on the province's aggregate resources. The background and goals of this program have been summarized previously (Bobrowsky *et al.*, 1995).

During 1995, progress was made on three fronts.

- Interested parties were invited to participate in a two-day forum and workshop on the aggregate resources of the province. The meeting addressed concerns and requirements in aggregate resource management. Case studies from Canadian and U.S. jurisdictions provided valuable background to the discussions.
- The digital inventory of private aggregate pits in British Columbia has been completed.
- Aggregate potential mapping has been initiated with a pilot study in the Prince George area.

## AGGREGATE FORUM

The Aggregate Forum and Workshop was held March 30-31, 1995, in Richmond. The forum was primarily sponsored by the Ministry of Energy, Mines and Petroleum Resources and the Ministry of Transportation and Highways. Co-sponsors included the Planners Institute of British Columbia, the Commission on Geological Sciences for Environmental Planning, the University of British Columbia (Department of Mining and Mineral Process Engineering), and the University of Northern British Columbia (Natural Resources and Environmental Studies).

The first day comprised an open forum, with 104 participants attending, all having an interest in the aggregate industry of British Columbia. They included aggregate producers, engineering and geotechnical consultants, community planners (Municipal, Regional and First Nations), academia (UBC, UNBC, SFU, UVic), provincial government (MEMPR, MoTH, MoF) and federal government (DIAND, NRC). Out-of-province participants came from Ontario, Alberta, Yukon, Washington State, California and the United States Geological Survey (Colorado, Arizona).

Fifteen talks were presented dealing with the aggregate market in Canada and the U.S.A. aggregate geology and inventory in British Columbia, the management of aggregate resources, and methods of mapping and assessing aggregate resource potential (Bobrowsky *et al.*, in preparation).

The second day consisted of a workshop with a smaller group of about forty participants, all interested specialists in the field of aggregate inventory and mapping. Participants were divided into three discussion groups which considered the need for, and make up of:

- a provincial aggregate inventory,
- qualitative aggregate resource potential maps, and
- quantitative aggregate resource potential maps.

The three groups presented summaries of their discussions to the workshop as a whole in the afternoon, for further input.

Broad concensus was reached during the two days of the forum concerning the need for a single province-wide inventory of aggregate pits. There was also strong support for aggregate potential mapping at 1:50 000 scale with the undertaking of a pilot project as a means of developing suitable methodologies.

## PROVINCIAL INVENTORY

Information about aggregate pits in British Columbia is collected and managed primarily by two ministries. The Ministry of Transportation and Highways gathers data on some 4000 to 5000 public pits in order to ensure an adequate supply of good quality gravel is available for construction, maintenance and rehabilitation of highways in the province. These data have been managed by the Ministry of Transportation and Highways using three systems: ADIS (aggregate deposit information system), ARMS (aggregate resource management system) and RAAMS (regional aggregate account management system). These are being replaced by a new system, GMSS, which is a compilation of the previous three separate systems. Assembly of this new database will allow for the elimination of errors in location and status of pits and the completion of missing data fields.

In British Columbia, aggregate pits are designated as mines. As such, the Ministry of Energy, Mines and Petroleum Resources is responsible for their planning, management and regulation, including permitting, health, safety and reclamation. Owners or operators of all private aggregate pits must file Notices of Work as part of the permitting and reclamation process. Our efforts to establish a provincial inventory of private pits (Matheson *et al.*, 1996) have been based on these files. Individual pit

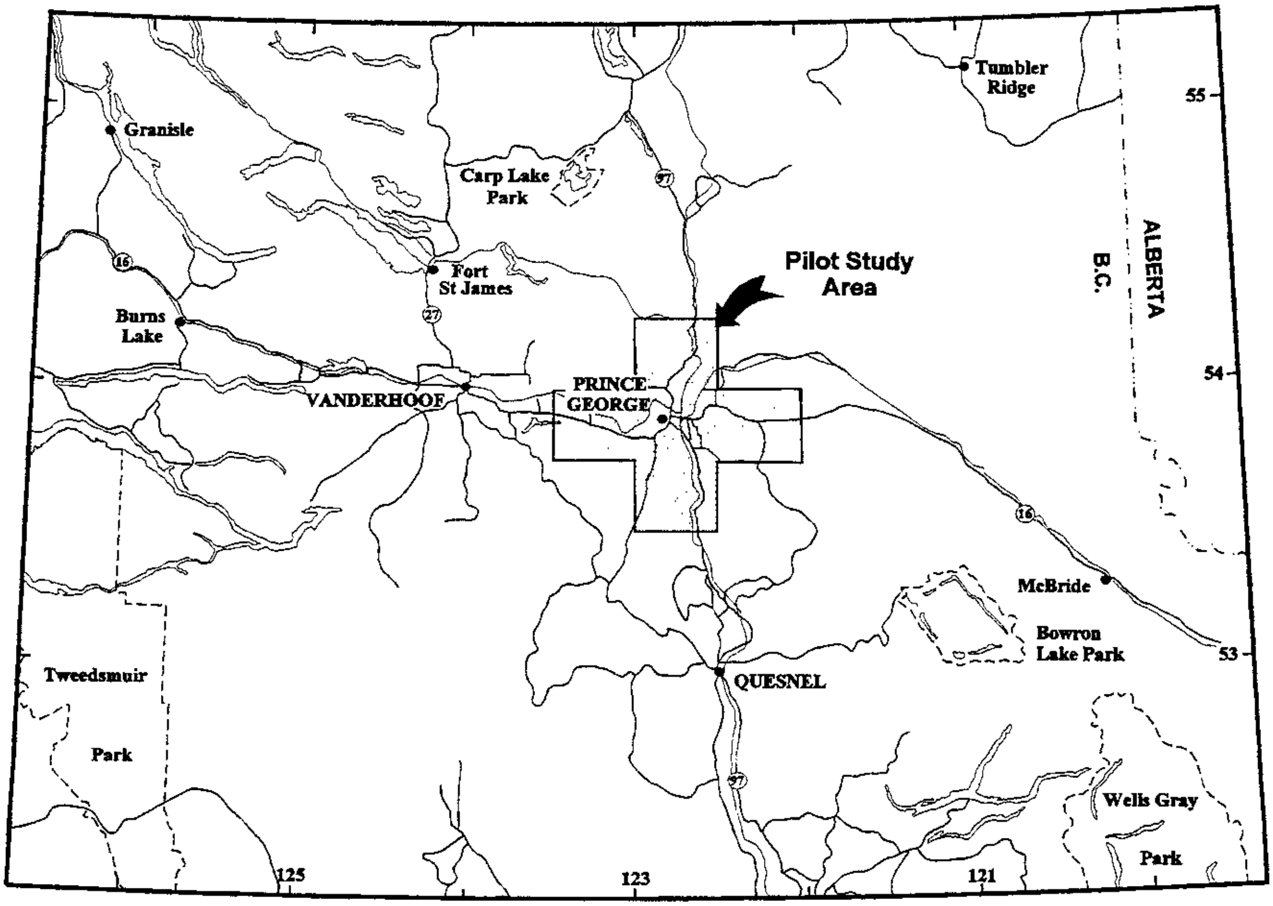


Figure 1. Location of the Prince George pilot study for aggregate potential maps.

identifications and locations were obtained, reviewed and upgraded. The locations were plotted on 1:50 000-scale base maps, digitized and compiled in a simple dBase format. In total, over six hundred currently permitted pits, and a lesser number of reclaimed pits, have been located accurately for inclusion in the database. Where possible, the landform associated with each pit has also been determined.

## AGGREGATE POTENTIAL MAPPING

Participants in the Aggregate Forum recognized the utility of aggregate potential maps for the good management of the resource and general landuse planning at the regional and local levels. Several approaches to assessing that potential have been made in other jurisdictions (*e.g.* Gartner *et al.*, 1981; Fox *et al.*, 1987; Bliss and Page, 1994). The Forum recommended a pilot project be undertaken as a means of evaluating the efficacy of these methods in British Columbia.

An aggregate potential map typically outlines areas of aggregate potential as polygons on the map and ranks the potential of the areas qualitatively from high to low. The parameters used in the derivation of the rankings, including landform type, quantity of sand *versus* gravel, volume estimate, thickness of deposit, etc., are also detailed on the map. On-site geotechnical evaluation is still required to quantitatively confirm the aggregate potential of any specific target. However, the maps provide a quick "first approximation" for alternative land use by also identifying areas which hold little or no potential for aggregate resources. Ultimately, such maps save those planners, developers and producers involved in aggregate considerable effort and cost by focusing attention on select areas.

The pilot study is being undertaken in the Prince George area, covering five 1:50 000-scale map sheets forming a cross centred on the city of Prince George (Figure 1) and including the major transportation corridors in the area. The study area has a reasonable endowment of aggregates but suffers from problems in the management of the resource and conflicts with other land uses. Methodologies developed here should also be applicable elsewhere in British Columbia. The project has the support and cooperation of the Ministry of Transportation and Highways, the Ministry of Forests, the City of Prince George, the Regional District of Fraser - Fort George, and faculty members of the University of Northern British Columbia. These partners will not only be invaluable sources of relevant technical data, but also provide input on the effectiveness of the presentation format of final products.

All data are being assembled in digital format, and will be managed and analysed in a geographic information system (ARC/INFO™). Resultant aggregate potential maps, with accompanying report and documentation, will be released as an Open File in 1996.


## ACKNOWLEDGMENTS

Greg McKillop provided continuing access to Ministry of Energy, Mines and Petroleum Resources Notice of Work files. Cal Kilby and Gavin Manson made significant contributions to locating and digitizing of aggregate pits. The paper benefited from review by J.M. Newell.


## REFERENCES


Bliss, J.D. and Page, N.J. (1994): Modeling Surficial Sand and Gravel Deposits; *Nonrenewable Resources*, Volume 3, pages 237-249.

Bobrowsky, P.T., Kilby C.E., Manson, G. and Matysek, P.F. (1995): British Columbia Aggregate Inventory Project; *in* Geological Fieldwork 1994, Grant, B. and Newell, J.M., Editors, *B.C Ministry of Energy, Mines and Petroleum Resources*, Paper 1995-1, pages 361-364.

Bobrowsky, P.T., Massey, N.W.D. and Matysek, P.F. (in preparation): Aggregate Forum: Developing an Inventory that Works for You!, Report of Proceedings; *B.C. Ministry of Energy, Mines and Petroleum Resources*, Information Circular.

Fox, J.C., Richardson, R.J.H. and Sham, P.C. (1987): Aggregate Resource Potential by Geological Ranking and Reserve Estimates; Peace River - High Level Area, Alberta; *Alberta Research Council*, 1 500 000-scale map.

Gartner, J.F., Mollard, J.D. and Roed, M.A. (1981): Ontario Engineering Geology Terrain Study Users' Manual; *Ontario Geological Survey*, Northern Ontario Engineering Geology Terrain Study 1.

Matheson, A., Massey, N.W.D., Bobrowsky, P.T., Kilby, C.E. and Manson, G. (1996): Agreggate Inventory of British Columbia - Private Pits; *B.C. Ministry of Energy, Mines and Petroleum Resources*, Open File 1996-5.

NOTES

# MINERAL POTENTIAL ASSESSMENT PROJECTS - AN UPDATE

By Ward E. Kilby

*Contribution to the Mineral Potential Project, funded in part by the Corporate Resource Inventory Initiative (CRII)*

*KEYWORDS:* Mineral assessment, geology compilation, expert estimation, world wide web.

## INTRODUCTION

During 1995, the third year of the Mineral Potential Project, the mineral assessment methodology was standardized, geological compilations were completed on schedule and expert estimations were completed on two new regions and more structured assessments completed on two other regions. In addition, the information collected during the analyses and the results of the analyses were made available on the Internet.

## 1995 PROGRESS

### *NORTHWEST BRITISH COLUMBIA GEOLOGICAL COMPILATION*

Geological compilation of the northwest region was started in April of 1995. This 155 000 square kilometre region is being compiled by seven Geological Survey Branch geologists led by Mitch Mihalynuk, with significant input from Geological Survey of Canada geologists (Figure 1). The compilation is scheduled for completion and release as an open file in January of 1996. The associated mineral assessment will be completed by April 1996.

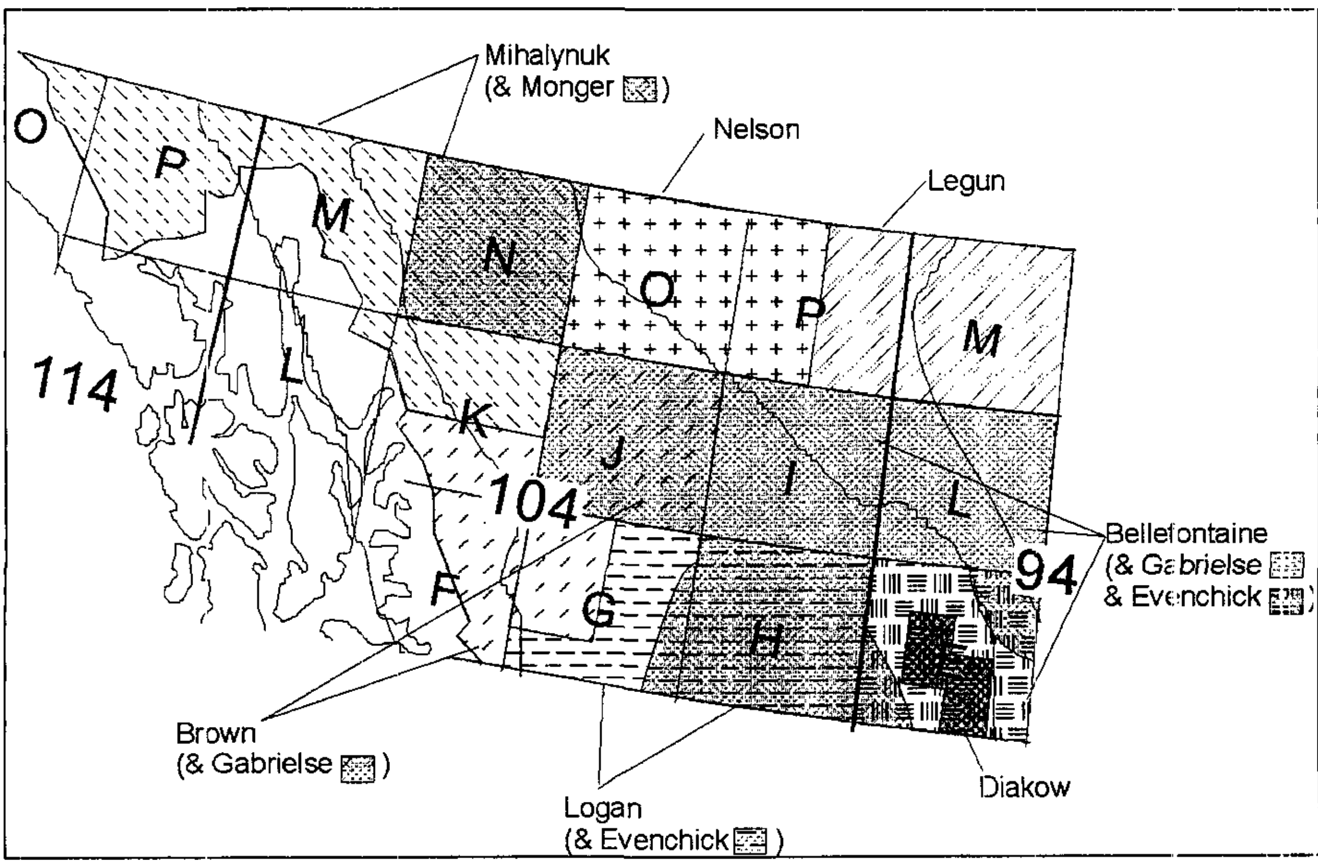


Figure 1. Northwest British Columbia Mineral Assessment Region, showing the geologist responsible for compilation in various sections of the project

## *NORTHEAST BRITISH COLUMBIA MINERAL ASSESSMENT*

During the last year, the geology for the northeast region was completed and released as two digital open files (McIntyre *et al.*, 1995; Bellefontaine *et al.*, 1995). In March 1995 an estimation workshop was held to obtain estimates of the potential for future mineral discoveries in this region. At the workshop, 24 estimators evaluated the 136 tracts in the region for 70 possible deposit types, generating 4050 individual estimates.

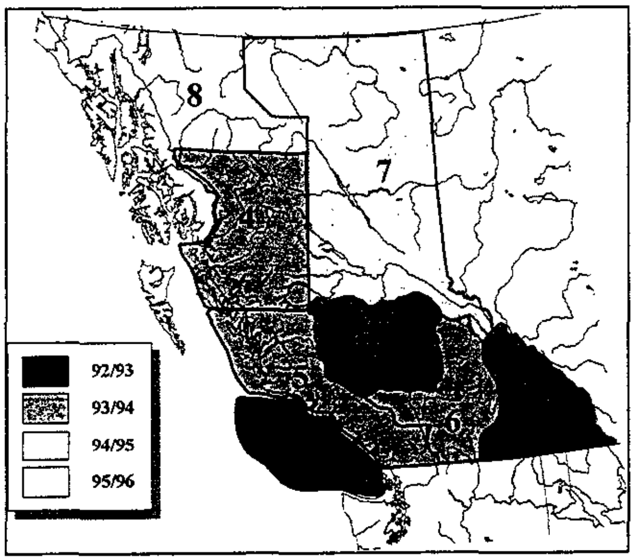


Figure 2. Locations of the various study areas. Mineral potential assessment regions; 1-Vancouver Island, 2- Cariboo-Chilcotin, 3- Kootenays, 4- Skeena-Nass, 5- Mid-Coast, 6- Thompson-Okanagan, 7- Northeast BC and 8- Northwest BC. The Muskwa - Kechika area occupies the northwestern part of the northeast region.

Estimates of future mineral discoveries and the final mineral assessment were made for the whole Northeast British Columbia Region and an extension into the Northwest British Columbia Region. This extension was added to address the urgent need for an analysis of the Muskwa-Kechika area (B.C. Ministry of Energy, Mines and Petroleum Resources, 1995). Geological compilations were not available for this extension at the time of the estimation workshop so estimates were made based on the 1:1 000 000 compilation of the Geological Survey of Canada (Journeay and Williams, 1995). The part of the Muskwa-Kechika area not compiled during the Northeast British Columbia project compilation was compiled as part of the Northwest British Columbia project (Figure 2). Expert estimations for this part of the area will be redone together with the rest of the northwest region in March of 1996.

## *REASSESSMENT OF REGIONS*

Starting with the Thompson-Okanagan expert-estimation workshop held in November of 1994, a new, more structured method of generating the estimates was used. This methodology improvement is described in a following section. The results of this workshop were significantly superior to earlier estimation efforts. As a result, a workshop was run in February 1995 to reassess the Skeena-Nass and Mid-Ccoast Regions using the improved format (Figure 2). During the current year it is planned to develop new estimates for the Vancouver Island, Cariboo and Kootenay regions and produce new evaluations. These reassessments will standardize the analysis of all regions to a single methodology. This will facilitate the comparison of tracts in neighbouring regions when land-use planning areas straddle boundaries of mineral potential regions.

## *DIGITAL OPEN FILE RELEASES*

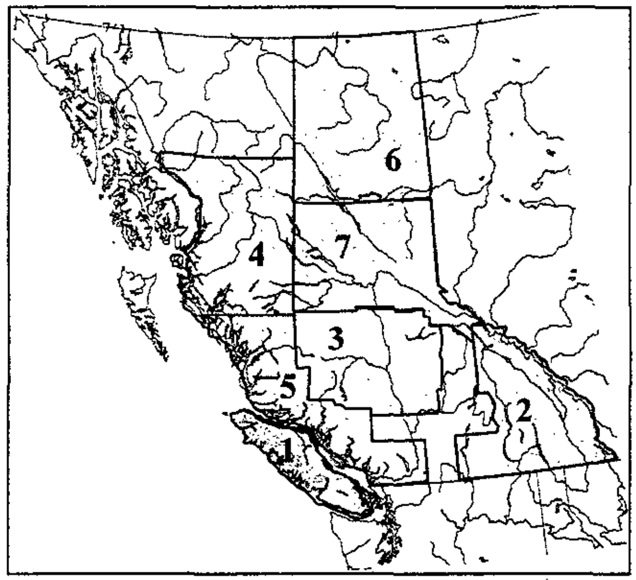


Figure 3. Map showing the locations of the Open File releases of geological compilations to date. Areas of digital geology releases; 1 - OF 1994-6 (Massey, 1994), 2 - OF 1994-7 (Schiarizza *et al.*, 1994), 3 - OF 1994-8 (Höy *et al.*, 1994), 4 - OF 1994-14 (MacIntyre *et al.*, 1994), 5 - OF 1994-17 (Bellefontaine and Alldrick, 1994), 6 - OF 1995-6 (MacIntyre *et al.*, 1995), 7 - OF 1995-24 (Bellefontaine *et al.*, 1995) and 8 - 1994-27 (Desjardins, 1994).

On completion of the geological compilation in each region, the information is made available by means of Open File Series releases. To date there have been eight such releases (Figure 3). Each release contains a set of diskettes holding the digital information, paper representations of the map legend, information sources and a copy of the digital data for reference. Some of the later releases contain a colour plotfile which can be used to produce a colour hardcopy map of the geology. This information can be used in CAD systems directly as it is presented, in an industry standard format (.DXF), or input into a GIS or desktop mapping system. Some additional effort will be required to build topology for the dataset in a GIS system, but the required information is provided in the releases. Comparable information in GIS-compatible format is now being made available on the Internet (see later section).

## *NEW REQUIREMENTS PLACED ON ASSESSMENTS*

Output from this project was designed to meet the requirements of the Commission on Resources and Environment's land-use planning process. This process was implemented at a regional scale of 1:250 000. Since the original three CORE regions of Vancouver Island, Cariboo-Chilcotin and Kootenays were started, no additional CORE-style land-use planning processes have been undertaken. In place of the regional CORE process many subregional Land and Resource Management Plan processes (LRMP) have been initiated (Figure 4). The scale of these planning processes is typically more detailed than the 1:250 000 used in the CORE analysis. The accuracy of the point information and the mineral assessment tract boundaries is adequate for use at the scales being used in the LRMPs. However, the size of the mineral assessment tract polygons may be a concern at these more detailed scales.

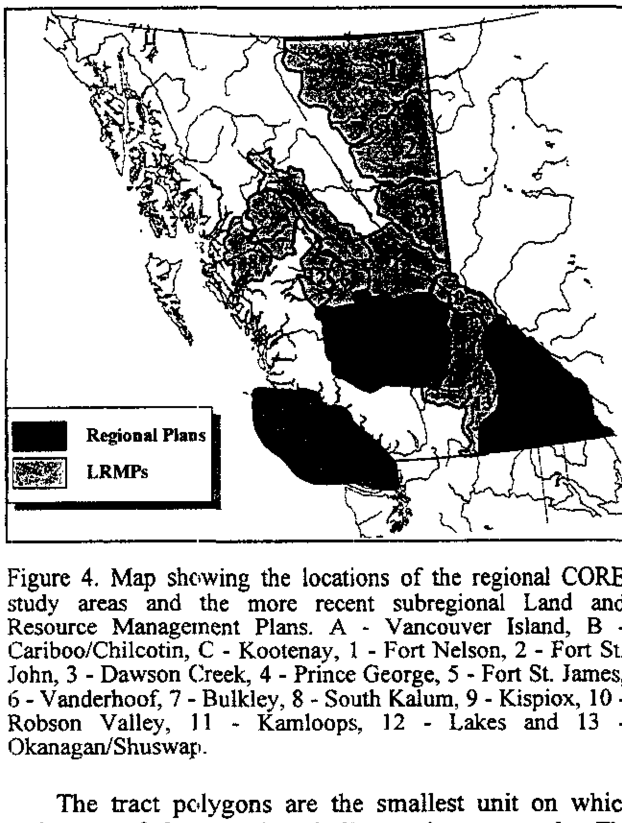


Figure 4. Map showing the locations of the regional CORE study areas and the more recent subregional Land and Resource Management Plans. A - Vancouver Island, B - Cariboo/Chilcotin, C - Kootenay, 1 - Fort Nelson, 2 - Fort St. John, 3 - Dawson Creek, 4 - Prince George, 5 - Fort St. James, 6 - Vanderhoof, 7 - Bulkley, 8 - South Kalum, 9 - Kispiox, 10 - Robson Valley, 11 - Kamloops, 12 - Lakes and 13 - Okanagan/Shuswap.

The tract polygons are the smallest unit on which estimates of future mineral discoveries are made. The estimation process treats the tract as a single homogenous unit. Estimated undiscovered deposits have no position within the tract but also cannot be assumed to be evenly distributed throughout the tract. When a LRMP is relatively small there may be few tracts in the study area. As a result there may not be sufficient detail available from the regional-scale analysis of the Mineral Potential Project to satisfy the more detailed land-use analysis being carried out for the LRMPs. This concern has not yet been expressed by land-use planners, but as more detailed analyses are performed, the value of the regional Mineral Potential Analysis will decrease. There are several options to address this problem, if it becomes a concern. Firstly, and most effective, would be the selection of smaller mineral assessment tracts based on smaller geological subdivisions and re-estimation of the potential discoveries in these smaller tracts. Alternatively, the deposit types estimated in the original tracts could be assigned, where possible, to "most likely" formations within the tract. In this way the finest resolution of the geological compilation would be made available.

# NEW METHODOLOGY

## *STRUCTURED ESTIMATION PROCESS*

Starting in November, 1994 a more structured method of collecting estimations was introduced. Earlier, industry and government experts received training on the estimation process and data packages for the region being estimated. They took this material away and made independent estimates for the tracts and deposit types for which they had significant expertise. As a result, not all tracts and deposit types received the same attention from the estimators.

A simple modification to this earlier process has resulted in a rigorous examination of all tracts and potential deposit types within a region. Now workshops of 3 to 5 days duration are held for each region, the estimators are divided into groups of three or four, and each group is responsible for estimating a class of deposits, for example skarns or porphyries. Usually there are five or six such groups, each working on a class of deposit types. The estimators in each group discuss the geology in each tract, using the information provided and adding their personal knowledge. Generally the groups work through the tracts in the region, examining each deposit type in their class of deposits, on a tract by tract basis. If they all agree that a particular deposit type is not possible in a tract, no estimate is made, but if one of the estimators feels there is a chance of a particular deposit type occurring in the tract, all the estimators in the group make a confidential estimate. As part of each estimate each estimator provides a confidential grading of the other estimators in the group, based on his or her perception of their knowledge of the tract and deposit type in question. These weights are used to combine the estimates generated by the group (see Grunsky and Kilby, 1996).

Advantages of this approach are:

- The estimation process is completed in less than five days.
- All tracts and deposit types are examined.
- Each estimate benefits from discussion between several experts (often more than 100 years of

collective experience is brought to play for a deposit type in a tract).
- A form of quality control is inherent in the expert-weighting process.

## WEIGHTING OF FULL PROBABILITY SPECTRUM

The subjective probability estimation process used provides a probability spectrum for each estimate; for each estimate, the number of deposits expected to be found in the future can be determined at various confidence values (Grunsky and Kilby, 1996). This probability spectrum of estimated deposits is used as input to the Mark 3 simulator (Root *et al.*, 1992) where it is combined with the deposit grade and tonnage probability information (Grunsky, 1995). Outputs from the simulator are probability spectrums for the tonnage of each commodity associated with the deposit type.

In earlier analyses, only the 50% confidence level was used for comparative purposes. It was found that a significant amount of information associated with low confidence levels was lost using this method. Now values from four confidence levels are used and weighted by their confidence in order to capture the full set of information that is available from the analysis. The confidence levels sampled are 90%, 50%, 10% and 1% and the associated weightings are .9, .5, .1, .01. These values can then be added to those from discovered deposits which have a 100% confidence level and weighting factor of 1.0.

## METAL AND INDUSTRIAL MINERALS MAPS

Metallic and industrial mineral commodities were grouped together during analysis early in the project. This grouping of two distinct types of commodities has caused difficulties in presenting meaningful results. Originally, end users desired only one map to represent mineral potential values. This requirement has changed and now more leeway is being allowed to accurately represent the various exploration and mining values of interest to the land-use planners.

In general, metallic commodities are sold into a general market with minimal processing and involving reletively low volumes. The ready market is there as long as the metellic element being sold is in demand and can be mined at a profit. Industrial minerals, on the other hand, tend to be far more dependent on specialized processing to meet limited specialized market requirements. Industrial minerals also tend to be bulk commodities, such as limestone, with very large tonnages of *in situ* resources, but with limited markets and transportation costs often rivaling mining costs.

To address these significant differences, two mineral assessment maps are now used to represent the mineral potential of a region; exactly the same tracts are used for each display.

## METALLIC MINERAL ASSESSMENT RANKING

The metallic mineral assessment ranking is made using the methodology described by Kilby (1995). The ranking is based on the gross in-place value of the metallic commodities in each tract, contained in both discovered and undiscovered deposits. The dollar value of the commodities in each deposit is used to generate a total dollar score for each tract. These dollar scores are then used to rank the tracts within the region.

## INDUSTRIAL MINERALS ASSESSMENT RANKING

The dollar value of the many industrial mineral commodities found in British Columbia is not an acceptable way to realistically compare their relative values. For example, it is relatively easy to locate a billion tonnes of limestone, but almost impossible to find a market for anywhere near this tonnage. Even at a very low dollar value per tonne, a deposit of this size would completely overshadow a much smaller deposit of some commodity that has a ready market. In this case, the large limestone deposit would be assigned a much higher value than the smaller deposit if simple dollar values were used to rank the commodities. An industrial mineral deposit ranking scheme has been established in an effort to overcome this problem.

A score of 1 to 100 is given to each type of industrial mineral deposit, ranking its perceived value. This value incorporates an estimate of product marketability if a deposit is found, and the overall value of the marketed product. The ranking has been done by experts in the industrial mineral field and a partial list is presented in Table 1.

**Table 1. Partial listing of industrial mineral deposit types with their ranking score.**

| Deposit Type | Ranking Score |
|---|---|
| Zeolites | 22.5 |
| Vermiculite | 27.5 |
| Mississippi Valley Type Barite | 35.0 |
| Residual Kaolin | 45.0 |
| Crystalline Flake Graphite | 65.0 |
| Asbestos | 95 |
| Diamond | 95 |

The final ranking score for industrial minerals is based on both discovered deposits and estimated future discoveries. For known deposits, the dollar value of all defined resources is summed for each tract, just as with metallic minerals. The tracts are ordered by this total discovered dollar value and then assigned an ordinal value from 1 to the total number of tracts (1 being the lowest).

The number of deposits expected to be discovered is multiplied by the industrial mineral deposit ranking value (Table 1) at four probability levels; these scores are compiled for each deposit type estimated in each tract. The probability levels used are .90,.50, .10 and .01. Once the values associated with all industrial mineral deposit types estimated have been compiled for each tract, the tracts are ranked by the scores associated with each of the four probability levels. An ordinal value from 1 to the total number of tracts is assigned to each tract for each of the four levels. The final ranking score for the tract is obtained by weighting the five ordinal scores and summing these values. The weighting values used for each probability level and the discovered deposits are the same as described in the above section on weighting the full probability spectrum.

## *PHASE 1 DISCONTINUED*

Phase 1 methodology, as described in Kilby (1995), was designed as an interim response to extremely short timelines. Its objective was to use existing information to estimate the tract ranking industry experts would produce through the more rigorous probability estimation process. The Phase 1 maps were easily understood by non-specialists, as simple weightings were applied to four historical parameters that had been collected for each tract. These maps have become popular with lay people and have in some cases been preferred over the much more predictive maps based on expert estimations. Every effort is now being made to discourage the use of these maps as indicative of the value of the landbase of a region.

The information used to compile the maps remains useful to represent the value of mineral exploration and mining in a region, but the Phase 1 derivative map produced from these data should no longer be used, as it has outlived its value. Much better maps are now available to illustrate the relative ranking of the landbase.

# MINERAL POTENTIAL INFORMATION DISTRIBUTION

## *OPEN FILE RELEASES ON DISKETTE*

Digital versions of the compiled geology have been released in the form of Open File publications since 1994. Eight such releases have been made (Figure 3), each covering a complete region or half a region. The information is placed on diskettes in a CAD format (.DXF) with supporting paper information such as a dump of the CAD linework, legend and reference list. The released information is adequate for incorporation into a GIS or simply used for CAD drawings.

## *ON-LINE ACCESS BY WWW - MINERAL POTENTIAL HOMEPAGE*

A Mineral Potential Homepage has been established on the World Wide Web to display and provide access to the results of the Mineral Potential Project and datasets generated by the project. The URL (Universal Resource Locator) for the site is http://www.empr.gov.bc.ca (Figure 5).

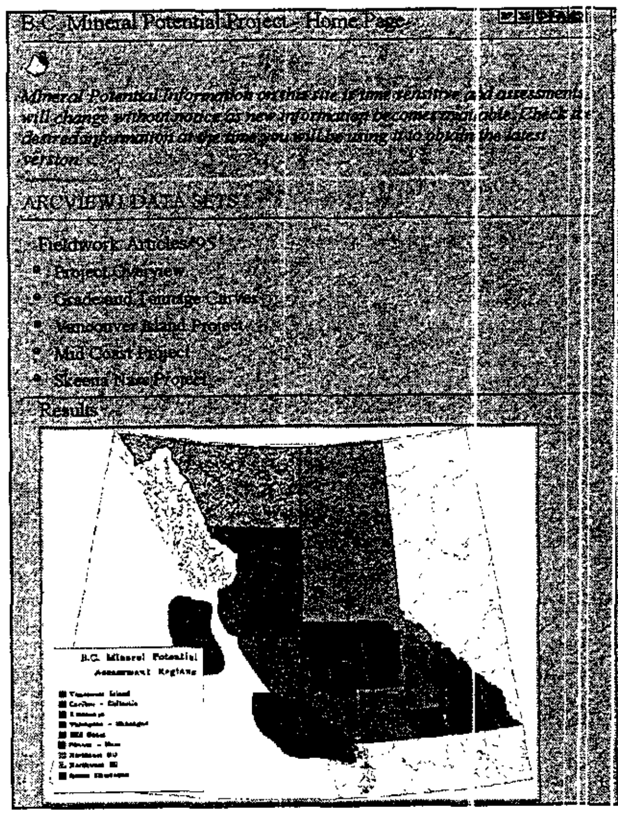

Figure 5. Mineral Potential Project World Wide Web homepage showing the various topics available.

### REPORTS AND ARTICLES

The homepage contains a section of hyperlinked articles describing various aspects of the Mineral Potential Project. The articles are hypertext copies from Geological Fieldwork 1994. Articles from Geological Fieldwork 1995, such as this one, will be added to this location.

### MINERAL ASSESSMENT MAPS (HYPERLINKED)

The results of the mineral assessments can be viewed interactively on the WWW site with a WWW browser. Colour maps of each analysed region are presented, showing the relative rankings of the tracts (Figure 6). The viewer can click on a tract of interest to obtain a table of information about the tract, such as the results of the

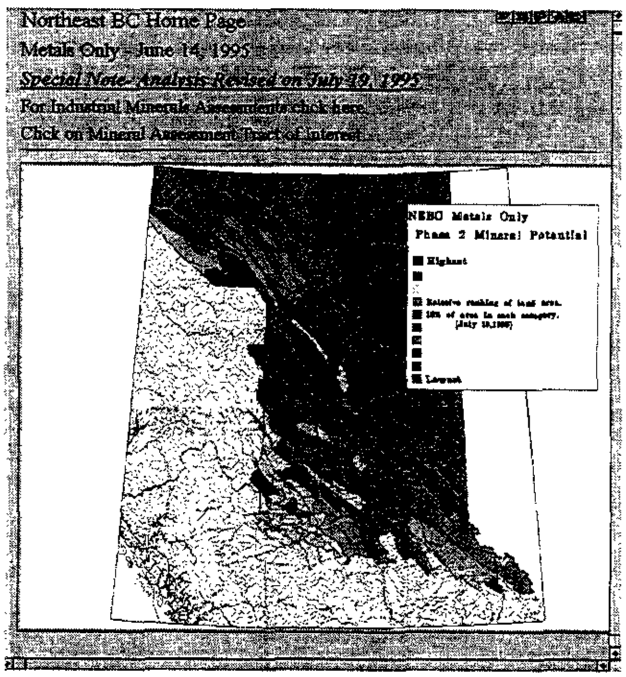


Figure 6. Example of a mineral assessment map accessible on the World Wide Web.

estimation process, mineral occurrences in the tract, tract area, value of past production, value of past exploration and the relative ranking of the tract (Figure 7).

## DOWN-LOADABLE DATA

In addition to being able to view the results of the mineral potential project interactively, information can be downloaded for subsequent analysis and use at no cost. The down-loadable data can be accessed through the Mineral Potential Homepage or through LANDDATA BC (accessible through the B.C. Government Homepage at http://WWW.GOV.BC.CA). All the datasets provided in this section have been placed in a single standard projection so they can be combined in any combination and retain their relative positions. The information is presented in one format at present: the Export (E00) format of ESRI. This allows easy importing to major GIS systems and is easily viewable by the freely available program ARCVIEW1 which can be accessed from the WWW site. This program runs on PC computers with the WINDOWS operating system. This powerful program allows users to produce a wide range of maps and derivative analyses from the datasets provided (Figure 8).

### *Mineral Assessments*

The results of the mineral assessment of each region are contained in individual ESRI Export files. A view file is attached in a single zipped file for convenience of downloading. The file contains information describing the shape of each mineral assessment tract and associated attribute information. The attribute information available

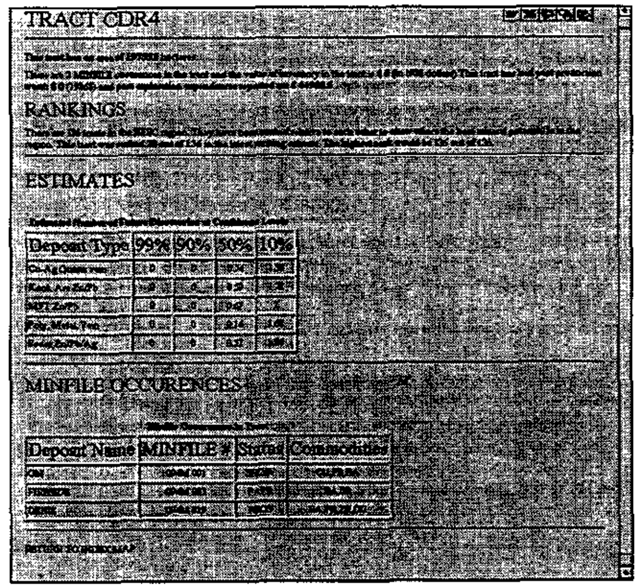


Figure 7. Example of a tract table which is hyperlinked to a tract on a mineral assessment map.

for each tract is: tract name, tract area, number of mineral occurrences in the tract, value of past production, value of past exploration reported, value of known resources (metallic), relative tract ranking with respect to metallic minerals, relative tract ranking with respect to industrial minerals, value of known resources (industrial minerals) and blank calculation fields.

Each of these attributes can be used for labeling, or to colour the tracts within the map area to illustrate the distribution of a desired variable, as shown in Figure 8.

### *Province-Wide Datasets*

Two base maps of the province are available for downloading. The file BC.zip contains a very simplified outline of the province with major waterways (see background of Figures 2 and 3). The file BCFULL.zip contains a much more detailed map of British Columbia useful, at scales as detailed as 1:500 000.

The file MINFILE.zip contains all the mineral occurrence data locations recorded in the MINFILE database (Jones and McPeek, 1992). In addition to the geographic location of the mineral occurrence, the following information is included in this subset of MINFILE: MINFILE number, map sheet name, deposit name, occurrence status, commodities and deposit type.

The file ARIS.zip contains the locations of all mineral assessment reports filed with the Ministry and recorded in the Assessment Report Information System (Kalnins and Wilcox, 1994). In addition to the geographic location of each report, the following information about the report is included in the file: Assessment Report number, confidentiality period, year of report and value of exploration work reported.

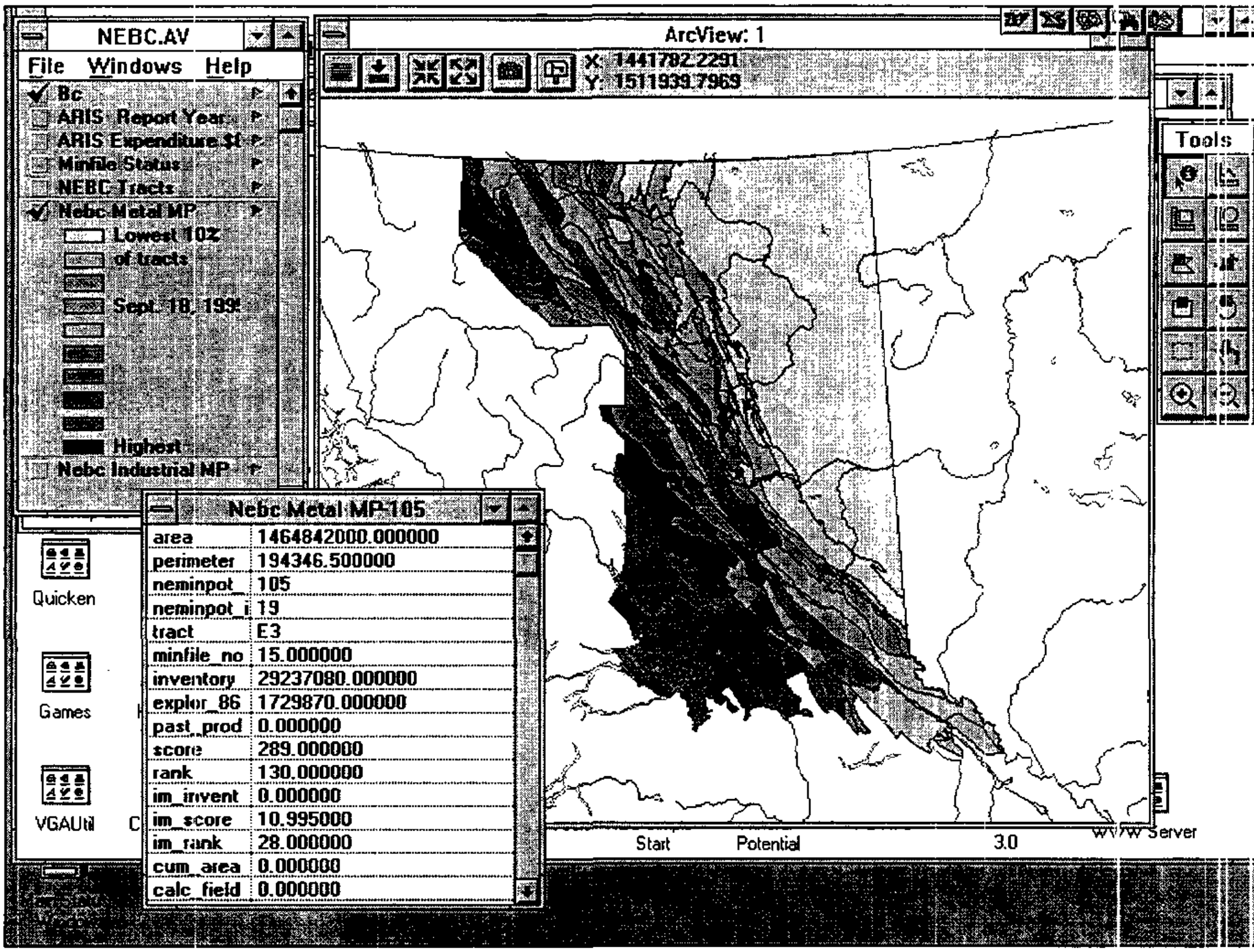


Figure 8. Arcview1 map of Northeast British Columbia Mineral Assessment data showing the map, legend, tool menu and the query menu.

The compiled geology for each region has been converted into the ESRI Export format. The regions have been divided into individual 1:250 000 map-sheet files to reduce file size and facilitate downloading over the Internet. Each map sheet is represented by three files; a geology polygon, geology linework and a view file are needed to completely illustrate the geology of a map sheet. The view files for all the maps within a region contain a standardized legend for the whole region. Views are also available that combine all the map sheets within a region. These geological maps are presented on an "as is" basis and are continually being upgraded.

## FUTURE

The next year of the project will see the completion of the analysis for the whole province. The Queen Charlotte Islands are all that will remain to be completed at the end of this year. By the end of next year all the mineral assessment data and compiled geology for the province will be available on the World Wide Web.

## REFERENCES

B.C. Ministry of Energy, Mines and Petroleum Resources (1995): The Muskwa - Kechika Area: Planning for Energy and Mineral Resources; *B.C. Ministry of Energy, Mines and Petroleum Resources,* Information Paper, 53 pages.

Bellefontaine, K.A. and Alldrick, D.J. (1994): Mineral Potential - Mid-Coast Area; *B.C. Ministry of Energy, Mines and Petroleum Resources*, Open File 1994-17.

Bellefontaine, K.A., Legun, A., Massey, N.W.D. and Desjardins, P. (1995): Mineral Potential - Digital Geological Compilation NEBC South 1/2; *B.C. Ministry of Energy, Mines and Petroleum Resources*, Open File 1995-24.

Desjardins, P. (1994); Digital Geology Polygons for Vancouver Island, Kootenay Region and Cariboo-Chilcotin Region; *B.C. Ministry of Energy, Mines and Petroleum Resources*, Open File 1994-27.

Grunsky, E.C. (1995): Grade and Tonnage Data for Mineral Deposit Models in British Columbia; *in* Geological Fieldwork 1994, Grant, B. and Newell, J.M., Editors, *B.C. Ministry of Energy, Mines and Petroleum Resources*, Paper 1995-1, pages 417-423.

Grunsky, E.C. and Kilby, W.E. (1996): Mineral Resource Estimation: An Evaluation of Responses from Northeast British Columbia; *in* Geological Fieldwork 1995, Grant, B. and Newell, J.M., Editors, *B.C. Ministry of Energy,* *Mines and Petroleum Resources*, Paper 1996-1, this volume.

Höy, T., Church, N., Legun, A., Glover, K., Gibson, G., Grant, B., Wheeler, J.O. and Dunn, K.P.E. (1994): Mineral Potential -Kootenay Area; *B.C. Ministry of Energy, Mines and Petroleum Resources*, Open File 1994-8.

Jones, L.D. and McPeek, C.B. (1992): MINFILE - A Mineral Deposit Information System for B.C.; *B.C. Ministry of Energy, Mines and Petroleum Resources*, Information Circular 1992-2.

Journeay, J.M. and Williams, S.P. (1995): GIS Map Library: A Window on Cordilleran Geology; *Geological Survey of Canada*, Open File 2948 (V. 1.0).

Kalnins, T.E. and Wilcox, A.F. (1994): A Primary Source of Exploration Data - Assessment Reports; *B.C. Ministry of Energy, Mines and Petroleum Resources*, pamphlet.

Kilby, W.E. (1995) Mineral Potential Project - Overview; *in* Geological Fieldwork 1995, Grant, B. and Newell, J.M., Editors, *B.C. Ministry of Energy, Mines and Petroleum Resources*, Paper 1996-1, pages 411-416.

MacIntyre, D., Ash, C. and Britton, J. (1994): Mineral Potential - Nass-Skeena Area; *B.C. Ministry of Energy, Mines and Petroleum Resources*, Open File 1994-14.

MacIntyre, D.G., Legun, A., Bellefontaine, K.S. and Massey,.N.W.D. (1995): Mineral Potential Project - Digital Geological Compilation NEBC North 1/2; *B.C. Ministry of Energy, Mines and Petroleum Resources*, Open File 1995-6.

Massey, N.W.D. (1994): Mineral Potential - Vancouver Island; *B.C. Ministry of Energy, Mines and Petroleum Resources*, Open File 1994-6.

Root, D.H., Menzie, W.D. and Scott, W.A. (1992): Computer Monte Carlo Simulation in Quantitative Resource Assessment; *Nonrenewable Resources*, Volume 1, No. 2, pages 125-138.

Schiarizza, P., Panteleyev, A., Gaba, B. and Glover, K. (1994): Mineral Potential - Cariboo-Chilcotin Area; *B.C. Ministry of Energy, Mines and Petroleum Resources*, Open File 1994-7.

# MINERAL RESOURCE ESTIMATION: AN EVALUATION OF RESPONSES FROM NORTHEAST BRITISH COLUMBIA

**E.C. Grunsky and W.E. Kilby**

KEYWORDS: Mineral resource assessment, estimator evaluation, Northeast British Columbia

## INTRODUCTION

The Mineral Potential Project is an initiative that provides predictions of resource abundance in the province and has been described by Kilby (1995). In this project, resource assessment is carried out on specified tracts of land, referred to as mineral assessment tracts. These tracts are generalizations of contiguous geological tracts that share a common tectonic history and metallogeny and whose boundaries reflect differences in lithology, structure and geological history (*see* Grunsky *et al.*, 1994; Church, 1995; Massey, 1995). Areas that have been covered to date include: Vancouver Island, Kootenay region, Cariboo region, Skeena-Nass region, Mid-coast, Thompson-Okanagan region, and northeast British Columbia (*see* Kilby, 1995, Figure 1).

The Mineral Potential Project adapted an approach similar to the methodology of the U.S. Geological Survey three-part assessment method as outlined by Singer (1993). The modified methodology used in British Columbia consists of:

- Creation of mineral assessment tracts;
- Grade and tonnage models are used that reflect the types of deposits that are expected in the area;
- An estimate of expected undiscovered deposits based on the grade and tonnage data.

In contrast to a purely statistical assessment based on a grid-cell approach, the mineral assessment tracts were created to reflect areas that contain specific characteristics related to metallogeny. The assessment is based on subjective probability applied to the prediction of undiscovered resources and known resources. The subjective approach to resource estimation requires that geologists make estimates on the likelihood of finding deposits, based on their knowledge of the geology and other information within each tract. These assessments were carried out in Mineral Resource Assessment Workshops.

## WORKSHOP METHOD

The workshop were introduced with lectures about the regional geology and known metallogeny. Geologists were assigned to working groups of three to four members. Each group represented knowledge and expertise with specific types of mineral deposits (e.g. industrial minerals, gold deposits, massive sulphide deposits). A facilitator was assigned to each group. The facilitator compiled the responses from the members and worked at resolving questions or difficulties that might be encountered in the group. Each group was given mineral resource assessment tract maps, geological maps, geochemical maps, geophysical maps, and a copy of the MINFILE database. Using these resources, the group members discussed the likelihood of mineral deposits of specific classes that might possibly be present. Through discussions, each member of the group was exposed to the other estimators' persnal knowledge of a given tract. Each member of the group would then, based on their knowledge, the information provided and the group discussion, make an independent confidential probabilistic estimation of undiscoveredl mineral deposits. This approach, modified from the RCON approach of Resource Science, Inc., (1994) weights the responses of individuals. The potential benefit of such weights is that an estimator who is highly respected (high scores) has more influence than an estimator who is considered to have less knowledge (lower scores) for a particular deposit model or mineral assessment tract.

## ESTIMATOR RESPONSE

A cornerstone of accurate estimates is the correct understanding of how a geologist perceives the likelihood of **at least one or more undiscovered deposits** occurring in a tract. Each workshop covered the process of assessment with careful instructions of how the resulting estimates are translated into a frequency distribution that is used in the simulation process. The use of grade and tonnage models is crucial to a meaningful estimate of resources, as the estimator must consider the size and grade of a deposit in order to make an estimate (Grunsky, 1995; Resource Science, Inc., 1994). In this study geologists used the median grade and tonnage as the basis for their estimates (Kilby, 1995). The estimates were then used as input to a Monte Carlo simulation program that computes expected grades and tonnage, given the probability of finding at least one deposit. A typical response is as shown in Figure 1. The interpretation of this response is as follows:

The geologist decided that the probabilities of finding one or more copper skarn deposits are:

- 85% probability that there is at least one undiscovered deposit.
- 44% probability that there are at least two undiscovered deposits present.
- 21% probability that there are three undiscovered deposits present.

From these estimates a probability distribution can be constructed that indicates the likelihood of undiscovered

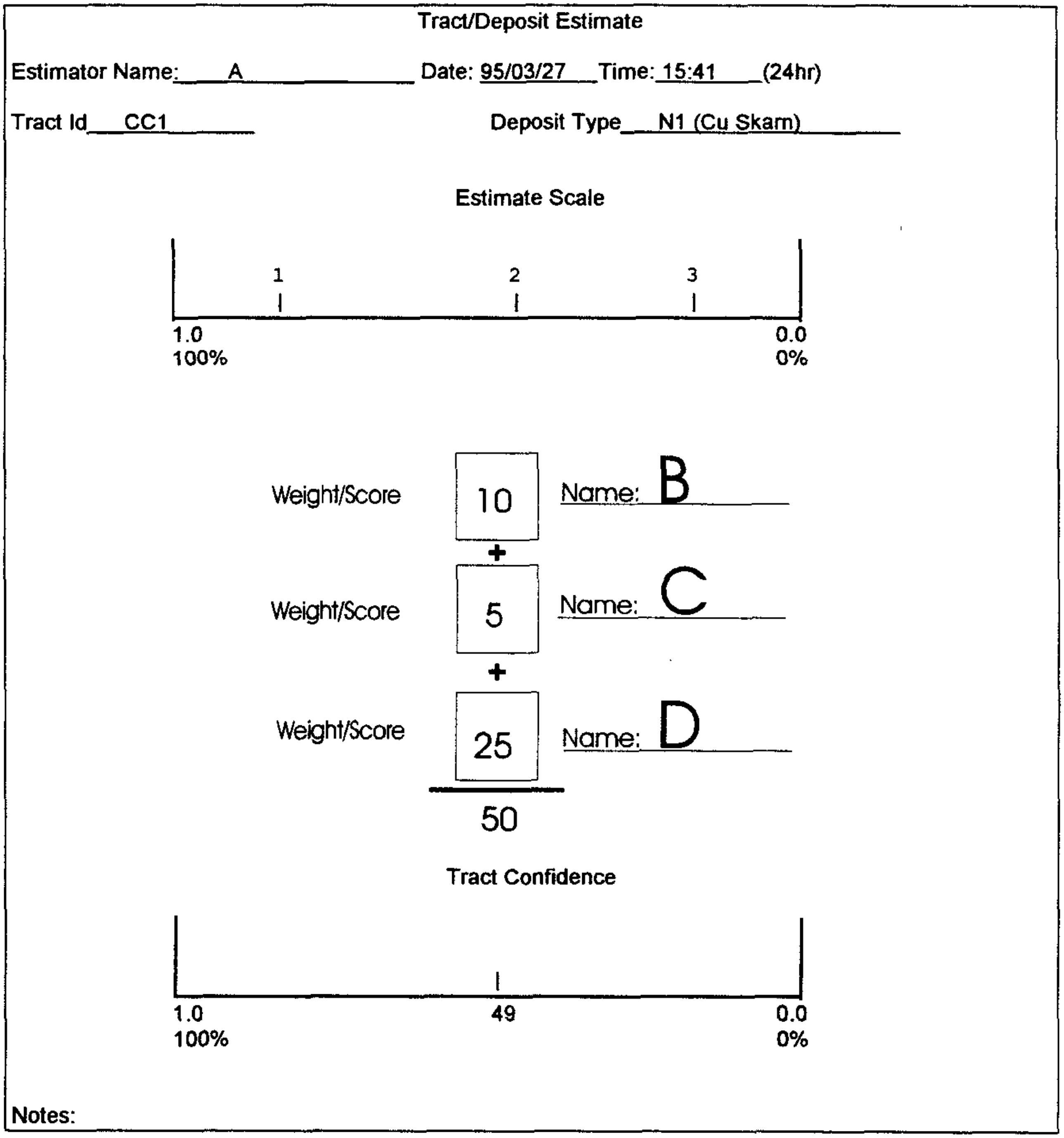
Tract/Deposit Estimate

Estimator Name: A Date: 95/03/27 Time: 15:41 (24hr)

Tract Id CC1 Deposit Type N1 (Cu Skarn)

Estimate Scale

1 2 3

1.0 0.0
100% 0%

Weight/Score 10 Name: B
+
Weight/Score 5 Name: C
+
Weight/Score 25 Name: D

50

Tract Confidence

1.0 49 0.0
100% 0%

Notes:

Figure 1. Estimator work sheet.

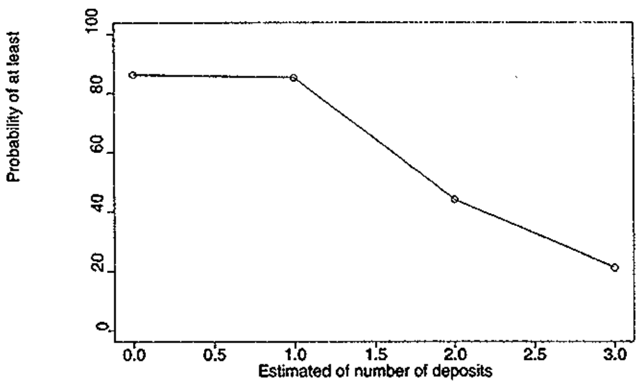


Figure 2. Cumulative probability distribution of estimator response for a specific tract and mineral deposit model.

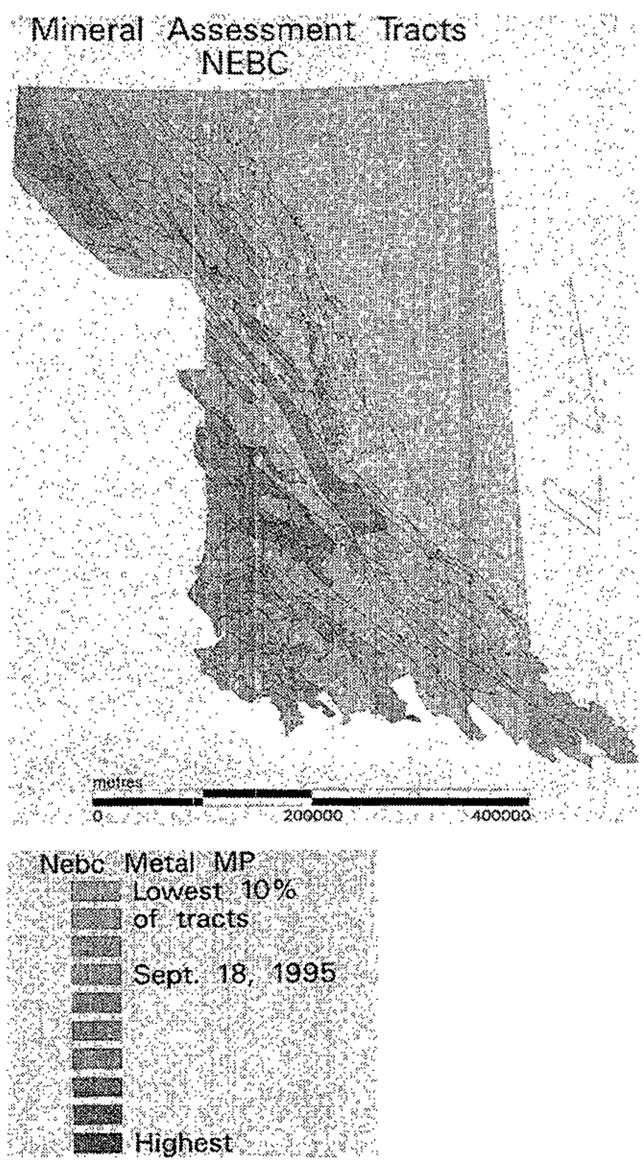


Figure 3. Map showing the Mineral Assessment Tract locations for Northeast B.C. The map is shaded according to mineral potential. Light areas have low mineral potential; dark areas have high mineral potential.

copper skarn deposits existing in this mineral assessment tract. A schematic of the initial estimate is shown in Figure 2. Using the procedure outlined by Root *et al.* (1992) the endpoints of the distribution can be defined and constructed so that probabilities and estimates are defined for the 99, 90, 50 and 10 percent probabilities. These computed values were used as a comparative basis between estimators, mineral deposit models and tracts. For each estimate, the geologist also assigned a weight to the other group members. The assigned weight may vary from 0 to 50 for the group members. The maximum score that any individual can assign another group member is 50. (As shown in Figure 1, the weights estimator A assigned to estimators B,C and D are 10, 5 and 25, respectively). Each estimator is automatically assigned a weight of 50. The total combined weight for any individual cannot exceed 100. For example if there are four members to a group, the maximum score that the group may obtain is a value of 400. Each group member will have individual weights that may vary from a minimum of 50 to a maximum of 200. Mathematically expressed, an estimate, P, made for a given tract, j, and mineral deposit model, k, with estimator, a, with weights from estimators i (i=1,2, ...,n-1) is defined as follows (equation 1):

$$E_a = 50^*P_{ajk} + \sum_{i=1}^{n} w_{ijk}{}^*P_{ajk} \qquad (1)$$

where P represents the probability and w is the assigned weight.

Estimates were made for each tract, for each mineral deposit type considered likely to occur within it. For northeast British Columbia., a total of 2533 estimates were made. Figure 3 shows the locations of the mineral assessment tracts in the northeast region. The number of estimates made for each of the tracts varied greatly. The estimates were compiled and entered into a database that served as input for the Monte Carlo simulation program. Note that the references made to estimators G1A, G1B, G1C, and G1D represent estimators A, B, C and D for Group 1, respectively.

The Monte Carlo simulation program was adapted from the Mark 3 Simulation program that was kindly provided by the U.S. Geological Survey. It was modified to accept grade and tonnage data from British Columbia mineral deposit models (Lefebure *et al.*, 1995). The program was originally written to accept estimates at 90, 50 and 10% probabilities. This was modified to accept up to ten estimates with probabilities defined by the marks placed on the scale, as shown in Figure 1. The assigned weights of the estimators are applied to the results of the simulation.

The process of Monte Carlo simulation involves a random selection from the probability distribution that is determined from the estimates for a given tract and deposit model. The distribution curve is sampled 4999 times. Each time it is sampled, the resulting probability is multiplied by

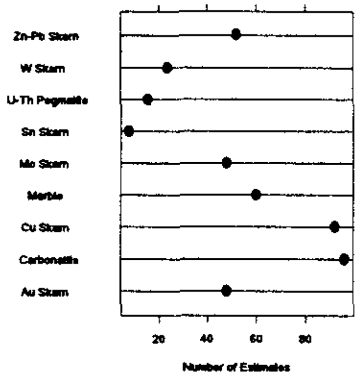


Figure 4. Number of estimates made by Group 1 for each mineral deposit model.

a randomly chosen grade and tonnage appropriate to the deposit model. This product is an estimate of the actual number of kilograms of metal. For each iteration, the product is summed. The final iteration produces a total expected number of kilograms of metal based on the distribution of the estimate.

## COMPILATION OF RESPONSES

The estimates have been compiled and analyzed, in part, using a graphical display package. Not all features of the responses can be shown here. A total of five groups provided estimates for the northeast British Columbia region. The results from Group 1 are presented here. Group 1 had a total of four estimators and assessed the potential for the following models: U-Th pegmatite, Cu skarn, Pb-Zn skarn, Au skarn, W skarn, Sn skarn, marble skarn and carbonatite deposits. The group made 444 estimates. Figure 4 shows how the estimates were distributed over the mineral deposit models assessed by the group.

## ESTIMATOR CONFIDENCE:

Figure 5 shows a plot of the overall confidences of estimates expressed by each estimator. Notice that most estimates are in the range of 25 to 60% for estimators A, B, and C. Estimator D displays a considerably higher amount of confidence relative to the others.. The interpretation that can be drawn from this figure is as follows:

- Estimators A and B share similar levels of confidence,
- Estimators C and D shows a more constrained range of confidences relative to estimators A and B,
- Estimator D shows a high degree of confidence relative to estimators A, B, and C.

One interpretation for very high confidences is that the estimator had some detailed knowledge about the mineral assessment tract and deposit model. Where confidences are very low, it can be inferred that the estimators did not feel comfortable with their level of knowledge or by what was discussed within the group for a given mineral assessment tract and deposit model.

A further analysis of confidence levels can be made by evaluating confidence as a function of mineral deposit model. This is illustrated in Figure 6 where the confidences of the estimators can be examined with respect to each of the mineral deposits. Estimators A and B show the greatest range in confidence. No clear comparisons or distinctions can be made between the four estimators, however, the figure clearly captures the range of confidence with respect to the mineral deposit models that were considered.

An important consideration is the confidence of estimators with respect to each other. Evaluation of the weight

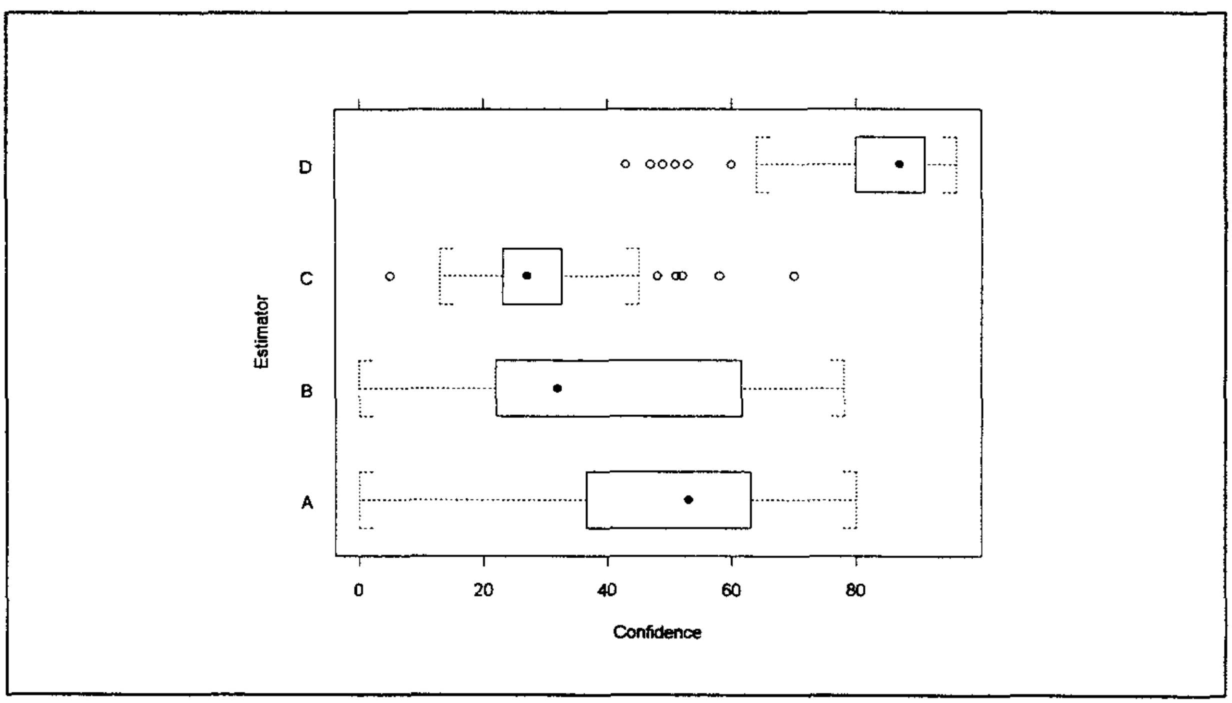


Figure 5. Boxplot showing the range of confidences expressed by each estimator for their own estimates.

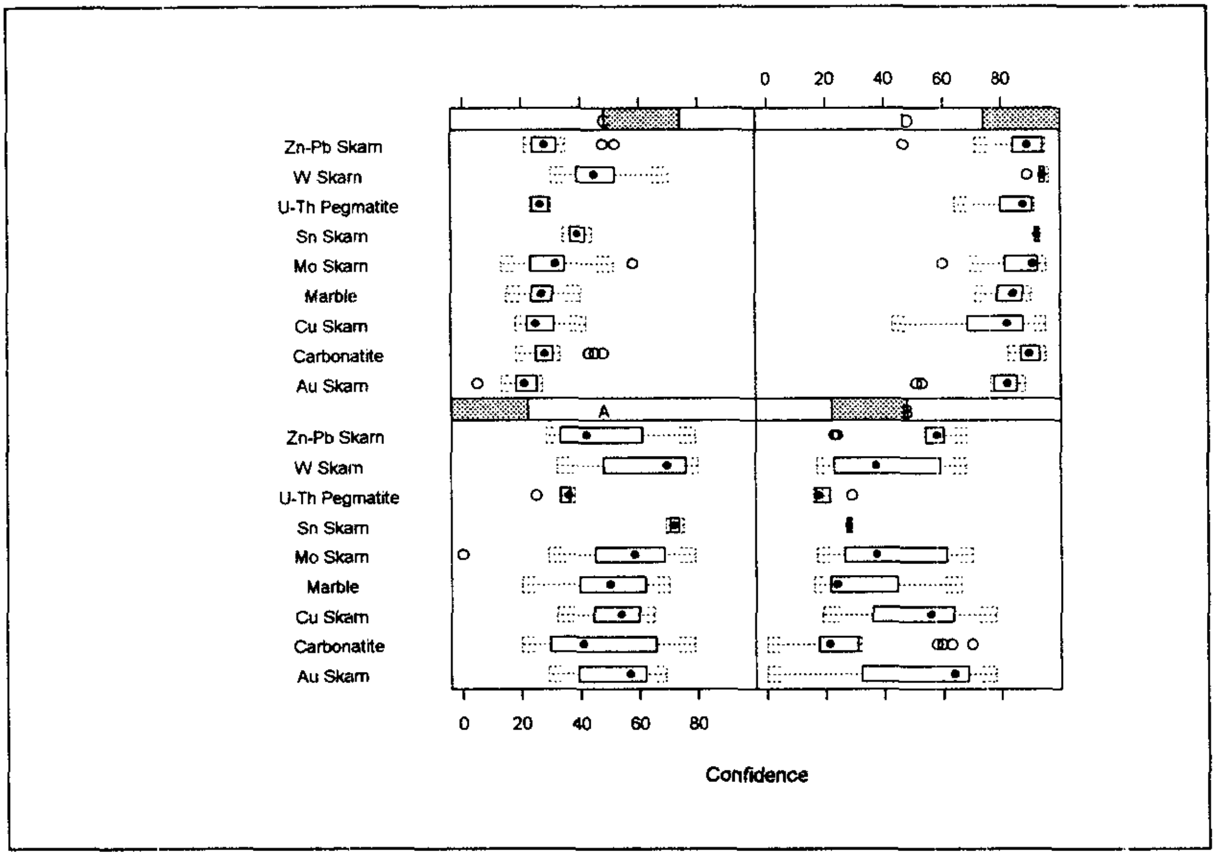


Figure 6. Boxplot showing confidence ranges for specific deposit types.

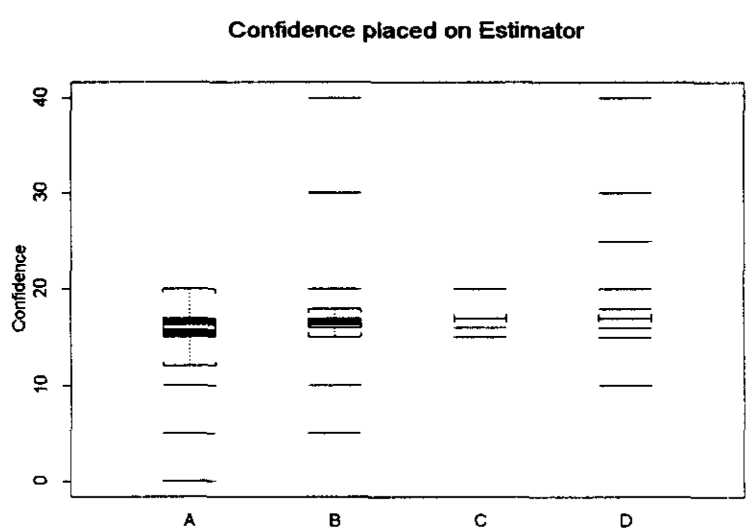


Figure 7. Boxplot showing how estimators were judged by each other. Each estimator can receive a maximum of 50 points from other group members,

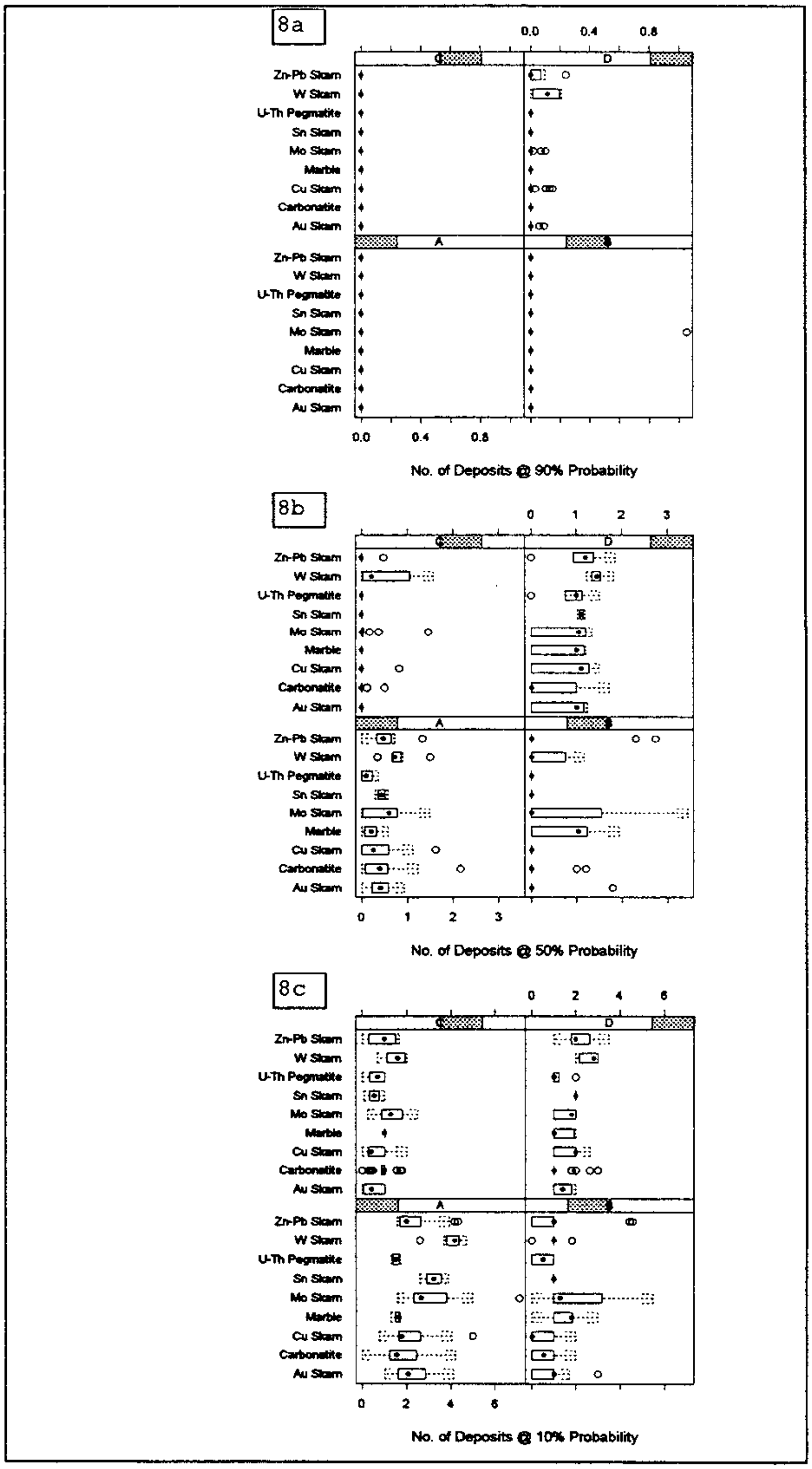


Figure 8. Number of estimates versus mineral deposit model for each of the estimators.

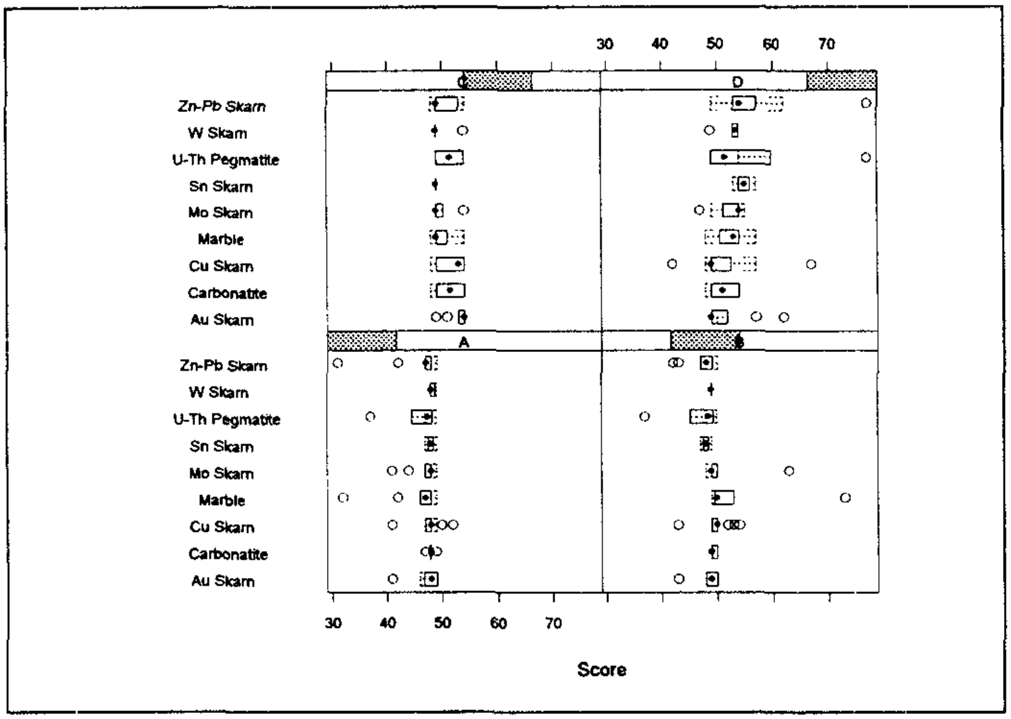


Figure 9. Scores assigned to each estimator for each deposit model. The maximum score that any estimator can obtain is 150. Note that most scores are in the range of 40 to 50. Estimator D obtained the highest scores. This suggests that the other estimators assigned more value to the estimates made by estimator D.

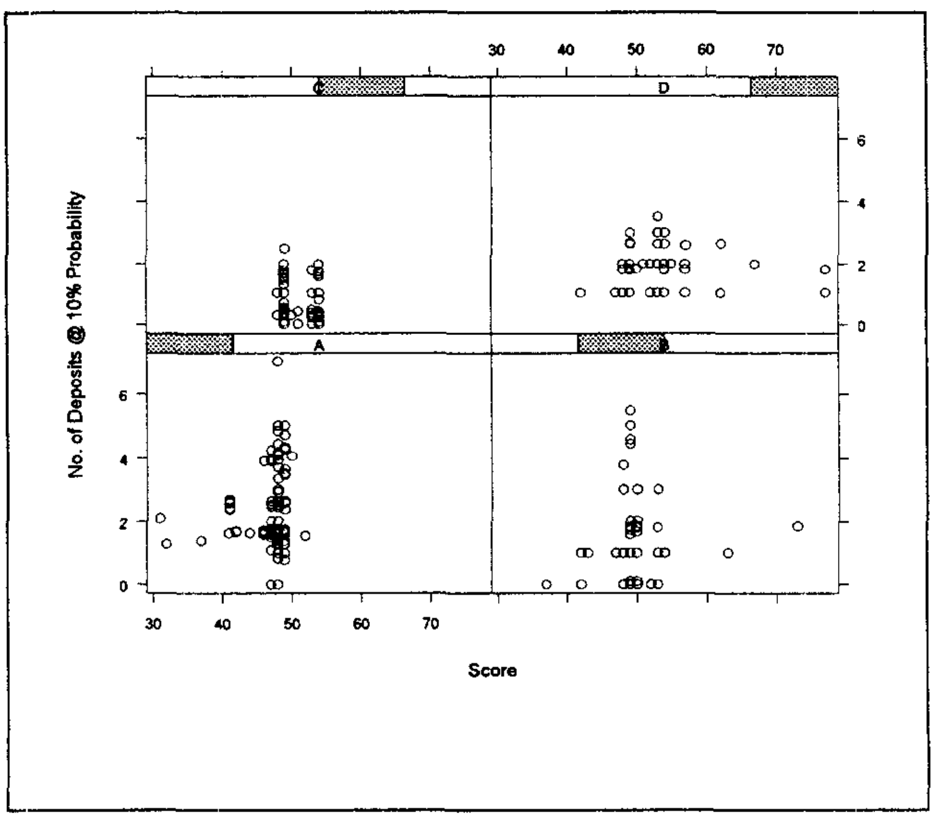


Figure 10. A plot of estimator scores versus the number of predicted deposits at the 10 % level of probability..

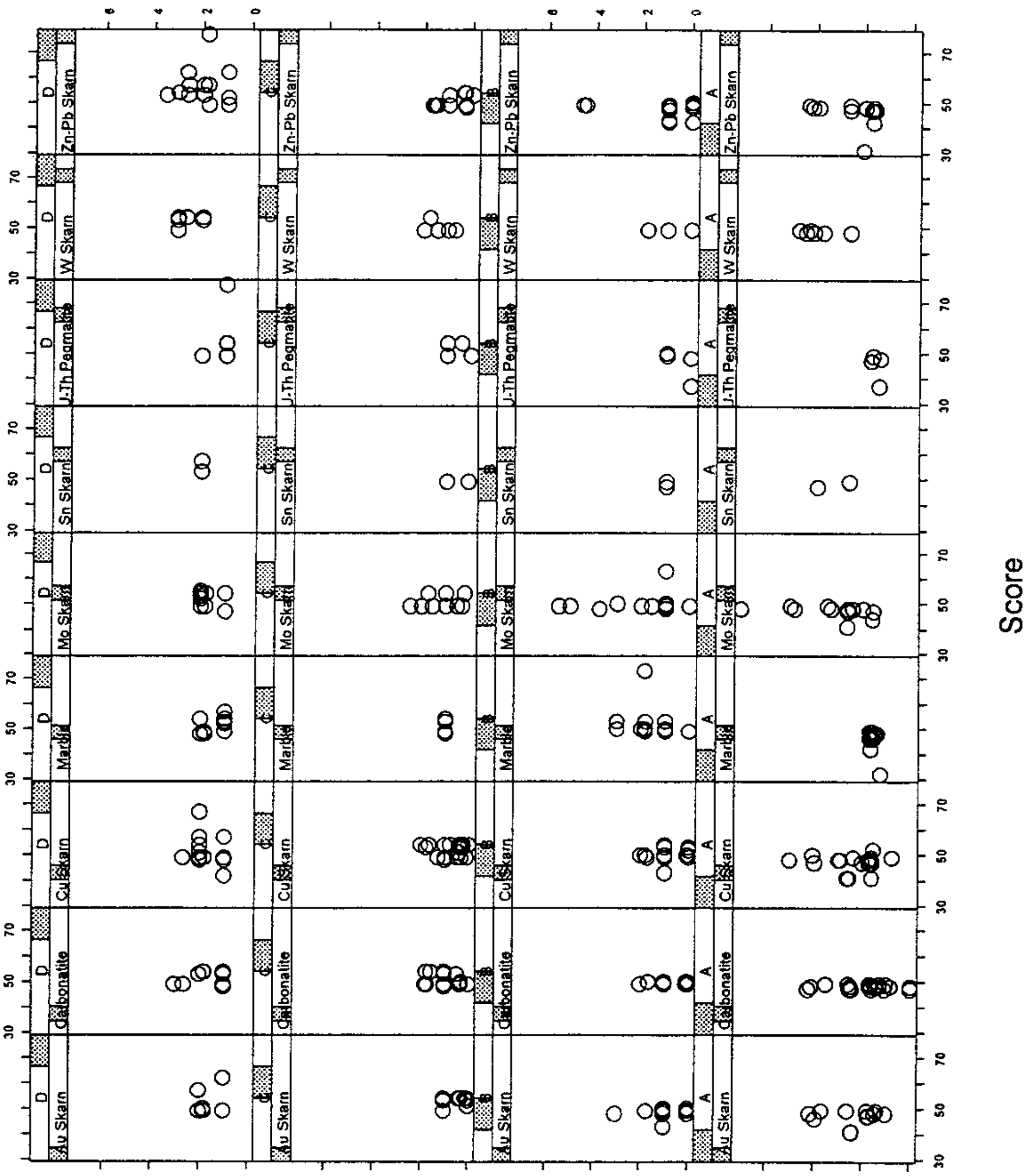


Figure 11. A plot of the number of predicted deposits at the 10% level of probability as a function of score for each mineral deposit profile and estimator.

(or score) that each estimator gives the others can be examined to see who in the group receives the most weight and who, the least weight. Figure 7 shows a compilation of weights that were assigned to each of the four estimators. For four estimators, the average weighting that could be assigned was 50/3 which means that two estimators would be given 17 points and one estimator would be given 16 points. A summary of the responses is as follows:

- Estimator B was given a low weighting for two estimates and very high weightings for three estimates,
- Estimator C shows little variation in the weighting assigned by others.
- Estimator D shows the greatest variation of weighting and received high weights for two estimates.
- Estimator A was given a low weighting for three particular estimates.

The variation in the weighting does not appear to be very dramatic and suggests that generally the estimators had consistent confidence in each other's ability. Alternatively, there may have been some reluctance to depart from a neutral weighting in expressing confidence in each other's estimates.

## ESTIMATES AT DIFFERENT PROBABILITY LEVELS

Figure 8 is a plot of the number of estimates made by each estimator for each model at three confidence levels. The number of estimates represents the number of ticks that were placed along the estimate scale as shown in Figure 1. Comparison of Figures 8a, b, and c provides an estimate how certain the estimators were of finding at least one deposit at the 90, 50 and 10% confidence levels. Figure 8a shows that only estimator D has made predictions of at least one deposit at 90% or better confidence for any of the skarn mineral deposit models. At the 50% and 10% levels of confidence, estimators B and C are more conservative than A or D, as shown in Figures 8b and 8c. However, estimator D does not predict more deposits than the others at the 10% level of confidence. This estimator displayed high levels of confidence in his/her own estimates (Figure 5) and has predicted a greater likelihood of finding additional deposits relative to the other group members, particularly at the greater than 50% level of confidence. The results of this analysis indicate that estimator D will predict more tonnes of metal than the other estimators, due to the higher probability of finding a deposit.

## EVALUATION OF THE ESTIMATES BASED ON ESTIMATOR SCORES

Although each estimator generated a range of estimates as illustrated in Figure 8, these results were modified based on the score that each estimator received as shown in equation 1. The scores can be summarized in terms of the mineral deposit models and the actual estimates made. Figure 9 shows a boxplot of scores given each estimator for each model. Examination of the figure indicates that the overall scores that each estimator received do not differ greatly. The mean scores for estimators A, B, C and D were 47, 49, 51 and 52, respectively. However, in Figure 8, it appears that estimator A received lower scores for several estimates and estimators C and D received higher. The scores can also be viewed in terms of the number of deposits predicted made by each of the estimators. Figure 10 is a scatterplot of score versus number of predicted deposits at the 10% probability level. This is analogous to the plot shown in Figure 8c. Examination of this figure shows that estimators A and B estimated a higher number of deposits than estimators C or D, but have a corresponding lower score. Figure 11 shows a further breakdown of the information illustrated by Figure 10. In this figure predictions at the 10% probability level are plotted with respect to each estimator and mineral deposit model. This permits a closer examination of score and prediction as a function of model and estimator.

## CONCLUDING COMMENTS

In the example described in this paper, it appears that there is not a great degree of variation between the estimates and scores of the four estimators. Of the four estimators, D appears to have had the highest degree of confidence. The self confidence expressed by estimator D also influenced the scores given D by the other group members. Estimator D, on the average was assigned a higher weight than the other three estimators. Also, because D has predicted the presence of deposits at a higher degree of probability, D will have more influence on the resulting tonnage estimates that are generated in the Monte Carlo simulation program. The assessments of the group of estimators described here require further analysis to capture the range of thinking that was expressed in the estimates. Further analysis is being carried out on the five groups that took part in the resource estimate workshop for northeast British Columbia. These results will be reported in the near future.

## REFERENCES


Church, B.N. (1995): Mineral Potential of the Okanagan-Similkameen-Boundary Area (82E, 82L/SE, SW, 92H/SE, NE); *in* Geological Fieldwork 1994, Grant, B. and Newell, J.M., Editors, *B.C. Ministry of Energy, Mines and Petroleum Resources*, Paper 1995-1, pages 424-434

Grunsky, E.C. (1995): Grade and Tonnage Data for British Columbia Mineral Deposit Models; *in* Geological Fieldwork 1994, Grant, B. and Newell, J.M., Editors, *B.C. Ministry of Energy, Mines and Petroleum Resources*, Paper 1995-1, pages 417-423.

Grunsky, E.C., Massey, N.W.D. and Kilby, W.E. (1994): Mineral Resource Assessment in British Columbia, The Mineral Potential Project; *Nonrenewable Resources*, Volume 3, No. 4, pages 271-283.

Kilby, W.E. (1995): Mineral Potential Project - Overview; *in* Geological Fieldwork 1994, Grant, B. and Newell, J.M., Editors, *B.C. Ministry of Energy, Mines and Petroleum Resources*, Paper 1995-1, pages 411-416.

Lefebure, D.V., Alldrick, G.J., Simandl, G.J. and Ray, G. (1995): British Columbia Mineral Deposit Profiles, *in* Geological Fieldwork 1994, Grant, B. and Newell, J.M., Editors. *B.C.*

*Ministry of Energy, Mines and Petroleum Resources*, Paper 1995-1, pages 469-490.

Massey, N.W.D. (1995): The Vancouver Island Mineral Potential Project (92B, C, E, F, G, K, L and 102I); *in* Geological Fieldwork 1994, Grant, B. and Newell, J.M., Editors, *B.C. Ministry of Energy, Mines and Petroleum Resources*, Paper 1995-1, pages 435-448.

Resource Science, Inc. (1994): Mineral Resource Evaluation Workshop, March 15-17, 1994, Victoria, British Columbia, *in* Mineral Resource Evaluation Workshop, *B.C. Ministry of Energy, Mines and Petroleum Resources.*

Root, D.H., Menzie, W.D. and Scott, W.A. (1992): Computer Monte Carlo Simulation in Quantitative Resource Assessment; *Nonrenewable Resources,* Volume 1, No. 2, pages 125-138.

Singer, D.A. (1993): Basic Concepts in Three-part Quantitative Assessments of Undiscovered Mineral Resources; *Nonrenewable Resources*, Volume 2, No. 2, pages 69-81.

# EXTERNAL PUBLICATIONS

Atwater, B.F., Nelson, A.R., Clague, J.J., Carver, G.A., Yamaguchi, D.K., Bobrowsky, P.T., Bourgeois, J., Darienzo, M.E., Grant, W.C., Hemphill-Haley, E., Kelsey, H.M., Jacoby, G.C., Nishenko, S.P., Palmer, S.P., Peterson, C.D. and Reinhart, M. (1995): Summary of Coastal Geologic Evidence for Past Great Earthquakes at the Cascadia Subduction Zone; *Earthquake Spectra*, Volume 11, No. 1 [Contribution No. 032].

Barcelo, C., Pawlowsky, V. and Grunsky, E.C. (1995): Classification Problems of Samples of Finite Mixtures of Compositions; *Mathematical Geology*, Volume 27, No. 1, pages 129-148 [Contribution No. 048].

Bobrowsky, P.T. and Liverman, D.G.E., Editors (1993): Applied Quaternay Research; *Quaternary International*, Volume 20, 1993 [Contribution No. 10].

Bobrowsky, P. and Clague, J. (1995): Quaternary Geology of Southern Vancouver Island; *Geological Association of Canada/Mineralogical Association of Canada* Annual Meeting 1995, Fieldtrip Guidebook B1, 16 pages [Contribution No. 067].

Brown D.A. and Klewchuk, P. (1994): Pb-Zn-Ba Mineralization at Wilds Creek: Relevance to Stratabound Deposits along the Western Purcell Anticlinorium; *in* Northwest Geology, *Montana State University*, Volume 23, pages 27-32 [Contribution No. 030]

Casselman, M.J., Newman, K.M., and McMillan, W.J. (1995): Highland Valley Porphyry Copper Deposits near Kamloops, British Columbia: A Review and Update with Emphasis on the Valley Deposit; *Canadian Institute of Mining and Metallurgy*, Special Volume No. 46 [Contribution No. 22].

Clague, J.J., Bobrowsky, P.T. and Hamilton, T.S. (1994): A Sand Sheet Deposited by the 1964 Alaska Tsunami at Port Alberni, British Columbia; *in* Estuarine, Coal and Shelf Science, *Academic Press Limited*, Volume 38, pages 413-421 [Contribution 003].

Clague, J.J., Bobrowsky, P.T. and Hyndman, R.D. (1995): The Threat of a Great Earthquake in Southwestern British Columbia; *in* B.C. Professional Engineer, *Association of Professional Engineers and Geoscientists of B.C., pages 1-5 [Contribution No. 35].*

Clague, J.J. and Bobrowsky, P.T. (1994): Evidence for a Large Earthquake and Tsunami 200-400 Years Ago on Western Vancouver Island, British Columbia; *Quaternary Research*, Volume 41, pages 176-184 [Contribution No. 008].

Clague, J.J. and Bobrowsky, P.T. (1994): Tsunami Deposits in Tidal Marshes on Vancouver Island, British Columbia; *Geological Society of America*, Bulletin, Volume 106, pages 1293-1303 [Contribution No. 009].

Cook, S.J. (1994): Lake Sediment Geochemistry: An Exploration Tool for Buried Epithermal Precious Metal Deposits in the Northern Interior Plateau, British Columbia; *Geological Society of America*, Abstracts with Programs, Volume 6 [Contribution No. 055].

Cook, S.J., Levson, V.M., Giles, T.R. and Jackaman, W. (1995): A Comparison of Regional Lake Sediment and Till Geochemistry Surveys: A Case Study from the Fawnie Creek Area, Central British Columbia; *Exploration and Mining Geology*, Volume 4, pages 93-110 [Contribution 056].

Dunne, K.P.E. and Grant, B., Editors (1993): Mid-Continent Diamonds; GAC-MAC Symposium Volume, *Mineral Deposits Division*, 160 pages [Contribution No. 068].

Fletcher, W.K., Cook, S.J., Hall, G.E.M., Scagel, R.K. and Dunn, C.E. (1995): Enrichment of Platinum and Associated Elements in Organic Seepage Soils of the Tulameen Ultramafic Complex, Southern British Columbia; *Journal of Geochemical Exploration*, Volume 54, pages 39-47 [Contribution No. 057].

Grant, B., Editor (1995): Final Program and Abstracts Victoria '95. GAC/MAC Annual Meeting, May 17-19, 1995; *Geological Association of Canada*, Volume 20, 124 pages [Contribution No. 069].

Grunsky, E.C. and Good, C. (1995): Establishing and Managing a FTP Site: The IAMG Case History; *Computers and Geosciences*, Volume 21, No. 6, pages 771-774 [Contribution No 047].

Höy, T., Turner, R. and Leitch, C., Anderson, D., Ransom, P.W., Pighin, D. and Brown, D. (1995): Depositional Environment, Alteration and Associated Magmatism, Sullivan and Related Massive Sulphide Deposits, Southeastern B.C.; *Geological Association of Canada/Mineralogical Association of Canada* Annual Meeting 1995, Fieldtrip Guidebook A1, 80 pages [Contribution No. 061].

Hussain, N., Mustard, P., Struik, L., Luternauer, J., Matysek, P., Sibbick, S., Bobrowsky, P., and Noble, W. (1994): Results of a Survey of Clients for a Proposed Georgia Basin Geoscience Atlas [Contribution No. 017].

Levson, V.M. and Blyth, H. (1993): Applications of Quaternary Geology to Placer Deposit Investigations in Glaciated Areas: A Case Study, Atlin, British Columbia; *Quaternary International*, pages 93-105, Volume 20 [Contribution No. 02_].

Levson, V.M., Monahan, P.A., Meldrum, D.G., Matysek, P.F, Watts, B.D., Yan, L. and Sy, A. (1995): Seismic Microzonation Mapping in Southwestern British Columbia: A Pilot Project; *Canadian Geotechnical Society*, Trends in Geotechnique, 48th Canadian Geotechnical Conference, Volume 2, pages 927-936 [Contribution No, 049].

Levson, V.M. and Rutter, N.W. (1995): Pleistocene Stratigraphy of the Athabasca River Valley Regin, Rocky Mountains, Canada; Geographie Physique et Quaternaire, Volume 49 No. 3, pages 381-399 [Contributin No. 050].

Levson, V.M. and Morison, S. (1995): Geology of Placer Deposits in Glaciated Environments; *in* Past Glacial Environments - Sediments, Forms and Techniques, Menzies, J., Editor, *Butterworth-Heinemann*, Chapter 16, pages 441-478 [Contribution No. 051].

Levson, V.M. (1995): Late Pleistocene Stratigraphy and Sedimentology of Coarse Clastic Deposits in the Central Canadian Rocky Mountains, Jasper; Ph.D. Dissertation, *University of Alberta*, 269 pages [Contribution No. 052].

Levson, V.M., Clague, J.J., and Fulton, R.J. (1995): Quaternary Geology and Placer Gold Deposits of Central British Columbia; *Geological Association of Canada/Mineralogical Asso-*

*ciation of Canada* Annual Meeting 1995, Fieldtrip Guidebook A4, 67 pages [Contribution No. 053].

Lowe, C., Best, M.E., Seemann, D.A. and Bobrowsky, P.T. (1995): Shallow Subsurface Mapping Using an Integrated Geophysical Approach, Northern Vancouver Island, British Columbia; *Geological Survey of Canada*, Open File 3195, 109 pages [Contribution No. 043].

McMillan, W.J. and Panteleyev, A. (1995): Porphyry Deposits of the Canadian Cordillera; *in* Porphyry Copper Deposits of the American Cordillera, Pierce, F.W. and Bolm, J.G., Editors, *Arizona Geological Society*, Digest 20, pages 203-218 [Contribution 069].

McMillan, W.J., Thompson, J.F.H., Hart, C.J.R. and Johnston, S.T. (1995): Porphyry Deposits of the Canadian Cordillera; *in* The Gangue, No. 50, *GAC Mineral Deposits Division*, page 1-4 [Contribution No. 037].

McMillan, W.J., Thompson, J.F.H., Hart, C.J.R. and Johnston, S.T. (1995): Regional Geological and Tectonic Setting of Porphyry Deposits in British Columbia and Yukon Territory, *Canadian Institute of Mining and Metallurgy*, Special Volume 46 [Contribution No. 022].

Norford, B.S. and Mihalynuk, M.G. (1994): Middle Ordovician Graptolites in the Alexander Terrane, Northwestern British Columbia; Implications for Terrane Relationships; *Canadian Journal of Earth and Sciences*, Volume 31, pages 1389-1396 [Contribution No. 012].

Owen, J.V., Dostal, J., and Church, B.N. (1994): Mineralogic Reaction Zones at a Calc-silicate/Metapelite Interface: An Example of Trace Element Mobility in a Metamorphic Environment; *Mineralogical Magazine*, Volume 58, pages 205-214 [Contribution No. 046].

Panteleyev, A., Godwin, C., Juras, S. and Fleming, J. (1995): Mineral Deposits of Vancouver Island; *Geological Association of Canada/Mineralogical Association of Canada* Annual Meeting 1995, Fieldtrip Guidebook B1, 80 pages [Contribution No. 065].

Preto, V., and McMillan, B. (1995): Mineralization and Geological Setting of Calcalkaline and Alkaline Porphyry Copper Deposits in Southern B.C.; *Geological Association of Canada/Mineralogical Association of Canada* Annual Meeting 1995, Fieldtrip Guidebook A3, 151 pages [Contribution No. 063].

Ray, G.E., Webster, I.C.L. and Ettlinger, A.D. (1995): The Distribution of Skarns in British Columbia and the Chemistry and Ages of their Related Plutonic Rocks; *Economic Geology*, Volume 90, pages 920-937 [Contribution No. 011].

Roback, R., Schiarizza, P., Nelson, J., Fyles, J., Ferri, F., Höy, T., Ash, C. and Danner, W.R. (1995): Late Paleozoic Arc and Oceanic Terranes and Their External Relationships, Southern Quesnellia; *Geological Association of Canada/Mineralogical Association of Canada* Annual Meeting 1995, Fieldtrip Guidebook B1, 79 pages [Contribution No. 066].

Ryan, B. (1995): Coal Deposits of the Elk Valley and Crowsnest Pass, Southeast B.C. and Southwest Alberta; *Geological Association of Canada/Mineralogical Association of Canada* Annual Meeting 1995, Fieldtrip Guidebook A2, 54 pages [Contribution No. 062].

Schiarizza, P., Garver, J.J., Journeay, J.M. and Monger, J.W.H. (1995): Geology and Tectonic Evolution of the Southern Coast Belt, Southwestern British Columbia; *Geological Association of Canada/Mineralogical Association of Canada* Annual Meeting 1995, Fieldtrip Guidebook A5, 88 pages [Contribution No. 064].

Schroeter, T., Editor (1995): Porphyry Deposits of the Northwestern Cordillera of North America; *Canadian Institute of Mining, Metallurgy and Petroleum*, CIM Special Volume 46, 908 pages plus 1:2000 000 scale map [Contribution No. 054].

Sibbick, S.J. and Laurus, K.A. (1995d) Natural Mercury Contamination in a Vancouver Island Drainage: Residence Sites, Origin and Implications for Estimates of Acceptable Background Mercury Levels; *Geological Association of Canada/Mineralogical Association of Canada* '95 Program with Abstracts, page A-97 [Contribution No. 058].

Sibbick, S.J. (1995) Prediction of Acid Rock Drainage Prone Regions Using Regional Geochemical Data; *in* Proceedings of Sudbury '95: Mining and the Environment, Hynes, T.P. and Blanchette, M.C., Editors, *CANMET*, 3 Volumes, pages 897-904 [Contribution No. 059].

Sibbick, S.J. and Laurus, K.A. (1995c) Accumulation of Gold and Heavy Minerals in a Northern Vancouver Island Stream; *Explore*, Number 86, pages 8-12 [Contribution No. 060].

Stinson, P. and Brown, D.A. (1994 ): Iron Mineralization and Ultramafic Dikes on Iron Range Mountain, Southeastern British Columbia; *in* Northwest Geology, *Montana State University*, Volume 23 [Contribution No. 029].

Umhoefer, P.J., Schiarizza, P. (1995): Latest Cretaceous to Early Tertiary Dextral Strike-Slip Faulting on the Southeastern Yalakom Fault System, Southeastern Coast Belt, British Columbia; *Geological Society of America*, Bulletin [Contribution No. 039].

British Columbia Geological Survey Branch, 1995.

Staff appearing in the photo from front to back and left to right are: Vic Levson, George Owsiacki, Ron Smyth, Paula Ashby, Ian Webster, Tom Schroeter, Christine Petrini, Laura De Groot, Ray Lett, Cindy McPeek, Trygve Höy, Larry Jones, Linda Hitchen, Gib McArthur, Dave Huntley, Pat Desjardins, Janet Holland, John Armitage, Don MacIntyre, Micah Beaudry, Andre Panteleyev, Dan Meldrum, Fil Ferri, Mike Fournier, Talis Kalnins, Chris Ash, Chris Rees, Theresa Leonard, Sherri Proceviat, Kim Passmore, Shirley Marshall, Eric Grunsky, Vic Preto, Peter Bobrowsky, Bob Lane, Doreen Fehr, Barry Ryan, Nick Massey, Neil Church, Wade Noble, Mac Chaudry, Ward Kilby, Dan Hora, Dorthe Jakobsen, Pat Monahan, Steve Sibbick, Steve Cook, Gary Payie, Alex Matheson, Dave Lefebure, Maurice Colpron, Kirk Hancock, George Simandl, Pat Stinson. Photo by Dick Player.

Staff missing are: Dani Alldrick, Donna Blackwell, Beverly Brown, Derek Brown, Pierino Chicorelli, Larry Diakow, Brian Grant, Marjorie Hunter, Wayne Jackaman, Brad Johnson, Andrew Legun, Jim Logan, Bill McMillan, Paul Matysek, Mitch Mihalynuk, Joanne Nelson, Graham Nixon, Gerry Ray, Paul Schiarizza, Martin Taylor, Verna Vilkos, Allan Wilcox.